Magmatic processes associated with the Voisey's Bay Ni-Cu-Co sulphide deposit, Labrador, Canada

Thesis

MAGMATIC PROCESSES ASSOCIATED WITH THE VOISEY'S BAY Ni-Cu-Co SULPHIDE DEPOSIT, LABRADOR, CANADA

A thesis presented for the degree of
Doctor of Philosophy

by

Aaron Venables

B.Sc. (Hons.) 1998

Department of Earth Sciences
The Open University
Milton Keynes, U.K.

November 2003

Abstract

The Voisey's Bay deposit is considered anomalous within the terms of World-Class magmatic Ni sulphide deposits as it is hosted by low-olivine, low-forsterite troctolites within an anorthosite complex - a combination not previously considered a viable prospect for economic Ni-sulphide mineralisation.

The accepted model for generation of a sulphide magma at Voisey's Bay has been contamination of the troctolite parental magma at mid-crustal levels by the sulphidic and graphitic Tasiuyak gneiss. Trace element and mineralogical data presented here suggest that sulphide immiscibility is the result of contamination of the Voisey's Bay magmas by Nain gneiss, probably at the base of the crust.

Olivine geochemistry suggests that the source of the Ni at Voisey's Bay is a now departed high-Mg# melt with forsterite $>Fo_{80}$. Trace element evidence implies that this melt was plume-like and derived from 7-8 percent partial melting at garnet/spinel facies. The melting temperature was ~1530°C, the pressure was ~3.25 GPa, the fO_2 ~QFM.

Pb isotope, trace element, olivine and sulphide geochemical data imply that there was a sulphide liquid present before the parental magmas encountered the Tasiuyak gneiss. Although the Tasiuyak gneiss has contaminated the Voisey's Bay silicate magmas, the extent of contamination is small and coincidental. The Voisey's Bay intrusion sulphides and silicates exhibit different Pb isotope ratios, this disequilibrium is explained in terms of immiscibility, density contrasts and contamination models.

Data presented in this thesis allow the relative timing of the main events in the forming of the Voisey's Bay deposit to be constrained and for a new model of deposit genesis to be proposed. This new model provides new criteria for exploring within anorthosite complexes for another Voisey's Bay- type magmatic Ni-sulphide deposit.

Acknowledgements

Thanks must go first to Peter Lightfoot and INCO; without their help and support, technical, financial, moral, academic and logistical this thesis could never have existed. I owe Peter and INCO a huge debt. Secondly, I'd like to be able to thank my supervisors Nick Rogers and Chris Hawkesworth; their support made my time at the OU the experience it was. In terms of supervision, I am very grateful to Ian Parkinson – his support, guidance and steadfast belief all through this project helped to make it possible. Ian also has my gratitude for tolerating my rants!

For support and guidance in labs, techniques and all things OU I am indebted to Andy Tindle, John Watson, Mabs Gilmour, Jo Rhodes, Kay Green and Michelle Higgins: I can't begin to list all the times that, individually you've helped me – the list would make another thesis!

For friendship, support and office-mate buffoonery special thanks have to go to Steve Smith, Jo Rhodes and Dan Croucher: you've all helped me survive the Milton Keynes experience! Housemates are similarly thanked, in case you've managed to forget, you are: James Fox, Andy Mac, Deborah Osberg, Mark Gaved, Cheryl Williams Russell Johnson, John Watson, Ziggy Pozzi-Walker, Mary Metz, and Marie-Noelle Guilbaud. There are others and I will identify them publicly and at my leisure! Someone who has never had the misfortune to share a house with me but deserves endless thanks for support both moral and financial and for being a really good mate is Justin: thanks mate.

Finally, Olwyn: without your support I don't think that I'd ever have finished this thesis, you stopped me quitting and helped provide inspiration and ideas. Thank you too for help with printing binding and collation type activities. What's more, if you hadn't nagged me I don't think that I'd ever have handed in the corrected version! Oh, and thanks for being you – it's what makes you special.

Table of Contents

List of Figures

CHAPTER 2

CHAPTER 3

CHAPTER 4

CHAPTER 5

CHAPTER 6

CHAPTER 7

Discussion and Conclusions

List of Tables

Chapter 1

Chapter 3

Chapter 1

Background to Magmatic Ni-Sulphide Deposits and Why Voisey's Bay is Different

1.1 General background

Nickel is an important industrial element used in the manufacture of corrosion resistant alloys, the blades of turbines and jet engines, batteries for electronic equipment and probably most familiarly, stainless steel. Because of the importance and diversity of uses for Ni, its value is high; over the last three years, its value has fluctuated between US$4500-10000 per imperial ton (Source: London Metal Exchange).

The Voisey's Bay intrusion is a world-class, Ni-Cu-Co magmatic sulphide deposit, currently estimated at 136.7 million tonnes of sulphide, grading at 1.59% Ni, 0.85% Cu and 0.09% Co including measured, indicated and inferred resources (Evans-Lambswood et al., 2000). Because of nickel's high value, its listing as a strategic metal, as a new deposit, Voisey's Bay resource is extremely important.

1.2 Outline of major Ni-Cu magmatic sulphide deposits

Types of geological settings

Magmatic Ni-sulphide deposits are associated with mafic or ultramafic rocks. This type of deposit is rare and not all mafic or ultramafic rocks have associated economic concentrations of Ni-sulphides.

The world's most significant Ni-Cu sulphide deposits can be confined to four petrologic/tectonic settings (Naldrett, 1989a; Naldrett, 1989b):

1. Deposits found within Archaean greenstone belts.

2. Deposits associated with rifted plate margins and ocean basins.
3. Deposits associated with cratonic areas.
4. Sulphide mineralisation in syn-orogenic mafic intrusions.

Archaean greenstone belts

The first of these categories, the Archaean greenstone belts have two main associations; those associated with komatiitic rocks and those with tholeiites (Naldrett, 1989a, 1989b). The komatiitic class is represented by the deposit at Kambalda, Australia (Gresham and Loftus-Hill, 1981). The tholeiite class is typified by the Pechanga deposit of the former USSR (Green and Melezhik, 1999).

Rifted plate margins and ocean basins

Deposits associated with rifted plate margins can be divided into those hosted by continental crust and those that are ophiolite-hosted. Ophiolites are not usually noted for their magmatic sulphide mineralisation but the Acoje Ni sulphide deposit in the Zambaldes ophiolite of the Philippines, described by Bacuta et al. (1987) is a definite example of this type. The continental crust-hosted type is represented by the Thompson belt, Manitoba Canada (Zurbrigg, 1963).

Cratonic associated deposits

This category includes deposits related to picritic-tholeiitic flood basalt magmatism, and large stratiform complexes. Naldrett (1997) includes anorthosite provinces in this category, presumably to account for the then recent discovery of Voisey's Bay. Of the deposits associated with picritic-tholeiitic flood basalts, Noril'sk–Talnakh is probably the most important (Naldrett and Lightfoot, 1999). The Duluth complex of the Keweenawan lavas of the United States (Weiblen and Morey, 1980) is also a representative of this type of deposit and although it has extensive disseminated Ni-Cu sulphide mineralisation, it is

currently sub-economic (Naldrett, 1997). The stratiform complexes are divided into those that have a sheet-like morphology and dyke-like bodies. The Bushveld and Stillwater complex are representative of the former (Czamanske and Zientek, 1985: Wager and Brown, 1968: Wisser and von Gruenewaldt, 1970), while the Great Dyke of Zimbabwe is a representative of the latter (Prendergast, 1988). However, both types are exploited primarily for their PGE mineralisation rather than Ni-sulphides. The Sudbury Igneous Complex has also been included in the sheet-like stratiform bodies. However, Sudbury must really be considered as a special case as it is now widely considered to be the result of meteorite impact (Dressler, 1984; Grieve, 1994) rather than the usual forms of mantle-derived magmatism that are invoked for magmatic sulphide deposits.

Syn-orogenic mafic intrusion hosted deposits

The final category, syn-orogenic mafic intrusions can be sub-divided into those that were emplaced during active compression and those that were emplaced during epiorogenic rebound. The former type, emplaced during the active phase, include the Moxie pluton in Maine, United States (Thompson and Naldrett, 1984) and the Caledonian intrusions of north-eastern Scotland (Fletcher et al., 1987). This type has proved to be host to only minor Ni-Cu-sulphide deposits (Naldrett, 1997). The latter type, often referred to as Alaskan type deposits (Irvine, 1974), have not proved to be significant as sources for Ni-Cu sulphides (Naldrett, 1997).

1.3 Features common to magmatic sulphide deposits

At this point, it is useful to summarise what is known about major magmatic Ni-Cu sulphide deposits from around the world and to investigate if the Voisey's Bay deposit conforms to the accepted models. Naldrett (1997, 1999) compiled a set of criteria by which new deposits could be judged to examine how well they conform to the pattern

defined by well-known magmatic sulphide deposits. These criteria have been reproduced and are presented as Table 1.1 below.

Several factors appear to be common to all the deposits. For example: a high Mg# magma (termed olivine-rich magma by Naldrett, 1999), a prominent crustal suture and a magma conduit. Other features that are common to most: a sulphur source in the country rock, interaction with country rocks, and chalcophile depletion in the parental silicate magma.

Key Factor	Noril'sk	Kambalda	Duluth	Jinchuan	Voisey's Bay
Olivine rich magma	Yes (Fo_{80})	Yes (Fo_{90-95})	Yes (Fo_{50-65})	Yes (Fo_{84})	Yes (Fo_{50-65})
Prominent crustal suture	Yes	Yes	Yes	Yes	Yes
Sulphur source in country rock	Yes	Yes	Yes	Not established	Yes
Chalcophile depletion	Yes	Yes	Not established	Not established	Yes
Interaction with country rocks seen	Yes	Yes	Yes	Not established	Yes
Magma conduit	Yes	Yes	Yes	Yes	Yes
Economic	Yes	Yes	No	Yes	Yes

Table 1.1 A comparison of major Ni-Cu sulphide deposits and factors in their genesis (from Naldrett, 1997, 1999). This demonstrates a number of common features that are implicated in the genesis of magmatic sulphide deposits. The forsterite contents in this table are taken directly from Naldrett (1999) and differ from the values found for Voisey's Bay in this study.

1.4 How well does the Voisey's Bay deposit fit the model?

The Voisey's Bay deposit appears to fit well with the other deposits in Table 1.1. However, the Voisey's Bay deposit is associated with an anorthosite complex – until the discovery of Voisey's Bay, anorthosite complexes were not considered favourable prospects for Ni-sulphide exploration. In addition, the rocks parental to the Voisey's Bay deposit are typified by low abundances of olivine. Moreover, Naldrett (1997) found that the olivine at Voisey's Bay is Fo_{50-65} rather than Fo_{80} or higher that is typical for other most sulphide deposits. The only deposit to share the low forsterite values is Duluth, a deposit that is at present sub-economic (Naldrett, 1997). Magmatic sulphide deposits are generally thought to form via sulphide liquid scavenging of chalcophile elements from silicate magmas, especially those rich in olivine. Because high Ni contents in olivine are associated with high forsterite values (e.g. Beattie et al., 1991; Hart and Davies, 1978), one

would expect a high Ni deposit such as Voisey's Bay to be associated with high forsterite olivine. Other world class magmatic Ni-Cu sulphide deposits are usually associated with high-forsterite mafic and ultramafic intrusions. For example, Kambalda, Noril'sk-Talnakh, Jinchuan etc. Thus, the low forsterite values at Voisey's Bay are intriguing.

Another puzzling aspect of the Voisey's Bay deposit is the role of crustal contamination. From the studies that have been carried out on other major Ni-sulphide deposits, e.g. Noril'sk, Kambalda, Duluth, Sudbury (Naldrett, 1995; Lesher and Groves, 1986; Ripley, 1981,1986: Irvine, 1975; Li and Naldrett 1983 respectively), it appears that interaction with country rocks was the cause of sulphide immiscibility. This interaction usually takes the form of assimilation of sulphur-bearing country rocks. However, sulphide immiscibility can be induced by the assimilation of either sulphur or silica; both in sufficient quantity can cause the generation of an immiscible sulphide liquid (O'Neill and Mavrognes, 2002). At Voisey's Bay, there is an ideal candidate as a contaminant to induce sulphide immiscibility in a mafic melt: the Tasiuyak gneiss – a sulphide-bearing, quartzo-feldspathic, Proterozoic paragneiss. Despite abundant petrologic and textural evidence suggesting extensive assimilation of the Tasiuyak gneiss by the Voisey's Bay magmas (e.g. Li and Naldrett, 1999; Li and Naldrett, 2000; Lightfoot and Naldrett, 1999; Naldrett, 1997 and Naldrett et al., 2000) the trace element and isotopic evidence remain ambiguous, suggesting that the Voisey's Bay magmas have had only an inconsequential interaction with the Tasiuyak gneiss (Amelin et al., 2000; Lambert et al., 2000; Li et al., 2000; Ripley et al., 1999).

1.5 Thesis aims

The points outlined above raise four main questions:

1. As anorthosite complexes are not usually held to be good prospects for Ni-sulphide mineralisation, presumably the parental magmas of the Voisey's Bay intrusion are unusual - what is the nature of the Voisey's Bay parental magmas?
2. The Voisey's Bay intrusion rocks have anomalously low forsterite contents for the host of a major Ni-sulphide deposit. Are these rocks the source of the Voisey's Bay Ni?
3. The Tasiuyak gneiss has all the attributes of an ideal contaminant to induce sulphide immiscibility but has little apparent influence on the composition of the Voisey's Bay intrusion. What is the contamination history of the Voisey's Bay intrusion?
4. Was the Tasiuyak gneiss the contaminant that induced sulphide immiscibility?

1.6 Thesis structure

Chapter 2 presents the background to the Voisey's Bay deposit in terms of host geology, regional geology and regional tectonic history. The controls on sulphide solubility are explored and the mechanism that would lead to sulphide immiscibility and forming of a Ni-sulphide deposit are considered.

Chapter 3 is an investigation of the nature of the Voisey's Bay intrusion rocks using new major and trace element data collected from several diamond drill cores.

Chapter 4 presents new olivine forsterite and Ni data for samples collected from diamond drill hole VB 96 266.

Chapter 5 is a detailed investigation of variations in sulphide chemistry using new data from samples across the Voisey's Bay deposit.

Chapter 6 presents new Pb isotope data for the Voisey's Bay sulphides and combines these with published data to gain insights to sulphide genesis.

Chapter 7 is a summary of the data presented in this thesis and details the conclusions that can be drawn, along with suggestions for further work.

Chapter 2

Geological Background of the Voisey's Bay Magmatic Sulphide Deposit and the Controls on Sulphide Solubility

2.1 Location of the Voisey's Bay intrusion

The Voisey's Bay deposit is located in western Labrador, Canada, approximately 56° 18' north and 62° 10' west (Figure 2.1) and is hosted by the Voisey's Bay intrusion (VBI), part of the Nain Plutonic Suite (NPS), a major mid-Proterozoic intrusive complex. The NPS intrudes a Paleoproterozoic suture between two major lithotectonic terrains, the Archaean

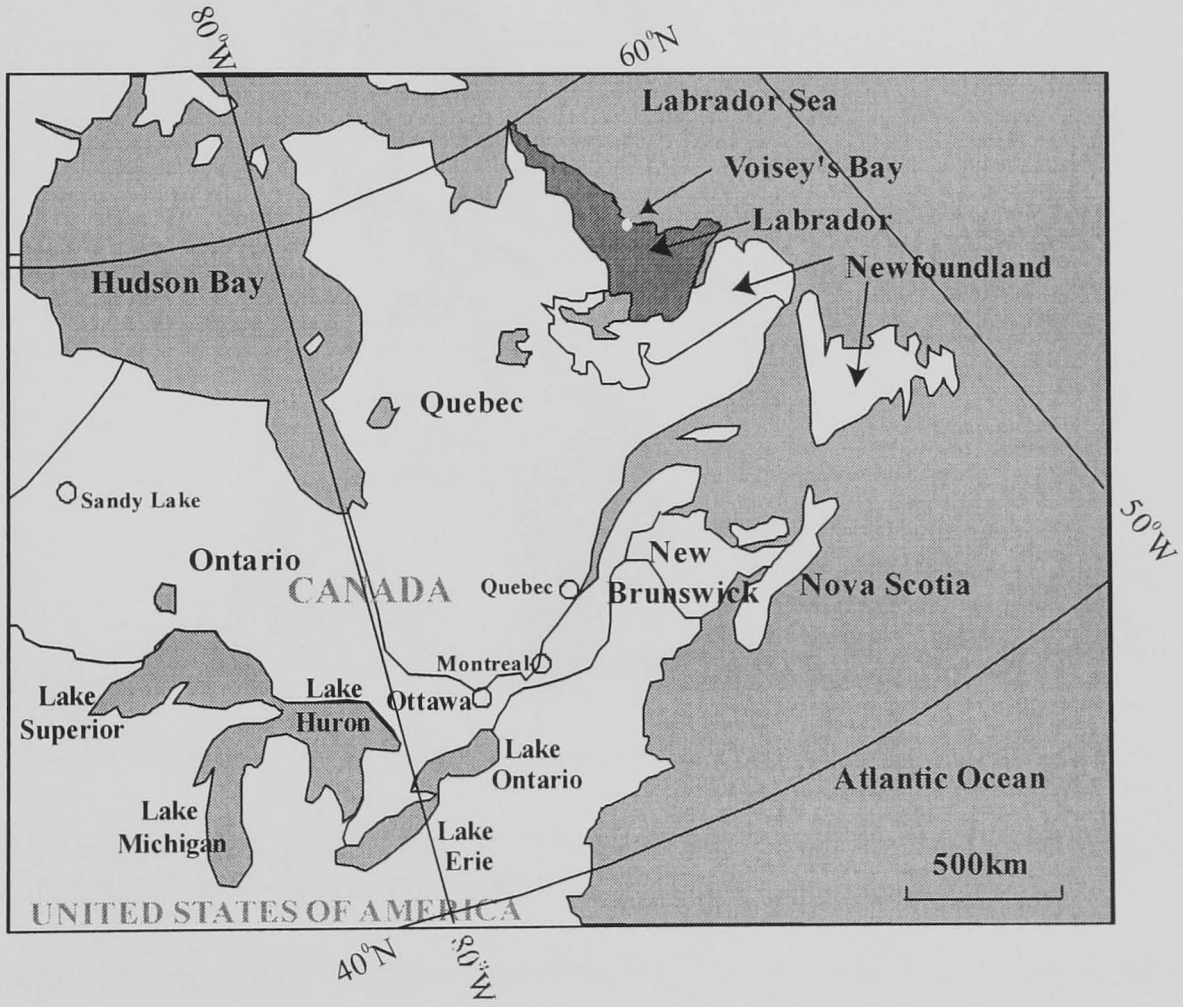

Figure 2.1 Map of eastern Canada illustrating the location of Voisey's Bay, Labrador.

Nain Province to the east and the Palaeoproterozoic and Archaean Churchill Province to the west (Figure 2.2).

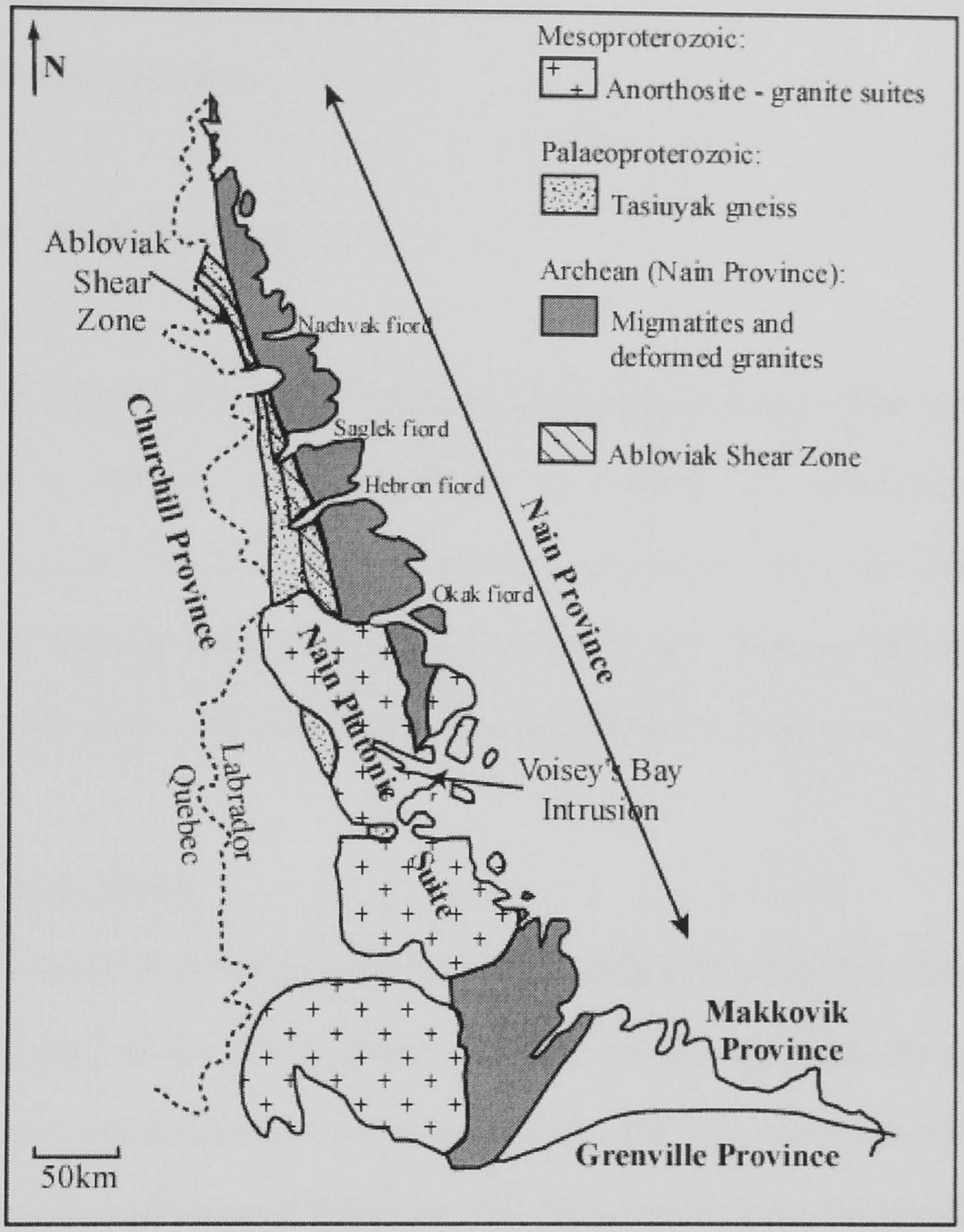

Figure 2.2 Schematic geological map of Labrador showing the province boundaries, political boundaries and extent of the Nain Plutonic Suite (NPS). (Redrawn from Ryan et al., 1995)

It is believed that the Voisey's Bay deposit formed as the result of a mantle-derived melt (part of the Nain Plutonic Suite magmatism) interacting with the Tasiuyak gneiss. The consequence of this interaction was the onset of sulphide immiscibility, chalcophile scavenging and the subsequent genesis of a Ni-Cu-Co, magmatic sulphide deposit. The country rock that is thought to have been the chief cause of sulphide immiscibility is the Tasiuyak gneiss, a locally sulphide and graphite-bearing garnetiferous, quartzo-feldspathic paragneiss (e.g. Evans-Lambswood et al., 2000; Li and Naldrett, 1999; Li and Naldrett,

2000; Li et al., 2001; Naldrett, 1997). The host magma and postulated source of the Ni, Cu, and Co is the Voisey's Bay intrusion, a poorly layered gabbroic and troctolitic intrusion, possibly the oldest member of the Nain Plutonic Suite. The NPS is a mid-Proterozoic massif anorthosite complex.

2.2 The Nain Plutonic Suite

2.2.1 Outline

The Nain Plutonic Suite is a complex of coalescing plutons that underlies around 19000km^2 of Labrador (Figure 2.2). The NPS is comprised of a varied collection of rocks, ranging from gabbroic to syenitic. Anorthositic and granitic rocks, approximately equal in abundance, make up around 90% of the NPS by area, the remaining 10% being comprised of more mafic rocks such as norites, gabbros and troctolites (Berg et al., 1994).

2.2.2 Tectonic setting

The NPS straddles the Palaeoproterezoic continental suture between the Archaean Nain Province, part of the North Atlantic Craton to the east, and the more complex Palaeoproterozoic Churchill Province to the west. The NPS was emplaced some 400 Ma after post-collisional rebound had ceased. It is therefore unlikely that the NPS magmatism is linked to the tectonic processes involved in collision. However, Berg (1994) has described the NPS as a 'stitching batholith' and infers that the junction between the Nain and Churchill provinces may have had some role in focusing the intrusion of the NPS event magmas.

2.2.3 Age of the Nain Plutonic Suite

Granitoid rocks exhibit both the oldest and the youngest ages of all the lithologies within the NPS, implying that this type of magma was produced throughout the history of the NPS event (Ryan, 2000). Because of this, the efforts to constrain the age of the NPS have

focussed on broadly granitic rocks. The oldest ages published so far for the NPS have been found in monzonitic rocks from around Webb Bay, that yielded zircon U-Pb ages of 1.35-1.34 Ga (Connolly and Ryan, 1994). A quartz monzodiorite from just north of Webb Bay was found to have an emplacement date of 1.33 Ga based on zircon and baddelyite U-Pb chronology (Hamilton et al., 1998). The Makhavinekh Lake Pluton to the west and intruding into the Voisey's Bay deposit has been found to have been emplaced at 1.322 Ga (Ryan, 2000). The youngest age so far derived for a NPS rock is for granite from Dog Island. This crystallised at 1.29 Ga (Ryan, 2000). In summary, it seems that the Nain Plutonic Suite magmatism started at around 1.35 Ga and continued until 1.29 Ga, some 60 million years later. It must also be noted that Ryan (2000) does not give any errors for these ages.

2.2.4 Petrogenesis

The petrogenesis of the NPS has been extensively investigated, most notably by Emslie et al. (1994). Since then the NPS has been reviewed by Bedard (2001) but essentially the conclusions have remained the same. Emslie et al. (1994) proposed that generation of the anorthosite complex started with plume-associated basaltic activity in the mantle and lower crust. The consequence of this activity was large-scale anatexis of lower crustal rocks, causing the production of a granitic magma. This granitic melt then ascended buoyantly, leaving behind a plagioclase-pyroxene-granulite residue. This is in many ways similar to the model outlined by Fountain et al. (1989) for the anatectic petrogenesis and melt segregation in granites. This process would have left a heated restite, which would have been available for assimilation by the ponded, basaltic, mantle-derived magma. Assimilation of the heated restite by the basic magma (that caused the partial melt via assimilation-fractional crystallisation processes) would have promoted plagioclase saturation. This would have resulted in plagioclase spending extended periods on the liquidus, generating an anorthositic parental magma. This proposed mechanism for the

generation of anorthosite is well-supported by the trace element data for the early-formed granites found at Voisey's Bay: these early–stage granites are depleted with respect to Eu and Sr implying that the restite retained plagioclase (Emslie et al., 1994). The recognition that some of the major granitoid plutons of the NPS are older than several of the more mafic members, also supports this model.

2.2.5 Emplacement Depth

The depth at which the NPS was intruded has been investigated by numerous authors. Berg and Wheeler (1976) found an osumilite-bearing assemblage adjacent to the Anaktalik Brook anorthosite, part of the VBI, and inferred that this indicated a temperature of 700-900°C and approximately 5 kbar total pressure. In a later paper, Berg (1977) concluded that the temperature ranged from 645–915°C and that the pressure was 3.7–6.6 kbar. These pressures and temperatures are slightly contradicted by Speer (1982). Speer studied the Snyder Group, a metamorphic terrain in the contact aureole of the nearby Kiglapait Intrusion. His study concluded that the peak metamorphic temperature was 900°C, and that the estimated equilibration pressure of the metamorphic assemblage was 2.2 kbar, using the Holdaway (1971) triple point geobarometer. In marked contrast to these are the conclusions reached by Emslie et al. (1994) concerning the pressures reached by the magmas that formed the NPS. Because the NPS magmas contain aluminous orthopyroxene megacrysts, typical of pressures of 6.2 to 11 kbar; considerably greater than those observed by the previous authors. However, it is likely that theses megacrysts are relicts of a previous high-pressure environment and were carried up from much greater depths in a mush of melt and crystallised material. With the perspective that massif anorthosite genesis occurred at the crust-mantle boundary and with the generation of large accumulations of melt at this interface, this would not perhaps be an unfeasible prospect.

2.3. The Nain – Churchill Province boundary

2.3.1 Outline

The first worker to recognise the Nain and Churchill Provinces as separate terrains was Taylor (1971, 1972). Taylor (1972, 1972) observed that two gneisses of contrasting character were divided by a roughly north-south trending boundary. He proposed that these two gneisses represent separate structural provinces of the eastern Canadian Shield: the Archaean Nain Province and the Palaeoproterozoic Churchill Province. Bridgewater et al. (1973) proposed that the Nain – Churchill boundary represented a major Palaeoproterozoic continental-suture with oblique strike-slip shear. Later work by Korstgard et al. (1987) continued within this theme and defined some of the structural elements that justify the tectonic model. Among the most important of these elements is the Abloviak Shear Zone (see Figure 2.2). This shear zone comprises of a belt of mylonitic rocks along the eastern edge of the Churchill Province with shallowly plunging lineations; the lineations mostly confined to the Tasiuyak gneiss. Taylor (1979) was able to show that the juncture between the Nain and Churchill Provinces was tectonic and this was subsequently named the Torngat Orogeny.

2.3.2 Geological Background

The Torngat Orogeny spans three principal lithotectonic elements. In the east (Nain Province) are the Archaean Nain gneisses and at least one set of deformed Palaeoproterozoic dolerite dykes. These are all unconformably overlain by the metamorphosed Ramah and Mugford Groups. The Ramah Group comprises a basal shelf sequence overlain by deeper water sequences. The Mugford Group has a basal shelf sequence that is overlain by predominantly volcanic rocks (Taylor, 1979). The western side (Churchill Province) of the orogeny is underlain by reworked Archaean gneisses and also contains deformed Palaeoproterozoic mafic dykes and folded remnants of shelf type metasedimentary rocks (Taylor, 1979). These have been interpreted as representing the

continuation of the Palaeoproterozoic Lake Harbour Group. Taylor (1979) was also able to delineate a broad belt of pelitic and paragneiss, subsequently named the Tasiuyak gneiss (Wardle, 1983), that runs from Nachvak Fiord south towards Nain and divides the Nain and Churchill Provinces (Figure 2.2).

2.3.3 Tectonic History

The tectonic history of the Torngat orogen, begins at approximately 1.88Ga with the intrusion of the enderbitic rocks, Figure 2.3a. These have been interpreted as dioritic plutons representative of a continental magmatic arc during westward subduction beneath the Churchill Province (Lightfoot and Naldrett, 1999).

The Nain-Churchill collision began at or before 1.86 Ga and continued through until 1.74 Ga in three distinct phases (Bertrand et al., 1993). In the first instance, collision caused crustal thickening, east to west shortening and associated metamorphism, lasting from 1.86 to 1.84 Ga (Figure 2.3b). This was followed by the onset of sinistral shearing from 1.84 to 1.82 Ga (Figure 2.3c), concentrated within a 10-15km wide zone now known as the Abloviak Shear Zone. The probable cause for this is the change in the locus of subduction and the accretion of juvenile material to the southern margin of the Nain Province. This would have had the result of driving the Nain Province northwards relative to the Churchill Province (Van Kranendonk, 1993). The final episode of tectonics was the uplift and exhumation, juxtaposing high-grade metamorphic rocks in the west against lower grade rocks in the east. This uplift may have been initiated by the collision of the Superior Province to the south and is thought to have persisted until 1.79 Ga (Ryan, 2000), Figure 2.3d. By 1.74 Ga the Torngat Orogeny was essentially over and the boundary had become quiescent.

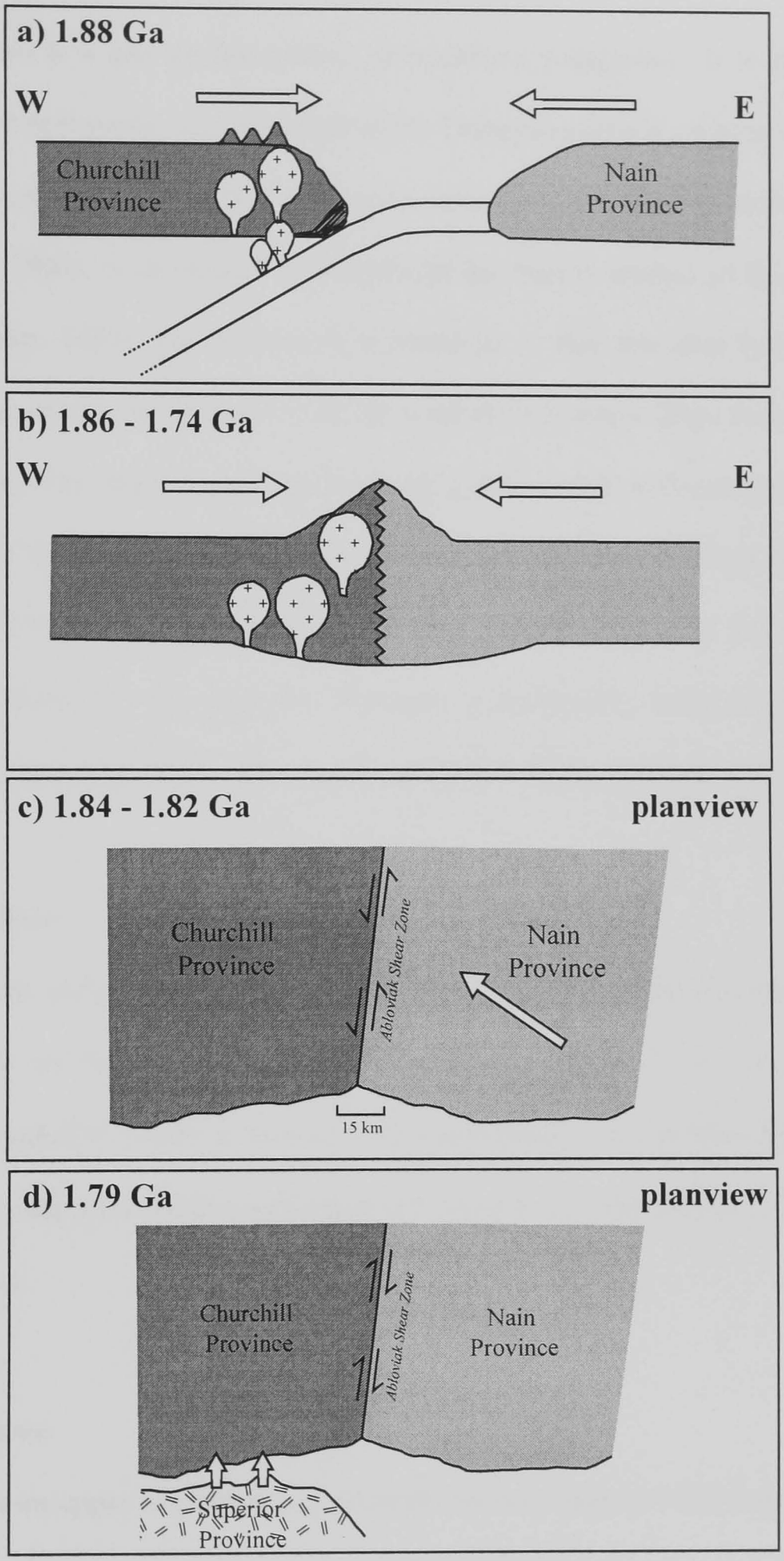

Figure 2.3 Cartoon depicting the tectonic evolution of the Churchill, Nain and Superior provinces. a) 1.88 Ga, oceanic crust is subducted beneath the Churchill Province. b)Collision begins between the Churchill Province to the east, and the Nain Province to the west at approximately 1.86 Ga. c)Collision is folowed by sinistral shearing at 1.84-1.82 Ga and the establishment of the Abloviak Shear Zone. d)The sense of shear is reversed as the Superior Province collides with the southern margin of the Churchill Province (1.79 Ga).

2.3.4 Tasiuyak gneiss

The Tasiuyak gneiss is a quartzo-feldspathic, garnetiferous paragneiss. It is also locally sulphide- and graphite-bearing. The protoliths of the Tasiuyak gneiss have been interpreted as a continental slope, turbiditic quartz arenite and pelite deposit (Van Kranendonk, 1993; Van Kranendonk, 1996), or as oceanic sediments on the eastern margin of the Churchill Province (Hoffmann, 1988). An alternative explanation is that this unit formed as an accretionary wedge during the subduction of the southeast Churchill (Rae) Province (Van Kranendonk, 1993). The exact age of the Tasiuyak gneiss is not well constrained but it must be older than the Torngat orogen (1.88-1.74 Ga) that deforms it. Work by Jackson and Hegner (1991) based on Nd isotopic systematics, suggests an age of 2.1 Ga for the Tasiuyak gneiss. However, this age may represent a composite, based on the mixed provenance of Archaean and Proterozoic material accreted during collision.

2.3.5 Enderbite gneiss

Within the Tasiuyak gneiss, there are large bodies of deformed orthopyroxene tonalities (enderbites). These are thought to represent the roots of a magmatic arc formed on the margin of the Churchill Province at around 1.88 Ga (Ermanovics and Van Kranendonk, 1990). These have undergone metamorphism in the Torngat orogeny and are referred to as the Enderbite gneiss.

2.3.6 The Nain gneiss

The Nain gneiss is an upper amphibolite to granulite facies, tonalitic rock that is believed to have been derived from plutonic protoliths emplaced between 3.85 and 3.1 Ga (Wardle and Wilton, 1995) and underwent widespread migmatism ~2.8 Ga (Vielzuf and Vidal, 1990). The Nain gneiss is unconformably overlain by rocks of the Ramah Group. This group consists of a basal shelf facies sequence of dolomitic sandstone, quartzite and dolomite. This in turn, is conformably overlain by the Nullataktok Formation, which

includes widespread massive to bedded pyrite–chert units. The Nullataktok Formation is succeeded by debris flow breccias of the Warspite Formation. These in turn are overlain by turbidites of the Cameron Brook and Typhoon Peak formations (Hoffman, 1987).

2.4. The Voisey's Bay Deposit

2.4.1 Deposit morphology

The Voisey's Bay intrusion trends more-or-less east-west for approximately 6km as defined by exploratory drilling (Evans-Lamswood et al., 2000). At the surface, its morphology is that of a 10–100m scale linear feature cutting across the country rocks. See Figure 2.4 for a deposit scale map. In three dimensions, the Voisey's Bay intrusion can be envisaged as a gently south-dipping, sheet-like structure that overturns through vertical to dip to the north. In addition, the axis of this hinge plunges to the east at about 30 degrees (Naldrett, 1997b). Lightfoot et al. (1999) proposed that the Voisey's Bay deposit took the form of two chambers connected by a conduit. Figure 2.5 is a schematic, west-facing representation of the morphology of the host intrusion. Later work by Evans–Lamswood et al. (2000) strongly supports this model and is able to divide the mineralisation styles and link these to position within the deposit. The massive mineralisation occurs in four zones. From west to east, the zones are the Reid Brook Zone, Mini Ovoid, Ovoid and the Eastern Deeps (Figure 2.4).

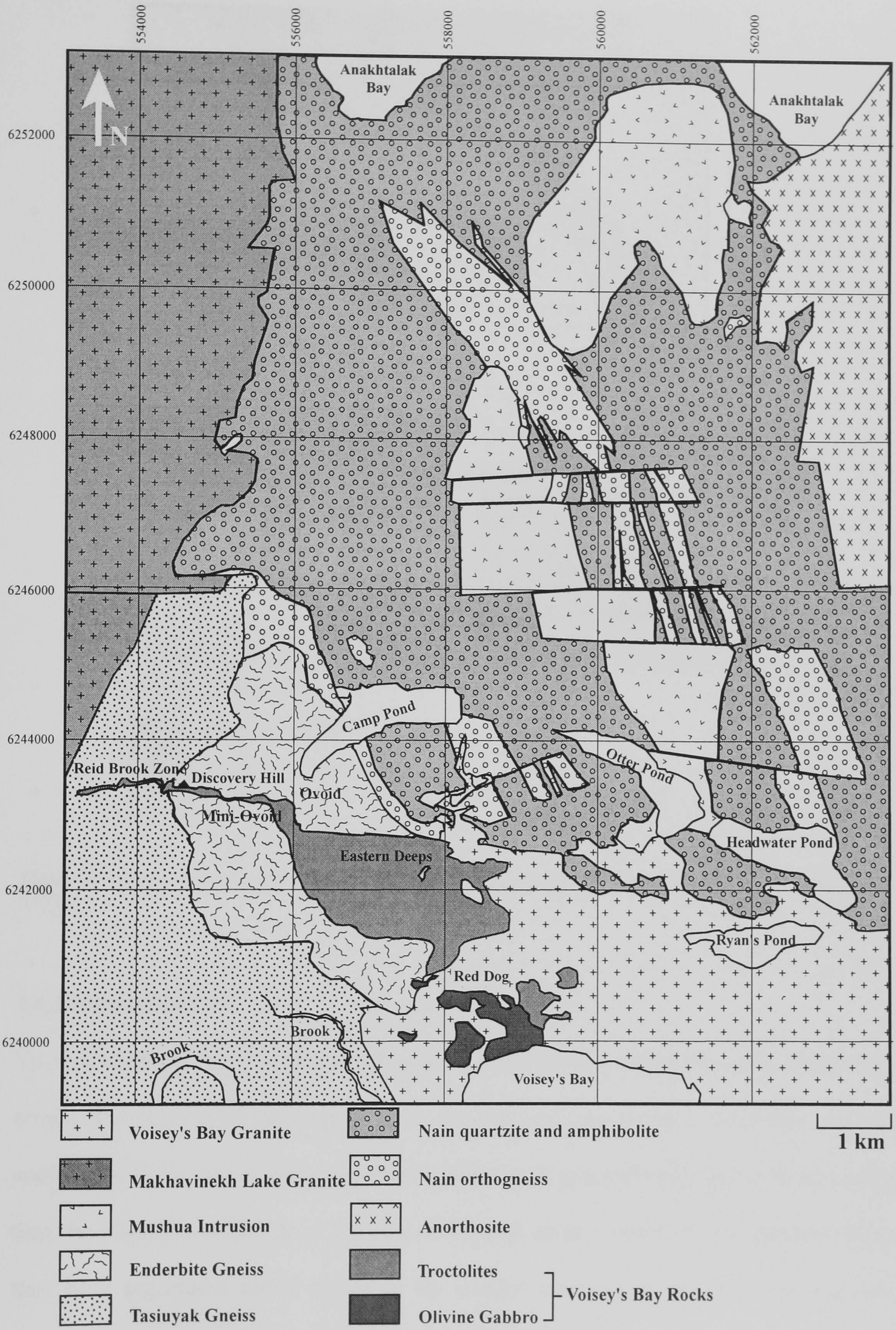

Figure 2.4 Geological map of the Voisey's Bay area showing the deposit zone names and Anakhtalak and Voisey's Bays. Redrawn from Voisey's Bay Nickel Company data.

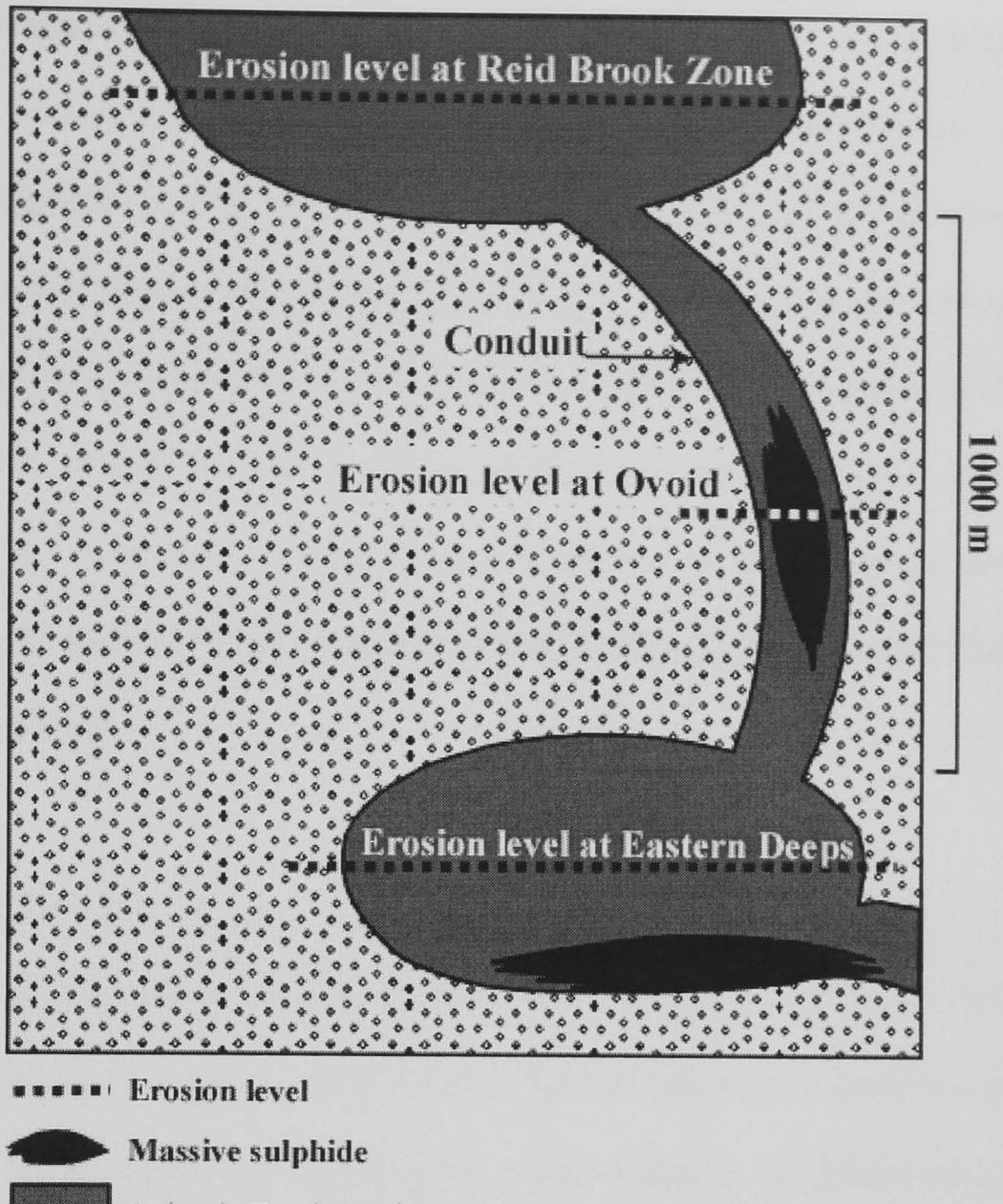

Figure 2.5 Schematic, west-facing cross section of the Voisey's Bay intrusion (after Lightfoot et al., 1999).

2.4.2 Mineralisation

Textural evidence at Voisey's Bay strongly suggests that the mineralisation is magmatic in origin. The mineralisation is present as disseminated and massive sulphides, with the controls on style appearing to be dynamic rather than gravitational. That is to say, rather than the sulphides collecting at the base of the deposit as a result of their greater density, they have segregated out at points in the conduit where is a change in flow (Evans-Lamswood et al, 2000). The primary sulphide minerals present are pyrrhotite, chalcopyrite and pentlandite. The relative proportions of these minerals are variable across the deposit. Additional accessory sulphide minerals include galena, sphalerite and cubanite. At

various locations across the deposit, most notably the Ovoid, magnetite can be very abundant. Voisey's Bay is exceptional when compared with similar sized magmatic sulphide deposits in that gravitational separation seems not to have been the primary mechanism for sulphide segregation. Rather it seems that the controlling factor for the location of massive sulphides was dynamic flow. Evans-Lamswood et al. (2000) proposed that the best analogy for the deposition of the sulphides is that of a fast-flowing stream depositing its sediments. Where there is a change in flow regime, sediments will be deposited. At Voisey's Bay, changes in conduit morphology are often marked by pods of massive sulphide.

2.4.3 Host Geology

The Voisey's Bay deposit is hosted within the Voisey's Bay intrusion. Formerly, this was known as the Reid Brook Intrusion (RBI). The RBI has been reclassified as two intrusions because isotopic and age studies have revealed that it is comprised of two separate intrusive events; the sub-economically mineralised Mushua Intrusion and the Voisey's Bay intrusion (Li et al., 2000).

In the area of the Ovoid and Discovery Hill, the VBI intrudes retrogressed orthogniess (enderbite) of the Churchill Province. To the east, the enderbite is in contact with the migmatitic, quartzofeldspathic, metagabbroic and metasedimentary gneisses of the Nain Province. To the west, the enderbite is in contact with the locally graphitic and garnetiferous Tasiuyak gneiss of the Churchill Province. There are two types of magmatic environment preserved within the VBI, sulphide-poor magma chambers and locally sulphide-rich magma conduits. Although the conduit and the chambers are spatially linked, Evans-Lamswood et al. (2000) points out that they may not be contemporaneous.

2.4.4 Age

Troctolites from the Voisey's Bay intrusion have yielded ages of 1.333 ±0.001 Ga based on zircon, apatite and baddelyite U-Pb geochronology (Amelin et al., 1999). This is corroborated by a study of Ryan (1995) that found zircons with an age of 1.338 Ga.

2.4.5 Setting within the NPS

The troctolitic rocks of the VBI have the least crustally contaminated and most mantle-like isotopic signature of all the NPS rocks so far investigated. In addition, they have the least crustally influenced trace element and REE profile when normalised to primitive mantle (Lightfoot and Naldrett, 1999). The VBI is also the oldest of the mafic members of the NPS yet found (Ryan, 2000).

2.4.6 Stratigraphy of the Voisey's Bay intrusion

The stratigraphy of the Voisey's Bay intrusion was first described in detail by Li and Naldrett (1999) and the description below follows their example so that consistency is maintained with other authors. (Thin section photomicrographs are presented in Appendix D.) The Voisey's Bay deposit is associated with a troctolitic body that forms an upper chamber, the Eastern Deeps, that is connected to a lower chamber (the Reid Brook Zone) by a troctolitic/gabbroic feeder sheet. This feeder sheet separates the two chambers by approximately 1000 metres in vertical extent.

At Voisey's Bay, there are several different intrusive rock types. Li and Naldrett (1999) based their description of the VBI rocks upon that of Streckeisen, (1976). The rocks thus described are olivine gabbro, normal troctolite, vary-textured troctolite, breccia sequence, and marginal phase. In addition, there are sets of mafic dykes, syenite dykes and intercalated layers of a rapakivi granite that all post-date the original intrusive event and are not involved in the mineralisation process. Because of this, their description is not included.

Olivine gabbro

The olivine gabbro is a common rock in the Voisey's Bay intrusion. It is an olivine-plagioclase cumulate with 50-70 modal percent plagioclase, 15-30 modal percent olivine, and 10-20 modal percent augite. Interstitial minerals are hornblende, biotite, ilmenite and sulphide. The interstitial material amounts to less than 20 modal percent. Augite occurs mainly as large crystals surrounding plagioclase and olivine poikilitically. Olivine frequently has a reaction rim of orthopyroxene, but serpentinisation is rare. Where serpentine is found it is usually associated with the contact of the younger Voisey's Bay granite.

Normal troctolite

The normal troctolite is medium grain-sized and of uniform texture. It consists of 20–40 modal percent cumulus olivine and 40–65 modal percent cumulus plagioclase. Plagioclase crystals are randomly orientated, 5–10mm long and are often partially enclosed in oikocrysts of olivine. Augite is rare, however, orthopyroxene can occur as reaction rims on olivine grains. Typically, these reaction rims encroach less than 5 percent of the grain volume. Biotite can constitute up to 8 modal percent as an interstitial material, frequently associated with oxides and sulphides. Ilmenite is the most common oxide mineral and constitutes around 2-5 modal percent.

Variable troctolite

The variable textured troctolite differs from the normal troctolite, in having up to 25 volume percent of gneissic inclusions and some blotches of sulphide. Plagioclase crystal size is also more variable, ranging from 5 mm to several cm. Large oikocrysts of plagioclase are observed enclosing euhedral olivine. Reaction rims of orthopyroxene on olivine are common. Interstitial augite, hornblende, biotite, and apatite are also more

abundant than in the normal troctolite. Biotite most frequently occurs in bands around the gneissic inclusions.

Breccia sequence

The breccia sequence rocks have greater than 25 volume percent of gneissic inclusions. The matrix of the breccia sequence is noritic because of hypersthene developing at the expense of olivine. Three types of inclusions are present, arranged in order of decreasing abundance they are: gneiss inclusions, ultramafic rocks, and sulphide-poor troctolite. The gneiss inclusions vary from a few mm to several cm. They frequently exhibit much evidence of melting. This melting generates a characteristic set of minerals that have been extensively described by Li and Naldrett (2000). The melting reaction is summarised below. Garnet is oxidised to hercynite and magnetite. Cordierite is dehydrated to hercynite. Plagioclase becomes richer in anorthite via a breakdown reaction to corundum. Hypersthene and K-feldspar react to produce hercynite. For a rigorous treatment of this topic see Li and Naldrett (2000). The ultramafic inclusions are wehrlite, dunite, and melatroctolite. The ultramafic inclusions range from 2-10 cm in diameter and are irregularly shaped. The olivine within the ultramafic inclusions is frequently serpentinised. The troctolite inclusions are irregularly shaped, several centimetres in diameter and have sharp edges. Minor alteration of the troctolite is often observed, with serpentinisation and sericitisation of the olivine and plagioclase respectively.

Marginal phase

The marginal phase is a fine-grained, non-cumulate ferrodiorite. It comprises 30–40 modal percent plagioclase, 25-40 percent hornblende, 10–15 percent biotite, 5-10 percent ilmenite, and less than 10 percent pyroxene. The marginal phase is generally structureless, but occasionally exhibits flow banding especially when associated with sulphides.

2.5 Sulphide Solubility in Silicate Magmas

2.5.1 Introduction

To form an economic magmatic sulphide deposit it is necessary that a mafic magma become saturated with sulphur and segregate droplets of an immiscible sulphide liquid. The immiscible sulphide phase then equilibrates with large volumes of silicate melt, depleting it of chalcophile elements and concentrating them within the sulphide droplets. If the appropriate conditions apply, the droplets of chalcophile-enriched sulphide will coalesce and become concentrated within a trap. This separation and concentration is believed to occur primarily via gravitational processes because of the pronounced density contrast between the sulphide and silicate phases. Kress (1997) gave a density contrast of 49 percent between sulphides and a typical MORB liquid at 1200°C, enough to allow gravitational separation. Recent work by de Bremond d'Ars et al. (2001) has confirmed that in a dynamic magma system, sulphides can be transported away from their source and then undergo gravitational separation and deposition.

2.5.2 Sulphur capacity of the silicate melt

The earliest work on the solubility of sulphur in silicate melts was derived not from rocks but smelter slags, the initial work was carried out by Abraham et al. (1960) and Fincham and Richardson (1954). These papers provided important insights into the mechanisms controlling sulphur solubility. Fincham and Richardson (1954) found that at temperatures of 1400-1500 °C and oxygen fugacities of less than 10^{-6} atmospheres, approximately equivalent to QFM (quartz-fayalite-magnetite) buffer, S dissolved primarily as sulphide (S^{2-}), reflecting the low activity of oxygen. At oxygen fugacities above the QFM buffer, Fincham and Richardson (1954) found that S was more commonly present as the sulphate ion (SO_4^{2-}). Fincham and Richardson (1954) went on to derive a relationship for the total amount of sulphur that the melt could dissolve. This was termed the sulphur capacity, C_s, and was a constant for melts of the same composition.

$$C_s = \left[S/ppm \left(\frac{fO_2}{fS_2} \right)^{1/2} \right] \quad (1)$$

Where S/ppm is the sulphur concentration in ppm, fO_2 is the oxygen fugacity and fS_2 is the sulphur fugacity.

2.5.3 Sulphide content at sulphide saturation (SCSS)

Although the work of Fincham and Richardson (1954) defined the sulphide capacity of a silicate melt as being proportional to the ratio of the oxygen and sulphur fugacities, it appears that the sulphide content at sulphide saturation (SCSS) is different. This is because there is an equilibrium between a sulphide and silicate liquid. Equation (1) suggests that the SCSS is dependent upon fO_2 and fS_2. However, Mavrogenes and O'Neill (1999) arrived at the relationship below using theoretical constraints and empirical evidence.

$$\ln[S/ppm]_{SCSS} = \frac{A}{T} + B + \frac{CP}{T} + \ln a_{FeS}^{sulphide} \quad (2)$$

Where T is temperature (K) and P is pressure (GPa). The A, B, and C parameters are related to the enthalpy, entropy and molar volume respectively of the silicate melt. The term $\ln a_{FeS}^{sulphide}$ is the natural logarithm of the activity of FeS in the sulphide liquid. Mavrogenes and O'Neill compared their own data with that already published (Wendlandt, 1982) and showed that for a given system, equation (2) provides a good estimate of SCSS. As is evident from equation (2), the chief controls on sulphide solubility at sulphide saturation are the composition of the silicate melt, temperature and pressure. Therefore, in a given P-T space, SCSS is independent of either fO_2 or fS_2, unless they affect the composition of the sulphide liquid and hence $a_{FeS}^{sulphide}$ (Mavrogenes and O'Neill, 1999).

2.5.4 Mechanism of sulphide dissolution

In the investigation of the Voisey's Bay deposit consideration will only be made of sulphur dissolving as sulphide (S^{2-}). This is because the fO_2 is at or below that of QFM, the redox state of most basaltic magmas (Wallace and Carmichael, 1992). Because the valance behaviour of S is controlled by the fO_2, at fO_2 typical of basaltic magmas, S is present chiefly as sulphide, its two-valance state. At fO_2 greater than QFM S is usually present as sulphate (SO_4^{2-}).

Haughton et al. (1974) were the first to provide extensive data on the solubility of sulphur within a silicate melt of naturally occurring composition, in equilibrium with a sulphide liquid. They discovered a strong, positive correlation between the sulphur and FeO content of the silicate material. Haughton et al. (1974) also noticed a lesser correlation with TiO_2. However, this was interpreted as being an artefact of the experimental conditions caused by ferropseudobrookite, a common component in high TiO_2 melts (Cooper, 2000). Prior to Haughton et al. (1974), MacLean (1969) published a paper on the system Fe-S-O-SiO_2. He discovered that the sulphur content of a silicate melt in equilibrium with a sulphide liquid decreased with increasing fO_2. He concluded that this was because sulphur dissolved in the silicate melt by displacing the oxygen bonded to Fe^{2+} as FeO. In support of this, Maclean (1969) demonstrated that an increase in oxygen partial pressure resulted in an increase of Fe^{3+} at the expense of Fe^{2+} in the melt, and hence a reduction in dissolved sulphur. Buchanan and Nolan (1979) carried out similar experiments to Haughton et al. (1974) and were able to demonstrate a positive correlation between FeO and the dissolved S content. Mathez (1976) found that the sulphur content of basalt glass increased significantly with increasing FeO content from ~0.105 weight percent S at 9.0 weight percent FeO to around 0.18 weight percent S at 12.9 weight percent FeO. This suggests that when S dissolves as

an S^{2-} ion, it does so primarily by replacing O^{2-} on the anion sublattice. This is described by the reaction below:

$$O^{2-} + \frac{1}{2}S_2 \Leftrightarrow S^{2-} + \frac{1}{2}O_2 \tag{3}$$

The equilibrium between silicate magma and a sulphide liquid suggested by the observations described above and outlined by Naldrett (1989) is described by equation (4).

$$FeO + \frac{1}{2}S_2 \Leftrightarrow FeS + \frac{1}{2}O_2 \tag{4}$$

2.5.5 The effect of temperature

It seems certain that temperature has a significant effect on a silicate magma's ability to dissolve S. Buchanan et al. (1983) investigated the solubility of S as a function of fS_2 in a basaltic melt containing 17 weight percent FeO at 1200, 1300 and 1400 °C. They found that the dissolved S content increased by a factor of 8.5 per 100 °C between 1000 °C and 1300 °C. From 1400 °C the S content increased by only 3 times per 100 °C. It must be noted that these analyses were carried out below sulphide saturation, as saturation proved difficult to achieve. Buchanan et al. (1983) did attempt to predict saturation values of the S content, but it is difficult to determine how reliable these data are. Haughton et al. (1974) found that tholeiitic melts having 10 weight percent FeO, dissolve about 0.04 weight percent S when saturated with FeS at 1200 °C and fO_2 $10^{-10.5}$ atmospheres (-2 log units relative to the QFM buffer). This compares with the work of Shima and Naldrett (1975) who found that a komatiitic melt with the same FeO content dissolved between 0.16 and 0.27 weight percent S at an fO_2 of –4 log units QFM and 1450 °C. Shima and Naldrett (1975) went on to indicate an increase of between 0.05 and 0.09 weight percent S per 100°C rise in temperature. Wendlandt (1982) carried out a series of experiments at 20 kb and varying temperatures using three natural specimens. Each of the experiments had a

different SiO_2 and FeO content which gives each a different SCSS. Wendlandt (1982) found that for each composition there was a strong, positive correlation between the temperature and the sulphide solubility and that the S solubility increased by around 0.06 weight percent per 100 °C rise in temperature.

2.5.6 The effect of pressure

Huang and Williams (1980), Wendlandt (1982), Mavrogenes and O'Neill (1999) and others have argued that the solubility of sulphide in a silicate melt decreases with increasing pressure. Wendlandt (1982) carried out a series of experiments in which he used a series of natural rocks and measured the SCSS while varying the pressure at a fixed temperature. He found that although C_s varied significantly with composition, the SCSS was clearly pressure dependent. This conclusion is supported by the work of Mavrogenes and O'Neill (1999) who carried out experiments with basaltic and picritic melts at various temperatures and pressures. They too found that C_s varied with composition but was pressure dependent. This is reflected in equation (2), which has a pressure term. Wendlandt (1982) found that SCSS decreased by 0.05 weight percent per kb increase at 1420 °C, while Mavrogenes and O'Neill (1999) found that the variation was 0.04 weight percent per kb decrease at the same temperature.

2.5.7 The effect of oxygen and sulphur fugacities

Fincham and Richardson (1954) found that the O_2 content of a silicate melt had a marked effect on its ability to dissolve sulphide. However, their work was chiefly concerned with silicate compositions that were of interest to metallurgists; i.e. either saturated with Fe or with Fe absent. Mavrogenes and O'Neill (1999) found that although the position of the sulphide saturation surface in P-T space is dependent upon O_2 and S_2 in the terms of the composition of the sulphide liquids, the value of SCSS in a silicate magma of fixed

composition is independent of fO_2 and fS_2. Mavrogenes and O'Neill (1999) went further, they stated that "At fO_2 below QFM oxidation-reduction effects cannot bring on sulphide saturation.... Because SCSS is insensitive to fO_2 apart from its effect of a_{FeS}." This is because S dissolves primarily by displacing the oxygen from FeO. A greater fO_2 will cause the Fe^{3+} component of the melt to increase at the expense of the Fe^{2+}, so decreasing the Fe^{2+} ion's availability for sulphide dissolution. In addition, the fO_2 and fS_2 of melts are linked, an increase in one causes a decrease in the other and in basaltic melts the ranges of fO_2 and hence fS_2 are relatively restricted.

2.5.8 The effect of composition

The chief control on sulphide solubility is the amount of FeO in the melt and S dissolves within silicate melts by displacing the oxygen on this molecule (Buchanan and Nolan, 1979b; Haughton et al., 1974; MacLean, 1969; O'Neill and Mavrogenes, 2002). It is important to consider any molecules or elements that might affect the activity of FeO and therefore the solubility of sulphide. Irvine (1975) investigated the role of SiO_2 contamination in the evolution of the Muskox layered intrusion. He concluded that SiO_2 played a pivotal role in inducing the onset of chromite, magnetite, and sulphide immiscibility. Irvine (1975) proposed that silica contamination reduced sulphide solubility by increasing the polymerisation of the silicate melt and reducing the number of bonding sites that can accept metal oxides and by implication sulphides. Hess (1980) gave an in-depth explanation of the effects of silica polymerisation of silicate melts and the implications that this might have for sulphide solubility. However, recent work by O'Neill and Mavrogenes (2002) has found that at 1400 °C and 1 bar the solubility of sulphide is dominated by the control exercised by the FeO content. This effect is so pronounced that when the FeO content of the melt is over ~10 weight percent, it is sufficient to make other compositional variations more-or-less irrelevant. Thus, any influence that the proportion of

bridging oxygens has on sulphide solubility, is completely swamped by the effect of *dilution* of the FeO by SiO_2 (O'Neill and Mavrogenes, 2002).

2.5.9 Likelihood of sulphide saturation at initial melting

Keays (1995) suggested that a major requirement for the generation of a magmatic sulphide deposit is that the parental magma must have been sulphide-undersaturated at the time of magma formation. He also asserted that sulphide-undersaturation must have persisted during transport through the crust so that the magma's budget of chalcophile elements remained undepleted. Keays (1995) also noted that the magmas that have a sufficient abundance of chalcophile elements for the generation of an economically viable magmatic sulphide deposit are high temperature, high MgO magmas, formed by extended mantle partial melting. Komatiites, picrites, and high MgO basalts are examples of the rock types that are usually given as suitable parental material for magmatic sulphide deposits (Lambert et al., 1999). Keays (1995) argued that that high degrees (~25 percent) of mantle partial melting depletes the source with respect to S and lead to the generation of sulphur-undersaturated magmas. He went on to argue that extended mantle melting was a prerequisite for the generation of magmatic sulphide deposits. Furthermore, Keays (1995) argued that a mantle melt of less than approximately 25 percent would have been sulphide saturated at source, consequently chalcophile-depleted and therefore unable to generate a magmatic Ni-sulphide deposit. Naldrett (1997) proposed that the total PGE content of 1-10 ppb of most basaltic magmas implied that an immiscible sulphide liquid was not present at their genesis and that they were therefore the product of extended mantle melting. Had an immiscible sulphide liquid been present at the source, this would have strongly depleted the PGE and other siderophile and chalcophile elements.

The S content of the mantle has been subject to much controversy and has been much debated in the last decade (e.g., Ionov et al.,1993; Lorand, 1993). McDonough and Sun

(1995) estimated that the upper mantle has a S abundance of 250±50ppm and work on fertile perdotites from orogenic massifs has suggested that the S content of the mantle is between 100-300ppm (e.g., Garuti et al., 1984; Lorand, 1991). Consequently, here a conservative S content of 200ppm will be assumed for mantle compositions.

To assess whether partial melting of the mantle would result in the generation of a sulphide saturated melt the extent of melting, depth, and hence temperature and pressure must be considered. Figure 2.6 (after McKenzie and Bickle, 1988) is a plot of four adiabatic ascent paths at different mantle potential temperatures (T_p), represented by the bold lines, plotted on a P-T diagram. The solidus and liquidus are marked as solid lines, while 10, 20, 30 and 40 percent increments of partial melting are represented as dotted lines. The transition between spinel and garnet facies is labelled and is represented by dashed and dotted lines obliquely across this figure. The data used in plotting Figure 2.6 allow the calculation of the SCSS for model basaltic and picritic melts according to Mavrogenes and O'Neill (1999).

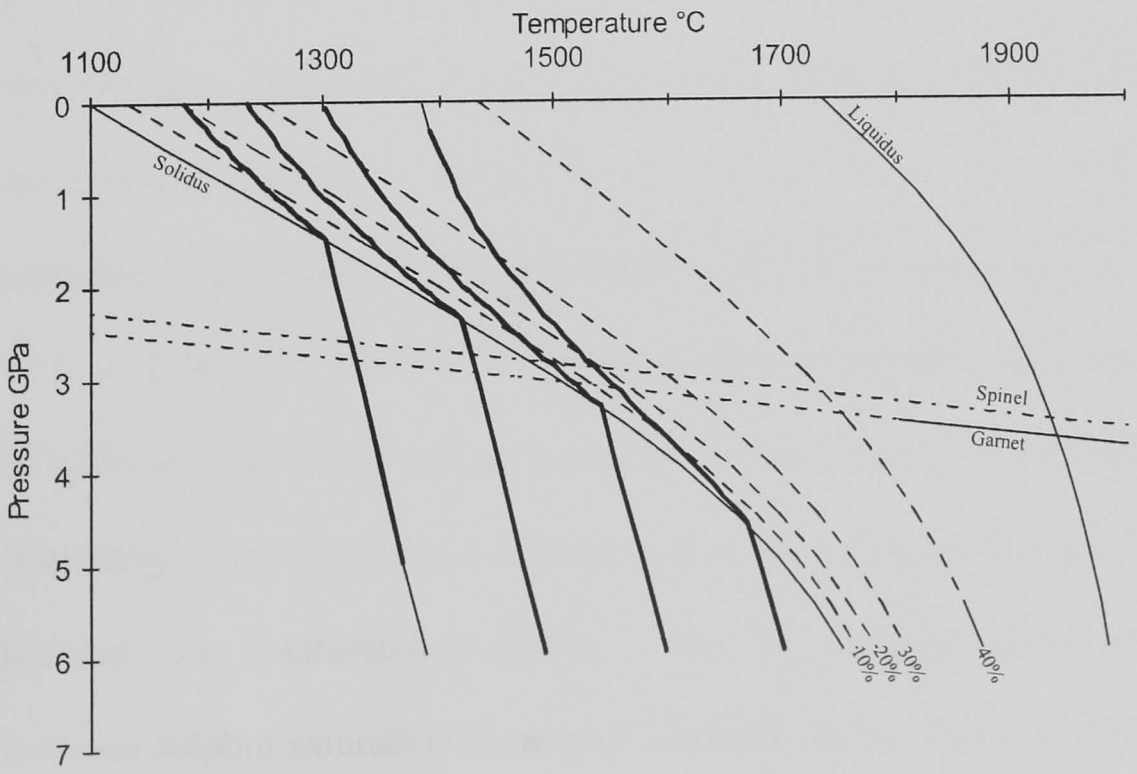

Figure 2.6 Graph of temperature versus pressure showing four adiabats crossing the dry solidus. The four adiabats have potential temperatures of 1280, 1380, 1480, and 1580 °C (after McKenzie and Bickle, 1988).

The parameters used by Mavrogenes and O'Neill (1999) for calculation of SCSS are:

A –6684	B 11.5	C -0.047 (basalt)
A 683	B 7.97	C -0.047 (picrite)

Substituting these parameters into equation (2), and the appropriate temperatures and pressures allows us to calculate the sulphide content at sulphide saturation content for the synthetic melts. The results of these calculations are plotted in Figures 2.7a and b, which give the SCSS on a P-T diagram for model basaltic and picritic melts respectively.

Figures 2.7a and b have curves plotted that illustrate the SCSS in ppm for each potential temperature adiabat. In addition to these, from each SCSS adiabat a solid line is plotted which corresponds to the modelled S contents in ppm for aggregate partial melting assuming a mantle S concentration of 200ppm. These are plotted using 1 percent increments of melting and assuming that each melt fraction is saturated with respect to S. For the higher temperature model basalts and all the picrites, the aggregate melt S concentration curves exhibit a pronounced inflection. This is a response to the exhaustion of S in the source. The basaltic model melts (Figure 2.7a) achieve a maximum S concentration of a little over 1000ppm, with little variation between the four potential temperature adiabats. However, the picritic melts have much more variable S concentration, between 1300 and 2800ppm, the higher concentrations achieved with melts of T_p of 1280 and 1380 °C. It is acknowledged in this case, only the mantle melts with T_p of 1480 or 1580°C are likely to generate picritic melts; the lower temperature melts are for illustration only. Regardless of these issues, the salient point is that regardless of whether the melt was S-saturated at source, neither the modelled basalt nor picrite model melt achieves sulphur saturation because of adiabatic ascent. The implication of this is, contrary to Keays (1995) and Naldrett (1997), even melts produced by small degrees of mantle melting can generate magmatic Ni-sulphide deposits

2.5.10 The effects of fractionation

When discussing sulphide saturation with respect to silicate melts, the effects of fractionation must not be ignored. Many authors have noted that the FeO content of silicate magmas has a pronounced effect on its SCSS (e.g. Buchanan and Nolan, 1979a; Haughton et al., 1974; O'Neill and Mavrogenes, 2002; Shima and Naldrett, 1975). Fractionation, especially tholeitic fractionation, can markedly influence the FeO content of a magma and thus have a major effect on the SCSS. In addition, fractionation is associated with a fall in magma temperature; this also affects the solubility of sulphide. In order to explore this topic, the model basalt and picrite of Mavrogenes and O'Neill (1999) were taken and using MELTS (Ghiorso and Sack, 1994) fractional crystallisation was simulated at 1 bar from the calculated liquidus temperature for each model composition. The MELTS output includes weight percent oxides and the temperature, so the SCSS could be calculated at increments of crystallisation using the FeO-based method of O'Neill and Mavrogenes (2002). However, this method does not include any consideration of temperature. To rectify this, a graph was plotted of temperature versus SCSS at 1 bar over the same temperature interval covered in the MELTS modelling, using the method of Mavrogenes and O'Neill (1999). A linear regression was plotted and the gradient of this regression used to calculate the change in SCSS at each temperature increment produced by MELTS. For both the model basalt and picrite, the R^2 value of the regression was at least 0.99. The two modelled melts were assumed to have S contents corresponding to the maximum predicted by Figures 2.7a and b. In the case of the picritic melts, only those with a T_p of 1480 and 1580°C were considered. Using these data, Figures 2.8a and b, graphs of temperature versus SCSS and S in ppm were generated. Figure 2.8a represents basaltic model melt and Figure 2.8b the picrite. Two curves have been plotted; the diamond-ornamented curve is the SCSS, based upon the FeO content of the magma and its temperature, calculated using O'Neill and Mavrogenes (2002) and Mavrogenes and O'Neill (1999). The filled-circle-ornamented curve is the modelled S concentration with a bulk

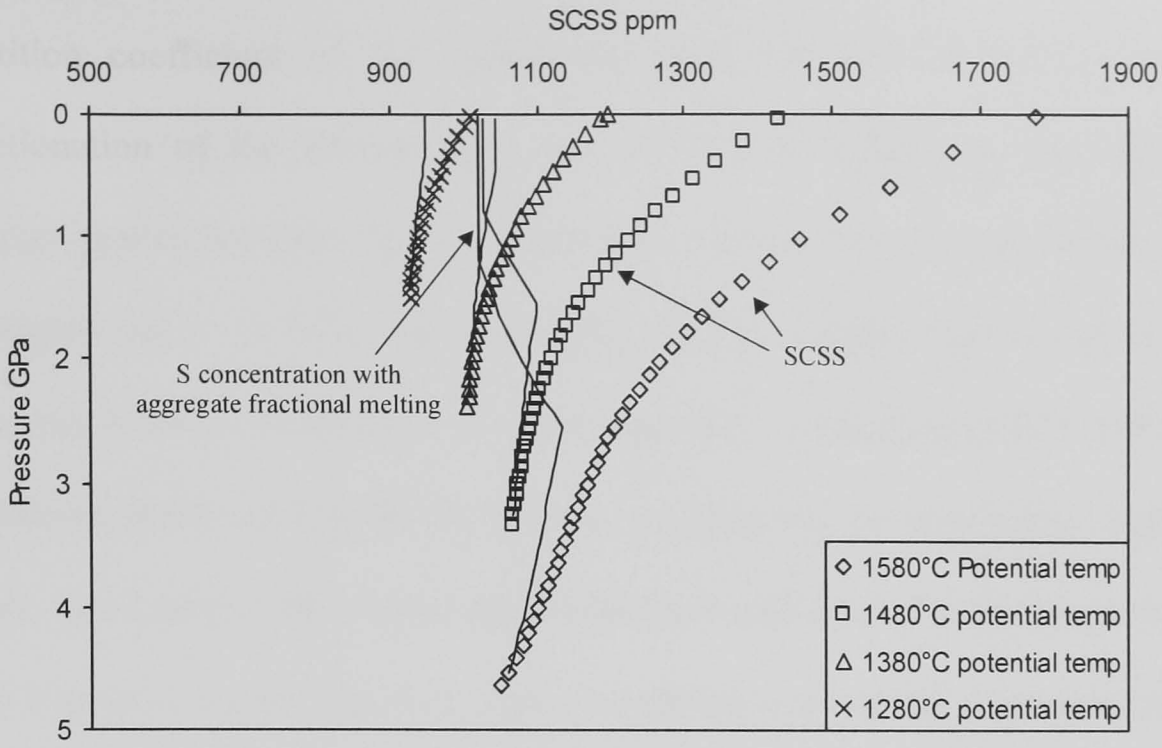

Figure 2.7a Graph of SCSS versus pressure for a model basaltic melt at potential temperatures between 1280 and 1580 °C. The ornamented curves represent the SCSS and are calculated using Mavrogenes and O'Neill (1999). The solid lines indicate the S concentration in the silicate magma as a result of aggregate melting. Inflections in the solid lines are the result of S being exhausted in the source and cessation of further melting at the base of the crust. This figure illustrates that although a melt might be sulphur-saturated at source, adiabatic ascent will result in sulphur-undersaturation.

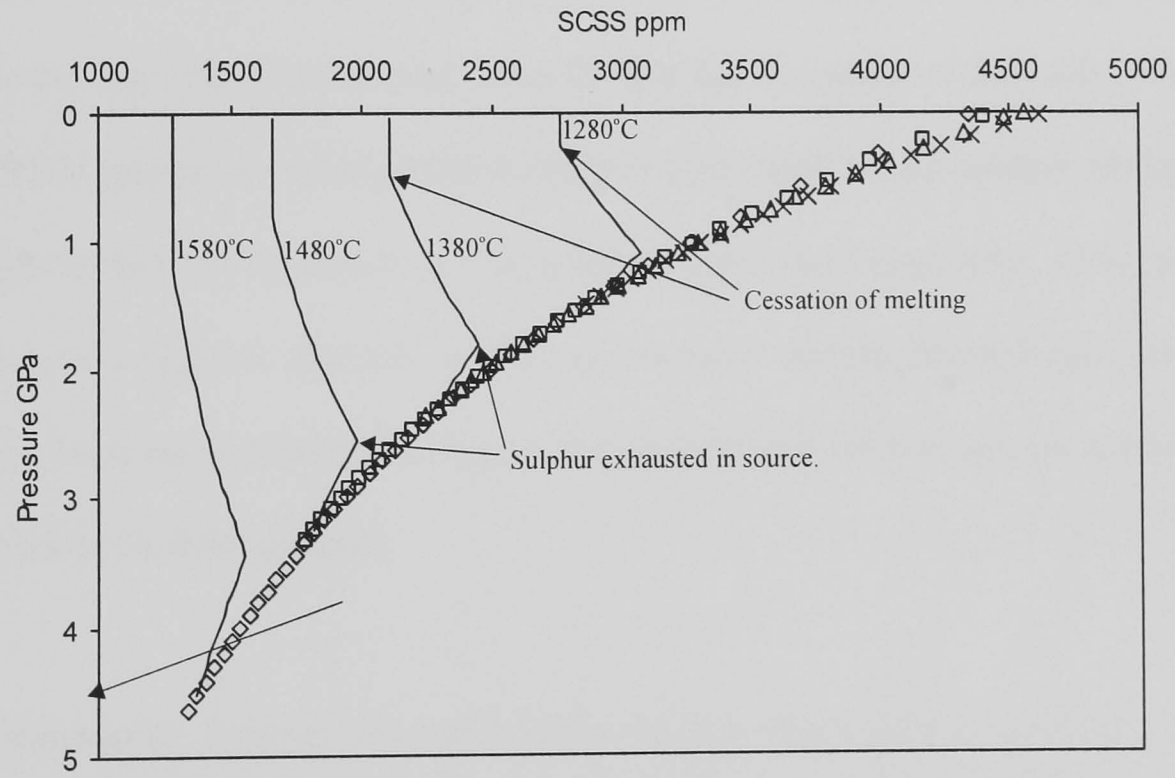

Figure 2.7b Graph of SCSS versus pressure for modelled picrite melts at mantle potential temperatures of 1280, 1380, 1480 and 1580 °C. The solid lines indicate S content of the agregate fractional melt assuming S saturation in each 1 percent melt fraction. The SCSS of the model picrite melts is not as stongly affected by reduction in pressure as the model basalt. Nevertheless, sulphide saturation will not be achieved in picrite melts by adiabatic ascent. It is noted that picritic melts are unlikely at mantle potential temperature of 1280 and 1380°C. These adiabats are included for the purposes of illustration only.

partition coefficient of 0.1, calculated using the data of Morgan (1986). During fractionation of the basaltic melt, the SCSS rises rapidly as the FeO content of the remaining melt increases; the S content also increases but less rapidly than the SCSS. This continues until ~1135°C when the FeO content of the melt begins to fall rapidly in response to the crystallisation of titanomagnetite. At around 1125°C the S content of the remaining melt exceeds the SCSS and consequently an immiscible sulphide liquid will form. On Figure 2.8b, plotted for the picrite model melt, the SCSS curve can be divided into 3 separate stages. The first, high temperature stage of this curve is dominated by olivine fractionation, with gently increasing SCSS in response to minor Fe enrichment. The second stage exhibits rapidly increasing SCSS as the Fe content of the residual liquid increases rapidly in response to plagioclase and clinopyroxene fractionation. Finally, the SCSS falls as the Fe content of the residual liquid diminishes as titanomagnetite comes onto the liquidus. The second curve depicts the S content of the melt. It is clear that the SCSS is greatly in excess of the S concentration until the Fe content of the residual liquid begins to fall in response to the crystallisation of titanomagnetite. However, this will not generate a high-Ni sulphide liquid, as extensive olivine fractionation has already taken place. Ni is compatible in olivine, so the fractionation of this mineral is an effective way of removing Ni from the melt.

To summarise, Figures 2.8a and b imply that it is impossible to generate a Ni-rich sulphide by fractionation of a mantle-derived melt. In both cases, SCSS exceeds the S content until fractionation is very advanced. For the basaltic model melt, it is unlikely that large concentrations of Ni would be present at the outset as the fractionation curve implies that either significant olivine has been retained in the source, or olivine fractionation has already taken place. For the picritic model melt, extensive olivine fractionation has taken place, depleting the melt of Ni before the onset of sulphide immiscibility.

2.5.11 Generation of an immiscible sulphide

Despite the likelihood that a small degree of mantle-partial melting will be sulphide-saturated at source, it will not generate a sulphide liquid because of adiabatic ascent (Mavrogenes and O'Neill, 1999). Fractionation of more extensive mantle-derived melt fractions will also fail to generate a Ni-rich sulphide melt as the onset of sulphide immiscibility post-dates Ni depletion in the melt by olivine fractionation. The implication of this is that the generation of a sulphide liquid must be the result of an external factor.

The easiest ways to initiate the onset of sulphide immiscibility is by the assimilation of a sulphur-rich country rock or by the injection of silicate-rich melt (Naldrett, 1997, 1999). Adding sulphur can initiate sulphide immiscibility by increasing the sulphide content beyond that of the SCSS. Adding SiO_2 causes sulphide over-saturation chiefly by diluting the FeO and reducing the magma's sulphide capacity. Because of the exponential nature of the relationship between FeO and S solubility, at FeO contents of greater than 10 percent, a small reduction in the FeO content by dilution will markedly reduce the solubility of sulphide. Because of this, relatively small amounts of additional silica can induce sulphide over-saturation and lead to the genesis of an immiscible sulphide liquid. Irvine (1975) proposed that the ingestion of silica rich material by a silicate melt at or near sulphide saturation would result in an immiscible sulphide liquid being formed. He attributed this to the change in the relative proportions of bridging, non-bridging, and free oxygen because of the increased polymerisation of the silicate melt reducing sulphide solubility. However, O'Neill and Mavrogenes (2002) have cast some doubt on Irvine's proposed mechanism. Instead, they postulated that the main control that increased silica exercises on sulphur solubility is that of a dilutant, by reducing the concentration of FeO.

2.5.12 Sulphur budget at Voisey's Bay

The Voisey's Bay deposit is currently estimated to hold 136.7 x 10^6 tonnes of sulphide ore grading at approximately 1.6 percent Ni. Because the ore includes silicate material, we need to calculate the total mass of sulphides included within the current estimated size. If it is assumed that Voisey's Bay sulphides are generally ~5 percent Ni in 100 percent sulphide and that the total mass of ore at Voisey's Bay is 136.7 x 10^6 tonnes, then the total mass of sulphide must be:

$$\left(\frac{1.367\times10^{8}\times1.6}{100}\right)=5\times\frac{X}{100}$$

$$\left(\frac{1.367\times10^{8}\times1.6}{5}\right)=X$$

$$=4.37\times10^{7}\,tonnes$$

Assuming the deposit is dominantly pyrrhotite, it is a simple matter to then calculate the total mass of S present. Pyrrhotite has a formula of Fe_7S_8-FeS with the stochiometric form of FeS being known as troilite. Therefore, taking the formula of pyrrhotite to be Fe_7S_8, the weight percent S can be calculated thus:

Molar mass S: 32.066

Molar mass Fe: 55.845

$$\text{Weight percent } S=\left(\frac{8(32.066)}{7(55.845)+8(32.066)}\right)\times100$$

$$=\left(\frac{256.528}{647.443}\right)\times100$$

$$=39.62\%$$

Knowing that S accounts for approximately 40 percent of the sulphide, it is straightforward to calculate the amount of sulphur present:

$$4.37 \times 10^7 \text{ tonnes sulphide} \times \frac{40}{100}$$

$$= 1.75 \times 10^7 \text{ tonnes sulphur}$$

Because we are assuming that the mantle contains 200ppm S and we have derived a value for the amount of S at Voisey's Bay, it is possible to calculate an estimate for the amount of mantle that would have had to have been partially melted to release the required amount of sulphur.

Density mantle rock:	3300 kgm^{-3}
Sulphur abundance:	200 ppm
Degree of partial melting:	10 percent

Because the mantle abundance of sulphur is ~200ppm, $1m^3$ of mantle rock will contain 0.66 kg of sulphur. However, in this case the source has only undergone a 10 percent partial melt and Keays (1995) found that for 10 percent partial melting ~40 percent of the mantle's sulphur budget is partitioned into the melt fraction.

It has been calculated here that the Voisey's Bay deposit contains 1.75×10^{10} kg of sulphur. Therefore, allowing for 40 percent of mantle sulphur being partitioned into the melt, the required amount of mantle material to generate the sulphur found at Voisey's Bay is:

$$\frac{1.75 \times 10^{10} kg}{\left(6.6 \times 10^{-1} kgm^{-3}\right) \times 0.4}$$

$$= 6.6 \times 10^{10} m^3$$

$$= 66 km^3$$

To generate the amount of sulphur found at Voisey's Bay there would need to be a 10 percent partial melt of 66 km^3. As this is a 10 percent partial melt, this would generate 6.6 km^3 of magma.

The volume of the Voisey's Bay intrusion is not well defined. However, it can be divided into separate sub-areas whose dimensions are known with a little more certainty (see the deposit map (Figure 2.4) for the names of these various areas). The Eastern Deeps and the Red Dog areas comprise a volume of around 1km x 3km x 5km. The Reid Brook zone sub-chamber is of a similar size and the conduit between the Reid Brook zone and Eastern Deeps is approximately 50 m wide, 2km long and greater than 1km deep (Lightfoot, pers comm.). As an approximation, the volume of the VBI can be defined as:

$$2 \times (1000m \times 3000m \times 5000m) + (50m \times 2000m \times 1500m)$$

$$= 3.0 \times 10^{10} m^3$$

$$= 30 km^3$$

This is evidently in excess of the volume of material produced by the mantle-melting sulphide budget model outlined above. The implication of this is that mantle melting can provide all the sulphur at Voisey's Bay and that no other source of sulphur need be invoked as a source of material for the Voisey's Bay deposit.

2.5.13 The nickel budget at Voisey's Bay

As there are approximately 136.7 x 10^6 tonnes of ore at Voisey's Bay, grading ~5 weight percent Ni then the total amount of Ni present is:

$$1.367 * 10^9 kg \times \frac{5}{100}$$

$$= 6.8 \times 10^7 kg$$

Because the levels of Ni in crustal rocks are low, around 20-100ppm for upper and lower crust respectively (Taylor and McLennan, 1985) it seems unlikely that this much Ni could have been derived from a crustal source. This assumption is based on the data of Lambert et al. (1999) suggesting that the amount of assimilation of two country rocks (the Nain and Tasiuyak gneisses) was only 2 percent or 14 percent by mass depending upon which was assimilated. In addition, all the country rocks that are considered potential contaminants are also low in nickel, generally around 50ppm maximum (Lightfoot, pers. comm). It is therefore reasonable to presume that the Ni in the deposit must have been sourced from mantle-derived melt.

Chapter 3

Whole Rock Geochemical Variations

3.1.1 Introduction

In Chapter 1, four main questions were posed. These concerned the nature of the melt parental to the Voisey's Bay intrusion troctolites and whether this melt could have been the source of the Ni in the Voisey's Bay magmatic sulphides. This chapter will use major and trace element data to investigate the nature of the magma parental to the Voisey's Bay intrusion and the contamination history of this magma. As an integral part of this approach the temperature, depth, and extent of melting that occurred during the generation of these magmas will be investigated. Because the Tasiuyak gneiss is graphite-bearing, assimilation of this rock should have an effect on the fO_2 regime of the Voisey's Bay intrusion. Moreover, the fO_2 of a magma has implications as to its genesis – MORB, OIB and plume-type magmas have characteristic oxygen fugacities (Wallace and Carmichael, 1992). Therefore, the fO_2 prevalent during the genesis of the Voisey's Bay intrusion is investigated.

All the trace element data in this chapter were collected by INCO during their exploration programme of the Voisey's Bay deposit and as part of the large-scale investigation of other NPS intrusions as potential hosts to Ni-sulphide mineralisation. These data are unpublished and are provided by Dr Peter Lightfoot of INCO Technical Services. The samples were analysed at the SGS XRAL laboratories using ICP-MS and XRF. The Nd and Sr isotope data are previously published (Amelin et al., 2000b; Emslie et al., 1994). All the standards and sample location data are in Appendix A, the sampling localities are illustrated on Figure 3.1, a sketch map of the Voisey's Bay intrusion.

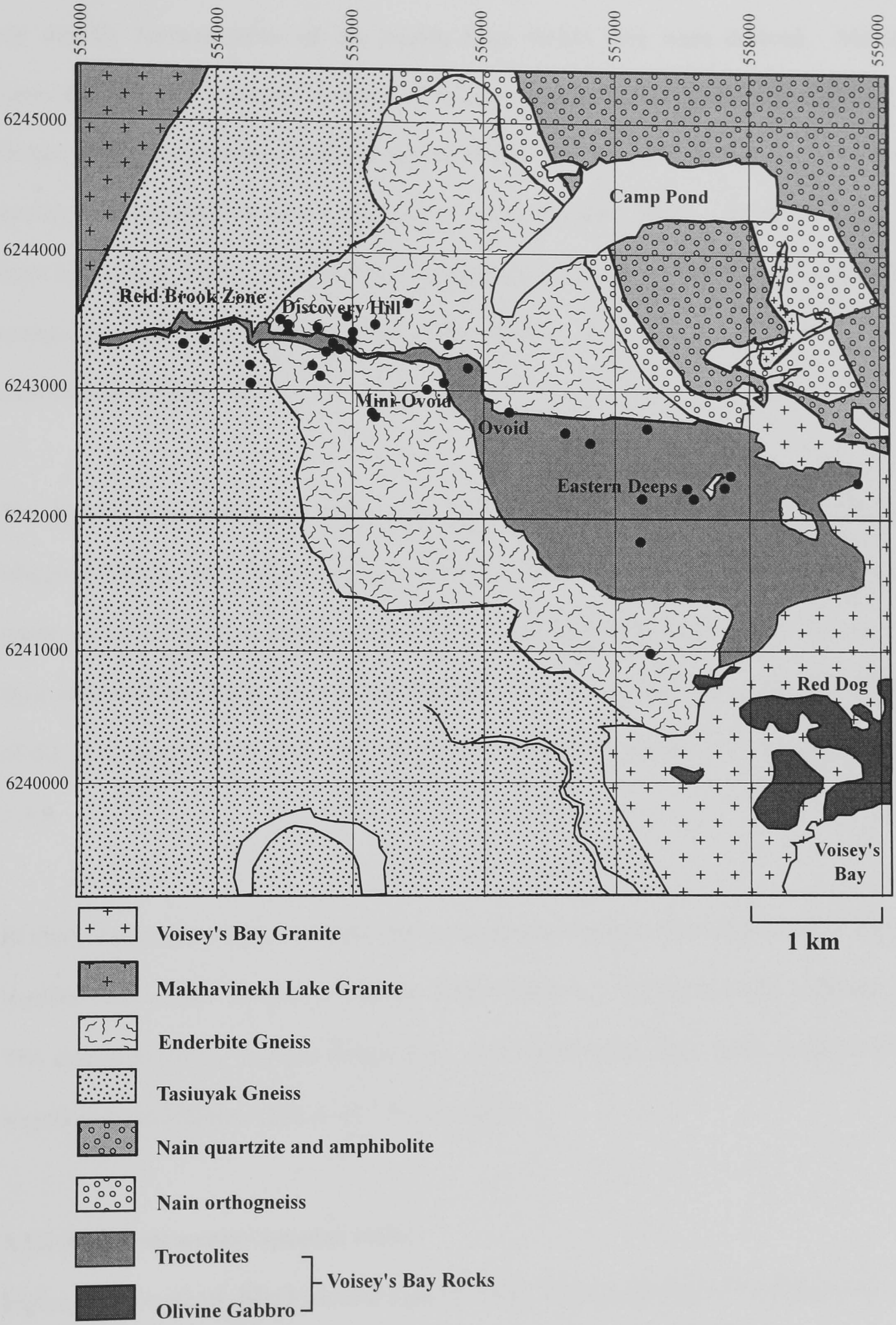

Figure 3.1 Map of the Voisey's Bay deposit with the names of the different areas. Locations of the drill hole from which samples were taken are shown as filled black circles. Details on the UTM coordinates and depth of each sample are included in Appendix A. Redrawn from Voisey's Bay Nickel Company data.

Because of their cumulate nature, the compositions of the Voisey's Bay intrusion rocks are not directly representative of the liquids from which they were derived. Moreover, cumulates are not a simple product of fractional crystallisation and accumulation. For instance, if some fraction of melt is trapped within the cumulate pile this can significantly modify the composition of the cumulus minerals (Barnes, 1986). Because of this, care must be taken in interpreting the data. Various methods exist to calculate a parental liquid composition from cumulates (Bedard, 1994; Bedard, 2001), of which Bedard (2001) is used in this chapter.

The Voisey's Bay intrusion rocks are chiefly troctolitic and gabbroic cumulates. The Marginal Phase, also referred to as a chilled margin (Li et al., 2000), is a fine-grained gabbro. The Ultramafic Inclusions are olivine-rich xenoliths found within the Troctolite, their compositions range from dunite through to melatroctolite. For a detailed description of the mineralogy of the rock types found at Voisey's Bay the reader is referred to section 2.4.6.

In this chapter, the various textural and mineralogical types of troctolitic rocks are grouped together and termed Troctolite because they behave as a compositionally coherent group. The marginal phase, Eastern Deeps dyke, and Ovoid dyke have been similarly grouped together as the Marginal Phase and Dykes (MPD).

3.1.2 Major elements - igneous rocks

Figures 3.2a-c show MgO plotted against SiO_2, CaO, and $Fe_2O_3(T)$ respectively. The quadrilateral superimposed on Figures 3.1a and b is defined by the composition of feldspar (An_{50}-An_{65}) and olivine (Fo_{65}-Fo_{80}). These values represent the likely range of compositions of the olivine and plagioclase found at Voisey's Bay. Both Figures 3.2a and b demonstrate that the Ultramafic Inclusions (UMI) have a greater proportion of olivine

than the Troctolite, and that the olivines in the UMI have a higher forsterite content. The MPD data fall outside the quadrilateral, trending to low CaO and SiO_2 values. Figure 3.2c, a graph of MgO plotted against Fe_2O_3, has two lines superimposed upon it. Trend A corresponds to addition of 10 percent increments of olivine Fo_{65} and trend B corresponds to the addition of 10 percent increments of olivine Fo_{80}. As might be expected from the previous figures, the data from the Troctolite and the UMI fit neatly between these two trends. This indicates that the Fe within these samples is contained within olivine. It is possible to estimate the modal olivine directly from this graph. Most of the Troctolite data fall between 20-25 percent olivine, consistent with the petrographic observations. The MPD data however, fall well outside the olivine-defined field indicating that another phase is controlling the distribution of Fe. Figure 3.3a plots loss on ignition (LOI) against Fe_2O_3. Once more, the MPD data fall on a different trend to the Troctolite and the UMI. The UMI data form a trend of increasing LOI with near constant Fe_2O_3. This trend is a reflection of the UMI's high olivine content, illustrating that olivine has been hydrated to serpentine. Because serpentine is a hydrous mineral the LOI process causes dehydration and therefore mass-loss. The MPD data have steeply increasing Fe_2O_3 coupled with increased LOI. This is a result of an increase in the modal abundance of sulphide. It is this high abundance of sulphide, and hence total Fe, in the MPD samples that gives the low SiO_2 and CaO contents observed in Figures 3.2a and b.

The conclusion that the high Fe_2O_3 content of a proportion of the MPD data is a response to high sulphide contents is supported by Figure 3.3b, a plot of Fe_2O_3 against total S. The effects of adding 10 percent increments of stoichiometric pyrrhotite (FeS) are plotted on this figure. Olivine and plagioclase are assumed to carry no S, therefore, although the Fe_2O_3 content will increase as the proportion of olivine rises, S should remain at zero. There is some agreement between the theoretical trend and the observed data for the high Fe_2O_3 MPD data. However, some of the MPD points fall between the trends expected for

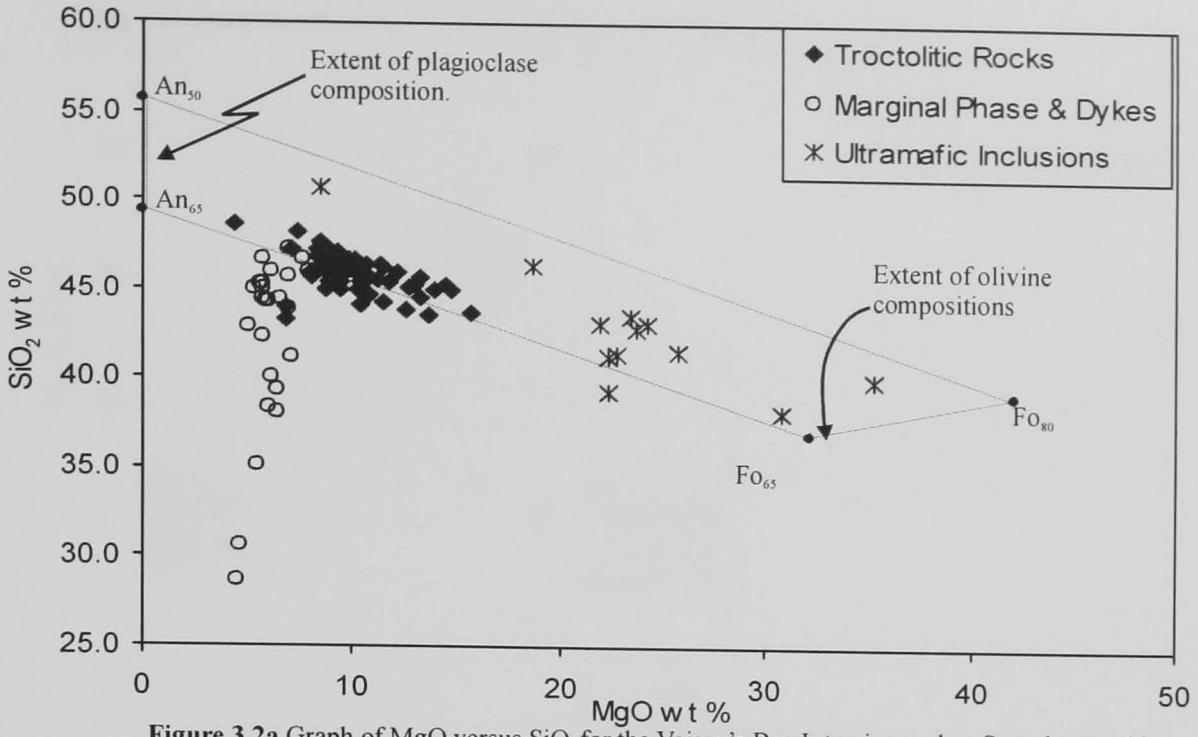

Figure 3.2a Graph of MgO versus SiO_2 for the Voisey's Bay Intrusion rocks. Superimposed is a quadrilateral defined by observed plagioclase and olivine compositions. The Troctolites data fall within the plagioclase-olivine defined quadrilateral. The MPD data fall outside the quadrilateral, this is discussed in the text.

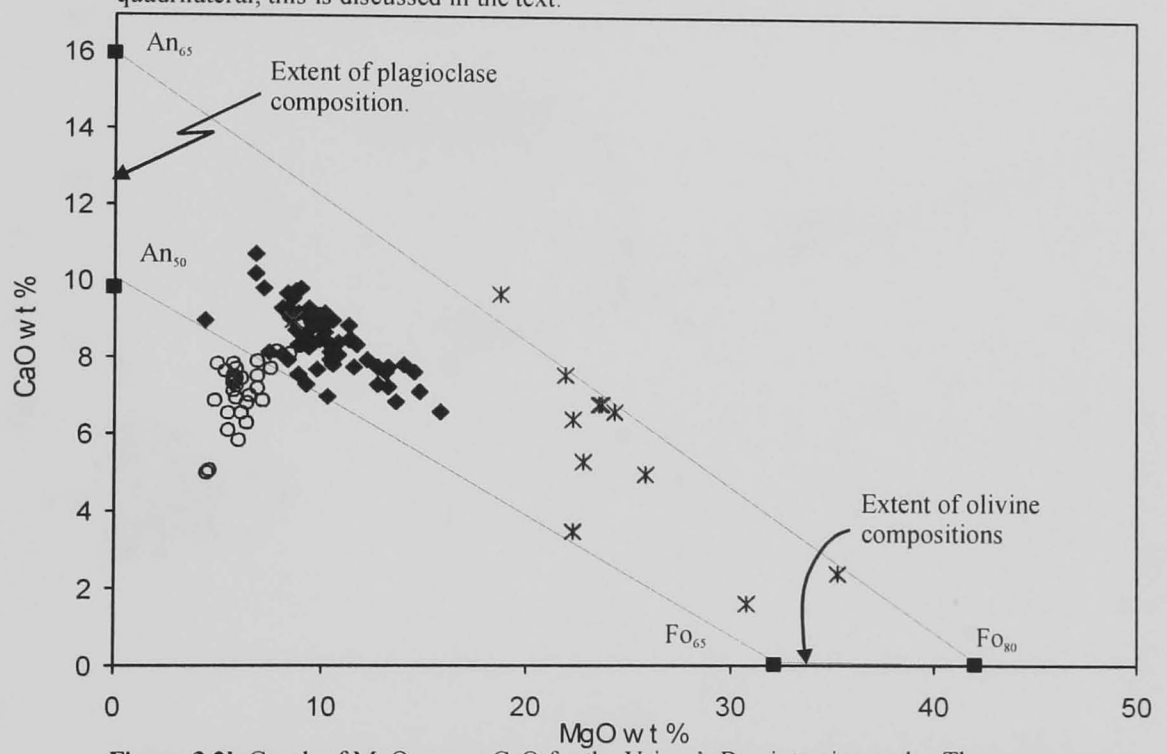

Figure 3.2b Graph of MgO versus CaO for the Voisey's Bay intrusion rocks. The superimposed quadrilateral is defined by the observed anorthite and forsterite values at Voisey's Bay. The UMI and Troctolites are contained within this field while the MPD tend to fall outside.

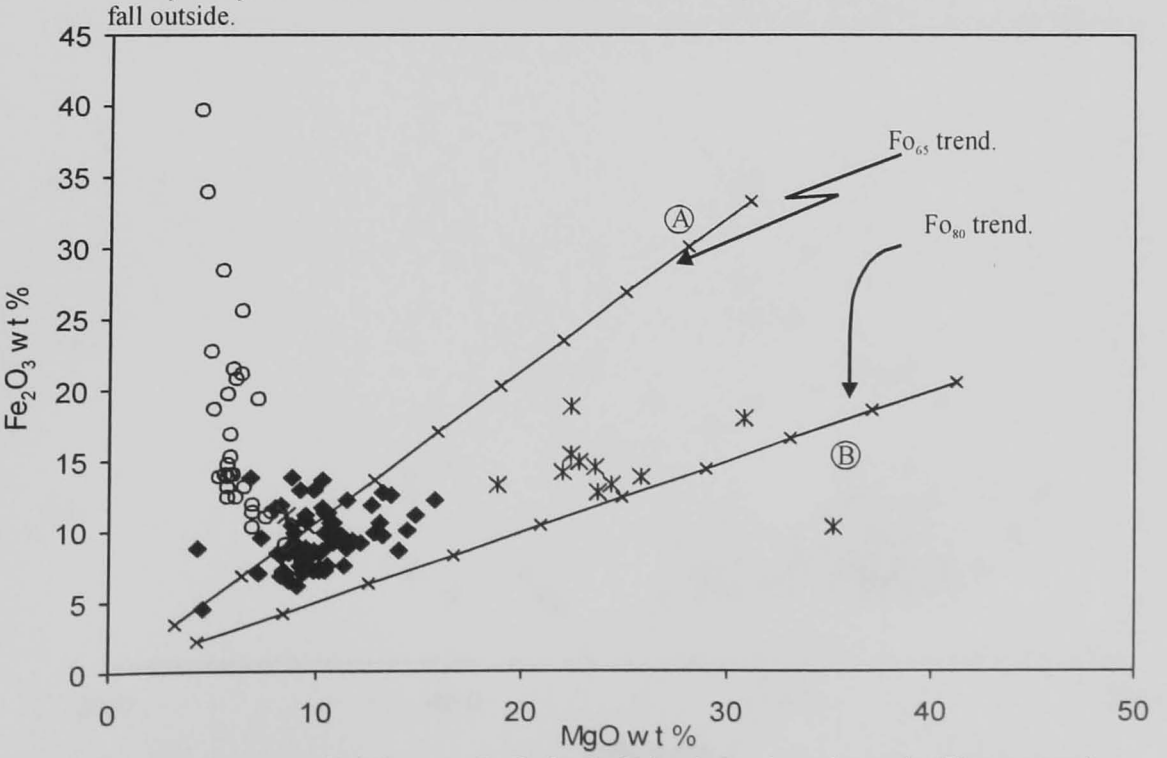

Figure 3.2c Graph of MgO versus Fe_2O_3 for the Voisey's Bay intrusion rocks. The two trends marked as lines represent the composition of a whole rock starting with 10 wt% olivine and increasing in 10 wt% increments. The upper trend is for olivine Fo_{65}, the lower, Fo_{80}.

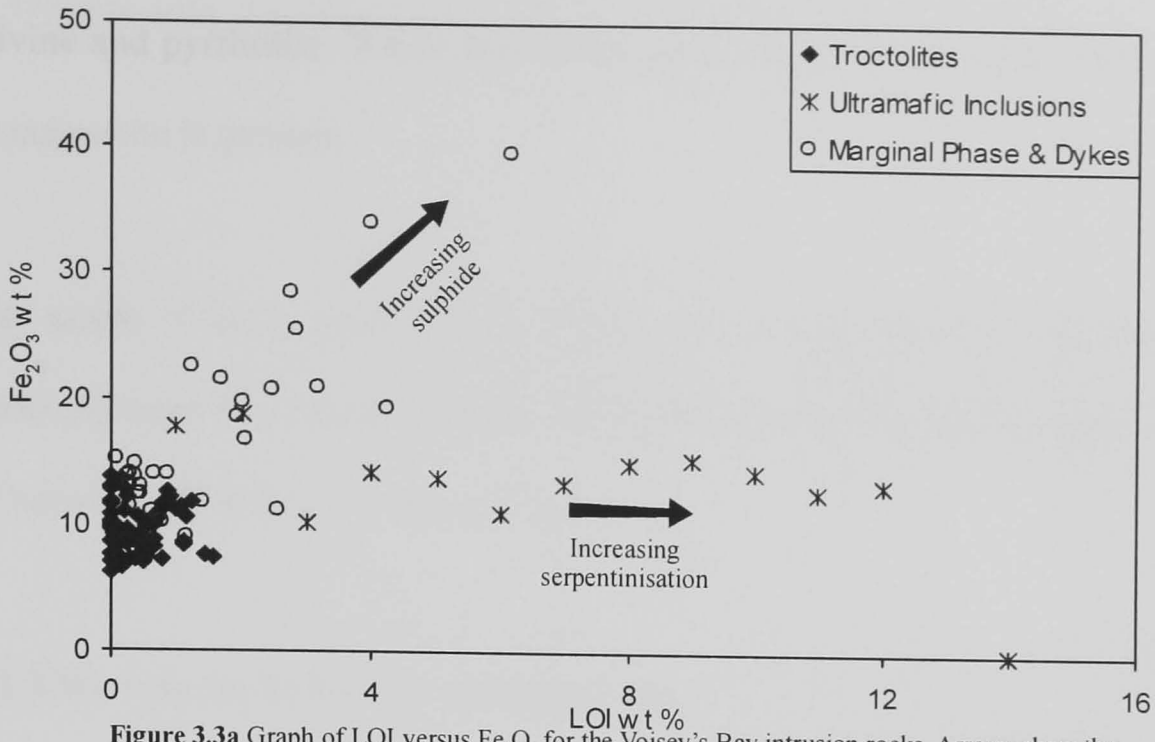

Figure 3.3a Graph of LOI versus Fe_2O_3 for the Voisey's Bay intrusion rocks. Arrows show the vectors resulting from increases in sulphide and serpentinised olivine. Notice that the UMI data have a trend of increasing LOI for constant Fe_2O_3, while the MP D exhibit LOI increasing with Fe_2O_3 content..

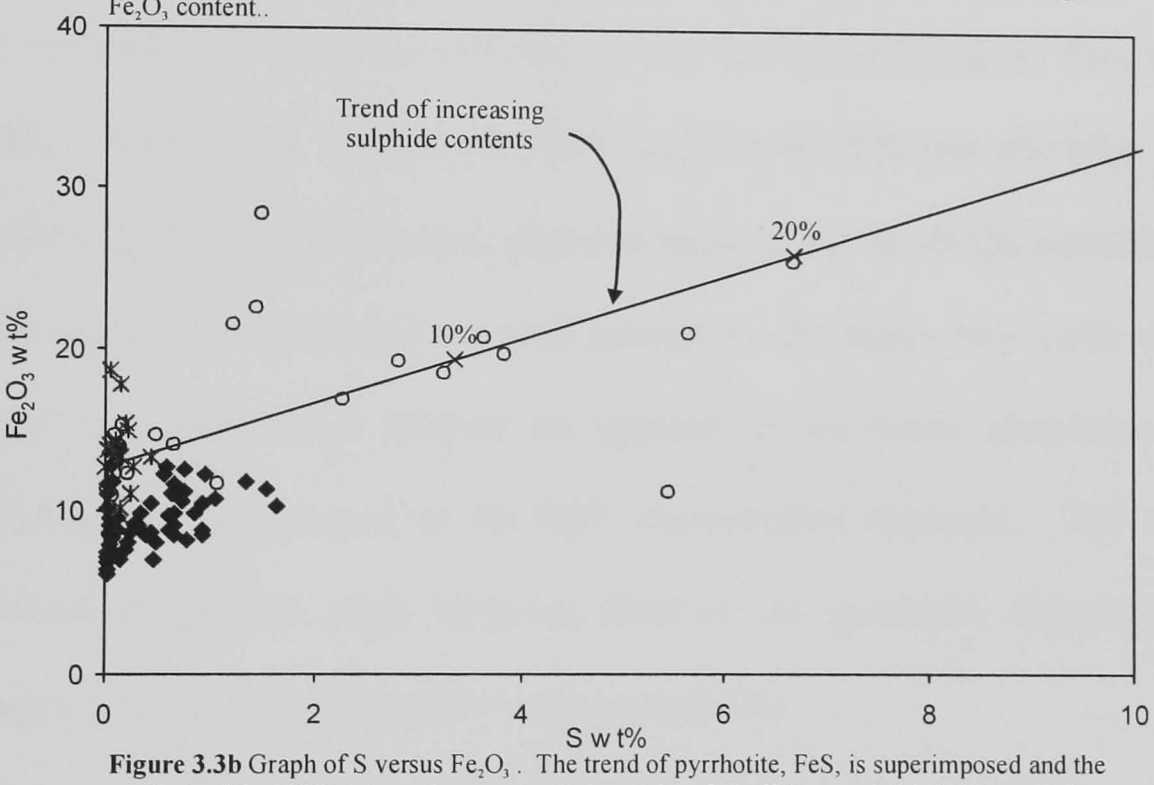

Figure 3.3b Graph of S versus Fe_2O_3 . The trend of pyrrhotite, FeS, is superimposed and the gradient of the MPD data are in agreement. Some data fall off the trend, this is interpreted as these samples containing an additional Fe rich phase, perhaps titanomagnetite.

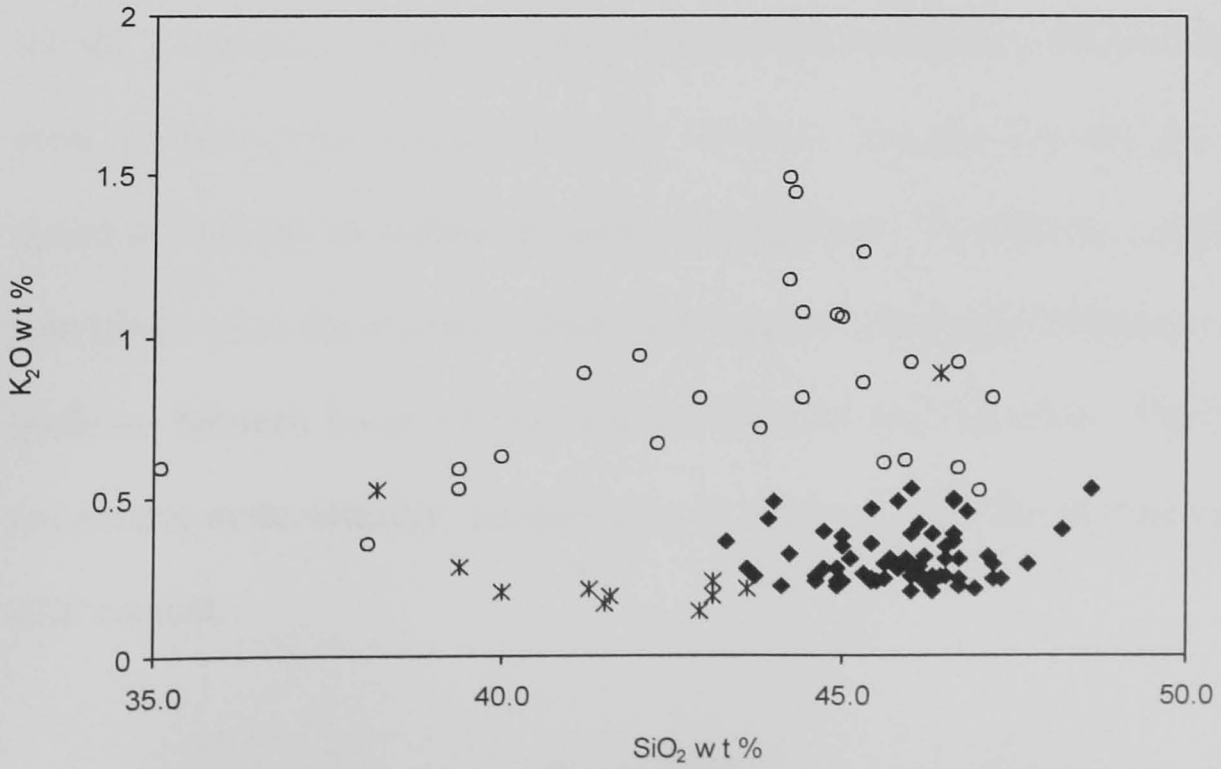

Figure 3.4 Graph of SiO_2 versus K_2O for the Voisey's Bay intrusion rocks. The Troctolites and the UMI have lower K_2O contents than the MPD data. The MPD data with low SiO_2 reflect high sulphide contents.

olivine and pyrrhotite. Where this occurs, it is likely that an additional Fe rich phase such as magnetite is present.

The graph of SiO_2 against K_2O, Figure 3.4, reveals that the Troctolite and UMI data generally have less than 0.5 weight percent K_2O, while the MPD generally have K_2O levels of between 0.5 and 1.6 weight percent.

3.1.3 Rare earth elements – igneous rocks

The rare earth element (REE) data presented in the following section are all normalised to C1 chondritic abundances according to the values published by Sun and McDonough, (1989). Figure 3.5a, presents the REE data for the different troctolite types as a range defined by the arithmetic mean plus and minus 2 σ. In all the troctolites, the light rare earth elements (LREE) are enriched relative to the heavy rare earth elements (HREE). There is a pronounced positive Eu anomaly in the lower abundance patterns, which becomes less pronounced as the REE concentration increases. The variable troctolite exhibits the greatest range, however, there are no systematic differences in REE curve shapes between the petrographic types of troctolite.

All the Ultramafic Inclusions data are presented in Figure 3.5b. The data exhibit much more variability than seen in any of the Troctolite data, the concentration of La relative to chondrite varying by almost an order of magnitude. Yb exhibits a higher concentration than observed in the troctolitic data, such that the Ultramafic Inclusions have flatter REE gradients between La to Yb than that observed for the Troctolite. The Eu anomaly does not behave systematically; samples may or may not have this feature regardless of their REE content.

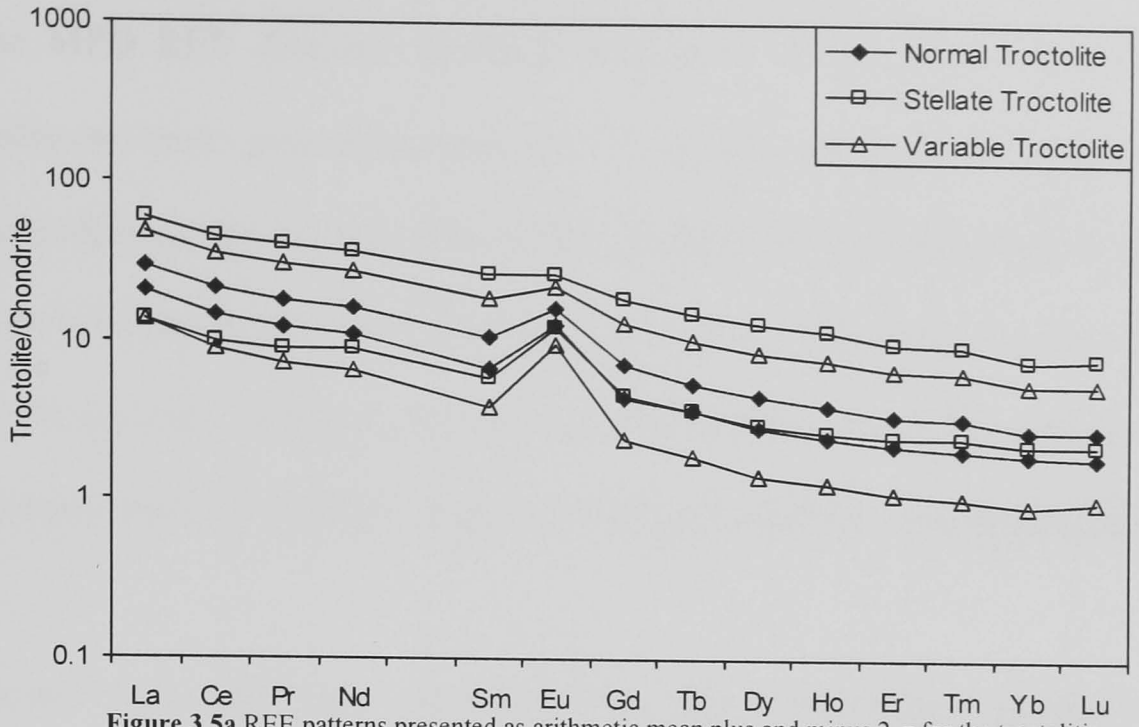

Figure 3.5a REE patterns presented as arithmetic mean plus and minus 2 σ for the troctolitic rocks of the Voisey's Bay Intrusion. All the data are LREE enriched relative to the HREE. All have a positive Eu anomaly, though this decreases with Eu abundance.

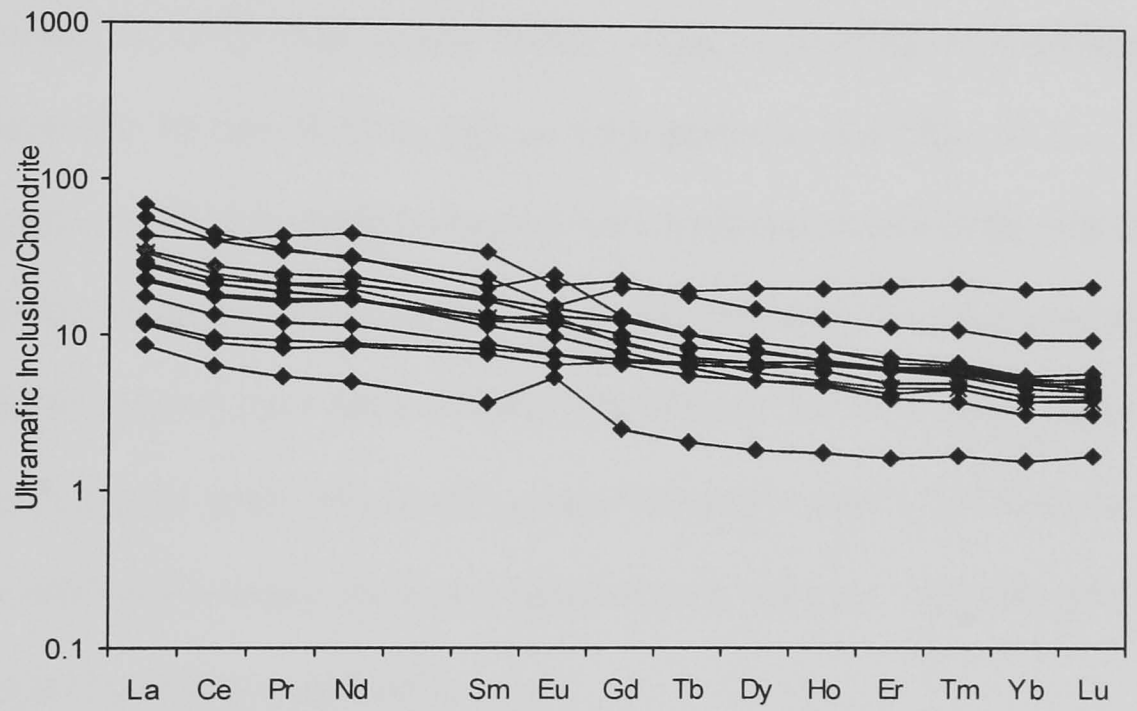

Figure 3.5b REE patterns for the UMI. These patterns are generally less LREE enriched than the Troctolites and do not display the systematic Eu behaviour seen above. All the data are shown.

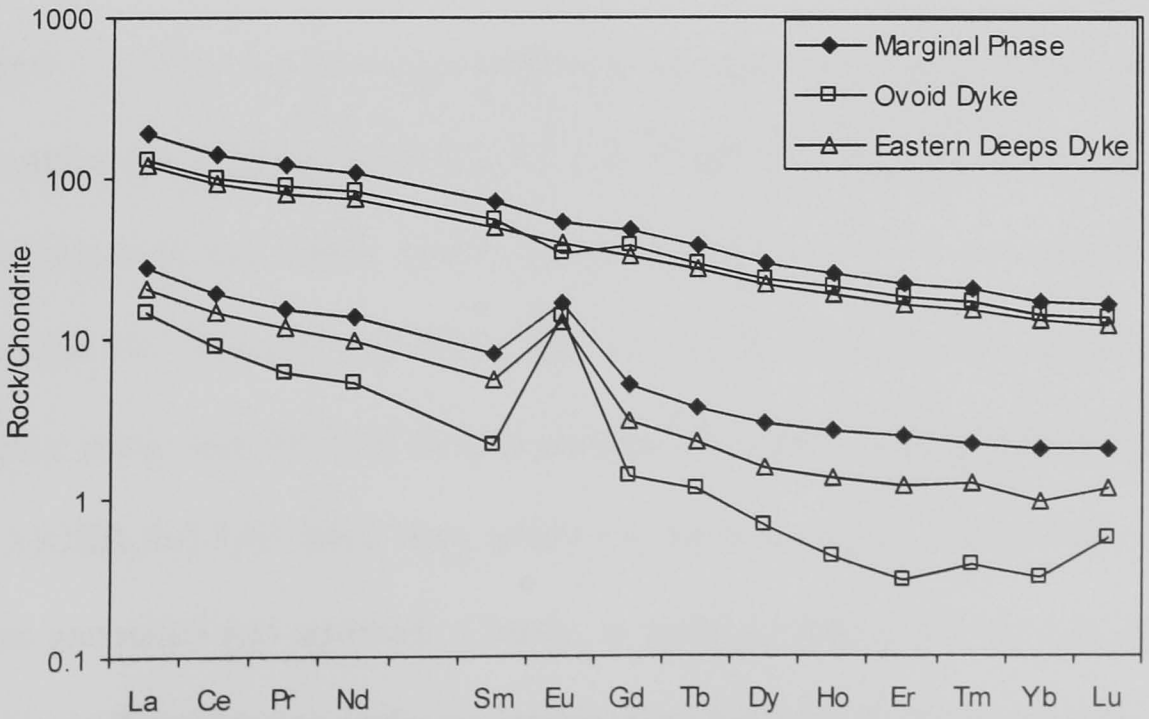

Figure 3.5c REE patterns for the Marginal Phase, Ovoid Dyke, and Eastern Deeps Dyke presented as arithmetic mean plus and minus 2 σ. The data exhibit LREE enrichment and have a positive Eu anomaly on the lower REE abundance samples. This Eu anomaly is absent on the higher REE abundance data.

The MPD REE data are presented in Figure 3.5c as ranges that are defined by the arithmetic mean plus and minus 2 σ. In general, these patterns are a little steeper than those observed for the troctolitic rocks. In detail, the data separate into two groups, one more enriched in REE than the other. As with the Troctolite, the more enriched group has no Eu anomaly. Whereas, the second less-enriched group has a pronounced positive Eu anomaly, the size of which increases as the general REE content diminishes.

Figure 3.6 is a plot $[La]_N$ versus $[La/Yb]_N$. The Voisey's Bay intrusion rocks form clusters that lie between $[La/Yb]_N$ 3–15. The Troctolite have $[La/Yb]_N$ values of around 10, whereas the MPD have slightly higher values of $[La/Yb]_N$ at10–15 times chondritic. The Ultramafic Inclusions data plot at approximately $[La/Yb]_N$ of 5. The $[La]_N$ for the Troctolite and Ultramafic Inclusions have a maximum of a little over 50, while the MPD data extend to 150 times chondritic. For the purposes of comparison, the compositions of MORB and OIB have been included; MORB and OIB were been chosen as comparators as they represent near-end-member compositions for basalts. The data for the Troctolite and the MPD fall between these two compositions, with the Troctolite plotting nearer MORB and MPD plotting nearer OIB.

When $[La/Yb]_N$ is plotted against $[Dy/Yb]_N$, Figure 3.7, the Troctolite and MPD data form a continuous series at $[Dy/Yb]_N$ 1.3-1.8. The UMI data have lower $[Dy/Yb]_N$ values than the Troctolite and MPD, falling between $[Dy/Yb]_N$ 1–1.7, with much more scatter than seen for the Troctolite and MPD. For clarity, the MPD and Troctolite have been outlined as one group and the UMI data as another. In addition, the $[La/Yb]_N$ and $[Dy/Yb]_N$ ratios of MORB and OIB have been added for the purposes of comparison. These points have been annotated and arrowed. Clearly, in terms of their $[La/Yb]_N$ and $[Dy/Yb]_N$ ratios, the Voisey's Bay intrusion rocks are intermediate between MORB and OIB.

Eu is unusual among the REE in that it has two valance states rather than only the 3^+ state that is common to the rest of the REE. At fO_2 typical of basaltic magmas (i.e. at QFM or below (Wallace and Carmichael, 1992)), Eu is also present as $Eu^{2+}$and thus substitute into plagioclase. Because of this, Eu can behave anomalously during magmatic processes. Relative to Eu^{3+} and the other REE, Eu^{2+} is compatible with plagioclase. As this mineral is the dominant component in troctolite, the behaviour of Eu, and particularly the magnitude of the Eu anomaly, can give important insights into magmatic processes. Eu/Eu* is the ratio of the measured Eu to expected Eu abundance, based on the abundances of Sm and Gd and provides a quantitative measure of the Eu anomaly. The Eu/Eu* is calculated using the geometric mean of the adjacent elements *i.e.*:

$$Eu / Eu^* = Eu_N / \sqrt{(Sm_N).(Gd_N)}$$ (Taylor and McLennan, 1985)

Thus, when Eu/Eu* is equal to one, the observed Eu concentration is equal to that expected from the adjacent elements. If Eu/Eu* is greater than 1, a greater abundance of Eu than expected is present. This is usually the result of plagioclase accumulation. If the Eu anomaly is below 1, plagioclase has been extracted from the melt and when Eu/Eu* is equal to 1, the rock in question has neither undergone nor is a product of plagioclase fractionation. Therefore, the Eu/Eu* can be used as an index of plagioclase fractionation.

Figure 3.8 is a graph of La_N versus Eu/Eu*. The Troctolite data form a curved trend from around Eu/Eu* 1 to 2.7. The La_N content of the Troctolite is inversely proportional to the size of the Eu anomaly, as the La_N contents decrease, the Eu/Eu* rises to a maximum of 2.7. At a Eu/Eu* of 1, the Troctolite La_N content is around 60 times chondritic. The UMI data plot in a separate cluster to the Troctolite, and exhibit little variation in Eu/Eu* with most of the points falling close to Eu/ Eu* = 1. The MPD data show less variability than the Troctolite, with Eu/Eu* that varies between 1-1.5. Similarly to the Troctolite, as the La_N content of the MPD samples diminishes, their Eu/Eu* increases. The result is the MPD data intersect the Troctolite data approximately midway along the Troctolite trend at La_N =

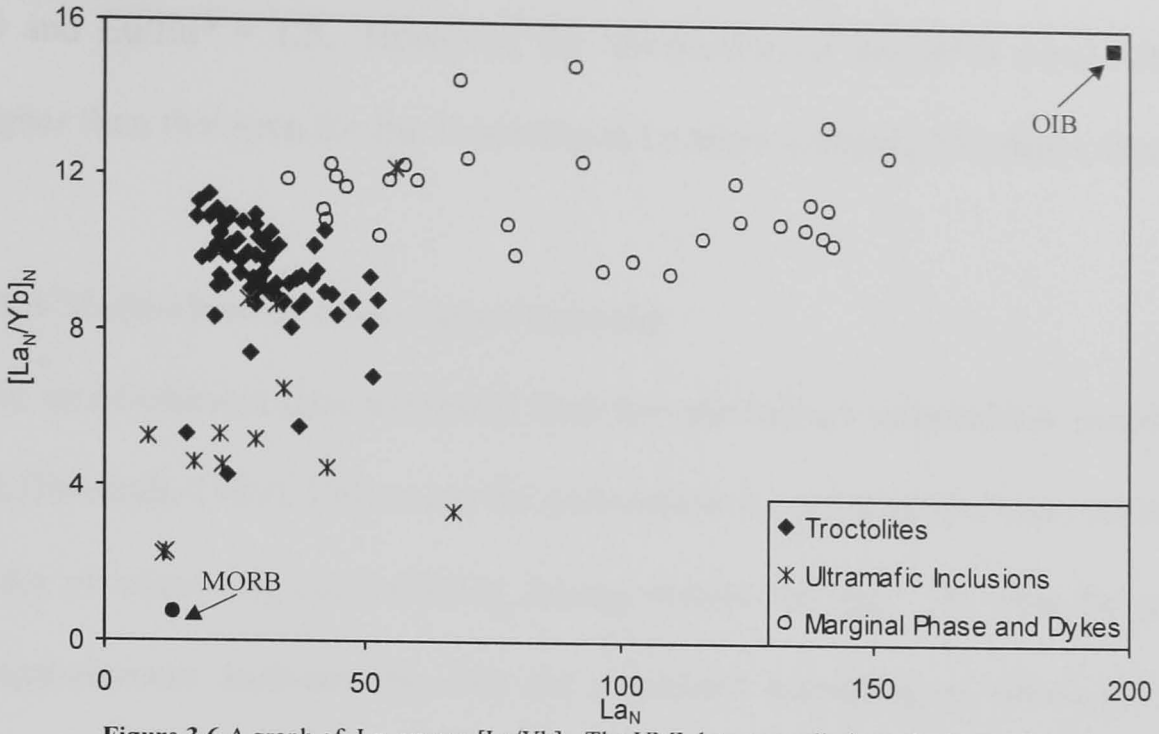

Figure 3.6 A graph of La_N versus $[La/Yb]_N$. The UMI data generally have the lowest La and La/Yb. The Troctolites data have higher La/Yb but similar range of values for La The MPD data have higher La/Yb and much higher La than either the Troctolites or the UMI. The compositions of MORB and OIB are included as comparison.

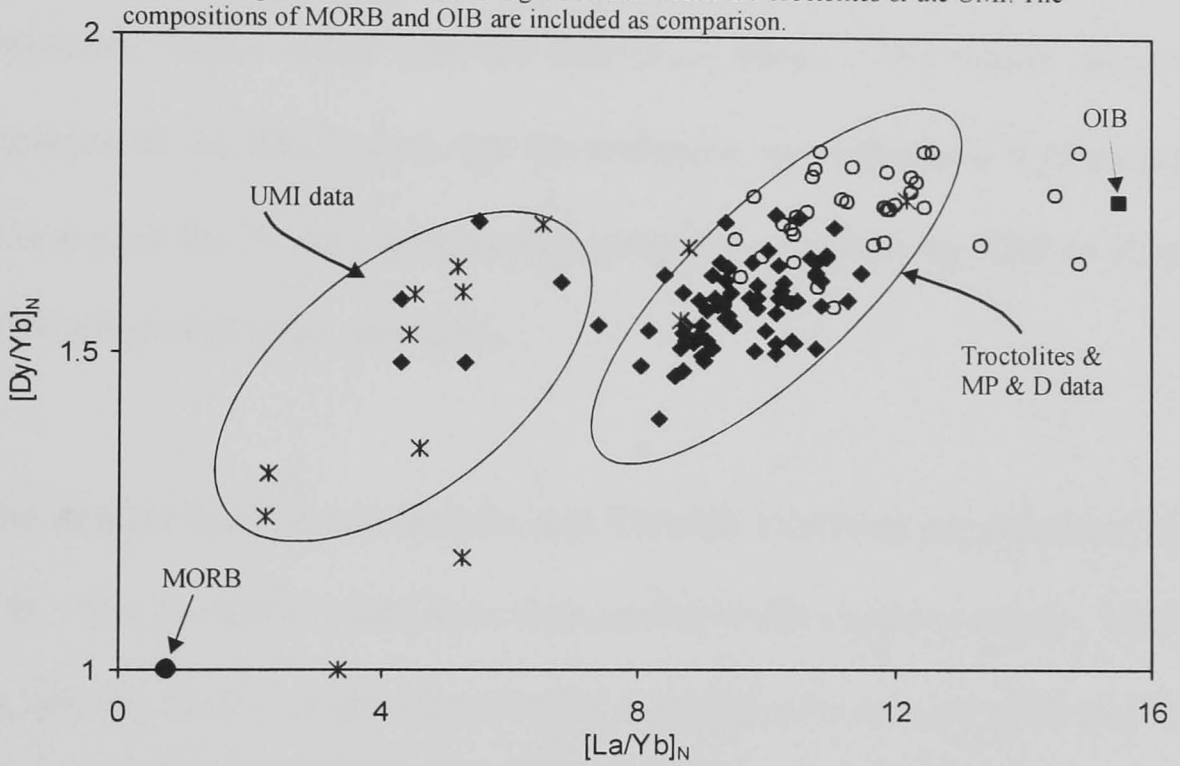

Figure 3.7 Graph of $[La/Yb]_N$ versus $[Dy/Yb]_N$. The Troctolites and MPD data form a continuous series, while the UMI data have lower $[Dy/Yb]_N$. The compositions of MORB and OIB are included for comparison and are arrowed.

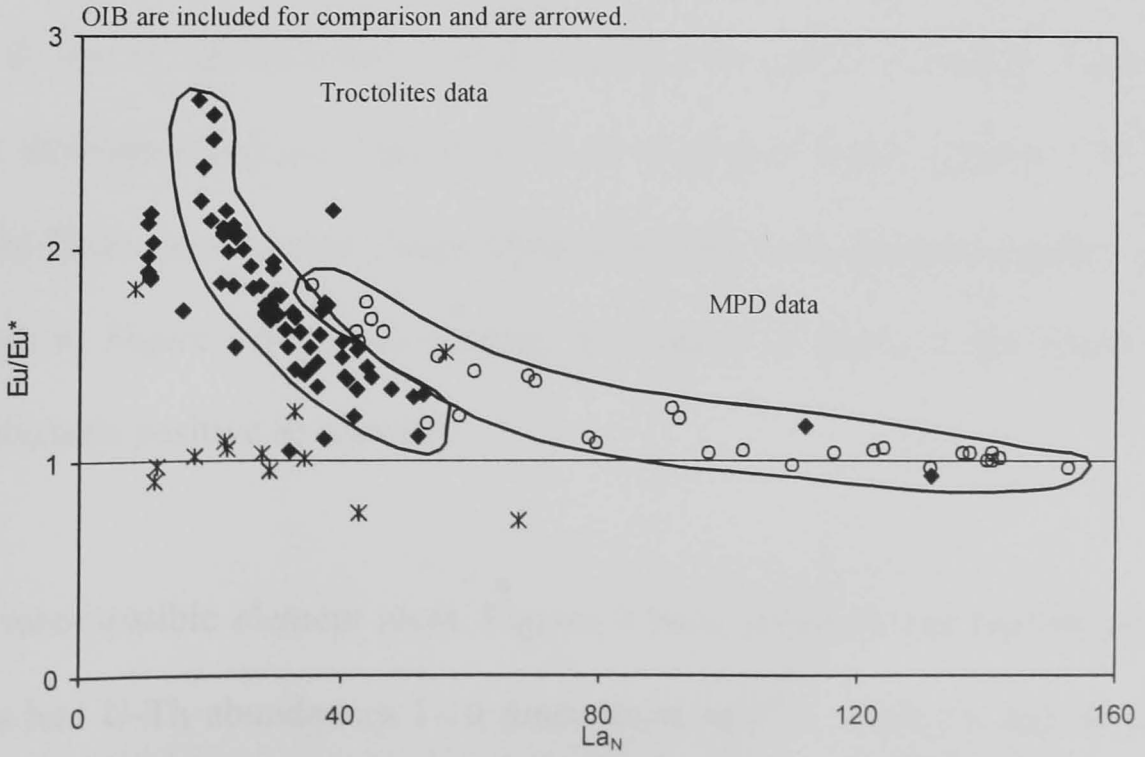

Figure 3.8 Graph of La_N versus Eu/Eu*. The Troctolites data form a line with decreasing Eu/Eu* corresponding to increasing La. The MPD data also have increasing La as Eu/Eu* decreases, but exhibit much higher La contents. The Eu/Eu* and La of the UMI do not appear to be dependant. The derivation Eu/Eu* is explained in the text.

40 and Eu/Eu* = 1.5. However, the intersection of the MPD trend with Eu/Eu* = 1, is higher than that seen for the Troctolite at La approximately 100 times chondritic.

3.1.4 Multi-element data – igneous rocks

The multi-element data presented here are normalised to primitive mantle (PM) (Sun and McDonough, 1989). Following the convention for plots of this type, the data are plotted in order of increasing compatibility during mantle melting. As with the previous REE and major-element analyses the data are organised according to lithology. For this section, wherever possible the data have been presented as ranges showing the maximum and minimum values rather than the individual traces. The ranges have been used as the variance on the data is such that the arithmetic mean minus 2 σ gives negative values. In this section the Zr data were plotted using data analysed by XRF as Zr data derived from ICP-MS proved to be unreliable.

The data for the Normal, Stellate, and Variable Troctolite are presented as ranges in Figure 3.9a. The troctolitic rocks have very similar multi-element patterns with peaks for Ba, K, Sr, and Ti, relative to the elements Th, U and to a lesser extent Nb and Ta. The UMI data show some similarities to the Troctolite patterns (Figure 3.9b). Peaks are present for Ba and K, and in approximately half the samples, Sr and Ti. However, these peaks are not as well developed and the impression is of an overall flatter pattern. The Marginal Phase, Ovoid Dyke, and Eastern Deeps Dyke data have been grouped together and presented as ranges in Figure 3.9c; these patterns are similar to those of the Troctolite but lack the pronounced positive Sr anomaly.

The incompatible element plots, Figures 3.9a-c, revealed that the Voisey's Bay intrusion rocks had U-Th abundances 1-10 times those of PM, while La and Ce abundances were typically almost an order of magnitude greater and have high K/Nb ratios. Therefore, a

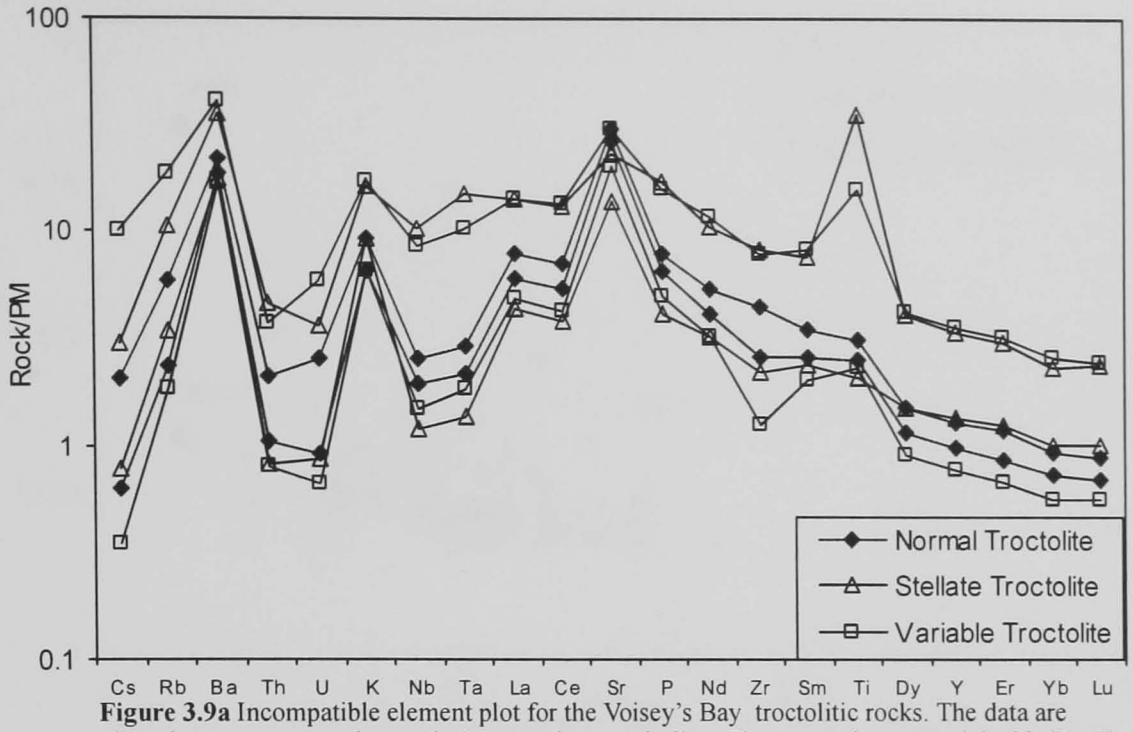

Figure 3.9a Incompatible element plot for the Voisey's Bay troctolitic rocks. The data are plotted as ranges as each samples' pattern is very similar. These samples are enriched in Ba, K, Sr and in some cases Ti. They are depleted in Th, U, Nb and Ta relative to the other elements.

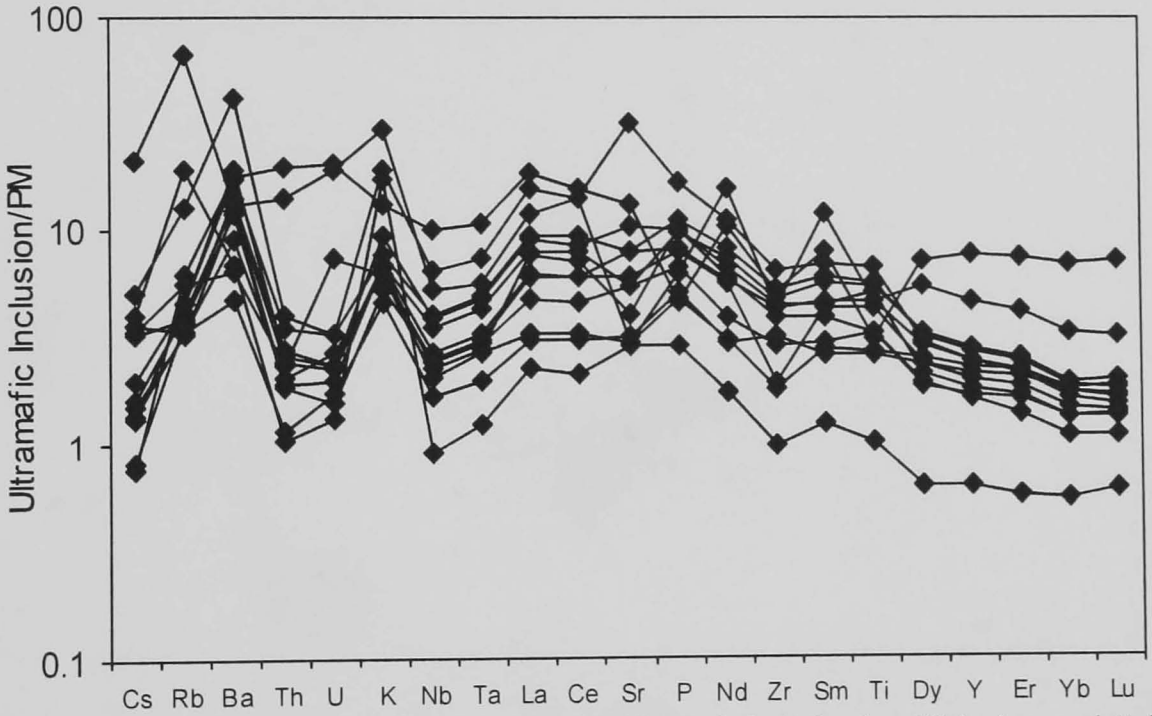

Figure 3.9b Incompatible element plot for the Ultramafic Inclusion data. All the data are plotted. These data exhibit more variability than the Troctolites, as a consequence the patterns cross cut. Despite this, some resemblance to the Troctolites data is visible.

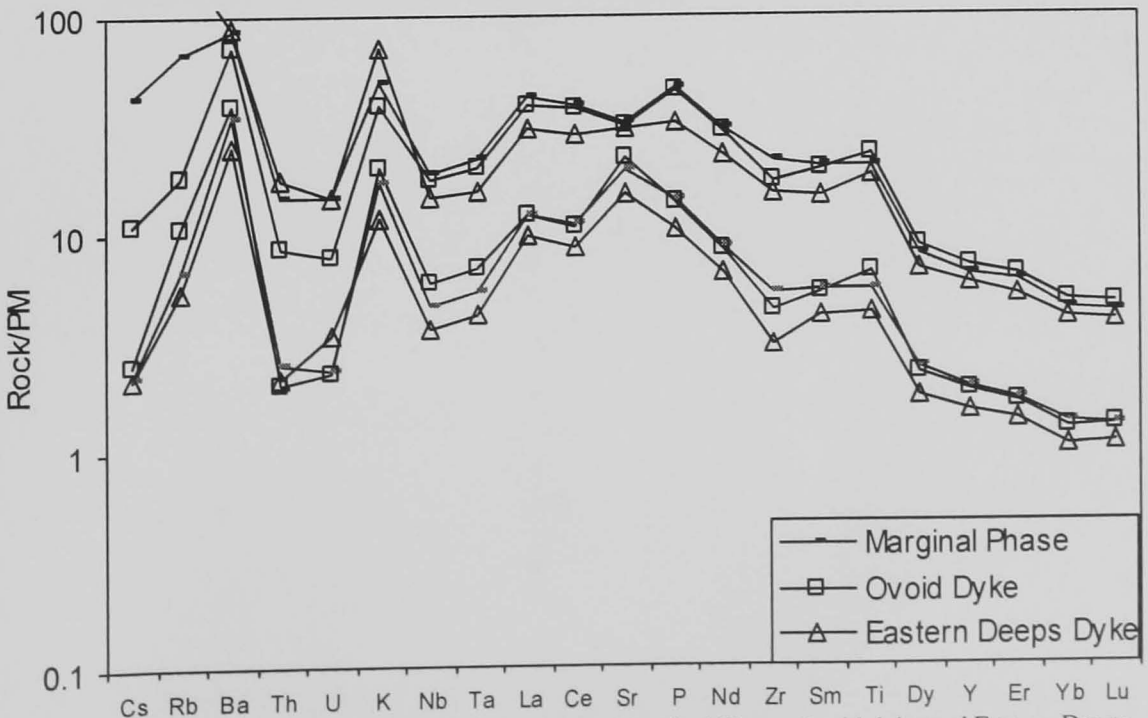

Figure 3.9c Incompatible element plot for the Marginal Phase, Ovoid dyke and Eastern Deeps dyke data. Because these data have similar patterns it is possible to plot them as ranges rather than individual traces. Notice that the pattern of relatively enriched and depleted elements is similar to the Troctolites, but that the abundance of each element tends to be higher.

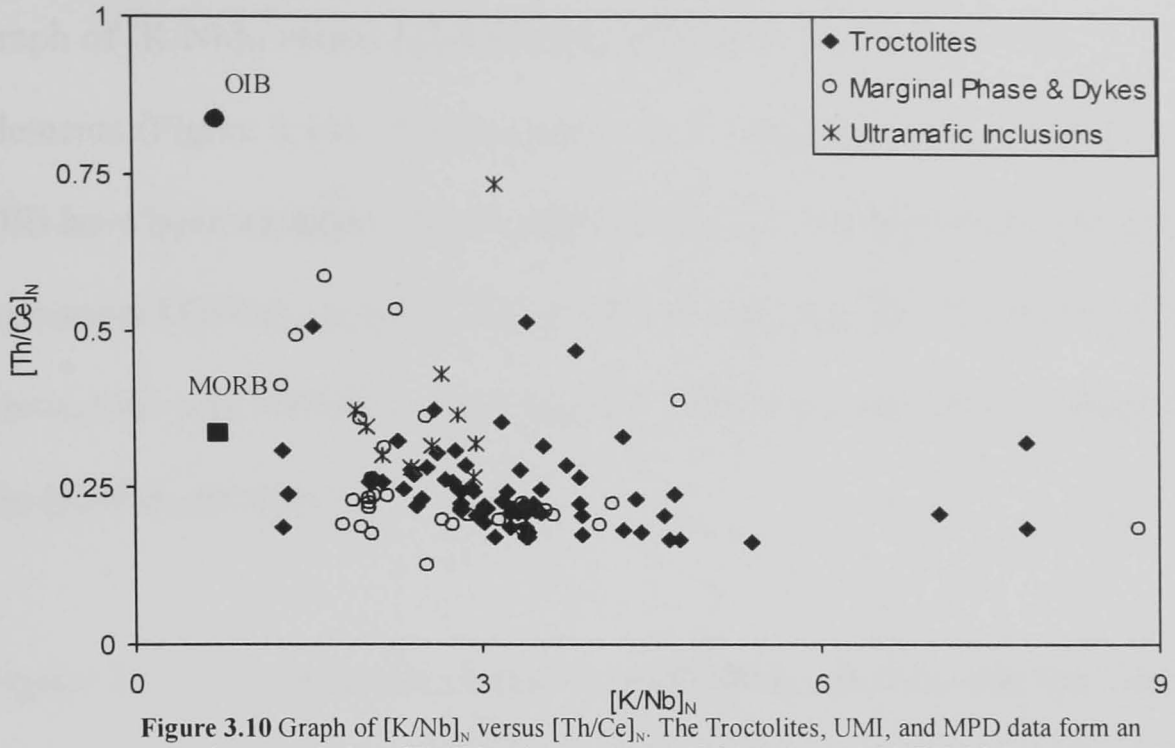

Figure 3.10 Graph of $[K/Nb]_N$ versus $[Th/Ce]_N$. The Troctolites, UMI, and MPD data form an array that extends form $[Th/Ce]_N$ od approximately 0.24 to almost 0.75. $[K/Nb]_N$ values vary between 1 and 9. MORB and OIB (Sun and McDonough, 1989) are included for comparison.

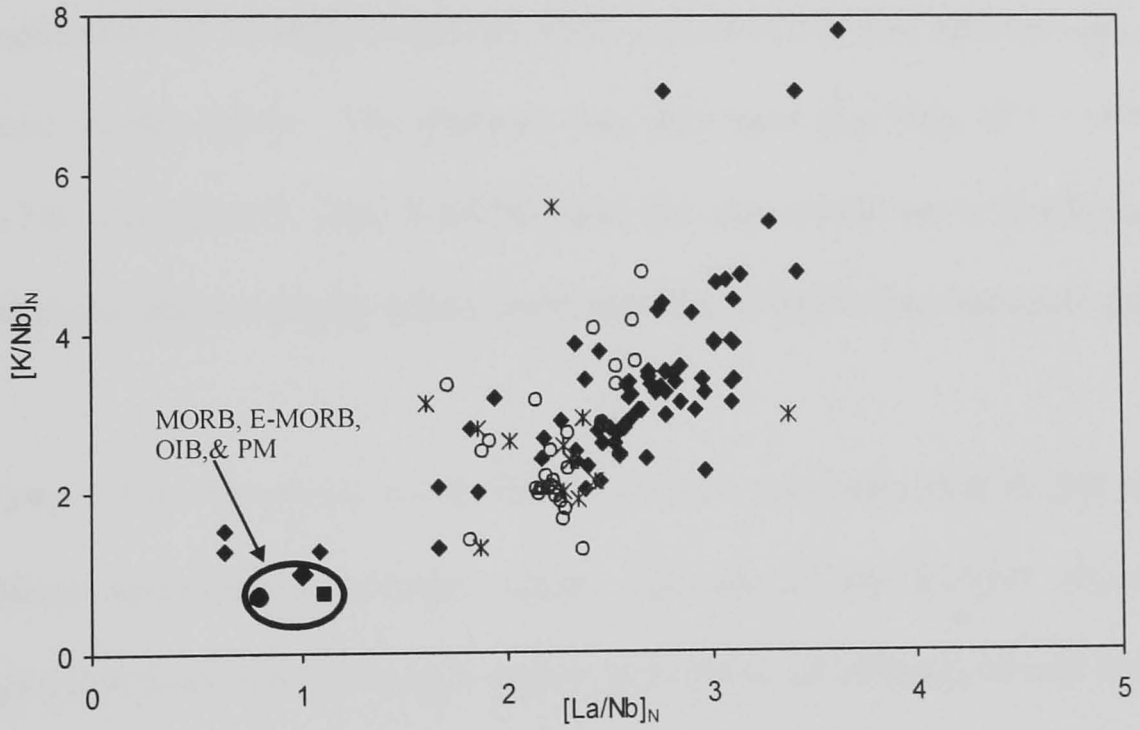

Figure 3.11 Graph of $[La/Nb]_N$ versus $[K/Nb]_N$ for the Voisey's Bay Intrusion Rocks. For the purposes of comparison, published data for OIB, MORB, and E-MORB are included (Sun and McDonough, 1989), and have been circled for clarity..

graph of $[K/Nb]_N$ versus $[Th/Ce]_N$ was plotted to investigate further the behaviour of these elements (Figure 3.10). For the purposes of comparison, the compositions of MORB and OIB have been included. The Troctolite, UMI, and MPD data form an array with its maximum $[Th/Ce]_N$ equal to that of MORB composition. The $[K/Nb]_N$ ranges from a little above OIB and MORB to $[K/Nb]_N$ of 9. $[Th/Ce]_N$, displays a poorly defined increase as the $[K/Nb]_N$ increases.

Figure 3.11 is a graph of $[La/Nb]_N$ versus $[K/Nb]_N$. In order that the Voisey's Bay intrusion rocks might be compared with comparatively well-understood rocks, the published compositions of MORB, E-MORB, OIB, and PM (Sun and McDonough, 1989) were also plotted on this figure. The Voisey's Bay data have $[La/Nb]_N$ of 1.7–4.8 and $[K/Nb]_N$ of 1.2–7.8. The MORB, OIB, E-MORB and PM data all cluster at $[La/Nb]_N$ and $[K/Nb]_N$ of around one and are clearly much lower than the Voisey's Bay intrusion samples.

Figures 3.12a-l combine the Eu/Eu* data that was presented in the REE section with different incompatible element ratios. The use of the Eu/Eu* allows the effects of plagioclase fractionation to be assessed and allows an estimate of whole rock incompatible element ratios before extensive plagioclase accumulation took place. On these diagrams, a line has been drawn at Eu/Eu* = 1 so that the composition prior to plagioclase accumulation is more easily seen. On Figures 3.12 a-j, a regression line has been drawn through the Troctolite data using ORIGIN 6.1 software and the slopes at ± 2 standard deviations have been added; on Figures 3.12k and l, a line has been drawn through at the median value and upper and lower limits estimated. Those Troctolite data that have been circled were omitted from the regression analyses. The justification for the omission of these data is that they are derived from inclusion-bearing variable troctolite and the inclusions that have caused deviation from the observed trend. Because the MPD and UMI data do not lie on a well-defined trend, regression analyses of these data was not attempted.

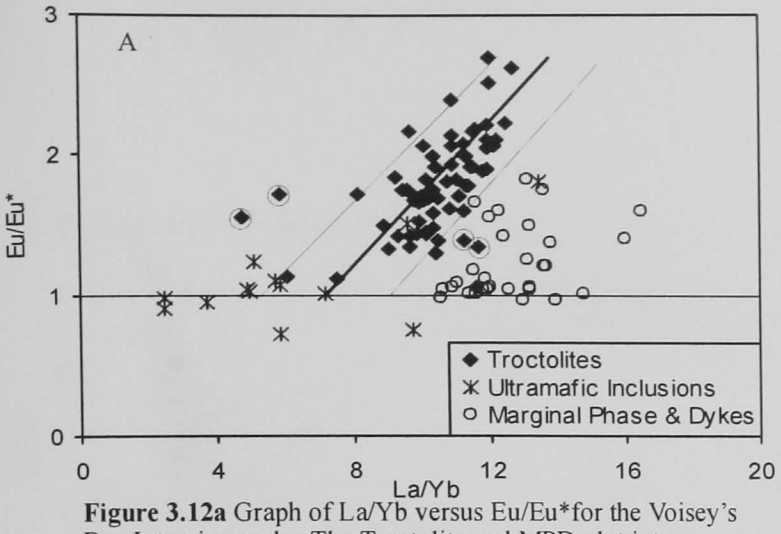

Figure 3.12a Graph of La/Yb versus Eu/Eu*for the Voisey's Bay Intrusion rocks. The Troctolite and MPD plot into separate areas. The La/Yb in the Troctolite increases with increasing Eu/Eu*. The intercept on the Eu/Eu* = 1 line was calculated using ORIGIN. Troctolite data that are circled were omitted from the regression analyses.

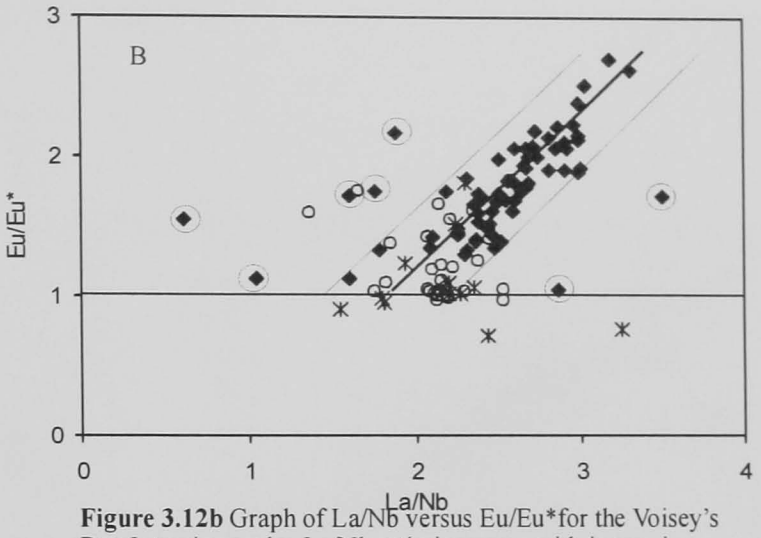

Figure 3.12b Graph of La/Nb versus Eu/Eu*for the Voisey's Bay Intrusion rocks. La/Nb ratio increases with increasing Eu/Eu*. The behaviour of the Troctolite and the MPD is similar.

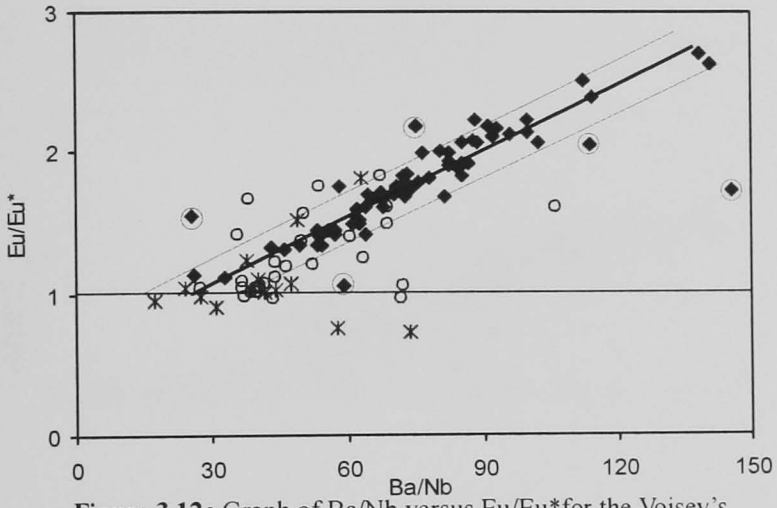

Figure 3.12c Graph of Ba/Nb versus Eu/Eu*for the Voisey's Bay intrusion rocks. Ba/Nb and Eu/Eu* increase in a systematic manner. The Troctolite and MPD behaviour are similar.

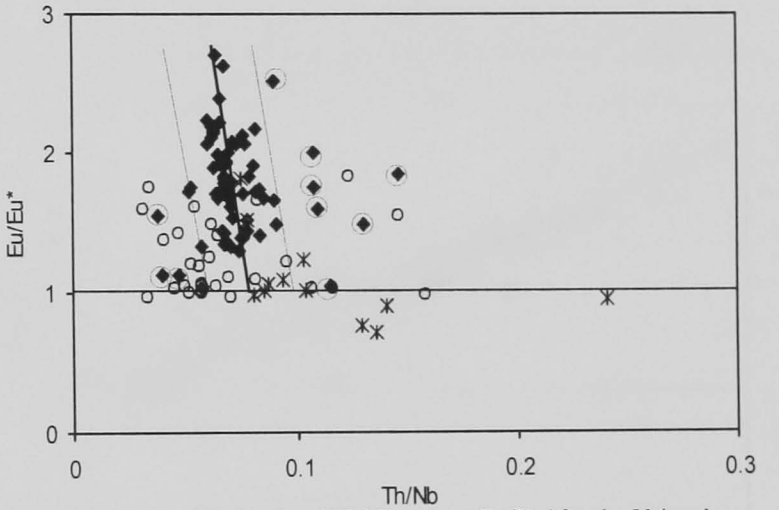

Figure 3.12d Graph of Th/Nb versus Eu/Eu*for the Voisey's Bay intrusion rocks. Th/Nb decreases with increasing Eu/Eu*. The Troctolite and MPD plot into separate areas.

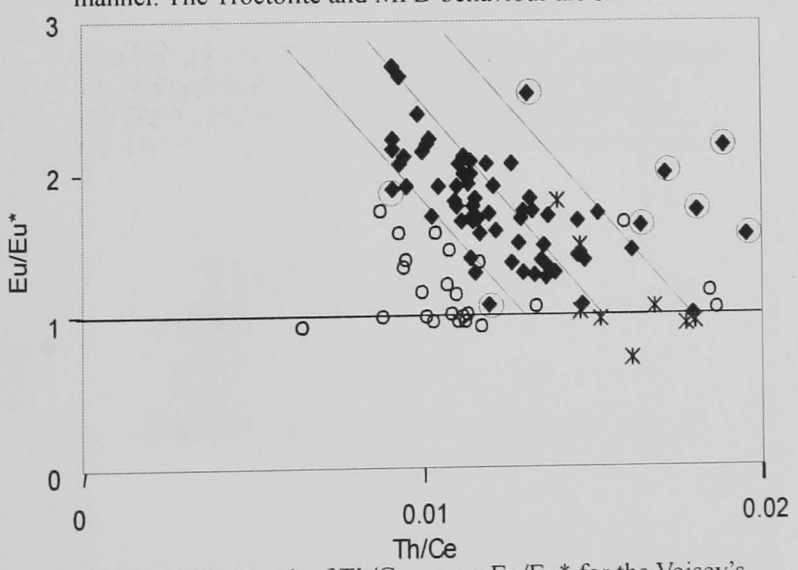

Figure 3.12e Graph of Th/Ce versus Eu/Eu* for the Voisey's Bay intrusion rocks. Th/Ce and Eu/Eu* are negatively correlated. The MPD and Troctolite have similar trends.

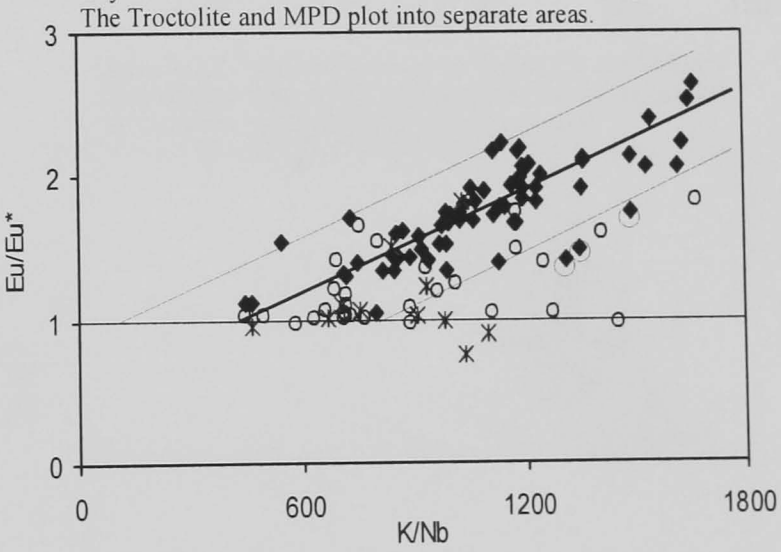

Figure 3.12f Graph of K/Nb versus Eu/Eu*for the Voisey's Bay intrusion rocks. As K/Nb increases, Eu/Eu* increases. The Troctolite and MPD have similar behaviour.

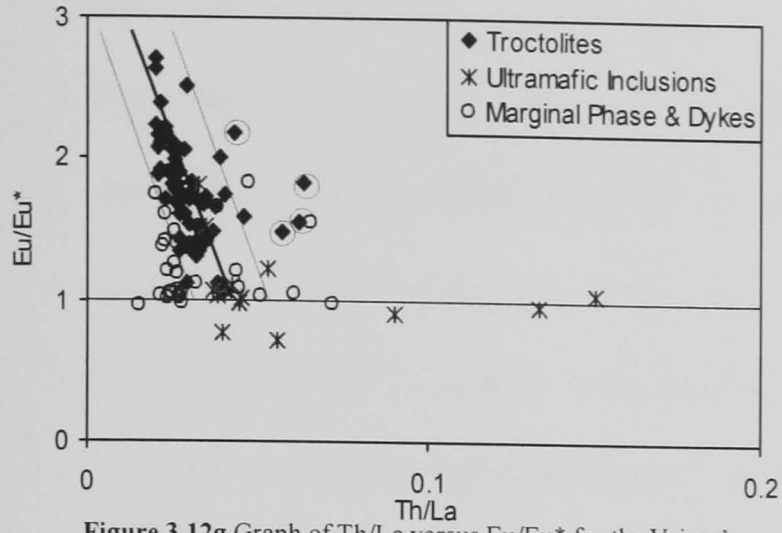

Figure 3.12g Graph of Th/La versus Eu/Eu* for the Voisey's Bay intrusion rocks. Increasing Eu/Eu* correlates to decreasing Th/La. The MPD data have a different trend.

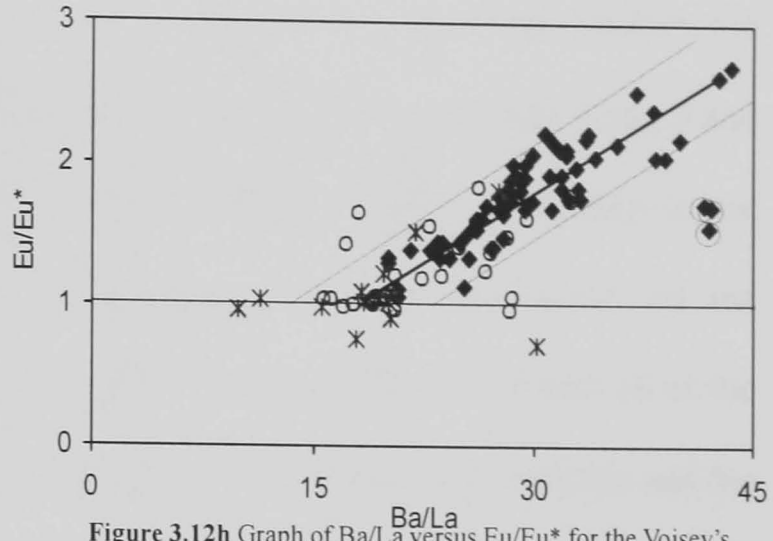

Figure 3.12h Graph of Ba/La versus Eu/Eu* for the Voisey's Bay intrusion rocks. Ba/La increases with Eu/Eu* and the Troctolite and MPD have a similar trend.

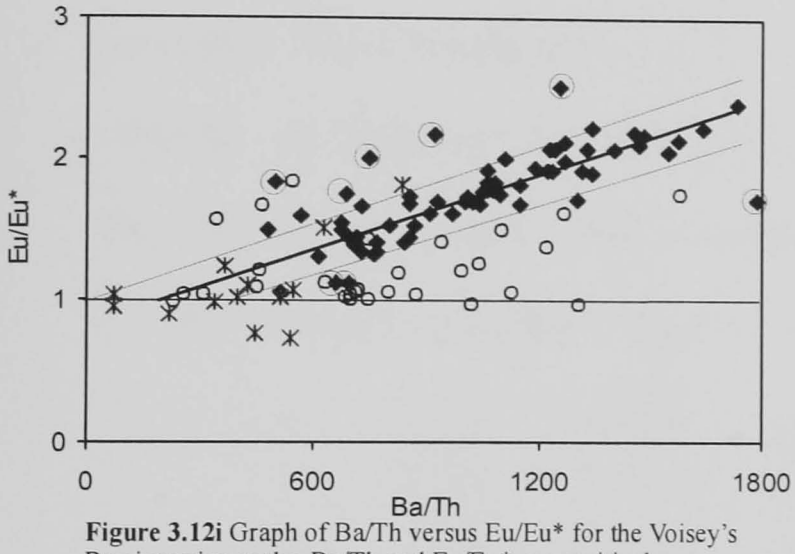

Figure 3.12i Graph of Ba/Th versus Eu/Eu* for the Voisey's Bay intrusion rocks. Ba/Th and Eu/Eu* are positively correlated. The Troctolite and MPD have similar trends.

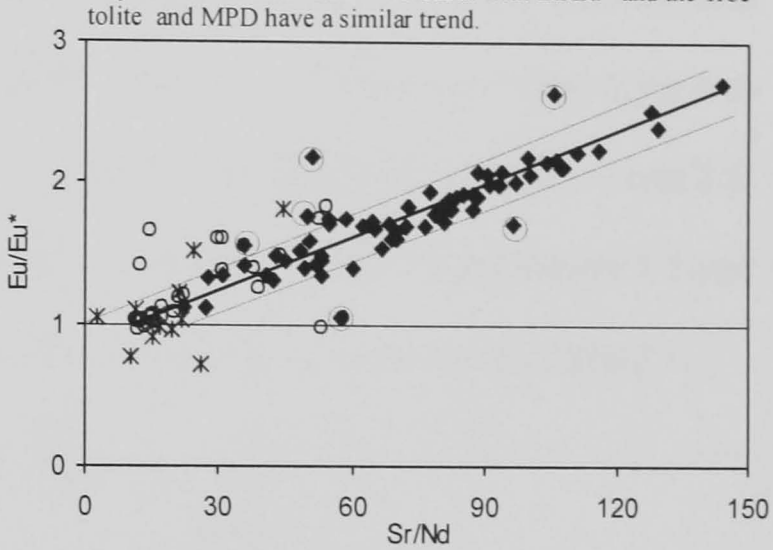

Figure 3.12j Graph of Sr/Nd versus Eu/Eu* for the Voisey's Bay intrusion rocks. Sr/Nd increases with increasing Eu/Eu*. The Troctolite and MPD plot on the same trend.

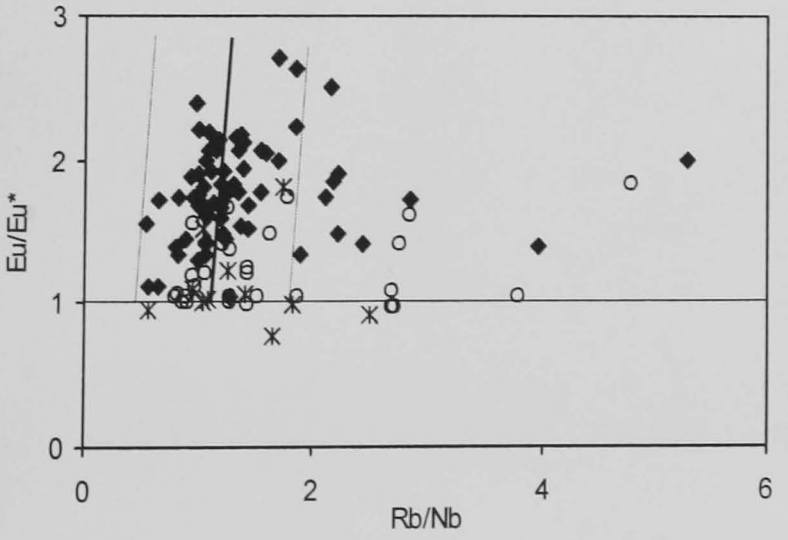

Figure 3.12k Graph of Rb/Nb versus Eu/Eu*for the Voisey's Bay Intrusion rocks. There is little dependence of Rb/Nb upon Eu/Eu*. The Troctolite and MPD behave as one group.

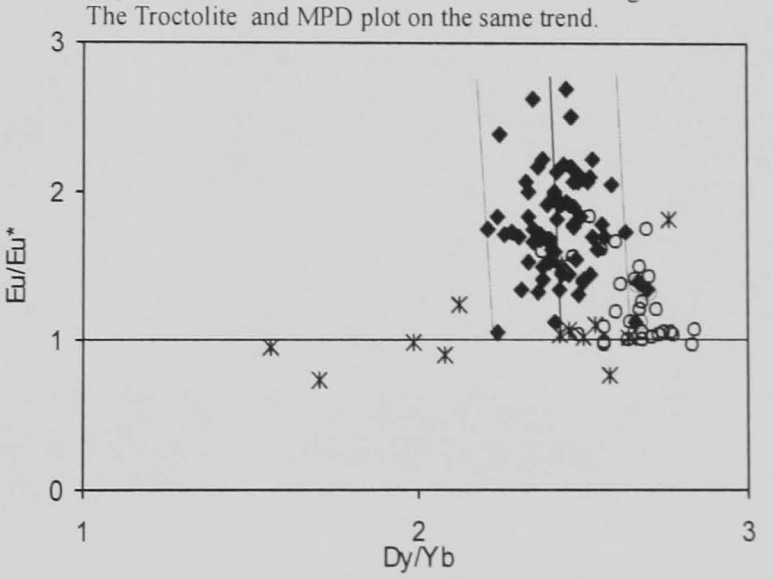

Figure 3.12l Graph of Dy/Yb versus EuEu* for the Voisey's Bay intrusion rocks. Dy/Yb remains approximately constant as Eu/Eu* increases for both Troctolite and MPD.

Figure 3.12a presents La/Yb versus Eu/Eu*. The La/Yb ratio increases in the Troctolite with increasing Eu/Eu*. However, in the MPD and the UMI there is no such relationship. The UMI exhibit little variation in Eu/Eu*, with most points on or near the Eu/Eu* = 1 line. However, the UMI data do vary with respect to La/Yb, the lowest value being 3 and the highest 12. The MPD vary in both La/Yb and Eu/Eu* but the relationship is not systematic, with La/Yb between 10 and 17 regardless of Eu/Eu*. At Eu/Eu* =1 the Troctolite La /Yb is 7.4±2. The MPD have La/Yb that varies between 10 and 16 at the same point. The graph of La/Nb versus Eu/Eu* (Figure 3.12b) shows the Troctolite and the MPD falling onto a similar trend, though the MPD La/Nb to Eu/Eu* appears less systematic. The UMI data however, do not have a systematic relationship between the two variables. At Eu/Eu* = 1, the Troctolite have La/Nb = 1.8, the MPD between 1.7 and 2.5. The UMI are very variable, those data that are near Eu/Eu* have La/Nb between 1.5 and 3.3. The results of the regressions plotted in figures 3.12a–k are presented in Table 3.1.

	Troctolite	MORB	OIB
La/Yb	7.4 ±2	0.8	17.1
La/Nb	1.8 ±0.3	1.1	0.8
Ba/Nb	26 ±8	2.7	7.3
Ba/Th	175 ±120	52.5	87.5
Rb/Nb	1.2 ±0.8	0.2	0.7
K/Nb	375 ±300	257.5	250.0
Th/Nb	0.09 ±0.01	0.05	0.08
Th/La	0.04 ±0.01	0.05	0.1
Sr/Nd	12 ±8	12.3	17.1
Th/Ce	0.017 ±0.003	0.016	0.05
Ba/La	18 ±5	2.52	9.5
Dy/Yb	2.3 ±0.2	1.49	2.59

Table 3.1 Regression analysis values for incompatible element ratios for the Troctolite ± 2 standard deviations at Eu/Eu* = 1. The values for MORB and OIB are included for comparison.

The ratios of Th/La, Sr/Nd, and Th/Ce are approximately equal to MORB values. In terms of La/Yb, Ba/Nb, Ba/Th, K/Nb, Th/Nb and Ba/La the Troctolite parental magma ratios are higher than both MORB and OIB values. The calculated La/Nb ratio is intermediate between MORB and OIB.

3.1.5.1 Country rocks

The purpose of presenting the data for the country rocks is to facilitate a discussion of the effects of the country rocks on the evolution of the magmatic rocks and massive sulphide deposits of the Voisey's Bay intrusion. Four country rock types are considered: the Nain, Tasiuyak, Enderbite and Uivak gneisses. The major and trace element data for the Nain, Tasiuyak and Enderbite gneisses are unpublished, but the Uivak gneiss data are from Schiotte et al. (1993). Although the Uivak gneiss is not exposed at Voisey's Bay, it is included here as it is considered a reasonable analogue for the regional basement at the time the Voisey's Bay intrusion was emplaced. The Uivak gneiss is the dominant component of the Archaean North Atlantic Craton and comprises two members, the Uviak I and Uivak II. The Uivak I is a ~3.7 Ga tonalitic-trondhjemitic-granodioritic gneiss, the less extensive Uivak II is a group of iron-rich porphyritic granodiorites and ferrodiorites (Wendt and Collerson, 1999). The Uivak II is believed to have been emplaced after the Uivak I had undergone at least one major metamorphic event. However, both Uivak I and II fall onto a 3.622 Ga Rb/Sr isochron (Bridgewater and Collerson, 1976).

3.1.5.2 Country rock major element data

Figure 3.13a is a graph of MgO weight percent versus SiO_2 weight percent for the Nain, Tasiuyak, Uivak, and Enderbite gneisses. The Tasiuyak and Uivak gneisses extend to high SiO_2 contents and range between 46-77 weight percent. The MgO content of the Tasiuyak varies between approximately 1-11 weight percent. The Uivak is less variable, plotting between 0-8 weight percent MgO. The Enderbite and Nain gneiss SiO_2 contents overlap those of the Tasiuyak and Uivak gneiss, though do not extent to such high values, falling between 40-66 weight percent. The MgO content of the Nain and Enderbite gneisses is more restricted than that of the Tasiuyak gneiss at 1-7 weight percent.

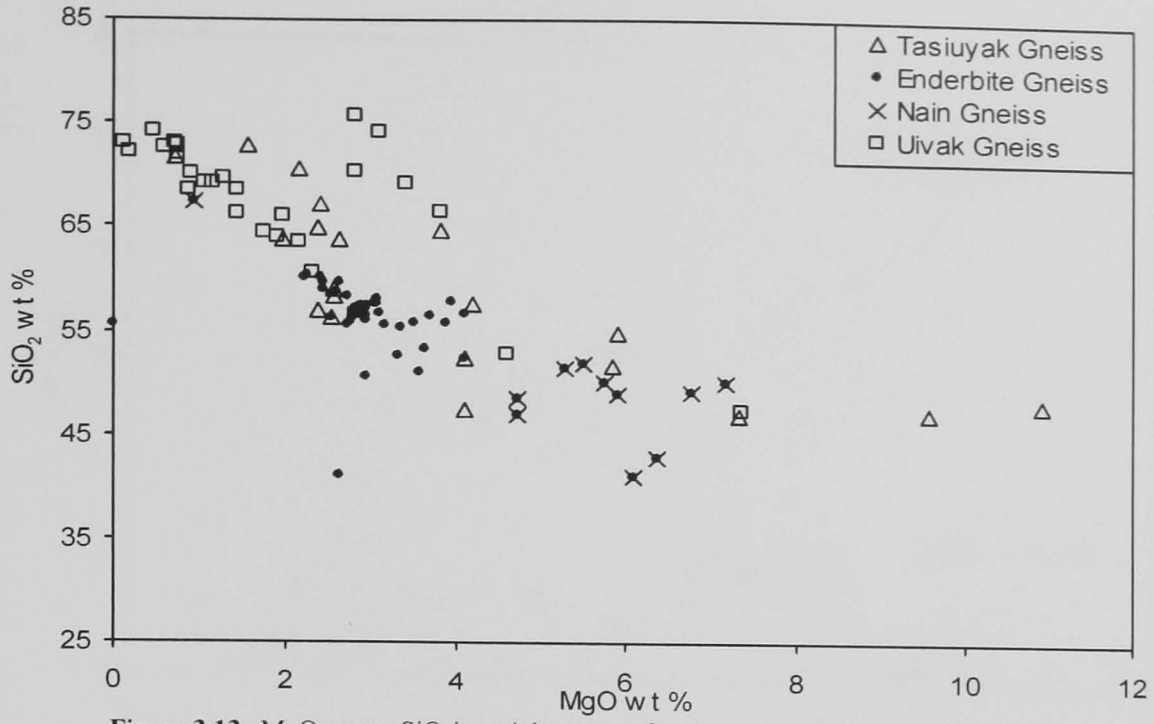

Figure 3.13a MgO versus SiO_2 in weight percent for the country rocks around Voisey's Bay. The Tasiuyak and Uivak gneisses have SiO_2 values of up to 75 weight percent. The Nain and Enderbite gneisses overlap the Uivak and Tasiuyak, with SiO_2 from 44- 60 weight percent. The Uivak gneiss data is from Schiotte et al. (1993); Bridgewater and Collerson (1976).

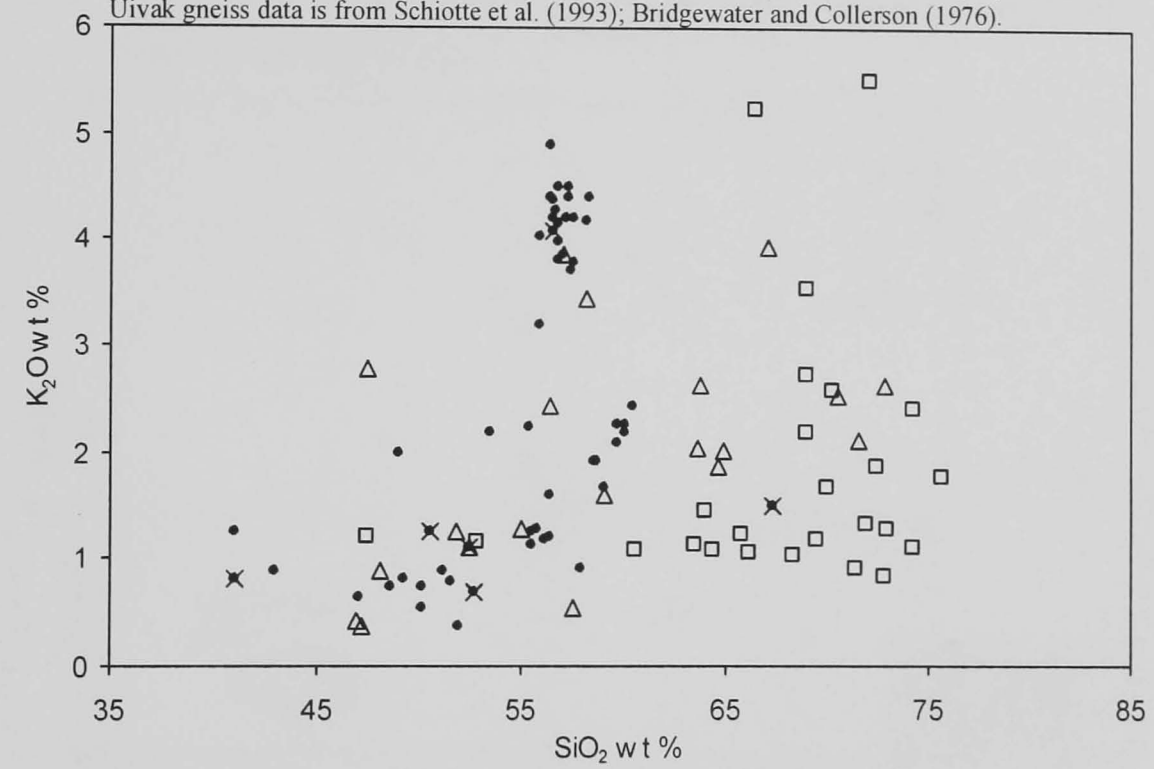

Figure 3.13b SiO_2 versus K_2O for the country rocks around the Voisey's Bay intrusion. The Nain, Tasiuyak, and Uivak gneisses have increasing K_2O with increasing SiO_2. The Enderbite gneiss has two populations, one high K_2O and with lower K_2O.

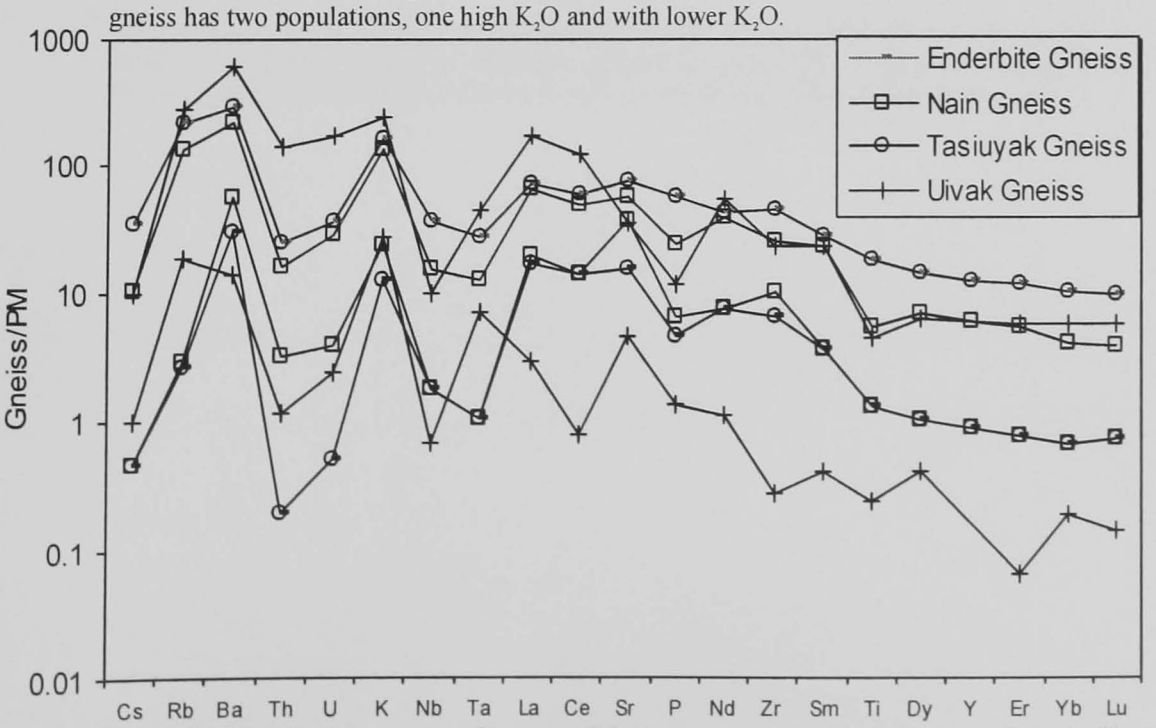

Figure 3.14 Graph of the ranges of incompatible element concentrations normalised to primitive mantle for the the Nain, Tasiuyak, Enderbite and Uivak gneisses. The gneisses have very similar multi-element patterns. These patterns are also similar to those of the Voisey's Bay intrusion rocks.

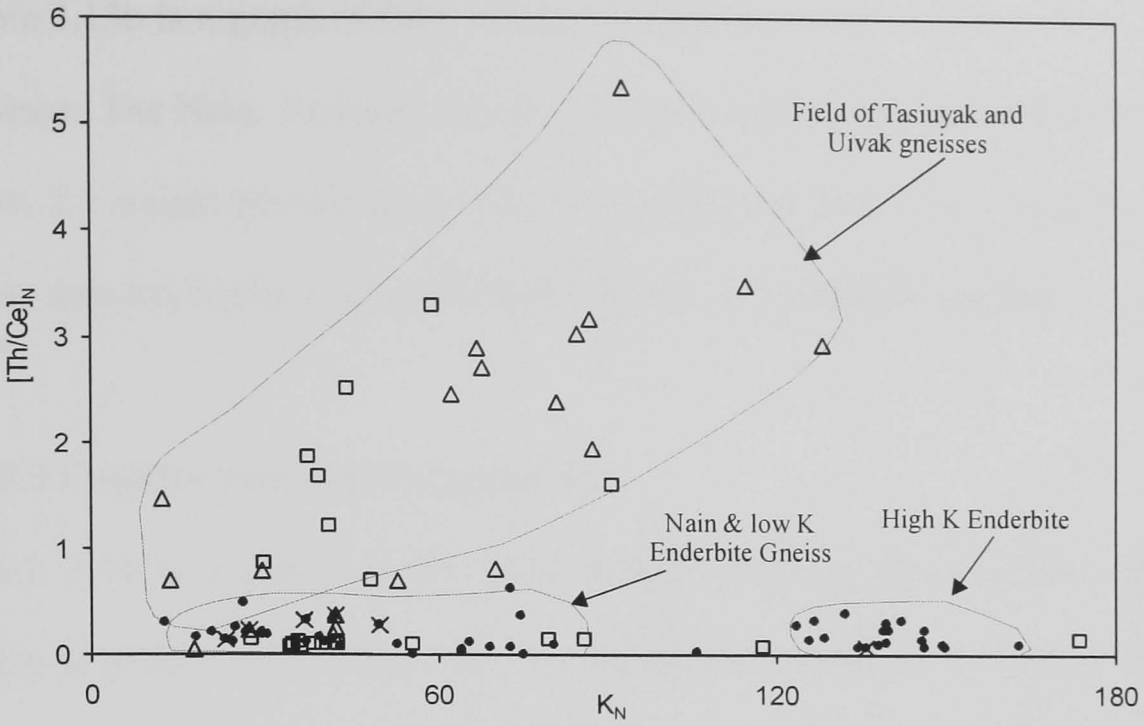

Figure 3.15 Graph of K_N versus $[Th/Ce]_N$ for the Nain, Tasiuyak, Uivak, and Enderbite gneisses. The Nain and low K Enderbite gneisses are coincident, while the Tasiuyak and Uivak gneiss data plot onto a separate trend. Uivak gneiss data from Schiotte et al. (1993); Bridgewater and Collerson (1976).

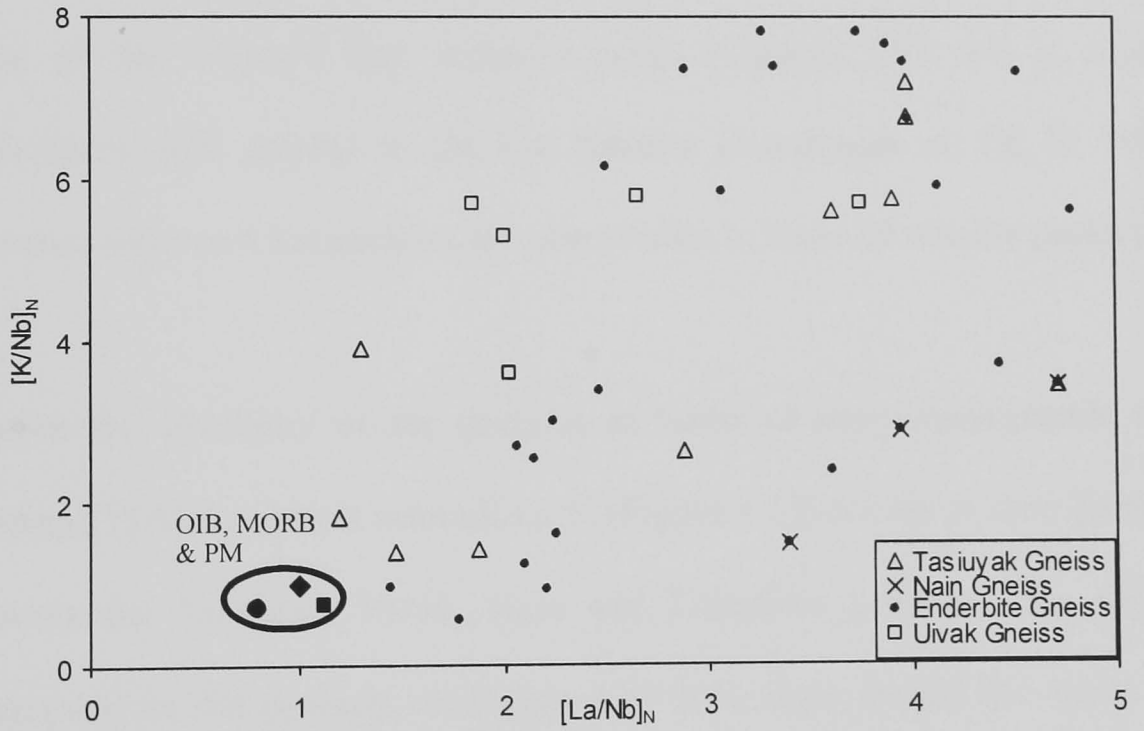

Figure 3.16 Graph of $[La/Nb]_N$ versus $[K/Nb]_N$ for the Tasiuyak, Nain, Enderbite, and Uivak gneisses. The composition of MORB, OIB, and PM are included for comparson. The gneisses have elevated $[La/Nb]_N$ and $[K/Nb]_N$ ratios relative to the mantle-derived compositions.

Figure 3.13b is a graph of SiO_2 versus K_2O for the Nain, Tasiuyak, Uivak, and Enderbite gneisses. The Nain, Tasiuyak, Uivak and approximately half the Enderbite gneiss data plot below 2.5 weight percent K_2O, with SiO_2 increasing with K_2O. A group of the Enderbite gneiss data has higher K_2O, with levels between 3.5-5 weight percent.

3.1.5.3 Country rock multi-element data

Figure 3.14 is a graph of the multi-element data for the Enderbite, Nain, Uivak and Tasiuyak gneiss. For all four gneisses, the data are presented as ranges. The most striking point about these data is the similarity between the patterns. All the gneisses have high K/Th, K/U, K/Nb and K/Ta ratios. Comparing the gneiss multi-element patterns with those of the Voisey's Bay intrusion rocks (Figures 3.9a and c) reveals similarities, particularly with respect to the low relative abundances of Th, U, Nb, and Ta. The intrusive rocks and the gneisses are also similar in terms of notable peaks for Ba and K.

Despite the similarity of the gneisses in terms of their incompatible element patterns, plotting $[Th/Ce]_N$ against normalised K (Figure 3.15) allows at least partial discrimination between the Tasiuyak, Uivak, Nain and Enderbite gneisses. The different fields that correspond to the gneisses on Figure 3.15 have been circled for clarity. The Enderbite gneiss has high and low K variants (Figure 3.13b). The high K form of the Enderbite gneiss plots separately with K values 120 times greater than PM, while the low K Enderbite gneiss is indistinguishable from the Nain gneiss data. The Tasiuyak gneiss has similar K levels to the Nain and low K Enderbite gneiss, but has markedly higher Th/Ce values. The Nain and Enderbite gneiss generally have $[Th/Ce]_N < 0.5$, while the Tasiuyak gneiss is generally between 0.5 and 5. The majority of the Uivak gneiss data are similar to the Tasiuyak gneiss. However, a proportion exhibits behaviour more like that of the Nain and low K Enderbite gneisses. Figure 3.11 presented $[La/Nb]_N$ versus $[K/Nb]_N$ for the Voisey's Bay intrusion rocks. Because it is likely that the magmas parental to the Voisey's

Bay intrusion assimilated the country gneisses, it will be informative to compare the gneisses against the same reference points. Figure 3.16 is a graph of $[La/Nb]_N$ versus $[K/Nb]_N$ for the country gneisses. In comparison, with MORB and OIB the gneiss data have elevated $[La/Nb]_N$ and $[K/Nb]_N$, with increases in $[La/Nb]_N$ corresponding to increases in $[K/Nb]_N$.

3.1.6 Sr and Nd isotope data

The data in this section are taken from Amelin et al. (2000a), Emslie et al. (1994), and Schiotte et al. (1993). These data are reviewed, because taken with the whole rock data they can considerably increase our understanding of the processes involved in the generation of the Voisey's Bay parental magmas and the genesis of the magmatic sulphides. Figures 3.17a-b present the Sr and Nd isotope data plotted using the epsilon notation for both Sr and Nd, corrected to the time of crystallisation. The time of crystallisation is taken to be 1.32 Ga (after (Amelin et al., 2000a) rather than the 1.334 Ga that is usually accepted as being the emplacement date for the Voisey's Bay intrusion (Amelin et al., 1999). Amelin (2000) reasoned that the Voisey's Bay intrusion remained above the closure temperature for Rb, Sr, Sm, and Nd for 13.4 million years after emplacement. To avoid complication the younger age of 1.32 Ga was used. Figure 3.17a presents the Sr and Nd isotope data for the Voisey's Bay intrusion rocks. The Troctolite data form a cluster between εSr +9 to +15 and εNd-0.2 to-1.9. The MPD data exhibit greater variation, with εSr between +6–+45 and εNd varies from +0.8 to –12. The Nd and Sr isotope data for the Nain, Tasiuyak, Uivak and Enderbite gneisses are illustrated in Figure 3.17b. The Tasiuyak gneiss data vary between εSr +130 to +315 and εNd –9 to –10. The Nain gneiss by comparison, exhibits less variation in εSr and greater variability in the εNd. The values are εSr +19 to +90 and εNd –12 to –19. The Enderbite gneiss εSr values are similar to those of the Nain gneiss, but with somewhat higher εNd. The values are εSr +13 to +57 and εNd-3

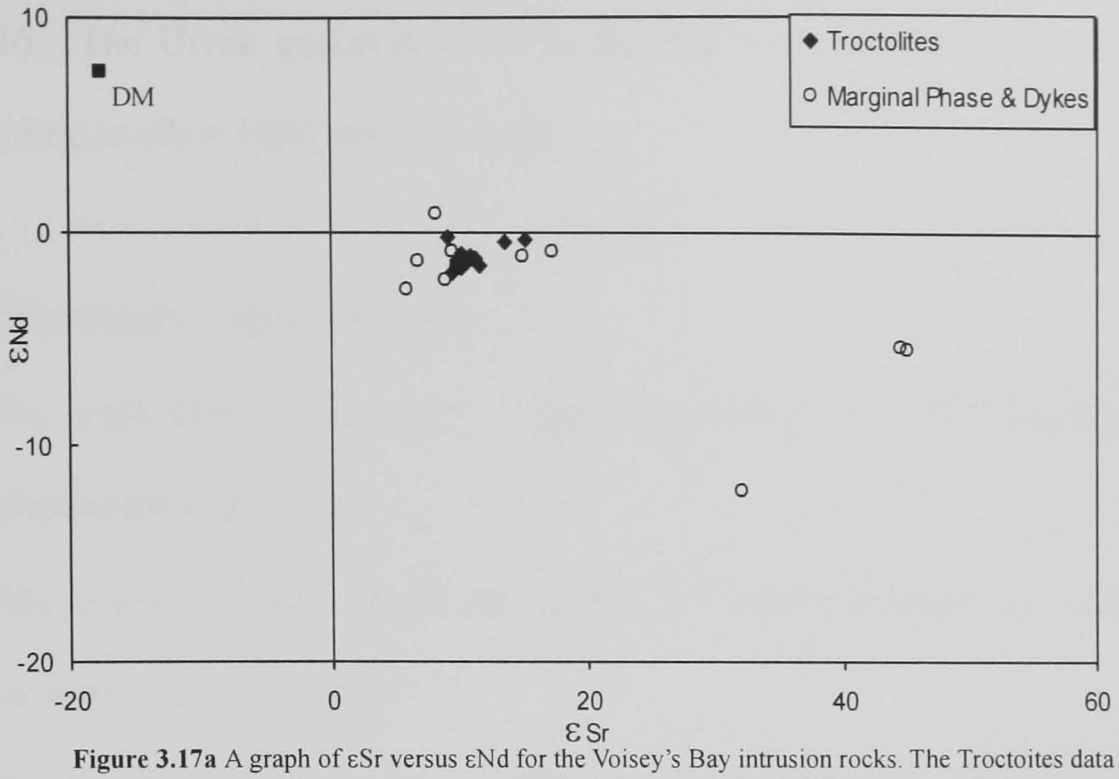

Figure 3.17a A graph of εSr versus εNd for the Voisey's Bay intrusion rocks. The Troctoites data make a group εSr of approximately 10 to 17 and εNd 0 to -3. The MPD data from εSr 5 to 45 and

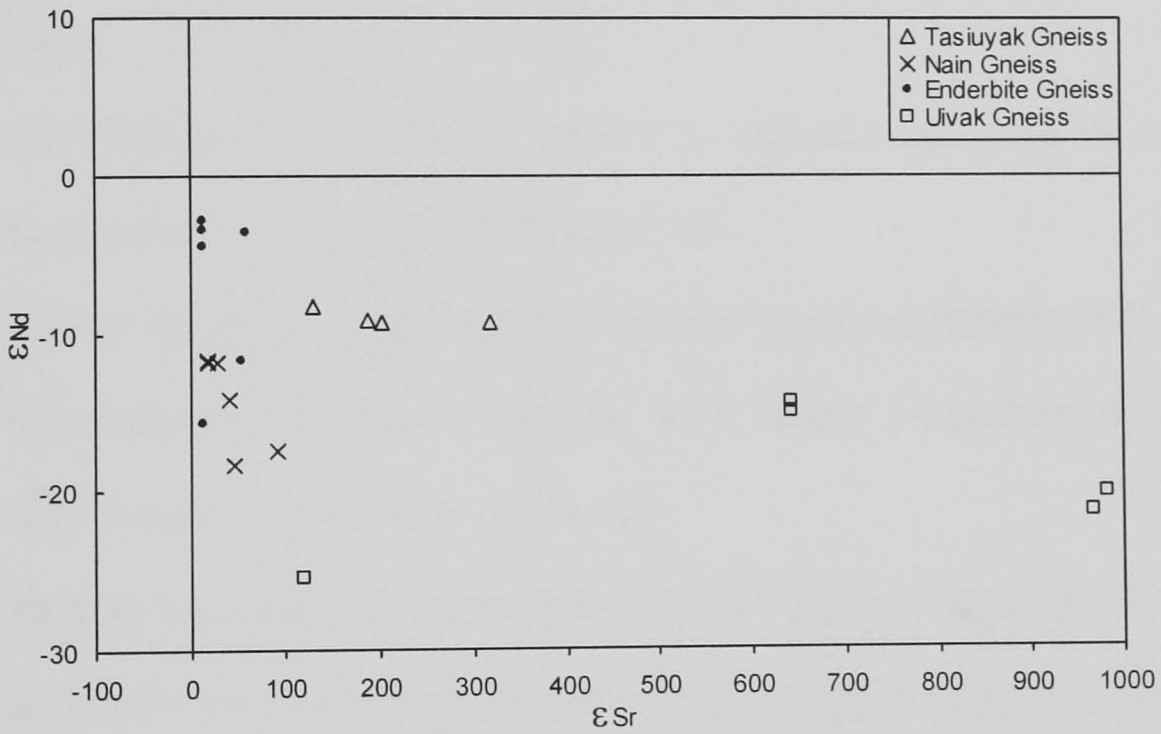

Figure 3.17b A graph of εSr versus ε Nd for the Tasiuyak, Nain, and Enderbite Gneiss. The Tasiuyak Gneiss has ε Sr of between 100 to 325 and epsilon Nd of -7 to -10. The Nain Gneiss has εSr of 20 to 100 and epsilon Nd 12 to 18. The Enderbite Gneiss has εSr of 20 to 60 and ε Nd of -3 to -16 (data from Amelin et al., 2000; Emslie et al., 1994; Schiotte et al., 1993).

to −16. The Uivak gneiss data fall to the end of the Tasiuyak and Nain gneiss trends extending to εSr = 1000 and εNd = -25.

3.1.7 Summary – igneous rocks

- The major element chemistry of the Voisey's Bay intrusion Troctolite is controlled by plagioclase and olivine.
- The major element chemistry of the MPD is controlled by olivine, plagioclase, sulphides and Fe-oxides.
- Relative to MORB the Voisey's Bay intrusion rocks have elevated La/Yb and Dy/Yb ratios.
- The MPD have a higher La/Yb and Dy/Yb ratios than the Troctolite and the Troctolite have higher La/Yb and Dy/Yb than the UMI.
- Eu/Eu* diagrams suggest that the Troctolite began crystallising from liquids with La approximately 60 times chondritic. MPD began crystallising from liquids with approximately 100 times chondritic La.
- Plotting trace element ratios against Eu/Eu* allows a composition for the magma parental to the Troctolite to be deduced. In terms of K versus K/Nb the Troctolite and UMI behave differently from the MPD
- The Voisey's Bay intrusion rocks have markedly greater K/Nb and La/Nb ratios than MORB, OIB, and E-MORB.
- The Troctolite have εSr and εNd between +9 to +15 and –9 to –10 respectively.
- The MPD have εSr and εNd between +6 to +45 and 0.8 to –12 respectively.

3.2. Discussion

3.2.1 Effects of Crystal Accumulation/Fractionation and the Composition of the Parental Magma

It has already been stated that the Voisey's Bay rocks are cumulates. Before any estimate can be made of the characteristics of the magma parental to these cumulates the effects of crystal accumulation and fractionation must be assessed. This is made easier, as the rocks at Voisey's Bay are dominated by troctolite - which comprises plagioclase and olivine. Therefore, only the effects of olivine and plagioclase fractionation and the proportion of trapped melt need be considered when making an estimate of the parental magma composition. Plagioclase and olivine fractionation do not affect trace element ratios until fractionation is very advanced. By contrast, variation in plagioclase and olivine abundance has a marked effect on the trace element ratios. The variation of trace element ratios with respect to plagioclase abundance (and by implication, olivine abundance) has already been considered in the section on Eu/Eu*. The results are presented in Figures 3.12 a- k, and the results summarised in Table 3.1. Table 3.2 takes the data for the Troctolite and compares it with that of the parental liquid proposed by Bedard (2001).

Ratio	Parental melt	Bedard	MORB	OIB	PM
La/Yb	7.4 ±0.8	7.2	0.55	6.61	0.93
La/Nb	1.8 ±0.3	1.55	1.07	0.77	0.96
Ba/Nb	26 ±8	21.5	2.70	7.29	9.80
Ba/Th	175 ±120	471.5	52.5	87.5	82.22
Rb/Nb	1.2 ±0.8	0.78	0.24	0.65	0.89
K/Nb	375 ±300	372.77	257	250	350
Th/Nb	0.09 ±0.01	0.05	0.05	0.08	0.12
Th/La	0.04 ±0.01	0.03	0.05	0.11	0.12
Sr/Nd	12 ±8	11.11	12.32	17.14	15.58
Th/Ce	0.018 ±0.003	0.013	0.016	0.050	1.00
Ba/La	18 ±5	13.8	2.52	9.46	10.17
Dy/Yb	2.3 ±0.2	2.18	1.49	2.59	1.49

Table 3.2 Calculated composition of the magma parental to the Troctolite in terms of trace element ratios. Also shown is the composition calculated by Bedard (2001) using published Kd values and normative mineralogy. For comparison, the composition of MORB, OIB and PM are included after Sun and McDonough (1989).

The calculated ratios for the Troctolite parental melt are in generally good agreement with those calculated by Bedard (2001). The only large difference occurs with Ba/Th, which is considerably lower than that estimated by Bedard (2001). The reasons for this are not clear; other ratios involving Ba or Th are close to Bedard's values and often similar to MORB or OIB. In his 2001 paper, Bedard grouped the Voisey's Bay intrusion rocks together differentiating them chiefly based on their K contents. However, here it has been observed that the Troctolite and the MPD have several major differences. In addition, Bedard used data from the nearby Mushaua intrusion. It is possible that the differences in the trace element ratios calculated here and by Bedard are due in part to his combining the two rock types and data from the Mushaua intrusion.

The Rb/Nb, Th/Nb, Th/La, Th/Ce, and Sr/Nd ratios calculated here are generally intermediate to MORB and OIB. La/Yb, La/Nb, Ba/Nb, Ba/Th, Ba/La and K/Nb are all in excess of the ratios found in MORB and OIB. Given that olivine fractionation and plagioclase fractionation will not greatly alter these ratios, the only way that the observed trace element ratios could arise is by contamination of the melt by crustal material.

3.2.3 Calculating the fO_2 of the Voisey's Bay intrusion

Figure 3.18 is a graph of $[Sr/Nd]_N$ plotted against Eu/Eu*, similar to Figure 3.12j. As the Eu/Eu* increases there is a corresponding, systematic increase in Sr/Nd ratio. This is a reflection of the control that plagioclase has on the rock composition. Superimposed upon this figure are three lines labelled A, B, and C. These lines correspond to hypothetical whole-rock compositions in which the plagioclase abundance is increased in 10 percent increments using mass-balance and were calculated using published partition coefficients. Table 3.3 lists these Kd values and the sources from which they were drawn (Drake and Weill, 1975; Fujimaki et al., 1984). The starting composition is calculated based upon averages of whole-rock data where the Eu/Eu* equals one. The added plagioclase is taken

to be in equilibrium with the same calculated composition. Line A represents the composition of a whole-rock whose plagioclase is derived from a liquid where all the Eu is present as Eu^{3+}. Line B represents a rock composition derived from a liquid where all the Eu is present as Eu^{2+}. Line C has been drawn through the observed data by adjusting the partition coefficient of Eu into the plagioclase until the calculated whole rock composition was in good agreement with the observed data. As the oxidation state of Eu is dependant upon the oxygen fugacity (Drake, 1975; Drake and Weill, 1975; Weill and Drake, 1973), the ratio of Eu^{2+}/Eu^{3+} in plagioclase and the corresponding liquid can be used to derive the oxygen fugacity (Drake, 1975). Because the Eu in Troctolite is controlled by plagioclase, the Eu content of olivine being negligible, we can use the partition coefficients of Eu into Troctolite to derive the Eu^{2+}/Eu^{3+} ratio in plagioclase and therefore the oxygen fugacity (fO_2).

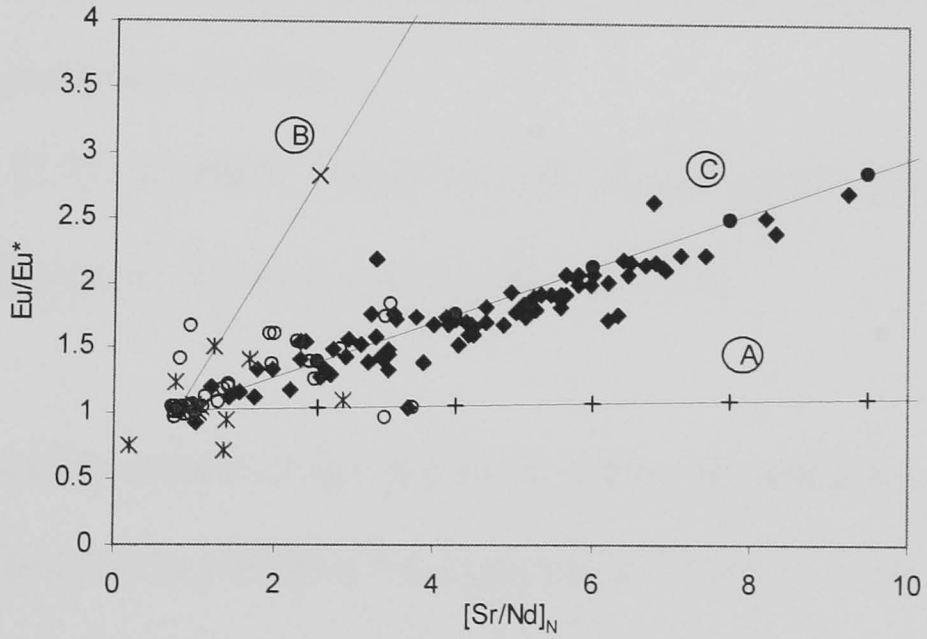

Figure 3.18 Graph of [Sr/Nd]N versus Eu/Eu*. Superimposed are three lines, A, B, C. Line A represents the gradient if all Eu were present as Eu^{3+}. Line B represents the composition if all Eu were present as Eu^{2+}, and line C is the trend of Eu with a distribution coefficient of 0.28.

	D value	Source
Eu^{2+}	1.214	(Fujimaki et al., 1984)
Eu^{3+}	0.079	(Drake and Weill, 1975)
Model Eu	0.28±0.02	Calculated

Table 3.3 Partition coefficients for Eu^{2+}, Eu^{3+} and modelled Eu used in the calculation of fO_2 discussed in the text.

The Eu^{2+}/Eu^{3+} ratio in the plagioclase is calculated by using the concentration of Eu in plagioclase resulting from a Eu partition coefficient of 0.28 with the expected Eu concentration by extrapolating between Sm and Gd *e.g.*:

$$\text{Eu concentration in whole rock} \times \frac{0.28}{\sqrt{[Sm]_N \cdot [Gd]_N}}$$

Once the Eu^{2+}/Eu^{3+} ratio has been calculated, it is substituted into the equation below and the fO_2 is calculated.

$$\text{Plagioclase } fO_2 = -4.60 \log \frac{Eu^{2+}}{Eu^{3+}} - 3.86 \text{ (Drake and Weill, 1975)}$$

Using the above equations, assuming a temperature of 1300°C and an intrusion depth of 10 km (Berg, 1976; Berg and Wheeler, 1976), the oxygen fugacity of the liquids parental to the Voisey's Bay Troctolite is around $+0.4 \pm 0.1$ log units relative to the quartz-fayalite-magnetite (QFM) buffer. The fO_2 at the QFM buffer being calculated using the equation below (Ballhaus et al., 1991).

$$82.77 + 0.00484T - (30681/T) - 24.24 LogT + 940P - 0.02P = fO_2 \text{ at QFM}$$

where T is temperature in K and P is pressure in GPa.

An alternative method of deriving the fO_2 using the calculated partition coefficients and mass-balance of the published *Kd* values for Eu^{2+} and Eu^{3+} (Table 3.3), is to reconcile them with the empirically derived partition coefficient *e.g.*:

$$Kd_{2+} X + Kd_{3+} (1 - X) = 0.28$$

Rearranging for X gives:

$$X = \frac{0.28 - Kd_{3+}}{Kd_{2+} - Kd_{3+}}$$

Substituting the values in Table 3.3 gives:

$$X = \frac{0.28 - 0.079}{1.214 - 0.079} = 0.177$$

Therefore, Eu^{2+}/Eu^{3+} is equal to:

$$\frac{0.177}{1-0.177} = 0.215$$

Because this considers the Eu^{2+}/Eu^{3+} ratio for the whole rock rather than for just plagioclase, it is necessary to use the alternative equation proposed by Drake (1975):

$$\text{Whole rock } fO_2 = -4.55 \log \frac{Eu^{2+}}{Eu^{3+}} - 10.89$$

Substituting in the value of Eu^{2+}/Eu^{3+}, gives an fO_2 of -0.6 ± 0.2 log units below the QFM buffer. Thus, the Eu barometer gives the fO_2 at the Voisey's Bay intrusion as being at QFM $\pm^{0.5}_{0.8}$ log units.

This fO_2 is considerably higher than that calculated by Brenan and Li (2000) using the partitioning of Ni between olivine and sulphide. Brenan and Li (2001) found that the range of fO_2 across the Voisey's Bay intrusion was between approximately –2 to –4 log units relative to QFM. However, Fleet (2001) raised serious concerns about the validity of Brenan and Li's method, their method based upon one derived by Brenan and Caciagli (2000). Fleet (2001) proposed that the apparent fO_2 dependence of Ni partitioning observed by Brenan and Li (2001) was an artefact of the experimental method. The fO_2 values calculated using the method of Drake (1975) are similar to those expected for OIB type melts at or near QFM (Wallace and Carmichael, 1992). Those of Brenan and Li (2001) are somewhat below those one might expect from MORB style magmatism which is typically 1–2 log units below QFM (Wallace and Carmichael, 1992). For both the results published by Brenan and Li (2001) and those calculated here to be valid requires that the genesis of the silicate rocks represents a separate system from that which generated the sulphides. However, textural evidence suggests that the sulphides and silicates at Voisey's Bay have interacted extensively. Thus, Brenan and Li's (2001) results must be regarded with some scepticism.

3.2.4 Contamination of the Voisey's Bay intrusion

Previously, it has been demonstrated that the magma parental to the Voisey's Bay Troctolite had elevated K/Nb, La/Nb, and diminished Th/Ce relative to MORB, OIB, and PM. It has also been demonstrated that the enrichment of Troctolite parental magma in K, La, and decrease in Th relative to Nb and Ce could not arise by the fractionation of olivine and plagioclase. Therefore, the observed enrichment in the Voisey's Bay intrusion parental magma must be the result of contamination of mantle derived melts, possibly by crustal material.

In the data presentation section it was shown that $[Th/Ce]_N$ provided a method of geochemically discriminating between the Tasiuyak, Nain, Uivak, and Enderbite gneisses. If the magma parental to the Voisey's Bay intrusion is the result of interaction between a mantle-derived melt with the Nain, Tasiuyak, Uivak, or Enderbite gneisses, a mixing line or lines will be apparent between the mantle-derived end member and the gneiss contaminant. On Figure 3.19, a graph of $[K/Nb]_N$ versus $[Th/Ce]_N$, mixing lines with ticks at 10 percent increments have been calculated and plotted between MORB and the mean compositions of the Nain, Tasiuyak, Uivak, and Enderbite gneisses. The Uivak gneiss mixing line appears to have little relevance to the Uivak data included on this plot. However, the Uivak gneiss has extremely variable composition and many data plot off the scale of this graph; see Figure 3.15 for clarification. Also included on Figure 3.19 is the calculated parental melt composition with 2 σ error bars. The calculated parental liquid composition plots nearest the Tasiuyak mixing line. However, the error bars on the parental liquid overlap all the gneiss mixing lines. Because of this uncertainty, it is impossible to say which of the gneisses is the chief contaminant in the genesis of the Troctolite parental magma. Figure 3.20 is a graph of $[La/Nb]_N$ plotted against $[K/Nb]_N$ for the Nain, Tasiuyak, Uivak, and Enderbite gneisses. The compositions of MORB, OIB, PM, and the calculated parental liquid for the Troctolite have also been included. The

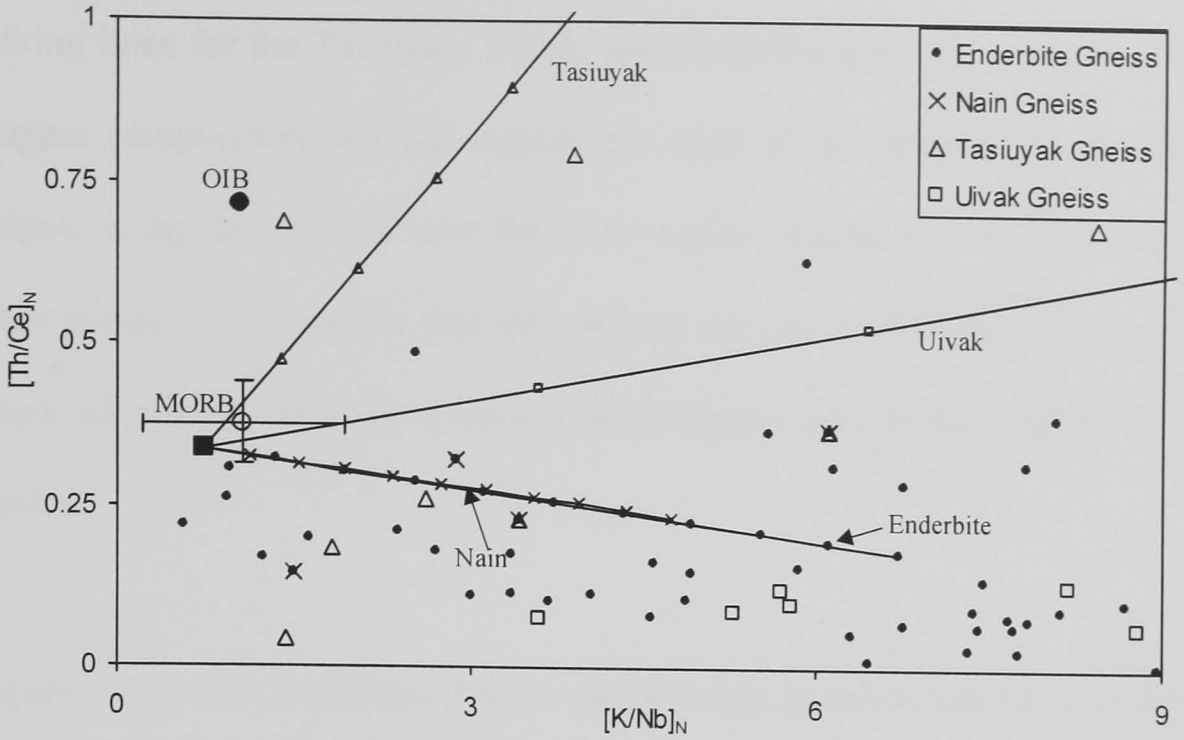

Figure 3.19 Graph of $[K/NB]_N$ versus $[Th/Ce]_N$ for the Nain, Tasiuyak, Uivak, and Enderbite gneisses. The compositions of MORB and OIB have been included as has the calculated parental melt composition. Error bars are 2 σ. The calculated parental liquid lies closest to the Tasiuyak gneiss. However, all the gneiss mixing lines plot within the parental liquid error bars. The ticks on the mixing lines are at 10 percent increments and correspond to the gneiss they represent.

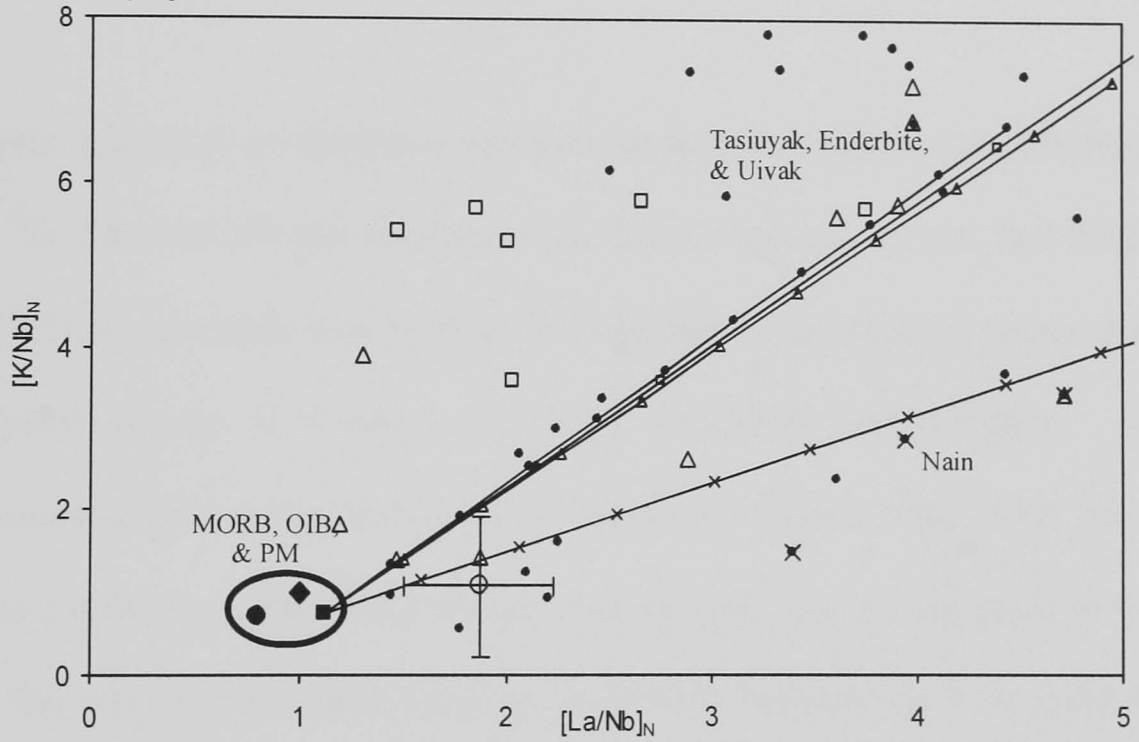

Figure 3.20 Graph of $[La/Nb]_N$ versus $[K/Nb]_N$ for the Nain, Tasiuyak, Enderbite and Uivak gneisses. The composition of MORB, OIB and the calculated parental liquid composition are included. Error bars on the parental liquid composition are 2 σ. Mixing lines have been calculated between MORB to the arithmetic mean of each of the gneisses. The ticks on the mixing lines corresponds to the ornament used for each of the gneisses. The calculated composition is closest to the Nain gneiss mixing line. The approximate amount of gneiss assimilated is 13 percent.

mixing lines for the Tasiuyak, Uivak, and Enderbite gneisses plot away from the parental magma composition and fall outside the limit of the error bars. However, the parental magma composition falls near the Nain gneiss mixing line, at approximately 13 percent Nain gneiss. This implies that the parental magma for the Voisey`s Bay Troctolite is the result of mixing between a mantle-derived melt and in the region of 13 percent Nain gneiss.

Figure 3.21a uses published data to plot a graph of εSr versus εNd (Amelin et al., 2000a; Emslie et al., 1994; Schiotte et al., 1993) for the Voisey's Bay intrusion and country rocks. Depleted mantle has been plotted for the purposes of comparison.

Figure 3.21b has mixing lines between the depleted mantle with MORB concentrations of Rb, Sr, Sm, and Nd and averages of the Nain, Tasiuyak, Uivak, and Enderbite gneisses. A MORB composition was chosen, as it appears to represent a reasonable analogue of the parental magma at Voisey's Bay prior to crustal contamination. The Voisey's Bay intrusion data do not coincide exactly with any of the mixing lines. However, the mixing lines for the Nain and Enderbite gneisses lie very close to the least contaminated samples. As the mixing lines have ticks at 10 percent increments, it is possible to estimate the approximate amount of contamination from the Nain gneiss. The mixing lines imply that between 10 and 20 percent of Nain gneiss has been assimilated by a MORB-like melt. A similar amount of assimilation of the Enderbite gneiss is also indicated, although the $[La/Nb]_N$ versus $[K/Nb]_N$ diagram (Figure 3.21) has already indicated that the Enderbite gneiss cannot be the main contaminant.

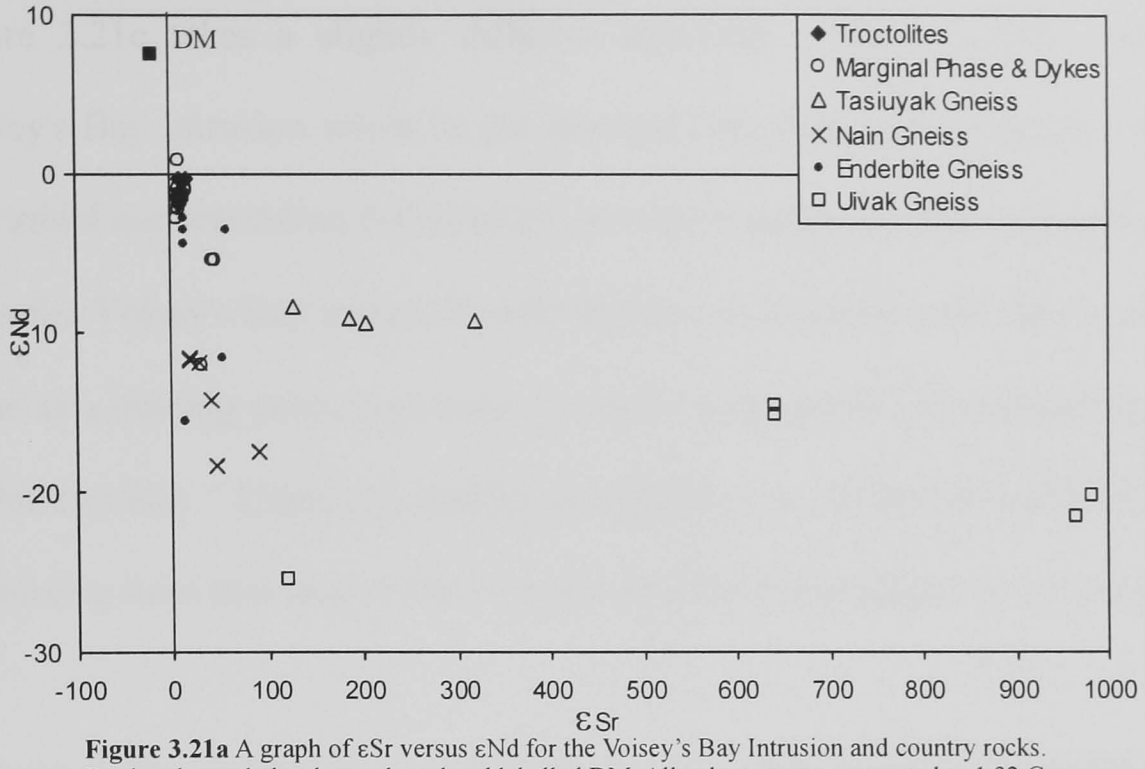

Figure 3.21a A graph of εSr versus εNd for the Voisey's Bay Intrusion and country rocks. Depleted mantle has been plotted and labelled DM. All values are age corrected to 1.32 Ga.

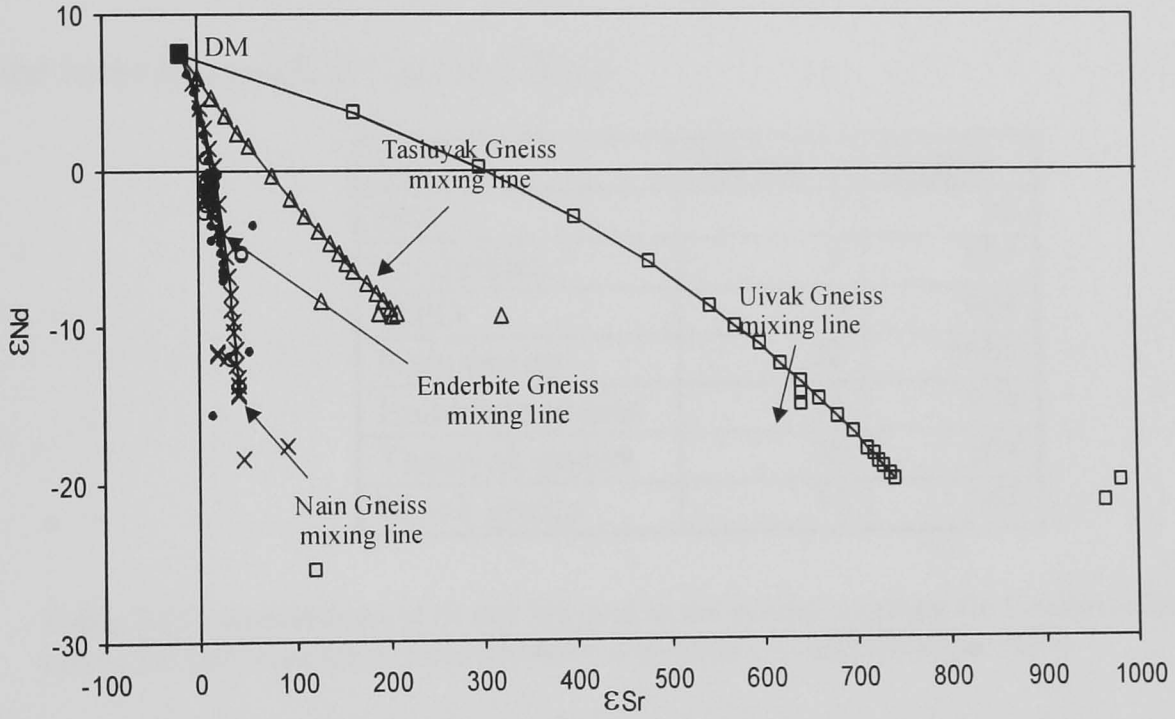

Figure 3.21b A graph of εSr versus εNd for the Voisey's Bay intrusion Rocks. Mixing lines from DM at 1.32 Ga to the average compositions of Nain, Tasiuyak, Uivak, and Enderbite Gneiss are shown. The mixing lines do not coincide with the isotopic composition of the Voisey's Bay intrusion rocks.

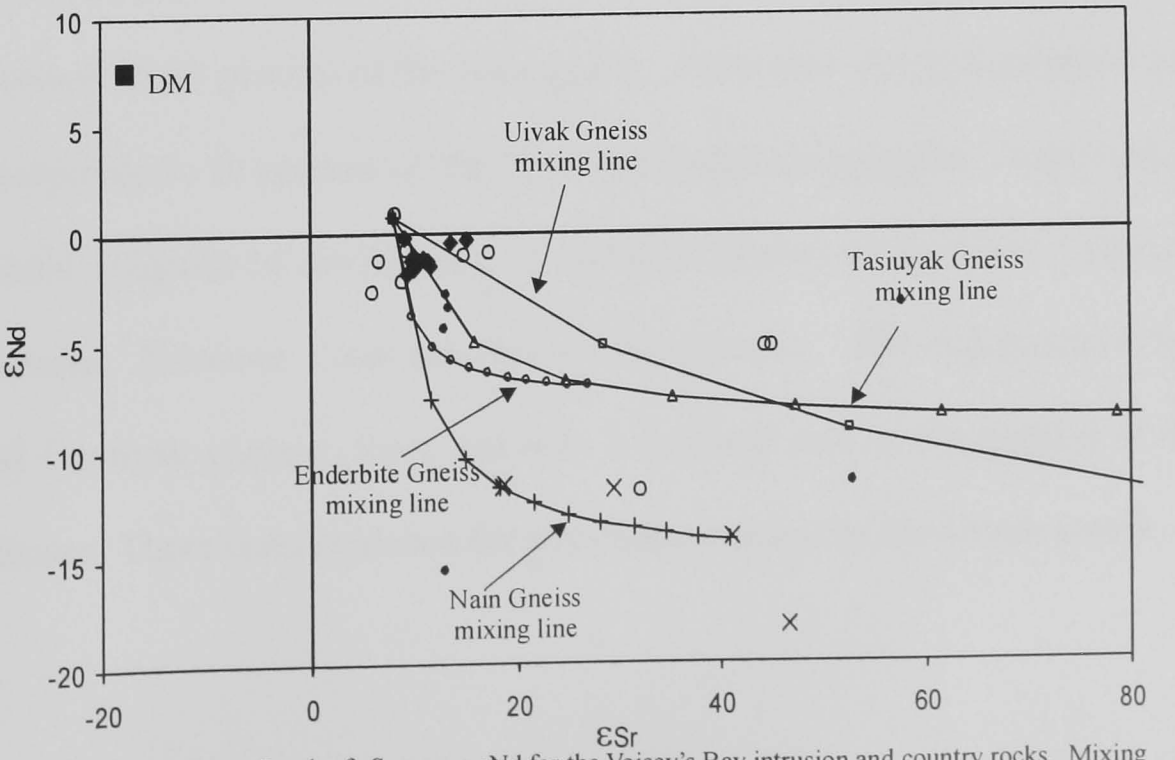

Figure 3.21c Graph of εSr versus εNd for the Voisey's Bay intrusion and country rocks. Mixing lines are plotted between the most 'uncontaminated' Voisey's Bay Intrusion sample and averages of the Nain, Tasiuyak, and Enderbite Gneisses.

Figure 3.21c takes a slightly different approach. Amelin (2000) suggested that the Voisey's Bay intrusion might be the result of two-stage contamination, with Nain gneiss-like initial contamination followed by later assimilation of Tasiuyak gneiss. Figure 3.21c takes the Voisey's Bay intrusion rock with the most positive εNd and least radiogenic εSr value as a starting point, reasoning that these represent the least contaminated rock found at Voisey's Bay. Using this starting composition, the Troctolite and MPD fall neatly onto the mixing lines that then continue to intersect their appropriate country rocks.

To lend clarity to the mixing lines Table 3.4 gives the concentrations of Sr and Nd for each of the rocks discussed in Figures 3.21a-c.

Rock	Nd ppm	Sr ppm
DM	7	90
Troctolites	8	551
MPD	3	994
Nain gneiss	32	1052
Enderbite gneiss	36	934
Tasiuyak gneiss	36	364
Uivak gneiss	11	257

Table 3.4 Concentrations of Sr and Nd used in the mixing equation for Figures 3.20a-c. The values for DM were taken from MORB values (Sun and McDonough, 1989).

This model suggests that the Troctolite and MPD are the result of a multi-stage contamination process. This process began with a mantle-derived melt assimilating between 10-20 percent of the Nain gneiss. After this, the contaminated magma went on to incorporate 3–10 percent of the Nain and Enderbite gneisses. Some samples of the MPD exhibit evidence of assimilation of up to 30 percent of the Nain, Tasiuyak and Enderbite gneisses. However, these samples are exceptional. The conclusion is that the Enderbite and Tasiuyak gneisses have had only a minimal role in the genesis of the Voisey's Bay silicates. There is no evidence for any contamination by the Uivak gneiss.

3.2.5 Melting regime

Section 3.1.2 presented the REE data for the Voisey's Bay intrusion rocks. The conclusions of that section were that all the intrusive rocks are enriched in the LREE relative to the HREE. The graphs of La/Yb and Dy/Yb (Figures 3.6 and 3.7) revealed that the Troctolite, the MPD, and UMI all had slightly different La/Yb and Dy/Yb ratios. The choice of these ratios is significant, as the REE from Dy to Yb are compatible in garnet (Irving and Frey, 1978). Melts derived from material with residual garnet would be depleted in Yb relative to Dy and La. Therefore, if garnet is present in the source of the melts parental to the Voisey's Bay intrusion this must be reflected in the La/Yb and Dy/Yb ratios. As garnet replaces spinel in the mantle in response to increases in pressure, the inferred presence or absence of garnet in the source would provide a useful indicator of depth of melting.

To examine this further, Figure 3.22a is a graph of normalised La/Yb versus Dy/Yb, similar to Figure 3.6. However, Figure 3.22a has curves superimposed upon it that compare the compositions of fractional non-modal melts derived from garnet bearing and spinel-bearing lherzolite. The starting composition was primitive mantle (McDonough and Sun, 1995) and the melting and mineral modes were as defined by Hauri and Hart (1994). The spinel lherzolite mineralogy was based upon the garnet lherzolite using the garnet break down reactions proposed by Hauri and Hart (1994). The mineral modes and melting modes are given in Table 3.5 below.

Mineral	Garnet lherzolite	Melt mode	Spinel lherzolite	Melt mode
Olivine	0.553	0.19	0.552	-0.30
Orthopyroxene	0.193	-0.50	0.247	0.40
Clinopyroxene	0.095	0.68	0.178	0.82
Garnet	0.159	0.63	0	0
Spinel	0	0	0.023	0.08

Table 3.5 Mineral modes and melting modes for garnet and spinel lherzolites (Hauri and Hart, 1994).

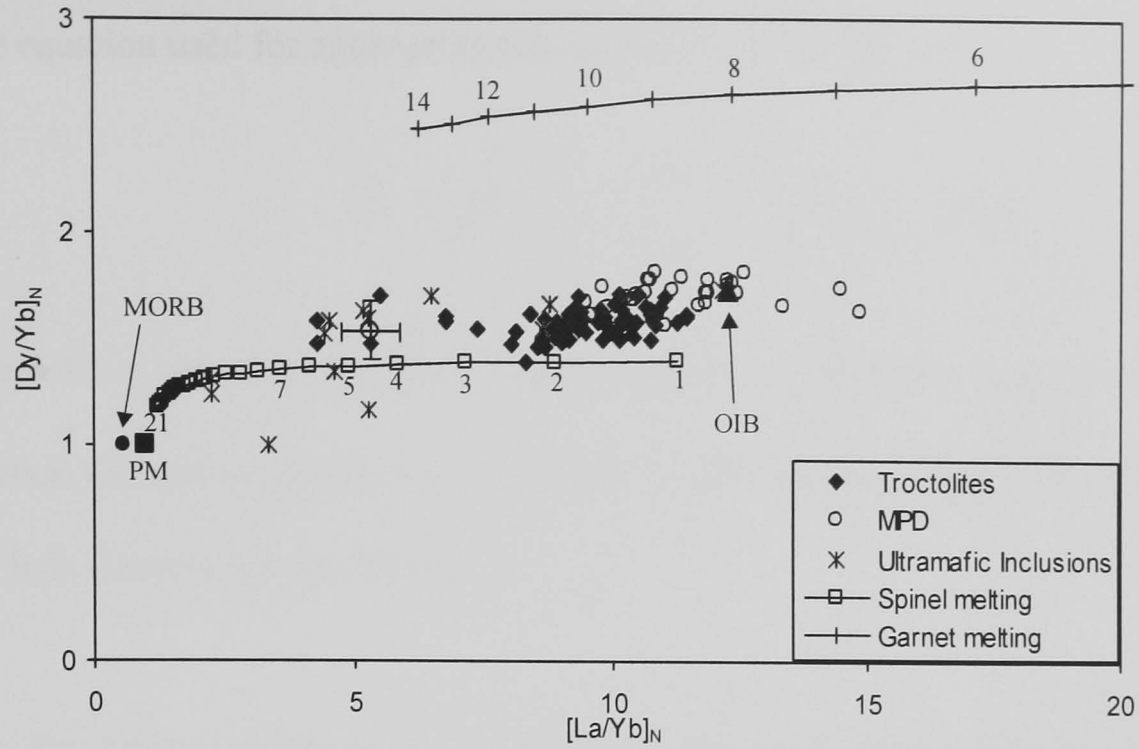

Figure 3.22a A graph of $[La/Yb]_N$ versus $[Dy/Yb]_N$ with curves plotted for non-modal melting of garnet and spinel lherzolite (Hauri and Hart, 1994). The Troctolites and the MPD fall between the spinel and garnet curves. The calculated parental melt composition is shown, with 2σ error bars. The inference is that melting from both spinel and garnet facies have contributed to the Troctolites and MPD magmas. The numbers beside the garnet and spinel melting traces refer to the degree of melting. In each case, the curve extends until clinopyroxene is exhausted in the source. The compositions of MORB and OIB (after Sun and McDonough, 1989) are included for comparison.

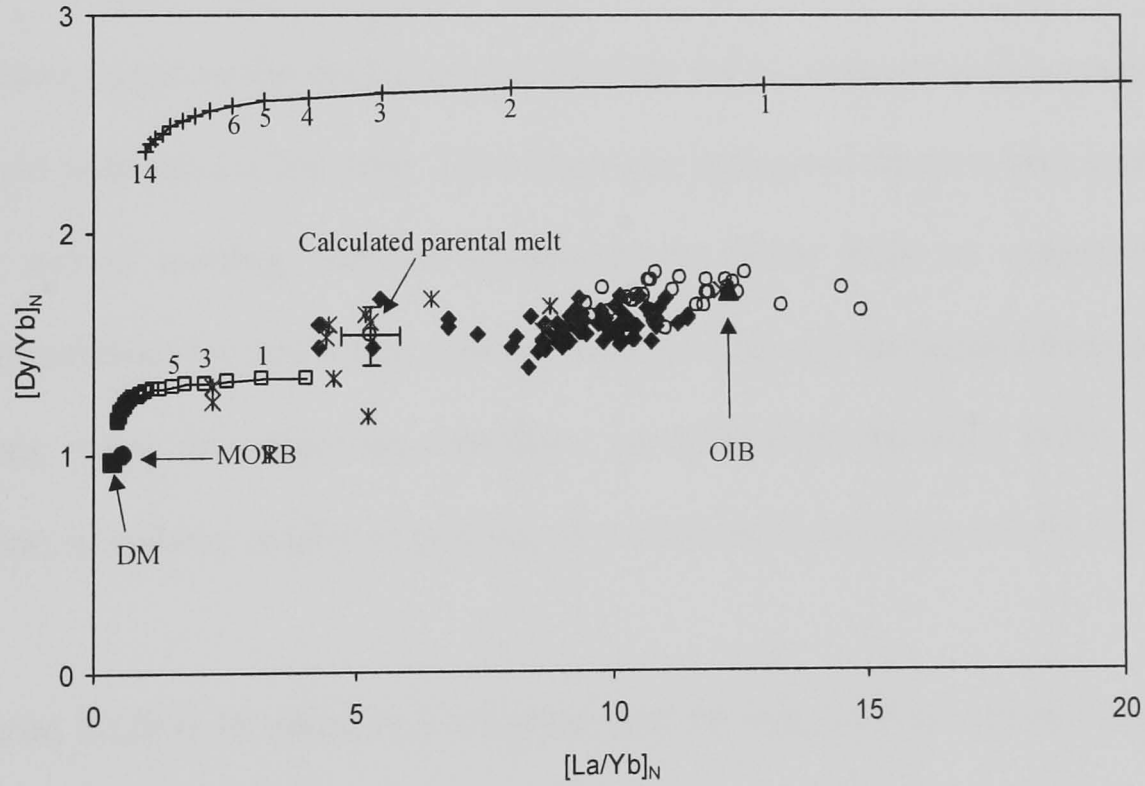

Figure 3.22b Graph of $[La/Yb]_N$ versus $[Dy/Yb]_N$ with modelled non-modal fractional melting in the garnet and spinel facies (after Hauri and Hart, 1994). The starting composition was taken to be depleted mantle (DM) (calculated after Hirschmann and Stolper, 1996). Figures on the modelled curves refer to fraction of melting. In comparison with the PM source, the apparent fraction of melting is much smaller. Total amount of melting is 14 percent for garnet facies and 21 percent for spinel facies.

The equation used for aggregated non-modal fractional melting is:

$$\overline{C}_l = \frac{C_o}{F}\left[1-\left(1-\frac{PF}{D_O}\right)^{\left(\frac{1}{P}\right)}\right] \quad \text{(Shaw, 1970)}$$

where C_o is the concentration in the source; $\overline{C}_l$ is the concentration in the liquid; F the fraction of melting; P the bulk distribution of the minerals that make up the melt; and D_o the bulk distribution coefficient.

The Troctolite and MPD data fall between the spinel melting and garnet-melting curves. The implication of this is that the source of the magma parental to the Troctolite and MPD began at garnet facies depths and continued into spinel facies with contributions from both. The MPD data have higher Dy/Yb than the Troctolite. A probable explanation is that melting began in the deeper, garnet stability facies, thus allowing a greater contribution of liquid with this Dy/Yb ratio. The Ultramafic Inclusions data are very scattered, falling into the garnet melting and the spinel-melting fields with no coherence. One possible interpretation for this is that some of these samples are the residue from a previous melting event, while the others are cumulates, possibly from the same event. The approximate extent of melting require to produce the calculated Troctolite parental melt is 7–8 percent.

Figure 3.22b is identical to 3.22a other than the nature of the source material. In this case, depleted mantle has been used. This composition was calculated from a starting point of PM after Sun and McDonough (1989). From this, 2 percent liquid was removed via non-modal batch melting. The mineral modes were 0.525 olivine, 0.23 orthopyroxene, 0.175 clinopyroxene, and 0.07 garnet. The proportions entering the melt were –0.1 olivine, 0.3 orthopyroxene, 0.4 clinopyroxene and 0.4 garnet (Hirschmann and Stolper, 1996). In comparison with Figure 3.22a, the extent of melting required to produce the Voisey's Bay intrusion magma is much reduced. Rather than the 7–8 percent of melting observed for

PM source, nearer 1–2 percent is indicated. In both diagrams, the calculated parental melt lies between OIB and MORB compositions.

3.2.6 Conclusions

Plotting trace element ratios against Eu/Eu* has provided a method of estimating the composition of the magma parental to the Voisey's Bay Troctolite. Having estimated a parental liquid composition, the hypothetical liquid was compared with MORB, OIB, and PM. In general, the liquid was found to have some of the characteristics of both MORB and OIB. This consideration of trace elements, particularly La_N versus Eu/Eu*, revealed that the Troctolite and the MPD had different parental magmas. Bedard (2001) also calculated a parental liquid composition for the Voisey's Bay intrusion and his proposed liquid was compared with that calculated here. The proposed liquids are very similar with the exception of Ba/Th. However, Bedard (2001) considered the Troctolite and the MPD together and included material from the nearby Mushaua intrusion. The Troctolite and the MPD had different parental magmas, and the parental liquid calculated is specific to the Troctolite and the Mushaua intrusion rocks represent a separate episode of magmatism. It is possible that some of the differences between Bedard's (2001) composition and that calculated here arise from these facts.

Using the Sr/Nd ratio and Eu/Eu* it is possible to calculate the fO_2 prevalent during the accumulation of the Troctolite. The two methods of calculating the fO_2 were found to agree within one log unit. The fO_2 based on plagioclase was found 0.4±0.1 log units above QFM. That based on whole rock was 0.6±0.2 log units below QFM, both approximately what is expected from OIB type melts and between 1–2 log units above that expected for MORB. This is in marked contrast to the results of Brenan and Li (2000) who used the partitioning of Ni between olivine and sulphide to calculate an fO_2 for the Voisey's Bay intrusion. They found that the fO_2 was between 2 and 4 log units below QFM. Because

textural evidence suggests that the sulphides and silicates interacted extensively, removing the possibility that the sulphides and silicates represent different systems, the present conclusions are preferred over those of Brenan and Li (2000).

The magmas parental to the Voisey's Bay intrusion have been contaminated by crustal material. The evidence for this is in the form of textures (Li et al., 2000; Naldrett et al., 1996), isotopic evidence (Amelin et al., 2000; Emslie et al., 1994) and trace elements (this study and Li et al., 2000). The calculated parental melt composition and trace element evidence demonstrated that the magmas parental to the Troctolite and the MPD had undergone contamination possibly with Nain gneiss before any contamination by the Tasiuyak and Enderbite gneisses. No evidence for contamination by the Uivak could be proved. Mass-balance calculations make it possible to estimate the extent of contamination by the Nain gneiss. This was found to be approximately 13 percent according to trace element evidence. Consideration of the Sr and Nd isotope evidence suggested that contamination of the Troctolite parental melt was a multi-stage process. The first stage was contamination of a mantle-derived melt by the Nain gneiss. Mass-balance calculations suggest that the amount of contamination was approximately 10-20 percent according to Sr and Nd isotopes. The Troctolite parental magma then underwent a further stage of contamination. This was relatively minor, being between 3–10 percent and incorporates Tasiuyak, Nain, and Enderbite gneisses.

The initial source of the magmas parental to the Voisey's Bay intrusion was the upper asthenosphere. Modelling mantle melting using REE data for garnet and spinel lherzolite appears to indicate that melting began in the garnet stability field and continued into the spinel stability field with contributions from both. The calculated parental melt for the Troctolite is the product of 7-8 percent melting or 1-2 percent melting depending whether PM or DM is used as the source. The Troctolite and the MPD have different La/Yb and

Dy/Yb ratios, which suggest that they represent different episodes of melting. The MPD appear to be products of deeper and therefore hotter melting than the Troctolite. In chapter 2, reference was made to the work of McKenzie and Bickle (1988) and the relationship of pressure, temperature and extent of melting. Figure 3.23 is a P-T diagram identical to Figure 2.6.

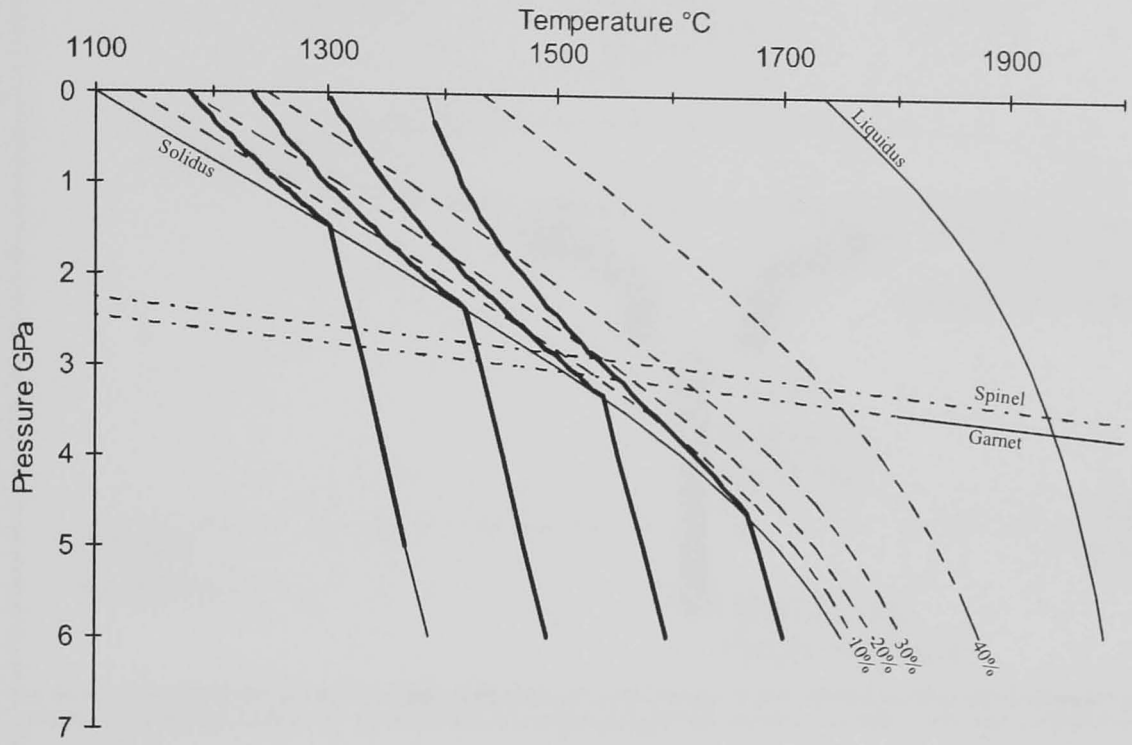

Figure 3.23 P-T diagram after McKenzie and Bickle (1988), showing 4 adiabats with T_p of 1280-1580°C. The dotted curves represent 10, 20, 30, and 40percent partial melts. The two dotted lines cutting obliquely across the diagram represent the transition between garnet and spinel facies. Taking the Voisey's Bay intrusion parental magma to be the product of 7-8 percent melting starting just within the garnet stability field, the estimated mantle temperature is 1530°C and pressure is ~3.25 GPa.

The parental magma of the Voisey's Bay troctolites is the product of 1-2 or 7-8 percent partial melting. Trace element evidence suggests that melting started just deeper than the spinel-garnet transition. Therefore, using this information and reading directly from Figure 3.22, the approximate pressure and mantle temperature during the initial melting was ~3 GPa and 1500°C. Given that the fO_2 of the Voisey's Bay intrusion was ~QFM, and that the source region for the melt was below the garnet/spinel transition, it is likely that the Voisey's Bay intrusion represents plume-like rather than MORB-like magmatism. Because of this, the source rock is unlikely to be MORB type material, i.e. probably more like PM than DM. Thus, the Voisey's Bay intrusion is the product of 7-8 percent mantle melting.

CONTAMINATION MODEL

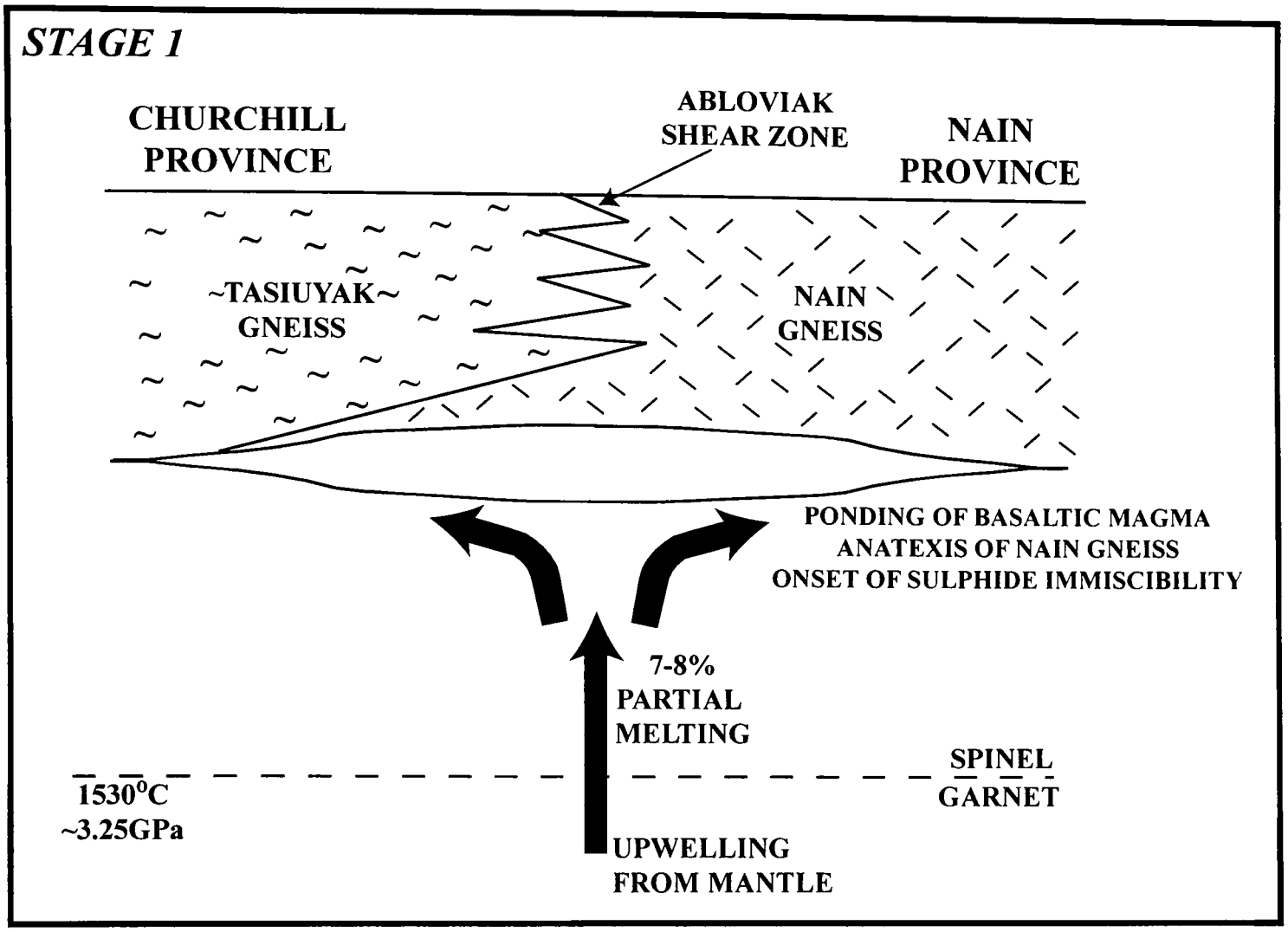

Figure 3.24 Cartoon of the mantle melting and contamination for the Voisey's Bay parental melts. Stage 1 Mantle melting begins in the garnet stability field at ~1530°C and 3.25GPa. Melting continues into spinel facies, with contributions from both. The melt ascends to the crust/mantle boundary, where it ponds and assimilates ~15 percent Nain gneiss. Stage 2 The melt is then emplaced via the Abloviak Shear Zone into a magma chamber within the crust, where it assimilates small quantities of Tasiuyak Gneiss.

To illustrate this melting and contamination model a cartoon has been drawn. Figure 3.24. Stage 1 shows upwelling mantle from below the spinel/garnet transition, at a pressure of ~3 GPa and temperature of 1500°C. The upwelling mantle passes through the spinel/garnet transition and melting continues. The melt fraction ponds at the base of the crust and begins to assimilate Nain gneiss via anatexis. Stage 2 illustrates the magma ascending to mid crustal magma chamber, where cold, dense, possibly sulphide-bearing fragments of Tasiuyak gneiss become detached from the roof and walls and sink to the bottom of the contaminated mafic magma.

3.2.7 Summary

- The Voisey's Bay intrusion magmas are the product of mantle-melting, with contributions from garnet and spinel facies.
- The fO_2 of the Voisey's Bay intrusion was QFM $\pm^{0.5}_{0.8}$ log units.
- The Voisey's Bay intrusion magmas are the result of 7-8 percent melting of PM type mantle.
- The P-T conditions during initial melting of the Troctolite parental magma were ~3 GPa and 1500°C.
- The Voisey's Bay intrusion is the product of a plume-like melt.
- The Troctolite and MPD are the product of different magmas, the MPD a response to deeper and hotter melting than the Troctolite.
- Based on trace element and Sr and Nd isotopic evidence, the Voisey's Bay parental magmas were contaminated with 10-20 percent of Nain gneiss-like crust.

Chapter 4

Forsterite and Nickel Variations in Olivine from Diamond Drill Hole VB 96 266

4.1.1 Introduction

One of the most important differences between the Voisey's Bay deposit and other world-class economic magmatic Ni-sulphide deposits is the forsterite content of the Voisey's Bay intrusion olivine (see Section 1.3, Table 1.1). The forsterite contents olivines in the Voisey's Bay troctolites are typically between Fo_{85-95}, whereas at Kambalda, Noril'sk-Talnakh, and Jinchuan forsterite contents of Fo_{80-95} are more typical. The Ni content of olivine has long been accepted as being a function of olivine's forsterite contents (e.g. Hart and Davis, 1979; Beattie et al., 1991). Therefore, when considering a magmatic Ni-sulphide deposit with markedly lower forsterite contents than those seen in similar deposits, the relationship between the sulphides and the host rocks must be investigated. Detailed olivine mineralogy also allows conclusions to be drawn as to the relative timing of emplacement of the various Voisey's Bay intrusion rocks. In addition, this study will enable the timing of the sulphide immiscibility in relation to the crystallisation of the different troctolitic and gabbroic rocks to be assessed.

The data in this section are derived from one drill core, VB 96 266. This core was drilled in the Eastern Deeps (see Figure 4.1 for location) and the sampled rock types include normal textured troctolite, variable troctolite, and breccia sequence material. Figure 4.2 is a schematic representation of the geometry of the Eastern Deeps prior to any erosion. Illustrated on this figure is a representation of the rock types included in the core VB 96 266.

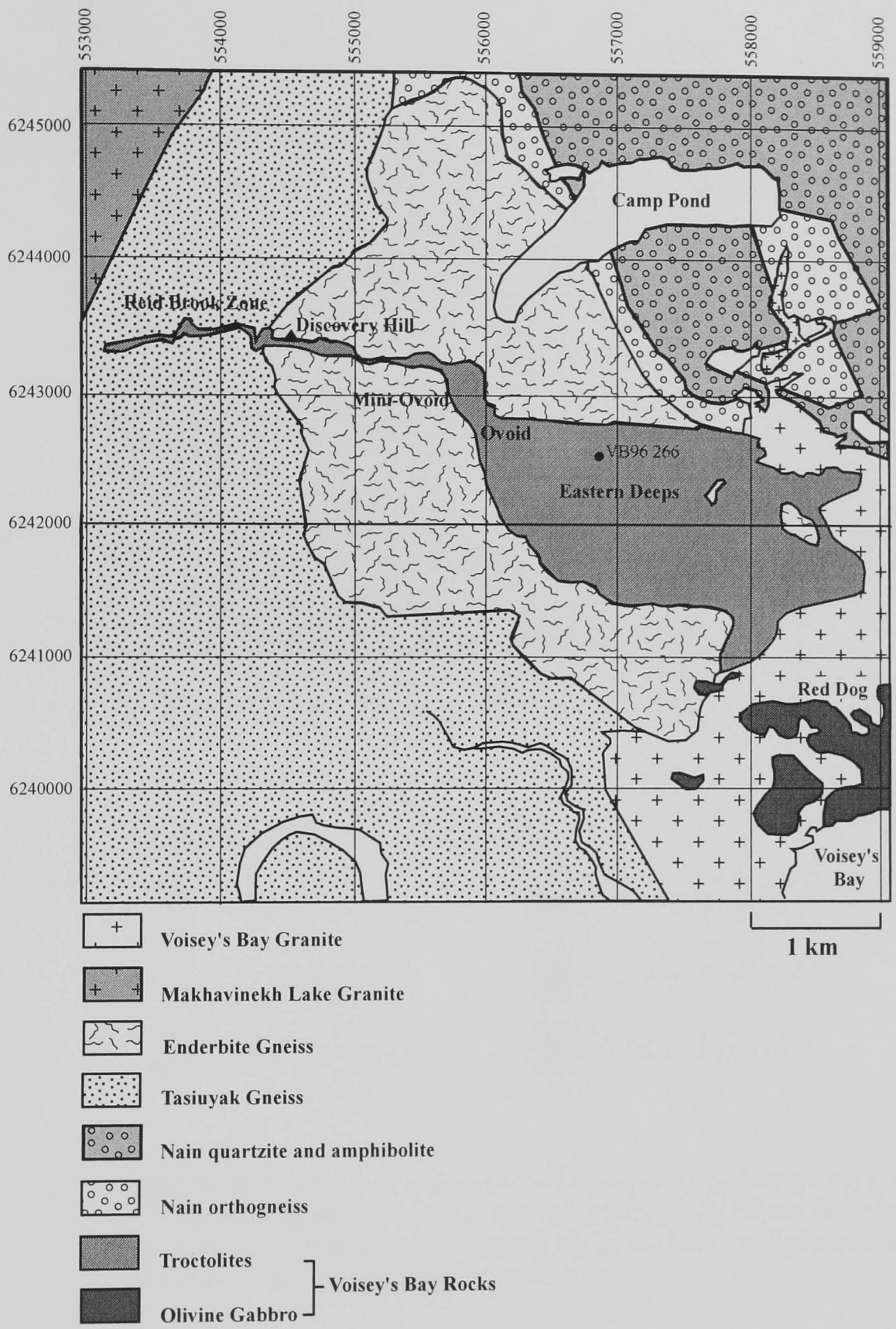

Figure 4.1 Map of the Voisey's Bay deposit with the names of the different areas. Redrawn from Voisey's Bay Nickel Company data.

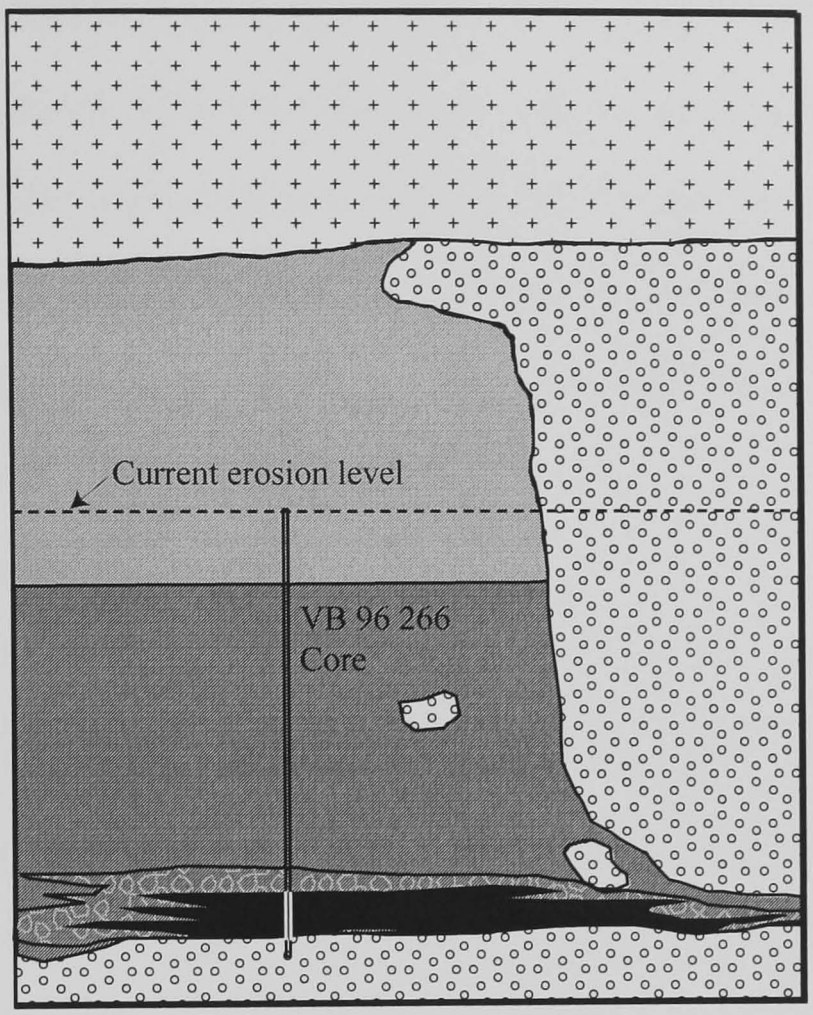

Figure 4.2 Schematic cross section of the Eastern Deeps area of the Voisey's Bay intrusion showing the different rock types sampled by hole VB 96 266. Erosion has removed material to the level indicated by the dotted line. The horizontal and vertical scales are identical though approximate.

4.1.2 Sources of data

All the olivine and sulphide data in this section were acquired at the Open University using the Cameca SX100 electron microprobe. The whole rock major and trace element data are the property of INCO and form part of their exploration operation in the Nain Plutonic Suite. The whole rock data are available through Dr Peter C. Lightfoot at INCO Technical Services Limited and were collected at the XRAL laboratories by XRF and ICP-MS. The data are unpublished and are presented in full in Appendix A.

4.1.3 Data presentation

Figure 4.3 is a plot of forsterite content versus depth. The data are presented based on host lithology. The different categories are normal troctolite, variable troctolite, and inclusion troctolite and breccia sequence. The normal troctolite have forsterite between Fo_{73-77}. The variable troctolite exhibits greater variation in its forsterite value, with the majority of values falling between Fo_{69-75}, though a few more extreme values are observed, ranging from Fo_{61-85}. In general, the forsterite values observed in the variable troctolite are a little lower than those in the normal troctolite. The breccia sequence forsterite contents are lower still, falling between Fo_{66-72}.

The graph of Ni in olivine (ppm) versus depth (m) (Figure 4.4), illustrates that the Ni contents of the olivine in drill core VB 96 266 are extremely variable. The Ni contents vary between a minimum of 55 ppm to 2216ppm. Most of the data fall between 900 and 1700 ppm. There is no systematic relationship between depth and Ni content in olivine.

Figure 4.5, a graph of forsterite value versus Ni ppm demonstrates that there is little correlation between olivine Ni content and forsterite value. This figure also serves to

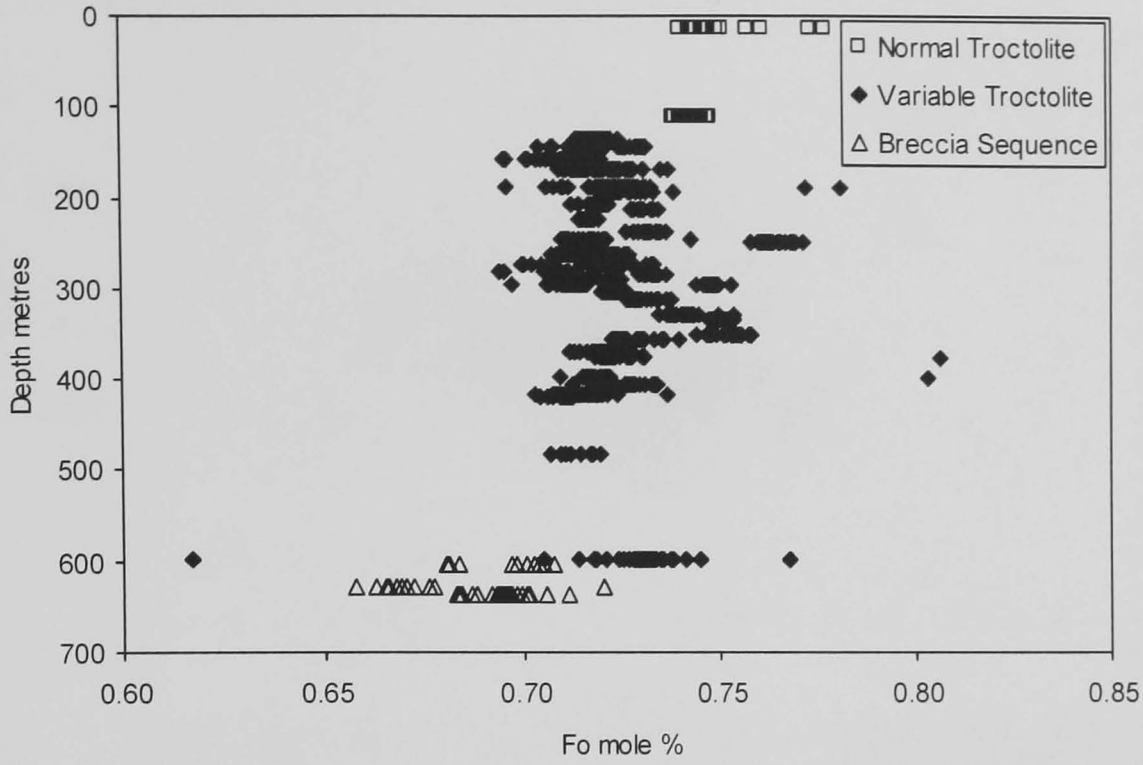

Figure 4.3 Graph of forsterite content versus depth in metres. The normal troctolite have the highest forsterite values. Variable troctolite forsterite is intermediate between normal troctolite and the breccia sequence.

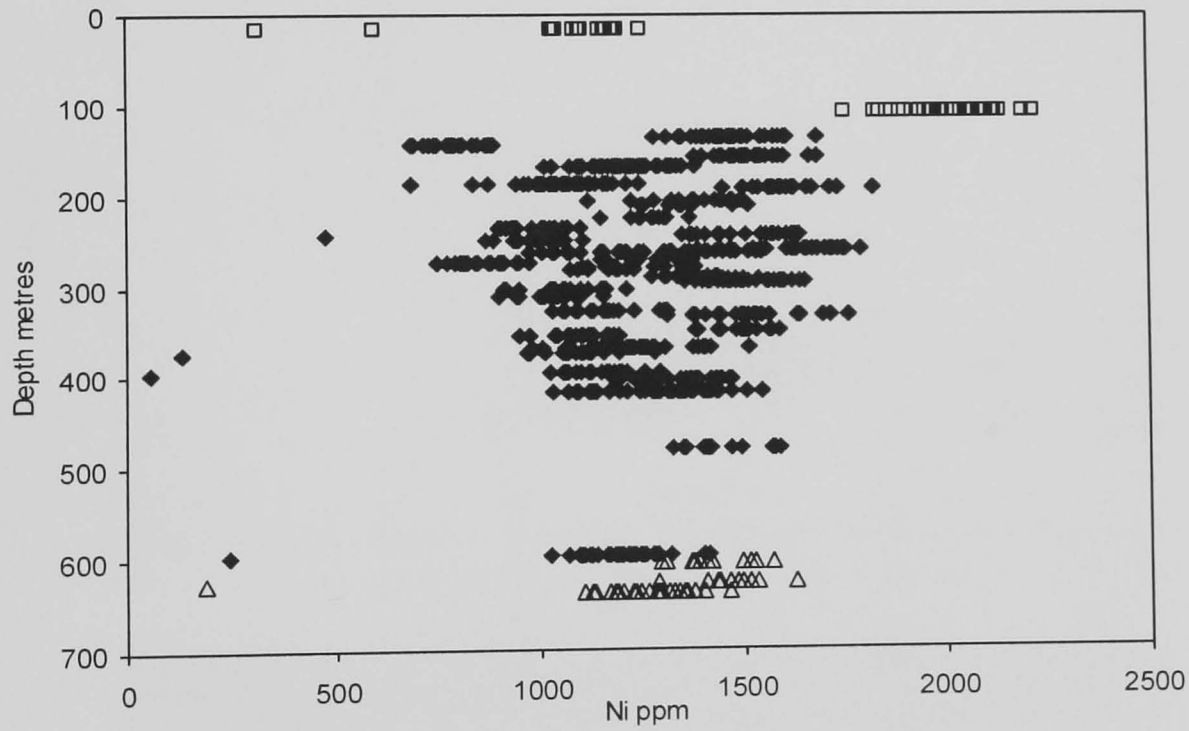

Figure 4.4 Graph of Ni in olivine versus depth in metres. The normal troctolite, variable troctolite, and breccia sequence olivine have broadly similar Ni content between 900 and 1700ppm. However, grains with marked variation are observed.

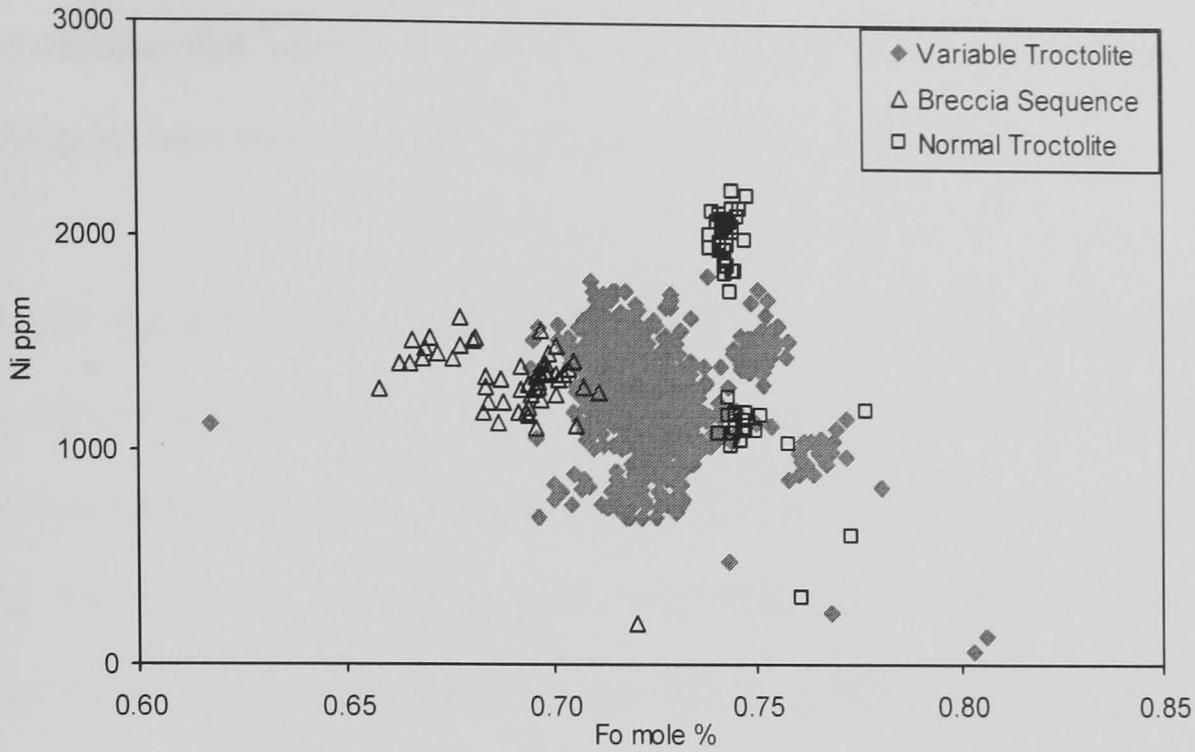

Figure 4.5 Graph of forsterite versus Ni in olivine. The normal troctolite, variable troctolite, and breccia sequence data plot into different groups, although there is significant overlap between these groups.

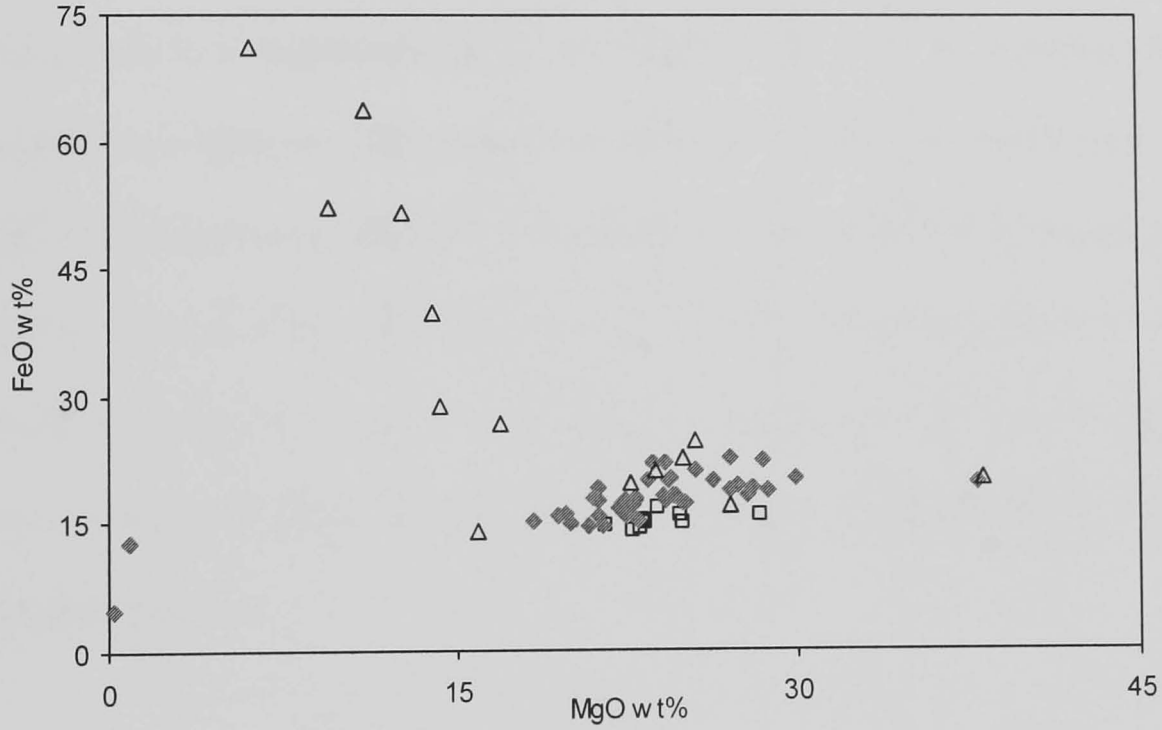

Figure 4.6 Graph of whole rock MgO versus FeO recalculated to exclude cumulate plagioclase. The normal and variable troctolite plot in a linear group between 15-40 weight percent MgO and 8-15 weight percent FeO.. The breccia sequence data are much more variable, with few plotting into the same group as the troctolites.

emphasise that olivine from the variable troctolite, normal troctolite, and breccia sequence have similar Ni contents but differing forsterite values.

Figure 4.6 is a graph of whole rock MgO versus FeO, where the analyses have been recalculated to exclude the contribution from cumulus plagioclase, sulphide and LOI. The cumulus plagioclase component is calculated by assuming its composition is equal to An_{60}, and that 90 percent of the Na is present in the form of plagioclase. The equivalent amounts of CaO, SiO_2, and Al_2O_3 are then removed from the whole rock total. Fe is corrected by assuming that all sulphide is in the form of stoichiometric pyrrhotite ($Fe_{(1-X)}S$). The remainder is then recalculated to 100 percent. Therefore, Figure 4.6 is a representation of the MgO versus FeO in cumulus olivine and the trapped melt fraction. The normal troctolite and variable troctolite form a linear group with MgO increasing with FeO. The MgO is between 20 and 40 weight percent and the FeO is between 8 and 28 weight percent. Within this group, the normal troctolite has slightly less FeO for a given MgO than the variable troctolite. The breccia sequence material is much more variable, this is a reflection of the differing mineralogy in the included material.

4.1.4 Conclusions

- Forsterite values vary with lithology and hence depth.
- Highest forsterite values are observed in the normal troctolite, lowest in the breccia sequence and intermediate values in the variable troctolite.
- Ni concentrations in olivine are broadly similar the normal troctolite, variable troctolite and breccia sequence.
- Ni concentrations are independent of forsterite values.

4.2 Discussion

4.2.1 Composition of primary olivine and parental liquids

Postcumulus equilibration between cumulate minerals and trapped remnant liquid fraction results in minerals with more fractionated compositions than the original primary phases. This phenomenon is referred to as the trapped liquid shift. Barnes (1986) demonstrated that if cumulus olivine were to equilibrate with a residual trapped liquid, the result would be a reduction in the cumulus forsterite content. Similarly, equilibration with a trapped liquid will also reduce the cumulus olivine's Ni content. Therefore, any attempt to model the composition of olivine within cumulus rocks must acknowledge the effects of a trapped melt fraction. Cawthorn et al., (1992) and Chai and Naldrett (1992) used the FeO and MgO contents of olivine cumulates to calculate the initial compositions of the Mount Ayliff intrusion, South Africa, and the Jinchuan intrusion, China respectively. Their method was based upon the fact that in a rock in which olivine is the only cumulus phase, bulk rock FeO and MgO contents will be related to the proportion of primary olivine and trapped liquid. When data derived from electron microprobe analyses of cumulate olivine grains are plotted onto an MgO/FeO diagram with the bulk rock data, both sets of data plot onto straight lines, albeit with different trends. If regression lines are plotted for the whole rock and olivine data, where these two lines intersect will correspond with the primary olivine composition. The composition of the parental liquid that was in equilibrium with the primary olivine can be calculated using the relationship proposed by Roeder and Emslie (1970). If this compositions is then plotted onto the MgO/FeO plot with the whole rock and olivine data, and the whole rock regression line is extrapolated towards the parental liquid composition line, it will intercept the point equivalent to the liquid MgO/FeO ratio from which the primary olivine crystallised. Figure 4.7 presents MgO versus FeO corrected data for whole rock analyses from the variable troctolite. These analyses are taken over a ~200m interval in which there was no observed change in mineralogy or texture.

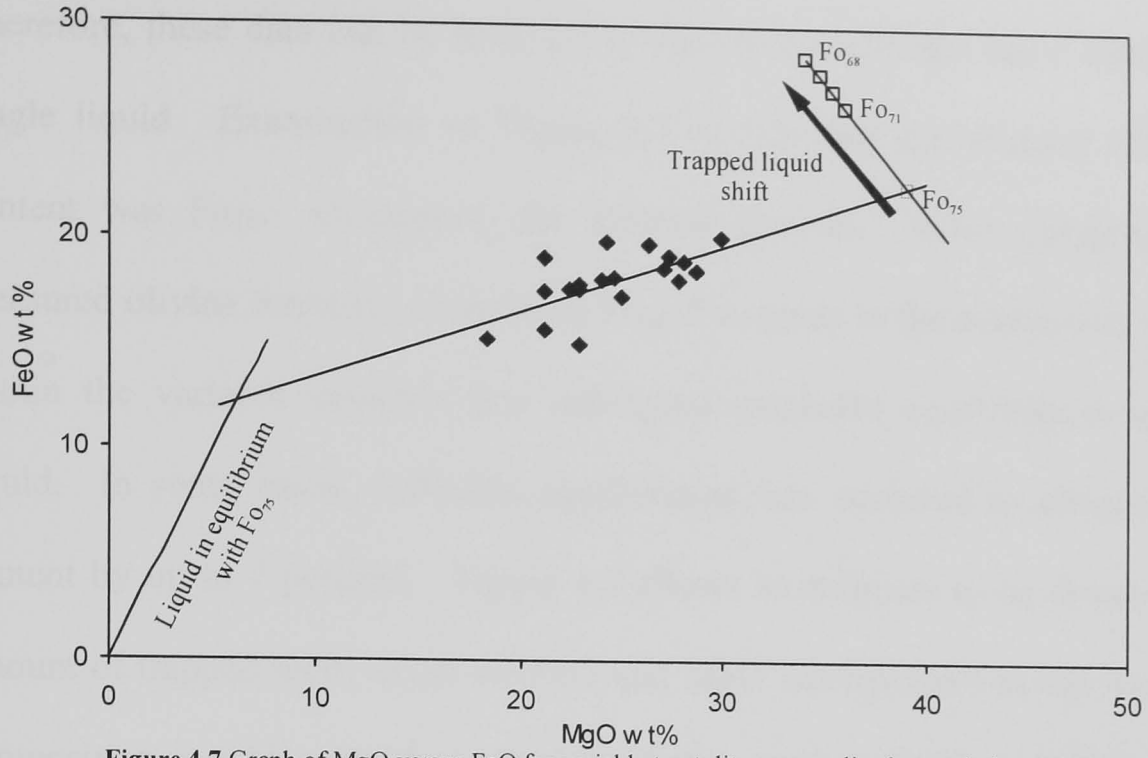

Figure 4.7 Graph of MgO versus FeO for variable troctolite renormalised to exclude sulphide and cumulus plagioclase. Where the whole rock regression line intersects the measured forsterite trend is inferred to be the primary olivine forsterite value. Where the whole rock regression line intersects the parental liquid equilibrium trend can be used to give the parental melt Fe:Mg ratio.

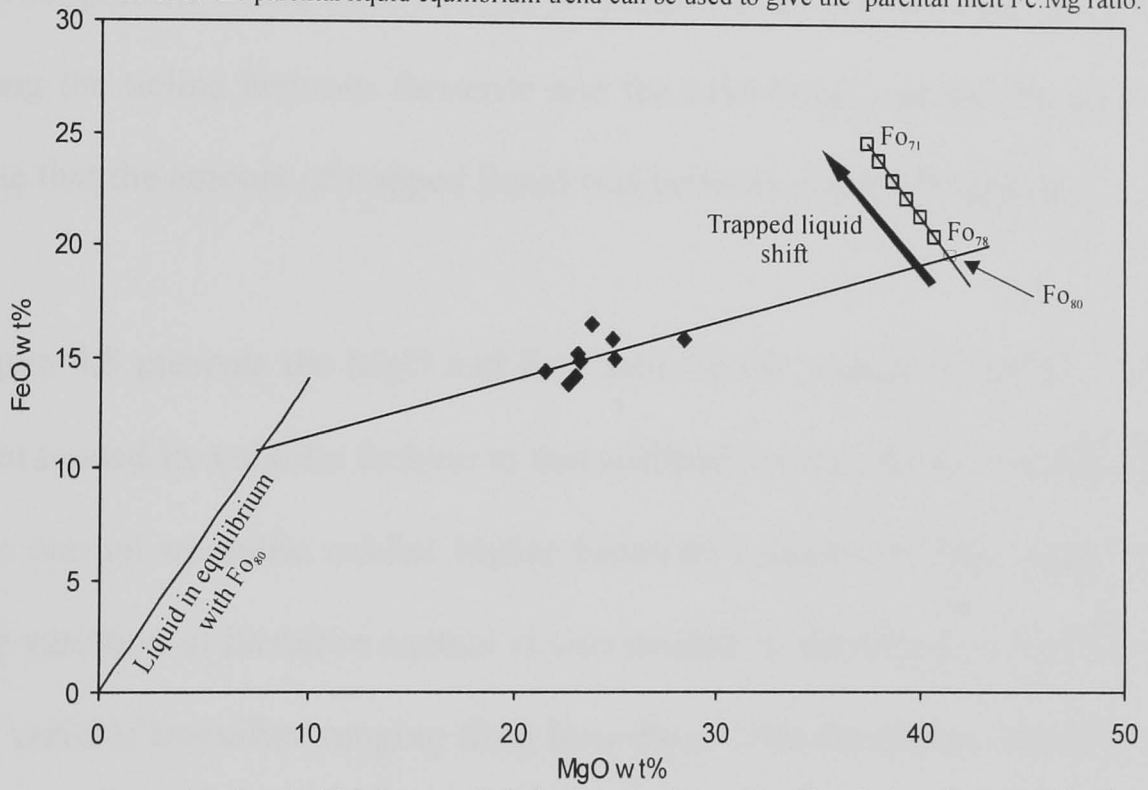

Figure 4.8 Graph of MgO versus FeO for the normal troctolite. The whole rock composition has been renormalised to exclude sulphide and cumulate plagioclase. The whole rock regression line's intersection with the forsterite trend is inferred to give the primary olivine forsterite value. The intersection between the whole rock trend and the trend for the liquid in equilibrium with the primary olivine gives the parental melt Fe:Mg ratio. The disparity between the primary olivine composition and the measured values is interpreted as the result of equilibration with a trapped melt fraction. (after Cawthorn et al., 1991; Chai and Naldrett, 1991; Li et al., 2000)

Therefore, these data can be assumed to represent rocks that have crystallised from a single liquid. Examination of Figure 4.7 reveals that the primary olivine forsterite content was Fo_{75}. Comparing the inferred primary olivine composition with the measured olivine forsterite contents of Fo_{68}–Fo_{73} leads to the conclusion that the olivine within the variable troctolite has undergone extensive equilibration with a trapped liquid. In some cases, sufficient equilibration has occurred to change the forsterite content by up to 7 percent. Figure 4.7 allows an estimate to be drawn regarding the amount of trapped melt. If all the FeO and MgO were present as olivine, the observed composition would coincide with that of the primary olivine. Additionally, all the olivine present would have a single forsterite value. As the observed data plot midway along the tieline between forsterite and the calculated parental liquid, it is possible to state that the amount of trapped liquid was between 30 and 50 percent.

Figure 4.8 presents the MgO and FeO data for the normal troctolite. These data have been treated in a similar fashion to that outlined for the variable troctolite in Figure 4.7. The normal troctolite exhibit higher forsterite contents in the primary olivine (Fo_{80}). The variation in forsterite content is also smaller in the normal troctolite compared with the variable troctolite, ranging from Fo_{71}–Fo_{78}. The maximum observed trapped liquid shift in the normal troctolite is 9 mole percent – 2 percent greater than that observed in the variable troctolite. Figures 4.7 and 4.8 also allow the Fe/Mg ratio and Mg# of the liquid in equilibrium with the primary olivine to be calculated. This can be calculated via the weight percent of the MgO and FeO read off the diagrams, or directly through the forsterite of the inferred primary olivine using the relationship proposed by Roeder and Emslie (1970).

These calculations are presented in Appendix C. The Mg# of the normal troctolite calculated in this fashion is 55. Carrying out the same calculation for the variable

troctolite reveals that its Mg# is 47. Because the Mg# of a melt falls as olivine fractionation progresses, the implication of the difference in primary olivine forsterite and corresponding parental melt Mg# is that the normal troctolite represents crystallisation from a less-evolved melt than does the variable troctolite. However, neither the trace element data presented in Chapter 2, nor the data presented here suggest that they are the products of separate parent magmas.

4.2.2 Ni contents of olivine

Figures 4.4 and 4.5 revealed that the olivine in the majority of troctolites have Ni contents between 900 and 1700 ppm, with some data plotting either side of these values. This is contrary to expectation; theory and empirical evidence suggest that as the forsterite content of olivine decreases so should its Ni (Beattie et al., 1991; Hart and Davies, 1978). Although the olivine in the normal troctolite, variable troctolite and breccia sequence have forsterite values that range from Fo_{62}–Fo_{78}, no systematic variation in Ni contents is observed. Figure 4.9 is a graph of forsterite versus Ni similar to Figure 6.5. However, in this case a curve modelling the expected Ni content of olivine as a melt crystallises plagioclase and olivine in a 1:1 ratio is included. The starting composition is Fo_{80}, 2600 ppm Ni in olivine, and 8 weight percent MgO in the melt. These are the same as those used by Li and Naldrett (1999) and the values for MgO, and olivine Ni and forsterite contents in layered intrusions described by Simkin and Smith (1970). Each cross on the curve indicates the effect of crystallising one weight percent of equal quantities of olivine and plagioclase. The Ni-Fo curve was calculated using partition coefficients derived with the equation proposed by Beattie et al. (1991), e.g.

$$D_i^{Ol-l} = A_i^{Ol-l} D_{Mg}^{Ol-l} + B_i^{Ol-l}$$

where: D_i^{Ol-l} is the partition coefficient of element *i* between olivine and liquid,

D_{Mg}^{Ol-l} is the partition coefficient of Mg between olivine and liquid,

A_i^{Ol-l} & B_i^{Ol-l} are constants.

The partition coefficient for Mg in olivine was calculated using the relationship outlined by Roeder and Emslie (1970). Also included are trajectories that would result from equilibration of olivine with a trapped melt fraction. These were calculated using a programme outlined by Barnes (1986). The trapped liquid shift is modelled from olivine Fo_{80}, Fo_{75}, and Fo_{70}. The parameters used for the trapped melt fraction are 12 weight percent FeO, a crystallising temperature of 1100 °C and clinopyroxene, orthopyroxene and olivine crystallising in the ratio 1:1:1. Plagioclase was not considered, as it affects neither the resultant forsterite nor Ni contents. It has already been shown that the normal troctolite primary olivine was Fo_{80}, and that variations in forsterite content are probably the result of trapped liquid shift. Considering Figure 4.9, the normal troctolite olivines plot some way below the trapped liquid shift trajectory. If trapped liquid shift were the only mechanism operating, one would expect forsterite contents to be markedly reduced, while Ni concentrations would be only a little lower than the starting composition. Consequently, it is quite clear that trapped liquid shift cannot account for the Ni concentration in the normal troctolite olivines. To diminish the Ni concentration in this way, equilibration with a sulphide liquid must have taken place. The variable troctolite primary olivine has a calculated forsterite value of Fo_{75}. Figure 4.9 demonstrates that the normal and much of the variable troctolite data plot about the trapped liquid shift line from Fo_{75}, with a significant proportion exhibiting elevated Ni contents. It appears that for those data with Ni concentrations in the range 900 –1200 ppm, their Fo/Ni balance may well be the result of trapped liquid shift. The data with Ni abundances in excess of 1200 ppm have gained Ni, perhaps via equilibration with a high Ni sulphide liquid. Conversely, the data with less than 800 ppm Ni have equilibrated with a low Ni sulphide.

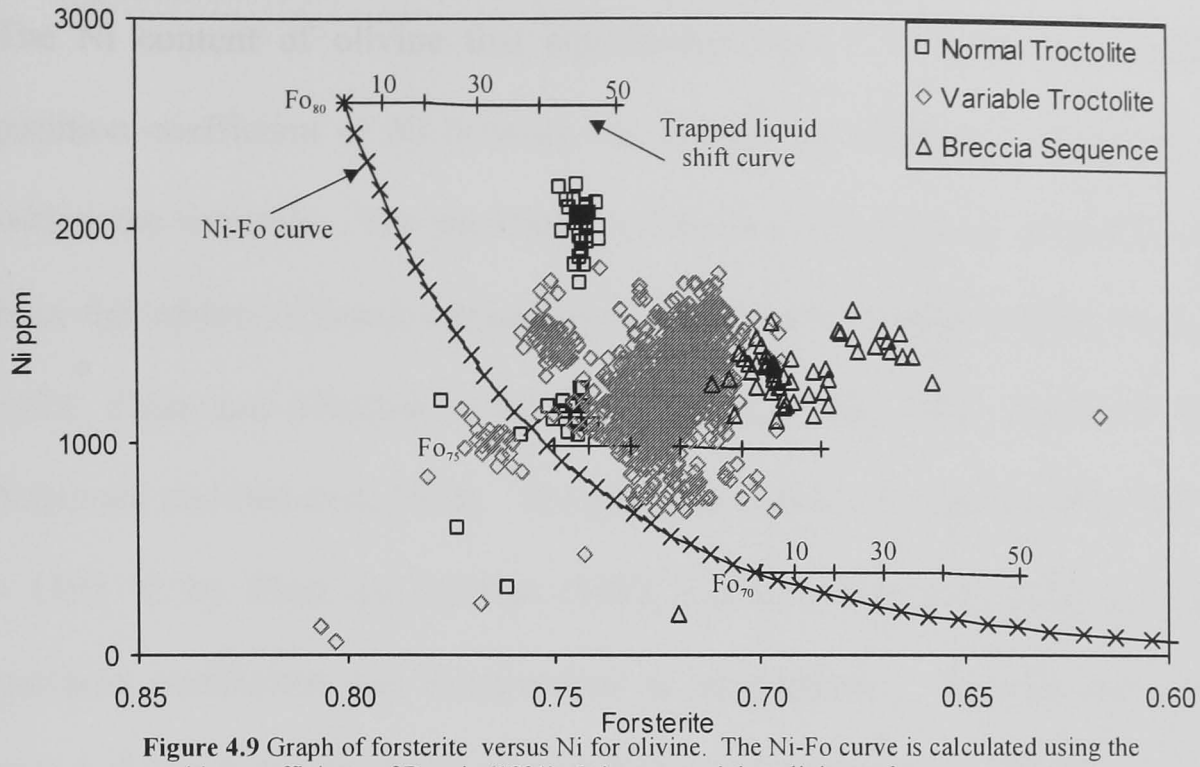

Figure 4.9 Graph of forsterite versus Ni for olivine. The Ni-Fo curve is calculated using the partition coefficients of Beattie (1991). It is assumed that olivine and plagioclase are crystallising in the ratio 1:1 from a liquid containing 8% MgO. The starting composition is Fo_{80} and 2600 ppm Ni. The trapped liquid shift curves are marked in increments of 10 percent and were calculated using Barnes (1986) assuming 12 percent FeO in the trapped liquid and olivine, orthopyroxene, and clinopyroxene crystallising in the ratio 1:1:1.

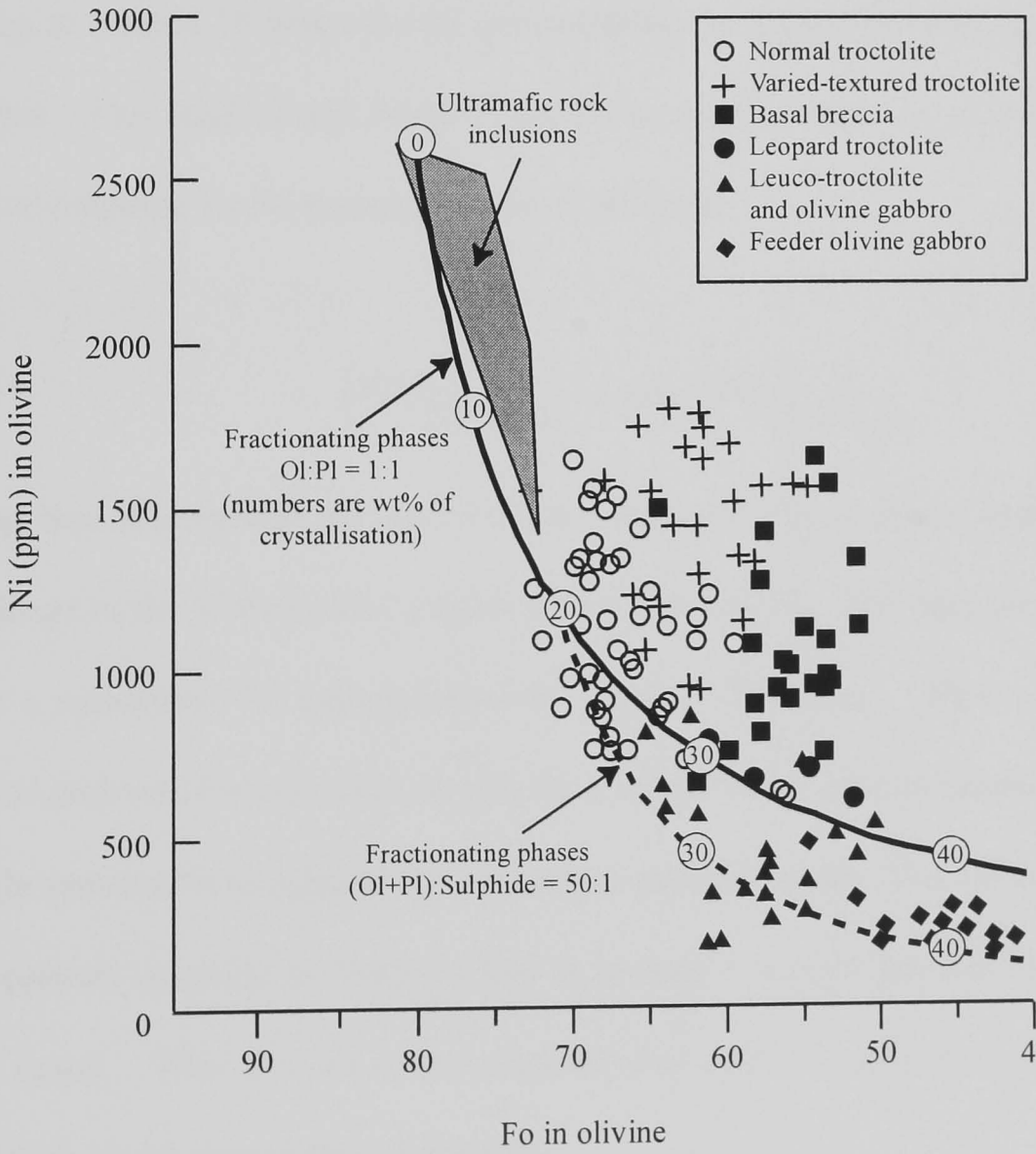

Figure 4.10 Graph of forsterite versus Ni in olivine taken from Li and Naldrett (1999). Included is a modelled curve based on a starting composition of 8 percent MgO, Fo_{80}, and 2600 ppm Ni in olivine. Olivine and plagioclase are assumed to crystallise in a 1:1 ratio. A significant proportion of the data plots below the modelled curve.

The Ni content of olivine that equilibrates with a Ni-sulphide is a product of the partition coefficient of Ni between the olivine and sulphide and the Ni concentration within the sulphide. The partition coefficient of Ni between sulphide and olivine has been the subject of much research (e.g. Brenan and Caciagli, 1998; Clark and Naldrett, 1972; Fleet and MacRae, 1988; Fleet and McRae, 1983; Fleet and McRae, 1987; Rajamani and Naldrett, 1978). The partition coefficient was found to be 27–38 at 1200 - 1395 °C by Fleet and McRae (1983, 1987), which lead them to suggest that the partition coefficient was independent of temperature. Brenan and Caciagli (1998), found that while the partition coefficient of Ni between sulphide and olivine was independent of temperature it appeared to decrease with increasing Ni in sulphide, falling to around 10 when the Ni concentration in the sulphide reached about 5 weight percent. This lead Li and Naldrett (1999) to propose that the partition coefficient for olivine-sulphide Fe-Ni exchange to be of the form:

$$\left(NiS/FeS\right)_{sulphide} \approx 10 \times \left(NiO/FeO\right)_{olivine}$$

Using this relationship Li and Naldrett estimated the partition coefficient for Ni-Fe exchange in the Voisey's Bay intrusion to be around 24. The variable troctolite olivines have a maximum Ni concentration of around 1800 ppm. Thus the olivines in the normal and variable troctolite need to have equilibrated with sulphides with around 4 –5 weight percent Ni to achieve their observed concentrations. The estimated Ni content in 100 percent sulphide at Voisey's Bay is around 5 weight percent Ni (P. C. Lightfoot pers. com). This is close to the required total and it is easy to conceive that locally, sulphides could exceed this Ni content.

This mechanism fails to explain the very low Ni content of the highest forsterite olivine observed in Figure 4.9. These very low Ni olivines plot far below the forsterite versus Ni curve. A possible explanation is that these grains represent remnants of an earlier

magma that equilibrated with a Ni-poor sulphide. Subsequent to this equilibration, the olivine grains were incorporated into the troctolites but remained isolated from the effects of trapped liquid shift. Olivine is frequently observed as a poikilitic texture within plagioclase in the variable troctolite (see section 2.5.6, also Li and Naldrett, 1999). Thus isolated, these grains were able to preserve their high forsterite and low Ni character.

Figure 4.10 is a graph of forsterite versus Ni in olivine, taken from Li and Naldrett's 1999 study of the Voisey's Bay and Mushua intrusions. As with Figure 4.9, an additional curve has been superimposed that represents Ni in olivine crystallising in a 1:1 ratio with plagioclase from a starting composition of 8 weight percent MgO, initial olivine of Fo_{80} and 2600 ppm Ni. The numbers on this curve refer to the weight percent of crystallisation. An important difference between the approach taken by Li and Naldrett (1999) and the one in this study is that Li and Naldrett (1999) used a fixed partition coefficient of 9 to model the behaviour of Ni between olivine and the silicate melt. This is despite the fact that the partition coefficient of Ni is well known to be dependent upon the MgO content of the melt (Hart and Davies, 1978; Beattie et al., 1991). In contrast to Figure 4.9, the data on Figure 4.10 scatter about the modelled trend rather than dominantly above it. For the data that fall below the Fo/Ni trend Li and Naldrett (1999) inferred that this was the result of olivine fractionating in equilibrium with a sulphide melt (signified by the dashed curve). This process generated a Ni-rich sulphide melt that then equilibrated with fresh olivine, upgrading their Ni contents. Figure 4.11 is a plot of Li and Naldrett's (1999) olivine data against the forsterite/Ni curve calculated using the olivine/melt partition coefficients derived by Beattie et al. (1991). Plotted in this way, the data plot on or above the Fo versus Ni curve in a similar way to Figure 4.9. In their 1999 paper, Li and Naldrett argued that the low Ni contents

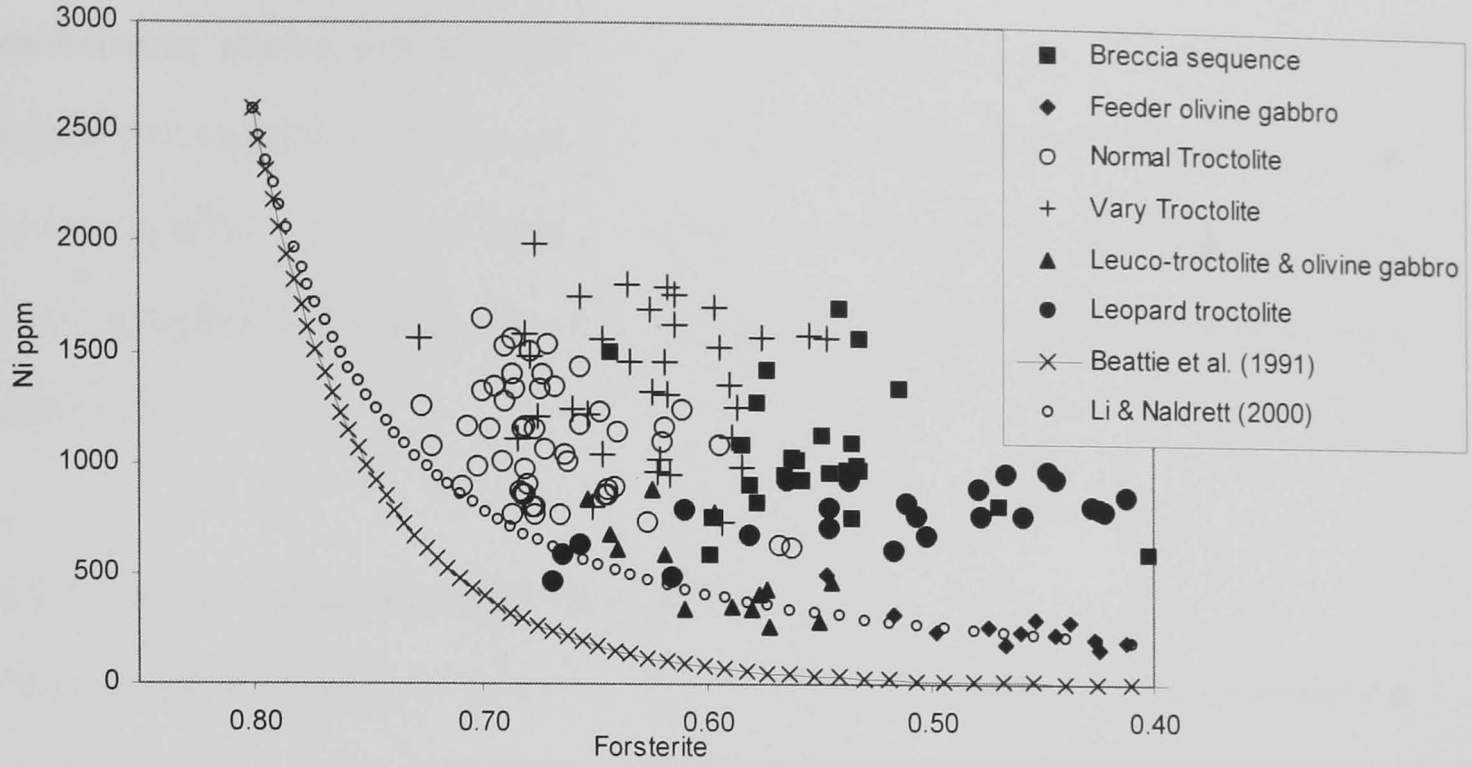

Figure 4.11 Graph of forsterite contents versus Ni in olivine using the data from Li and Naldrett (1999). The fractionation curve is calculated according to Li and Naldrett (1999) starting conditions is shown as is a similar curve calculated according to the equations of Beattie et al. (1991). In contrast to Figure 4.10, Li and Naldrett's (1999) data plot on or above the Fo/Ni curve using their starting conditions (open circle ornament). Relative to Beattie et al. (1991)(crossed ornament), the data are enriched with Ni relative to their forsterite content.

observed in the leuco troctolite, feeder olivine gabbro and olivine gabbro were the result of silicate and sulphide co-fractionation. However, when plotted using an MgO-dependent Ni partition coefficient, it is clear that rather than being depleted in Ni, these rocks are enriched. Thus, rather than the olivine fractionating with a sulphide melt and losing Ni, as proposed by Li and Naldrett (1999), the majority of the Voisey's Bay olivines have equilibrated with a high Ni-sulphide, becoming enriched in Ni. Contrary to Li and Naldrett's (1999) model of a sulphide liquid forming as the olivine fractionated, it appears that a sulphide liquid was present before the troctolites and olivine gabbro formed.

An additional result of plotting Li and Naldrett's data is that it is impossible to match their results. Figure 4.10, taken directly from Li and Naldrett's 1999 paper, clearly shows 22 different data in the series "Leuco-troctolite and olivine gabbro". However, the data tables included in this paper have only 15 data for this category. These are the

data that help to define the group that Li and Naldrett argue is formed as a result of co-fractionating olivine and sulphide. On close examination, the fosterite/Ni curve in Figure 4.10 and that calculated using a Ni partition coefficient of 9 in Figure 4.11 can be seen to differ. Using the starting compositions proposed by Li and Naldrett (1999) it was impossible to replicate this curve. It has not been possible to account for these differences.

4.2.3 Timing of sulphide magma generation

The data that have been discussed so far indicate that when the troctolites crystallised a Ni-rich sulphide magma was present. The high forsterite, low Ni olivine grains that are observed in the normal and variable troctolite are probably included Ni-depleted olivine grains from preceding magma pulses. This requires that an earlier injection of magma had equilibrated with sulphide liquid, upgrading the sulphide liquid with respect to Ni. This early, Ni-donating, silicate magma was then displaced as a later pulse of magma replaced it. This later pulse equilibrated with the now, Ni-rich sulphide liquid. At the same time the new pulse of magma began to fractionate olivine and plagioclase to form the troctolitic rocks.

4.2.4 Timing of silicate rock genesis

Li and Naldrett (1999) carried out a similar investigation to that presented here. In their study, they analysed samples of feeder olivine gabbro and olivine gabbro along with troctolite and breccia sequence material. Throughout their analyses, Li and Naldrett (1999) reported that the olivine gabbros contained olivines with low forsterite contents relative to the troctolitic rocks. Based on their data and the data described here, it would appear that the olivine gabbros are the manifestation of an earlier episode of magmatism than that which generated the troctolitic rocks. This statement is based on the differences in the forsterite values in the different units and the observation that

early fractionates from a magma have higher forsterite. The olivine gabbros are also fine grained, indicating that they underwent more rapid cooling relative to the troctolites. As such, the olivine gabbros must have encountered cool host rocks - suggesting that the gabbros were the first of the Voisey's Bay intrusion rocks to be emplaced. As their forsterite content is lower than that of the troctolitic rocks, they must be derived from a different parental magma. The normal troctolite parental magma, with an Mg# of 55 was then emplaced. During its emplacement the normal troctolite parental magma equilibrated with the Ni-rich sulphides formed by the olivine gabbros. This depleted the Ni content of the normal troctolite olivine. The normal troctolite was in its turn displaced by the variable troctolite, with an Mg# of 47. Because the normal and variable troctolite have such similar trace element profiles it is probable that they share the same genesis. The variable troctolite parental magma also equilibrated with the sulphide liquid, also enhancing its Ni content. The final phase of magmatism generated the breccia sequence, also probably derived from the same source as the variable and normal troctolite and equilibrating with sulphide during its emplacement. Because of the nature of the breccia sequence samples it is not possible to calculate the initial liquid Mg#. However, on the basis of the breccia sequence's observed range of forsterite contents (Fo_{65-72}), lower than either the normal or variable troctolite, its position as the final phase of the genesis of the Voisey's Bay intrusion appears logical.

Because the breccia sequence represents the last stage of magmatism, and a Ni rich sulphide liquid was present when the breccia sequence was emplaced, it seems unlikely that the Tasiuyak gneiss could have initiated the generation of a sulphide liquid. This statement is lent additional credence when the findings of Chapter 2 are considered: the breccia sequence is the only material with a clear Tasiuyak gneiss signature.

A cartoon depicting the probable sequence of events based upon deductions from olivine forsterite and Ni contents is presented as Figure 4.12a-d. In this model, a high MgO magma is ponded at the crust/mantle boundary. By anatexis of the overlying crustal rocks, it achieves sulphide saturation and an immiscible sulphide liquid is generated (Figure 4.12a). This magma, accompanied by its immiscible sulphide liquid, is injected into a higher-level magma chamber and begins to assimilate Tasiuyak Gneiss (Figure 4.12b). Through a process of thermal convection and perhaps some magma replenishment, the sulphide liquid is upgraded with respect to Ni (Figure 4.12b). A second, major pulse of magmatism then takes place (Figure 4.12c) and the earlier pulse(s) of magma are displaced. The existing sulphide liquid and new magma begin to equilibrate as the new magma fractionates olivine and plagioclase. Because the sulphide liquid is already high in Ni, the newly crystallising olivines have enhanced levels of this metal. By a process of plagioclase flotation (Morse, 1969) the normal troctolite forms at the top of the magma chamber. This is followed by the variable textured troctolite and then the breccia sequence material (Figure 4.12d).

4.2.5 Conclusions

All the Voisey's Bay intrusion troctolite-hosted olivines have equilibrated with a sulphide liquid. Furthermore, the troctolite-hosted olivine can be placed into three groups. The first, largest group comprises olivine that is enriched in Ni relative to its forsterite content compared with modelled fractionation trends. The second, much smaller group has higher forsterite, but relative to its forsterite has lower Ni than expected. The first group is the result of olivine equilibrating with high-Ni sulphide magmas. The latter group has the highest forsterite and among the lowest Ni of all the olivines analysed. These olivines are interpreted to be relict grains from an earlier pulse of magma that equilibrated with a Ni-poor sulphide, have preserved their Ni-depleted character and have been incorporated into the troctolites.

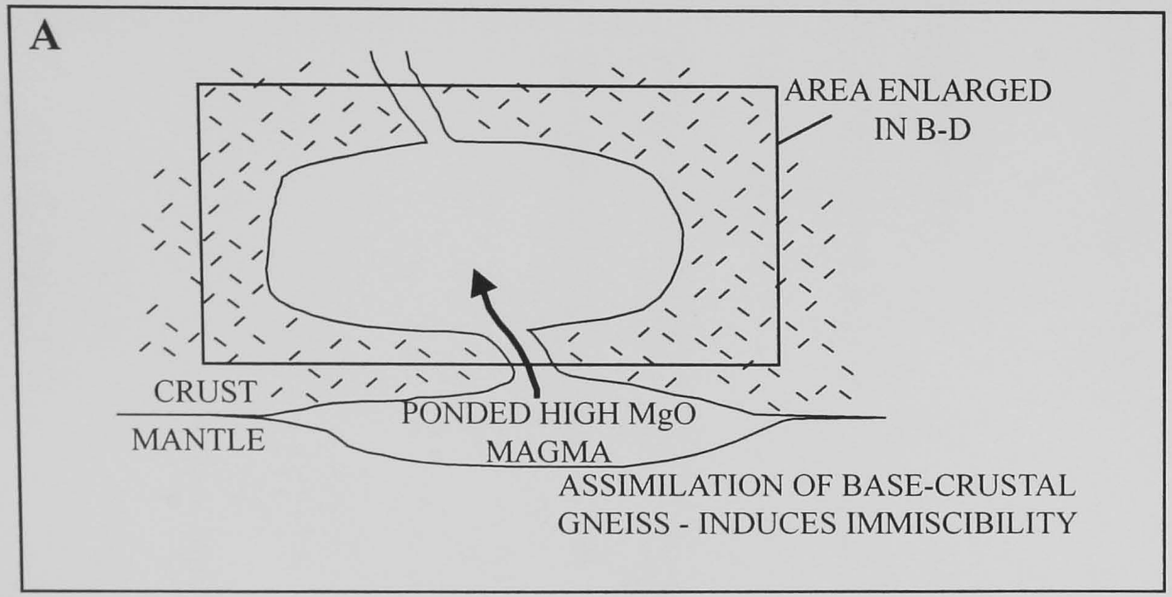

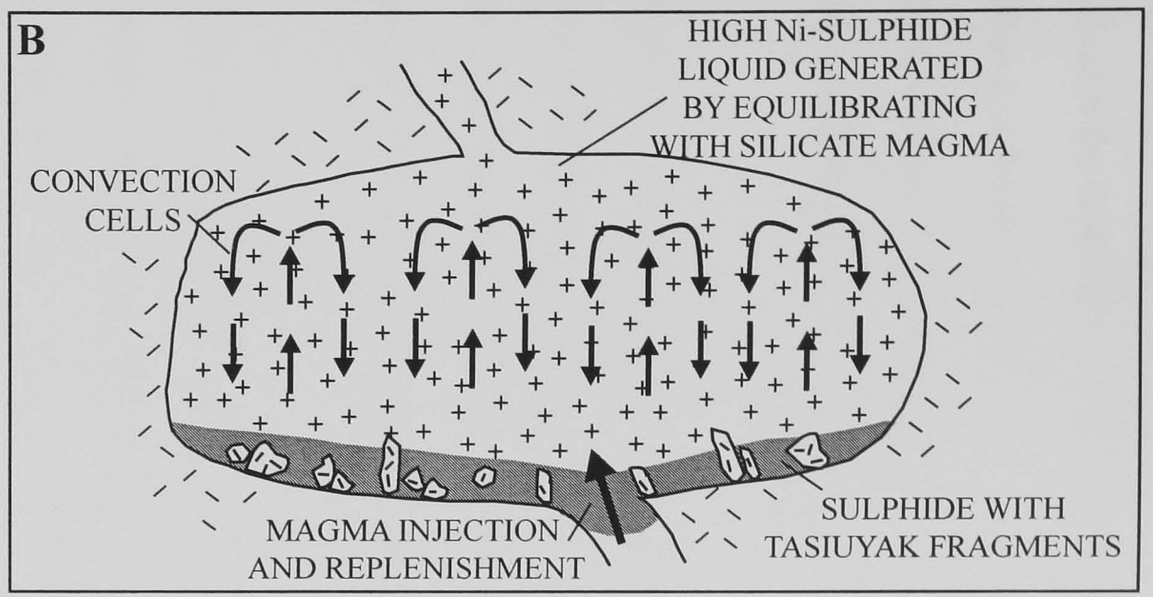

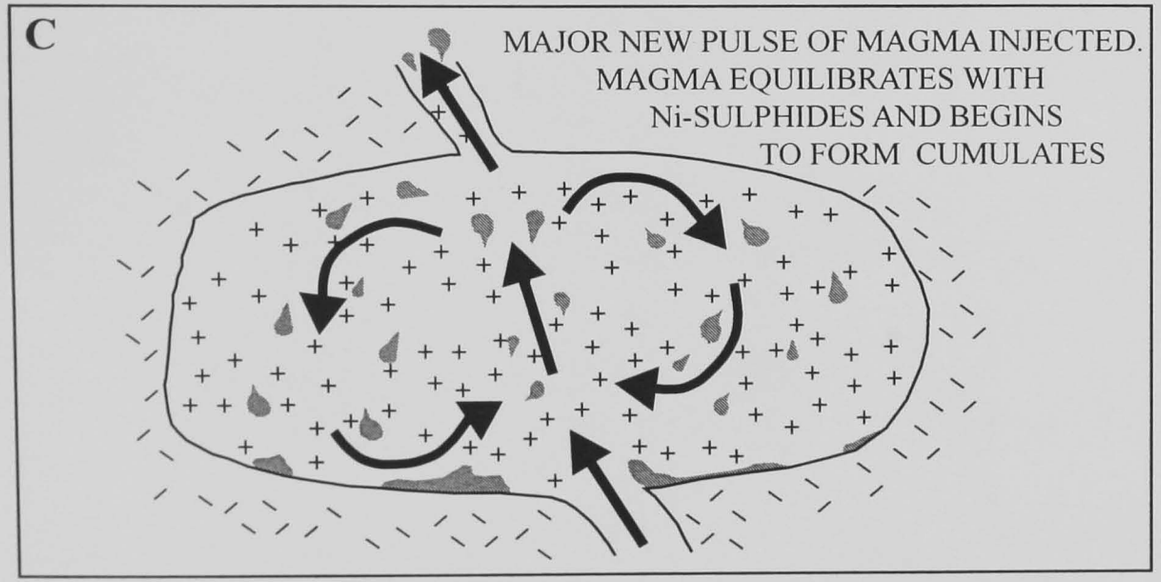

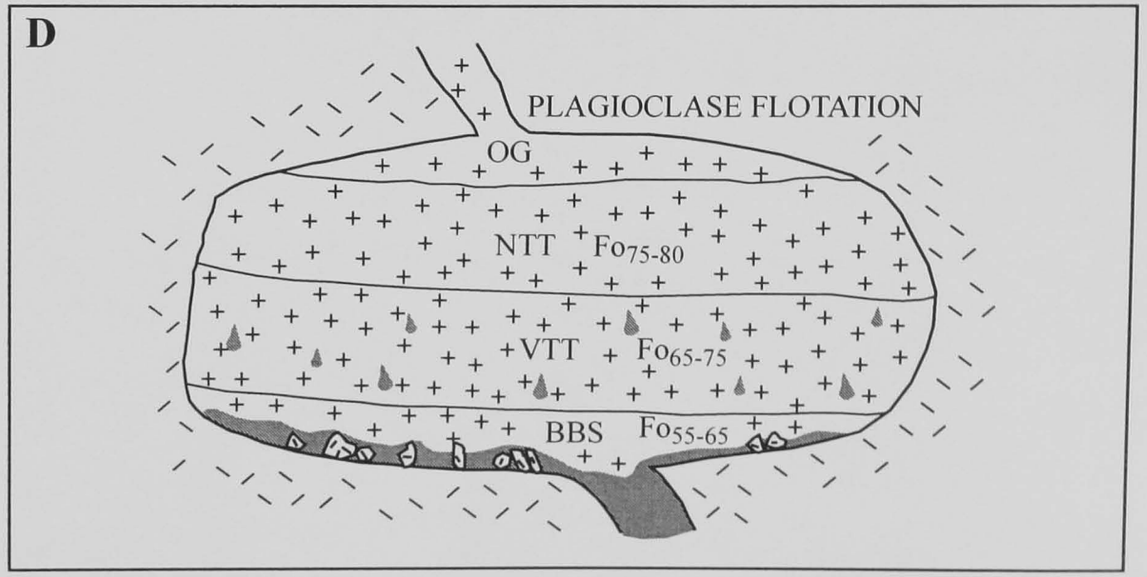

Figure 4.12a-d Cartoon of the timing of Voisey's Bay Intrusion crystallisation and sulphide segregation. A) High Mg# melt ponds at the crust/mantle boundary and assimilates crust initiating sulphide immiscibility. B) Silicate and sulphide magmas are injected into higher-level magma chamber and begin to assimilate Tasiuyak gneiss. Via convection and magma replenishment the sulphides are upgraded with Ni. C) A second pulse of magma is injected and the earlier pulse is displaced. The sulphide liquid and new magma begin to equilibrate. D) By plagioclase flotation the normal troctolite forms at the top of the magma chamber, followed by the variable troctolite and finally the breccia sequence.

Because the troctolitic rocks exhibit evidence of equilibrating with a high-Ni sulphide magma, a Ni-rich sulphide magma must have been present before the emplacement of the troctolites. As all the troctolitic rocks have equilibrated with a Ni-rich sulphide, it is impossible that the troctolites are the source of the Ni in the Voisey`s Bay deposit.

Based on calculated parental melt Mg#, relative positioning and the assumption that the normal troctolite, variable troctolite, and breccia sequence are consanguineous, it is proposed that the relative timing of these rocks' crystallisation was thus: olivine gabbro, normal troctolite, variable troctolite, and breccia sequence.

Given the sequence of crystallisation above, it is probable that a sulphide liquid was present before the assimilation of Tasiuyak gneiss. Because the sulphide liquid was present before the assimilation of the Tasiuyak gneiss, this lithology cannot have induced sulphide immiscibility.

4.2.6 Summary

- The troctolites have equilibrated with a Ni-rich sulphide.
- The troctolites are not the source of Ni for the Voisey's Bay deposit.
- The source of the Ni is a now-departed olivine-rich high-Mg# magma.
- The Tasiuyak gneiss cannot have induced sulphide immiscibility.

Chapter 5

Geochemical Variation in the Voisey's Bay Intrusion Sulphides

5.1.1 Introduction

Chapters 3 and 4 have both suggested that the Tasiuyak gneiss has had little influence on the mineralisation at Voisey's Bay: it seems that rather than being the contaminant that induced sulphide immiscibility across the Voisey's Bay deposit, the Tasiuyak gneiss has had only local influence. If this is the case then differences should be apparent in the geochemistry of the sulphide minerals. In addition, the Ni, Co, and Cu content of the sulphides is a result of the Ni, Co, and Cu content of the silicates with which they have equilibrated – the concentrations of these elements varying with the Mg# of the silicate magma. Thus, investigation of the sulphide metal contents will give insights into the nature of the magma that donated the Ni to the sulphides. Therefore, the purpose of this chapter is to investigate the variations of sulphide mineral geochemistry and relate these to the role of the Tasiuyak gneiss in sulphide genesis and evolution. In addition, the metal contents of the sulphides will be examined to gain further knowledge of the sulphide/silicate interactions.

The analytical approach taken in this chapter is novel; previously the geochemical analyses of sulphides have used samples with a mass of up to several kilograms, with the analysis carried out using a variety of techniques. Data obtained in this manner were then normalised to 100 percent sulphide, which gives the composition of bulk sulphide. Carrying out the investigation into bulk sulphide geochemical variations in this way makes observing differences in sulphide mineral composition impossible. Consequently, the decision was made to carry out a detailed analytical programme by analysing polished thin

sections from a range of localities across the deposit. It is acknowledged that this type of analytical programme is particularly labour intensive, but the observations possible with this technique could not be made otherwise.

The sulphide minerals at Voisey's Bay are found in two characteristic styles:

1) Massive sulphides, where the sulphide minerals make up the bulk of the rock volume with little or no silicate mineral component.

2) Disseminated sulphides where the rock is dominantly silicate with sulphide minerals as a subordinate phases. The disseminated sulphides at Voisey's Bay are further divided based on the lithologic host. The first subdivision includes those sulphides that are associated with the troctolitic to gabbroic rocks of the Voisey's Bay intrusion. The second comprises sulphides associated with the breccia sequence rocks.

The sulphide mineralogy at Voisey's Bay is simple, dominated by pyrrhotite ($Fe_{(1-x)}S$), chalcopyrite ($CuFeS_2$), and pentlandite ($(Fe,Ni)_9S_8$). Minerals observed in minor quantities and reported by other authors include sphalerite (ZnS), galena (PbS), mackinawite (Fe_9S_8), linnaeite ($(Co, Ni, Cu, Cr)_3 S_4$), and cubanite ($CuFe_2S_3$) (Naldrett et al., 2000). Because of the simplicity and ubiquity of the sulphide mineralogy at Voisey's Bay, analyses of the three dominant minerals provides an ideal and comprehensive basis for comparison between the different areas and styles of mineralisation of the deposit.

However, chalcopyrite has a restricted range of values for its major element chemistry, having 24-25 atomic percent Fe, 25-26 atomic percent Cu, and S at 49-50 atomic percent. In addition, there is very little variation in the trace element chemistry in chalcopyrite, Co and Ni are sometimes present, but this is not always the case. Co and Ni occurrence and

abundance of in chalcopyrite does not appear to be systematic, consequently, data for Breccia sequence and Eastern Deeps chalcopyrite are not presented here, though for completeness these analyses are included in Appendix A.

The samples used for the analyses were prepared as polished thin sections, with an increased thickness of around 40 microns compared with conventional petrographic 30-micron sections. This was to ensure that there was a sufficient volume of material for reliable data acquisition. The analyses were carried out on the Open University's Cameca SX100 electron microprobe with analytical conditions set at a filament current of 20 nanoamperes, an accelerating potential difference of 20 kilovolts and a beam spot size of 10 microns.

5.1.2 Results

The results are divided into two sections.

1) The first section deals with data derived from breccia sequence rocks and massive sulphides from across the whole of the Voisey's Bay deposit. The data are grouped according to the area of the deposit that the samples were collected. Figure 5.1 is a map of the deposit with the names of the various deposit areas. Also shown on this map are the locations of the diamond drill holes from which samples were taken; these are indicated by black circles.
2) The second section investigates samples from one area of the Voisey's Bay deposit, the Eastern Deeps. Here the data are divided on texture and lithologic host. The disseminated sulphide data are presented as breccia sequence and as troctolite-hosted. The troctolite-hosted samples are derived from the variable textured troctolite described in Section 2.4.6.

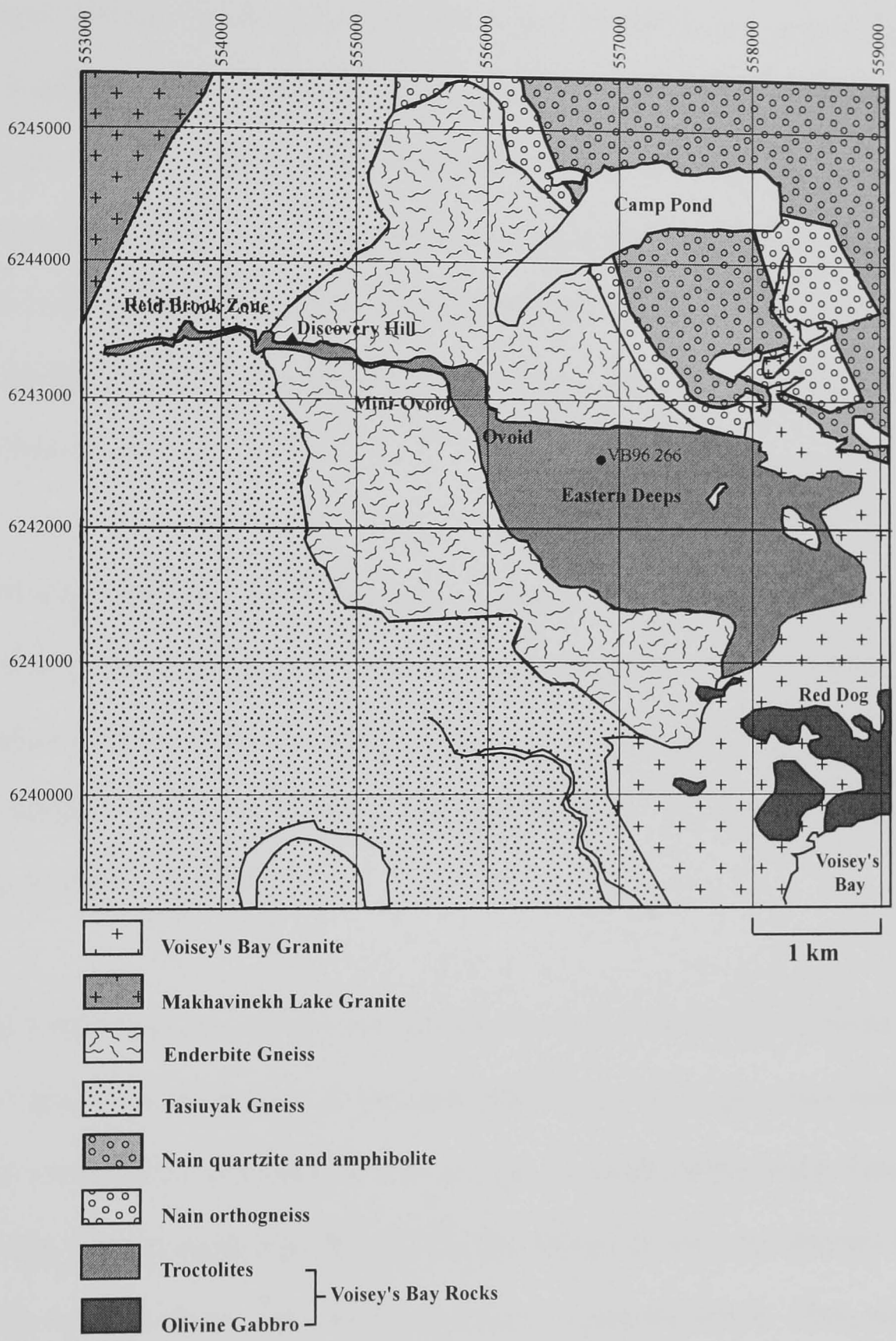

Figure 5.1 Map of the Voisey's Bay deposit with the names of the different areas. Redrawn from Voisey's Bay Nickel Company data.

5.1.3 Breccia sequence data

Pyrrhotite from the breccia sequence form a tightly constrained linear group with a negative slope between ~51-55 atomic percent S and ~45-48 atomic percent Fe (Figure 5.2a). The lowest S values are attributed to the Eastern Deeps and the highest values to the Western Dyke samples. The rest of the analyses form an array between the limits described. Also plotted on Figure 5.2a is the composition of pyrrhotite as predicted by the relationship $Fe_{(1-X)}S$. This forms a perfectly straight line between 45-49 atomic percent Fe and 51-55 atomic percent S. The data from the Voisey's Bay plot consistently below the predicted composition.

Figure 5.2b illustrates that the nickel content of the Voisey's Bay breccia sequence pyrrhotite is restricted, varying between 0.1-0.6 atomic percent. The highest Ni contents are observed in the Ovoid and Far Eastern Deeps. From these data, the breccia sequence pyrrhotite samples from the Voisey's Bay intrusions do not show any systematic relationship between Fe and Ni.

The plot of total metals against atomic sulphur for breccia sequence pyrrhotite (Figure 5.2c) shows that when all metals are included, there is excellent agreement between the composition predicted for pyrrhotite by $Fe_{(1-X)}S$ and the analysed pyrrhotite from breccia sequence rocks. The deviation from the theoretical composition that was observed for the same samples when Fe alone was considered is now completely absent. Thus, any deficit in Fe in breccia sequence pyrrhotite is compensated by increases in Ni and Co.

Figure 5.2d uses the notation Delta Po to explore the compositional variations of breccia sequence pyrrhotite. The notation Delta Po is based upon the deviation of observed

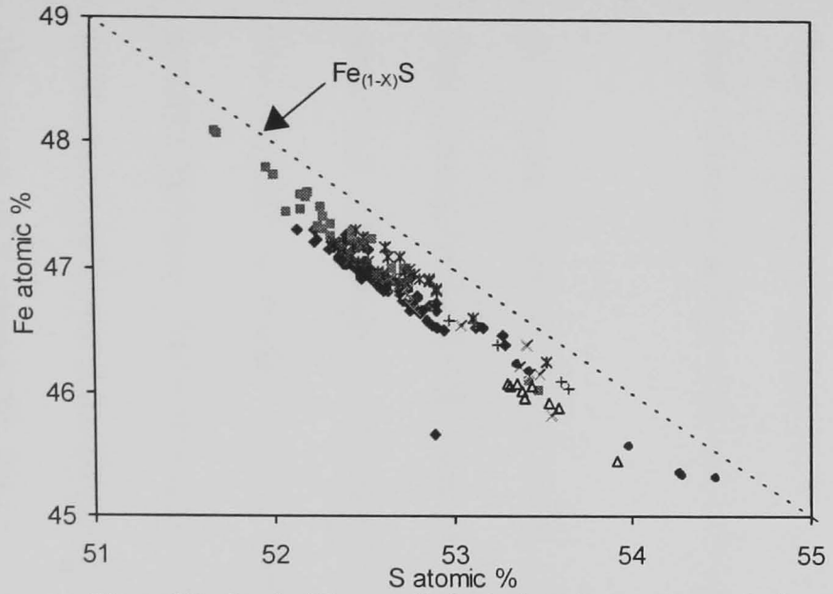

Figure 5.2a Graph of S versus Fe for the breccia sequence pyrrhotite. For comparison, the theoretical composition of pyrrhotite has been plotted and is labelled $Fe_{(1-X)}S$. The breccia sequence data have less Fe than predicted by the relationship $Fe_{(1-X)}S$.

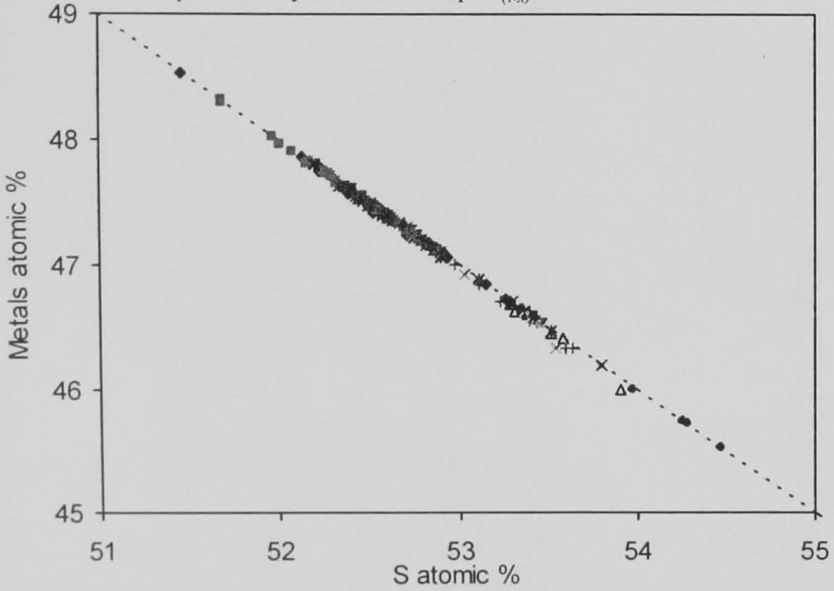

Figure 5.2c Graph of S versus total metals (Fe + Ni + Co) in breccia sequence pyrrhotite. For comparison, the theoretical composition of pyrrhotite is included as a dotted line. If all metals are included, the observed pyrrhotite compositions agree well with theoretical values.

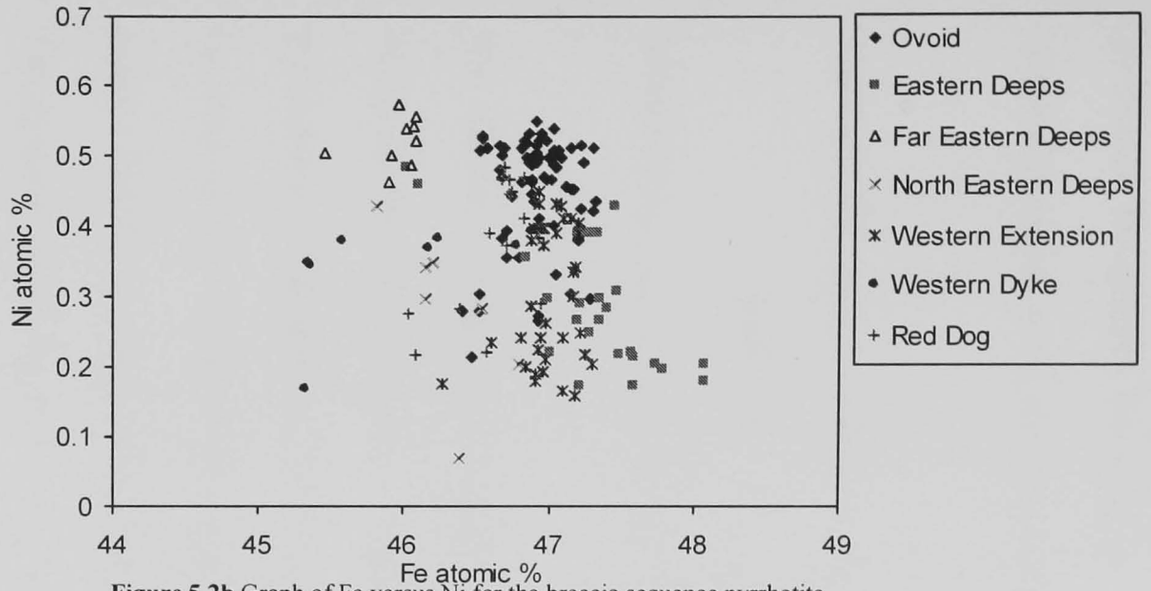

Figure 5.2b Graph of Fe versus Ni for the breccia sequence pyrrhotite. The maximum Ni content is observed in the Far Eastern Deeps and Ovoid samples.

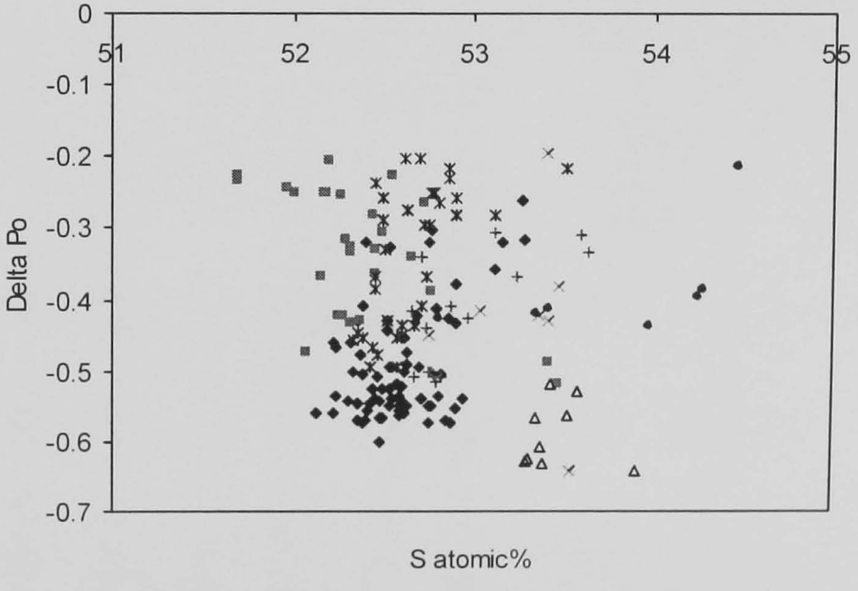

Figure 5.2d Graph of S versus delta Po for breccia sequence pyrrhotite. Delta Po is explained in the text. The Ovoid and Far Eastern Deeps samples have the greatest Delta Po with the remainder of the data scattered above.

pyrrhotite Fe content for a measured S content from that predicted by $Fe_{(1-X)}S$. The Fe content (predicted) for a measured S component can be expressed as:

$$Fe_{(Pred)} = 100 - S$$

The Delta Po notation can be expressed as:

$$Delta\ Po = Fe_{(Observed)} - (100 - S) = Fe_{(Observed)} - Fe_{(Predicted)}$$

Where $Fe_{(Observed)}$ is the measured Fe component of pyrrhotite.

The degree of separation expressed by the Delta Po notation is the amount of Fe that is being substituted for by Ni, Co, and Cu. Typically, in the Voisey's Bay breccia sequence pyrrhotites, Ni abundance is 0.1 to 0.6 atomic percent, Co an order of magnitude less and Cu may or may not be present in similar amounts to Co. The Voisey's Bay data all have greater than 51 atomic percent S and show a Delta Po that varies between –0.2 and –0.65. The greatest Delta Po is observed in the Ovoid and Far Eastern Deeps samples and the least Delta Po is found in the Western Extension. There is an even distribution of data between the end members. Therefore, in the Voisey's Bay breccia sequence, the conditions that causes a deficit in Fe abundance in pyrrhotite are variable.

In Figure 5.3a, a graph of S versus Fe for massive sulphide pyrrhotite, a similar discrepancy between the measure Fe content of pyrrhotite and that predicted by theory is observed. However, in this case the Fe content of pyrrhotite has a slightly different range and extends to higher levels, 46.5–48.5 atomic percent rather than 45.5–48.0 atomic percent that was observed in the breccia sequence data. Correspondingly, the S contents of the massive sulphide data are reduced, ~51–53 atomic percent.

The graph of S versus Ni, Figure 5.3b, reveals that the massive sulphide samples typically have a more restricted range of Ni contents than breccia sequence material, the massive

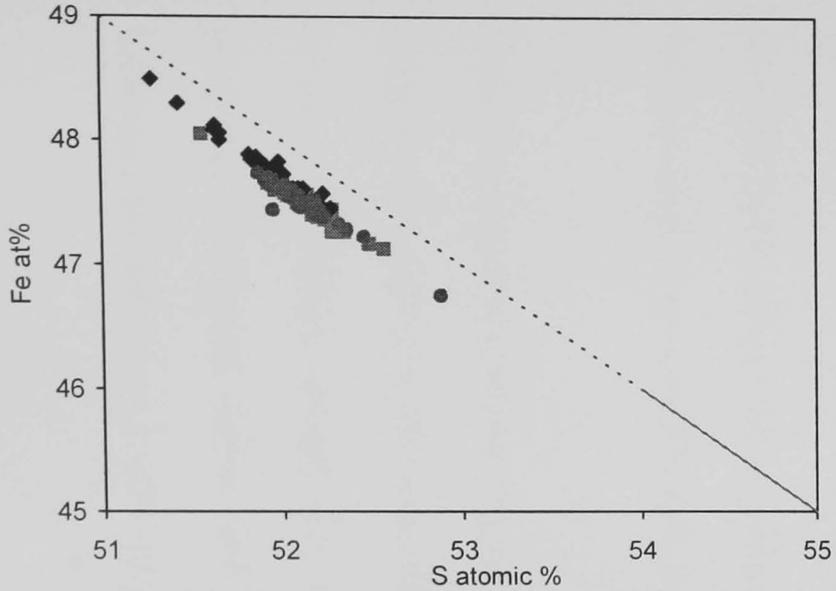

Figure 5.3a Graph of S versus Fe for massive sulphide pyrrhotite. For comparison, the theoretical pyrrhotite composition according to $Fe_{(1-x)}S$ has been plotted as a dotted line. The measured data fall consistently below the predicted composition.

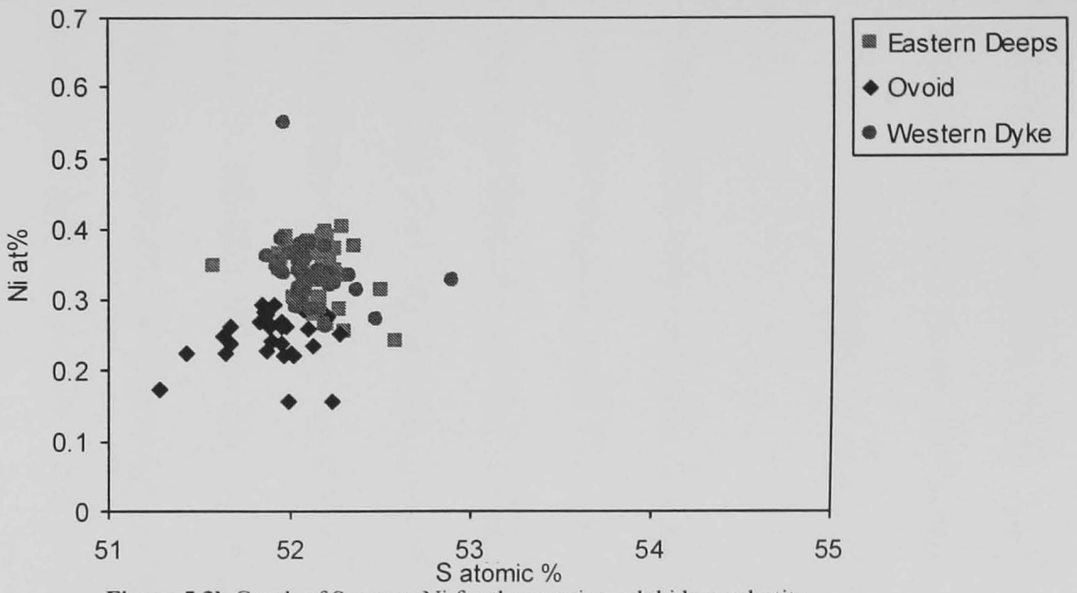

Figure 5.3b Graph of S versus Ni for the massive sulphide pyrrhotite. The data exhibit some variation with the Ovoid data having the least Ni and the Eastern Deeps and Western Dyke having the most.

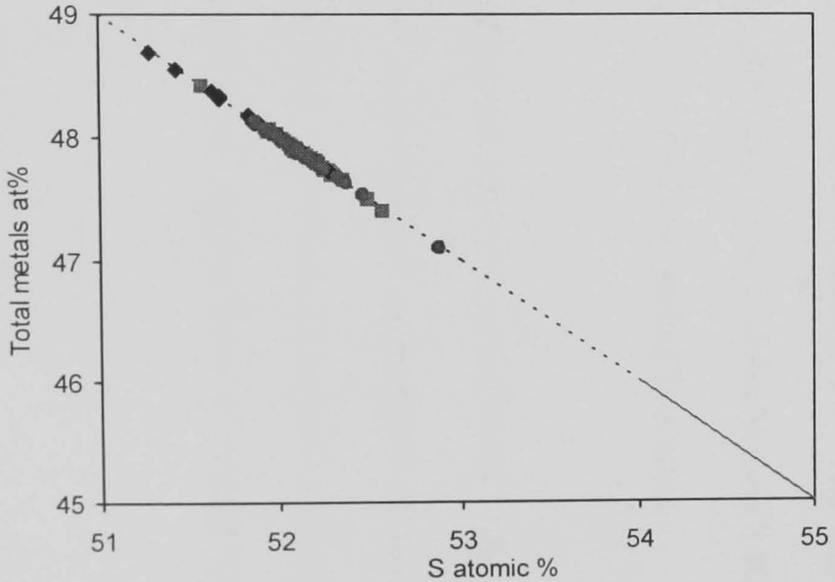

Figure 5.3c Graph of S versus total metals (Fe + Ni + Co) for the massive sulphide pyrrhotite. With Ni, Co, and Fe included in the metal budget the observed data exhibit good agreement with the predicted composition of pyrrhotite shown here as a dotted line.

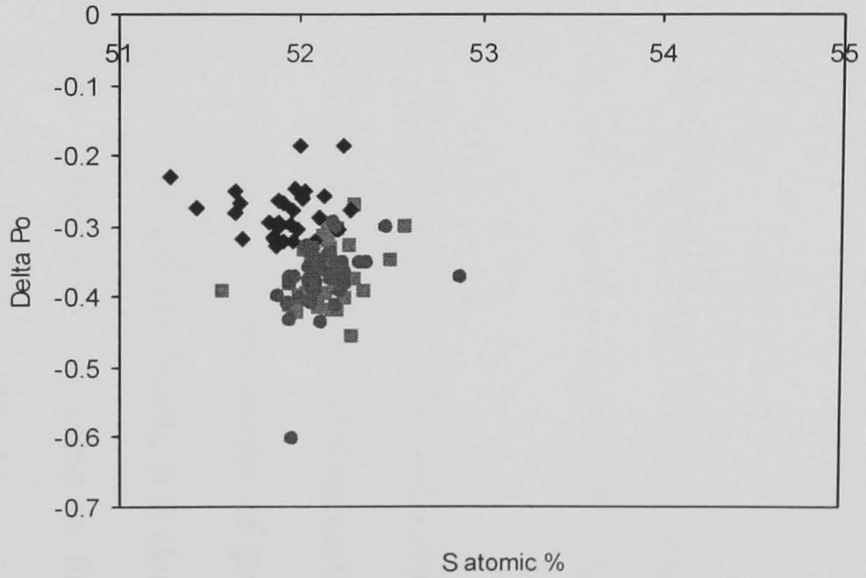

Figure 5.3d Graph of S versus delta Po for the massive sulphide pyrrhotite. The Delta Po notation is explained in the text. The data exhibit a range of values, the Ovoid having the smallest Delta Po and the Eastern Deeps and Western Dyke having the greatest.

sulphides varying between ~0.2 – 0.4 atomic percent. The greatest abundance of Ni is found in the Western Dyke and Eastern Deeps samples and the least in samples derived from the Ovoid. Summing Ni and Co (Figure 5.3c) demonstrates that a similar process of Ni and Co substituting for Fe in pyrrhotite is taking place in the massive sulphides.

Figure 5.3d uses the Delta Po notation and demonstrates that the massive sulphides have a restricted range of Delta Po when compared with the breccia sequence data. The massive sulphide Delta Po varies between –0.2 to -0.45.

In Figure 5.4a, the variation of Fe versus Ni in Breccia sequence pentlandite is examined. This figure illustrates that the data for both the Voisey's Bay and Mushua intrusions fall onto a straight line with a strongly negative slope. The composition of pentlandite, according to its formula is plotted on this figure and labelled $(Fe,Ni)_9S_8$. It is clear that the gradient defined by the Voisey's Bay intrusion samples is very close to that of the predicted composition, the difference being a consistent Ni deficit. The Voisey's Bay data plot between 25-28 atomic percent Ni, and 23-25 atomic percent Fe. The two samples from the North Eastern Deeps differ significantly from the rest of the Voisey's Bay, being lower in both Ni and Fe. The deficit is balanced by relatively high Co contents.

If the Co and Ni for breccia sequence pentlandite are summed, as in Figure 5.4b, there is a much closer agreement between the observed and predicted compositions. The separation of the North Eastern Deeps data has disappeared and overall, the data are more tightly clustered. The metal deficit that was observed in Figure 5.4a is completely offset, indicating that the Co was substituting for Ni.

In contrast to pyrrhotite, breccia sequence pentlandite data do not exhibit the diminishing Fe component with respect to the predicted composition as sulphur content increases (Figure 5.4c). The Fe and S content of pentlandite do not appear to be mutually dependent. The only variations observed in pentlandite are systematic variation between Fe and Ni, in line with pentlandite stoichiometry, and to a certain extent Co substituting for Ni.

5.1.4 Eastern Deeps data

The next series of figures examines variation in sulphide composition from one part of the Voisey's Bay deposit, the Eastern Deeps, where all the types of mineralisation occuring at Voisey's Bay are found. For example, disseminated troctolite-hosted sulphides, disseminated breccia sequence, and massive sulphide are all present. The approach taken in this section is to compare critical compositional variation between the two disseminated sulphides and the massive sulphide minerals.

Figure 5.5 illustrates the variation in Fe contents with depth for Eastern Deeps pentlandite. The breccia sequence and massive sulphide data are quite tightly constrained at 23.8-27.2 atomic percent Fe. However, the troctolite-hosted data exhibit a markedly greater variation. This variation does not appear to have any depth dependence. A similar lack of composition-upon-depth dependence is repeated for the other elements analysed in Eastern Deeps pentlandite. As such, this information is of little value so will not be represented graphically but is included in Appendix A.

The next series of figures plot the major elements against each other for pyrrhotite and pentlandite in the Eastern Deeps. Not all the possible permutations of elements will be

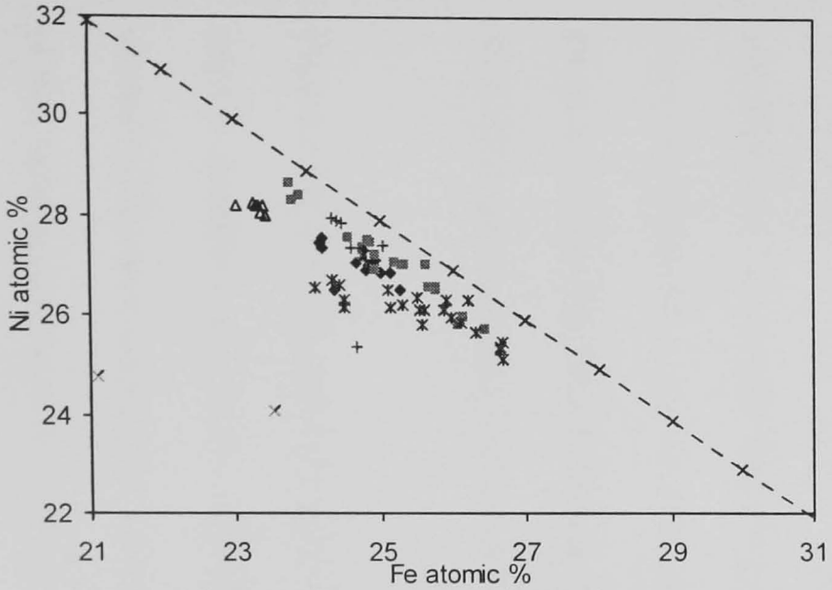

Figure 5.4a Graph of Fe versus Ni for the breccia sequence pentlandite. The composition of pentlandite according to $(Fe,Ni)_9S_8$ is illustrated for comparison. The measured data plot beneath the predicted composition.

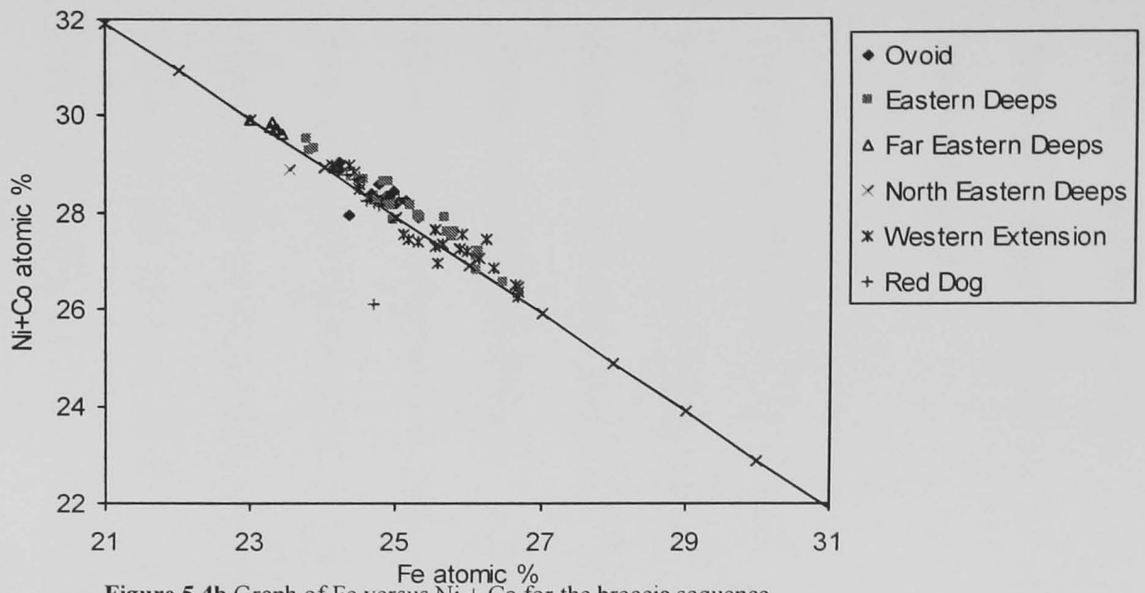

Figure 5.4b Graph of Fe versus Ni + Co for the breccia sequence pentlandite. When Co and Ni are summed the observed composition of pentlandite exhibits a good agreement with the predicted composition according to $(Fe, Ni)_9S_8$.

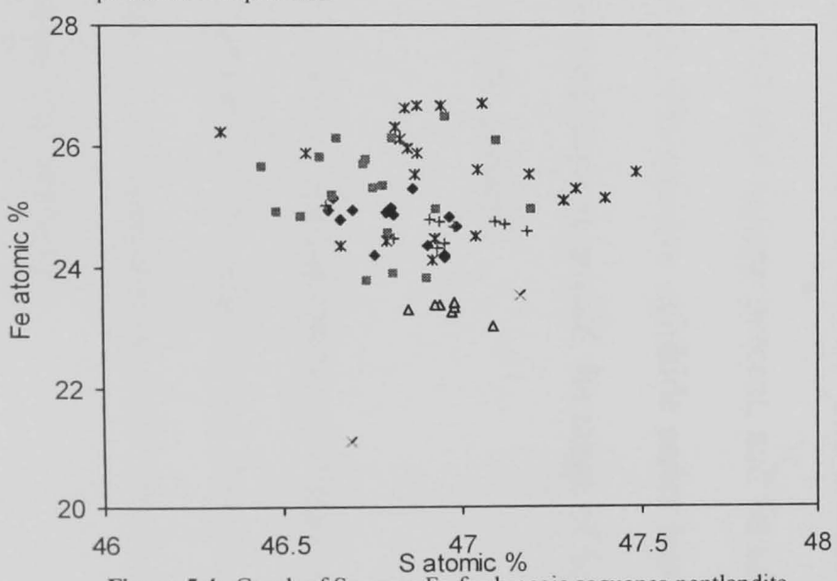

Figure 5.4c Graph of S versus Fe for breccia sequence pentlandite. The data have restricted variation in S values, illustrating good agreement with $(Fe, Ni)_9S_8$.

plotted as not all show any systematic variation. In particular, variation with respect to Co has been discarded. This is because for most examples Co was near constant, or exhibited random variation.

Figure 5.6a illustrates the almost perfect linear negative relationship between the S and Fe content of Eastern Deeps pyrrhotite. Also included on this figure is the trend for the theoretical composition of pyrrhotite, predicted from its formula $Fe_{(1-X)}S$. This trend is shown as a dotted line and is arrowed. The observed data show a marked similarity to the predicted compositions. However, as the sulphur content of Eastern Deeps pyrrhotite increases, a deviation from the $Fe_{(1-X)}S$ develops. As the S content of pyrrhotite increases, the deviation of observed Fe content from the predicted increases. The troctolite-hosted series has the greatest variation in S and Fe content of the three series analysed, with a range of S content from 43.5-53.8 atomic percent. This series also has the greatest range in Fe content, from 46.2-50.9 atomic percent. By contrast, the breccia sequence and the massive sulphide data are much more restricted in both Fe and S. The breccia sequence samples have S contents that vary between 51.7-53.4 atomic percent, and Fe content that varies between 48.1 and 46.0 atomic percent. The massive sulphide series has a similar range of values for both S and Fe, and is perhaps more restricted. Its range of S content is 51.6-52.6 and Fe varies between 47.1-48.0 atomic percent.

Figure 5.6b is S versus total metals (Fe + Ni + Co) for Eastern Deeps pyrrhotite. The data exhibit excellent agreement with the line defined by the relationship $Fe_{(1-X)}S$. As the S content of Eastern Deeps pyrrhotite increases, Fe is substituted by other metals, the extent of this substitution apparently being a product of the S content.

Figure 5.6c uses the notation Delta Po. Delta Po is plotted against atomic percent S so that the relationship between increasing S and deviation of Fe from the predicted value may be explored properly. If the measured data were in perfect agreement with the composition predicted by $Fe_{(1-X)}S$, then all the points would fall along the Delta Po = 0 line. This is not the case. As the sulphur content of pyrrhotite increases there is a corresponding decrease in the Delta Po value. Up to approximately 52 atomic percent S, the decrease in Delta Po is gradual and apparently linear. At 52 atomic percent, S this behaviour changes and much greater variation in Delta Po is observed. It appears from this data that for Eastern Deeps pyrrhotite the control on substitution of Fe by Ni and Co remains systematic until 52 atomic percent S. At this point, an additional control begins to operate and the previous systematic behaviour is disrupted.

Figure 5.7a is a graph of Fe against Ni, both in atomic percent, for Eastern Deeps pentlandite. There is a good correlation between Fe and Ni, with Ni decreasing as Fe increases. The high-Ni end of the line is occupied by breccia sequence points. These are partly overlapped by points from the massive sulphide series, although the massive sulphide data continue to lower Ni concentrations. The troctolite-hosted data have a greater variation in their values than that observed for either the breccia sequence or massive sulphides. The Fe and Ni values for pentlandite as predicted by the formula $(Fe,Ni)_9S_8$, are plotted as a dotted line to allow comparison with the measured data. Most of the measured data exhibit less Ni that that predicted by the pentlandite formula.

Figure 5.7b presents Fe versus Ni + Co for Eastern Deeps pentlandite compared with the theoretical pentlandite compositions predicted by $(Fe,Ni)_9S_8$. Here, better agreement with the observed and predicted data is seen. This suggests that some substitution between Ni

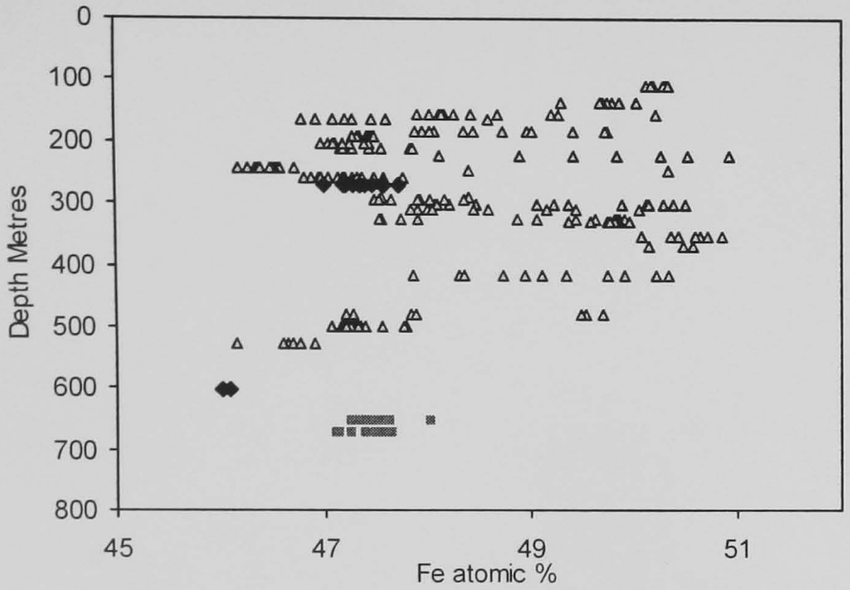

Figure 5.5 Graph of Fe versus depth in metres for Eastern Deeps pyrrhotite. The troctolite-hosted samples exhibit much variation. Less variation is observed in massive sulphide and breccia sequence samples.

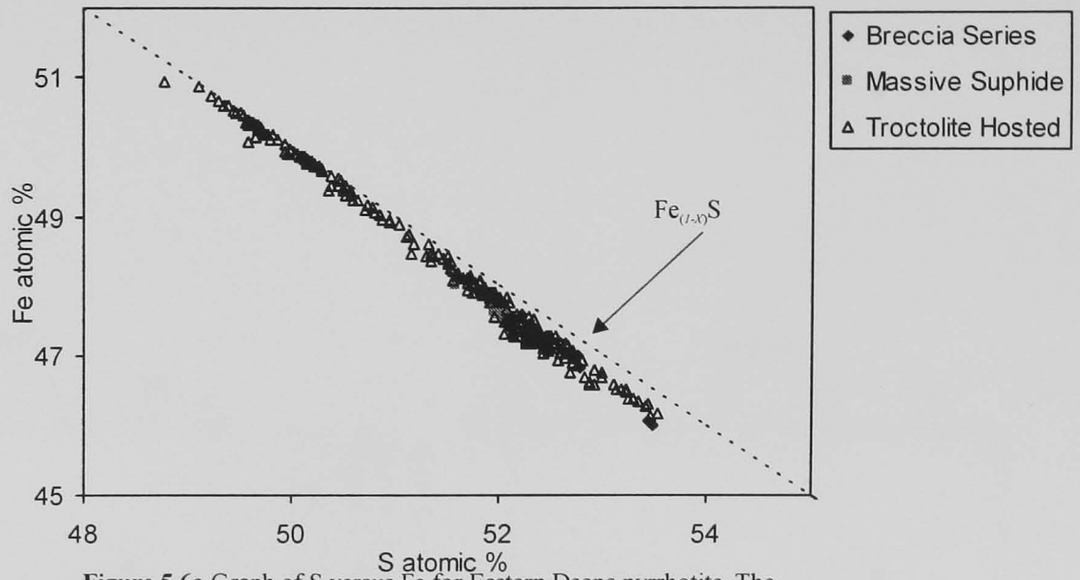

Figure 5.6a Graph of S versus Fe for Eastern Deeps pyrrhotite. The composition of pyrrhotite according to $Fe_{(1-X)}S$ is plotted as a dotted line. In comparison with the theoretical pyrrhotite, the observed data exhibit a decrease in Fe with increasing S content.

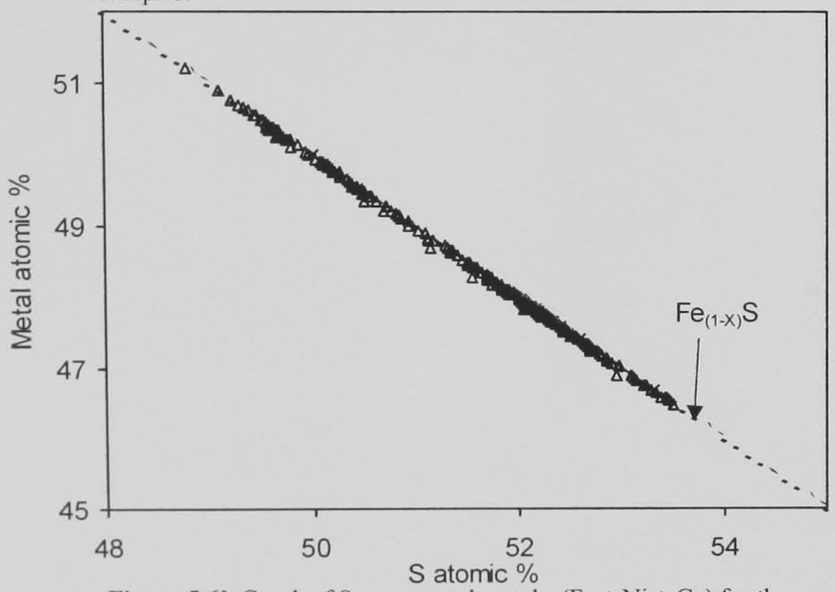

Figure 5.6b Graph of S versus total metals (Fe + Ni + Co) for the Eastern Deeps pyrrhotite. With Ni and Co included, the increasing deviation away from the predicted pyrrhotite composition with increasing S content is removed. This implies that at higher S content Ni and Co substitute for Fe.

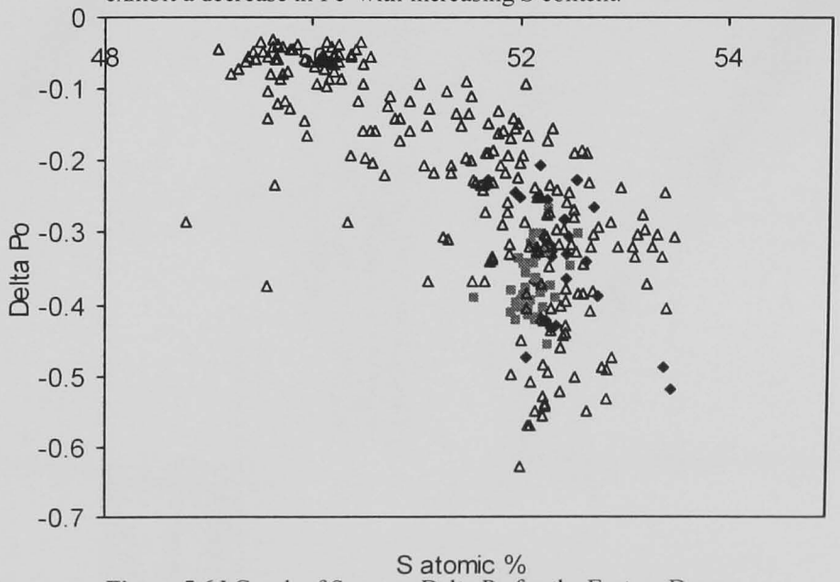

Figure 5.6d Graph of S versus Delta Po for the Eastern Deeps pyrrhotite. The troctolite hosted samples exhibit the greatest variation. Breccia sequence and massive sulphide samples have similar values, clustering around -0.3 to -0.4.

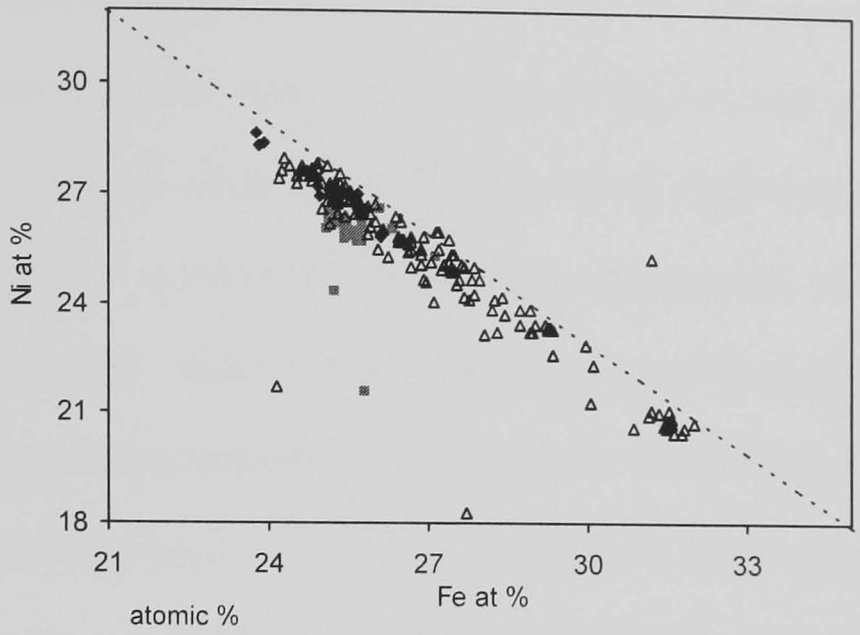

Figure 5.7a Graph of Fe versus Ni for Eastern Deeps pentlandite. For comparison, the theoretical composition of pentlandite according to $(Fe, Ni)_9S_8$ has been plotted as a dotted line. The measured data have a Ni deficit compared with the calculated composition.

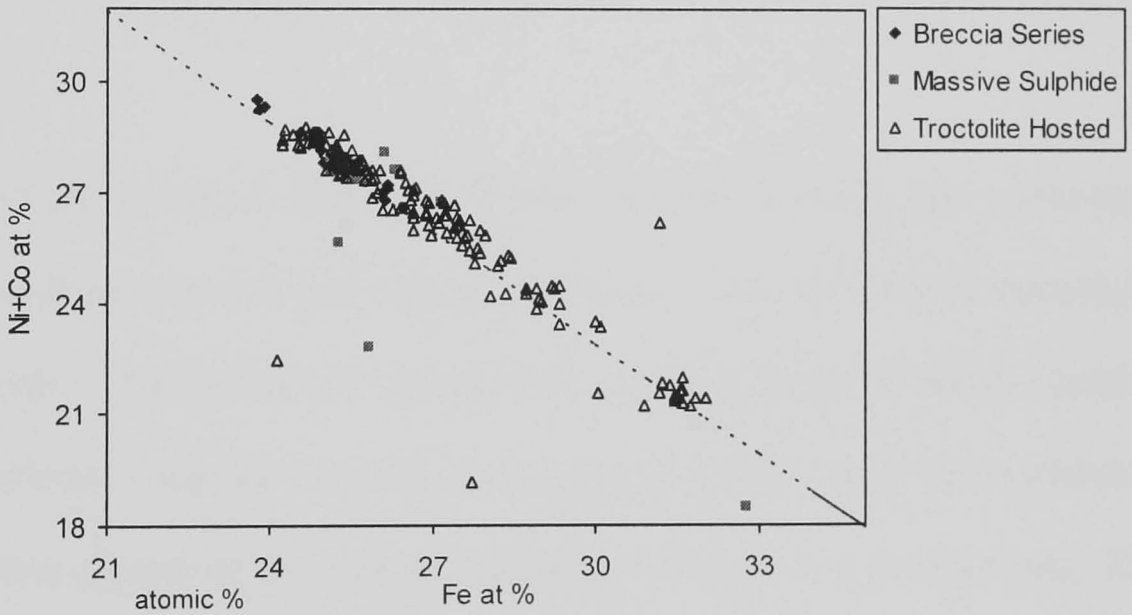

Figure 5.7b Graph of Fe versus Ni + Co for the Eastern Deeps pentlandite. When Ni and Co content of pentlandite are combined, there is better agreement with the predicted pentlandite composition shown here as a dotted line.

and Fe and Co may be taking place. However, the deviation of Ni content from the predicted composition is similar throughout the range of compositions. None of the changes with increasing S that were seen in Voisey's Bay breccia sequence pyrrhotite (Figures 5.2a and 5.2c) are observed in Eastern Deeps pentlandite. However, some compositional variation is apparent in Eastern Deeps pentlandite; the Fe varies over a range of 8 atomic percent while the S varies only around 2 atomic percent. This is compared with a range of approximately 6 atomic percent for both elements in pyrrhotite. This difference in compositional variation is a factor of the chemistry and structural differences between the two minerals; in pyrrhotite the substitution is between Fe and S, pentlandite substitution is between Fe and Ni.

5.1.5 Conclusions

The investigation of the pyrrhotite data has revealed that the Voisey's Bay pyrrhotite composition deviates away from that predicted by its formula. This deviation is expressed as a deficit in Fe content, the shortfall being negated by substitution by Ni and to a lesser extent Co. Where extensive data are available, they have shown that largely the anomalous behaviour of pyrrhotite appears to be linear and systematic. However, at approximately 52 atomic percent S in the Eastern Deeps, a change is observed and the Delta Po increases markedly. This change in behaviour was not observed for the breccia sequence or massive sulphide pyrrhotite.

Investigation of the pentlandite data revealed that similar deviation of measured data from predicted composition was observed. In this case, the Ni deficit was entirely balanced by the inclusion of Co. No systematic variation in Ni or Co variation could be discerned.

5.1.6 Summary

- Pyrrhotite Fe contents deviate from those predicted by its formula.
- The Fe deficit is balanced by substitution by Ni + Co.
- At lower S contents, the Fe deficit behaviour of pyrrhotite appears to be systematic and dependent upon S contents. When S contents are approximately 52 atomic percent, the relationship S content and Fe deficit changes.
- Pentlandite measured Ni contents are below that predicted by its formula.
- The Ni deficit of pentlandite appears to be constant across the range of observed pentlandite compositions.

5.2 Discussion

5.2.1 Introduction

In this section, the variation that was observed in pentlandite and pyrrhotite composition from the Voisey's Bay intrusion will be discussed. Before this can be considered, the mechanisms that control sulphide liquid and sulphide mineral composition must be considered. Firstly, the relationship between the siderophile elements and MgO content of the silicate melt and solids with which the sulphide liquids have equilibrated will be investigated. Next, the partitioning of siderophiles between sulphide and silicates will be discussed along with the implications of sulphide - silicate equilibration. Sulphide liquid fractionation will also be discussed in terms of the effects upon sulphide mineral composition. Finally, the observed variation in Voisey's Bay pyrrhotite and pentlandite compositions will be discussed with respect to the controls and effects outlined above. To finish this chapter, conclusions will be drawn as to the nature of the source of the siderophile elements, the effects of sulphide fractionation, and the influences of any external controls.

5.2.2 Metal content of silicate melts

A magmatic sulphide acquires its siderophile elements via interaction with silicate magmas. This section investigates the relationship between silicate fractionation in terms of MgO and Ni content.

The amount of Ni within a mantle-derived silicate melt is dependent upon the Mg content of the melt (Barnes, 1986). The Mg content of a primary mantle-derived melt is dependent upon the pressure and temperature at which initial melting took place (e.g. Jacques and Green, 1980). After melting has occurred the Mg content of the melt will be quickly

reduced if fractional crystallisation of olivine takes place. Figure 5.8 is a plot of weight percent MgO against Ni in ppm for a series of hypothetical melts that are in equilibrium with mantle olivine. This figure was prepared using the equations proposed by (Beattie et al., 1991). The assumptions made in this model are that the first fraction of olivine to crystallise will be in equilibrium with mantle olivine. This first olivine fraction is forsterite 90 and has a Ni content of 3200 ppm as this is thought to be representative of mantle composition (I. J. Parkinson, pers. comm.). Figure 5.8 shows clearly that as the MgO content of melt increases in response to elevated melting temperatures, there is a corresponding increase in its Ni abundance. The effects of olivine fractionation are shown on Figure 5.9, which uses methods for calculating D values of Ni in olivine of Beattie et al. (1991). The curving traces depicted by the filled circles represent increments of 1 percent fractional crystallisation of olivine. Because both Ni and Mg are compatible in olivine, the crystallisation of olivine rapidly depletes the melt of Ni and Mg. A sulphide liquid will be able to achieve higher Ni concentrations if it interacts with a silicate melt which has not undergone a significant extent of olivine fractionation. For comparison, Figure 5.10 shows MgO versus Co plotted against melt MgO for melts in equilibrium with mantle olivine. It was assumed that mantle olivine has approximately 100 ppm Co (O. Alard, pers. comm.). As in Figure 5.9, the partition coefficients were calculated using the method proposed by Beattie et al. (1991). Figure 5.10 demonstrates that as olivine fractionates, the Co component of the melt diminishes. However, because the partition coefficient for Co is less than that of Ni, the diminution of Co in the melt is much less rapid than that seen for Ni. Consequently, after olivine fractionation has taken place, the concentration of Co in the melt may exceed that of Ni. Figure 5.11 combines figures 5.9 and 5.10 to illustrate the effects of olivine fractionation upon Ni and Co melt concentrations and clearly shows that at around 7% MgO, Co concentration exceeds Ni concentration. Thus, to generate a high

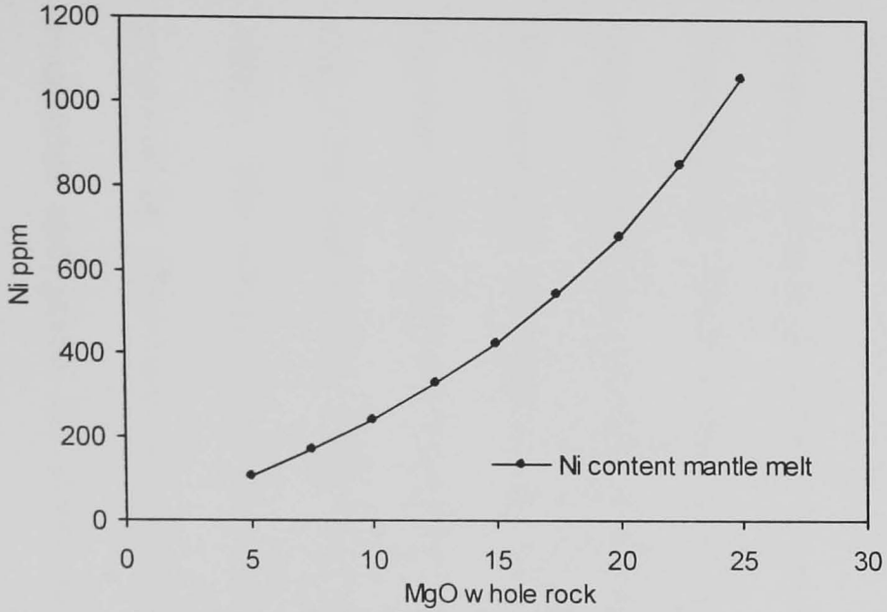

Figure 5.8 Graph of MgO versus Ni for melts in equilibrium with mantle olivine. As the MgO increases the Ni content of the melt also rises. This figure assumes olivine has Fo90 and 3200 ppm Ni (after Beattie et al., 1991)

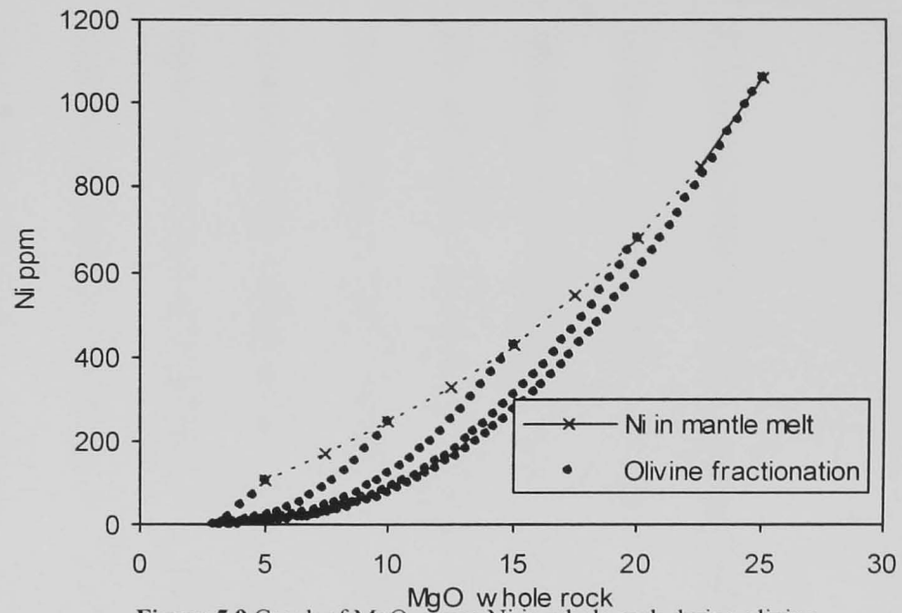

Figure 5.9 Graph of MgO versus Ni in whole rock during olivine fractionation. The starting composition is in equilibrium with mantle olivine and the filled circles represent whole rock Ni content at 1% increments of olivine fractionation.

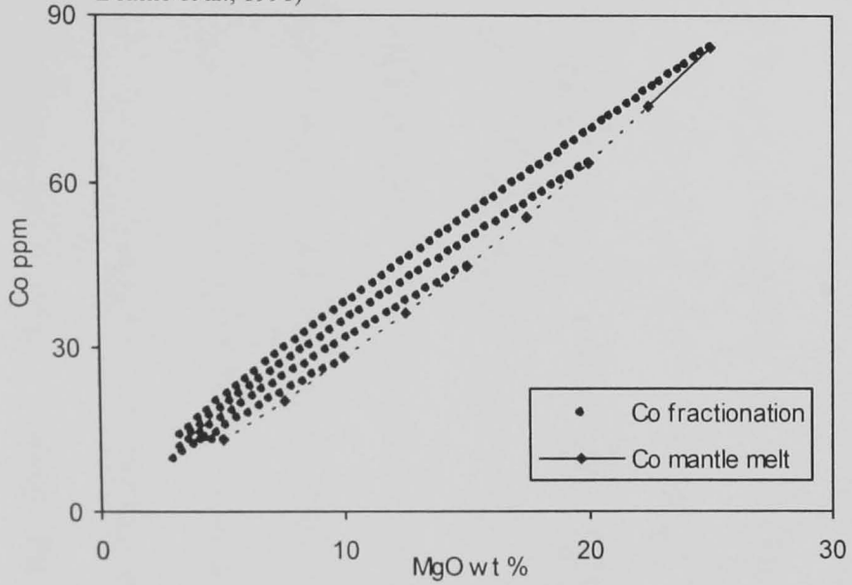

Figure 5.10 Graph of MgO versus Co for starting compositions in equilibrium with mantle olivine. Each solid circle represents 1 % increments of olivine crystallisation. Crystallisation is modelled from starting compositions of 5, 10, 15, 20, and 25% MgO.

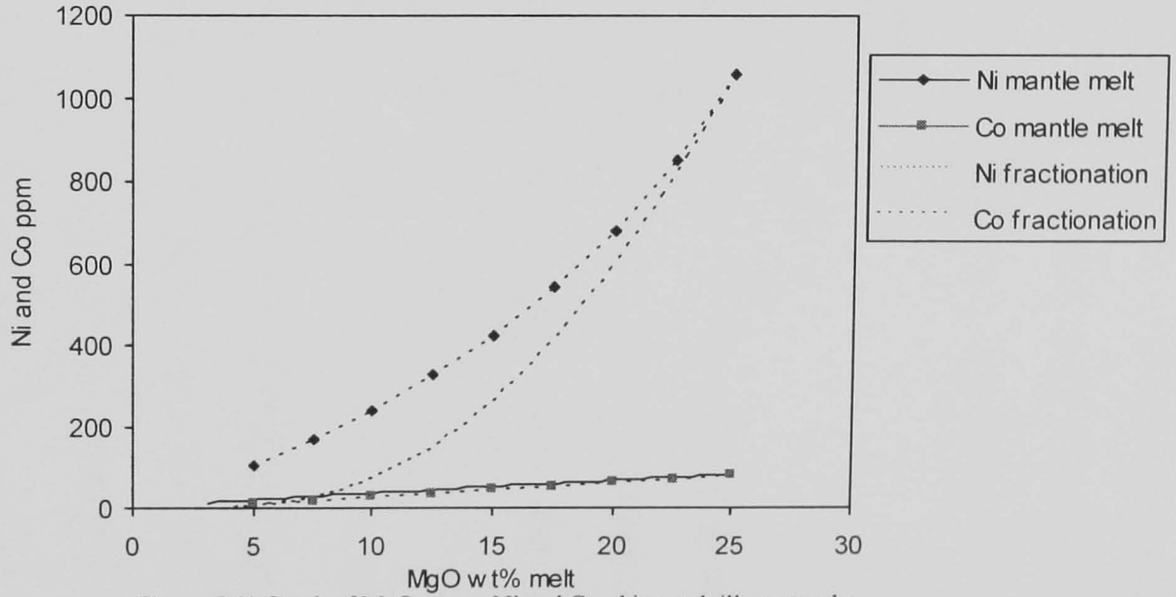

Figure 5.11 Graph of MgO versus Ni and Co, this graph illustrates the effect of crystallising olivine in 1% increments from a starting composition of 25% MgO.

Ni sulphide, the sulphide liquid should interact with a silicate magma that represents high temperature mantle melting and low degrees of olivine fractionation. If a sulphide liquid equilibrates with silicates that have undergone prior olivine fractionation, the resultant sulphide liquid will have a decreased Ni/Co ratio.

5.2.3 Sulphide-silicate partition coefficients and sulphide-silicate ratio (R factor)

Magmatic Ni-sulphides acquire their Ni via interaction with Ni-rich silicate magma. Brenan and Caciagli (2000) found that the partition coefficient for Ni between sulphide and silicate melts was not temperature dependent, a finding supported by the work of Fleet and MacRae (1987, 1988). Brenan and Caciagli (2001) found that the fO_2 and the Ni content of the sulphide liquid exercised strong controls upon the partition coefficient for Ni between olivine and sulphide liquid. In their paper, Brenan and Cacliagli (2000) showed that the partition coefficient for Ni increased linearly with the Ni content of the sulphide liquid and followed a power-law increase with decreasing fO_2. However, this was strongly contradicted in a comment paper by Fleet (2001). Fleet (2001) argued that the results Brenan and Cacliagli (2000) results were spurious and the artefact of experimnetal method. Instead Fleet (2001) maintained that the partition coefficient of Ni between olivine and sulphide liquid was between 25-35 and was independent of the composition of olivine, the Ni content of the sulphide liquid and the fO_2 of the sulphide liquid. Fleet based his argument upon his long record of research in this field and numerous papers on the subject (e.g. Fleet and McRae, 1987; Fleet and MacRae, 1988; Fleet et al., 1977; Fleet and Stone, 1990). The values proposed by Fleet and others of around 25-35 are similar to those proposed by (Rajamani and Naldrett, 1978). Consequently, in the absence of a clear consensus and given the doubt raised on Brenan and Cacliagli (2000), the partition coefficient of Ni between olivine and sulphide is used here 25.

The ratio of silicate to sulphide masses is usually referred to as the R factor (Campbell and Naldrett, 1979). This ratio is a reflection of the volume of the melting event, the mass of sulphide liquid generated, and the physical dynamics of the flow system through which the sulphide and silicate magmas are then transported. In the context of magmatic sulphides, R factor refers specifically to the ratios of sulphide and silicate magmas that have equilibrated, allowing the sulphide to strip the silicate of its chalcophile and siderophile elements. For the greatest silicate to sulphide mass ratio, and hence the greatest possible Ni contents, a sulphide liquid should be transported in turbulent rather than laminar flow. The turbulence ensures that the sulphide liquid has the greatest possible opportunity to equilibrate with a largest possible volume of silicate magma before sulphide silicate segregation (Naldrett, 1999). An alternative process that would allow equilibration is for the sulphide liquid to become segregated in a trap located within a conduit. Successive pulses of chalcophile and siderophile laden silicate magma passing through the conduit equilibrating with the trapped sulphide, increasing the Ni content of the sulphide liquid (Naldrett, 1999).

Figure 5.12a shows the Ni content in ppm of a hypothetical sulphide liquid that has equilibrated with varying masses of silicate magma. In each case, the silicate magma has a fixed Ni concentration, taken from the Ni concentrations calculated for Figures 5.8 and 5.9. The curve with the lowest Ni abundance was derived using the Ni content for the 5% MgO mantle melt in the preceding figures. The remaining curves use the calculated Ni abundances at 10, 15, 20, and 25% MgO respectively. Figure 5.12a confirms that interaction of high Ni silicate magmas with sulphide liquids results in the generation of higher Ni sulphide liquids than if the same interaction were to have taken place with a low-Ni silicate.

Figure 5.12b examines the result of equilibrating a sulphide liquid with a silicate magma that has undergone significant olivine fractionation markedly diminishing the Ni content relative to Co. In this case, the degree of fractionation has driven the Ni and Co to 7 and 20 ppm respectively within the silicate. The result is that the levels of both Ni and Co are less than 300 ppm in the sulphide, with the Co content exceeding that of Ni. It is acknowledged that this model lacks a rigorous treatment of the processes involved in a fractionating magma. This was not the purpose of this model. The primary aim was to demonstrate that it is possible to vary the composition of a sulphide liquid by altering the composition of the silicate liquid from which it derives its chalcophile and siderophile elements.

5.2.4 Fractionation of sulphide liquids

MSS (monosulphide solution) – a high temperature sulphide mineral isostructural with NiAs and with the composition of $Fe_{(1-X)}S$ to $Ni_{(1-X)}S$ - is the first phase to crystallise from a sulphide liquid (Kullerud et al., 1969; Naldrett, 1969). Naldrett, (1969) demonstrated that the oxygen fugacity (fO_2), the sulphur fugacity (fS_2) and the activity of FeO (aFeO) in the silicate melt all had a role in controlling the composition of MSS within the limits defined by the formula $Fe_{(1-X)}S$.

In Figure 5.13a (after Naldrett, 2000), a section of the system Fe-S-O is considered. The aFeO in silicate melts is defined by the activity coefficient, which for FeO is very close to 1 (Roeder, 1974). If a sulphide liquid is in equilibrium with a silicate magma the aFeO will be the same in both (Naldrett et al., 1967). Because the activity coefficient is close to 1, the activity of FeO in silicate liquids may be taken as being equivalent to the mole fraction. If the contribution of Ni and Cu is ignored, the composition of MSS will fall onto

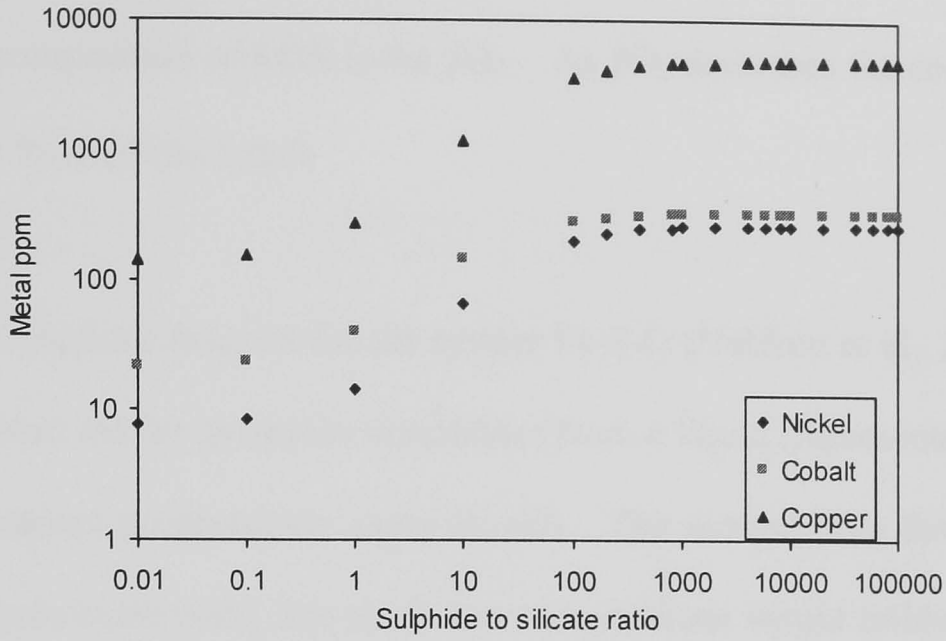

Figure 5.12b Graph of R value versus sulphide metal content for a sulphide melt equilibrating with at silicate magma that has undergone olivine fractionation. Partition coefficient calculated after Beattie et al. (1991).

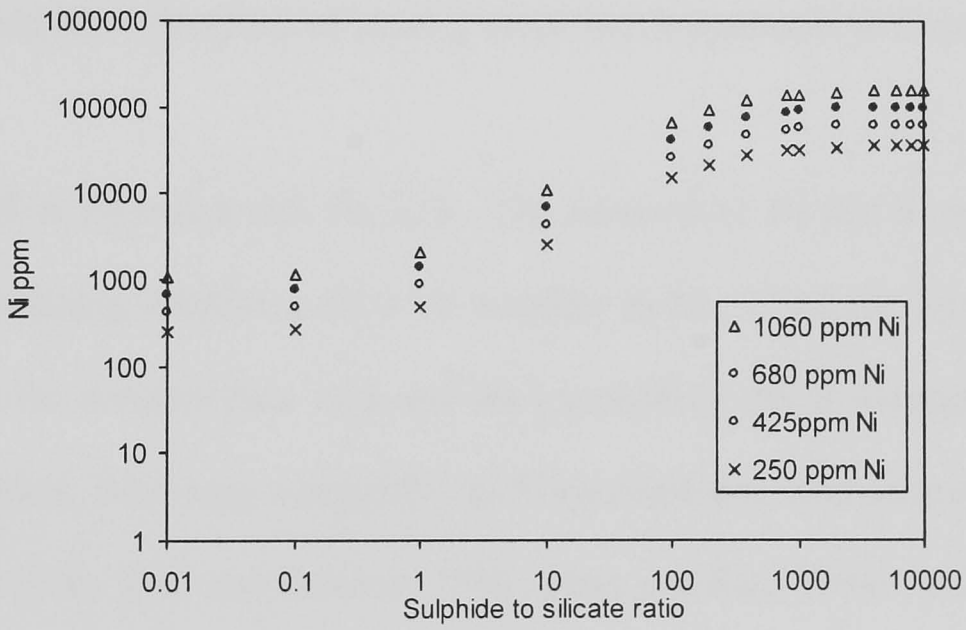

Figure 5.12a Graph of R value for sulphide melts equilibrating with silicate magmas of differing Ni content. After Campbell and Naldrett (1979); Lesher and Burnham (1999).

the curve aFeO = 0.1 for a liquid with 10 mole percent FeO. One of the most important controls on the composition of MSS is the fO_2. As fO_2 decreases the composition of the liquid will move from points 1 to 5.

Figure 5.13b is a liquidus diagram for the system Fe-S-O (Naldrett et al., 2000). From this figure it can be seen that as pyrrhotite crystallises from a liquid (represented by points 1 to 5) the liquid becomes progressively more Fe-rich. The dashed lines from points 1 to 5 represent the approximate paths that pyrrhotite compositions would follow as this mineral crystallises. The arrows on these dashed lines show the direction that the composition of MSS will move as pyrrhotite crystallises. Figure 5.13b implies that as pyrrhotite crystallises from MSS the liquid will be driven to higher values of fO_2 and a higher fO_2 in the liquid would have the effect of causing more S-rich pyrrhotite to form.

The first MSS is Fe and S-rich $Fe_{(1-X)}S$. The removal of Fe and S as MSS crystallises causes the remaining sulphide melt to be enriched in Ni. The behaviour of Ni in MSS is controlled by the concentration of S and the temperature. Ni is incompatible in S under-saturated systems, becoming compatible in S saturated and over-saturated systems (Ebel and Naldrett, 1996; Ebel and Naldrett, 1997; Fleet and Pan, 1994; Li et al., 1996). With increasing S content in MSS, Ni becomes more compatible, the partition coefficient varying between 0.71-1.43 (Ebel and Naldrett, 1997). The reasons for this behaviour are structural; MSS and pyrrhotite share the $Fe_{(1-X)}S$ formula and the same superstructure, similar to the NiAs structure. This $Fe_{(1-X)}S$ solid solution is formed by ordering the vacancies on the Fe position with VI co-ordination (Vaughan and Craig, 1978). This arrangement requires some Fe^{3+} ions in the same layer as the vacancies in order to maintain the charge balance. Thus, the number of vacancies and Fe^{3+} ions increase with the

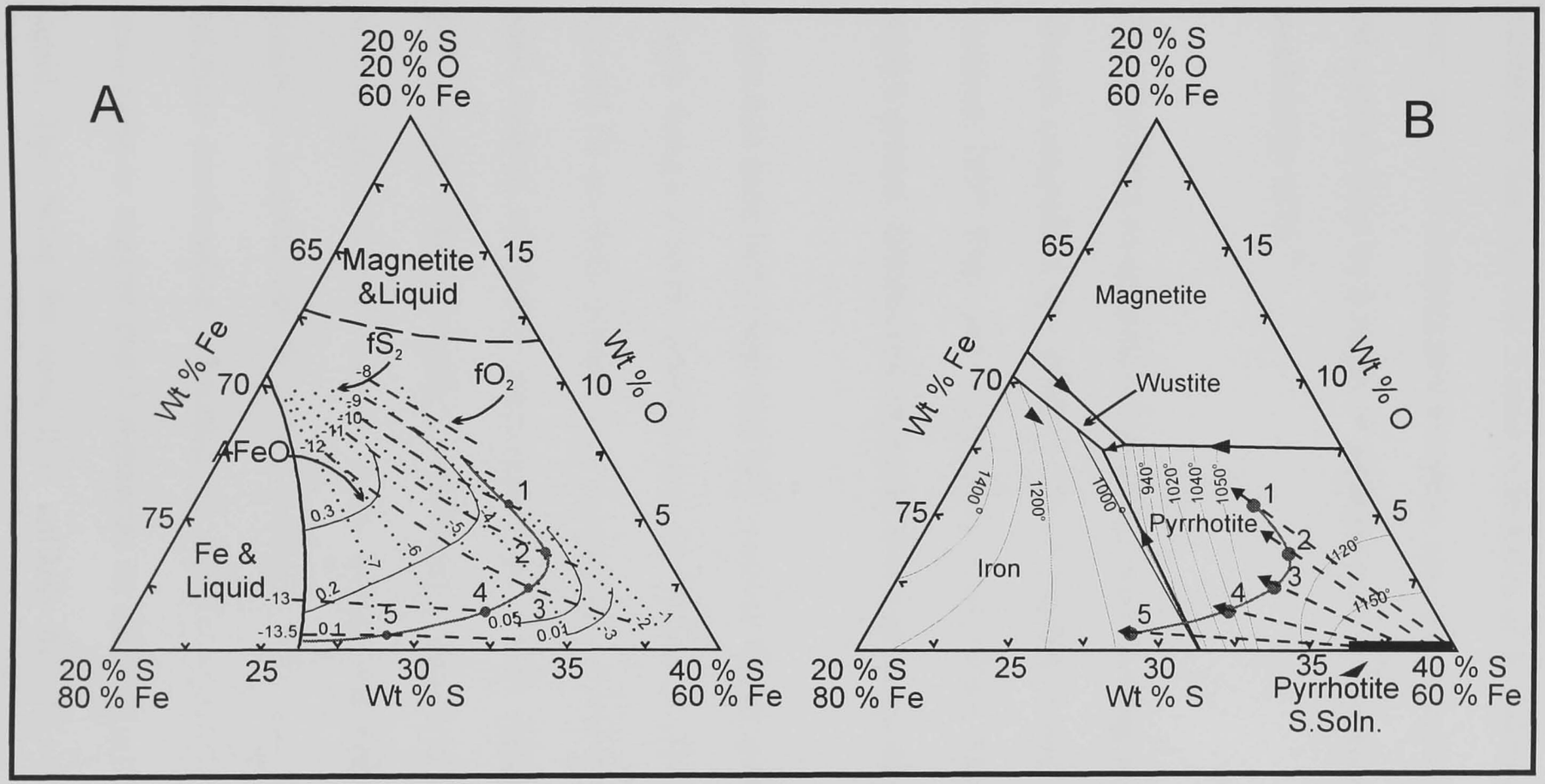

Figure 5.13a A section of the system Fe-S-O at 1100°C where the dashed lines are contours of fO_2, the dotted lines fS_2, and the solid lines are activity of FeO. The points 1-5 represent points of decreasing fO_2 intersecting the aFeO = 0.1 curve.

Figure 5.13b Liquidus diagram for the system Fe-S-O. The dashed lines intersecting the points 1-4 represent the approximate paths that pyrrhotite compositions follow as pyrrhotite crystallises from sulphide liquid. The arrows indicate the direction that the composition of the liquid will move as pyrrhotite crystallises
(after Naldrett, 2000).

S content. The Ni^{2+} ion (0.69Å) is smaller than the Fe^{2+} ion (0.77 Å) but similar to the Fe^{3+} ion (0.64 Å) in octahedral co-ordination (Henderson, 1982). Because of this, it is much easier to incorporate Ni^{2+} into S-rich MSS or pyrrhotite, with abundant Fe^{3+} and site vacancies than into the S-poor defect-free or low-defect equivalent. For two pyrrhotites with similar S contents and therefore similar vacancies on the Fe lattice, variations in the Ni content must be a result of differences in the Ni content of the sulphide liquid and the availability of Fe^{3+}.

The first MSS to crystallise will reflect the S concentration of the sulphide liquid. As S is always compatible into MSS, a high S sulphide liquid results in high S MSS (Ebel and Naldrett, 1997; Fleet and Pan, 1994; Li et al., 1996). This means, for fractionation within a high S system, that the remaining sulphide liquid will be depleted in Fe, Ni, and S.

Little data have been published with regard to the behaviour of Co in the system Fe-Ni-Cu-Co-S, though it seems probable that the behaviour of Co should be similar to that of Ni. Co and Ni are both bivalent ions in sulphide, and their ionic radii are similar; Ni has an ionic radius of 0.69Å compared with 0.75Å for cobalt in six-fold co-ordination (Henderson, 1982). Indeed, Co partitioning behaviour between sulphide and silicate was seen to follow that of Ni in the study of Rajamani and Naldrett (1978), and there is little reason to suppose that these two elements' behaviour should become de-coupled during sulphide fractionation. Because the MSS at Voisey's Bay is high-S and high-Ni, it is reasonable to suggest that it represents an early-stage precipitate from a high-S sulphide liquid. This being the case, it is unlikely that Ni, and perhaps Co would have been incompatible in MSS until the abundance of S in the sulphide liquid had been much diminished.

5.2.5 Variation in Pyrrhotite Fe:S ratio

In Figure 5.2a it was observed that variation in pyrrhotite Fe/S ratio largely conforms to the relationship $Fe_{(1-X)}S$. However, lower Fe contents than predicted by the formula were observed. Figure 5.2c examined the relationship between the mole fraction of S and total metals for pyrrhotite and found that an excellent agreement with the theoretical composition, suggesting that as S increased Fe was being substituted by other metals. This raises two main questions:

1) What controls the ratio of Fe and S?
2) What controls the substitution of Fe by other metals?

Referring to Figure 5.6c, one can see that the pyrrhotite data from the Eastern Deeps form an array. This array has systematic behaviour between 51-52 atomic percent S. At 52 atomic percent S a marked deviation in Delta Po was observed. The gradual decrease in Delta Po with increasing S content is likely to be a response to sulphide liquid fractionation. Fractionation of sulphide liquids increases the sulphide-liquid fO_2, driving pyrrhotite compositions to increasingly S-rich/Fe-poor values. Thus the sudden change in behaviour at 52 atomic percent S must be a manifestation of some other control acting upon the fractionating sulphide liquid.

Several recent studies suggest that there has been considerable interaction between the magmas involved in the genesis of the Voisey's Bay deposit and the sulphidic and graphitic Tasiuyak gneiss, (e.g. Li and Naldrett, 1999; Lightfoot and Naldrett, 1997; Naldrett, 1999). Indeed, Ripley, (1999) suggested that much of the S in the Voisey's Bay sulphides may have been derived from the Tasiuyak gneiss. Naldrett (2000) proposed that different mineralising environments exist at Voisey's Bay and went on to suggest that

when the magmas parental to the Voisey's Bay deposit reacted with the different parts of the Tasiuyak gneiss on a local scale, the resultant sulphide liquids did not become homogenised throughout the system. In the same paper (Naldrett, 2000), postulated that as the Tasiuyak gneiss has an unequal distribution of graphite, it is very likely that some parts of the Voisey's Bay deposit would be more reduced than others. Thus, the sulphides that have formed as a result of interaction with a more graphite-rich representative of the Tasiuyak gneiss will be expected to have a more Fe-rich pyrrhotite than sulphides that have reacted with graphite-poor material.

5.2.5.1 Ni content of Pyrrhotite

As pyrrhotite has many similarities in terms of structure and composition with MSS (Vaughan and Craig, 1978), it is appropriate to consider the compatibility of Ni into MSS as an analogue for the compatibility of Ni into pyrrhotite. In sulphur-poor MSS, Ni is incompatible, partitioning into the coexisting sulphide liquid. In S-rich MSS, this situation is reversed and Ni becomes more compatible into the MSS, fractionating out of the coexisting sulphide liquid (Li et al., 1996).

The discussion in section 5.2.4 demonstrated that Ni substitutes for Fe^{3+} in pyrrhotite and that the abundance of Fe^{3+} and Ni increased in proportion to pyrrhotite S content. The availability of Fe^{3+} is a reflection of the fO_2; a decrease in fO_2 would result in a corresponding lessening in the availability of Fe^{3+}. Consequently, at a given pyrrhotite S content, a decrease in fO_2 would result in increased Ni substitution.

Figure 5.14 is a graph of S versus Delta Po. This diagram is based upon Figure 5.6c, but has had arrows superimposed to illustrate the effects of sulphide fractionation and decrease

in fO_2. As sulphide fractionation progresses, the S content of pyrrhotite rises, in line with the findings of Naldrett (2000), summarised in Figure 5.13b. As long as no external influence alters the fO_2, there will be a progressive increase in S content of pyrrhotite. However, Figure 5.14 illustrates that there is a marked decrease in Delta Po at 52 atomic percent S. Figures 5.2b and 5.2d demonstrated that decreases in Delta Po were linked with increases in Ni content. It is argued here that the increased substitution of Ni for Fe as illustrated in Figure 5.14 is a response to diminished fO_2 - a reduction in fO_2 decreases the availability of the Fe^{3+} ion so allowing Ni substitution. Therefore, when there are sudden increases in Ni content of pyrrhotite at the constant S, this may be the result of an externally induced reduction event. In this case, it seems probable that this is a response to the assimilation of graphitic Tasiuyak gneiss. However, it is evident that much sulphide fractionation had already occurred before the sulphide magma encountered the graphite-bearing Tasiuyak gneiss.

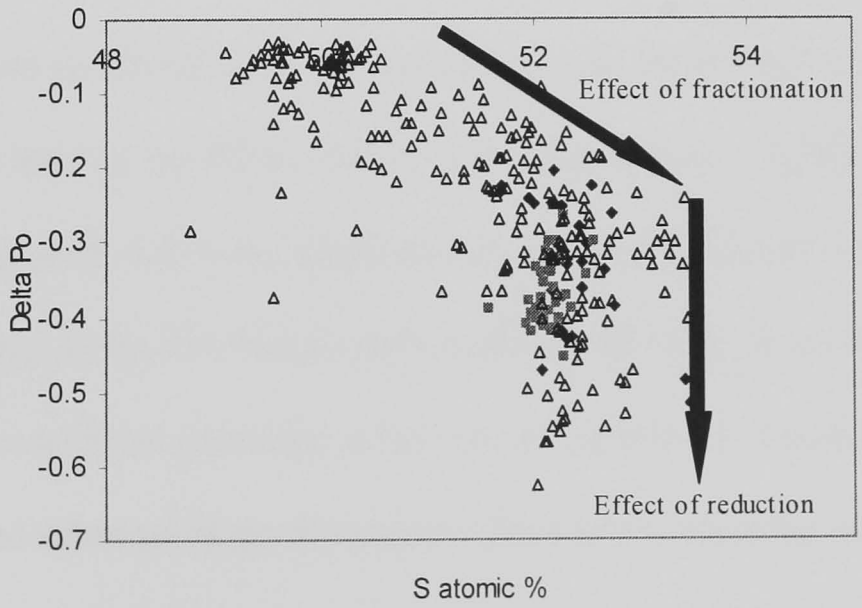

Figure 5.14 Graph of Delta Po versus atomic percent S. This figure has arrows superimposed that indicate the effects of sulphide fractionation and externally influenced fO_2 variation. This is particularly developed at 52 atomic percent S.

5.2.6 Exsolution of pentlandite

The Ni in sulphide liquids is more compatible at high temperatures and low S concentrations, whereas in MSS the reverse is true (Li et al., 1996). As Ni-Cu magmatic sulphide liquids solidify the earliest mineral to crystallise is MSS (Naldrett et al., 2000). After MSS has crystallised from the sulphide liquid, the Ni which is incompatible in the NiAs type structure begins to exsolve (Sugaki and Kitakaze, 1998). Sugaki and Kitakaze (1998) found that an unquenchable high temperature form of pentlandite with a cubic unit cell exists with an upper stability limit of 865°C. This is in marked contrast with the work of Kullerud (1964) who found that pentlandite had an upper stability limit of around 610°C. Sugaki and Kitakaze (1998) proposed that the upper stability limit described by Kullerud (1963) represented the transition from a high to low form. Therefore, for the Voisey's Bay intrusion, which has a solidification temperature of over 1000°C (Naldrett et al., 2000), pentlandite formed not as a liquidus phase but via a solid solution process.

Pentlandite forms via a solid solution process from MSS. Ni and Co fractionate preferentially into pentlandite. In ideal conditions all the Ni and Co in MSS will diffuse into pentlandite leaving the MSS with $Fe_{(1-X)}S$ composition. Therefore, the timing and rate of pentlandite growth will have implications for the Ni content of the remaining MSS. Because pyrrhotite is the low-temperature analogue of MSS, the composition of pyrrhotite will reflect the conditions prevalent at the time of pentlandite exsolution. This is providing there has been no subsequent metamorphism that has modified the sulphide compositions.

As temperature falls, the stability field of MSS retreats to more S-rich compositions (Kelly and Vaughan, 1983). In experimental studies it has been demonstrated that homogenous MSS will exsolve pentlandite if it is annealed at temperatures below 600°C (Kelly and

Vaughan, 1983), and the remaining MSS will move towards a more Fe-poor, S-rich composition as a result (Kelly and Vaughan, 1983). If the MSS is then allowed to cool further, this process of pentlandite exsolution continues and the MSS becomes progressively more Fe-depleted and S-rich.

The compositions and the structures of the MSS phase and pentlandite differ greatly. The former has the NiAs type structure, and the latter has a cubic structure with the metals in tetrahedral co-ordination (Vaughan and Craig, 1978). Consequently, the exsolution of pentlandite from MSS requires that a nucleation event take place. This nucleation event requires that small clusters of atoms agglomerate and stabilise with the pentlandite structure within the MSS matrix. This involves the diffusion of Fe and Ni, and to a lesser extent S, atoms through the MSS lattice. For this to occur necessitates the operation of some driving force. The nature of this force may be appreciated by studying Figure 5.15 from Kelly and Vaughan (1983). This shows the solvii for MSS and pentlandite in terms of atomic percentage S plotted against temperature in °C. As the temperature falls, the MSS + pentlandite solvus retreats to more S-rich compositions. Consider a MSS with 50.65 atomic percent S at approximately 500°C. It can be seen that this composition would fall onto the MSS plus pentlandite equilibrium. If the temperature were then to fall to 400 °C where the equilibrium composition is 51 atomic percent S. The MSS composition of 50.65 atomic percent S would not be in the equilibrium, forcing the system to exsolve Fe and Ni to reduce the metal sulphide (Me:S) ratio and regain equilibrium. Thus, there is a net driving force for exsolution. The nature of this force is - ΔG_{vol} (Kelly and Vaughan, 1983). It can be seen from Figure 5.15, for exsolution to proceed there must be a degree of under-cooling below the MSS-pentlandite solvus. As the degree of under-cooling increases so does the driving force for exsolution, and hence the rate of pentlandite growth.

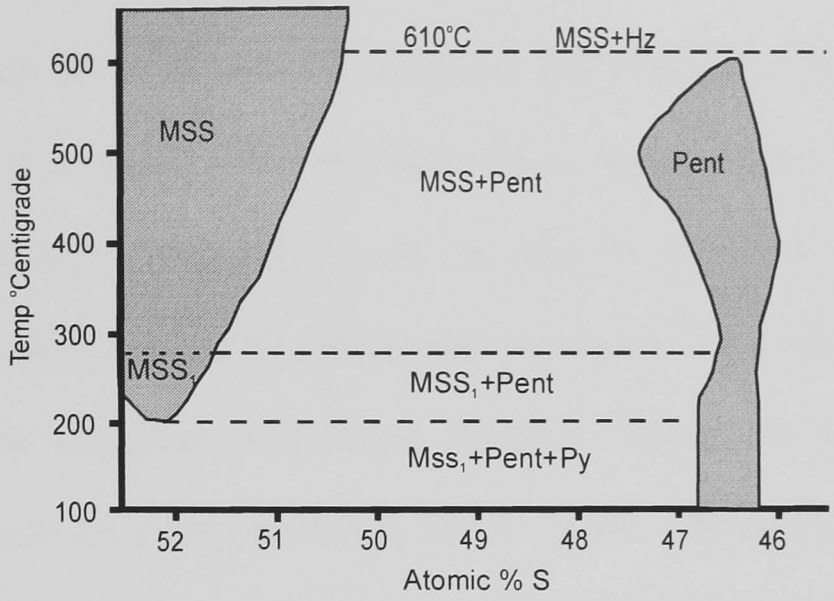

Figure 5.15 MSS and pentlandite solvii in terms of atomic percent S and temperature in °C. The uppermost dotted line represents the upper stability limit according to Kullerud (1963). The two lower dotted lines represent the fields of stability for MSS and pentlandite and MSS plus pentlandite plus pyrite. (After Kelly and Vaughan, 1983)

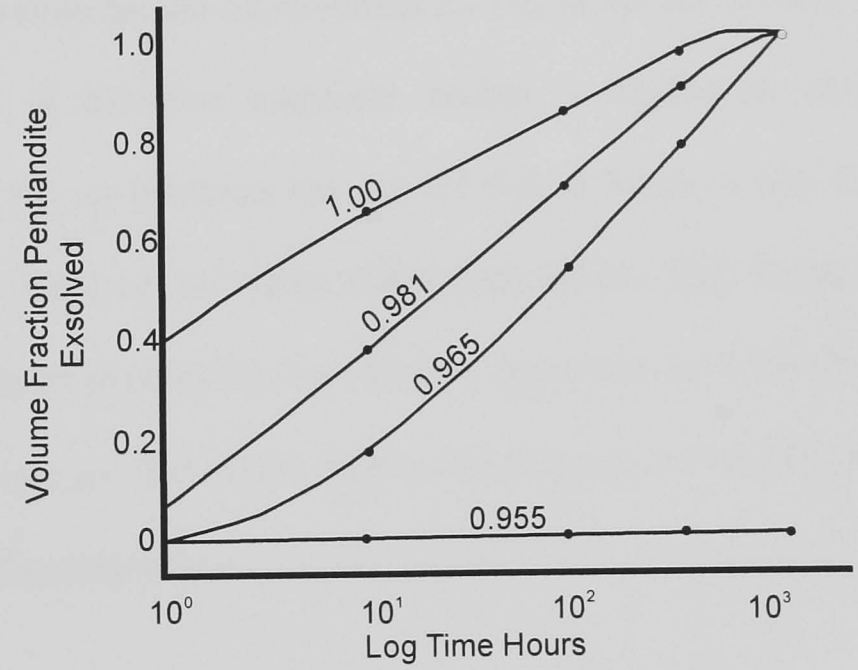

Figure 5.16 Volume fraction pentlandite exsolved against log time in hours at 400°C. The traces represent different Me:S ratios and illustrate that as the Me:S ratio increases so does the exsolution rate (from Kelly and Vaughan, 1983).

The composition of the MSS has an effect upon the rate of pentlandite exsolution. Figure 5.16 is a plot of volume fraction of pentlandite exsolved plotted against log time in hours for a variety of MSS compositions with the same Fe:Ni ratio at 400 °C. Examination of this figure reveals that as the Me:S ratio increases, the observed rate of pentlandite exsolution also increases (Kelly and Vaughan, 1983). At 400 °C. the equilibrium composition is 51.16 atomic percent S, Me:S = 0.955. The exsolution for this composition is plotted onto the figure and remains at zero throughout the duration of the analyses because no pentlandite is exsolved.

An important point to raise is the timescales of equilibration implied by Figure 5.16. The maximum duration for the equilibration for any of the Me:S ratios are under 10^3 hours. The cooling time of intrusive magmatic bodies is dependent upon size and temperature gradient, but for an intrusion the size of that at Voisey's Bay the cooling time must be measured in terms of 10^3 years rather than hours. This being the case, given that the exsolution rate of pentlandite from MSS is dependent upon the degree of under-cooling, it might be expected that all the Ni would be exsolved from the MSS lattice and be present in the form of pentlandite.

5.2.7 Compositional variation of pentlandite

The composition of pentlandite varies in two ways. Firstly, the Fe content of Voisey's Bay Intrusion pentlandite varies between $Fe_{0.40\text{-}64}$. Secondly, the Ni within pentlandite undergoes a variable amount of substitution by Co. For the Voisey's Bay intrusion the Co content of pentlandite varies between 0.246-7.41 atomic percent. These observations raise three questions:

1) What controls the Fe/Ni ratio of pentlandite?

2) What controls the Co content of pentlandite?

3) What insights can this give us into the genesis of magmatic sulphides?

5.2.8 Fe, Ni, and Co variation in pentlandite

The Fe/Ni ratio in pentlandite is controlled largely by the amount of Ni that is available during the exsolution of pentlandite from MSS (Riley, 1977; Ueno, 2000; Durazzo and Taylor, 1982). Similarly, the behaviour of Co in pentlandite is not governed by the fS_2 or temperature but reflects the Co content of MSS from which the pentlandite exsolved (Kaneda et al., 1986). Because the pentlandite at Voisey's Bay has high Ni/Co ratios and Fe/Ni ratios that are close to equality, this suggests that the sulphides were not the product of extreme fractionation.

5.2.9 Metal contents of 100 percent sulphide

When investigating the nature of the silicate melt from which a magmatic sulphide is derived, it is usually the Ni/Cu ratio in 100 percent sulphide that is considered (e.g. Naldrett, 1989). This is usually measured on whole rocks using techniques such as XRF, INAA, ICP-MS and Leco furnace analysis. As was stated in the introduction, this gives different insights from those using the ultra-detailed approach of electron microprobe analysis of individual sulphide grains that has been undertaken here. However, it is useful at this stage to compare the data presented in this chapter, with published whole rock analysis of metals in 100 percent sulphide from the various magmatic sulphide deposits around the world and unpublished whole rock sulphide data for the Voisey's Bay deposit.

Figure 5.17 presents the Voisey's Bay whole rock data renormalised to 100 percent sulphide with data from komatiite- and flood basalt-hosted deposits from around the world (data from Naldrett, 1989).

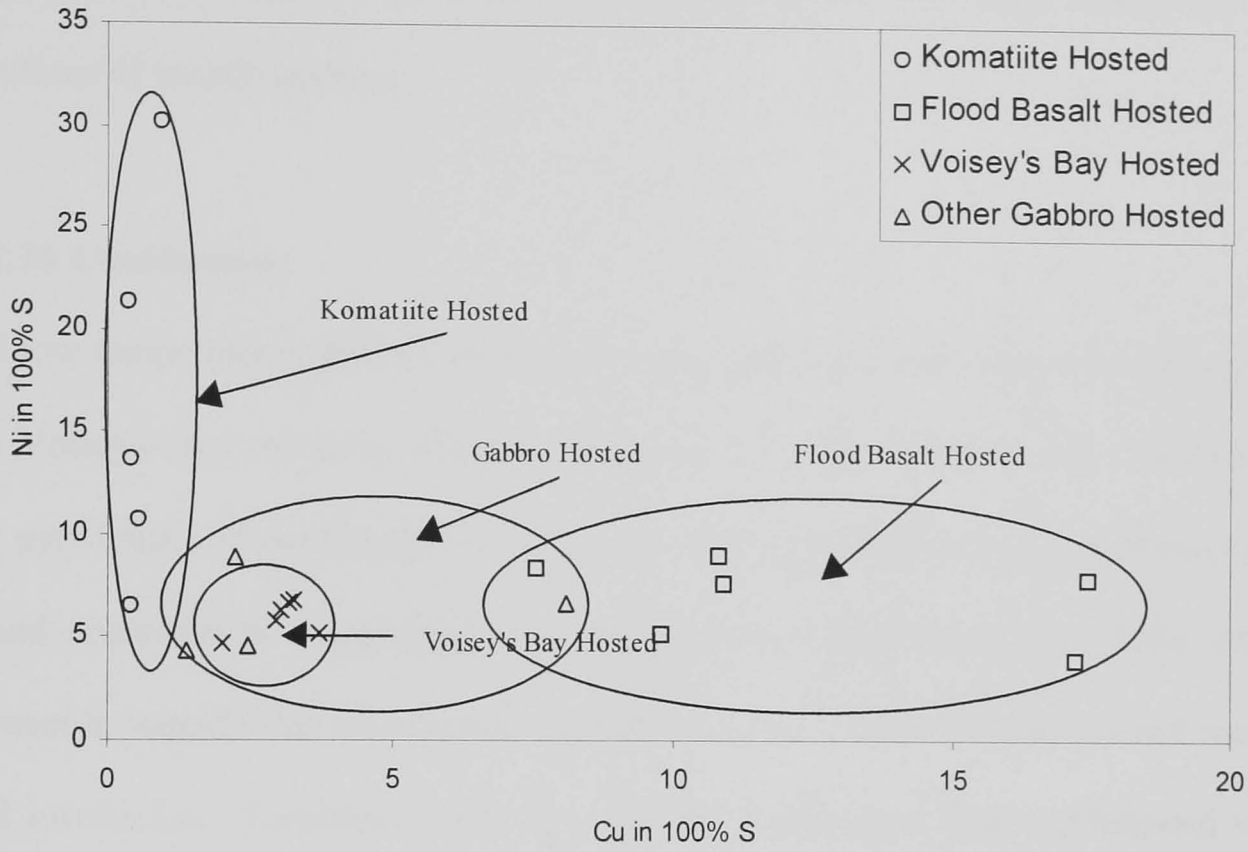

Figure 5.17 Graph of Cu in 100 percent S versus Ni in 100 percent S for flood basalt, komatiite and Voisey's Bay hosted sulphides. The in terms of Ni/Cu ratios the Voisey's Bay sulphides are intermediate to flood basalt and komatiite hosted sulphides. The implication is that the Voisey's Bay sulphides are derived from a melt with higher Mg# the flood basalts.

It is clear that the komatiite-, Gabbro-, and flood basalt-hosted deposits occupy quite different areas of the graph. However, the Voisey's Bay data coincide with the Gabbro-hosted towards the komatiite-hosted end of the field. The Ni contents of a mafic silicate melt are related to the Mg# (see chapter 4), and because Cu is incompatible in olivine (Beattie et al., 1991) as the Mg# of a melt increases, so will its Ni/Cu ratio. Thus, the arguments presented in chapter 4 and Figure 5.17 suggests that deposits with a high Ni/Cu ratio are derived from melts with high Mg#s. Therefore, the Voisey's Bay deposit must have been derived from interaction with a high-Mg# melt. An additional facet to this argument is that the Voisey's Bay sulphides are low in PGEs (Lightfoot, P. C., pers.

comm.). Keays (1995) suggested that magmatic sulphide liquids that are low in the PGE are derived from restricted degrees of mantle melting – as long as there are residual sulphides in the source the PGEs are retained in the restite. Thus, the inference is that the Ni and PGE contents of the Voisey's Bay sulphides are the result interaction with small fractions of mantle melting.

5.2.10 Conclusions

All low temperature sulphide phases exsolve in the solid state. Because the cooling rate of the Voisey's Bay intrusion allowed sufficient time for exsolution and diffusion processes, the pyrrhotite and pentlandite compositions have to be considered with respect to sulphide liquid composition. Consideration of pentlandite compositions and Ni/Cu ratios in 100 percent S, suggest that the sulphide liquid from which the MSS was derived was rich in Ni and low in Co. To achieve this, the sulphide liquid must have equilibrated with a high Mg#, high Ni, relatively unfractionated silicate magma. In addition, the PGE contents of the sulphides suggest that the fraction of mantle melting that donated the Ni to the sulphides was restricted.

Because the pyrrhotite at Voisey's Bay is high S and high Ni this implies that the MSS was the result of early crystallisation from a sulphide melt. The pyrrhotite compositions in the Eastern Deeps suggest that the main control on the fO_2 within the sulphides was sulphide fractionation. There is evidence of an extended period of sulphide fractionation taking place before an abrupt change in fO_2. This change in fO_2 has been interpreted as resulting from the assimilation of graphitic Tasiuyak gneiss. Therefore, as there was a sulphide liquid present before assimilation of Tasiuyak gneiss, the Tasiuyak gneiss cannot have caused sulphide immiscibility.

Chapter 6

Pb-Pb Isotope Variation in Voisey's Bay Intrusion Sulphides and Silicates

6.1.1 Introduction

This chapter uses Pb isotopes to investigate the contamination history of the Voisey's Bay sulphides. It builds upon a small-scale study carried out for INCO by the University of Toronto on sulphides from the Tasiuyak gneiss-hosted sulphides and Voisey's Bay intrusion-hosted disseminated and massive sulphides. This initial study used 10 samples taken from two diamond drill cores at the Reid Brook Zone and three from the Ovoid. The Tasiuyak sulphides were exclusively from the Reid Brook Zone, while the magmatic sulphide samples were taken from the two Reid Brook Zone cores and an additional three from the Ovoid. In contrast, this new study examines the Pb isotopes of the Voisey's Bay sulphides in much more detail with 26 different samples taken from 12 diamond drill cores. The samples used include Tasiuyak gneiss sulphides that have been collected from six different locations across the deposit. Similarly, the analysis of the intrusive rock-hosted sulphides uses disseminated and massive samples from locations right across the Voisey's Bay deposit. Full details of the locations and depths from which the samples were collected are provided in Appendix A. In addition, Figure 6.1 is a sketch map of the Voisey's Bay intrusion and the locations of the sampled diamond drill holes for both the INCO and Open University samples are shown.

Two types of study can be performed using Pb isotopes: age determinations and estimation of the initial Pb isotopic composition of samples to gain insights into the sources of their lead. Here, Pb isotopes are used for the latter purpose, as the age of the Voisey's Bay deposit is well constrained at 1.333±0.001 Ga using U/Pb systematics on baddeleyite (Amelin et al., 1999).

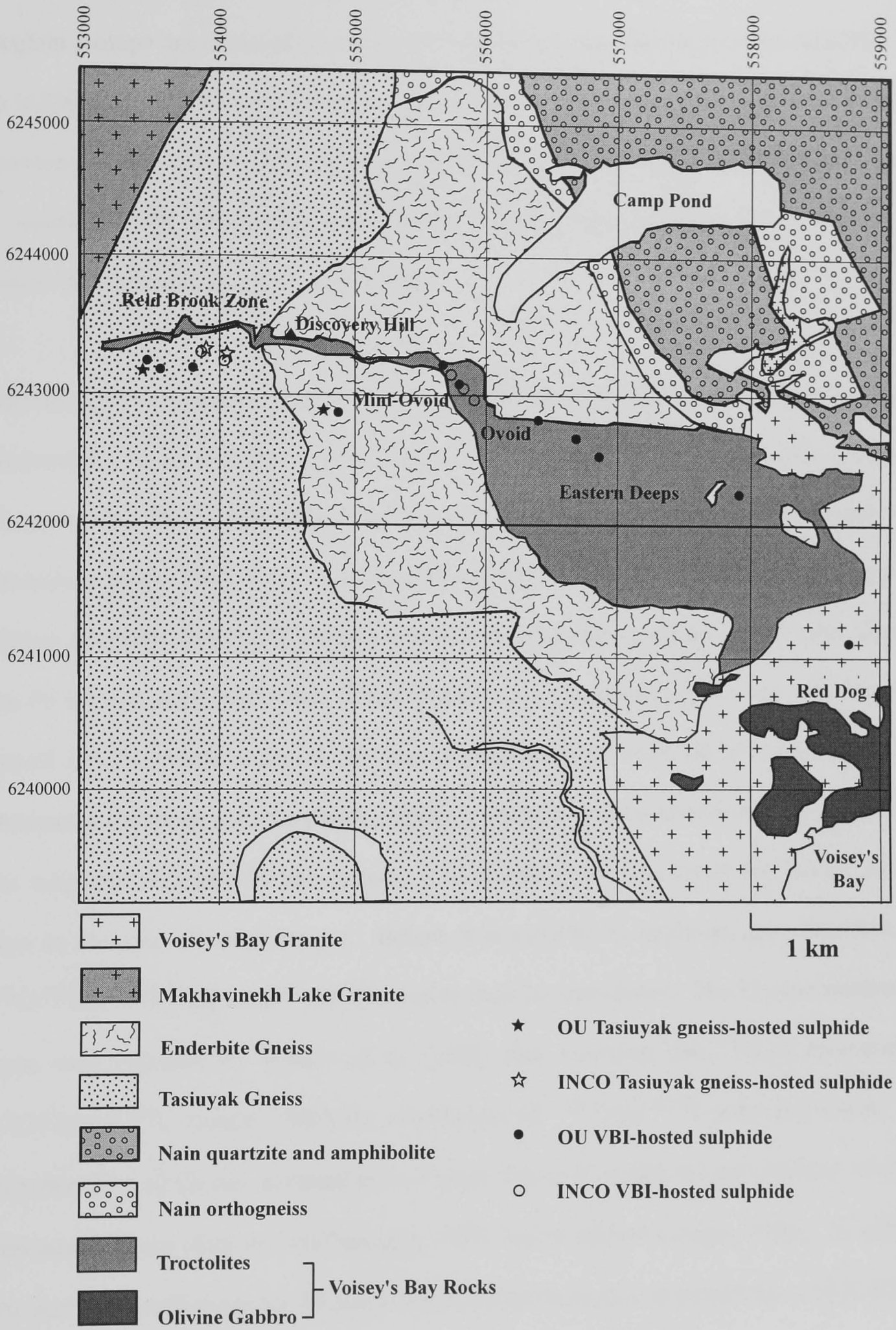

Figure 6.1 Map of the Voisey's Bay deposit with the names of the different areas, also illustrated are the locations of the diamond drill holes from which samples were taken. The prefixes OU and INCO refer to the analyses locations, see text for details. Redrawn from Voisey's Bay Nickel Company data.

Unlike other commonly used decay systems such as Re-Os, where both parent and daughter isotope are chalcophile and Sm-Nd where parent and daughter are lithophile, in the U-Th-Pb system the parent elements are lithophile and daughter element is chalcophile. Because Pb is present in both sulphide and silicate lithologies the U-Th-Pb system is ideal to investigate the relationship between the Voisey's Bay intrusion, the sulphides, the mantle-derived melt, and the country rocks.

Sulphides are considered to have so little U and Th that radiogenic Pb growth can be discounted. As an illustration of this point, analyses of sulphides in meteorites provided the primordial Pb isotope ratios used for current estimates of the age of the Earth (e.g. Tatsumoto et al., 1973; Chen and Wasserburg, 1983). However, this is not the case for silicate minerals; their U-Th contents are such that radiogenic decay significantly changes the Pb isotope ratios with time. Consequently, in a magmatic system, the sulphides will record the Pb isotope ratios at the time of emplacement while the silicate minerals Pb isotopes will change with the passage of time. Therefore, when considering Pb isotope data for magmatic sulphide-silicate systems it is necessary to age-correct the silicate isotope date to the date of emplacement. Before it is possible to apply an age correction, the $^{238}U/^{204}Pb$, $^{235}U/^{204}Pb$, and $^{232}Th/^{204}Pb$ ratios must be considered. The U concentrations in ppm were included by Amelin et al. (2000) and assuming that ^{235}U is equivalent to 1/137.88 of ^{238}U (Faure, 1986) the abundances of ^{235}U and ^{238}U were calculated. The concentration of Th was assumed to be 3 times that of U as this is representative of crustal and mantle rocks (Sun and McDonough, 1989; Taylor and McLennen, 1985). In addition, the partition coefficients for Th and U are found quite similar in plagioclase and K feldspar in the rock types found at Voisey's Bay (McKenzie and O'Nions, 1991).

In Chapter 2, it was demonstrated that for a mantle-derived melt to generate an immiscible Ni-rich sulphide it was necessary to contaminate the magma with additional S or SiO_2. In

sufficient quantity, both will induce the generation of an immiscible sulphide. At present, most authors favour the Tasiuyak gneiss as the contaminant that induced sulphide saturation (e.g. Lambert et al., 2000; Li et al., 2000; Li and Naldrett, 1999; Li and Naldrett, 2000; Naldrett, 1997; Ripley et al., 1999; Ryan, 1995; Wilton, 1996). Reasons for this include textural observations, sulphur and Re-Os isotopic evidence, and that the Tasiuyak gneiss is sulphide-bearing. However, in Chapter 3, data were presented that demonstrated the magmas parental to the Voisey's Bay intrusion were contaminated predominantly with Nain gneiss (~15 percent) and very minor quantities of Tasiuyak gneiss (~3 percent).

Because the Voisey's Bay intrusion was derived from a mantle-melt (*c.f.* Chapter 3), and the sulphides at Voisey's Bay are the result of contamination of that melt with either sulphur and/or silica, the Pb isotope profile of the Voisey's Bay sulphides should lie on a mixing line between the Pb isotopic composition of the mantle-melt and the contaminants. Therefore, the approach taken in this chapter is to compare the Pb isotope composition of sulphide and silicate samples from the Voisey's Bay intrusion and the local gneisses. Because the Nain, Tasiuyak, and Enderbite gneiss all have different histories, and the U-Th-Pb system is sensitive to intracrustal differentiation processes (Doe and Zartman, 1979), the gneisses will have differing Pb isotope ratios. Thus, comparison of the initial Pb isotope ratios of the sulphides and silicates of the Voisey's Bay intrusion with those of the country rocks will highlight which has been the contaminant that generated an immiscible sulphide liquid.

To provide a basis for comparison, the Stacey and Kramers (1975) two-stage growth curve and the expected Pb-Pb gradients for a 1.33 Ga mantle-derived melt have been included. The 1.33 Ga gradient was calculated using $^{235}U/^{204}Pb$, $^{238}U/^{204}Pb$, and $^{232}Th/^{204}Pb$ starting parameters for Stacey and Kramers (1975) second stage. If the Voisey's Bay intrusion rocks were the product of only mantle melting, they will plot on or near the $^{206}Pb/^{204}Pb$

versus $^{207}Pb/^{204}Pb$ gradients calculated using the Stacey and Kramers (1975) starting parameters for a 1.33 Ga melt. However, as it is believed that the Voisey's Bay intrusion magmas are the product of mantle-derived melt contaminated with various crustal rocks, provided the compositions of the contaminants differ from the mantle in terms of their Pb isotopes, contamination of a mantle-derived melt will cause a deviation from the gradient calculated according to Stacey and Kramers (1975).

The equations used to calculate the initial Pb isotope ratios in the silicates were of the form:

$$\left(\frac{^{206}Pb}{^{204}Pb}\right)_P = \left(\frac{^{206}Pb}{^{204}Pb}\right)_I + \frac{^{238}U}{^{204}Pb}\left(e^{\lambda_{238}t} - 1\right)$$

Where λ_{238} is the decay constant for ^{238}U (1.55125×10^{-10}, Faure, 1986), and t is the time since closure of the system in years. The subscripts *P* and *I* refer to present and initial ratios respectively. The appropriate decay constants and isotope ratios were inserted following Faure (1986).

6.1.2 Sources of data

The Pb isotope data for sulphides are derived from two different sources. The first set was collected at the Open University using MC-ICP-MS. The other was made available by Dr Peter C. Lightfoot (PCL) at INCO Technical Services Limited. Both sets are unpublished. The Pb isotope data collected at the Open University and those supplied by PCL are presented in Appendix A. The methodology of the Pb isotope sample preparation and information on reproducibility are presented in Appendix B.

6.1.3 Data presentation

Figure 6.2 presents a graph of Eastings versus Δ Pb for the data analysed on behalf of INCO and at the Open University. The Eastings are the east-west UTM co-ordinates of the drill holes sampled during the programme of Pb isotope analyses. The notation Δ Pb is the difference between the measured $^{207}Pb/^{204}Pb$ ratio of a given sample and the 1.33 Ga isochron for the same $^{206}Pb/^{204}Pb$ ratio.

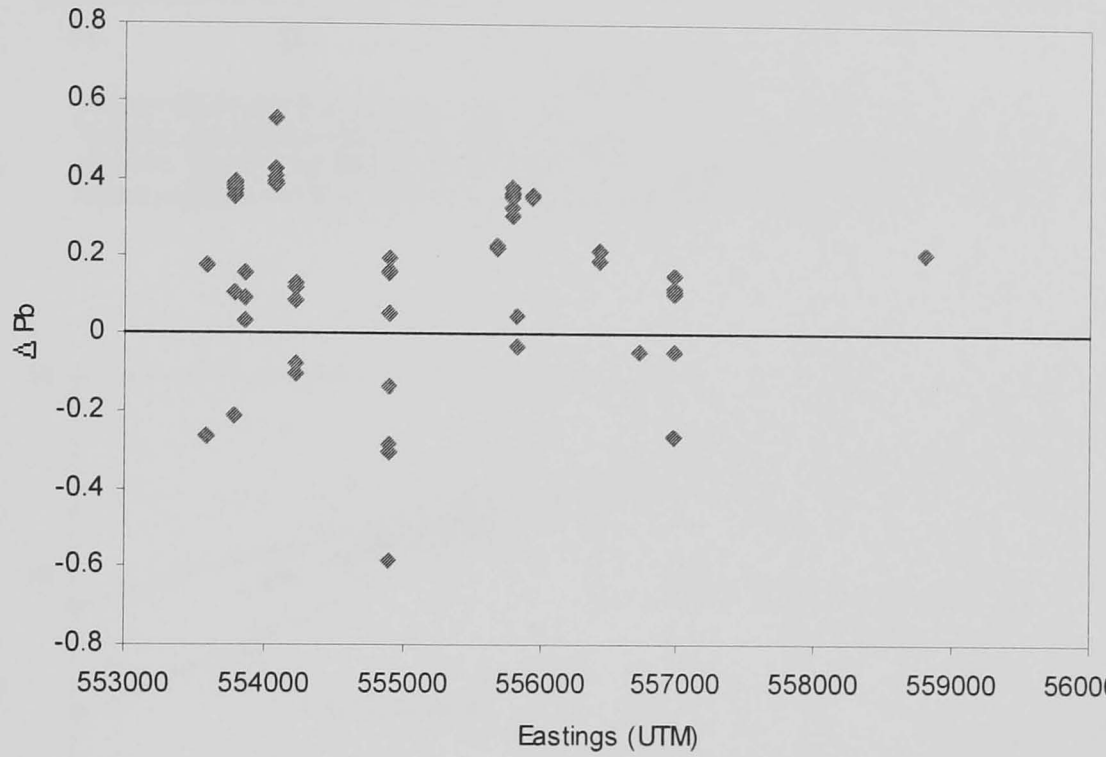

Figure 6.2 Graph of east west UTM co-ordinate versus Δ Pb for all OU and INCO sulphide samples analysed during the Pb isotope investigation. The Δ Pb is the difference between the observed $^{207}Pb/^{204}Pb$ ratio and that for the 1.33 Ga isochron. There is no correlation between sample location and $^{207}Pb/^{204}Pb$ ratio.

Figure 6.3a is a graph of present day $^{206}Pb/^{204}Pb$ versus $^{207}Pb/^{204}Pb$ for Voisey's Bay and Tasiuyak gneiss hosted sulphides. The filled symbols represent the data collected at the Open University, while the open symbols represent that data collected at the University of Toronto. The crosses labelled *OU Reproducibility* and *INCO Reproducibility* represent the errors on repeated analyses of NBS981 carried out at the Open University and the University of Toronto respectively. The error bars represent two standard errors. The VBI and Tasiuyak gneiss hosted sulphide data form a secondary isochron at a lower gradient and scattering below the 1.33 Ga isochron. The Voisey's Bay intrusion and Tasiuyak gneiss data overlap, but the Tasiuyak gneiss data appear to consist of two groups, one group that

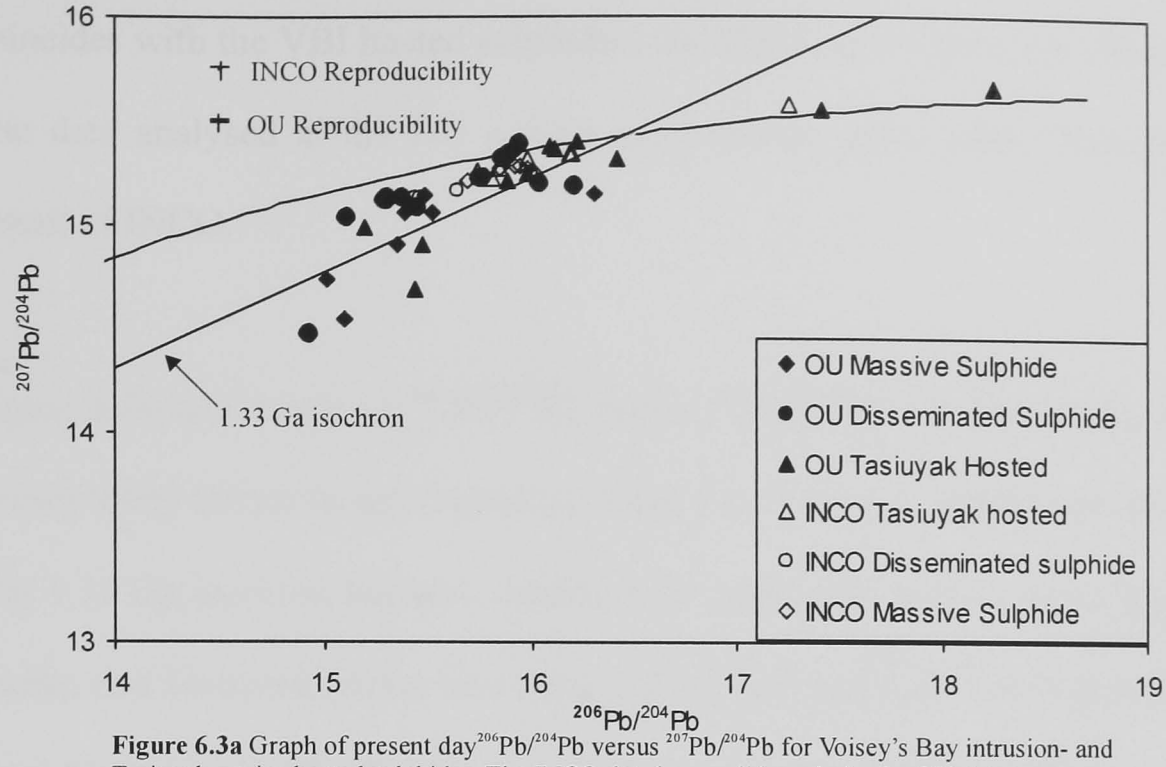

Figure 6.3a Graph of present day $^{206}Pb/^{204}Pb$ versus $^{207}Pb/^{204}Pb$ for Voisey's Bay intrusion- and Tasiuyak gneiss-hosted sulphides. The INCO data have solid symbols, the OU data open symbols. The VBI and Tasiuyak gneiss ranges of Pb isotope values overlap, but the Tasiuyak-hosted sulphides extend to more radiogenic values of $^{206}Pb/^{204}Pb$ and $^{207}Pb/^{204}Pb$.

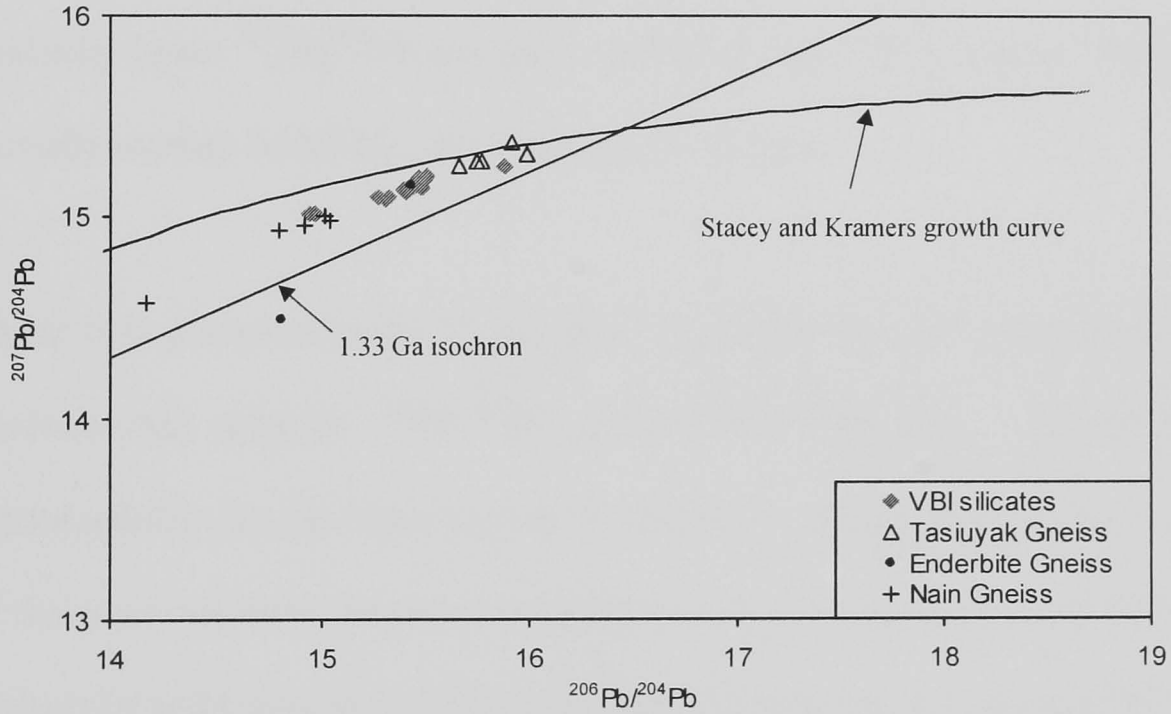

Figure 6.3b Graph of $^{206}Pb/^{204}Pb$ versus $^{207}Pb/^{204}Pb$ at 1.33 Ga for the silicates as analysed by Amelin et al. (2000). The Voisey's Bay intrusion and Enderbite gneiss silicates have coincident Pb isotope profiles. The Tasiuyak gneiss has noticeably higher $^{206}Pb/^{204}Pb$, but this is less pronounced in terms of $^{207}Pb/^{204}Pb$.

coincides with the VBI hosted sulphides, the other with much more radiogenic $^{206}Pb/^{204}Pb$. The data analysed at the OU exhibit considerably more scatter than those analysed on behalf of INCO.

Figure 6.3b is a graph of $^{206}Pb/^{204}Pb$ versus $^{207}Pb/^{204}Pb$ for the silicate minerals from the Voisey's Bay intrusion and Enderbite, Nain, and Tasiuyak gneisses recalculated to 1.33 Ga. The 1.33 Ga isochron has been included for reference. The Voisey's Bay intrusion, Nain gneiss, and Tasiuyak gneiss data form a secondary isochron with a gradient less steep than the 1.33 Ga isochron. The least radiogenic end of the secondary isochron is formed by the Nain gneiss and the most radiogenic by the Tasiuyak gneiss. Of the two Enderbite gneiss data, one is coincident with the VBI silicates; the other has similar $^{206}Pb/^{204}Pb$ but distinctly lower $^{207}Pb/^{204}Pb$ and plots well below the 1.33 isochron. The VBI silicate data partially overlap both Nain and Tasiuyak gneiss data.

Figure 6.4a presents the INCO and Open University Voisey's Bay intrusion- and Tasiuyak gneiss-hosted sulphide $^{206}Pb/^{204}Pb$ versus $^{208}Pb/^{204}Pb$ data. As for Figure 6.3a, the reproducibility for the Open University and INCO data is presented as a cross. The limbs of the cross represent the two standard errors on repeated analyses of NBS981 at the Open University and University of Toronto. Taken as a whole, the sulphide Pb isotope data form an array generally slightly above the 1.33 Ga isochron, albeit an array with a distinct bulge to higher $^{208}Pb/^{204}Pb$ at $^{206}Pb/^{204}Pb$ ~16. Similarly to Figure 6.4a, the Tasiuyak gneiss-hosted sulphide data overlap those of the Voisey's Bay intrusion, but appear to comprise two groups; one coincident with the VBI sulphides and one with more radiogenic $^{206}Pb/^{204}Pb$ and $^{208}Pb/^{204}Pb$ ratios. However, it appears that the gradient on which these data plot is close to that of the main group of points. In contrast, the data presented in Figure 6.4b, the VBI, Nain, Tasiuyak and Enderbite gneiss silicate $^{206}Pb/^{204}Pb$ versus

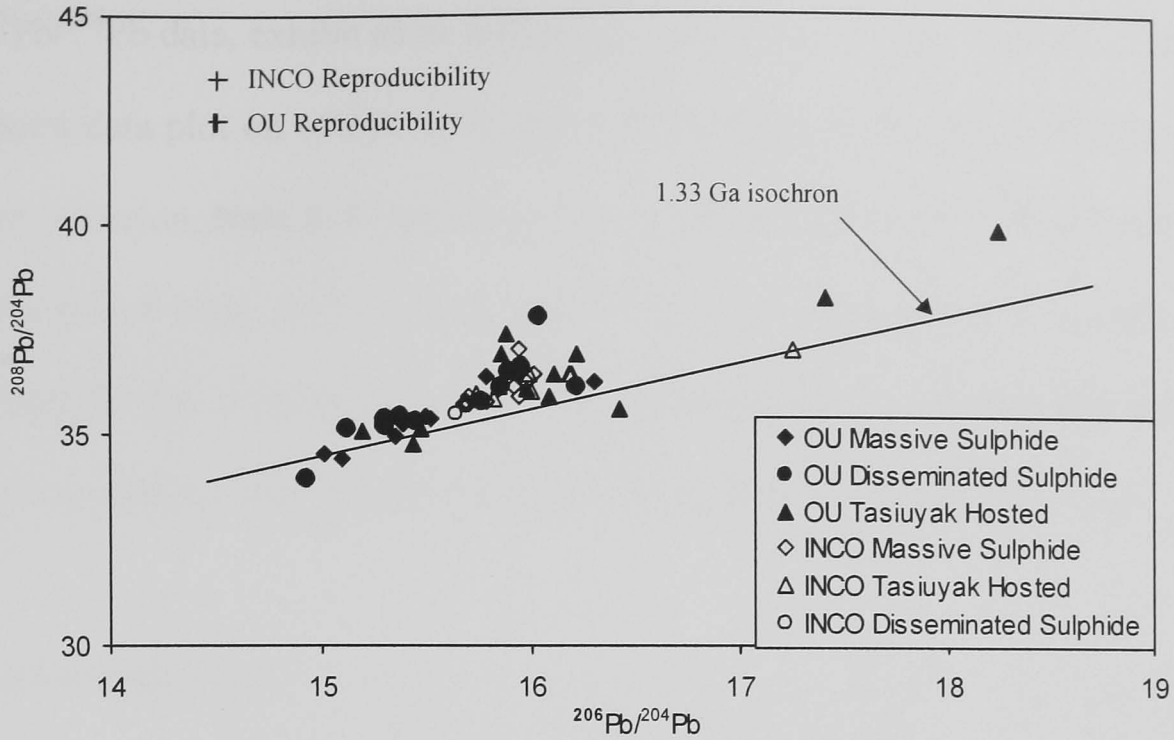

Figure 6.4a Graph of $^{206}Pb/^{204}Pb$ versus $^{208}Pb/^{204}Pb$ for the VBI- and Tasiuyak gneiss-hosted sulphides. The Tasiuyak gneiss data extend to more radiogenic values of $^{206}Pb/^{204}Pb$ and $^{208}Pb/^{204}Pb$ than the Voisey's Bay intrusion data.

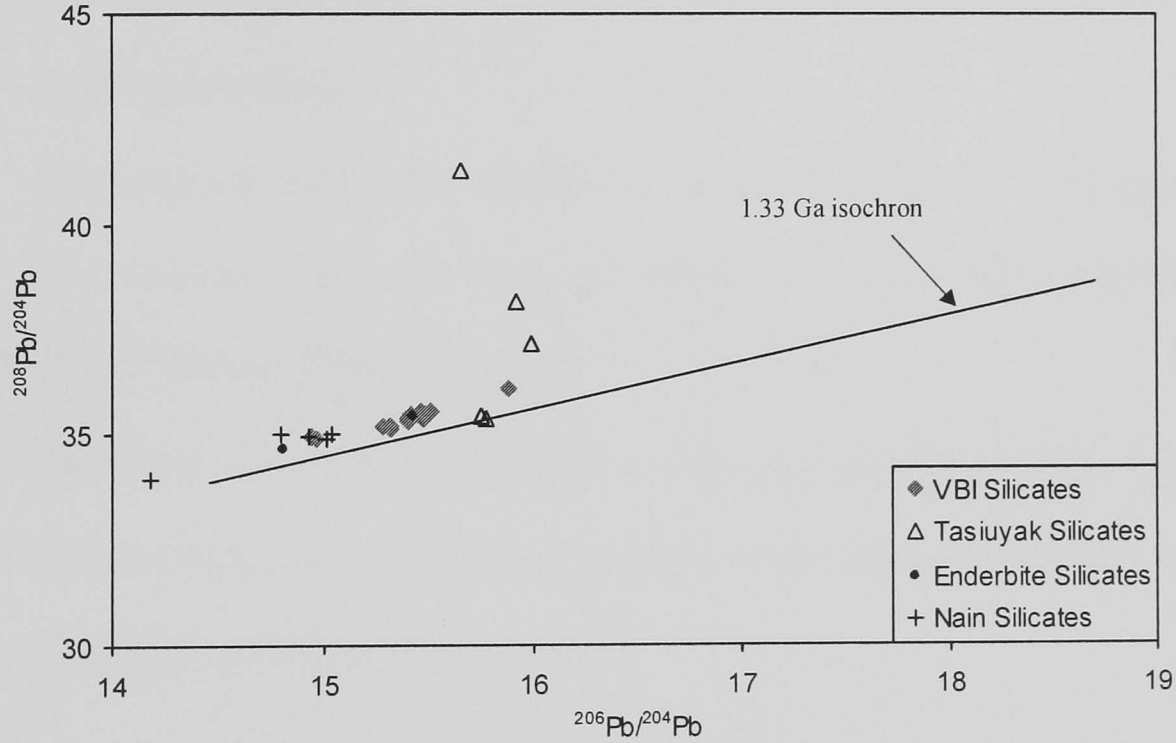

Figure 6.4b Graph of $^{206}Pb/^{204}Pb$ versus $^{208}Pb/^{204}Pb$ at 1.33Ga for silicates at Voisey's Bay as analysed by Amelin et al. (2000). The Voisey's Bay intrusion and Enderbite gneiss silicates form one array while the Tasiuyak gneiss data form another.

$^{208}Pb/^{204}Pb$ data, exhibit clear differences. The Voisey's Bay intrusion, Nain, and Enderbite gneiss data plot on one gradient and the Tasiuyak gneiss data on the other. The Voisey's Bay intrusion, Nain and Enderbite gneiss gradients are exactly coincident and make a well-constrained array, with the Nain gneiss having the least radiogenic values and the VBI and Enderbite data overlapping. However, the Tasiuyak gneiss data define a trend with a near-vertical gradient and extend to much more radiogenic $^{208}Pb/^{204}Pb$ values.

6.1.4 Conclusions

- The Pb isotope ratios of the sulphides at Voisey's Bay have no relationship to their location.
- The Pb isotopes ratios of the Voisey's Bay and Tasiuyak gneiss sulphides exhibit significant overlap.
- The Tasiuyak gneiss data appear to form two groups; one overlapping the Voisey's Bay intrusion sulphide data, the other with much more radiogenic $^{206}Pb/^{204}Pb$, $^{207}Pb/^{204}Pb$ and $^{208}Pb/^{204}Pb$ ratios
- The VBI silicates overlap the Nain and Tasiuyak gneiss Pb isotope values.
- The OU data more extreme values than the INCO data, these values are not an artefact of experimental method.

6.2.1 Discussion

Figures 6.3a and b and 6.4a and b demonstrated that the Voisey's Bay intrusion, Tasiuyak, Nain and Enderbite gneiss sulphides and silicates have characteristic Pb isotope ratios and that the Pb isotope ratios for the VBI overlapped those of the country rocks. To generate a magmatic Ni-sulphide deposit requires contamination of a mantle-derived melt by a silica or sulphur bearing material. Therefore, one would expect that the sulphide data would fall

onto trends on $^{206}Pb/^{204}Pb$ versus $^{207}Pb/^{204}Pb$ and $^{208}Pb/^{204}Pb$ diagrams that represented mixing lines between the contaminant(s) that induced sulphide immiscibility and that of the parental mantle-derived melt. These mixing lines can also be termed secondary isochrons. However, the gradients of secondary isochrons on $^{206}Pb/^{204}Pb$ versus $^{207}Pb/^{204}Pb$ diagrams have age significance – the older the material the steeper the gradient and measurement of this gradient can yield age information. Therefore, regression lines have been calculated for the sulphide and silicate Pb isotope data and these regression lines have been analysed using ISOPLOT/EX (Ludwig, 1999) to provide a framework within which to discuss the data.

Figure 6.5a presents the $^{206}Pb/^{204}Pb$ versus $^{207}Pb/^{204}Pb$ data for the Voisey's Bay intrusion- and Tasiuyak gneiss-hosted sulphides. The VBI-hosted sulphide secondary isochron intersects the Tasiuyak gneiss and the 1.33 Ga point on the two-stage growth curve, but has a distinctly lower gradient than the 1.33 Ga isochron. Using ISOPLOT/EX (Ludwig, 1999) to investigate this secondary isochron yields an apparent age for the VBI sulphides of 3.619 ± 0.190 Ga, considerably older than the emplacement date of the Voisey's Bay intrusion.

The Voisey's Bay intrusion, Tasiuyak and Nain gneiss silicate data are presented in Figure 6.5b, a graph of $^{206}Pb/^{204}Pb$ versus $^{207}Pb/^{204}Pb$. A secondary isochron has been drawn by calculating a linear regression through the VBI silicate data. The gradient of this regression line is obviously shallower that that of the 1.33 isochron. Applying ISOPLOT/EX (Ludwig, 1999) to the VBI silicate data yields an apparent age of 3.299 ±0.210 Ga – again much older than the emplacement age of the Voisey's Bay intrusion but younger than that observed for the sulphides.

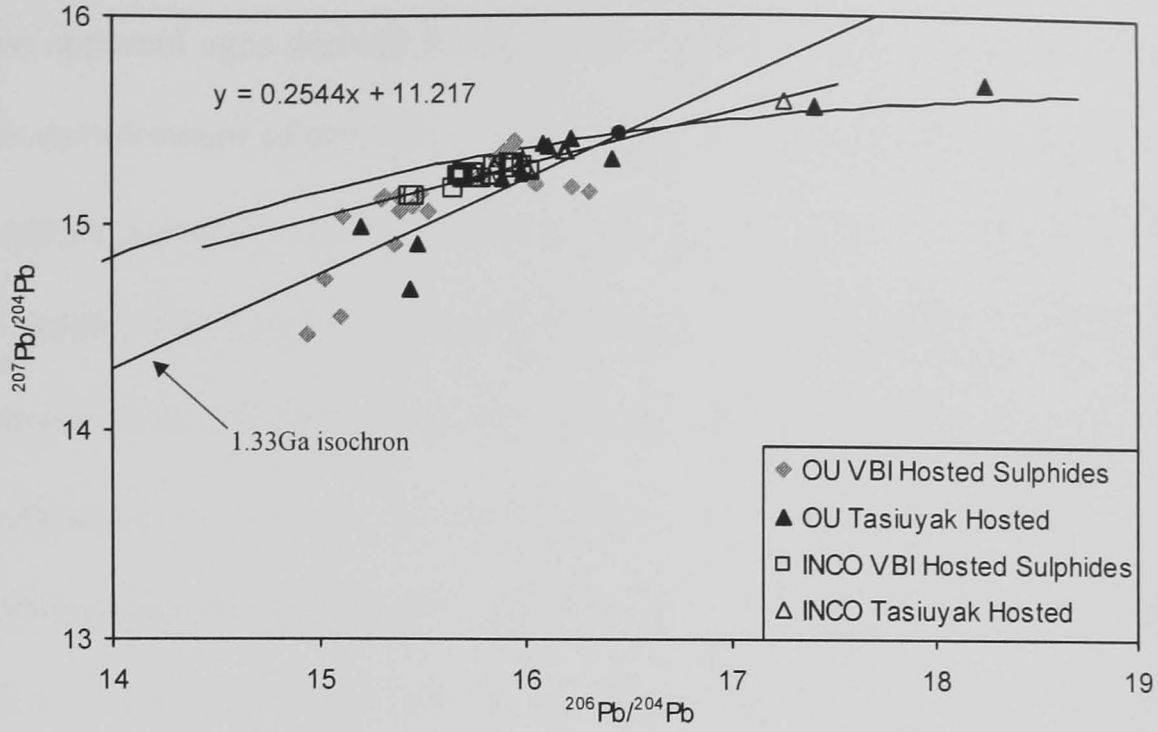

Figure 6.5a Graph of $^{206}Pb/^{204}Pb$ versus $^{207}Pb/^{204}Pb$ for the Voisey's Bay intrusion and Tasiuyak gneiss sulphide data. The Voisey's Bay intrusion sulphide data scatter around and below a secondary isochron defined by the INCO VBI sulphide data. The slope of the secondary isochron is lower than that of the 1.33Ga isochron.

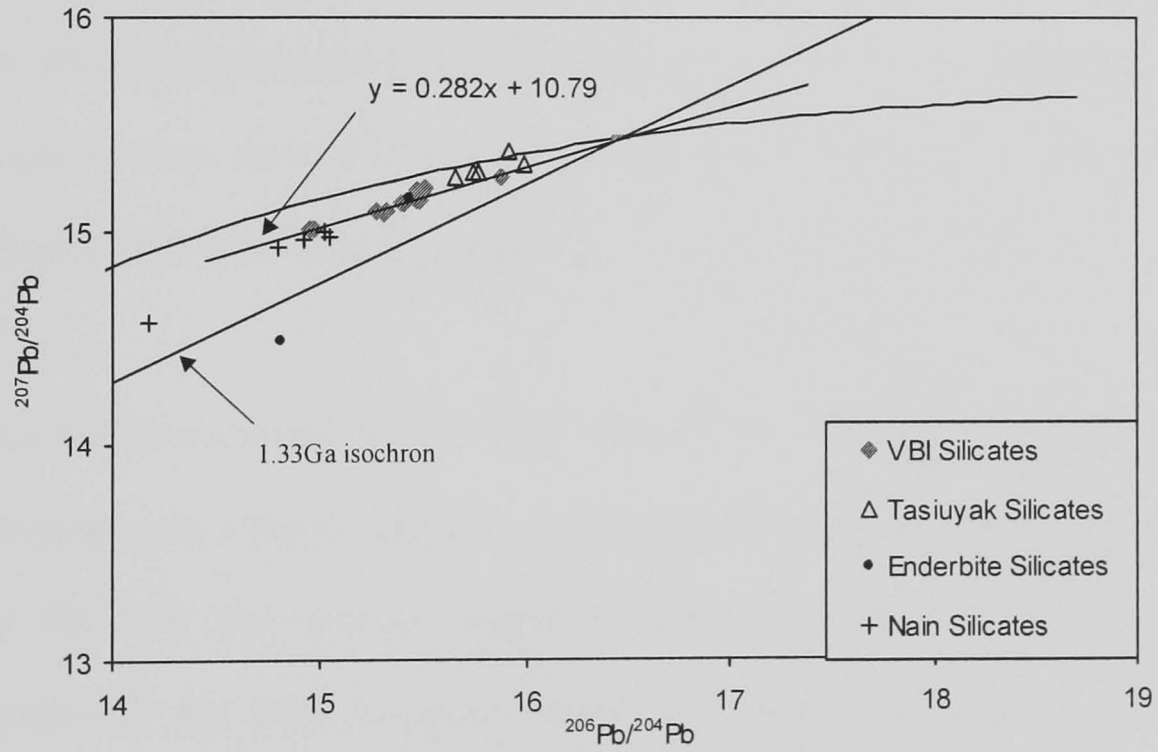

Figure 6.5b Graph of $^{206}Pb/^{204}Pb$ versus $^{207}Pb/^{204}Pb$ for the VBI- and Tasiuyak silicates, and Nain gneiss silicates at 1.33 Ga. The VBI silicate data are intermediate between the Nain gneiss silicate data, the Tasiuyak gneiss silicate data, and the 1.33 Ga point on the growth curve. The gradient of the VBI silicate data secondary isochron is shallower than the 1.33Ga

The apparent ages derived for the VBI sulphides and silicates are quite clearly older than the emplacement of the Voisey's Bay intrusion. The most likely reason for this is that the magmas parental to the VBI rocks must have had a lower μ ($^{238}U/^{204}Pb$) value than 9.735 as proposed by Stacey and Kramers (1975). This conclusion is supported by the work of Amelin et al. (2000), who found that the VBI parental melt had μ ~7.8-8.0. A probable explanation for this low value is that the primary melt assimilated old crustal material with unradiogenic Pb isotope ratios, thus driving the $^{206}Pb/^{204}Pb$ ratio of the melt to the left of the 1.33 Ga point on the two-stage Pb-Pb growth curve. If this assimilation had not taken place, the $^{206}Pb/^{204}Pb$ ratios at the time of emplacement would coincide with the 1.33 Ga point on the growth curve. The textures of the VBI sulphides and silicates indicate that they were emplaced at the same time. However, the gradients of their secondary isochrons are different, the sulphides having a steeper gradient. One possible explanation is that the sulphides have incorporated material with higher $^{206}Pb/^{204}Pb$, $^{207}Pb/^{204}Pb$ ratios than the silicates, thus increasing the gradient.

Figure 6.6a is a graph of $^{206}Pb/^{204}Pb$ versus $^{208}Pb/^{204}Pb$ for the Voisey's Bay sulphides and Tasiuyak gneiss hosted sulphides. In contrast to previous figures, this graph includes data for the Nain and Tasiuyak gneiss silicates recalculated to 1.33 Ga. As previously mentioned, the VBI sulphides exhibit a pronounced 'bulge' in $^{208}Pb/^{204}Pb$ ratio at $^{206}Pb/^{204}Pb$ ~16. With the inclusion of the Tasiuyak gneiss silicate data, this increase in $^{208}Pb/^{204}Pb$ ratio matches similar Pb isotope ratios in the Tasiuyak silicates. This is highlighted on Figure 6.6a with an arrow labelled *Influence of Tasiuyak silicates*. The remainder of the VBI and the Tasiuyak sulphide data extend sub-parallel to the 1.33 Ga isochron until it intercepts the Nain gneiss data. The inference of this is that the Pb isotope ratios of these sulphides are the result of assimilation of Nain gneiss. This point is emphasised the superimposed arrow labelled *Influence of Nain silicates*. This suggests that the Pb isotope ratios of the sulphides associated with the VBI are the result of mixing

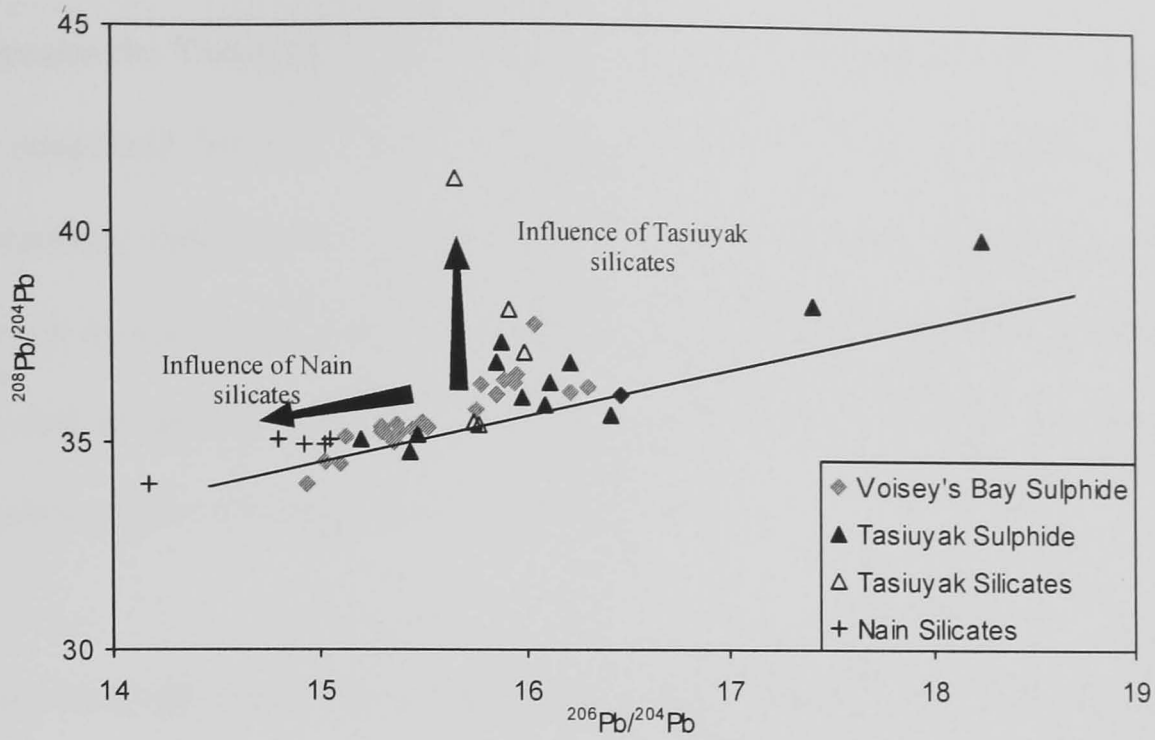

Figure 6.6a Graph of $^{206}Pb/^{204}Pb$ versus $^{208}Pb/^{204}Pb$ for the VBI- and Tasiuyak gneiss-hosted sulphides, and Nai and Tasiuyak gneiss silicates. The VBI-hosted sulphide Pb isotope data overlaps the Tasiuyak gneiss-hosted sulphide and Nain and Tasiuyak gneiss silicate data.

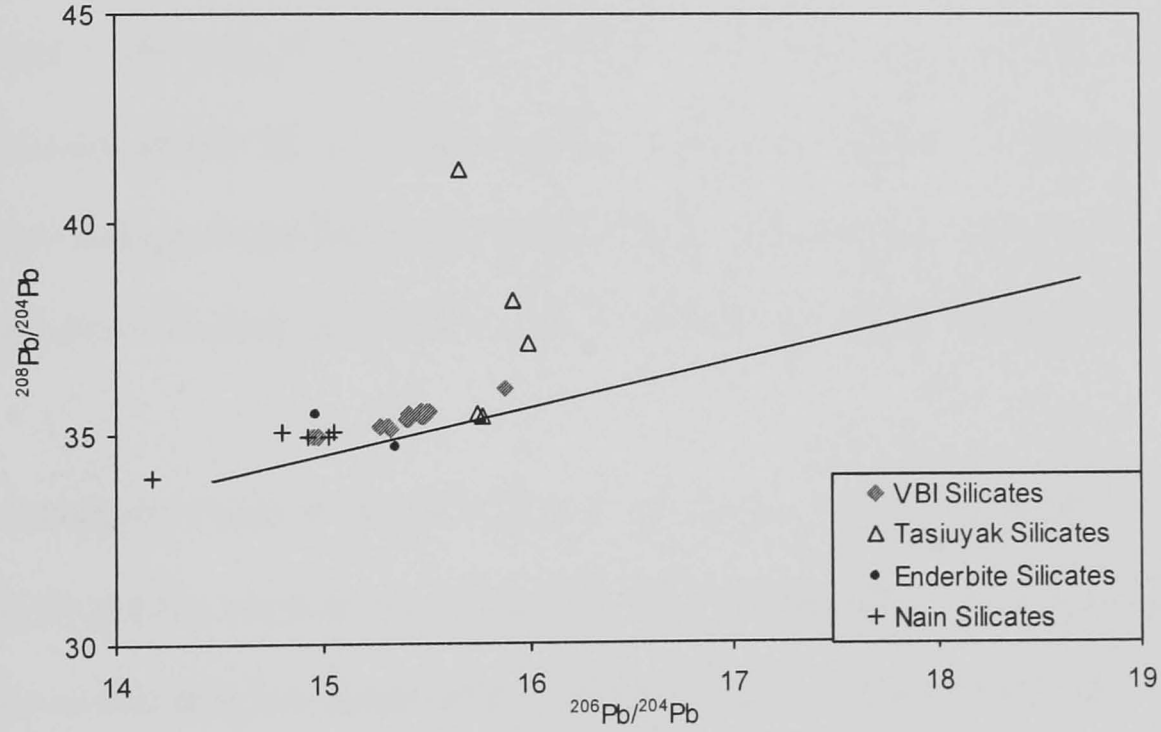

Figure 6.6b Graph of $^{206}Pb/^{204}Pb$ versus $^{208}Pb/^{204}Pb$ for the VBI, Tasiuyak gneiss, and Nain gneiss silicates. The Voisey's Bay silicates plot between the Nain gneiss and the least radiogenic Tasiuyak gneiss data and have a different gradient to the VBI-hosted sulphides.

between the Tasiuyak gneiss, the Nain gneiss and a mantle-derived melt. This observation is supported by the $^{206}Pb/^{204}Pb$ versus $^{207}Pb/^{204}Pb$ data presented in Figure 6.5a: the secondary isochron formed by the VBI-hosted sulphide data plot intersects the Tasiuyak gneiss data and the Pb growth curve at 1.33 Ga. The inference being that the sulphides are a result of mixing between a component with low $^{206}Pb/^{204}Pb$ and $^{207}Pb/^{204}Pb$, the Tasiuyak gneiss, and a 1.33 Ga mantle derived melt.

The Tasiuyak gneiss-hosted sulphides plot into two groups; this is seen most clearly when considering $^{208}Pb/^{204}Pb$ ratios. One group has Pb isotope ratios approximately coincident with the VBI silicates and sulphides, while the other has markedly higher $^{208}Pb/^{204}Pb$ ratios. The reasons for this are unclear, no differences in mineralogy or habit were observed during the selection or picking of these samples. It seems probable that these more radiogenic ratios are the result of post-emplacement decay of U and deposition of later sulphide minerals, possibly by a fluid medium. This area may justify further research.

Considering Figure 6.5b, the VBI silicates lie on a line that between the 1.33 Ga point on the Pb growth curve at one end and the Nain gneiss at the other. The Tasiuyak gneiss also lies on this line, but examination of Figure 6.6b reveals that the Tasiuyak gneiss can have had little influence on the VBI Pb ratios. Because the majority of the Tasiuyak silicate data are so radiogenic and their gradient so steep, significant contributions by the Tasiuyak gneiss to the Voisey's Bay intrusion silicates Pb budget would be easily detected. Had anything other than the least-radiogenic Tasiuyak been assimilated, the gradient of the Voisey's Bay intrusion silicates would trend well above the two-stage growth curve in a manner similar to the Pb data for the sulphides. However, as there is little reason to suppose that the least-radiogenic material would be assimilated preferentially, it is unlikely that the Tasiuyak has contributed significantly to the Pb budget of the Voisey's Bay silicates. Based on this reasoning, the unradiogenic component that shifted the VBI

silicate $^{206}Pb/^{204}Pb$ ratios to the left of the 1.33 Ga point on the Pb growth curve is likely to have been the Nain rather than the Tasiuyak gneiss. Therefore, in contrast to the Voisey's Bay intrusion sulphides, the silicates appear to be the product of significant mixing between only a mantle-derived component and the Nain gneiss.

Attention was drawn to the fact that the samples analysed at the Open University exhibit considerably more scatter than those analysed on behalf of INCO. It is believed that this scatter is a reflection on the sampling strategies employed in the two studies. All the data from the INCO study was derived from samples taken from five cores; two at the Reid Brook Zone and three from the Ovoid. In contrast, the samples analysed at the Open University were taken from 12 cores from localities all across the Voisey's Bay deposit. This greater scatter observed for the OU-analysed samples is thus a truer representation of the variation of the Voisey's Bay sulphide Pb isotope ratios.

Section 6.2.2 Summary

It appears that the Pb isotope profile of the silicates and sulphides at Voisey's Bay are representative of different mixing events. The Voisey's Bay silicates represent mixing between a mantle-derived component and a rock with a similar Pb isotope profile to the Nain gneiss. The only possible contribution from the Tasiuyak silicates to the Voisey's Bay intrusion silicates is either tiny amounts of Tasiuyak gneiss, or only the least-radiogenic end member. The Voisey's Bay sulphides are a little more complex. On both $^{206}Pb/^{204}Pb$ versus $^{207}Pb/^{204}Pb$ and $^{208}Pb/^{204}Pb$ diagrams, the VBI-hosted sulphide data overlap the Tasiuyak gneiss sulphides, the Nain gneiss silicates, though with a gradient close to that of the VBI silicates. This suggests that a significant proportion of the Pb budget in the Voisey's Bay intrusion sulphides is derived via interaction with the Tasiuyak gneiss, the remainder being the result of mixing between the Nain gneiss and mantle-derived component. The inference of this is that the Tasiuyak gneiss donated its Pb to the

VBI sulphides with little contribution to the VBI silicates. One mechanism that has been suggested to account for this is preferential extraction of Tasiuyak sulphides by the VBI sulphide melt (Lightfoot, pers. comm.). However, the melting temperature of the system Fe-S-O at one atmosphere is 915 °C (Naldrett, 1989). At these temperatures, some fusion of felsic components is expected (Yoder and Tilley, 1962), particularly as the Voisey's Bay intrusion magmas were not dry (Li and Naldrett, 1999; Li and Naldrett, 2000). Because of this, assimilation of sulphide will inevitably cause the assimilation of felsic components: this would be detected in the Pb isotope and trace element geochemistry of the intruding magmas. Little evidence of Tasiuyak gneiss assimilation is detected in either the Pb isotope or the trace element geochemistry of the Voisey's Bay intrusion magmas. Thus, it can only conclude that the Tasiuyak gneiss was incorporated only by a sulphide liquid and that interaction with the magmas parental to the troctolitic rocks was minimal.

This requires a mechanism for assimilation of Tasiuyak gneiss material by the magmatic sulphides but not by the silicates be proposed. Figure 6.7 is a schematic representation of a hypothetical magma chamber in the Voisey's Bay intrusion conduit system. Cold, dense sulphide-bearing fragments of Tasiuyak Gneiss become detached from the roof and walls and sink to the base of the magma chamber. An existing sulphide liquid has also collected on the floor of the magma chamber. Consequently, the dense, sulphide bearing, Tasiuyak gneiss fragments are immersed in the sulphide liquid and are digested by it. Sulphide liquid has a pronounced density contrast with silicate liquids, this, combined with sulphide/silicate immiscibility would be sufficient to ensure that the two systems would develop different Pb isotope ratios.

The implication of this model is that a sulphide liquid was present before the mantle-derived melt parental to the VBI encountered the Tasiuyak gneiss. Because a sulphide liquid was already present when the Tasiuyak gneiss began to be assimilated, the Tasiuyak

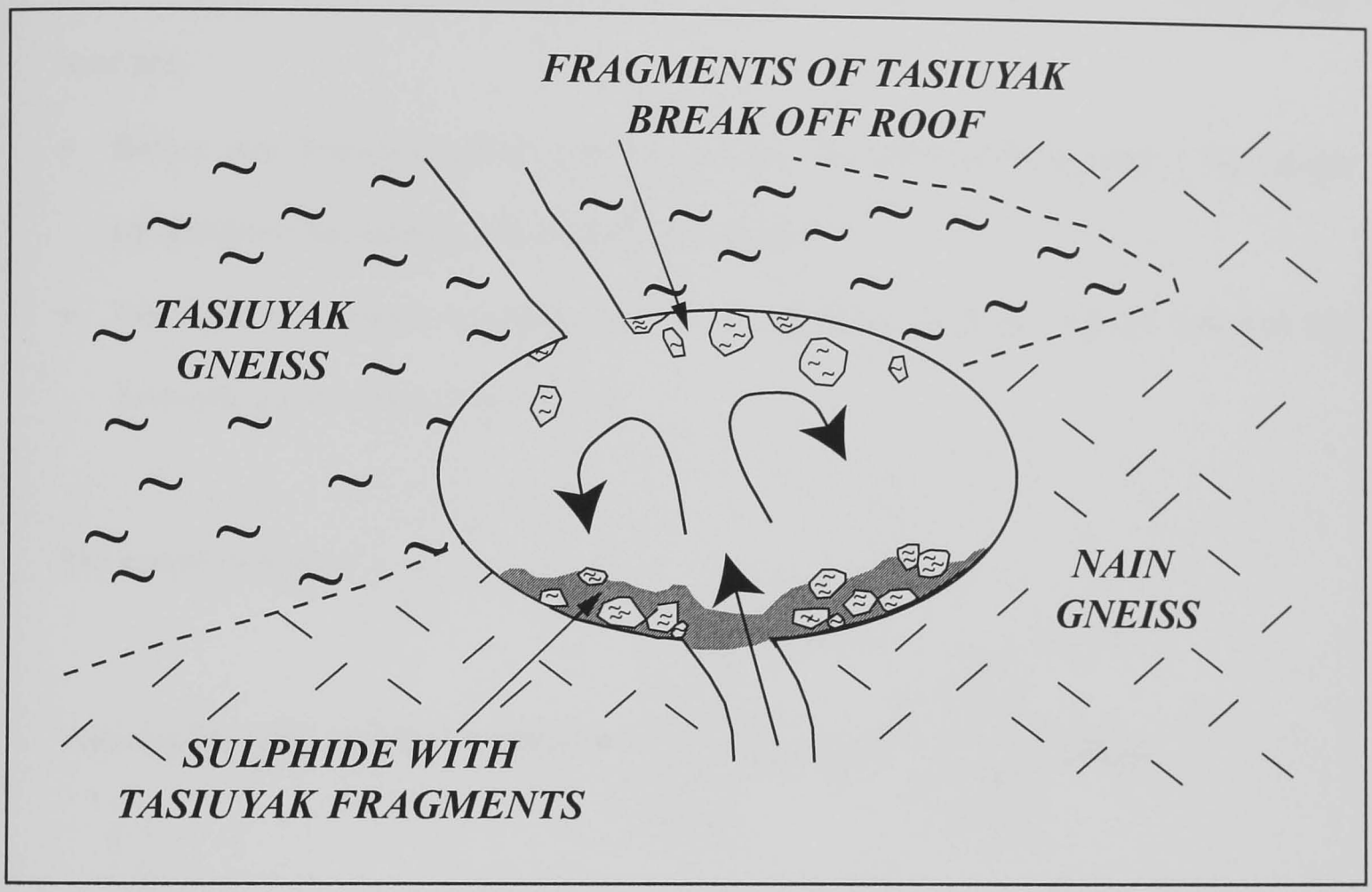

Figure 6.7 Cartoon illustrating the mechanism for sulphide/silicate Pb isotope disequilibrium. A mantle-derived melt, with an accompanying immiscible sulphide liquid is emplaced into a mid-crustal magma chamber. Cold, dense fragments of sulphide bearing Tasiuyak gneiss fall from the roof and walls of the magma chamber and sink through to the floor. Because sulphide liquid has a pronounced density contrast with silicate liquids (~49% Kress, 1997), they tend to segregate at the base of any magma chamber. Consequently, the clasts of Tasiuyak gneiss are immersed in the sulphide liquid and are digested. Because of the density contrast, and sulphide/silicate immiscibility, there is little mixing between the two systems. In this way, the isotopic disequilibrium is preserved.

gneiss cannot have caused the onset of sulphide immiscibility in the Voisey's Bay parental magmas. Because the $^{208}Pb/^{204}Pb$ ratios of the Nain, Tasiuyak and VBI silicates are different, they provide a method of estimating the amount of Tasiuyak gneiss assimilated by the VBI sulphides. The amount of Tasiuyak gneiss assimilated by the VBI sulphides can be estimated using mass balance and averaged Pb isotope ratios. The assumptions used are:

- Before any Tasiuyak gneiss was assimilated, the sulphide liquid had a Pb isotope composition identical to that of the VBI silicates.
- The Tasiuyak gneiss sulphides at 1.33 Ga had the same Pb isotope ratios as the Tasiuyak gneiss silicates at 1.33 Ga.

The equation used is:

$$\text{Amount Tasiuyak gneiss assimilated} = \frac{\left(\frac{^{208}Pb}{^{204}Pb}\right)_P^{\text{VBI sulphide}} - \left(\frac{^{208}Pb}{^{204}Pb}\right)_I^{\text{VBI silicates}}}{\left(\frac{^{208}Pb}{^{204}Pb}\right)_I^{\text{Tasiuyak silicates}} - \left(\frac{^{208}Pb}{^{204}Pb}\right)_I^{\text{VBI silicates}}}$$

Using the above equation, the amount of Tasiuyak gneiss assimilated by the VBI sulphides is ~25-30 percent.

Chapter 7

Discussion and conclusions

7.1 Introduction

The aim of this thesis has been to gain a better understanding of the nature of the Voisey's Bay parental magmas, the nature of the contamination that induced sulphide immiscibility, and the timing of sulphide saturation. This has been achieved through the combined use of major and trace element data, olivine chemistry, sulphide mineralogy data and Pb-Pb isotope data. These were used to answer the questions posed in Chapter 1:

1. What was the nature of the Voisey's Bay parental magma(s)?
2. Are the troctolites the source of the Ni at Voisey's Bay?
3. What is the contamination history of the Voisey's Bay intrusion?
4. Was the Tasiuyak gneiss the contaminant that induced sulphide immiscibility?

The discussion below will summarise the insights from each chapter and investigate whether these questions have been answered.

7.2 Nature of the Voisey's Bay parental magma

In Chapter 3, the nature of the magmas parental to the Voisey's Bay intrusion was investigated. Using selected trace element ratios and Eu/Eu* it was possible to characterise the magma parental to the troctolitic rocks. Using this calculated parental melt composition it was possible to deduce a pressure and temperature at which the parental magma was formed. Melting started in the garnet stability field at a temperature of approximately 1500°C and pressure of ~3GPa, melting continued into the spinel stability field. Because the parental melt composition plotted between those expected for garnet and spinel facies melt it was surmised that there had been melt contributions from both.

Using Eu/Eu* and Sr/Nd ratios, the fO_2 of the Voisey's Bay intrusion was found to be QFM $\pm^{0.5}_{0.8}$ log units, typical of OIB rather than MORB (Wallace and Carmichael, 1992). Because of this, the inferred depth of melting, and the εSr and εNd evidence it is likely that the Voisey's Bay magmas were not the product of 1-2 percent MORB-type melting, but instead were derived from 7-8 percent melting of a PM (Sun and McDonough, 1989) type source. Therefore, it is proposed that the Voisey's Bay intrusion is the product of plume-like magmatism.

The forsterite contents and whole rock Mg/Fe ratio of the troctolites allowed the calculation of the Mg# of their parental melts. This was 55 for the normal troctolite and 47 for the variable troctolite. It is probable that the troctolite parental magma was preceded by magma that was less evolved. This is likely, as the relict olivine grains that were described in Chapter 4 had forsterite contents of $Fo_{80,}$ in excess of those of the troctolites. It also seems as if the Voisey's Bay magmas form a consanguineous series, each more evolved than the last. This being the case, the magma(s) that generated the Ni-rich sulphides at Voisey's Bay almost certainly had forsterite contents in the range Fo_{80}-Fo_{90}, directly comparable to the magmas that host the world's other magmatic Ni-sulphide deposits.

The electron microprobe analysis of sulphide minerals revealed that the metals were derived via interaction with a high-Mg#, high-Ni silicate melt. When Voisey's Bay whole rock normalised to 100 percent sulphide were compared with similar data from magmatic Ni-sulphide deposits from around the world, it was found that Voisey's Bay was comparable to low-Mg# komatiite- and high-Mg# gabbro-hosted deposits. This supports the conclusion arrived at through trace element data and olivine data that the Voisey's Bay deposit was derived from a high Mg# melt.

7.3 Are the troctolites the source of the Ni?

The Voisey's Bay olivines gave considerable insights to the mineralisation and petrogenesis and metallogenesis of the Voisey's Bay intrusion and deposit respectively. It was found that olivines form the Voisey's Bay troctolites had been ubiquitously enriched in Ni compared with their expected contents based on forsterite/Ni relationships. It was inferred that this was the result of the magma parental to the Voisey's Bay troctolites interacting and equilibrating with a Ni-rich sulphide liquid. The inevitable conclusion is that the Voisey's Bay troctolites cannot be the source of the Ni in the eponymous deposit. Because the troctolites equilibrated with a Ni-rich sulphide liquid, a sulphide liquid must have been present and upgraded with respect to Ni before the troctolites or the magma parental to them was emplaced. Therefore, a previous magma or magmas must have generated and equilibrated with an immiscible, Ni-rich sulphide liquid and the troctolites cannot be the source of the Ni.

7.4 Contamination history of the Voisey's Bay magmas

Having derived a robust parental melt composition allowed the input from the various potential contaminants to be assessed. It was found that the Voisey's Bay magmas are the products of a two-stage contamination process. The first stage comprising plume-like magma with approximately 15 percent contamination of Nain gneiss, the second comprises minor contamination with Nain, Tasiuyak, and Enderbite gneiss. Comparison with Sr/Nd isotope data found that contamination by 10-20 percent Nain gneiss was indicated. Evidence of second stage of contamination was discussed, but was found to be minor, with a maximum of 3-10 percent of Nain, Tasiuyak or Enderbite gneiss being possible. A cartoon illustrating the proposed sequence of events from mantle melting through to two-stage contamination is reproduced in Figure 7.1 and 7.2.

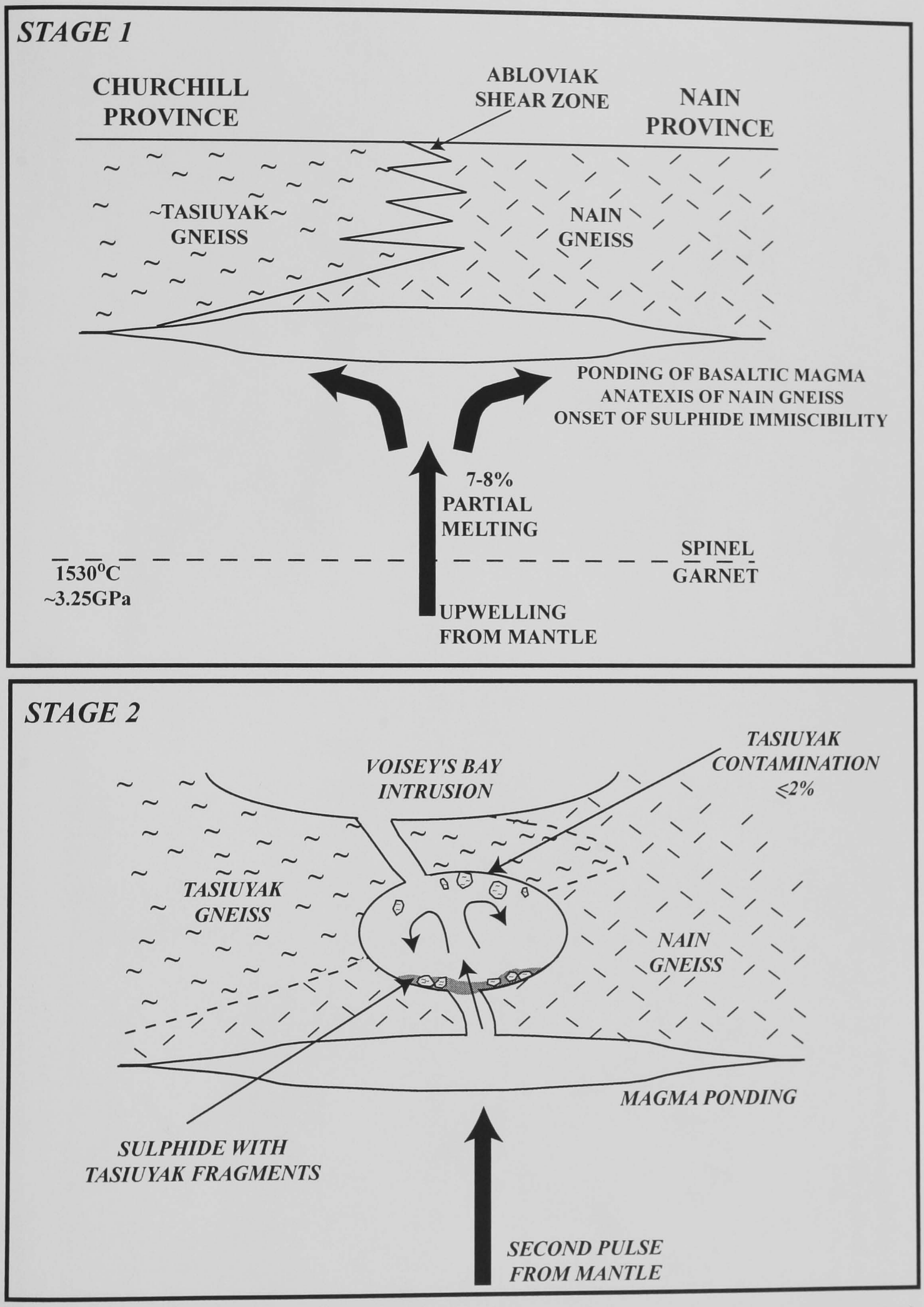

Figure 7.1 Cartoon of the mantle melting and contamination for the Voisey's Bay parental melts. Stage 1 Mantle melting begins in the garnet stability field at ~1530°C and 3.25GPa. Melting continues into spinel facies, with contributions from both. The melt ascends to the crust/mantle boundary, where it ponds and assimilates ~15 percent Nain gneiss. Stage 2 The melt is then emplaced within the crust via the Abloviak Shear Zone where it assimilates small quantities of Tasiuyak Gneiss.

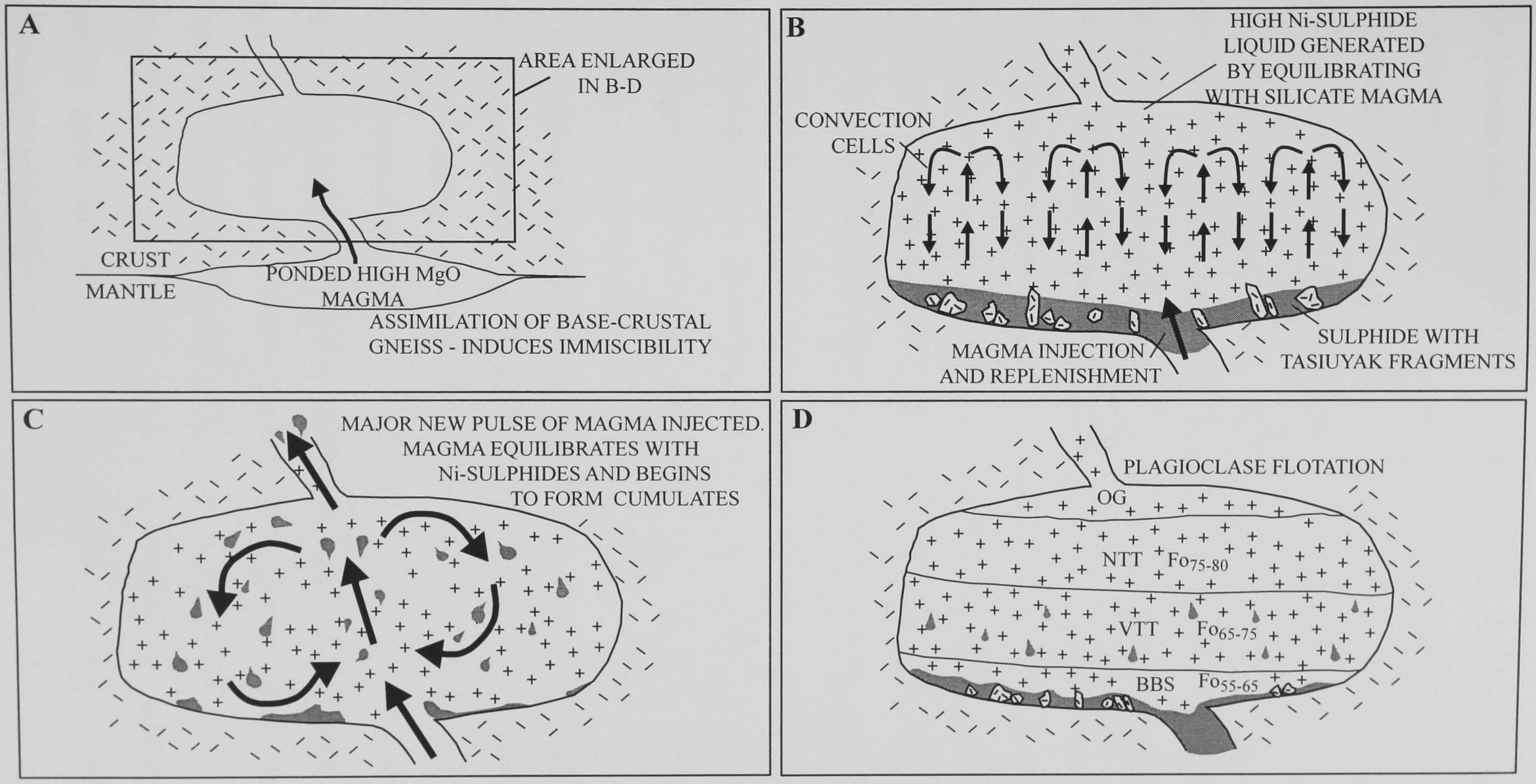

Figure 7.2a-d Cartoon of the timing of Voisey's Bay Intrusion crystallisation and sulphide segregation. A) High Mg# melt ponds at the crust/mantle boundary and assimilates crust initiating sulphide immiscibility. B) Silicate and sulphide magmas are injected into higher-level magma chamber and begin to assimilate Tasiuyak gneiss. Via convection and magma replenishment the sulphides are upgraded with Ni. C) A second pulse of magma is injected and the earlier pulse is displaced. The sulphide liquid and new magma begin to equilibrate. D) By plagioclase flotation the normal troctolite forms at the top of the magma chamber, followed by the variable troctolite and finally the breccia sequence.

The Pb isotope data suggest that the Voisey's Bay silicates, at most, have incorporated only the least-radiogenic Tasiuyak gneiss. Despite this, the Voisey's Bay sulphides have a clear Tasiuyak gneiss influence upon their Pb isotope ratios. The inference of this is that the sulphide and silicate systems have different contamination histories. One possible explanation is presented in Figures 7.1 and 7.2, cartoons of the magmatic evolution and contamination at Voisey's Bay. Figure 7.1 describes how a mantle-derived melt ponds at the base of the crust, assimilating Nain gneiss. The magma then ascends to a magma chamber, where cold, dense fragments of Tasiuyak gneiss are detached from the sides and roof of the magma chamber. These fragments sink through the contaminated magma to lie at the base, where disseminated sulphides collect around them. Because the magmas are still hot, the fragments of Tasiuyak gneiss are digested, imparting much of their Pb and their characteristic Pb isotope ratios to the Voisey's Bay magmatic sulphides. Because of the sulphides density contrast with the silicates, coupled with their mutual immiscibility, the Pb isotopes of the two systems remain separate. Therefore, the sulphides acquire a distinct Tasiuyak gneiss Pb isotope signature while the Voisey's Bay silicates retain only evidence of contamination with the Nain gneiss. The similarity between the magmatic and Tasiuyak sulphides Pb ratios can be explained by the sulphides assimilating quantities of sulphide-bearing Tasiuyak gneiss. Estimating the amount of Tasiuyak gneiss assimilated by the VBI-hosted sulphides is difficult. However, because U and Th are incompatible in sulphides, and assuming the silicate contamination of the sulphides is negligible, the post-contamination radiogenic Pb growth within the sulphides will be minimal. Thus, with these assumptions it is possible it was possible to give an estimate Tasiuyak gneiss contamination of the VBI sulphides based on mass-balance calculations. Using average, initial $^{206}Pb/^{204}Pb$ and $^{208}Pb/^{204}Pb$ values for the Voisey's Bay intrusion silicates and Tasiuyak gneiss and VBI sulphides the approximate amount of Tasiuyak gneiss contamination of the VBI sulphides is ~25-30 percent.

Figure 7.2a-d presents a model for the crystallisation history of the Voisey's Bay intrusion silicates and sulphides. Figure 7.2a mantle-derived magmas were ponded at the base of the crust, assimilated ~15 percent of Nain gneiss and achieved sulphide immiscibility. They were then emplaced into a lower-crustal magma chamber (7.2b). Here, by thermal convection, and perhaps periodic magma replenishment, the sulphide liquid was upgraded with Ni. Simultaneously, fragments of sulphide bearing Tasiuyak gneiss were detached from the roof of the magma chamber, to sink to its base an be immersed in the sulphide liquid. A major new pulse of magma is then injected into the magma chamber displacing the original magma and taking the sulphide into suspension (Figure 7.2c). The now, high-Ni sulphide liquid partially equilibrates with the new silicate magma. In the process of this partial equilibration, the sulphide liquid donates some of its Ni to the new magma. The magma chamber cools and begins to crystallise the sequence of rocks observed at Voisey's Bay (Figure 7.12d).

7.5 Was the Tasiuyak gneiss the cause of sulphide immiscibility?

The olivine and Pb isotope data have demonstrated that a sulphide liquid must have been present prior to the crystallisation of the troctolites. In addition, the sulphide data revealed that the sulphide liquid had undergone considerable fractionation, when at 52 atomic percent S the pyrrhotite Ni content markedly increased. This sudden increase was interpreted as the result of graphite bearing Tasiuyak gneiss being assimilated, causing a decrease in sulphide fO_2 and hence a decrease in Fe^{3+} availability. The model invoked for the contamination history of the silicates and the sulphides using Pb isotope data requires that the sulphide liquid assimilate Tasiuyak gneiss. An important conclusion arising from these observations is that a sulphide liquid was present before Voisey's Bay intrusion magmas encountered the Tasiuyak gneiss. Consequently, the Tasiuyak gneiss could not have been the contaminant that induced sulphide immiscibility.

7.6 Towards a new model for magmatic sulphide genesis at Voisey's Bay

At this point, it may be appropriate to consider the model that has been suggested for the mineralisation process at Voisey's Bay. The Voisey's Bay deposit was thought to be the result of assimilation of the graphitic and sulphidic Tasiuyak gneiss into the magmas parental to the troctolitic rocks of the Voisey's Bay intrusion, leading to the precipitation of an immiscible sulphide. The Voisey's Bay intrusion was emplaced through a major continental suture, the Abloviak Shear Zone. This suture is thought to have acted as a conduit that focussed the magmatism and created a dynamic environment keeping the sulphide liquid in suspension due to turbulent flow (e.g. Naldrett et al., 1996). When the conduit opened into a magma chamber, the flow rate decreased and the sulphides dropped out of suspension to form basal accumulations, where the sulphides were upgraded by subsequent flows of magma (Evans-Lambswood et al., 2000).

The source of the Ni is not the troctolitic rocks – it was an earlier pulse of magma, of which only traces remain. This magma was high-Mg# and had forsterite contents in excess of Fo_{80}. This magma achieved sulphur saturation and sulphide immiscibility by crustal contamination. The sulphur saturation was not produced via contamination by the Tasiuyak gneiss in a mid-crustal magma chamber, but by the Nain gneiss, possibly at the crust/mantle boundary. The sulphide and the silicate magmas were emplaced in a mid-crustal magma chamber where the sulphides were upgraded with respect to Ni by equilibration with subsequent magma flows and thermal convection. After the sulphide/silicate equilibration had taken place and a high Ni-sulphide formed, the initial magma(s) were displaced by the magma that was parental to the troctolites. It is likely that this later magma was more evolved than those that generated the sulphide liquid. As a result, rather than donating Ni to the sulphides, the troctolite parental magmas acquired this element. It is undoubted that the Tasiuyak has contaminated the Voisey's Bay silicates and sulphides. However, the contamination of the former is minor at 3 percent, and that of the

latter, although major is merely coincidental when considered in the context of Ni-sulphide deposit genesis.

7.7 How does the Voisey's Bay deposit differ from other magmatic Ni-sulphide deposits?

The model for the genesis of a magmatic Ni-sulphide requires a mafic or ultramafic melt, a crustal suture or conduit, and a contaminant, either silicic or sulphurous. Prior to this study, the Voisey's Bay deposit was considered anomalous because of its association with an anorthosite complex and because of its apparent low-forsterite, low-olivine, Ni-donor lithology. In terms of the contaminant previously thought to have induced sulphide immiscibility however, it conformed well, as the contaminant, the Tasiuyak gneiss, is both silicic and sulphidic. The requirement for a crustal suture was also fulfilled – the Abloviak Shear Zone being ideal for focussing the flow of mantle-derived melts. The model proposed as a result of this study suggests that the Voisey's Bay deposit conforms rather better to the model defined by other world-class Ni-sulphide deposits than previously thought. The association of the Ni-sulphides at Voisey's Bay and the low-olivine, low-forsterite troctolitic rocks is almost entirely fortuitous. The magma that generated the Voisey's Bay deposit, if it were still present, would be entirely unremarkable in the company of the other host rocks for Ni-sulphide deposits, being both high-Mg# and high-Ni.

7.8 What about exploration for Ni-sulphides in other anorthosite complexes?

Prior to the discovery of the Voisey's Bay deposit, anorthosites were not considered promising prospects for Ni-sulphide mineralisation. With the benefit of what has been learned from Voisey's Bay, what can be said for exploration in similar complexes? Firstly, anorthosite complexes can be hosts to major magmatic Ni-sulphide mineralisation. To generate a magmatic Ni-sulphide, all that is required is that large volumes of high Mg#

melt interact with crustal material. However, if the extent of melting that generated the Voisey's Bay intrusion is typical of mafic intrusions within anorthosite complexes, deposits such as this are not suitable targets for PGEs. This is because at small melt fraction, below approximately 20 percent melting, the PGEs are retained in the mantle (Keays, 1995).

As anorthosite complexes can now be considered legitimate targets for Ni-sulphide mineralisation, it is appropriate to define a list of criteria by which they should be examined. It is necessary that a conduit exist to channel mantle-derived melts through the crust so that they might encounter a suitable contaminant and a trap to retain the sulphide liquids. To this end, it is essential that the anorthosite complex be located over a fault or suture that extend to the lower crust to focus magma flow. The complex must comprise of mafic intrusions as well as anorthosites – mafic rocks are required as a source of Ni. From the experience at Voisey's Bay, potential host rocks should not be discounted on the basis of low olivine or forsterite – these could be indicators of an earlier episode of magma that was sufficiently Mg- and Ni-rich. The mafic intrusions must comprise the earliest evidence of magmatism within the complex; sulphide saturation and the generation of an immiscible sulphide must occur early if the sulphides are to be upgraded with respect to Ni. An appropriate contaminant must be nearby, however, given the experience at Voisey's Bay it seems that many crustal-derived gneisses can be considered suitable.

7.9 Implications for further study

This thesis has demonstrated that the Voisey's Bay deposit is the product of a more complex history than thought by previous authors. The nature of the melt that was the source of the Ni at Voisey's Bay is worthy of further study. Much emphasis has been placed upon the necessity at Voisey's Bay of mantle-derived melts ponding at the crust/mantle interface. As well as being an essential stage in the petrogenesis and metallogenesis of the Voisey's Bay deposit, this also has implications for the study of

anorthosite complexes – a still enigmatic phenomenon in the Earth Sciences. One way that the existence of ponded high-Mg# melts can be investigated is via detailed, deep-crustal seismic surveying and perhaps gravimetric investigations. Should the result be proved positive, this may also have implications for the discovery of the next Voisey's Bay. An additional area of study that would prove useful is to link Pb isotope ratios to the composition of the sulphide minerals. This study has demonstrated that the Ni content of pyrrhotite varied maekedly ar 52 atomic percent S and this variation was interpreted as being due to the influence of the graphitic Tasiuyak gneiss on the fO_2. If this interpretation is correct, a corresponding variation in $^{208}Pb/^{204}Pb$ ratio should be observed.

References

Abraham K. P., Davies M. W., and Ricahrdson F. D. (1960) Sulfide capacities of silicate melts. *Journal of the Iron and Steel Institute* **196**, 309-312.

Amelin Y., Li C., and Naldrett A. J. (1999) Geochronology of the Voisey's Bay intrusion, Labrador, Canada, by precise U-Pb dating of coexisting baddelyite, zircon and apatite. *Lithos* **47**, 33-51.

Amelin Y., Li C., Valeyev O., and Naldrett A. J. (2000) Nd-Pb-Sr isotopic systematics of crustal assimilation in the Voisey's Bay and Mushua intrusions Labrador, Canada. *Economic Geology* **95**, 815-830.

Asimow A. D., Hirschmann M. M., and Stolper E. M. (2001) Calculation of peridotite partial melting from thermodynamic models of minerals and melts, IV. Adiabatic decompression and the composition and mean properties of mid-ocean ridge basalts. *Journal of Petrology* **42**(5), 963-998.

Bacuta G. C., Gibbs A. K., Kay R. W., and Kuoubm B. R. (1987) Platinum group element abundance in chromite deposits of the Acoje ophialite block. Zambales ophialite complex, Phillippines. In *Geo-Platinum 87* (ed. H. M. Prichard, P. J. Potts, J. F. W. Bowles, and S. J. Cribb), pp. 381-382. Elsevier Scientific Publications, Essex, UK.

Ballhaus C., Berry R. F., and Green D. H. (1991) High pressure experimental calibration of the orthopyroxene spinel oxygen geobarometer; implications for the oxidation state of the upper mantle. *Contributions to Mineralogy and Petrology,* **107**(1), 27-40.

Barnes S. J. (1986) The effect of trapped liquid crystallization on cumulus mineral compositions in layered intrusions. *Contributions to Mineralogy and Petrology* **93**, 524-531.

Beattie P., Ford C., and Russell D. D. (1991) Partition coefficients for olivine-melt and orthopyroxene-melt systems. *Contributions to Mineralogy and Petrology* **109**, 212-224.

Bedard J. H. (1994) A procedure for calculating the equilibrium distribution of trace elements among the minerals of cumulate rocks, and the concentration of trace elements in the coexisting liquids. *Chemical Geology* **118**, 143 - 153.

Bedard J. H. (2001) Parental magmas of the Nain Plutonic Suite anorthosites and mafic cumulates: a trace element modelling approach. *Contributions to Mineralogy and Petrology* **141**, 747-771.

Berg J. H. (1976) Regional geobarometry in the contact aureoles of the anorthositic Nain complex, Labrador. *Journal of Petrology* **18**(3), 399-430.

Berg J. H. (1977) Dry granulite mineral assemblages in the contact aureoles of the Nain Complex, Labrador. *Contributions to Mineralogy and Petrology* **64**, 33-52.

Berg J. H., Emslie R. F., Hamilton M. A., Morse S. A., Ryan R. F., and Wiebe R. A. (1994) Anorthositic, granitoid and related rocks of the Nain Plutonic Suite. In *International Geological Correlation Programme IGCP Projects #290 and#315.*

Berg J. H. and Wheeler E. P. (1976) Osumilite of deep seated origin in the contact aureole of the anorthositic Nain complex, Labrador. *American Mineralogist* **61**, 29-37.

Bertrand J. M., Roddick J. C., Van Kranendonk M. J., and Ermanovics I. (1993) U-Pb geochronology of deformation and metamorphism across a central transect of the Paleoproterozoic Torngat Orogen, North River map area, Labrador, Canada. *Canadian Journal of Earth Sciences* **30**, 1470-1489.

Brenan J. M. and Caciagli N. C. (1998) Fe-Ni exchange between olivine and sulphide liquid: Implications for oxygen barometry in sulphide-saturated magas. *Geochimica et Cosmochimica Acta* **64**(2), 307-320.

Brenan J. M. and Li C. (2000) Constraints on oxygen fugacity during sulfide segregation in the Voisey's Bay Intrusion, Labrador, Canada. *Economic Geology* **95**, 901-913.

Bridgewater D. and Collerson K. D. (1976) The major petrological and geochemical characters of the 3,600 m.y. Uivak gneisses from Labrador. *Contributions to Mineralogy and Petrology.* **54**, 43-59.

Bridgewater D., Escher A., and Watterson J. (1973) Tectonic displacement and thermal activity in two contrasting Proterozoic mobile belts from Greenland. *Philosophical Transactions of the Royal Society of London* **A273**. 513-533.

Buchanan D. L. and Nolan J. (1979) Solubility of sulfur and sulfide immiscibility in synthetic tholeiitic melts and their relevance to Bushveld complex rocks. *Canadian Mineralogist* **17**, 483-494.

Buchanan D. L., Nolan J., Wilkinson N., and De Villiers J. P. R. (1983) An experimental investigation of sulphur solubility as a function of temperature in synthetic silicate melts. *Special Publication of the Geological Society of South Africa* **7**, 383-391.

Campbell I. H. and Naldrett A. J. (1979) The influence of silicate:sulfide ratios on the geochemistry of magmatic sulfides. *Economic Geology* **74**. 1503-1506.

Cawthorn R. G., Sander B. K., and Jones I. M. (1992) Evidence for the trapped liquid shift effect in the Mount Ayliff intrusion, South Africa. *Contributions to Mineralogy and Petrology* **111**, 194-202.

Chai G. and Naldrett A. J. (1992) The Jinchuan ultramafic intrusion: cumulate of a high-Mg basaltic magma. *Journal of Petrology* **33**, 277-303.

Chen J. H. and Wasserburg G. J. (1983) The least radiogenic Pb in iron meteorites. *Fourteenth Lunar and Planetary Science Conference*, 103-104.

Clark T. and Naldrett A. J. (1972) The Distribution of Fe and Ni between synthetic olivine and sufide at 900 degrees C. *Economic Geology* **67**, 939-952.

Connelly J. N. and Ryan A. B. (1994) Late Archean and Proterozoic events in the central Nain Craton. *Secretariat Lithoprobe Report* **36**, 90-112.

Cooper M. (2000) The Sudbury Igneous Complex: Insights Into Melt Sheet Evolution and Ore Genesis. Ph.D., The Open University.

Craig J. R. and Kullerud G. (1969) Phase relations in the Cu-Fe-Ni-S system and their application to magmatic ore deposits. *Economic Geology Special Monograph* **4**, 344-358.

Czamanske G. K. and Zientek M. L. (1985) The Stillwater Complex, Montana: geology and guide. *Montana Bureau Of Mines Geology (special publication)* **92**, 396.

de Bremond d'Ars J., Arndt N. T., and Hallot E. (2001) Analog experimental insights into the formation of magmatic sulfide deposits. *Earth and Planetary Science Letters* **186**, 371-381.

Dickin A. P. (1995) *Radiogenic Isotope Geology*. Cambridge University Press.

Doe B. R. and Zartman R. E. (1979) Plumbotectonics 1, the Phanerozoic. In *Geochemistry of Hydrothermal Ore Deposits.* (ed. H. L. Barnes), pp. 22-70. Wiley.

Drake M. J. (1975) The oxidation state of europium as an indicator of oxygen fugacity. *Geochimica et Cosmochimica Acta* **39**, 55 - 64.

Drake M. J. and Weill D. F. (1975) Partition of Sr, Ba, Ca, Y, Eu^{2+}, Eu^{3+}, and other REE between plagioclase feldspar and magmatic liquid: an experimental study. *Geochimica et Cosmochimica Acta* **39**, 689 - 712.

Dressler B. O. (1984) The effects of the Sudbury event and the intrusion of the Sudbury Igneous complex on the footwall rocks of the Sudbury structure. In *The Geology and Ore Deposits of the Sudbury Structure*. Vol. 1 (ed. A. J. Naldrett, E. G. Pye, and P. E. Giblin), pp. 97-136. Ontario Geological Survey.

Dunn T. and Sen C. (1994) Mineral/matrix partition coefficients for orthopyroxene, plagioclase, and olivine in basaltic to andesitic systems: a combined analytical and experimental study. *Geochimica et Cosmochimica Acta* **58**, 717-733.

Durazzo A. and Taylor L. A. (1982) Exsolution in the MSS-pentlandite system: textural and genetic implications for Ni-sulfide ores. *Mineralium Deposita* **17**, 313-332.

Ebel D. S. and Naldrett A. J. (1996) Fractional crystallization of sulfide liquids at high temperature. *Economic Geology* **91**.

Ebel D. S. and Naldrett A. J. (1997) Crystallization of sulfide liquids and the interpretation of ore composition. *Canadian Journal of Earth Science* **34**, 352-365.

Emslie R. F., Hamilton M. A., and Theriault R. J. (1994) Petrogenesis of a mid-Proterozoic anorthosite-mangerite-charnockite-granite (AMCG) complex: isotopic and chemical evidence from the Nain Plutonic Suite. *The Journal Of Geology* **102**, 539-558.

Ermanovics I. and Van Kranendonk M. J. (1990) The Torngat Orogen in the North River - Nutak transect area of Nain and Churchill provinces. *Geoscience Canada* **17**, 279-283.

Evans A. M. (1993) *An Introduction to Ore Geology*. Blackwell.

Evans-Lambswood D. M., Butt D. P., Jackson R. S., Lee D. V., Muggeridge M. G., Wheeler R. I., and Wilton D. H. C. (2000) Physical controls associated with the distribution of sulphides in the Voisey's Bay Ni-Cu-Co deposit, Labrador. *Economic Geology* **95**, 749-769.

Faulkner E. L. (1969) Genetic implications of cobalt and nickel distribution in sulphide deposits of the Coronation Mine. *Geological Survey of Canada* **68**(5), 155-180.

Faure G. (1986) *Principles of Isotope Geology*. John Wiley and Sons.

Fincham C. J. B. and Richardson F. D. (1954) The behaviour of sulphur in silicate and aluminate melts. *Proceedings of the Royal Society* **A 223**, 40-62.

Fleet M. E. (2001) A comment on "Fe-Ni exhange between olivine and sulphide liquid: implications for oxygen barometry in sulphide saturated magmas" by Brenan and Caciagli (2000). *Geochimica et Cosmochimica Acta* **65**(23), 4425-4427.

Fleet M. E. and MacRae N. D. (1988) Partition of Ni between olivine and sulfide: equilibria with sulfide oxide liquids. *Contributions to Mineralogy and Petrology* **100**(462-469).

Fleet M. E., MacRae N. D., and Herzberg C. T. (1977) Partition of nickel between olivine and sulfide: a test for immiscible sulfide liquids. *Contributions to Mineralogy and Petrology* **65**, 191-197.

Fleet M. E. and McRae N. D. (1983) Partition of Ni between olivine and its application to Ni-Cu sulfide deposits. *Contributions to Mineralogy and Petrology* **83**, 75-81.

Fleet M. E. and McRae N. D. (1987) Partition of Ni between olivine and sulfide: the effect of temperature fO_2, and fS_2. *Contributions to Mineralogy and Petrology* **95**, 336-342.

Fleet M. E. and Pan Y. (1994) Fractional crystallization of anhydrous sulfide liquid in the system Fe-Ni-Cu-S, with application to magmatic sulfide deposits. *Geochimica et Cosmochimica Acta* **58**(16), 3369-3377.

Fleet M. E. and Stone W. E. (1990) Nickeliferous sulfides in xenoliths, olivine megacrysts and basaltic glass. *Contributions to Mineralogy and Petrology* **105**, 629-636.

Fletcher T. A., Boyce A. J., and Fallick A. E. (1987) A sulphur isotope study of Ni-Cu mineralisation in the Huntly-Knock Caledonian mafic and ultramafic intrusions of northeast Scotland. *Journal of the Geological Society of London* **146**, 675-684.

Fountain J. C., Hodge D. S., and Shaw R. P. (1989) Melt segregation in anatectic granites: a thermo-mechanical model. *Journal of Volcanology and Geothermal Research.* **39**(2), 279-296.

Fujimaki H., Tatsumoto T., and Aoki K. (1984) Partition coefficients of Hf, Zr, and the REE between phenocrysts and groundmass. Proceedings of the fourteenth Lunar and Planetary Science Conference, Part 2. *Journal of Geophysical Research* **89**(supplement), B662-B672.

Gaetani G. A. and Grove T. L. (1997) Partitioning of moderately siderophile elements among olivine, silicate melt, and sulfide melt: constraints on core formation in the Earth and Mars. *Geochimica et Cosmochimica Acta* **61**(9), 1829-1846.

Galer S. G. C. and Abouchami W. (1998) Practical application of lead triple spiking for correction of instrumental mass discrimination. *Mineralogical Magazine* **62A**, 491-492.

Garuti G., Gorgoni C., and Sighinolfi G. P. (1984) Sulfide mineralogy and chalcophie and siderophile element abundances in the Ivrea-Verbano mantle perodotites (Western Italian Alps). *Earth and Planetary Science Letters* **61**, 1829-1846.

Ghiorso M. S. and Sack R. O. (1994) Chemical mass transfer in magmatic processes. IV. A revised and internally consistant thermodynamics model for the interpolation and extrapolation of liquid /solid equilibria in magmatic systems at elevated temperatures and pressures. Contributions to Mineralogy and Petrology.

Green A. H. and Melezhik V. A. (1999) Geology of the pechanga ore deposits - a review with comments on ore forming processes. In *Dynamic Processes in Magmatic Ore Deposits and Their Application in Mineral Exploration*, Vol. Short Course Volume 13 (ed. R. R. Keays, C. M. Lesher, P. C. Lightfoot, and C. E. G. Farrow), pp. 287-328. Geological Association of Canada.

Gresham J. J. and Loftus-Hills G. D. (1981) The Geology of the Kambalda nickel field, Western Australia. *Economic Geology* **76**, 1373-1416.

Grieve R. A. F. (1994) An impact model for the Sudbury Structure. In *Sudbury-Noril'sk Symposium*, Vol. 5 (ed. A. J. Naldrett, E. G. Pye, and P. E. Giblin), pp. 119-132. Ontario Geological Survey.

Hamilton M. A., Emslie R. F., and Ryan B. (1998a) U-Pb evidence for Paleoproterozoic anorthosite and granitic magmatism predating the emplacement of the Mesoproterozoic Nain Plutonic Suite, Labrador. *G.A.C. - M.A.C.*, A- 71.

Hamilton M. A., Ryan A. B., Emslie R. F., and Ermanovics I. F. (1998b) Identification of Paleoproterozoic anorthosite and monzonitic rocks in the vicinity of the Mesoproterozoic Nain Plutonic Suite, Labrador: U-Pb evidence. *Current Research, Geological Survey of Canada, Report 11.* **1998F**, 23-40.

Harris D. C. and Nickel E. H. (1972) Pentlandite compositions and associations in some mineral deposits. *Canadian Mineralogist* **11**, 861-878.

Hart S. R. and Davies K. E. (1978) Nickel partitioning between olivine and silicate melt. *Earth and Planetary Science Letters* **40**, 203-219.

Hart S. R. and Davis K. E. (1979) Reply to D.B.Clarke and M.J. O'Hara, "Nickel and the existence of high MgO liquids in nature.". *Earth and Planetary Science Letters* **44**, 159-161.

Haughton D. R., Roeder P. L., and Skinner B. J. (1974) Solubility of sulfur in mafic magmas. *Economic Geology* **69**, 451-467.

Hauri E. H. and Hart S. R. (1994) Constraints on melt migration from mantle plumes: a trace element study of peridotite xenoliths from Savai'i, Western Samoa. *Journal of Geophysical Research* **99**(B12), 24301-24321.

Henderson P. (1982) *Inorganic Geochemistry*. Pergamon Press.

Hess P. C. (1980) Polymerization Model for Silicate Melts. In *The Physics of Magmatic Processes* (ed. R. B. Hargreaves), pp. 3-44. Princeton University Press.

Hirschmann M. M. and Stolper E. M. (1996) A possible role for garnet pyroxenite in the origin of the "garnet signature" in MORB. *Contributions to Mineralogy and Petrology* **124**, 185-208.

Hoffman P. F. (1987) Early Proterozoic foredeeps, foredeep magmatism and Superior-type iron formation of the Canadian Shield. In *Proterozoic Lithospheric Evolution.* (ed. A. Kroner), pp. 85-98. American Geophysical Unioun.

Hoffmann P. F. (1988) United plates of America, the birth of a craton: Early Proterozoic assembly and growth of Laurentia. *Annual Review Of Earth and Planetary Sciences* **16**, 543-603.

Huang W. L. and Williams R. J. (1980) Melting relations of portions of the system Fe-S-Si-O to 32kb with implications to the nature of the mantle-core boundary. *Lunar and Planetary Science Conference XI*, 486-488.

Hunter D. R. (1976) Some enigmas of the Bushveld Complex. *Economic Geology* **71**, 229-248.

Ionov P., Hoefs J., Wedepohl K. H., and Wiechet U. (1993) Content of sulphur in different mantle reservoirs: reply to comment on the paper "Content and isotopic composition of sulphur in ultramafic xenoliths from Central Asia". *Earth and Planetary Science Letters* **119**, 635-640.

Irvine T. N. (1974) Ultramafic and gabbroic rocks in the Aiken Lake and McConnell Creek map areas, British Columbia. *Report of Activities; Part A, April to October 1973; Petrology. Geological Survey of Canada.* **74-1**, 149-152.

Irvine T. N. (1975) Crystallization sequences in the Muskox intrusion and other layered intrusions-II. Origin of chromitite layers and similar deposits of other magmatic ores. *Geochimica et Cosmochimica Acta* **39**, 991-1020.

Irving A. J. and Frey F. A. (1978) Distribution of trace elements between garnet megacrysts and host volcanic liquids of kimberlitic to rhyolitic composition. *Geochimica et Cosmochimica Acta* **42**, 771 - 787.

Jackson G. and Hegner E. (1991) Evolution of Late Archaean to Early Proterozoic crust based on Nd isotopic data for Baffin Island and northern Quebec and Labrador. *Geological Association of Canada Progress Abstracts.* **16**, A59.

Jaques A. L. and Green D. H. (1980) Anhydrous melting of peridotite at 0-15Kb pressure and the genesis of tholeiitic basalts. *Contributions to Mineralogy and Petrology* **73**, 287-310.

Kaneda H., Takenouchi S., and Shoji T. (1986) Stability of pentlandite in the Fe-Ni-Co-S system. *Mineralium Deposita* **21**, 169-180.

Keays R. R. (1995) The role of komatiitic and picritic magmatism and S-saturation in the formation of ore deposits. *Lithos* **34**, 1-18.

Kelly D. P. and Vaughan D. J. (1983) Pyrrhotine-pentlandite ore textures: a mechanistic approach. *Mineralogical Magazine* **47**, 453-463.

Korstgard J., Ryan B., and Wardle R. (1987) The boundary between Proterozoic and Archaean crustal blocks in central West Greenland and northern Labrador. In *Evolution of the Lewisian and Comparable Precambrian High Grade Terrains.* (ed. R. G. Park and J. Tarney), pp. 247-249. The Geological Society of London.

Kress V. (1997) Thermochemistry of sulfide liquids I. The system O-S-Fe at 1 bar. *Contributions to Mineralogy and Petrology* **127**, 176-186.

Kullerud G., Yund R. A., and Moh G. H. (1969) Phase relations in the Cu-Fe-S, Cu-Ni-S and Fe-Ni-S systems. *Economic Geology Special Monographs* **4**, 323-343.

Lambert D. D., Frick L. R., Li C., Foster J. G., and Naldrett A. J. (2000) Re-Os isotope systematics of the Voisey's Bay Ni-Cu-Co magmatic sulfide system. Labrador, Canada: II. Implications for parental magma chemistry, ore genesis and metal redistribution. *Economic Geology* **95**, 867-888.

Lesher C. M. and Burnham O. M. (1999) Mass balance and mixing in magmatic sulphide systems. In *Dynamic Processes in Magmatic Ore Deposits And Their Application To Mineral Exploration*, Vol. 13 (ed. R. R. Keays, C. M. Lesher, P. C. Lightfoot, and C. E. G. Farrow), pp. 413-449. Geological Association of Canada.

Lesher C. M. and Groves D. I. (1986) Controls on the formation of Komatiite-associated nickel-copper sulfide deposits. In *Geology and Metallogeny of Copper Deposits* (ed. G. H. Freidrich, A. D. Genkin, A. J. Naldrett, J. D. Ridge, R. H. Sillitoe, and F. M. Vokes), pp. 43-62. Springer-Verlag.

Li C., Barnes S. J., Makovicky E., Rose-Hanson J., and Makovicky M. (1996) Partitioning of nickel, copper, iridium, rhenium, platinum , and palladium between

monosulphide solid solution and sulfide liquid: effects of composition and temperature. *Geochimica et Cosmochimica Acta* **60**(7), 1231-1238.

Li C., Lightfoot P. C., Amelin Y., and Naldrett A. J. (2000) Contrasting Petrological and geochemical relationships in the Voisey's Bay and Mushuau Intrusions, Labrador, Canada: implications for ore genesis. *Economic Geology* **95**, 771-799.

Li C. and Naldrett A. J. (1983) Sulfide capacity of magma: a quantitative model and its application to the formation of sulfide ores at Sudbury. *Economic Geology* **88**, 1253-1260.

Li C. and Naldrett A. J. (1999) Geology and petrology of the Voisey's Bay intrusion: reaction of olivine with sulfide and silicate liquids. *Lithos* **47**, 1-31.

Li C. and Naldrett A. J. (2000) Melting reactions of gneissic inclusions with enclosing magma at Voisey's Bay, Labrador, Canada: implications with respect to ore genesis. *Economic Geology* **95**(4), 801-814.

Li C., Naldrett A. J., and Ripley E. M. (2001) Critical factors for the formation of a nickel-copper deposit in an evolved magma system: lessons from a comparison of the Pants Lake and Voisey's Bay sulfide occurances in Labrador, Canada. *Mineralium Deposita* **36**, 85-92.

Lightfoot P. C. and Naldrett A. J. (1999) Geological and geochemical relationships in the Voisey's Bay Intrusion, Nain Plutonic Suite, Labrador, Canada. In *Geological Association of Canada short course Notes*, Vol. 13 (ed. R. R. Keays, C. M. Lesher, P. C. Lightfoot, and C. E. G. Farrow), pp. 1-31.

Lorand J. P. (1991) Sulphide petrology and sulphide geochemistry of orogenic lherzolites: a comparative study of the Pyrenean bodies (France). *Journal of Petrology* **Special Issue Orogenic lherzolites**, 56-77.

Lorand J. P. (1993) Comment on the paper "Content and isotopic composition of ultramfic xenoliths from Central Asia" by Ionov, D., Hoefs, J., Wedepohl, K. H. and Wiechert, U. *Earth and Planetary Science Letters* **119**, 627-634.

Ludwig K. R. (1999) ISOPLOT/EX a geochronological toolkitfor Microsoft Excel. Berkley Geochronolgy Center Special Publication.

MacLean W. H. (1969) Liquidus phase relations in the FeS-FeO-Fe_3O_4-SiO_2 system and their application in geology. *Economic Geology* **64**, 865-884.

Mathez E. A. (1976) Sulfur solubility and magmatic sulfides in submarine basalt glass. *Journal of Geophysical Research* **81**, 4269-4276.

Mavrogenes J. A. and O'Neill H. S. C. (1999) The relative effects of temperature and oxygen fugacity on the solubility of sulfide in mafic magmas. *Geochimica et Cosmochimica Acta* **63**(7/8), 1173-1180.

McDonough W. F. and Sun S. S. (1995) The composition of the Earth. *Chemical Geology* **120**, 223-253.

McKenzie D. and Bickle M. J. (1988) The volume and composition of melt generated by extension of the lithosphere. *Journal of Petrology* **29**, 625-679.

McKenzie D. and ONions R. K. (1991) Partial melt distributions from inversions of rare earth element concentrations. *Journal of Petrology* **32**, 1021-1091.

Morgan J. W. (1986) Ultramafic xenoliths: clues to the Earth's late accretionary history. *Journal of Geophysical Research* **91**(B12), 12375-12387.

Morse S. A. (1969) Layered intrusions and anorthosite genesis. *Memoir of the New York State Museum and Science Service* **18**, 175-187.

Naldrett A. J. (1969) A portion of the system Fe-S-O between 900 °C and 1080°C and its application to sulfide ore magmas. *Journal of Petrology* **10**, 171-201.

Naldrett A. J. (1989a) Magmatic deposits associated with mafic rocks. In *Ore Deposition Associated With Magmas*, Vol. 4 (ed. J. A. Whitney and A. J. Naldrett), pp. 1-3. Society of Economic Geologists.

Naldrett A. J. (1989b) *Magmatic Sulfide Deposits*. Oxford University Press.

Naldrett A. J. (1997) Key Factors in the genesis of Ni-Cu-PGE deposits: implications for exploration. In *Seventeenth Ore Deposits Workshop*, Vol. 1 (ed. A. J. Naldrett), pp. 471. University of Toronto.

Naldrett A. J. (1999) World-class Ni-Cu-PGE deposits: key factors in their genesis. *Mineralium Deposit* **34**, 227-240.

Naldrett A. J., Fedorenko V. A., ,, Lightfoot P. C., Kunilov V. A., Gorbachev N. S., Doherty W., and Johan Z. (1995) Ni-Cu-PGE deposits of the Noril'sk region, Siberia: their formation in conduits for flood basalt volcanism. *Transactions of the Institute of Mining and Metallogy* **104**, B18-B36.

Naldrett A. J., Keats H., Sparkes K., Moore R., and McKenzie C. (1997) Voisey's Bay, Canada: implications for exploration. *Minerals Industry International*(January), 66-70.

Naldrett A. J. and Lightfoot P. C. (1999) Ni-Cu-PGE deposits of the Noril'sk region, Siberia: their formation in conduits for flood basalt volcanism. In *Dynamic Processes in Magmatic Ore Deposits and their Application in Mineral Exploration*, Vol. Short course Volume 13 (ed. R. R. Keays, C. M. Lesher, P. C. Lightfoot, and C. E. G. Farrow), pp. 195-249. Geological Association of Canada.

Naldrett A. J., Singh J., Krstic S., and Li C. (2000) The mineralogy of the Voisey's Bay Ni-Cu-Co deposit, northern Labrador, Canada: The influence of oxidation state on textures and mineral compositions. *Economic Geology* **95**, 889 -900.

O'Neill H. S. C. (1991) The origin and early history of the Earth - a chemical model. Part 2. *Geochimica et Cosmochimica Acta* **55**, 1159-1172.

O'Neill H. S. C. and Mavrogenes J. A. (2002) The sulfide capacity and sulfur content at sulfur saturation of silicate melts at 1400 degrees C and 1 bar. *Journal of Petrology* **43**, 1049-1087.

Oversby V. M. (1970) The isotopic composition of lead in iron meteorites. *Geochimica et Cosmochimica Acta.* **34**, 65-75.

Prendergast M. D. (1988) The geology and economic potential of the PGE-rich main sulfide zone of the Great Dyke, Zimbabwe. *Geo-platinum '87*, 281-302.

Rajamani V. and Naldrett A. J. (1978) Partitioning of Fe, Co, Ni, and Co between sulfide liquid and basaltic melts and the composition of Ni-Cu sulfide deposits. *Economic Geology* **73**, 82-93.

Riley J. F. (1977) The pentlandite group $(Fe,Ni,Co)_9S_8$: new data and an appraisal of structure-composition relationships. *Mineralogical Magazine* **41**(319), 345-349.

Ripley E. M. (1981) Sulfur isotopic abundances of the Dunka Road Cu-Ni deposit, Duluth Complex, Minnesota. *Economic Geology* **76**, 619-620.

Ripley E. M. (1986) Applications of stable isotope studies to problems of magmatic sulfide ore genesis with special reference to the Duluth Complex, Minnesota. In *Geology and Metallogeny of Copper Deposits* (ed. G. H. Freidrich, A. D. Genkin, A. J. Naldrett, J. D. Ridge, R. H. Sillitoe, and F. M. Vokes), pp. 24-42. Springer-Verlag.

Ripley E. M., Park Y. R., Li C., and Naldrett A. J. (1999) Sulfur and oxygen isotopic evidence of country rock contamination in the Voisey's Bay Ni-Cu-Co deposit, Labrador, Canada. *Lithos* **47**, 53-68.

Roeder P. L. (1974) Activity of iron and olivine solubility in basaltic liquids. *Earth and Planetary Science Letters* **23**, 397-410.

Roeder P. L. and Emslie R. F. (1970) Olivine-liquid equilibrium. *Contributions to Mineralogy and Petrology* **29**, 275-289.

Ryan B. (2000) The Nain Churchill boundary and the Nain Plutonic Suite: a regional perspective on the geologic setting of the Voisey's Bay Ni-Cu-Co deposit. *Economic Geology* **95**, 703-724.

Ryan B., Krogh T. E., Heaman L., Scharer U., Philippe S., and Olivier G. (1991) On recent geochronological studies in the Nain Province, Churchill Province and Nain

Plutonic Suite, north-central Labrador. *Current Research, Newfoundland Department of Mines and Energy, Geological Survey Branch.* **91-1**, 257-261.
Ryan B., Wardle R. J., Gower C. F., and Nunn G. A. G. (1995) Nickel-copper-sulphide mineralization in Labrador: the Voisey Bay discovery and its exploration implications. *Newfoundland Department of Natural Resources, Geological Survey; Report.* **95**(1), 177-204.
Schiotte L., Hansen B. T., Shirey S. B., and Bridgewater D. (1993) Petrological and whole rock isotopic characteristics of tectonically juxtaposed Archaean gneisses of the Okak area of the Nain Province, Labrador: relavance for terrane models. *Precambrian Research* **63**, 293-323.
Shaw D. M. (1970) Trace element fractionation during anatexis. *Geochimica et Cosmochimica Acta* **34**, 237-234.
Shima H. and Naldrett A. J. (1975) Solubility of sulfur in an ultramafic melt and the relevance of the system Fe-S-O. *Economic Geology* **70**, 960-967.
Simkin T. and Smith J. V. (1970) Minor element distribution in olivine. *Journal of Geology* **78**, 304-325.
Speer J. A. (1982) Metamorphism of the pelitic rocks of the Snyder Group in the contact aureole of the Kiglapait layered intrusion, Labrador: effects of buffering partial pressures of water. *Canadian Journal of Earth Science* **19**, 1888-1909.
Stacey J. S. and Kramers J. D. (1975) Approximation of a terrestrial lead isotope evolution by a two stage model. *Earth and Planetary Science Letters* **26**, 207-221.
Streckeisen A. (1976) To each plutonic rock its proper name. *Earth Science Reviews* **12**, 1-33.
Sugaki A. and Kitakaze A. (1998) High form of pentlandite and its thermal stability. *American Mineralogist* **83**, 133-140.
Sun S. S. and McDonough W. F. (1989) Chemical and isotopic systematics of ocean basalts: implications for mantle compositions and processes. In *Magmatism In the Ocean Basins*, Vol. 42 (ed. A. D. Saunders and M. J. Norry), pp. 313-345. Geological Society of London/Blackwell Scientific.
Tatsumoto M., Knight R. J., and Allegre C. J. (1973) Time differences in the formation of meteorites as determined from the ratio of lead-207 to lead-206. *Science* **180**, 1279-1283.
Taylor F. C. (1971) A revision of Precambrian structural provinces in northeastern Quebec and Northern Labrador. *Canadian Journal of Earth Sciences.* **8**, 579-584.
Taylor F. C. (1972) A revision of Precambrian structural provinces in northeastern Quebec and Labrador: reply. *Canadian Journal of Earth Sciences* **9**, 930-932.
Taylor F. C. (1979) *Reconnaissance Geology of part of the Precambrian Shield, Northeastern Quebec, Northern Labrador and Northwestern Territories.* Geological Survey of Canada.
Taylor S. R. and McLennan S. M. (1985) *The Continental Crust: Its Composition and Evolution.* Blackwell.
Thompson J. F. H. and Naldrett A. J. (1984) Sulphide silicate reactions as a guide to Ni-Cu-Co mineralisation in central Maine, USA. In *Sulphide Deposits in Mafic and Ultramafic Rocks*, pp. 103-113. Institute of Mining and Metallogy.
Ueno T., Ito S., Nakatsaki S., Nakano K., Harada T., and Yamazaki T. (2000) Phase equilibria in the system Fe-Ni-S at 500^{o}C and 400^{o}C. *Journal of Mineralogical and Petrological Sciences* **95**, 145-161.
Van Kranendonk M. J. (1996) Tectonic evolution of the Paleoproterozoic Torngat Orogen: Evidence from pressure-temperature-time-deformation paths in the North River map area, Labrador. *Tectonics* **15**(4), 843-869.
Van Kranendonk M. J., St-Onge M. R., and Henderson J. R. (1993) Paleoproterozoic tectonic assemblage of northeast Laurentia through multiple indentations. *Precambrian Research* **63**, 325-347.

Vaughan D. J. and Craig J. R. (1978) *Mineral Chemistry of Metal Sulphides*. Cambridge University Press.
Vielzuf D. and Vidal P. (1990) Granulites and crustal evolution. In *Mathematical and Physical Sciences C*, Vol. 311, pp. 157-169.
Wager L. R. and Brown G. M. (1968) *Layered Igneous Intrusions*. Oliver and Boyd.
Wallace P. and Carmichael I. S. E. (1992) Sulfur in basaltic magmas. *Geochimica et Cosmochimica Acta* **56**, 163-184.
Wardle R. J. (1983) Nain-Churchill Province cross-section, Nachvak Fiord, northern Labrador. *Current Research Newfoundland Department of Mines and Energy, Mineral Development Division* **Report 86-1**, 68-89.
Wardle R. J. and Wilton D. H. C. (1995) The Geology And Mineral Deposits Of Labrador: The Nain Province,. In *The Geology And Mineral Deposits Of Labrador: A Guide for the Exploration Geologist.*, pp. 14-22. Geological Survey, Department of Natural Resources, Government of Newfoundland and Labrador.
Weiblen P. W. and Morey G. B. (1980) A summary of the stratigraphy, petrology, and structure of the Duluth Complex. *Ammerican Journal of Science* **280-A**(88-133).
Weill D. F. and Drake M. J. (1973) Europium anomaly in plagioclase feldspar: experimental results and semiquantitative model. *Science* **180**, 1059 - 1060.
Wendlandt R. F. (1982) Sulfide saturation of basalt and andesite melts at high pressures and temperatures. *American Mineralogist* **67**, 877-885.
Wendt J. I. and Collerson K. D. (1999) Early Archeaen U/Pb fractionation and timing of late Archeaen high-grade metamorphism in the Saglek-Hebron segment of the North Atlantic Craton. *Precambrian Research* **93**, 281-297.
Wilton D. H. C. (1996) Metallogenic overview of the Nain Province, northern Labrador. *CIM Bulletin* **89**(997), 43-52.
Wisser D. J. L. and von Gruenewaldt G. (1970) Syposium on the Bushveld and other layered complexes. *Geological Society of South Africa (special publication)* **1**, 763.
Yoder H. S. and Tilley C. E. (1962) Origin of basaltic magmas: an experimental study of natural and synthetic rock systems. *Journal of Petrology* **3**, 342-352.
Zurbrigg H. F. (1963) Thomson mine geology. *Transactions of the Canadian Institute of Mining and Metallogy* **66**, 227-236.

Appendix A Data tables.

The data here are divided into separate tables according to their chapters. Table A.2 presents the major and trace element analyses for whole rocks. The major element data are presented as oxides and are expressed as weight percent values, while trace elements are presented as parts per million. The major element data are normalised to 100 percent after loss on ignition (LOI) analyses were carried out. However, the LOI prior to normalisation are included.

Throughout Table A.2, abbreviations have been used for the various rock types found at Voisey's Bay. These abbreviations are summarised below:

NTT	Normal textured troctolite.
VTT	Variable textured troctolite.
IVT	Inclusion-bearing variable troctolite.
BBS	Breccia sequence.
Mushaua	Troctolitic and gabbroic rocks from the Mushaua intrusion.
Nain	Nain gneiss.
Tasiuyak	Tasiuyak gneiss.
Enderbite	Enderbite gneiss.

Table A.2 also includes information on the sampling locality. This is expressed as the drill core identifier, e.g. VB 96 266. Additionally, the grid reference is given. This coincides with the grid numbering system shown on all the maps reproduced in thesis and is expressed in universal transverse Mercator (UTM) coordinates.

Table A3 gives the analyses for olivine by electron microprobe analyses. These data are expressed in weight percent. The detection limits for the Open University's Cameca SX100 electron microprobe are given in ppm in table A1 below.

Element	K	Na	Mg	Si	P	Cl	Cr	Ni	Ba	Al	Ca	Ti	Mn	Fe
Detection Limits	130	154	117	116	115	187	253	127	358	100	139	165	139	168

Table A.1 Detection limits for various elements on the Open University's Cameca SX100 electron microprobe.

Table A4 gives the analyses for sulphides as carried out by electron microprobe. Data are presented in duplicate columns. The first set gives totals and element abundances in weight percent. The second set gives the element abundances expressed as atomic proportions. These have been normalised to 100 percent. For each polished thin section, the host material with respect to sulphide has been stated. These are abbreviated to the forms below:

Troc Troctolite/gabbro hosted.

BBS Breccia sequence hosted.

MASU Massive sulphide.

Although data is presented for S, Fe, Co, Ni and Cu, the analyses included Ti, Zn, and Pb. However, the abundances of the latter group elements were always less than 0.02 weight percent. Therefore, in the interests of brevity these data were not included.

Tables A5a-b give the Pb isotope analyses. The Pb isotope data are expressed as ratios so are without units. Table A5a presents the sulphide data analysed at the Open University using MC-ICP-MS, and Table A5B presents the sulphide data analysed on behalf of INCO at the University of Toronto using thermal ionisation mass spectrometry (TIMS). The University of Toronto/INCO data are unpublished. In both tables A5a and b, the UTM coordinates of the diamond drill hole are included.

Table A6 presents the data resulting from the electron microprobe analysis of hercynitic spinel grains found chiefly within the Breccia sequence rocks. These data were not presented in the main thesis as it was not possible during the writing of this work to correlate the observed variations with the parameters considered here. However, it is now the author's opinion that the variations in spinel chemistry may well relate to variation in the FO2 prevalent during the formation of the spinels from their precursor minerals. This merits further work and this combined with the wish to document the scope of the analyses undertaken is the reason for the inclusion of these data here.

Table A.2 Whole rock major and trace element data

SAMPLE	RX 321028	RX 321029	RX 321030	RX 321031	RX 321032	RX 321033	RX 321034	RX 321199
Rock type	NTT	NTT	NTT	NTT	NTT	NTT	NTT	STT
Drill hole	VB 96 266	VB 96 266	VB 96 266	VB 96 266	VB 96 266	VB 96 266	VB 96 266	VB 96 266
Depth	14	31	44.3	55.5	71.5	77	101	335
Easting	556965.8	556965.8	556965.8	556965.8	556965.8	556965.8	556965.8	556965.8
Northing	6242466.0	6242466.0	6242466.0	6242466.0	6242466.0	6242466.0	6242466.0	6242466.0
SiO_2	48.1	47.3	47.0	47.5	47.6	47.2	47.9	43.9
TIO_2	0.7	0.6	0.6	0.6	0.6	0.5	0.5	8.7
Al_2O_3	22.5	21.5	21.0	21.7	21.4	20.9	22.8	12.4
Cr_2O_3	0.0	0.0	0.0	0.0	0.0	0.0	0.0	0.0
Fe_2O_3	6.6	7.6	7.8	7.3	7.3	7.7	6.2	13.9
MnO	0.1	0.1	0.1	0.1	0.1	0.1	0.1	0.2
MgO	8.8	10.4	11.0	10.4	10.7	11.5	9.2	6.9
CaO	9.9	9.4	9.4	9.4	9.3	9.0	10.0	10.8
Na_2O	2.9	2.8	2.8	2.8	2.7	2.7	3.0	2.7
K_2O	0.2	0.3	0.2	0.2	0.3	0.2	0.2	0.4
P_2O_5	0.2	0.1	0.1	0.1	0.1	0.1	0.1	0.3
Total	100.0	100.0	100.0	100.0	100.0	100.0	100.0	100.0
LOI	0.2	0.6	0.4	0.8	0.4	0.0	0.0	0.0
Sc	6.7	6.2	6.2	5.8	6.2	5.8	5.1	62.3
Cr	68	76	71	61	70	67	54	142
Co	42	48	50	47	49	54	44	56
Ni	259	297	323	302	325	364	287	56
Cu	12.0	14.7	12.1	12.0	12.0	11.9	9.2	183.9
Rb	1.699	3.776	1.936	2.463	2.821	1.842	1.509	4.306
Sr	607	591	564	575	592	591	643	296
Y	6.0	5.4	5.2	4.9	5.2	4.6	4.5	15.6
Zr	39	50	38	42	29	30	42	75
Nb	1.82	1.72	1.60	1.60	1.67	1.40	1.53	6.73
Cs	0.02	0.07	0.04	0.05	0.04	0.03	0.03	0.06
Ba	154.0	146.3	138.1	135.9	133.9	130.2	134.0	177.3
La	5.45	4.99	4.79	4.55	4.57	4.19	4.36	7.03
Ce	12.61	11.41	11.05	10.40	10.45	9.62	9.79	18.32
Pr	1.69	1.50	1.46	1.39	1.38	1.28	1.29	2.74
Nd	7.42	6.69	6.46	6.13	6.11	5.58	5.81	13.27
Sm	1.56	1.41	1.33	1.27	1.26	1.15	1.19	3.46
Eu	0.92	0.83	0.81	0.81	0.79	0.77	0.81	1.25
Gd	1.44	1.24	1.26	1.15	1.15	1.04	1.05	3.36
Tb	0.21	0.18	0.17	0.16	0.17	0.16	0.15	0.50
Dy	1.14	1.00	1.02	0.93	0.95	0.86	0.87	3.08
Ho	0.22	0.20	0.19	0.19	0.18	0.16	0.16	0.60
Er	0.58	0.51	0.51	0.47	0.48	0.42	0.42	1.46
Tm	0.08	0.08	0.07	0.07	0.07	0.06	0.06	0.21
Yb	0.46	0.42	0.42	0.38	0.41	0.36	0.37	1.16
Lu	0.07	0.06	0.06	0.06	0.06	0.05	0.05	0.18
Ta	0.12	0.11	0.11	0.10	0.12	0.09	0.10	0.58
Th	0.12	0.14	0.11	0.10	0.18	0.09	0.10	0.27
U	0.02	0.03	0.02	0.03	0.05	0.02	0.03	0.06

SAMPLE	RX 321063	RX 321194	RX 321199	RX 321163	RX 321164	RX 321165	RX 321166	RX 321169
Rock type	STT	STT	STT	STT	STT	STT	STT	STT
Drill hole	VB 96 266	VB 96 266	VB 96 266	VB 96 266	VB 96 266	VB 96 266	VB 96 266	VB 96 266
Depth	583.1	38	335	21	30	49	67	80
Easting	556965.8	556965.8	556965.8	556965.8	556965.8	556965.8	556965.8	556965.8
Northing	6242466.0	6242466.0	6242466.0	6242466.0	6242466.0	6242466.0	6242466.0	6242466.0
SiO_2	52.7	44.5	43.9	47.4	46.8	47.1	45.7	46.0
TIO_2	0.4	8.5	8.7	1.9	3.2	1.7	2.4	2.9
Al_2O_3	21.5	12.2	12.4	17.8	17.5	16.7	16.8	16.5
Cr_2O_3	0.0	0.0	0.0	0.0	0.1	0.1	0.0	0.0
Fe_2O_3	4.6	14.0	13.9	12.0	11.9	13.0	13.8	13.9
MnO	0.1	0.2	0.2	0.1	0.1	0.1	0.2	0.2
MgO	4.6	6.8	6.9	8.4	8.2	9.9	10.4	8.9
CaO	11.9	10.3	10.8	8.0	8.3	7.8	7.1	7.7
Na_2O	3.9	2.9	2.7	3.5	3.5	2.9	3.1	3.1
K_2O	0.3	0.5	0.4	0.5	0.3	0.5	0.4	0.5
P_2O_5	0.1	0.1	0.3	0.3	0.2	0.2	0.2	0.3
Total	100.0	100.0	100.0	100.0	100.0	100.0	100.0	100.0
LOI	0.6	0.0	0.0	0.0	0.8	0.0	0.2	0.0
Sc	23.5	61.6	62.3	15.1	21.1	17.7	13.1	17.5
Cr	147	155	156	153	153	153	154	154
Co	304	38	142	331	468	386	358	266
Ni	23	53	56	57	58	62	69	60
Cu	36.4	27.9	55.7	89.9	94.5	96.9	115.1	89.4
Rb	175.442	67.046	183.891	53.137	52.517	49.153	83.705	59.976
Sr	429	311	296	449	441	409	420	406
Y	6.2	12.1	15.6	11.9	8.4	9.4	7.1	13.2
Zr	25	70	75	81	65	49	39	55
Nb	0.85	7.39	6.73	3.98	3.32	3.02	3.12	5.39
Cs	0.03	0.05	0.06	0.04	0.08	0.08	0.07	0.09
Ba	123.4	188.1	177.3	227.4	223.9	188.5	181.1	233.1
La	2.97	4.47	7.03	8.37	5.31	6.78	5.46	9.61
Ce	6.72	11.24	18.32	20.08	12.60	15.96	12.81	23.21
Pr	0.92	1.72	2.74	2.77	1.77	2.14	1.73	3.23
Nd	4.45	8.69	13.27	12.56	8.04	9.59	7.71	14.61
Sm	1.08	2.34	3.46	2.76	1.83	2.20	1.60	3.07
Eu	0.63	1.22	1.25	1.24	1.01	1.03	0.91	1.31
Gd	1.18	2.48	3.36	2.61	1.77	2.03	1.59	2.96
Tb	0.18	0.37	0.50	0.38	0.26	0.30	0.24	0.44
Dy	1.14	2.33	3.08	2.25	1.54	1.81	1.34	2.52
Ho	0.23	0.45	0.60	0.43	0.30	0.34	0.27	0.49
Er	0.61	1.20	1.46	1.13	0.78	0.90	0.69	1.25
Tm	0.09	0.17	0.21	0.16	0.11	0.13	0.10	0.18
Yb	0.50	0.94	1.16	0.90	0.65	0.76	0.57	1.07
Lu	0.08	0.15	0.18	0.13	0.10	0.11	0.09	0.16
Ta	0.06	0.62	0.58	0.30	0.27	0.23	0.24	0.38
Th	0.07	0.28	0.27	0.27	0.17	0.39	0.17	0.31
U	0.02	0.05	0.06	0.05	0.04	0.08	0.03	0.06

SAMPLE	RX 321168	RX 321197	RX 321036	RX 321006	RX 321035	RX 321037	RX 321016	RX 321017
Rock type	STT	STT	VTT	VTT	VTT	VTT	VTT	VTT
Drill hole	VB 96 266	VB 96 266	VB 96 266	VB 96 266	VB 96 266	VB 96 266	VB 96 266	VB 96 266
Depth	93	204	115.5	355.7	109	128	136.3	143
Easting	556965.8	556965.8	556965.8	556965.8	556965.8	556965.8	556965.8	556965.8
Northing	6242466.0	6242466.0	6242466.0	6242466.0	6242466.0	6242466.0	6242466.0	6242466.0
SiO_2	46.6	48.9	46.4	46.3	46.7	47.8	47.3	47.3
TIO_2	1.9	1.3	0.5	1.0	0.5	0.7	1.1	1.0
Al_2O_3	17.3	19.9	18.8	18.1	21.1	22.2	21.4	21.1
Cr_2O_3	0.0	0.0	0.0	0.0	0.0	0.0	0.0	0.0
Fe_2O_3	13.1	9.7	8.9	10.2	8.7	7.1	8.4	7.7
MnO	0.1	0.1	0.1	0.1	0.1	0.1	0.1	0.1
MgO	9.4	7.5	14.4	13.0	10.6	8.7	8.5	9.5
CaO	7.4	8.3	8.1	8.0	9.2	9.8	9.6	9.5
Na_2O	3.3	3.7	2.5	2.7	2.7	3.0	3.0	3.2
K_2O	0.5	0.4	0.2	0.3	0.2	0.3	0.4	0.4
P_2O_5	0.3	0.2	0.1	0.2	0.1	0.2	0.2	0.3
Total	100.0	100.0	100.0	100.0	100.0	100.0	100.0	100.0
LOI	0.2	0.0	1.1	0.6	0.2	0.0	0.7	1.6
Sc	12.7	10.5	6.0	9.9	5.8	6.6	8.7	7.5
Cr	260	313	88	164	89	69	82	65
Co	61	48	66	76	82	44	79	50
Ni	105	76	462	762	1932	232	1195	222
Cu	46.8	27.6	10.5	203.2	532.6	19.0	555.4	36.1
Rb	5.025	3.215	2.154	2.619	1.595	3.348	11.922	6.034
Sr	434	496	530	508	583	624	645	608
Y	12.6	9.0	3.7	8.8	4.4	6.5	9.5	9.5
Zr	94	51	27	37	36	54	53	54
Nb	4.72	3.25	1.17	2.98	1.40	2.19	3.02	3.19
Cs	0.10	0.04	0.02	0.02	0.02	0.03	0.14	0.24
Ba	250.4	228.9	116.3	158.4	129.2	158.4	162.2	158.2
La	9.85	7.08	3.46	6.69	4.07	5.75	7.56	7.92
Ce	23.62	16.58	7.77	15.73	9.27	13.42	18.00	18.88
Pr	3.24	2.23	1.05	2.10	1.22	1.78	2.40	2.52
Nd	14.10	9.98	4.57	9.54	5.40	7.94	10.76	11.46
Sm	3.05	2.11	0.92	1.98	1.11	1.66	2.25	2.44
Eu	1.29	1.17	0.64	0.92	0.74	0.91	1.00	1.01
Gd	2.85	1.97	0.83	1.89	1.04	1.49	2.15	2.19
Tb	0.42	0.29	0.12	0.27	0.15	0.21	0.31	0.32
Dy	2.35	1.69	0.70	1.66	0.84	1.26	1.79	1.83
Ho	0.46	0.32	0.13	0.32	0.16	0.24	0.34	0.34
Er	1.23	0.85	0.34	0.85	0.40	0.63	0.89	0.89
Tm	0.18	0.12	0.05	0.12	0.06	0.09	0.13	0.13
Yb	1.02	0.68	0.28	0.66	0.33	0.51	0.67	0.68
Lu	0.15	0.11	0.04	0.11	0.05	0.08	0.10	0.11
Ta	0.32	0.22	0.09	0.20	0.10	0.14	0.20	0.22
Th	0.33	0.22	0.07	0.23	0.09	0.15	0.23	0.22
U	0.07	0.04	0.02	0.05	0.02	0.03	0.06	0.05

SAMPLE	RX 321018	RX 321019	RX 321020	RX 321021	RX 321008	RX 321009	RX 321010	RX 321011
Rock type	VTT	VTT	VTT	VTT	VTT	VTT	VTT	VTT
Drill hole	VB 96 266	VB 96 266	VB 96 266	VB 96 266	VB 96 266	VB 96 266	VB 96 266	VB 96 266
Depth	143.5	156.5	167	187	192.5	206.5	211.5	224
Easting	556965.8	556965.8	556965.8	556965.8	556965.8	556965.8	556965.8	556965.8
Northing	6242466.0	6242466.0	6242466.0	6242466.0	6242466.0	6242466.0	6242466.0	6242466.0
SiO_2	47.9	47.1	47.3	47.4	47.6	47.2	45.6	47.2
TIO_2	0.6	0.5	0.8	0.9	0.7	0.7	0.7	0.8
Al_2O_3	22.0	21.7	21.3	21.0	21.2	21.8	19.5	20.8
Cr_2O_3	0.0	0.0	0.0	0.0	0.0	0.0	0.0	0.0
Fe_2O_3	7.2	9.0	8.3	8.2	7.8	8.7	11.7	8.7
MnO	0.1	0.1	0.1	0.1	0.1	0.1	0.1	0.1
MgO	9.6	9.0	9.4	9.6	10.0	8.3	10.7	10.1
CaO	9.4	9.4	9.4	9.3	9.2	9.6	8.6	9.0
Na_2O	2.9	2.9	3.0	3.0	2.8	3.2	2.8	3.0
K_2O	0.2	0.3	0.3	0.3	0.5	0.3	0.2	0.3
P_2O_5	0.1	0.1	0.2	0.2	0.1	0.2	0.1	0.2
Total	100.0	100.0	100.0	100.0	100.0	100.0	100.0	100.0
LOI	0.5	0.7	0.5	0.5	1.5	1.1	1.1	0.3
Y								
Sc	6	6	8	8	6	6	7	6
Cr	61	74	125	83	79	74	101	60
Co	51	92	72	57	58	83	128	70
Ni	207.7	1651.2	849.1	512.7	519.8	1644.7	2429.2	751.1
Cu	27.343	619.022	362.448	146.323	140.863	657.151	1004.975	259.504
Rb	2	3	3	3	9	3	2	3
Sr	624.5	638.9	627.6	617.3	600.9	617.0	554.0	591.5
Y	5	4	6	7	5	6	5	7
Zr	18.00	43.00	40.00	43.00	52.00	56.00	36.00	51.00
Nb	1.46	1.26	2.03	2.53	1.75	2.10	1.54	2.43
Cs	0.0	0.0	0.0	0.0	0.3	0.0	0.0	0.0
Ba	140.37	141.27	145.85	162.33	133.65	159.06	139.79	164.85
La	4.37	3.81	5.19	6.07	4.68	5.61	4.18	6.28
Ce	9.92	8.63	11.96	14.21	10.82	13.06	9.45	14.64
Pr	1.30	1.13	1.60	1.89	1.43	1.73	1.23	1.94
Nd	5.81	5.01	7.19	8.54	6.43	7.68	5.57	8.45
Sm	1.19	1.07	1.49	1.76	1.32	1.63	1.18	1.85
Eu	0.79	0.83	0.86	0.96	0.85	0.90	0.81	0.94
Gd	1.10	0.94	1.40	1.70	1.28	1.47	1.08	1.72
Tb	0.16	0.13	0.20	0.25	0.18	0.22	0.16	0.23
Dy	0.91	0.78	1.17	1.40	1.00	1.26	0.88	1.34
Ho	0.17	0.15	0.22	0.26	0.19	0.23	0.17	0.26
Er	0.44	0.38	0.57	0.71	0.51	0.64	0.45	0.68
Tm	0.06	0.05	0.08	0.10	0.07	0.09	0.06	0.10
Yb	0.37	0.32	0.47	0.55	0.41	0.49	0.36	0.56
Lu	0.05	0.05	0.07	0.08	0.06	0.07	0.06	0.08
Ta	0.09	0.09	0.13	0.17	0.12	0.14	0.10	0.16
Th	0.11	0.11	0.14	0.16	0.12	0.15	0.10	0.17
U	0.024	0.029	0.029	0.037	0.030	0.036	0.025	0.042

SAMPLE	RX 321012	RX 321013	RX 321041	RX 321015	RX 321042	RX 321043	RX 321044	RX 321045
Rock type	VTT	VTT	VTT	VTT	VTT	VTT	VTT	VTT
Drill hole	VB 96 266	VB 96 266	VB 96 266	VB 96 266	VB 96 266	VB 96 266	VB 96 266	VB 96 266
Depth	236.8	244	260.6	262	271.5	274	280	283.5
Easting	556965.8	556965.8	556965.8	556965.8	556965.8	556965.8	556965.8	556965.8
Northing	6242466.0	6242466.0	6242466.0	6242466.0	6242466.0	6242466.0	6242466.0	6242466.0
SiO_2	47.7	46.4	46.4	47.1	47.9	48.2	47.8	46.5
TIO_2	0.7	0.7	0.8	0.8	0.6	0.9	0.5	0.6
Al_2O_3	21.6	19.7	20.6	20.9	23.5	21.9	21.7	19.8
Cr_2O_3	0.0	0.0	0.0	0.0	0.1	0.0	0.0	0.0
Fe_2O_3	7.4	9.9	10.6	8.9	7.1	7.0	7.3	9.4
MnO	0.1	0.1	0.1	0.1	0.1	0.1	0.1	0.1
MgO	9.6	11.4	9.0	9.7	7.2	8.4	10.0	12.0
CaO	9.4	8.6	9.0	9.1	10.0	9.9	9.3	8.5
Na_2O	3.1	2.8	3.0	3.0	3.2	3.2	3.0	2.8
K_2O	0.3	0.2	0.3	0.3	0.2	0.3	0.2	0.2
P_2O_5	0.1	0.1	0.2	0.2	0.1	0.2	0.1	0.1
Total	100.0	100.0	100.0	100.0	100.0	100.0	100.0	100.0
LOI	0.1	0.6	0.7	0.6	0.1	0.2	0.2	0.1
Sc	6.6	7.0	6.9	7.2	5.1	8.7	5.6	6.3
Cr	82	92	72	68	696	81	84	124
Co	55	88	116	72	62	44	53	73
Ni	320	1200	2533	881	893	200	259	740
Cu	48.3	431.4	1064.4	321.1	299.1	23.2	26.3	225.1
Rb	1.964	1.916	2.242	2.519	1.771	2.042	1.163	1.561
Sr	641	563	559	586	629	625	603	531
Y	6.1	5.7	7.0	7.4	3.5	7.0	3.9	4.4
Zr	23	47	62	62	46	44	19	27
Nb	1.97	1.84	2.26	2.39	1.05	2.16	1.18	1.34
Cs	0.02	0.03	0.03	0.03	0.03	0.02	0.02	0.02
Ba	161.2	143.3	154.1	152.3	145.8	152.4	135.0	133.5
La	5.53	4.93	5.61	5.86	3.35	5.39	3.54	3.75
Ce	12.64	11.43	13.27	13.81	7.47	12.67	7.91	8.50
Pr	1.69	1.51	1.81	1.87	1.00	1.73	1.05	1.14
Nd	7.70	6.83	8.03	8.49	4.38	7.77	4.66	5.11
Sm	1.60	1.45	1.73	1.80	0.91	1.65	1.01	1.10
Eu	0.96	0.83	0.92	0.92	0.78	0.92	0.75	0.72
Gd	1.47	1.36	1.61	1.68	0.85	1.58	0.90	0.97
Tb	0.21	0.19	0.24	0.24	0.12	0.22	0.13	0.15
Dy	1.18	1.11	1.34	1.38	0.68	1.38	0.73	0.83
Ho	0.23	0.22	0.26	0.27	0.13	0.26	0.15	0.16
Er	0.59	0.58	0.71	0.67	0.33	0.68	0.36	0.42
Tm	0.08	0.08	0.10	0.10	0.05	0.10	0.05	0.06
Yb	0.48	0.46	0.56	0.54	0.28	0.53	0.33	0.34
Lu	0.07	0.07	0.09	0.09	0.04	0.08	0.05	0.05
Ta	0.13	0.13	0.16	0.16	0.08	0.14	0.08	0.09
Th	0.13	0.13	0.15	0.17	0.07	0.15	0.08	0.09
U	0.03	0.03	0.03	0.04	0.01	0.03	0.02	0.02

SAMPLE	RX 321046	RX 321047	RX321001	RX 321002	RX 321003	RX 321004	RX 321005	RX 321007
Rock type	VTT	VTT	VTT	VTT	VTT	VTT	VTT	VTT
Drill hole	VB 96 266	VB 96 266	VB 96 266	VB 96 266	VB 96 266	VB 96 266	VB 96 266	VB 96 266
Depth	290	296	304.5	312.2	327	332.5	343.5	350.5
Easting	556965.8	556965.8	556965.8	556965.8	556965.8	556965.8	556965.8	556965.8
Northing	6242466.0	6242466.0	6242466.0	6242466.0	6242466.0	6242466.0	6242466.0	6242466.0
SiO_2	47.1	47.3	47.0	46.8	46.5	45.0	46.9	45.7
TIO_2	0.7	0.8	0.6	0.9	0.7	0.6	0.8	0.5
Al_2O_3	20.9	21.3	19.9	19.7	18.5	15.9	19.0	17.4
Cr_2O_3	0.0	0.0	0.0	0.0	0.0	0.0	0.0	0.0
Fe_2O_3	9.0	8.7	9.0	9.4	9.8	12.6	9.3	11.3
MnO	0.1	0.1	0.1	0.1	0.1	0.1	0.1	0.1
MgO	9.8	8.8	11.6	11.1	13.5	16.2	12.3	15.0
CaO	9.0	9.4	8.6	8.6	7.9	6.8	8.1	7.2
Na_2O	3.0	3.1	2.8	2.9	2.7	2.4	3.0	2.5
K_2O	0.3	0.3	0.2	0.3	0.2	0.3	0.3	0.2
P_2O_5	0.1	0.2	0.1	0.2	0.1	0.1	0.3	0.1
Total	100.0	100.0	100.0	100.0	100.0	100.0	100.0	100.0
LOI	0.3	0.0	0.1	0.2	0.3	0.9	0.1	1.0
Sc	6.5	7.2	6.9	8.5	7.7	7.7	7.7	5.9
Cr	79	81	138	150	169	175	173	110
Co	79	77	64	72	72	106	64	98
Ni	1271	1259	473	737	514	1410	384	1538
Cu	459.2	510.9	93.0	231.3	89.9	430.4	50.3	493.0
Rb	1.988	2.237	1.721	3.416	1.775	3.769	2.620	1.713
Sr	577	590	568	559	523	451	532	479
Y	6.0	7.1	5.1	7.8	5.3	5.4	9.6	4.7
Zr	38	28	27	45	41	26	66	50
Nb	1.82	2.19	1.58	2.52	1.68	1.74	3.23	1.50
Cs	0.02	0.03	0.02	0.05	0.02	0.06	0.02	0.01
Ba	154.5	154.3	139.9	155.4	137.9	127.2	173.8	131.2
La	4.85	5.57	4.10	5.98	4.20	4.00	7.64	4.07
Ce	11.38	13.05	9.55	13.98	9.58	9.22	18.05	9.36
Pr	1.53	1.75	1.26	1.88	1.28	1.23	2.43	1.24
Nd	6.77	7.75	5.66	8.36	5.76	5.63	10.84	5.44
Sm	1.46	1.67	1.18	1.78	1.21	1.17	2.26	1.08
Eu	0.88	0.90	0.77	0.87	0.76	0.68	1.00	0.72
Gd	1.35	1.58	1.11	1.71	1.14	1.08	2.13	1.05
Tb	0.20	0.23	0.17	0.24	0.16	0.16	0.30	0.15
Dy	1.13	1.38	0.95	1.45	0.98	1.01	1.82	0.90
Ho	0.22	0.26	0.19	0.28	0.18	0.19	0.34	0.16
Er	0.58	0.68	0.48	0.74	0.51	0.53	0.92	0.45
Tm	0.09	0.11	0.07	0.11	0.07	0.07	0.13	0.06
Yb	0.47	0.55	0.41	0.60	0.41	0.43	0.73	0.36
Lu	0.07	0.08	0.06	0.09	0.06	0.07	0.11	0.06
Ta	0.12	0.15	0.11	0.17	0.11	0.13	0.21	0.10
Th	0.13	0.15	0.11	0.18	0.11	0.25	0.25	0.11
U	0.03	0.03	0.02	0.04	0.02	0.08	0.06	0.02

SAMPLE	RX 321173	RX 321198	RX 321196	RX 321022	RX 321023	RX 321024	RX 321026	RX 321027
Rock type	VTT	VTT	VTT	VTT	VTT	VTT	VTT	VTT
Drill hole	VB 96 266	VB 96 266	VB 96 266	VB 96 266	VB 96 266	VB 96 266	VB 96 266	VB 96 266
Depth	224	284	80	369	375	397	404.8	415
Easting	556965.8	556965.8	556965.8	556965.8	556965.8	556965.8	556965.8	556965.8
Northing	6242466.0	6242466.0	6242466.0	6242466.0	6242466.0	6242466.0	6242466.0	6242466.0
SiO_2	47.6	49.9	48.7	45.5	47.4	46.1	47.8	46.2
TIO_2	1.1	2.9	0.7	0.9	1.1	0.7	1.0	0.6
Al_2O_3	20.0	19.6	21.5	17.4	19.9	18.2	20.1	19.7
Cr_2O_3	0.0	0.0	0.0	0.0	0.0	0.0	0.0	0.0
Fe_2O_3	8.8	9.0	7.3	12.2	8.6	10.7	8.7	10.9
MnO	0.1	0.1	0.1	0.1	0.1	0.1	0.1	0.1
MgO	9.7	4.4	8.6	13.1	10.3	13.2	10.1	11.0
CaO	9.0	9.2	9.2	7.6	8.8	7.8	8.7	8.3
Na_2O	3.0	4.1	3.4	2.6	3.1	2.7	3.0	2.9
K_2O	0.4	0.5	0.3	0.4	0.4	0.3	0.3	0.2
P_2O_5	0.2	0.2	0.2	0.2	0.3	0.2	0.2	0.1
Total	100.0	100.0	100.0	100.0	100.0	100.0	100.0	100.0
LOI	0.1	0.5	0.3	1.3	0.3	0.4	0.4	1.2
Sc	10.6	21.2	7.6	8.7	9.4	7.0	8.7	7.2
Cr	85	85	79	132	95	89	88	142
Co	50	35	45	125	54	85	57	97
Ni	197	24	176	2797	303	1196	355	1882
Cu	17.4	29.1	14.0	1156.1	36.8	378.7	54.3	712.2
Rb	4.702	5.285	2.858	6.604	4.113	2.358	3.719	2.106
Sr	542	511	583	483	564	502	545	515
Y	10.0	9.7	6.6	8.3	12.2	6.5	9.3	3.7
Zr	77	85	53	61	89	58	46	29
Nb	3.27	3.87	2.07	2.72	4.17	2.10	3.08	1.15
Cs	0.10	0.08	0.06	0.14	0.04	0.03	0.08	0.06
Ba	204.0	289.4	169.8	173.4	191.7	147.8	188.4	161.6
La	7.98	7.23	5.49	6.42	9.57	5.28	7.50	3.79
Ce	18.91	16.72	12.63	15.31	22.82	12.43	17.42	8.33
Pr	2.58	2.24	1.70	2.07	3.04	1.65	2.30	1.10
Nd	11.32	10.06	7.52	9.26	13.42	7.33	10.26	4.88
Sm	2.35	2.23	1.61	1.98	2.86	1.55	2.22	0.99
Eu	1.13	1.55	0.99	0.89	1.20	0.84	1.04	0.81
Gd	2.21	2.13	1.50	1.89	2.77	1.47	2.08	0.90
Tb	0.32	0.32	0.22	0.28	0.39	0.21	0.31	0.13
Dy	1.87	1.85	1.23	1.58	2.29	1.22	1.77	0.70
Ho	0.36	0.36	0.23	0.30	0.44	0.23	0.34	0.14
Er	0.97	0.93	0.63	0.79	1.16	0.62	0.89	0.35
Tm	0.14	0.13	0.09	0.11	0.16	0.09	0.13	0.05
Yb	0.80	0.75	0.50	0.67	0.92	0.53	0.73	0.30
Lu	0.12	0.11	0.08	0.10	0.14	0.08	0.11	0.05
Ta	0.21	0.29	0.14	0.19	0.27	0.15	0.22	0.08
Th	0.26	0.32	0.14	0.23	0.31	0.16	0.28	0.08
U	0.09	0.05	0.03	0.05	0.06	0.03	0.06	0.02

SAMPLE	RX 321025	RX 321049	RX 321048	RX 321050	RX 321054	RX 321051	RX 321052	RX 321055
Rock type	VTT	VTT	VTT	VTT	VTT	VTT	VTT	VTT
Drill hole	VB 96 266	VB 96 266	VB 96 266	VB 96 266	VB 96 266	VB 96 266	VB 96 266	VB 96 266
Depth	417	424	428	440	452.6	453	464	481
Easting	556965.8	556965.8	556965.8	556965.8	556965.8	556965.8	556965.8	556965.8
Northing	6242466.0	6242466.0	6242466.0	6242466.0	6242466.0	6242466.0	6242466.0	6242466.0
SiO_2	46.1	46.1	48.3	47.2	46.6	45.3	47.2	45.2
TIO_2	0.8	3.6	0.8	0.7	1.0	0.7	0.8	0.9
Al_2O_3	19.3	16.2	20.6	20.4	19.6	17.1	19.3	16.6
Cr_2O_3	0.0	0.0	0.0	0.0	0.0	0.0	0.0	0.1
Fe_2O_3	10.9	11.3	8.1	10.2	11.0	12.9	10.0	12.9
MnO	0.1	0.1	0.1	0.1	0.1	0.1	0.1	0.1
MgO	11.1	9.6	9.5	9.2	9.6	13.4	10.6	14.1
CaO	8.3	9.5	8.8	8.6	8.5	7.3	8.4	7.1
Na_2O	2.8	2.9	3.4	3.3	3.1	2.6	3.1	2.6
K_2O	0.3	0.3	0.3	0.3	0.4	0.3	0.3	0.3
P_2O_5	0.2	0.3	0.1	0.1	0.2	0.1	0.2	0.2
Total	100.0	100.0	100.0	100.0	100.0	100.0	100.0	100.0
LOI	0.7	0.2	0.1	0.7	0.0	0.0	0.0	0.9
Sc	7.9	28.1	8.2	6.4	8.1	8.0	8.1	9.4
Cr	141	269	173	258	111	340	102	394
Co	96	56	52	90	105	101	70	113
Ni	1618	245	249	1662	2129	1316	870	1677
Cu	611.8	52.3	22.8	715.4	878.2	500.2	285.1	638.2
Rb	2.757	3.415	2.249	2.420	3.559	2.001	2.269	1.862
Sr	530	439	552	539	567	445	503	471
Y	6.9	16.3	5.3	5.0	7.8	5.3	6.9	6.6
Zr	53	83	33	14	36	31	43	56
Nb	2.31	6.10	1.68	1.54	2.48	1.68	2.19	2.24
Cs	0.06	0.04	0.02	0.03	0.06	0.02	0.02	0.02
Ba	150.8	200.8	171.5	174.4	180.5	143.4	177.5	159.1
La	5.42	9.75	4.48	4.48	6.17	4.35	5.69	5.32
Ce	12.65	24.32	10.22	10.22	14.53	10.13	13.52	12.36
Pr	1.68	3.46	1.38	1.38	1.94	1.35	1.83	1.66
Nd	7.57	16.09	6.10	5.95	8.70	6.13	8.07	7.29
Sm	1.60	3.71	1.30	1.25	1.87	1.31	1.70	1.60
Eu	0.85	1.35	0.86	0.82	0.98	0.75	0.90	0.87
Gd	1.55	3.68	1.25	1.19	1.72	1.20	1.55	1.47
Tb	0.22	0.53	0.18	0.17	0.25	0.18	0.23	0.22
Dy	1.28	3.13	1.03	0.97	1.49	0.96	1.30	1.26
Ho	0.24	0.62	0.19	0.18	0.28	0.19	0.26	0.24
Er	0.64	1.57	0.52	0.46	0.76	0.50	0.66	0.65
Tm	0.09	0.23	0.07	0.07	0.11	0.07	0.09	0.09
Yb	0.55	1.30	0.41	0.38	0.63	0.43	0.54	0.55
Lu	0.08	0.19	0.06	0.06	0.09	0.06	0.08	0.08
Ta	0.42	0.12	0.10	0.17	0.12	0.15	0.16	0.25
Th	0.29	0.13	0.11	0.21	0.13	0.16	0.19	0.29
U	0.06	0.03	0.02	0.04	0.03	0.03	0.04	0.06

SAMPLE	RX 321057	RX 321064	RX 321065	RX 321072	RX 321071	RX 321159	RX 321075	RX 321067
Rock type	VTT	VTT	VTT	VTT	VTT	VTT	IVTT	IVTT
Drill hole	VB 96 266	VB 96 266	VB 96 266	VB 96 266	VB 96 266	VB 96 266	VB 96 266	VB 96 266
Depth	529	590.4	597.4	627	637	727	648	604.5
Easting	556965.8	556965.8	556965.8	556965.8	556965.8	556965.8	556965.8	556965.8
Northing	6242466.0	6242466.0	6242466.0	6242466.0	6242466.0	6242466.0	6242466.0	6242466.0
SiO_2	46.1	47.0	46.0	47.8	45.2	47.0	35.0	41.9
TIO_2	1.3	0.5	0.9	0.9	1.0	1.2	1.2	2.1
Al_2O_3	18.5	18.5	17.6	20.3	18.4	18.8	14.9	20.2
Cr_2O_3	0.0	0.0	0.0	0.0	0.1	0.0	0.0	0.1
Fe_2O_3	11.6	11.8	10.1	9.4	12.5	10.3	34.2	16.5
MnO	0.1	0.1	0.1	0.1	0.1	0.1	0.2	0.1
MgO	10.8	10.5	14.6	9.1	11.7	10.8	5.0	8.0
CaO	8.0	8.1	7.7	8.6	7.9	8.1	6.3	6.5
Na_2O	3.0	3.1	2.4	3.2	2.6	3.1	2.5	2.6
K_2O	0.4	0.2	0.3	0.5	0.3	0.4	0.4	1.4
P_2O_5	0.2	0.2	0.2	0.2	0.2	0.3	0.2	0.5
Total	100.0	100.0	100.0	100.0	100.0	100.0	100.0	100.0
LOI	0.8	0.0	0.1	0.5	0.3	0.0	3.7	1.5
Sc	10.9	8.3	8.8	8.8	9.4	10.0	5.5	13.0
Cr	227	100	90	114	349	105	98	375
Co	95	94	69	81	115	63	569	176
Ni	1481	1582	421	1358	1778	367	6059	3537
Cu	537.3	813.9	29.1	723.7	567.0	53.0	3243.5	2413.8
Rb	4.485	2.686	2.695	5.589	3.478	3.185	5.193	31.618
Sr	514	431	475	526	493	524	437	450
Y	10.6	6.5	7.9	9.2	8.7	11.8	7.1	17.3
Zr	71	44	61	73	70	88	56	127
Nb	3.65	2.09	2.52	2.67	2.91	3.87	2.79	9.74
Cs	0.06	0.04	0.05	0.10	0.05	0.02	0.09	0.66
Ba	204.0	123.8	144.2	196.8	179.9	209.6	180.1	409.3
La	8.21	5.99	6.18	7.04	6.90	8.92	21.08	24.67
Ce	19.42	13.43	14.84	15.93	16.27	21.22	43.27	55.46
Pr	2.61	1.73	2.04	2.08	2.16	2.90	4.86	7.06
Nd	11.50	7.52	9.17	8.96	9.76	12.83	17.93	28.97
Sm	2.51	1.50	1.96	1.93	2.07	2.77	2.76	5.78
Eu	1.14	0.50	0.88	1.09	1.03	1.17	0.96	1.60
Gd	2.33	1.43	1.77	1.89	1.91	2.59	2.30	4.80
Tb	0.34	0.21	0.26	0.28	0.29	0.37	0.30	0.66
Dy	2.02	1.16	1.50	1.64	1.61	2.25	1.48	3.44
Ho	0.38	0.24	0.29	0.34	0.32	0.43	0.28	0.65
Er	1.03	0.62	0.77	0.90	0.85	1.12	0.67	1.67
Tm	0.14	0.09	0.11	0.13	0.13	0.16	0.10	0.23
Yb	0.83	0.52	0.61	0.74	0.67	0.93	0.57	1.31
Lu	0.12	0.08	0.09	0.12	0.10	0.13	0.09	0.20
Ta	0.14	0.16	0.18	0.19	0.26	0.16	0.18	0.58
Th	0.24	0.17	0.29	0.32	0.27	0.21	1.07	3.89
U	0.06	0.04	0.10	0.13	0.06	0.03	0.09	0.40

SAMPLE	RX 321077	RX 321076	RX 321160	RX 321161	RX 321066	RX 321200	RX 321201	RX 321038
Rock type	IVTT	IVTT	IVTT	IVTT	IVTT	LT	LT	UM
Drill hole	VB 96 266	VB 96 266	VB 96 266	VB 96 266	VB 96 266	VB 96 266	VB 96 266	VB 96 266
Depth	662.5	N.A.	920	947	602	335	341	132
Easting	556965.8	556965.8	556965.8	556965.8	556965.8	556965.8	556965.8	556965.8
Northing	6242466.0	6242466.0	6242466.0	6242466.0	6242466.0	6242466.0	6242466.0	6242466.0
SiO_2	22.9	29.4	31.7	28.0	38.9	32.3	29.7	40.1
TIO_2	2.2	1.2	0.8	1.9	1.4	1.8	1.8	0.2
Al_2O_3	8.7	12.4	15.0	10.8	18.7	13.1	11.6	5.5
Cr_2O_3	0.0	0.0	0.0	0.0	0.0	0.0	0.0	0.1
Fe_2O_3	56.7	44.4	39.0	47.1	24.5	39.3	43.8	18.7
MnO	0.3	0.2	0.1	0.2	0.1	0.1	0.1	0.2
MgO	2.6	4.3	4.2	4.3	5.4	4.7	5.0	32.3
CaO	4.3	5.3	6.2	4.8	7.7	5.8	5.4	1.7
Na_2O	1.8	2.3	2.4	2.2	2.8	2.2	1.9	0.7
K_2O	0.3	0.3	0.3	0.4	0.4	0.4	0.3	0.5
P_2O_5	0.3	0.2	0.2	0.3	0.2	0.3	0.2	0.1
Total	100.0	100.0	100.0	100.0	100.0	100.0	100.0	100.0
LOI	6.1	7.2	4.8	5.6	2.7	5.9	6.1	3.3
Sc	7.7	5.5	4.3	6.7	6.9	7.6	7.0	6.2
Cr	241	272	177	77	223	105	97	896
Co	943	803	652	706	395	568	648	141
Ni	6074	6066	6051	6049	6250	6012	6010	1455
Cu	2663.1	3356.4	2692.4	2690.7	2199.1	2657.5	2655.8	97.3
Sc								
Rb	3	2	3	3	6	4	4	12
Sr	216.1	326.4	399.4	298.3	505.8	351.1	318.8	60.3
Y	8	6	6	7	7	9	7	3
Zr	47.00	32.00	57.00	45.00	53.00	54.00	63.00	11.00
Nb	3.64	2.49	2.06	3.40	3.08	3.74	3.30	0.65
Cs	0.0	0.1	0.0	0.1	0.1	0.1	0.1	0.1
Ba	156.82	155.19	160.28	174.34	195.89	195.24	157.62	47.57
La	7.85	6.62	7.55	6.83	6.93	8.13	6.63	1.57
Ce	19.12	15.23	16.05	16.23	15.76	20.11	16.15	3.74
Pr	2.66	1.98	2.07	2.21	2.06	2.75	2.21	0.51
Nd	11.53	8.79	8.83	9.82	9.22	11.96	9.73	2.30
Sm	2.37	1.74	1.79	2.11	1.94	2.55	2.05	0.55
Eu	0.90	0.83	0.86	0.87	1.01	1.07	0.90	0.31
Gd	2.17	1.56	1.58	1.86	1.70	2.24	1.84	0.51
Tb	0.31	0.23	0.21	0.26	0.25	0.34	0.27	0.08
Dy	1.69	1.21	1.16	1.42	1.35	1.85	1.44	0.46
Ho	0.33	0.24	0.22	0.28	0.26	0.35	0.27	0.10
Er	0.80	0.57	0.56	0.70	0.67	0.87	0.68	0.27
Tm	0.12	0.09	0.08	0.10	0.10	0.12	0.10	0.04
Yb	0.63	0.47	0.44	0.53	0.53	0.69	0.55	0.27
Lu	0.10	0.07	0.06	0.08	0.08	0.10	0.09	0.04
Ta	0.26	0.18	0.15	0.25	0.22	0.25	0.23	0.05
Th	0.39	0.44	0.85	0.22	0.43	0.23	0.18	0.09
U	0.09	0.07	0.07	0.06	0.06	0.06	0.11	0.03

SAMPLE	RX 321088	RX 321090	RX 321091	RX 321092	RX 321086	RX 321087	RX 321093	RX 321094
Rock type	UM	UM	UM	UM	UM	UM	UM	UM
Drill hole	VB 96 247	VB 96 247	VB 96 247	VB 96 247	VB 96 249	VB 96 249	VB 96 254	VB 96 254
Depth	249	940	946	947	827	828	868	869
Easting	557782.7	557782.7	557782.7	557782.7	557596.6	557596.6	557696.9	557696.9
Northing	6242163.0	6242163.0	6242163.0	6242163.0	6242209.8	6242209.8	6242114.6	6242114.6
SiO_2	41.2	42.7	44.4	43.5	51.3	47.6	44.4	44.1
TIO_2	1.2	0.8	1.1	0.7	0.6	1.0	0.9	1.2
Al_2O_3	8.7	3.8	7.4	7.1	15.2	6.1	6.7	5.5
Cr_2O_3	0.3	0.3	0.3	0.3	0.1	0.3	0.3	0.3
Fe_2O_3	19.6	10.9	14.5	14.4	11.1	13.6	15.9	16.5
MnO	0.2	0.1	0.2	0.2	0.2	0.2	0.2	0.2
MgO	23.3	37.7	22.6	27.0	8.6	19.2	24.4	23.8
CaO	3.6	2.5	7.8	5.2	9.1	9.9	5.7	6.8
Na_2O	1.4	0.8	1.3	1.3	3.3	1.1	1.1	1.1
K_2O	0.3	0.2	0.2	0.2	0.4	0.9	0.2	0.2
P_2O_5	0.2	0.2	0.2	0.1	0.1	0.1	0.1	0.2
Total	100.0	100.0	100.0	100.0	100.0	100.0	100.0	100.0
LOI	4.4	4.8	1.5	2.4	0.6	1.2	6.6	4.9
Sc	10.4	11.6	33.8	20.3	35.1	38.5	22.8	29.8
Cr	1728	1663	1943	1998	368	1697	1655	1840
Co	129	108	89	102	46	82	96	101
Ni	1078	2061	1092	1233	141	940	1222	1076
Cu	98.1	39.1	107.9	45.1	64.7	199.8	103.5	179.3
Sc								
Rb	3	3	3	2	4	43	2	2
Sr	220.1	84.9	168.9	113.3	272.4	61.9	125.6	114.3
Y	8	7	12	8	34	21	9	12
Zr	50.00	43.00	59.00	32.00	57.00	48.00	21.00	54.00
Nb	2.77	1.60	2.86	1.70	7.04	3.73	1.77	2.48
Cs	0.1	0.1	0.0	0.0	0.0	0.7	0.1	0.0
Ba	135.10	92.46	118.97	64.21	123.96	90.64	84.02	99.02
La	6.18	5.21	6.46	3.28	12.67	8.01	4.14	5.43
Ce	14.82	12.85	16.51	8.14	27.52	24.49	10.55	13.81
Pr	2.00	1.76	2.31	1.12	3.40	4.13	1.54	2.00
Nd	9.02	8.09	10.99	5.30	14.04	20.94	7.65	9.85
Sm	1.96	1.74	2.69	1.32	3.55	5.29	1.90	2.51
Eu	0.76	0.57	0.87	0.44	0.91	1.23	0.68	0.79
Gd	1.81	1.61	2.60	1.31	4.20	4.63	1.88	2.52
Tb	0.27	0.23	0.39	0.21	0.74	0.67	0.28	0.38
Dy	1.57	1.38	2.37	1.37	5.33	3.97	1.74	2.40
Ho	0.30	0.27	0.46	0.28	1.16	0.72	0.34	0.46
Er	0.80	0.66	1.14	0.76	3.56	1.98	0.88	1.18
Tm	0.12	0.10	0.16	0.12	0.55	0.29	0.13	0.17
Yb	0.65	0.54	0.90	0.65	3.42	1.63	0.71	0.95
Lu	0.10	0.08	0.13	0.10	0.52	0.24	0.11	0.15
Ta	0.19	0.11	0.20	0.12	0.44	0.23	0.13	0.17
Th	0.22	0.21	0.30	0.18	1.69	1.20	0.15	0.23
U	0.05	0.05	0.07	0.06	0.43	0.40	0.03	0.05

SAMPLE	RX 321095	RX 321096	RX 321097	RX 321099	RX 321100	RX 321101	RX 321109	RX 321157
Rock type	UM	UM	UM	UM	CHILL	CHILL	CHILL	CHILL
Drill hole	VB 96 254	VB 96 254	VB 96 254	VB 96 265	VB-95-139	VB-95-139	VB-95-139	VB-95-202
Depth	891	949	950	369	163	165	176	242
Easting	557696.9	557696.9	557696.9	555438.2	556169.2	556169.2	556169.2	557212 3
Northing	6242114.6	6242114.6	6242114.6	6243667.5	6242802.3	6242802.3	6242802.3	6242557.0
SiO_2	45.1	44.8	44.6	47.6	45.4	47.9	45.3	41.1
TIO_2	0.9	0.5	0.5	1.3	3.8	3.2	4.3	3.6
Al_2O_3	5.7	7.7	7.2	20.7	16.2	17.0	16.0	14.3
Cr_2O_3	0.3	0.3	0.3	0.0	0.0	0.0	0.0	0.0
Fe_2O_3	14.9	13.3	13.8	10.0	14.4	12.6	15.0	23.6
MnO	0.2	0.2	0.2	0.1	0.2	0.2	0.2	0.2
MgO	24.3	24.7	25.2	7.5	6.1	5.9	5.8	5.1
CaO	7.0	7.1	6.8	8.2	7.9	7.5	7.6	7.2
Na_2O	1.2	1.2	1.1	3.7	3.6	4.1	3.7	3.4
K_2O	0.2	0.1	0.2	0.6	1.5	0.9	1.1	0.6
P_2O_5	0.1	0.1	0.1	0.3	1.0	0.7	1.0	0.9
Total	100.0	100.0	100.0	100.0	100.0	100.0	100.0	100.0
LOI	1.1	3.2	2.0	0.8	0.7	0.4	0.4	2.6
Sc	30.2	27.0	25.8	8.5	19.4	16.3	20.5	19.7
Cr	2093	2028	2074	58	64	89	70	140
Co	104	91	108	68	47	46	47	318
Ni	1349	1137	1426	548	67	69	70	4455
Cu	221.3	62.8	268.9	346.5	132.2	126.2	108.6	1678.6
Rb	2.082	2.172	3.590	7.989	36.429	15.518	10.907	8.690
Sr	168	67	63	656	482	526	462	413
Y	11.0	9.6	10.2	10.9	28.5	23.8	28.2	29.1
Zr	48	35	20	72	177	156	157	187
Nb	1.93	1.19	1.44	4.61	13.49	12.07	12.38	10.81
Cs	0.05	0.12	0.11	0.16	0.66	0.27	0.17	0.14
Ba	84.6	32.8	44.5	289.1	590.5	469.6	491.0	398.6
La	4.22	2.13	2.22	10.54	28.73	26.51	25.85	24.74
Ce	10.81	5.41	5.78	24.83	69.01	60.73	63.17	60.10
Pr	1.58	0.77	0.85	3.30	9.33	7.91	8.72	8.33
Nd	7.82	3.96	4.14	14.79	40.69	33.73	38.72	37.02
Sm	2.02	1.15	1.24	3.08	8.73	6.94	8.11	7.87
Eu	0.72	0.38	0.43	1.42	2.57	2.18	2.62	2.38
Gd	2.10	1.40	1.45	2.69	7.56	5.99	7.37	7.16
Tb	0.32	0.24	0.25	0.39	1.08	0.84	1.04	1.04
Dy	2.12	1.69	1.84	2.16	5.84	4.74	5.71	5.75
Ho	0.40	0.36	0.37	0.39	1.05	0.87	1.05	1.07
Er	1.04	0.99	1.06	1.02	2.83	2.39	2.67	2.72
Tm	0.15	0.15	0.16	0.14	0.37	0.32	0.37	0.39
Yb	0.85	0.85	0.88	0.78	2.06	1.80	2.06	2.07
Lu	0.12	0.13	0.14	0.11	0.29	0.26	0.30	0.31
Ta	0.13	0.08	0.11	0.30	0.87	0.75	0.82	0.76
Th	0.16	0.10	0.20	0.35	0.45	0.63	0.56	1.26
U	0.04	0.04	0.16	0.07	0.15	0.18	0.14	0.31

SAMPLE	RX 321128	RX 321127	RX 321134	RX 321133	RX 321155	RX 321123	RX 321102	RX 321103
Rock type	CHILL	CHILL	CHILL	CHILL	CHILL	CHILL	Ovoid Dyke	Ovoid Dyke
Drill hole	VB-95-202	VB-95-202	VB-95-211	VB-95-211	VB-95-222	VB 96 265	VB-95-139	VB-95-139
Depth	743	744	137.5	139	326.5	373	166	168
Easting	557212.3	557212.3	555835.6	555835.6	555149.1	555438.2	556169.2	556169.2
Northing	6242557.0	6242557.0	6243237.9	6243237.9	6243574.0	6243667.5	6242802.3	6242802.3
SiO_2	48.1	45.4	47.6	45.7	46.7	43.9	45.5	46.4
TIO_2	1.1	4.3	1.7	4.2	3.3	3.4	4.9	3.4
Al_2O_3	20.3	16.4	19.3	16.2	17.5	16.3	18.6	17.3
Cr_2O_3	0.0	0.0	0.0	0.0	0.0	0.0	0.0	0.0
Fe_2O_3	9.2	14.4	11.1	15.0	14.3	17.6	11.7	13.4
MnO	0.1	0.2	0.1	0.2	0.1	0.2	0.1	0.2
MgO	8.7	6.0	7.7	5.8	5.7	6.1	7.2	5.9
CaO	8.3	7.6	7.8	7.4	6.7	7.2	7.5	8.0
Na_2O	3.5	3.5	3.7	3.6	3.8	3.5	3.5	3.8
K_2O	0.5	1.5	0.6	1.1	1.3	1.0	0.7	0.9
P_2O_5	0.3	0.7	0.4	0.9	0.5	0.8	0.3	0.8
Total	100.0	100.0	100.0	100.0	100.0	100.0	100.0	100.0
LOI	0.3	0.6	0.4	0.9	1.3	2.1	0.3	0.3
Sc	7.4	18.7	9.4	19.6	11.7	16.7	10.2	17.7
Cr	36	69	120	66	87	60	70	63
Co	55	55	70	51	94	133	58	46
Ni	181	95	526	130	1729	1938	78	61
Cu	44.5	101.4	390.1	186.2	1156.0	2884.3	28.7	50.8
Rb	4.234	42.270	6.839	15.469	20.895	12.814	8.893	8.788
Sr	677	496	628	488	639	482	595	524
Y	8.8	24.1	11.8	28.7	13.5	24.6	8.4	27.2
Zr	59	170	91	237	144	142	49	148
Nb	3.32	11.18	4.78	12.78	7.34	10.24	5.01	10.72
Cs	0.07	1.35	0.10	0.14	0.14	0.14	0.36	0.09
Ba	239.5	450.2	302.5	455.3	505.8	393.3	268.6	446.4
La	8.40	23.08	11.36	26.53	17.17	21.90	8.26	23.32
Ce	19.64	55.49	27.08	63.78	38.53	53.03	19.36	57.07
Pr	2.65	7.55	3.61	8.72	4.94	7.30	2.59	7.81
Nd	11.67	33.14	16.15	38.74	20.72	32.48	11.32	34.78
Sm	2.44	7.01	3.41	8.13	4.09	6.98	2.31	7.40
Eu	1.24	2.26	1.48	2.52	1.55	2.23	1.25	2.45
Gd	2.16	6.16	2.99	7.25	3.51	6.13	2.07	6.71
Tb	0.31	0.88	0.42	1.06	0.49	0.88	0.31	0.95
Dy	1.71	4.86	2.32	5.78	2.67	4.93	1.64	5.51
Ho	0.32	0.92	0.43	1.08	0.48	0.94	0.30	1.01
Er	0.81	2.30	1.10	2.70	1.27	2.36	0.78	2.68
Tm	0.11	0.31	0.15	0.39	0.18	0.34	0.11	0.36
Yb	0.64	1.76	0.87	2.14	1.04	1.90	0.61	1.94
Lu	0.09	0.26	0.13	0.31	0.15	0.27	0.09	0.29
Ta	0.22	0.79	0.32	0.91	0.50	0.73	0.41	0.70
Th	0.21	0.56	0.29	0.61	0.40	0.85	0.17	0.62
U	0.05	0.15	0.07	0.16	0.11	0.16	0.05	0.14

SAMPLE	RX 321104	RX 321105	RX 321106	RX 321107	RX 321108	RX 321117	RX 321118	RX 321119
Rock type	Ovoid Dyke	Ovoid Dyke	Ovoid Dyke	Ovoid Dyke	Ovoid Dyke	ED Dyke	ED Dyke	ED Dyke
Drill hole	VB-95-139	VB-95-139	VB-95-139	VB-95-139	VB-95-139	VB 96 265	VB 96 265	VB 96 265
Depth	170	171	172	174	175	361	363	367
Easting	556169.2	556169.2	556169.2	556169.2	556169.2	555438.2	555438.2	555438.2
Northing	6242802.3	6242802.3	6242802.3	6242802.3	6242802.3	6243667.5	6243667.5	6243667.5
SiO_2	46.0	45.3	46.0	46.9	45.6	47.0	48.4	43.5
TIO_2	3.7	3.8	3.9	1.4	4.4	3.5	2.4	3.6
Al_2O_3	16.8	15.8	16.6	19.6	17.7	17.9	19.2	15.8
Cr_2O_3	0.0	0.0	0.0	0.0	0.0	0.0	0.0	0.0
Fe_2O_3	14.1	15.6	14.0	12.0	13.3	12.6	10.4	18.8
MnO	0.2	0.2	0.2	0.1	0.1	0.1	0.1	0.1
MgO	5.9	6.0	5.5	7.1	6.7	6.3	7.1	5.1
CaO	7.7	7.4	7.8	8.1	7.1	7.6	7.7	7.9
Na_2O	3.7	3.8	3.9	3.8	3.9	3.5	3.6	3.5
K_2O	1.1	1.2	1.1	0.6	0.8	0.9	0.8	0.8
P_2O_5	0.9	1.0	0.9	0.3	0.4	0.6	0.4	0.7
Total	100.0	100.0	100.0	100.0	100.0	100.0	100.0	100.0
LOI	0.4	0.1	0.3	1.4	0.5	0.5	0.8	2.0
Sc	17.5	18.2	19.4	8.1	13.2	14.7	9.7	23.1
Cr	64	51	63	39	74	102	184	61
Co	47	50	46	90	55	50	51	175
Ni	62	58	53	1060	130	81	101	3027
Cu	41.1	52.6	53.4	428.9	107.6	60.3	36.6	1567.1
Rb	10.603	11.535	10.770	6.914	9.195	11.216	14.542	17.428
Sr	502	469	497	641	544	547	622	518
Y	29.5	31.4	31.0	10.7	12.7	17.6	11.3	24.2
Zr	190	181	174	69	98	114	84	134
Nb	12.01	12.67	12.39	4.24	7.14	7.86	5.30	9.35
Cs	0.08	0.09	0.09	0.11	0.11	0.10	0.15	0.78
Ba	488.0	504.8	499.9	290.8	356.5	411.1	321.5	381.2
La	25.66	26.68	26.35	10.33	13.18	17.42	12.97	19.29
Ce	62.42	65.32	64.40	24.61	30.99	41.31	29.34	47.20
Pr	8.61	9.01	8.86	3.28	4.10	5.58	3.80	6.56
Nd	38.13	39.81	39.37	14.64	17.78	24.93	16.46	30.17
Sm	8.08	8.58	8.52	2.97	3.72	5.16	3.32	6.45
Eu	2.60	2.68	2.64	1.37	1.56	1.89	1.40	2.11
Gd	7.28	7.68	7.56	2.68	3.25	4.45	2.80	5.87
Tb	1.05	1.10	1.08	0.38	0.46	0.63	0.40	0.86
Dy	5.94	6.35	6.09	2.10	2.50	3.47	2.15	4.87
Ho	1.10	1.13	1.12	0.40	0.46	0.65	0.42	0.89
Er	2.89	3.07	3.03	0.98	1.20	1.62	1.01	2.29
Tm	0.39	0.41	0.41	0.14	0.17	0.23	0.15	0.32
Yb	2.18	2.34	2.27	0.79	0.96	1.27	0.81	1.78
Lu	0.32	0.34	0.34	0.12	0.15	0.19	0.12	0.26
Ta	0.79	0.83	0.83	0.29	0.52	0.56	0.35	0.64
Th	0.70	0.73	0.71	0.27	0.29	0.41	0.34	0.54
U	0.15	0.17	0.16	0.06	0.08	0.10	0.08	0.12

SAMPLE	RX 321120	RX 321121	RX 321122	RX 321125	RX 321112	RX 321113	RX 321114	RX 321115
Rock type	ED Dyke	ED Dyke	ED Dyke	ED Dyke	ED Dyke	ED Dyke	ED Dyke	ED Dyke
Drill hole	VB 96 265	VB 96 265	VB 96 265	VB 96 265	VB 96 270	VB 96 270	VB 96 270	VB 96 270
Depth	369	370	371	376	70.3	102	105	115
Easting	555438.2	555438.2	555438.2	555438.2	553775.5	553775.5	553775.5	553775.5
Northing	6243667.5	6243667.5	6243667.5	6243667.5	6243434.7	6243434.7	6243434.7	6243434.7
SiO_2	30.5	37.0	33.2	40.3	42.2	42.7	42.2	43.4
TIO_2	2.7	3.3	2.6	4.4	0.9	2.2	3.0	3.0
Al_2O_3	11.4	13.6	13.4	15.5	17.4	16.3	15.8	15.6
Cr_2O_3	0.0	0.0	0.0	0.0	0.0	0.0	0.0	0.0
Fe_2O_3	42.2	29.9	36.8	22.6	22.5	20.0	21.8	20.2
MnO	0.1	0.2	0.1	0.2	0.1	0.1	0.1	0.2
MgO	4.7	5.7	5.0	6.3	6.9	7.4	6.5	5.9
CaO	5.3	6.4	5.5	6.1	6.8	7.1	6.9	7.3
Na_2O	2.3	2.8	2.5	2.2	2.5	2.8	2.5	3.0
K_2O	0.4	0.6	0.5	2.3	0.6	0.9	0.7	0.7
P_2O_5	0.4	0.5	0.4	0.2	0.2	0.5	0.6	0.6
Total	100.0	100.0	100.0	100.0	100.0	100.0	100.0	100.0
LOI	4.3	2.9	6.2	2.8	4.0	1.7	3.2	2.5
Sc	9.4	13.2	9.4	9.5	5.6	13.5	17.4	18.4
Cr	88	67	85	59	64	84	126	109
Co	548	361	475	166	283	164	206	208
Ni	6339	6379	8709	2011	5044	2349	3465	3574
Cu	2730.9	2335.2	4005.0	2113.6	2332.0	1424.1	2003.4	2156.3
Rb	4.574	6.677	5.424	121.925	12.373	22.143	15.724	13.540
Sr	317	400	340	335	479	452	384	415
Y	11.1	16.8	11.0	8.0	6.7	18.1	22.0	26.2
Zr	34	96	63	63	40	118	138	167
Nb	4.78	6.85	5.08	5.83	2.59	8.26	10.40	9.44
Cs	0.07	0.10	0.12	5.09	0.12	0.30	0.15	0.18
Ba	222.4	302.8	224.5	616.5	174.1	305.0	287.0	350.8
La	10.00	14.73	10.95	7.93	6.65	14.98	18.24	20.68
Ce	24.52	35.79	26.31	19.47	15.17	36.03	43.73	49.87
Pr	3.37	4.89	3.53	2.58	1.98	4.93	5.93	6.78
Nd	14.97	22.78	15.33	11.20	8.88	22.25	26.63	30.10
Sm	3.15	4.84	3.27	2.31	1.82	4.78	5.75	6.51
Eu	1.18	1.64	1.21	1.10	1.02	1.62	1.83	2.00
Gd	2.93	4.18	2.83	1.92	1.58	4.31	5.07	5.95
Tb	0.42	0.60	0.41	0.29	0.23	0.62	0.75	0.89
Dy	2.26	3.28	2.16	1.54	1.28	3.49	4.27	5.03
Ho	0.43	0.63	0.43	0.29	0.24	0.66	0.82	0.95
Er	1.05	1.63	1.06	0.77	0.64	1.69	2.11	2.46
Tm	0.15	0.23	0.14	0.12	0.09	0.25	0.30	0.34
Yb	0.87	1.24	0.81	0.65	0.51	1.36	1.72	1.96
Lu	0.13	0.18	0.13	0.10	0.08	0.20	0.24	0.28
Ta	0.35	0.49	0.37	0.50	0.17	0.49	0.60	0.64
Th	0.27	0.48	0.49	0.18	0.32	0.67	1.11	1.49
U	0.07	0.11	0.11	0.21	0.08	0.25	0.26	0.31

SAMPLE	RX 321116	RX 321179	RX 321180	RX 321181	RX 321182	RX 321183	RX 321184	RX 321185
Rock type	ED Dyke	Mushaua	Mushaua	Mushaua	Mushaua	Mushaua	Mushaua	Mushaua
Drill hole	VB 96 270	S95-6	S95-6	S95-6	S95-6	S95-6	S95-6	S95-6
Depth	148.5	7	26	50	53	61	70	93
Easting	553775.5	555837.1	555837.1	555837.1	555837.1	555837.1	555837.1	555837.1
Northing	6243434.7	6243322.9	6243322.9	6243322.9	6243322.9	6243322.9	6243322.9	6243322.9
SiO_2	39.3	39.5	42.5	43.9	38.8	45.1	40.2	41.0
TIO_2	1.6	0.5	0.5	1.1	0.7	0.4	0.6	0.6
Al_2O_3	15.9	5.5	11.1	11.6	4.4	15.8	6.3	7.8
Cr_2O_3	0.0	0.0	0.0	0.0	0.0	0.0	0.0	0.0
Fe_2O_3	26.3	23.4	18.5	19.1	26.4	15.1	23.6	21.9
MnO	0.1	0.2	0.2	0.2	0.3	0.2	0.2	0.2
MgO	6.5	27.2	20.5	16.2	26.1	14.1	24.9	23.5
CaO	7.0	2.5	4.8	5.3	2.1	6.8	2.9	3.4
Na_2O	2.7	1.0	1.7	2.2	0.9	2.4	1.2	1.3
K_2O	0.4	0.1	0.2	0.3	0.2	0.2	0.2	0.1
P_2O_5	0.2	0.1	0.1	0.1	0.1	0.1	0.1	0.1
Total	100.0	100.0	100.0	100.0	100.0	100.0	100.0	100.0
LOI	2.0	0.0	0.0	0.0	0.0	0.0	0.0	0.0
Sc	9.7	12.5	11.1	16.9	14.7	9.6	13.7	12.5
Cr	203	51	43	45	56	35	50	47
Co	375	173	133	113	178	95	163	151
Ni	4967	769	594	415	631	368	648	592
Cu	2035.7	19.8	19.1	34.3	23.2	16.2	20.7	20.3
Rb	3.438	1.577	1.421	3.325	2.164	1.358	2.066	1.631
Sr	392	119	231	237	89	318	128	158
Y	8.7	7.4	6.9	13.4	9.4	5.6	8.8	7.5
Zr	54	39	52	93	63	21	59	49
Nb	3.63	1.79	1.64	3.73	2.40	1.28	2.13	1.83
Cs	0.07	0.02	0.02	0.04	0.03	0.02	0.03	0.02
Ba	182.9	67.7	86.0	186.1	87.0	109.3	90.3	88.1
La	8.04	3.82	3.80	7.33	5.22	3.59	5.14	4.11
Ce	18.82	9.15	8.63	16.77	12.14	7.86	11.64	9.45
Pr	2.49	1.20	1.13	2.21	1.58	1.02	1.53	1.23
Nd	10.97	5.28	5.07	9.52	6.92	4.48	6.77	5.42
Sm	2.33	1.20	1.16	2.18	1.62	0.98	1.47	1.25
Eu	1.10	0.46	0.60	1.05	0.53	0.64	0.55	0.55
Gd	2.00	1.27	1.21	2.26	1.63	0.99	1.57	1.28
Tb	0.30	0.21	0.19	0.37	0.25	0.15	0.24	0.20
Dy	1.66	1.34	1.21	2.40	1.65	0.99	1.57	1.36
Ho	0.31	0.27	0.25	0.48	0.34	0.20	0.32	0.27
Er	0.81	0.80	0.73	1.42	0.98	0.57	0.93	0.78
Tm	0.12	0.12	0.11	0.21	0.15	0.09	0.14	0.12
Yb	0.67	0.75	0.68	1.25	0.90	0.54	0.84	0.71
Lu	0.10	0.12	0.10	0.20	0.14	0.08	0.13	0.12
Ta	0.25	0.11	0.11	0.23	0.15	0.10	0.13	0.12
Th	0.53	0.19	0.15	0.36	0.23	0.13	0.23	0.17
U	0.11	0.06	0.04	0.08	0.05	0.03	0.06	0.04

SAMPLE	RX 321186	RX 321187	RX 321175	RX 321176	RX 321177	RX 321178	RX 321174	RX 321154
Rock type	Mushaua	Mushaua	Mushaua	Mushaua	Mushaua	Mushaua	Mushaua	BBS
Drill hole	S95-6	S95-6	S95-8	S95-8	S95-8	S95-8	S95-8	VB-95-211
Depth	114	143	115	118	125	129	142	135.5
Easting	555837.1	555837.1	555831.6	555831.6	555831.6	555831.6	555831.6	555835.6
Northing	6243322.9	6243322.9	6243051.5	6243051.5	6243051.5	6243051.5	6243051.5	6243237.9
SiO_2	48.0	42.0	40.5	46.8	48.6	51.1	49.3	42.3
TIO_2	1.0	0.5	0.5	0.4	0.7	0.9	3.6	2.5
Al_2O_3	19.9	5.4	7.5	20.6	19.6	15.8	15.2	22.2
Cr_2O_3	0.0	0.4	0.2	0.0	0.0	0.0	0.0	0.0
Fe_2O_3	11.0	16.3	20.2	11.1	11.7	13.0	14.2	16.6
MnO	0.1	0.2	0.2	0.1	0.1	0.1	0.1	0.1
MgO	7.5	31.7	26.8	9.0	7.2	7.0	4.7	5.2
CaO	8.9	2.7	3.0	8.8	8.1	8.0	8.2	6.7
Na_2O	3.2	0.7	0.9	3.1	3.7	3.4	3.7	3.1
K_2O	0.3	0.1	0.2	0.2	0.3	0.5	0.2	0.7
P_2O_5	0.1	0.1	0.1	0.1	0.1	0.1	0.8	0.6
Total	100.0	100.0	100.0	100.0	100.0	100.0	100.0	100.0
LOI	0.0	8.6	7.2	0.9	0.0	0.8	0.0	1.8
Sc	12.8	14.7	9.3	6.9	10.0	25.0	23.3	14.6
Cr	42	1135	1170	257	213	308	47	185
Co	57	111	141	95	95	105	45	195
Ni	169	1609	1047	976	888	1279	56	2954
Cu	25.4	128.8	111.0	708.4	742.3	884.9	57.0	1725.8
Rb	3.465	1.815	2.218	1.456	1.942	4.173	1.914	17.675
Sr	427	66	123	420	386	407	541	438
Y	13.7	6.6	7.7	5.9	7.2	15.7	20.7	19.7
Zr	73	29	67	50	29	91	162	163
Nb	3.44	1.19	1.94	1.42	1.80	3.14	13.59	11.19
Cs	0.03	0.05	0.04	0.02	0.02	0.04	0.03	0.22
Ba	174.9	43.2	58.4	101.2	141.2	202.4	202.5	351.6
La	7.89	2.86	3.90	3.63	4.22	7.18	17.96	25.67
Ce	18.04	6.63	9.50	8.16	9.23	16.53	41.24	59.03
Pr	2.36	0.87	1.28	1.03	1.19	2.22	5.74	7.61
Nd	10.17	4.04	5.67	4.69	5.20	10.17	26.69	32.20
Sm	2.29	0.96	1.30	1.05	1.17	2.41	5.85	6.39
Eu	1.06	0.37	0.44	0.75	0.88	1.01	1.61	1.79
Gd	2.38	1.09	1.37	1.06	1.21	2.58	5.54	5.34
Tb	0.37	0.17	0.22	0.17	0.19	0.41	0.77	0.74
Dy	2.42	1.21	1.36	1.06	1.23	2.71	4.21	3.83
Ho	0.48	0.24	0.28	0.20	0.26	0.56	0.78	0.74
Er	1.40	0.70	0.81	0.62	0.76	1.63	1.93	1.82
Tm	0.20	0.11	0.11	0.09	0.11	0.24	0.25	0.26
Yb	1.18	0.64	0.70	0.53	0.66	1.44	1.42	1.51
Lu	0.18	0.10	0.11	0.08	0.11	0.22	0.21	0.21
Ta	0.21	0.08	0.13	0.09	0.12	0.19	0.81	0.79
Th	0.37	0.16	0.21	0.14	0.16	0.33	0.37	3.86
U	0.08	0.04	0.05	0.04	0.04	0.08	0.07	0.47

SAMPLE	RX 321156	RX 321158	RX 321070	RX 321073	RX 321085	RX 321084	RX 321083	RX 321081
Rock type	BBS	BBS	BBS	BBS	Tasiuyak	Tasiuyak	Tasiuyak	Tasiuyak
Drill hole	VB-95-202	VB-95-202	VB 96 266	VB 96 266	AG95-2	AG95-2	AG95-2	AG95-2
Depth	632	239	529	640.5	66	130.7	150.3	153.3
Easting	557212.3	557212.3	556965.8	556965.8	555640.9	555640.9	555640.9	555640.9
Northing	6242557.0	6242557.0	6242466.0	6242466.0	6243331.5	6243331.5	6243331.5	6243331.5
SiO_2	42.8	41.8	42.3	33.1	51.6	66.1	59.8	60.8
TIO_2	1.8	4.0	2.3	1.7	1.4	0.7	0.8	0.9
Al_2O_3	18.7	15.3	24.5	14.5	16.9	12.3	14.2	15.1
Cr_2O_3	0.0	0.0	0.0	0.0	0.0	0.0	0.0	0.0
Fe_2O_3	17.4	21.4	12.8	37.1	15.1	12.1	14.0	12.2
MnO	0.1	0.2	0.1	0.2	0.0	0.0	0.1	0.1
MgO	8.1	5.2	5.3	4.0	4.4	2.0	2.5	2.7
CaO	7.2	7.3	6.9	6.4	4.6	2.0	2.4	2.3
Na_2O	2.9	3.3	3.3	2.3	2.8	2.0	2.3	2.3
K_2O	0.6	0.7	2.0	0.4	3.0	2.7	4.0	3.6
P_2O_5	0.3	0.8	0.4	0.3	0.0	0.0	0.0	0.0
Total	100.0	100.0	100.0	100.0	100.0	100.0	100.0	100.0
LOI	0.6	1.6	1.2	4.3	7.8	3.4	5.3	4.8
Sc	11.4	17.5	11.5	6.5	14.6	4.6	8.4	10.3
Cr	155	84	191	74	183	103	132	133
Co	166	250	92	578	47	38	44	35
Ni	2664	3485	1070	5032	184	153	156	124
Cu	1436.5	1346.4	555.7	2224.8	303.0	209.2	195.9	161.0
Rb	8.826	7.339	61.345	3.259	122.865	77.225	122.158	103.127
Sr	499	453	518	402	171	185	204	210
Y	10.8	22.6	15.5	8.0	5.4	5.2	7.0	8.8
Zr	80	138	159	51	257	189	230	226
Nb	4.76	9.10	11.11	3.33	9.53	8.11	6.71	7.41
Cs	0.10	0.09	2.02	0.05	1.04	0.29	0.43	0.34
Ba	243.3	364.0	490.0	193.9	374.4	671.7	804.0	793.9
La	9.80	18.73	29.25	7.87	67.35	44.71	42.30	52.62
Ce	23.16	45.78	63.33	18.81	138.43	85.56	79.06	102.29
Pr	3.13	6.32	7.87	2.51	16.53	9.51	8.72	11.54
Nd	13.56	28.60	31.89	11.25	60.57	33.38	30.38	40.65
Sm	2.80	6.17	5.87	2.32	8.28	5.11	4.10	5.72
Eu	1.17	2.01	1.61	1.11	1.29	1.39	1.46	1.54
Gd	2.56	5.62	4.50	2.09	4.39	3.40	2.42	3.61
Tb	0.37	0.80	0.60	0.30	0.43	0.40	0.29	0.45
Dy	2.06	4.51	3.08	1.60	1.24	1.32	1.24	1.84
Ho	0.39	0.85	0.55	0.30	0.20	0.19	0.25	0.32
Er	1.04	2.17	1.43	0.79	0.51	0.46	0.77	0.89
Tm	0.15	0.30	0.20	0.11	0.08	0.07	0.14	0.15
Yb	0.85	1.64	1.10	0.62	0.55	0.47	0.93	1.02
Lu	0.13	0.24	0.16	0.09	0.10	0.08	0.15	0.17
Ta	0.32	0.64	0.69	0.22	0.34	0.33	0.22	0.28
Th	0.64	0.64	8.17	0.30	35.52	12.99	11.11	17.18
U	0.10	0.17	0.58	0.08	1.05	0.87	0.73	0.85

SAMPLE	RX 321082	RX 321151	RX 321149	VX33146	VX34378	VX34751	VX34749	VX33163
Rock type	Tasiuyak	Tasiuyak	Tasiuyak	Tasiuyak	Tasiuyak	Tasiuyak	Tasiuyak	Tasiuyak
Drill hole	AG95-2	VB-95-193	VB-95-193	VB-97-369	VB-95-108	VB-97-400	VB-97-400	VB-97-374
Depth	167.5	207	230	652.9	511.1	149.3	144.2	96.6
Easting	555640.9	554453.0	554453.0	554898.1	554946.9	554546.3	554546.3	553972.7
Northing	6243331.5	6243577.4	6243577.4	6243185.8	6243550.2	6243232.4	6243232.4	6243386.3
SiO_2	68.4	60.9	49.3	73.5	73.7	71.1	66.3	59.8
TIO_2	0.8	0.5	1.0	0.3	0.4	0.6	0.9	0.5
Al_2O_3	14.2	17.2	11.8	14.1	12.9	13.5	15.0	11.4
Cr_2O_3	0.0	0.0	0.1	0.0	0.0	0.0	0.0	0.0
Fe_2O_3	6.7	5.7	12.2	2.4	4.6	6.1	6.8	18.9
MnO	0.1	0.1	0.2	0.0	0.0	0.1	0.1	0.2
MgO	2.4	2.7	11.2	0.7	1.6	2.2	2.4	2.7
CaO	1.6	6.1	11.4	2.9	1.6	1.7	3.3	2.0
Na_2O	1.8	4.9	1.8	4.0	2.6	2.1	3.0	1.8
K_2O	4.0	1.7	0.9	2.2	2.7	2.6	2.1	2.6
P_2O_5	0.1	0.3	0.1	0.1	0.0	0.0	0.2	0.2
Total	100.0	100.0	100.0	100.0	100.0	100.0	100.0	100.0
LOI	1.0	1.0	1.0	0.9	1.1	0.4	0.7	6.0
Sc	24.7	12.8	27.8	4.4	11.2	13.3	11.6	11.3
Cr	113	39	775	12	88	104	93	92
Co	8	29	53	6	9	13	15	71
Ni	25	330	372	5	28	40	39	198
Cu	26.1	267.3	136.8	9.8	17.5	28.9	69.1	964.5
Rb	40.450	13.817	23.865	46.028	56.009	73.169	74.931	74.272
Sr	488	1030	1083	226	268	292	490	209
Y	14.3	6.8	10.7					
Zr	283	31	57		172	211	244	
Nb	4.50	5.69	4.88	3.15	9.19	10.75	9.89	8.04
Cs	0.34	0.25	0.12	0.10	0.16	0.13	0.34	1.46
Ba	400.6	400.9	548.7	655.8	947.2	926.8	898.6	567.5
La	28.81	25.80	34.51	15.16	35.18	37.43	90.86	30.79
Ce	62.16	50.29	67.58	28.52	63.95	71.66	168.57	56.51
Pr	26.21	7.53	5.71	7.92	12.30	2.24	2.81	6.35
Nd	29.71	21.56	30.45	10.17	21.97	28.08	64.52	26.47
Sm	5.51	3.36	4.98	1.54	3.45	4.55	8.64	5.26
Eu	1.62	1.21	1.18	1.73	2.41	0.83	0.62	1.54
Gd	6.45	4.37	2.33	3.55	7.54	3.08	1.34	3.50
Tb	0.86	0.61	0.29	0.45	0.99	0.51	0.16	0.56
Dy	2.90	1.26	2.02	0.81	3.44	3.89	3.40	4.92
Ho	1.12	0.51	0.24	0.39	0.91	0.68	0.16	0.73
Er	1.25	0.63	1.00	0.45	2.15	2.54	2.06	2.97
Tm	0.64	0.16	0.10	0.15	0.34	0.28	0.07	0.34
Yb	0.94	0.58	0.89	0.41	2.37	2.52	2.21	3.35
Lu	0.13	0.09	0.13	0.07	0.35	0.39	0.35	0.54
Ta	0.30	0.31	0.26	0.20	0.48	0.57	0.33	0.49
Th	2.05	0.56	1.20	1.11	5.98	10.40	23.32	6.47
U	0.32	0.25	0.60	0.24	1.16	0.90	1.46	5.22

SAMPLE	VX34748	VX36414	VX34714	VX33145	VX34747	VX34716	VX36466	RX 321126
Rock type	Tasiuyak	Tasiuyak	Tasiuyak	Tasiuyak	Tasiuyak	Tasiuyak	Tasiuyak	Nain
Drill hole	VB-97-400	VB-95-213	VB-97-385	VB-97-369	VB-97-400	VB-97-390	VB-97-428	VB-96-265
Depth	139.9	352.5	815.5	647.5	130.1	344.2	566.8	382
Easting	554546.3	552128.2	555143.1	554898.1	554546.3	554266.1	554266.0	555438.2
Northing	6243232.4	6242488.1	6242897.7	6243185.8	6243232.4	6243135.3	6243039.6	6243667.5
SiO_2	65.7	65.9	58.1	51.9	55.7	47.1	48.5	57.8
TIO_2	0.5	0.5	0.9	2.1	1.1	1.9	0.3	0.8
Al_2O_3	14.7	16.6	16.9	14.0	15.5	13.6	10.2	17.7
Cr_2O_3	0.0	0.0	0.0	0.0	0.0	0.0	0.3	0.0
Fe_2O_3	8.4	7.5	6.7	15.0	9.5	16.7	9.7	6.0
MnO	0.1	0.1	0.1	0.2	0.1	0.2	0.1	0.1
MgO	2.7	3.9	4.2	5.8	6.0	7.4	9.8	2.9
CaO	2.7	1.4	8.5	6.2	7.0	11.3	20.3	5.1
Na_2O	3.0	2.2	3.9	3.3	3.6	1.3	0.3	5.0
K_2O	2.1	1.9	0.5	1.3	1.3	0.4	0.4	4.2
P_2O_5	0.1	0.0	0.2	0.2	0.2	0.1	0.0	0.5
Total	100.0	100.0	100.0	100.0	100.0	100.0	100.0	100.0
LOI	3.2	0.5	0.8	0.0	0.4	0.4	0.9	0.6
Sc	11.2	18.6	16.5	30.0	24.1	42.4	30.6	9.9
Cr	113	203	100	33	278	164	1847	60
Co	26	34	17	55	32	54	91	18
Ni	114	153	51	62	131	125	793	38
Cu	441.0	76.7	14.4	60.2	52.5	82.8	445.3	52.4
Rb	40.450	62.845	59.986	4.650	45.740	27.681	12.138	85.902
Sr	488	346	161	244	319	439	192	984
Y								14.7
Zr	31	233	136	160		212	83	252
Nb	4.50	7.72	7.73	8.81	16.27	11.51	6.93	9.87
Cs	0.34	0.30	0.15	0.03	1.00	0.13	0.07	0.33
Ba	400.6	702.1	490.3	249.1	422.8	676.9	117.2	1257.4
La	28.81	38.35	29.07	15.83	18.69	32.00	9.80	44.63
Ce	62.16	73.12	56.41	34.02	49.29	72.34	25.92	89.26
Pr	7.63	18.58	6.98	7.53	7.91	6.09	3.98	10.54
Nd	29.71	28.54	22.58	15.89	29.16	35.06	16.80	39.84
Sm	5.51	4.49	3.79	3.27	6.76	6.32	4.51	6.37
Eu	1.50	1.92	1.70	1.21	1.58	1.16	1.14	1.90
Gd	3.89	5.84	5.26	4.37	3.47	3.03	3.03	4.48
Tb	0.62	0.67	0.85	0.61	0.43	0.41	0.48	0.58
Dy	2.83	2.24	2.29	2.88	4.92	4.26	4.93	2.88
Ho	0.87	0.72	1.08	0.51	0.47	0.48	0.61	0.52
Er	1.22	1.39	1.50	1.69	2.44	2.37	2.76	1.36
Tm	0.40	0.33	0.49	0.16	0.24	0.24	0.25	0.19
Yb	0.94	1.71	1.76	1.61	2.13	2.13	2.54	1.14
Lu	0.13	0.27	0.28	0.25	0.29	0.32	0.37	0.18
Ta	0.30	0.41	0.47	0.41	1.05	0.44	0.38	0.43
Th	2.05	9.52	6.61	0.07	0.43	0.91	0.85	0.28
U	0.32	1.89	0.65	0.05	0.19	0.20	0.13	0.12

SAMPLE	RX 321191	RX 321193	RX 321152	RX 321153	RX 321150	RX 321193	RX 321150	VX35249
Rock type	Nain	Nain	Nain	Nain	Nain	Enderbite	Enderbite	Enderbite
Drill hole	VB-95-169	VB-96-263	VB-96-261	VB-96-261	VB-96-263	VB-96-263	VB-96-263	VB-97-402
Depth	186	838	453	454	750	838	750	1058.7
Easting	555234.6	557985.2	556718.7	556718.7	557985.2	557985.2	557985.2	558893.0
Northing	6243024.5	6242178.4	6242741.4	6242741.4	6242178.4	6242178.4	6242178.4	6242230.4
SiO_2	68.6	53.7	43.3	53.1	53.7	53.7	53.7	52.1
TIO_2	0.3	1.1	0.9	0.7	0.9	1.1	0.9	1.0
Al_2O_3	16.5	18.2	14.4	17.0	17.7	18.2	17.7	20.0
Cr_2O_3	0.0	0.0	0.0	0.0	0.0	0.0	0.0	0.0
Fe_2O_3	2.9	9.5	28.6	13.8	8.6	9.5	8.6	7.9
MnO	0.0	0.1	0.1	0.1	0.1	0.1	0.1	0.1
MgO	0.9	3.4	2.8	3.1	4.2	3.4	4.2	3.6
CaO	3.7	7.8	5.2	5.8	8.5	7.8	8.5	9.1
Na_2O	5.4	5.1	3.7	4.8	4.9	5.1	4.9	4.9
K_2O	1.5	0.7	0.9	1.3	1.1	0.7	1.1	0.9
P_2O_5	0.1	0.3	0.2	0.3	0.4	0.3	0.4	0.4
Total	100.0	100.0	100.0	100.0	100.0	100.0	100.0	100.0
LOI	0.4	0.0	3.1	2.7	0.5	0.0	0.5	0.3
Sc	5.3	23.8	7.0	9.5	19.0	23.8	19.0	17.0
Cr	18	49	68	52	106	49	106	36
Co	6	23	366	91	24	23	24	25
Ni	13	24	4688	1926	53	24	53	34
Cu	18.3	29.0	605.3	2061.0	137.2	29.0	137.2	112.4
Rb	7.715	1.833	13.817	23.865	10.653	1.833	10.653	13.958
Sr	769	1219	1030	1083	1227	1219	1227	1333
Y	4.0	24.8	6.8	10.7	25.9	24.8	25.9	17.7
Zr	111	284	186	239	227	284	227	183
Nb	1.30	11.15	5.69	4.88	9.14	11.15	9.14	6.21
Cs	0.05	0.02	0.25	0.12	0.05	0.02	0.05	0.08
Ba	1074.0	1580.6	400.9	548.7	684.6	1580.6	684.6	791.2
La	13.74	36.40	25.80	34.51	34.75	36.40	34.75	34.06
Ce	24.17	77.26	50.29	67.58	86.84	77.26	86.84	71.59
Pr	2.59	9.74	5.71	7.92	12.30	9.74	12.30	8.51
Nd	9.91	39.80	21.56	30.45	52.89	39.80	52.89	35.28
Sm	1.62	7.41	3.36	4.98	10.25	7.41	10.25	6.35
Eu	1.16	2.56	1.18	1.73	2.41	2.56	2.41	2.04
Gd	1.30	6.25	2.33	3.55	7.54	6.25	7.54	4.72
Tb	0.17	0.88	0.29	0.45	0.99	0.88	0.99	0.65
Dy	0.76	4.93	1.28	2.10	5.07	4.73	4.84	3.34
Ho	0.14	0.95	0.24	0.39	0.91	0.95	0.91	0.67
Er	0.37	2.51	0.63	1.00	2.43	2.35	2.33	1.72
Tm	0.06	0.34	0.10	0.15	0.34	0.34	0.34	0.24
Yb	0.33	1.84	0.58	0.89	1.98	1.84	1.98	1.47
Lu	0.05	0.26	0.09	0.13	0.28	0.26	0.28	0.20
Ta	0.04	0.45	0.31	0.26	0.52	0.45	0.52	0.22
Th	0.32	0.53	0.56	1.20	1.34	0.53	1.34	0.60
U	0.08	0.25	0.25	0.60	0.17	0.25	0.17	0.16

SAMPLE	RX 313204	RX 321153	RX 313198	VX34745	VX34331	RX 321152	VX34713	VX34746
Rock type	Enderbite	Enderbite	Enderbite	Enderbite	Enderbite	Enderbite	Enderbite	Enderbite
Drill hole	VB-96-316	VB-96-261	VB-96-332	VB-97-400	VB-95-123	VB-96-261	VB-97-385	VB-97-400
Depth	715	454	747	114.1	170.6	453	811.4	127.0
Easting	557211.0	556718.7	557201.0	554546.3	554848.4	556718.7	555143.1	554546.3
Northing	6241889.0	6242741.4	6242121.2	6243232.4	6243551.7	6242741.4	6242897.7	6243232.4
SiO_2	54.6	53.1	56.0	61.6	56.2	43.3	60.1	59.5
TIO_2	0.9	0.7	0.9	0.7	0.9	0.9	0.7	0.7
Al_2O_3	18.9	17.0	18.5	17.6	18.9	14.4	18.1	18.5
Cr_2O_3	0.0	0.0	0.0	0.0	0.0	0.0	0.0	0.0
Fe_2O_3	7.2	13.8	6.8	4.5	6.5	28.6	5.5	5.1
MnO	0.1	0.1	0.1	0.1	0.1	0.1	0.1	0.1
MgO	3.7	3.1	3.4	2.3	3.2	2.8	2.6	2.6
CaO	7.2	5.8	6.5	5.6	7.0	5.2	5.7	6.2
Na_2O	4.7	4.8	5.1	4.8	5.7	3.7	4.7	5.1
K_2O	2.2	1.3	2.3	2.5	1.1	0.9	2.1	2.0
P_2O_5	0.5	0.3	0.5	0.3	0.4	0.2	0.3	0.3
Total	100.0	100.0	100.0	100.0	100.0	100.0	100.0	100.0
LOI	0.3	2.7	0.1	0.5	1.3	3.1	0.6	0.3
Sc	13.0	9.5	11.0	8.5	11.1	7.0	8.9	8.5
Cr	55	52	49	28	34	68	30	29
Co	25	91	22	12	19	366	14	13
Ni	50	1926	97	21	28	4688	23	23
Cu	66.0	2061.0	449.0	50.6	44.5	605.3	12.8	13.8
Rb	42.836	23.865	43.312	37.563	14.342	13.817	21.644	19.134
Sr	1256	1083	1240	962	1181	1030	1082	1046
Y	14.3	10.7	14.7	12.5	11.0	6.8	10.6	10.1
Zr	209	239	211	185	152	186	198	191
Nb	6.73	4.88	9.54	6.64	6.54	5.69	7.29	7.27
Cs	0.33	0.12	0.32	0.06	0.07	0.25	0.08	0.03
Ba	1527.0	548.7	1217.0	1444.6	951.0	400.9	2056.3	1525.1
La	37.26	34.51	44.03	34.63	38.22	25.80	42.28	36.63
Ce	79.81	67.58	93.65	75.39	73.67	50.29	80.13	72.74
Pr	9.74	7.92	10.92	9.19	8.48	5.71	9.08	8.63
Nd	39.79	30.45	44.46	37.51	33.79	21.56	35.20	34.41
Sm	6.58	4.98	7.35	6.33	5.52	3.36	5.50	5.45
Eu	2.00	1.73	1.99	1.65	1.79	1.18	2.21	1.74
Gd	4.75	3.55	4.94	4.27	3.88	2.33	3.84	3.63
Tb	0.58	0.45	0.63	0.52	0.47	0.29	0.44	0.42
Dy	2.95	2.02	3.03	2.54	2.30	1.26	2.25	2.06
Ho	0.54	0.39	0.57	0.47	0.42	0.24	0.41	0.37
Er	1.27	1.00	1.45	1.24	1.05	0.63	1.02	0.93
Tm	0.19	0.15	0.20	0.17	0.14	0.10	0.14	0.14
Yb	1.14	0.89	1.20	0.96	0.86	0.58	0.92	0.81
Lu	0.16	0.13	0.17	0.14	0.12	0.09	0.12	0.11
Ta	0.22	0.26	0.36	0.20	0.24	0.31	0.25	0.23
Th	0.25	1.20	1.64	0.37	0.40	0.56	0.26	0.18
U	0.11	0.60	0.31	0.11	0.05	0.25	0.15	0.04

SAMPLE	VX34386	VX34703	VX34368	VX34334	VX34380	VX34330	VX33173	VX34712
Rock type	Enderbite	Enderbite	Enderbite	Enderbite	Enderbite	Enderbite	Enderbite	Enderbite
Drill hole	VB-95-108	VB-97-388	VB-95-106	VB-95-123	VB-95-108	VB-95-123	VB-97-378	VB-97-385
Depth	475.5	318.1	270.1	285.4	477.9	165.3	25.9	806.2
Easting	554946.9	554751.9	554947.0	554848.4	554946.9	554848.4	554752.0	555143.1
Northing	6243550.2	6243132.2	6243500.9	6243551.7	6243550.2	6243551.7	6243133.0	6242897.7
SiO_2	61.0	57.2	56.8	59.9	59.2	57.0	59.6	60.6
TIO_2	0.7	0.8	0.8	0.7	0.8	0.8	0.7	0.7
Al_2O_3	18.2	19.6	18.7	18.4	15.8	19.1	18.4	18.1
Cr_2O_3	0.0	0.0	0.0	0.0	0.0	0.0	0.0	0.0
Fe_2O_3	5.0	5.3	7.5	5.2	6.8	6.0	5.2	4.9
MnO	0.1	0.1	0.1	0.1	0.1	0.1	0.1	0.1
MgO	2.5	2.6	2.8	2.5	4.0	3.0	2.6	2.4
CaO	4.9	6.7	6.4	6.1	7.8	7.1	6.0	5.7
Na_2O	5.2	5.7	5.3	5.3	4.4	5.4	5.1	5.0
K_2O	2.3	1.6	1.3	1.7	0.9	1.2	2.0	2.3
P_2O_5	0.3	0.3	0.3	0.3	0.2	0.4	0.3	0.3
Total	100.0	100.0	100.0	100.0	100.0	100.0	100.0	100.0
LOI	2.1	0.6	1.0	0.4	1.6	0.5	0.7	0.5
Sc	7.9	8.6	8.2	8.2	15.0	9.2	8.8	7.8
Cr	33	30	43	23	63	31	35	41
Co	13	15	42	14	18	17	15	14
Ni	24	24	856	40	40	31	28	32
Cu	35.1	13.2	2508.2	83.0	85.2	26.1	16.1	47.2
Rb	33.679	23.216	18.977	16.563	20.890	13.918	24.103	25.553
Sr	980	1262	1326	1252	386	1452	1214	1150
Y	8.6	11.5	8.2	8.7	16.1	8.5	8.0	8.3
Zr	181	251	108	150	167	139	209	174
Nb	5.98	10.23	6.01	6.13	7.98	6.14	5.91	5.43
Cs	0.13	0.08	0.30	0.05	0.10	0.09	0.06	0.05
Ba	1419.8	974.5	1136.3	1292.8	328.5	1015.4	1639.3	1742.0
La	31.46	43.66	33.04	35.52	15.84	36.34	33.47	33.91
Ce	65.77	90.94	65.16	70.34	34.67	71.45	65.48	68.98
Pr	7.64	10.62	7.63	8.06	3.99	8.39	7.88	7.86
Nd	30.43	39.74	30.79	32.08	15.90	33.30	32.04	30.49
Sm	4.76	6.09	4.82	5.02	3.17	5.17	5.17	4.76
Eu	1.57	1.63	1.71	1.60	1.08	1.74	1.66	1.66
Gd	3.26	4.03	3.32	3.33	3.07	3.40	3.47	3.14
Tb	0.38	0.46	0.36	0.38	0.48	0.41	0.39	0.36
Dy	1.83	2.16	1.71	1.79	2.82	1.84	1.79	1.69
Ho	0.33	0.41	0.30	0.31	0.60	0.31	0.32	0.30
Er	0.78	1.03	0.73	0.78	1.57	0.79	0.72	0.73
Tm	0.10	0.14	0.10	0.10	0.24	0.10	0.10	0.10
Yb	0.66	0.89	0.64	0.65	1.51	0.65	0.59	0.61
Lu	0.09	0.13	0.09	0.08	0.23	0.09	0.09	0.09
Ta	0.14	0.37	0.22	0.16	0.37	0.21	0.16	0.16
Th	0.02	0.45	0.46	0.04	0.29	0.56	0.09	0.03
U	0.02	0.11	0.23	0.01	0.12	0.09	0.02	0.02

SAMPLE	VX34391	VX34344	VX34315	VX36402	RX313681	VX35231	VX35242	VX35206
Rock type	Enderbite	Enderbite	Enderbite	Enderbite	Enderbite	Enderbite	Enderbite	Enderbite
Drill hole	VB-95-160	VB-95-168	VB-95-153	VB-96-273	VB-95-027	VB-95-146	VB-95-136	VB-95-133
Depth	116.2	412.2	138.3	446.6	94.9	52.4	198.4	32.8
Easting	554799.5	555050.1	554797.7	555737.6	555781.9	554999.7	554997.5	554996.4
Northing	6243553.2	6243577.6	6243377.4	6242965.0	6243057.8	6243530.9	6243444.0	6243426.3
SiO_2	61.0	56.9	56.4	56.8	58.1	58.1	57.4	58.1
TIO_2	0.7	0.8	0.8	0.8	0.8	0.8	0.8	0.8
Al_2O_3	18.1	19.6	20.1	17.7	17.5	17.6	16.5	17.5
Cr_2O_3	0.0	0.0	0.0	0.0	0.0	0.0	0.0	0.0
Fe_2O_3	4.7	5.6	5.5	6.6	6.1	6.0	6.5	6.3
MnO	0.1	0.1	0.1	0.1	0.1	0.1	0.1	0.1
MgO	2.2	2.9	2.8	3.6	3.0	3.1	4.1	2.8
CaO	5.7	7.0	7.2	6.1	5.4	5.4	5.9	5.1
Na_2O	5.0	5.6	5.5	4.7	4.8	4.8	4.3	4.9
K_2O	2.2	1.2	1.3	3.2	3.8	3.8	3.9	3.9
P_2O_5	0.3	0.4	0.4	0.5	0.4	0.4	0.5	0.4
Total	100.0	100.0	100.0	100.0	100.0	100.0	100.0	100.0
LOI	0.8	0.9	0.5	0.3	0.3	0.3	0.5	0.4
Sc	7.4	8.9	8.6	10.4	9.1	9.6	12.2	8.9
Cr	28	26	25	73	51	66	156	57
Co	14	18	17	23	17	16	22	17
Ni	23	26	28	47	36	41	82	58
Cu	10.4	26.0	16.1	27.7	170.4	39.4	78.6	188.8
Rb	35.682	12.119	11.925	69.884	113.663	104.354	119.369	110.684
Sr	1251	1476	1575	1149	958	917	910	851
Y	8.3	8.8	8.1	14.9	15.1	14.8	15.1	15.0
Zr	153	88	88	194	182	250	159	386
Nb	8.80	5.89	6.69	10.33	13.05	12.03	6.55	15.66
Cs	0.25	0.08	0.08	0.25	1.13	0.39	1.10	0.43
Ba	1545.8	1010.4	1081.4	1538.9	1407.3	1362.9	1397.1	1295.7
La	35.05	37.70	35.71	45.04	50.18	45.97	41.30	46.42
Ce	71.28	75.22	70.97	92.03	102.25	92.97	84.74	93.99
Pr	8.27	8.69	8.19	10.64	11.43	10.87	10.08	10.83
Nd	32.33	34.53	32.44	41.83	43.62	42.10	39.77	42.11
Sm	5.21	5.47	5.06	6.63	6.78	6.68	6.55	6.61
Eu	1.61	1.88	1.79	1.93	1.84	1.87	1.92	1.71
Gd	3.46	3.53	3.33	4.75	4.94	4.57	4.65	4.39
Tb	0.40	0.40	0.39	0.59	0.57	0.57	0.57	0.57
Dy	1.80	1.90	1.68	2.80	2.91	2.92	2.93	2.87
Ho	0.32	0.33	0.29	0.54	0.53	0.56	0.57	0.55
Er	0.71	0.81	0.74	1.41	1.45	1.44	1.48	1.50
Tm	0.10	0.11	0.09	0.19	0.20	0.22	0.22	0.21
Yb	0.60	0.62	0.58	1.29	1.31	1.31	1.37	1.33
Lu	0.08	0.09	0.08	0.19	0.19	0.20	0.20	0.20
Ta	0.43	0.24	0.22	0.33	0.50	0.50	0.32	0.63
Th	2.15	0.39	0.27	0.13	1.40	0.62	1.33	0.70
U	0.76	0.11	0.06	0.08	0.55	0.19	0.49	0.29

SAMPLE	VX35224	VX35216	RX 321126	VX36454	VX34326	VX34338	VX35213	VX34329
Rock type	Enderbite	Enderbite	Enderbite	Enderbite	Enderbite	Enderbite	Enderbite	Enderbite
Drill hole	VB-95-134	VB-95-138	VB-96-265	VB-97-426	VB-95-114	VB-95-117	VB-95-133	VB-95-123
Depth	97.7	111.8	382	742.5	36.6	38.4	163.5	9.9
Easting	554895.8	554895.4	555438.2	557209.6	554844.6	554847.4	554996.4	554848.4
Northing	6243478.2	6243526.6	6243667.5	6240966.9	6243324.2	6243451.9	6243426.3	6243551.7
SiO_2	57.8	56.8	57.8	57.8	58.3	57.5	58.1	58.2
TIO_2	0.7	0.9	0.8	0.8	0.8	0.8	0.8	0.8
Al_2O_3	17.2	16.5	17.7	17.3	17.3	17.6	17.2	17.4
Cr_2O_3	0.0	0.0	0.0	0.0	0.0	0.0	0.0	0.0
Fe_2O_3	6.8	7.1	6.0	6.2	6.0	6.1	6.5	6.1
MnO	0.1	0.1	0.1	0.1	0.1	0.1	0.1	0.1
MgO	2.9	3.9	2.9	3.2	3.1	3.0	3.0	3.1
CaO	5.1	5.6	5.1	5.2	5.1	5.3	5.1	5.0
Na_2O	4.9	4.4	5.0	4.7	4.8	4.8	4.6	4.7
K_2O	4.1	4.1	4.2	4.2	4.2	4.3	4.3	4.3
P_2O_5	0.4	0.5	0.5	0.5	0.5	0.5	0.5	0.5
Total	100.0	100.0	100.0	100.0	100.0	100.0	100.0	100.0
LOI	0.4	0.0	0.6	0.4	0.4	0.5	0.3	0.5
Sc	9.0	11.6	9.9	10.9	9.5	9.7	9.3	9.8
Cr	76	129	60	102	92	84	87	96
Co	32	21	18	22	18	18	24	16
Ni	314	70	38	52	58	67	154	52
Cu	1535.5	97.0	52.4	117.6	60.9	130.7	1197.7	80.0
Rb	118.816	126.583	85.902	108.016	125.894	112.737	121.788	123.895
Sr	874	807	984	884	960	868	828	817
Y	14.8	17.1	14.7	15.3	13.4	13.5	14.1	13.8
Zr	240	298	252		199	241	247	233
Nb	11.67	12.48	9.87	12.13	8.39	8.59	10.54	9.00
Cs	0.76	0.43	0.33	0.21	0.73	0.56	0.65	0.68
Ba	1304.8	1257.9	1257.4	1495.0	1430.8	1449.5	1339.6	1345.4
La	45.11	46.69	44.63	41.16	41.58	43.38	42.43	39.85
Ce	91.55	95.67	89.26	87.53	83.24	87.10	84.45	78.95
Pr	10.74	11.45	10.54	9.93	9.41	9.72	9.96	8.87
Nd	41.27	44.97	39.84	39.18	36.38	38.20	37.92	34.54
Sm	6.61	7.23	6.37	6.29	5.81	6.01	6.18	5.73
Eu	1.81	1.76	1.90	1.67	1.71	1.68	1.68	1.60
Gd	4.42	4.93	4.48	4.28	4.13	4.29	4.28	3.90
Tb	0.56	0.63	0.58	0.57	0.52	0.53	0.53	0.51
Dy	2.82	3.24	2.70	2.93	2.54	2.67	2.71	2.58
Ho	0.56	0.64	0.52	0.58	0.49	0.50	0.52	0.51
Er	1.43	1.71	1.33	1.43	1.31	1.33	1.44	1.34
Tm	0.21	0.26	0.19	0.22	0.18	0.18	0.21	0.19
Yb	1.35	1.54	1.14	1.43	1.21	1.21	1.30	1.26
Lu	0.19	0.23	0.18	0.22	0.17	0.16	0.20	0.18
Ta	0.50	0.48	0.43	0.45	0.35	0.27	0.44	0.37
Th	1.70	0.36	0.28	0.39	0.95	0.46	1.24	0.88
U	0.68	0.15	0.12	0.20	0.39	0.14	0.50	0.41

SAMPLE	VX35205	VX34357	VX34373	VX35212	VX34345	VX34346	VX34328	VX34337
Rock type	Enderbite	Enderbite	Enderbite	Enderbite	Enderbite	Enderbite	Enderbite	Enderbite
Drill hole	VB-95-129	VB-95-106	VB-95-108	VB-95-133	VB-95-168	VB-95-144	VB-95-123	VB-95-112
Depth	71.2	24.2	155.2	175.3	317.7	121.7	97.4	161.2
Easting	554993.7	554947.0	554946.9	554996.4	555050.1	554894.6	554848.4	554846.1
Northing	6243356.1	6243500.9	6243550.2	6243426.3	6243577.6	6243577.1	6243551.7	6243377.8
SiO_2	57.4	57.3	58.4	58.8	57.7	58.1	57.9	57.5
TIO_2	0.8	0.8	0.8	0.7	0.8	0.8	0.9	1.0
Al_2O_3	16.9	16.8	17.1	17.5	17.6	17.4	17.5	17.3
Cr_2O_3	0.0	0.0	0.0	0.0	0.1	0.0	0.0	0.0
Fe_2O_3	7.2	6.3	6.2	5.7	6.0	5.9	6.1	7.0
MnO	0.1	0.1	0.1	0.1	0.1	0.1	0.1	0.1
MgO	2.9	3.7	2.9	2.7	2.8	2.8	2.9	2.8
CaO	5.1	5.4	4.9	4.8	5.0	5.0	4.8	4.5
Na_2O	4.6	4.5	4.7	4.7	4.8	4.7	4.8	4.5
K_2O	4.3	4.4	4.5	4.4	4.5	4.6	4.6	5.0
P_2O_5	0.5	0.5	0.5	0.4	0.5	0.5	0.4	0.4
Total	100.0	100.0	100.0	100.0	100.0	100.0	100.0	100.0
LOI	0.3	0.5	0.6	0.2	0.8	0.6	0.4	0.6
Sc	9.1	10.2	9.3	8.2	9.3	9.3	9.5	9.9
Cr	79	129	87	73	77	80	92	81
Co	22	20	17	16	17	16	17	29
Ni	155	75	48	60	44	45	50	352
Cu	1039.6	76.1	127.1	281.3	85.3	87.0	146.4	652.6
Rb	121.708	136.697	125.318	125.066	126.721	134.538	143.799	6.405
Sr	798	1018	827	803	888	911	764	593
Y	15.7	15.3	15.6	12.9	15.2	14.8	14.6	15.9
Zr	323	229	268	159	311	272	358	
Nb	12.94	9.82	11.03	8.12	14.09	10.96	13.65	5.15
Cs	0.78	0.61	0.47	0.58	0.25	0.43	0.46	0.05
Ba	1287.2	1385.6	1276.5	1351.2	1306.7	1343.0	1262.8	277.9
La	46.63	50.08	42.75	38.54	45.28	46.57	43.01	12.21
Ce	95.06	102.49	86.20	77.53	91.64	93.77	86.05	29.62
Pr	11.16	12.03	9.78	9.04	10.54	10.85	9.80	10.56
Nd	42.77	47.05	37.72	34.68	40.99	41.79	37.44	16.97
Sm	6.79	7.14	6.21	5.45	6.42	6.57	6.20	3.52
Eu	1.76	1.86	1.74	1.67	1.75	1.85	1.63	1.65
Gd	4.60	4.75	4.51	3.68	4.63	4.59	4.35	4.66
Tb	0.60	0.59	0.56	0.48	0.59	0.59	0.55	0.59
Dy	3.03	2.98	3.06	2.46	3.03	3.01	2.76	2.51
Ho	0.58	0.55	0.59	0.49	0.57	0.56	0.54	0.57
Er	1.54	1.44	1.55	1.26	1.51	1.49	1.42	1.54
Tm	0.22	0.22	0.22	0.19	0.22	0.21	0.20	0.21
Yb	1.33	1.37	1.42	1.15	1.26	1.35	1.34	1.48
Lu	0.22	0.19	0.20	0.18	0.20	0.19	0.20	0.21
Ta	0.49	0.34	0.50	0.36	0.52	0.46	0.51	0.25
Th	1.43	0.71	0.61	0.83	0.29	0.46	0.31	0.16
U	0.33	0.27	0.28	0.33	0.14	0.20	0.22	0.10

Table A.2 Olivine electron microprobe data

TS number	SiO_2	TiO_2	Al_2O_3	MgO	CaO	MnO	FeO	NiO	Total	Fo #	Depth	Rock
98/AV/289	39.09	0.01	0.00	38.20	0.03	0.28	22.73	0.14	100.5	75	15	NT
98/AV/289	39.14	0.01	0.00	38.26	0.01	0.27	22.58	0.15	100.4	75	15	NT
98/AV/289	38.77	0.01	0.01	38.25	0.00	0.29	23.33	0.15	100.8	75	15	NT
98/AV/289	38.73	0.00	0.00	38.31	0.02	0.29	23.49	0.14	101.0	74	15	NT
98/AV/289	38.51	0.00	0.00	38.23	0.01	0.28	23.60	0.16	100.8	74	15	NT
98/AV/289	38.97	0.00	0.00	38.38	0.01	0.31	23.58	0.13	101.4	74	15	NT
98/AV/289	39.18	0.00	0.00	38.39	0.01	0.30	23.66	0.16	101.7	74	15	NT
98/AV/289	39.03	0.01	0.00	38.24	0.02	0.30	23.35	0.14	101.1	74	15	NT
98/AV/289	38.95	0.01	0.00	38.26	0.01	0.29	23.60	0.15	101.3	74	15	NT
98/AV/289	40.06	0.00	0.00	37.46	0.06	0.25	21.34	0.13	99.3	76	15	NT
98/AV/289	38.98	0.01	0.01	38.29	0.02	0.29	23.40	0.15	101.2	74	15	NT
98/AV/289	38.98	0.02	0.01	37.43	0.03	0.28	23.40	0.14	100.3	74	15	NT
98/AV/289	38.99	0.00	0.00	38.29	0.01	0.29	23.59	0.15	101.3	74	15	NT
98/AV/289	38.98	0.00	0.00	38.38	0.00	0.28	23.26	0.13	101.0	75	15	NT
98/AV/289	39.22	0.00	0.01	38.45	0.03	0.29	23.21	0.14	101.3	75	15	NT
98/AV/289	38.75	0.00	0.00	38.50	0.02	0.28	23.24	0.14	100.9	75	15	NT
98/AV/289	38.88	0.02	0.00	38.42	0.02	0.29	23.19	0.15	101.0	75	15	NT
98/AV/289	38.87	0.06	0.01	38.63	0.03	0.29	23.28	0.15	101.3	75	15	NT
C97 1103	38.06	0.03	0.00	37.77	0.01	0.28	23.83	0.26	100.2	74	109	NT
C97 1103	39.11	0.01	0.01	38.11	0.03	0.30	23.66	0.26	101.5	74	109	NT
C97 1103	38.62	0.00	0.00	37.92	0.25	0.29	23.24	0.26	100.6	74	109	NT
C97 1103	39.15	0.03	0.00	38.10	0.02	0.29	23.78	0.26	101.6	74	109	NT
C97 1103	38.97	0.03	0.00	38.40	0.02	0.28	23.79	0.26	101.8	74	109	NT
C97 1103	39.05	0.01	0.00	38.47	0.01	0.30	23.62	0.26	101.7	74	109	NT
C97 1103	39.27	0.02	0.00	38.24	0.02	0.30	23.74	0.27	101.8	74	109	NT
C97 1103	39.08	0.02	0.00	38.31	0.02	0.29	23.78	0.25	101.7	74	109	NT
C97 1103	39.09	0.00	0.00	38.45	0.02	0.30	23.81	0.23	101.9	74	109	NT
C97 1103	38.79	0.01	0.00	38.38	0.03	0.29	23.70	0.24	101.5	74	109	NT
C97 1103	39.28	0.00	0.00	38.49	0.02	0.29	23.42	0.27	101.8	75	109	NT
C97 1103	39.23	0.00	0.00	38.21	0.01	0.32	23.60	0.25	101.6	74	109	NT
C97 1103	39.07	0.01	0.01	38.58	0.02	0.30	23.23	0.25	101.5	75	109	NT
C97 1103	39.14	0.01	0.00	38.34	0.03	0.30	23.45	0.23	101.5	74	109	NT
C97 1103	39.15	0.02	0.00	38.33	0.02	0.30	23.83	0.25	101.9	74	109	NT
C97 1103	39.40	0.01	0.09	38.08	0.04	0.29	23.51	0.26	101.7	74	109	NT
C97 1103	39.29	0.01	0.01	37.73	0.02	0.27	23.79	0.25	101.4	74	109	NT
C97 1103	39.08	0.01	0.00	38.33	0.02	0.29	23.83	0.27	101.8	74	109	NT
C97 1103	39.15	0.03	0.00	38.74	0.01	0.28	23.27	0.28	101.8	75	109	NT
C97 1103	39.17	0.01	0.00	38.46	0.01	0.29	23.58	0.26	101.8	74	109	NT
C97 1103	39.24	0.02	0.00	38.45	0.01	0.30	23.68	0.26	101.9	74	109	NT
C97 1103	39.15	0.04	0.00	38.31	0.01	0.29	23.72	0.26	101.8	74	109	NT
C97 1103	38.99	0.05	0.00	38.14	0.01	0.29	23.72	0.27	101.5	74	109	NT
C97 1103	39.04	0.00	0.00	38.10	0.02	0.29	23.57	0.26	101.3	74	109	NT
C97 1103	38.98	0.00	0.00	38.38	0.02	0.28	23.53	0.28	101.5	74	109	NT
C97 1103	39.29	0.00	0.00	38.71	0.00	0.28	23.43	0.27	102.0	75	109	NT
C97 1103	39.06	0.01	0.00	38.30	0.01	0.29	23.44	0.27	101.4	74	109	NT
C97 1103	39.29	0.00	0.00	38.33	0.02	0.27	23.60	0.25	101.8	74	109	NT
C97 1103	39.33	0.01	0.00	38.47	0.02	0.30	23.74	0.26	102.1	74	109	NT
C97 1103	39.32	0.00	0.00	38.45	0.02	0.28	23.77	0.24	102.1	74	109	NT
C97 1103	38.93	0.00	0.00	38.24	0.03	0.30	23.56	0.24	101.3	74	109	NT
C97 1103	39.40	0.02	0.00	38.56	0.01	0.29	23.57	0.23	102.1	74	109	NT
C97 1103	39.14	0.00	0.00	38.26	0.02	0.32	23.54	0.22	101.5	74	109	NT
C97 1086	38.22	0.00	1.36	35.59	0.04	0.29	25.06	0.18	100.7	72	136.3	VT
C97 1086	38.79	0.00	0.00	36.34	0.02	0.26	25.22	0.19	100.8	72	136.3	VT
C97 1086	38.53	0.00	0.19	36.03	0.01	0.29	25.50	0.19	100.7	72	136.3	VT

TS number	SiO_2	TiO_2	Al_2O_3	MgO	CaO	MnO	FeO	NiO	Total	Fo #	Depth	Rock
C97 1086	38.80	0.00	0.00	36.57	0.01	0.28	25.42	0.19	101.3	72	136.3	VT
C97 1086	38.60	0.00	0.00	36.41	0.02	0.29	25.61	0.19	101.1	72	136.3	VT
C97 1086	38.89	0.00	0.01	36.77	0.01	0.28	25.44	0.20	101.6	72	136.3	VT
C97 1086	39.05	0.01	0.00	36.59	0.01	0.29	25.57	0.21	101.7	72	136.3	VT
C97 1086	38.61	0.00	0.00	36.52	0.01	0.27	25.55	0.20	101.2	72	136.3	VT
C97 1086	38.89	0.00	0.00	36.65	0.02	0.26	25.40	0.21	101.4	72	136.3	VT
C97 1086	38.79	0.00	0.01	36.55	0.01	0.28	25.63	0.20	101.5	72	136.3	VT
C97 1086	38.45	0.00	0.00	36.66	0.01	0.29	25.44	0.20	101.1	72	136.3	VT
C97 1086	38.90	0.00	0.00	36.51	0.02	0.29	25.40	0.19	101.3	72	136.3	VT
C97 1086	38.74	0.02	0.00	36.74	0.06	0.26	25.37	0.19	101.4	72	136.3	VT
C97 1086	38.62	0.01	0.00	36.33	0.00	0.28	25.62	0.18	101.0	72	136.3	VT
C97 1086	38.47	0.01	0.01	35.89	0.02	0.29	25.30	0.18	100.2	72	136.3	VT
C97 1086	38.89	0.02	0.00	36.74	0.02	0.29	25.49	0.18	101.6	72	136.3	VT
C97 1086	38.92	0.00	0.00	36.68	0.01	0.28	25.37	0.19	101.5	72	136.3	VT
C97 1086	39.05	0.02	0.00	36.98	0.02	0.29	25.44	0.19	102.0	72	136.3	VT
C97 1086	38.84	0.02	0.00	36.71	0.01	0.27	25.53	0.18	101.6	72	136.3	VT
C97 1086	38.74	0.00	0.01	36.90	0.00	0.29	25.32	0.19	101.5	72	136.3	VT
C97 1086	38.60	0.00	0.00	37.08	0.00	0.28	25.35	0.17	101.5	72	136.3	VT
C97 1086	38.79	0.00	0.00	36.58	0.01	0.28	25.45	0.17	101.3	72	136.3	VT
C97 1086	39.08	0.01	0.00	36.78	0.01	0.28	25.40	0.19	101.8	72	136.3	VT
C97 1086	38.93	0.01	0.00	36.76	0.00	0.27	25.46	0.19	101.6	72	136.3	VT
C97 1086	38.75	0.00	0.01	36.49	0.01	0.29	25.51	0.19	101.2	72	136.3	VT
C97 1086	38.86	0.02	0.01	36.65	0.01	0.29	25.45	0.18	101.5	72	136.3	VT
C97 1086	38.64	0.00	0.00	36.56	0.00	0.27	25.37	0.20	101.0	72	136.3	VT
C97 1086	38.67	0.00	0.05	36.57	0.02	0.29	25.43	0.19	101.2	72	136.3	VT
C97 1086	38.82	0.01	0.00	36.71	0.01	0.27	25.45	0.19	101.4	72	136.3	VT
C97 1086	38.66	0.00	0.00	36.20	0.01	0.28	25.70	0.17	101.0	72	136.3	VT
C97 1086	38.83	0.01	0.00	36.32	0.01	0.28	25.78	0.18	101.4	72	136.3	VT
C97 1086	38.73	0.00	0.00	36.03	0.01	0.29	25.75	0.18	101.0	71	136.3	VT
C97 1086	38.70	0.00	0.00	36.11	0.03	0.28	25.71	0.19	101.0	71	136.3	VT
C97 1086	38.60	0.01	0.01	36.46	0.01	0.27	25.56	0.18	101.1	72	136.3	VT
C97 1086	38.71	0.00	0.00	36.63	0.00	0.28	25.40	0.18	101.2	72	136.3	VT
C97 1086	38.99	0.00	0.02	36.95	0.00	0.28	25.32	0.19	101.7	72	136.3	VT
C97 1086	38.86	0.00	0.01	36.65	0.02	0.28	25.52	0.19	101.5	72	136.3	VT
C97 1086	38.95	0.00	0.00	36.93	0.01	0.29	25.27	0.17	101.6	72	136.3	VT
C97 1086	38.80	0.00	0.01	36.70	0.00	0.28	25.64	0.20	101.6	72	136.3	VT
C97 1086	38.70	0.01	0.00	36.58	0.01	0.29	25.64	0.19	101.4	72	136.3	VT
C97 1086	39.08	0.00	0.00	36.81	0.01	0.29	25.66	0.19	102.0	72	136.3	VT
C97 1086	38.73	0.01	0.00	35.23	0.07	0.24	23.84	0.18	98.3	72	136.3	VT
C97 1086	38.82	0.00	0.00	36.89	0.01	0.27	25.42	0.18	101.6	72	136.3	VT
C97 1086	38.89	0.01	0.00	36.96	0.02	0.28	25.37	0.16	101.7	72	136.3	VT
C97 1086	39.14	0.00	0.00	37.07	0.00	0.29	25.32	0.17	102.0	72	136.3	VT
C97 1086	39.04	0.00	0.00	37.00	0.02	0.29	25.43	0.19	102.0	72	136.3	VT
C97 1086	39.22	0.01	0.00	36.94	0.02	0.29	25.40	0.18	102.0	72	136.3	VT
C97 1087	38.08	0.00	0.00	35.88	0.01	0.25	26.33	0.11	100.6	71	143	VT
C97 1087	37.84	0.00	0.00	36.48	0.01	0.27	25.85	0.11	100.6	72	143	VT
C97 1087	38.30	0.00	0.01	36.48	0.00	0.27	25.57	0.10	100.7	72	143	VT
C97 1087	38.06	0.00	0.01	36.32	0.02	0.27	25.79	0.10	100.6	72	143	VT
C97 1087	38.45	0.00	0.00	36.05	0.01	0.26	25.99	0.10	100.8	71	143	VT
C97 1087	38.56	0.01	0.00	36.59	0.01	0.27	26.15	0.09	101.7	71	143	VT
C97 1087	38.75	0.01	0.00	36.40	0.02	0.27	25.76	0.10	101.3	72	143	VT
C97 1087	38.51	0.00	0.00	35.93	0.01	0.28	26.46	0.11	101.3	71	143	VT
C97 1087	38.78	0.01	0.00	36.93	0.02	0.25	25.38	0.09	101.5	72	143	VT
C97 1087	38.80	0.00	0.01	36.71	0.04	0.26	25.71	0.09	101.6	72	143	VT

TS number	SiO_2	TiO_2	Al_2O_3	MgO	CaO	MnO	FeO	NiO	Total	Fo #	Depth	Rock
C97 1087	38.61	0.00	0.00	36.27	0.03	0.26	26.04	0.09	101.3	71	143	VT
C97 1087	38.49	0.00	0.00	36.40	0.01	0.28	25.96	0.10	101.2	71	143	VT
C97 1087	38.59	0.02	0.01	36.40	0.02	0.26	25.80	0.09	101.2	72	143	VT
C97 1087	38.70	0.00	0.00	36.61	0.01	0.28	25.76	0.09	101.5	72	143	VT
C97 1087	38.65	0.00	0.00	36.71	0.01	0.28	25.78	0.09	101.5	72	143	VT
C97 1087	37.44	0.01	0.02	35.29	0.00	0.26	26.39	0.10	99.5	70	143	VT
C97 1087	38.42	0.00	0.00	36.03	0.02	0.26	26.46	0.11	101.3	71	143	VT
C97 1087	41.28	0.00	0.40	37.14	0.01	0.25	23.86	0.11	103.1	74	143	VT
C97 1087	38.75	0.01	0.00	36.53	0.01	0.26	25.47	0.09	101.1	72	143	VT
C97 1088	38.96	0.00	0.00	37.54	0.01	0.30	24.62	0.11	101.5	73	143.5	VT
C97 1088	39.17	0.01	0.00	37.54	0.03	0.29	24.83	0.10	102.0	73	143.5	VT
C97 1088	38.92	0.00	0.03	37.60	0.01	0.31	24.75	0.09	101.7	73	143.5	VT
C97 1088	38.94	0.00	0.00	37.73	0.03	0.30	24.67	0.11	101.8	73	143.5	VT
C97 1088	38.12	0.00	0.00	36.81	0.02	0.29	24.80	0.09	100.1	73	143.5	VT
C97 1088	38.84	0.01	0.01	37.26	0.01	0.29	24.82	0.11	101.3	73	143.5	VT
C97 1088	38.97	0.00	0.01	37.26	0.03	0.29	24.87	0.10	101.5	73	143.5	VT
C97 1088	38.67	0.00	0.00	37.63	0.03	0.28	24.59	0.10	101.3	73	143.5	VT
C97 1088	38.65	0.00	0.00	37.49	0.01	0.28	24.86	0.11	101.4	73	143.5	VT
C97 1088	39.03	0.01	0.00	37.46	0.04	0.27	25.13	0.10	102.0	73	143.5	VT
C97 1088	39.20	0.00	0.00	37.73	0.02	0.29	25.16	0.10	102.5	73	143.5	VT
C97 1088	39.00	0.00	0.01	37.46	0.02	0.31	25.18	0.10	102.1	73	143.5	VT
C97 1088	38.91	0.07	0.03	37.51	0.03	0.30	25.31	0.09	102.2	73	143.5	VT
C97 1088	39.18	0.00	0.00	37.58	0.04	0.31	25.30	0.10	102.5	73	143.5	VT
C97 1088	38.83	0.03	0.01	37.45	0.00	0.30	25.24	0.11	102.0	73	143.5	VT
C97 1088	38.76	0.00	0.00	37.54	0.02	0.30	25.40	0.11	102.1	72	143.5	VT
C97 1088	39.04	0.00	0.00	37.38	0.01	0.27	25.14	0.10	101.9	73	143.5	VT
C97 1088	38.97	0.00	0.00	37.76	0.02	0.28	24.79	0.09	101.9	73	143.5	VT
C97 1089	38.51	0.00	0.05	35.64	0.04	0.31	26.42	0.18	101.2	71	156.5	VT
C97 1089	39.21	0.01	0.01	35.97	0.02	0.30	26.64	0.18	102.3	71	156.5	VT
C97 1089	38.77	0.00	0.00	36.01	0.03	0.31	26.55	0.19	101.9	71	156.5	VT
C97 1089	38.89	0.02	0.00	35.79	0.05	0.30	26.88	0.20	102.1	70	156.5	VT
C97 1089	38.87	0.02	0.01	35.77	0.02	0.31	26.69	0.19	101.9	70	156.5	VT
C97 1089	38.96	0.00	0.01	36.05	0.02	0.32	27.03	0.19	102.6	70	156.5	VT
C97 1089	38.86	0.00	0.00	35.84	0.02	0.30	27.19	0.19	102.4	70	156.5	VT
C97 1089	38.94	0.00	0.00	35.78	0.04	0.33	27.18	0.20	102.5	70	156.5	VT
C97 1089	39.38	0.00	0.02	36.64	0.02	0.30	26.03	0.19	102.6	72	156.5	VT
C97 1089	39.24	0.01	0.11	36.64	0.02	0.30	26.06	0.20	102.6	71	156.5	VT
C97 1089	39.19	0.00	0.00	36.47	0.02	0.31	26.10	0.20	102.3	71	156.5	VT
C97 1089	39.31	0.00	0.00	36.38	0.03	0.30	25.89	0.20	102.1	71	156.5	VT
C97 1089	39.50	0.00	0.00	36.51	0.02	0.30	26.07	0.19	102.6	71	156.5	VT
C97 1089	39.27	0.00	0.00	36.56	0.03	0.28	25.78	0.19	102.1	72	156.5	VT
C97 1089	39.40	0.00	0.00	36.57	0.02	0.30	25.83	0.19	102.3	72	156.5	VT
C97 1089	39.09	0.00	0.01	35.42	0.02	0.30	27.51	0.20	102.5	70	156.5	VT
C97 1089	39.17	0.01	0.00	35.69	0.01	0.32	27.85	0.19	103.2	70	156.5	VT
C97 1089	0.20	0.00	0.02	0.04	52.00	0.02	0.06	0.00	52.3	63	156.5	VT
C97 1089	39.14	0.01	0.01	36.38	0.00	0.32	26.69	0.20	102.7	71	156.5	VT
C97 1089	39.12	0.02	0.03	36.38	0.02	0.30	26.77	0.19	102.8	71	156.5	VT
C97 1089	39.00	0.00	0.00	36.57	0.02	0.33	26.43	0.21	102.6	71	156.5	VT
C97 1089	37.73	0.01	0.01	34.14	0.02	0.28	24.83	0.18	97.2	71	156.5	VT
C97 1089	39.22	0.00	0.00	36.43	0.00	0.31	26.44	0.21	102.6	71	156.5	VT
C97 1089	39.12	0.00	0.00	36.44	0.01	0.34	26.66	0.20	102.8	71	156.5	VT
C97 1089	39.12	0.01	0.00	36.85	0.03	0.31	26.26	0.20	102.8	71	156.5	VT
C97 1089	39.18	0.00	0.00	36.78	0.03	0.30	26.31	0.19	102.8	71	156.5	VT
C97 1089	39.22	0.00	0.01	37.01	0.02	0.31	26.20	0.19	103.0	72	156.5	VT

TS number	SiO_2	TiO_2	Al_2O_3	MgO	CaO	MnO	FeO	NiO	Total	Fo #	Depth	Rock
C97 1089	39.12	0.00	0.00	36.99	0.01	0.31	25.96	0.18	102.6	72	156.5	VT
C97 1089	39.49	0.01	0.01	36.93	0.01	0.32	26.02	0.18	103.0	72	156.5	VT
C97 1089	39.49	0.00	0.00	37.11	0.02	0.30	26.03	0.20	103.2	72	156.5	VT
C97 1089	39.35	0.00	0.00	37.30	0.01	0.30	25.81	0.19	103.0	72	156.5	VT
C97 1090	38.62	0.01	0.00	36.15	0.05	0.34	25.41	0.14	100.7	72	167	VT
C97 1090	38.37	0.01	0.00	36.22	0.04	0.31	25.55	0.15	100.6	72	167	VT
C97 1090	38.68	0.00	0.00	36.50	0.05	0.30	25.32	0.13	101.0	72	167	VT
C97 1090	38.52	0.00	0.00	36.45	0.26	0.31	25.13	0.14	100.8	72	167	VT
C97 1090	38.63	0.00	0.00	36.32	0.02	0.33	25.29	0.16	100.7	72	167	VT
C97 1090	38.59	0.01	0.00	36.64	0.04	0.32	25.26	0.14	101.0	72	167	VT
C97 1090	38.20	0.01	0.00	36.31	0.04	0.31	25.17	0.15	100.2	72	167	VT
C97 1090	38.54	0.00	0.00	36.73	0.04	0.32	25.11	0.14	100.9	72	167	VT
C97 1090	38.67	0.03	0.01	36.76	0.03	0.30	25.47	0.14	101.4	72	167	VT
C97 1090	39.86	0.01	0.00	38.44	0.02	0.30	24.43	0.15	103.2	74	167	VT
C97 1090	38.73	0.00	0.00	36.54	0.02	0.32	25.67	0.15	101.4	72	167	VT
C97 1090	38.91	0.01	0.00	36.45	0.02	0.32	25.68	0.13	101.5	72	167	VT
C97 1090	38.62	0.00	0.00	36.52	0.13	0.30	25.69	0.17	101.4	72	167	VT
C97 1090	38.49	0.00	0.01	36.39	0.01	0.31	25.81	0.15	101.2	72	167	VT
C97 1090	38.61	0.01	0.01	36.20	0.02	0.31	25.89	0.16	101.2	71	167	VT
C97 1090	38.96	0.01	0.00	36.27	0.02	0.31	26.04	0.15	101.8	71	167	VT
C97 1090	38.58	0.04	0.00	36.17	0.02	0.31	25.81	0.16	101.1	71	167	VT
C97 1090	38.88	0.00	0.00	36.28	0.03	0.30	26.35	0.14	102.0	71	167	VT
C97 1090	38.65	0.00	0.00	36.23	0.02	0.32	26.18	0.15	101.6	71	167	VT
C97 1090	38.93	0.01	0.00	36.53	0.03	0.32	26.00	0.17	102.0	71	167	VT
C97 1090	38.80	0.00	0.00	36.40	0.02	0.31	25.61	0.15	101.3	72	167	VT
C97 1090	38.75	0.00	0.00	36.63	0.01	0.31	25.33	0.16	101.2	72	167	VT
C97 1090	39.16	0.00	0.00	36.76	0.02	0.30	25.63	0.15	102.0	72	167	VT
C97 1090	38.98	0.01	0.00	37.03	0.02	0.31	25.68	0.16	102.2	72	167	VT
C97 1090	38.81	0.01	0.00	36.80	0.01	0.32	25.73	0.16	101.8	72	167	VT
C97 1090	38.89	0.00	0.00	36.72	0.02	0.31	25.50	0.16	101.6	72	167	VT
C97 1090	38.90	0.00	0.00	37.14	0.01	0.31	24.86	0.15	101.4	73	167	VT
C97 1090	39.27	0.00	0.00	37.24	0.02	0.30	24.73	0.16	101.7	73	167	VT
C97 1090	39.26	0.00	0.00	37.08	0.02	0.30	24.69	0.15	101.5	73	167	VT
C97 1090	38.88	0.00	0.00	36.85	0.03	0.30	24.95	0.17	101.2	72	167	VT
C97 1090	38.84	0.04	0.02	36.71	0.02	0.30	25.00	0.17	101.1	72	167	VT
C97 1090	38.63	0.00	0.00	36.08	0.02	0.31	26.32	0.16	101.5	71	167	VT
C97 1090	39.00	0.00	0.00	36.69	0.02	0.31	25.84	0.16	102.0	72	167	VT
C97 1090	39.02	0.00	0.00	36.50	0.02	0.31	25.77	0.16	101.8	72	167	VT
C97 1090	38.97	0.01	0.00	36.41	0.04	0.31	25.77	0.16	101.7	72	167	VT
C97 1090	38.78	0.00	0.00	36.50	0.02	0.32	25.82	0.16	101.6	72	167	VT
C97 1090	38.30	0.01	0.00	36.10	0.01	0.29	25.92	0.15	100.8	71	167	VT
C97 1090	38.83	0.00	0.01	36.48	0.01	0.30	25.92	0.16	101.7	72	167	VT
C97 1090	39.04	0.00	0.00	37.12	0.03	0.28	24.86	0.17	101.5	73	167	VT
C97 1090	38.59	0.00	0.00	36.63	0.01	0.30	25.07	0.16	100.7	72	167	VT
C97 1090	39.12	0.00	0.00	37.19	0.01	0.29	24.80	0.17	101.6	73	167	VT
C97 1090	39.06	0.00	0.00	37.32	0.01	0.29	25.22	0.14	102.0	73	167	VT
C97 1090	39.06	0.02	0.00	36.92	0.02	0.29	25.18	0.16	101.6	72	167	VT
C97 1090	38.97	0.02	0.00	37.15	0.00	0.30	24.85	0.16	101.4	73	167	VT
C97 1090	37.27	0.01	0.00	35.76	0.02	0.31	25.03	0.16	98.6	72	167	VT
C97 1090	39.09	0.00	0.00	36.86	0.02	0.29	25.30	0.17	101.7	72	167	VT
C97 1090	38.75	0.00	0.00	37.13	0.02	0.30	25.25	0.15	101.6	72	167	VT
C97 1090	39.17	0.00	0.00	37.25	0.01	0.31	25.12	0.18	102.0	73	167	VT
C97 1091	38.78	0.01	0.02	36.79	0.03	0.29	24.63	0.14	100.7	73	187	VT
C97 1091	39.17	0.00	0.00	37.06	0.04	0.31	24.64	0.13	101.3	73	187	VT

TS number	SiO_2	TiO_2	Al_2O_3	MgO	CaO	MnO	FeO	NiO	Total	Fo #	Depth	Rock
C97 1091	38.67	0.00	0.04	36.77	0.05	0.32	24.78	0.13	100.7	73	187	VT
C97 1091	39.03	0.00	0.01	37.04	0.02	0.30	24.55	0.13	101.1	73	187	VT
C97 1091	38.54	0.02	0.00	36.62	0.04	0.31	24.43	0.12	100.1	73	187	VT
C97 1091	38.63	0.01	0.00	36.79	0.02	0.32	24.53	0.13	100.4	73	187	VT
C97 1091	38.78	0.01	0.00	36.95	0.03	0.30	24.68	0.14	100.9	73	187	VT
C97 1091	38.53	0.00	0.02	36.63	0.04	0.31	24.74	0.14	100.4	73	187	VT
C97 1091	39.02	0.01	0.00	36.96	0.01	0.31	24.74	0.14	101.2	73	187	VT
C97 1091	39.01	0.00	0.00	36.75	0.01	0.31	24.80	0.13	101.0	73	187	VT
C97 1091	38.95	0.00	0.00	37.03	0.01	0.29	24.85	0.14	101.3	73	187	VT
C97 1091	39.27	0.00	0.00	37.59	0.02	0.29	24.65	0.14	102.0	73	187	VT
C97 1091	39.04	0.00	0.01	37.52	0.02	0.28	24.49	0.14	101.5	73	187	VT
C97 1091	38.72	0.01	0.00	37.52	0.01	0.28	24.40	0.14	101.1	73	187	VT
C97 1091	39.04	0.00	0.00	37.36	0.02	0.29	24.95	0.14	101.8	73	187	VT
C97 1091	37.87	0.00	0.00	35.79	0.02	0.31	24.94	0.12	99.0	72	187	VT
C97 1091	39.01	0.03	0.00	37.34	0.02	0.30	25.00	0.14	101.8	73	187	VT
C97 1091	39.18	0.02	0.00	37.41	0.01	0.31	24.85	0.13	101.9	73	187	VT
C97 1091	39.06	0.00	0.00	37.46	0.02	0.31	24.74	0.14	101.7	73	187	VT
C97 1091	38.42	0.02	0.00	36.40	0.02	0.30	24.69	0.13	100.0	72	187	VT
C97 1091	39.01	0.03	0.00	37.01	0.02	0.32	24.89	0.13	101.4	73	187	VT
C97 1091	38.97	0.01	0.00	37.01	0.02	0.31	25.10	0.13	101.5	72	187	VT
C97 1091	39.09	0.01	0.00	37.14	0.02	0.32	25.28	0.12	102.0	72	187	VT
C97 1091	39.08	0.00	0.00	37.11	0.01	0.30	25.19	0.13	101.8	72	187	VT
C97 1091	39.24	0.00	0.00	37.15	0.01	0.32	25.16	0.13	102.0	72	187	VT
C97 1091	38.86	0.01	0.00	36.79	0.02	0.31	25.37	0.12	101.5	72	187	VT
C97 1091	38.74	0.02	0.00	36.70	0.03	0.32	25.42	0.13	101.4	72	187	VT
C97 1091	38.76	0.01	0.00	36.90	0.03	0.31	25.37	0.13	101.5	72	187	VT
C97 1091	38.74	0.03	0.00	36.50	0.02	0.33	25.73	0.13	101.5	72	187	VT
C97 1091	39.03	0.10	0.02	36.52	0.03	0.32	25.57	0.15	101.7	72	187	VT
C97 1091	38.60	0.01	0.01	36.38	0.02	0.29	25.61	0.15	101.1	72	187	VT
C97 1091	38.71	0.00	0.00	36.40	0.02	0.34	25.50	0.14	101.1	72	187	VT
C97 1091	38.78	0.00	0.01	36.18	0.03	0.32	26.07	0.13	101.5	71	187	VT
C97 1091	38.70	0.00	0.00	36.05	0.02	0.31	26.25	0.13	101.4	71	187	VT
C97 1091	38.87	0.00	0.00	36.85	0.02	0.30	25.01	0.14	101.2	72	187	VT
C97 1091	38.91	0.00	0.01	36.63	0.01	0.33	25.04	0.14	101.1	72	187	VT
C97 1091	39.00	0.01	0.00	37.23	0.01	0.29	24.86	0.15	101.6	73	187	VT
C97 1091	38.90	0.01	0.01	37.19	0.01	0.31	25.03	0.13	101.6	73	187	VT
C97 1091	38.91	0.01	0.01	37.06	0.01	0.29	24.85	0.13	101.3	73	187	VT
C97 1091	39.04	0.01	0.00	37.01	0.02	0.30	25.10	0.14	101.6	72	187	VT
C97 1091	39.09	0.01	0.00	37.16	0.03	0.31	25.13	0.13	101.9	73	187	VT
C97 1091	38.98	0.00	0.00	37.05	0.02	0.31	25.14	0.13	101.6	72	187	VT
C97 1091	39.01	0.03	0.00	37.10	0.01	0.31	25.06	0.14	101.6	73	187	VT
C97 1091	39.03	0.00	0.00	37.08	0.01	0.31	25.21	0.14	101.8	72	187	VT
C97 1091	39.25	0.00	0.00	37.05	0.01	0.33	25.15	0.14	101.9	72	187	VT
C97 1091	38.99	0.03	0.00	37.10	0.02	0.31	25.21	0.14	101.8	72	187	VT
C97 1091	39.17	0.00	0.00	37.02	0.02	0.30	25.23	0.14	101.9	72	187	VT
C97 1091	39.06	0.00	0.00	36.95	0.02	0.31	25.32	0.13	101.8	72	187	VT
C97 1091	38.26	0.00	0.00	34.89	0.02	0.29	25.81	0.15	99.4	71	187	VT
C97 1091	38.79	0.06	0.00	36.88	0.02	0.31	25.41	0.14	101.6	72	187	VT
C97 1091	38.91	0.01	0.00	37.01	0.02	0.32	25.51	0.14	101.9	72	187	VT
C97 1091	38.81	0.01	0.00	37.17	0.03	0.31	25.20	0.15	101.7	72	187	VT
C97 1091	38.20	0.00	0.00	36.17	0.02	0.29	24.59	0.14	99.4	72	187	VT
C97 1091	38.46	0.00	0.00	36.10	0.00	0.33	26.21	0.14	101.2	71	187	VT
C97 1091	38.34	0.01	0.00	35.00	0.03	0.31	25.75	0.13	99.6	71	187	VT
C97 1091	38.97	0.00	0.01	36.90	0.02	0.32	25.63	0.15	102.0	72	187	VT

TS number	SiO_2	TiO_2	Al_2O_3	MgO	CaO	MnO	FeO	NiO	Total	Fo #	Depth	Rock
C97 1091	39.16	0.00	0.01	37.08	0.06	0.32	24.91	0.15	101.7	73	187	VT
C97 1091	38.97	0.02	0.00	37.15	0.01	0.32	24.94	0.14	101.5	73	187	VT
C97 1091	38.91	0.05	0.00	37.13	0.02	0.32	25.10	0.16	101.7	72	187	VT
C97 1091	37.46	0.00	0.00	35.53	0.03	0.29	24.10	0.12	97.5	72	187	VT
C97 1078	39.00	0.00	0.00	37.39	0.02	0.25	25.02	0.19	101.9	73	192.5	VT
C97 1078	39.06	0.00	0.01	37.22	0.02	0.25	25.31	0.20	102.1	72	192.5	VT
C97 1078	39.35	0.00	0.00	37.82	0.01	0.26	24.50	0.21	102.1	73	192.5	VT
C97 1078	39.27	0.00	0.01	37.59	0.01	0.26	24.93	0.22	102.3	73	192.5	VT
C97 1078	39.07	0.02	0.00	37.17	0.01	0.26	25.18	0.21	101.9	72	192.5	VT
C97 1078	39.16	0.02	0.00	37.96	0.00	0.27	23.95	0.23	101.6	74	192.5	VT
C97 1078	39.36	0.00	0.00	37.56	0.01	0.27	24.92	0.22	102.3	73	192.5	VT
C97 1078	39.19	0.01	0.00	37.36	0.00	0.28	24.95	0.21	102.0	73	192.5	VT
C97 1078	39.50	0.01	0.00	37.39	0.02	0.27	24.80	0.21	102.2	73	192.5	VT
C97 1078	39.22	0.00	0.00	37.49	0.01	0.25	25.01	0.20	102.2	73	192.5	VT
C97 1078	39.06	0.02	0.01	36.94	0.00	0.26	25.48	0.21	102.0	72	192.5	VT
C97 1078	39.14	0.00	0.00	36.97	0.00	0.24	25.18	0.20	101.7	72	192.5	VT
C97 1078	38.98	0.01	0.00	36.73	0.01	0.25	25.47	0.21	101.7	72	192.5	VT
C97 1078	39.07	0.00	0.00	37.25	0.02	0.26	25.19	0.20	102.0	73	192.5	VT
C97 1078	39.23	0.01	0.00	37.04	0.03	0.26	25.33	0.20	102.1	72	192.5	VT
C97 1078	39.07	0.00	0.00	36.97	0.02	0.26	25.14	0.19	101.7	72	192.5	VT
C97 1078	39.30	0.00	0.00	37.33	0.02	0.26	24.59	0.19	101.7	73	192.5	VT
C97 1078	39.15	0.00	0.00	37.53	0.01	0.27	24.54	0.20	101.7	73	192.5	VT
C97 1078	39.09	0.00	0.02	37.02	0.02	0.26	25.16	0.19	101.8	72	192.5	VT
C97 1078	38.96	0.03	0.01	37.08	0.01	0.26	25.23	0.20	101.8	72	192.5	VT
C97 1079	38.63	0.02	0.00	36.34	0.02	0.31	25.16	0.19	100.7	72	206.5	VT
C97 1079	38.69	0.00	0.00	36.45	0.02	0.32	25.14	0.19	100.8	72	206.5	VT
C97 1079	38.62	0.00	0.00	36.57	0.02	0.33	25.14	0.18	100.9	72	206.5	VT
C97 1079	38.73	0.00	0.00	36.38	0.03	0.31	25.18	0.18	100.8	72	206.5	VT
C97 1079	38.83	0.00	0.00	36.31	0.00	0.32	25.59	0.18	101.2	72	206.5	VT
C97 1079	38.79	0.00	0.00	36.50	0.02	0.33	25.58	0.19	101.4	72	206.5	VT
C97 1079	38.76	0.11	0.00	36.53	0.01	0.34	25.61	0.17	101.5	72	206.5	VT
C97 1079	38.76	0.01	0.00	36.44	0.02	0.35	25.64	0.17	101.4	72	206.5	VT
C97 1079	38.79	0.00	0.01	36.65	0.04	0.32	25.44	0.18	101.4	72	206.5	VT
C97 1079	38.64	0.01	0.00	36.50	0.03	0.33	25.49	0.18	101.2	72	206.5	VT
C97 1079	38.87	0.00	0.00	36.55	0.01	0.32	25.30	0.19	101.2	72	206.5	VT
C97 1079	38.64	0.00	0.00	36.02	0.02	0.32	25.61	0.14	100.8	71	206.5	VT
C97 1079	38.69	0.00	0.01	36.68	0.01	0.31	25.18	0.19	101.1	72	206.5	VT
C97 1079	38.65	0.01	0.00	36.44	0.02	0.34	25.62	0.16	101.3	72	206.5	VT
C97 1079	38.84	0.00	0.00	36.63	0.03	0.33	25.62	0.19	101.6	72	206.5	VT
C97 1079	38.89	0.12	0.72	35.81	0.00	0.32	25.03	0.18	101.1	72	206.5	VT
C97 1079	38.69	0.01	0.00	36.56	0.02	0.31	25.69	0.18	101.5	72	206.5	VT
C97 1079	38.94	0.01	0.00	36.71	0.02	0.33	25.48	0.18	101.7	72	206.5	VT
C97 1079	38.77	0.01	0.00	36.62	0.02	0.32	25.49	0.19	101.4	72	206.5	VT
C97 1080	38.89	0.00	0.00	37.35	0.02	0.33	24.92	0.19	101.7	73	211.5	VT
C97 1080	38.89	0.00	0.00	37.47	0.02	0.29	24.86	0.18	101.7	73	211.5	VT
C97 1080	39.30	0.01	0.01	37.69	0.02	0.30	24.78	0.17	102.3	73	211.5	VT
C97 1080	38.92	0.00	0.00	37.77	0.01	0.30	24.91	0.19	102.1	73	211.5	VT
C97 1080	39.23	0.02	0.00	38.07	0.01	0.31	24.95	0.17	102.8	73	211.5	VT
C97 1080	39.00	0.05	0.00	37.95	0.01	0.29	24.58	0.16	102.0	73	211.5	VT
C97 1080	39.02	0.00	0.00	37.84	0.16	0.30	24.37	0.16	101.9	73	211.5	VT
C97 1080	39.35	0.03	0.00	37.73	0.01	0.29	24.90	0.17	102.5	73	211.5	VT
C97 1080	39.24	0.00	0.00	37.89	0.01	0.29	24.61	0.17	102.2	73	211.5	VT
C97 1080	39.33	0.06	0.01	37.87	0.01	0.30	24.82	0.17	102.6	73	211.5	VT
C97 1080	38.94	0.04	0.00	37.93	0.02	0.31	24.65	0.16	102.0	73	211.5	VT

TS number	SiO_2	TiO_2	Al_2O_3	MgO	CaO	MnO	FeO	NiO	Total	Fo #	Depth	Rock
C97 1080	39.24	0.00	0.00	37.72	0.03	0.29	24.78	0.17	102.2	73	211.5	VT
C97 1081	38.38	0.00	0.00	36.51	0.02	0.33	25.77	0.16	101.2	72	224	VT
C97 1081	38.74	0.00	0.01	36.91	0.02	0.32	25.65	0.16	101.8	72	224	VT
C97 1081	38.76	0.01	0.00	36.87	0.02	0.32	25.88	0.17	102.0	72	224	VT
C97 1081	38.38	0.00	0.00	36.72	0.01	0.34	25.86	0.17	101.5	72	224	VT
C97 1081	38.53	0.02	0.00	36.82	0.02	0.32	26.13	0.16	102.0	72	224	VT
C97 1081	38.89	0.01	0.01	36.99	0.03	0.33	26.02	0.17	102.4	72	224	VT
C97 1081	38.89	0.00	0.00	36.76	0.01	0.31	25.70	0.16	101.8	72	224	VT
C97 1081	38.59	0.00	0.00	36.74	0.00	0.33	26.15	0.17	102.0	71	224	VT
C97 1081	38.37	0.01	0.00	36.70	0.01	0.31	25.91	0.16	101.5	72	224	VT
C97 1081	38.98	0.00	0.00	37.03	0.02	0.30	25.87	0.15	102.4	72	224	VT
C97 1081	38.76	0.00	0.02	37.07	0.02	0.32	25.73	0.16	102.1	72	224	VT
C97 1081	38.71	0.00	0.00	36.70	0.01	0.32	26.00	0.17	101.9	72	224	VT
C97 1082	38.80	0.00	0.00	37.86	0.02	0.30	24.64	0.13	101.7	73	236.8	VT
C97 1082	38.57	0.01	0.00	37.60	0.03	0.29	24.46	0.12	101.1	73	236.8	VT
C97 1082	39.12	0.00	0.00	37.77	0.02	0.31	24.59	0.12	101.9	73	236.8	VT
C97 1082	39.10	0.00	0.01	37.96	0.02	0.30	24.45	0.13	102.0	73	236.8	VT
C97 1082	39.14	0.01	0.01	37.91	0.02	0.30	24.47	0.14	102.0	73	236.8	VT
C97 1082	39.13	0.03	0.01	38.01	0.01	0.28	24.47	0.13	102.1	73	236.8	VT
C97 1082	39.21	0.02	0.00	38.23	0.02	0.30	24.38	0.13	102.3	74	236.8	VT
C97 1082	38.98	0.00	0.00	37.94	0.02	0.31	24.44	0.12	101.8	73	236.8	VT
C97 1082	39.17	0.02	0.01	37.91	0.03	0.29	24.27	0.13	101.8	74	236.8	VT
C97 1082	38.93	0.00	0.00	37.96	0.03	0.30	24.70	0.13	102.1	73	236.8	VT
C97 1082	39.15	0.01	0.00	37.83	0.02	0.30	24.84	0.14	102.3	73	236.8	VT
C97 1082	39.00	0.01	0.00	37.69	0.02	0.30	24.74	0.12	101.9	73	236.8	VT
C97 1082	38.72	0.02	0.00	37.53	0.03	0.30	24.77	0.11	101.5	73	236.8	VT
C97 1082	38.77	0.00	0.00	37.64	0.02	0.31	24.87	0.13	101.7	73	236.8	VT
C97 1082	39.01	0.00	0.01	37.52	0.02	0.31	24.50	0.12	101.5	73	236.8	VT
C97 1082	38.48	0.05	0.01	37.32	0.01	0.30	25.05	0.12	101.3	73	236.8	VT
C97 1082	38.98	0.00	0.00	37.69	0.03	0.30	24.52	0.12	101.6	73	236.8	VT
C97 1082	39.00	0.04	0.01	37.85	0.02	0.30	24.63	0.13	102.0	73	236.8	VT
C97 1082	38.75	0.03	0.00	37.63	0.03	0.31	25.03	0.12	101.9	73	236.8	VT
C97 1082	38.99	0.01	0.00	37.91	0.03	0.29	24.81	0.13	102.2	73	236.8	VT
C97 1083	39.07	0.02	0.01	36.48	0.05	0.30	25.31	0.18	101.4	72	244	VT
C97 1083	38.98	0.00	0.00	36.67	0.05	0.31	25.32	0.17	101.5	72	244	VT
C97 1083	39.09	0.00	0.00	36.82	0.03	0.32	25.41	0.17	101.8	72	244	VT
C97 1083	38.95	0.02	0.00	36.83	0.04	0.30	25.33	0.18	101.6	72	244	VT
C97 1083	38.88	0.00	0.01	36.49	0.01	0.33	25.63	0.19	101.5	72	244	VT
C97 1083	39.00	0.01	0.01	36.63	0.02	0.32	25.94	0.21	102.1	72	244	VT
C97 1083	38.74	0.00	0.01	36.23	0.01	0.34	26.35	0.20	101.9	71	244	VT
C97 1083	39.01	0.00	0.00	36.27	0.02	0.32	26.19	0.21	102.0	71	244	VT
C97 1083	38.88	0.01	0.00	36.54	0.03	0.33	25.61	0.20	101.6	72	244	VT
C97 1083	38.80	0.00	0.01	36.15	0.02	0.35	26.15	0.18	101.7	71	244	VT
C97 1083	38.95	0.00	0.00	36.51	0.02	0.32	26.19	0.20	102.2	71	244	VT
C97 1083	38.96	0.01	0.00	36.33	0.01	0.33	26.19	0.21	102.0	71	244	VT
C97 1083	38.82	0.00	0.00	36.85	0.02	0.31	25.76	0.21	102.0	72	244	VT
C97 1083	39.18	0.02	0.01	36.69	0.02	0.32	25.72	0.21	102.2	72	244	VT
C97 1083	39.00	0.02	0.00	36.48	0.02	0.33	26.29	0.18	102.3	71	244	VT
C97 1083	38.86	0.00	0.00	36.23	0.02	0.33	26.28	0.21	101.9	71	244	VT
C97 1083	39.03	0.00	0.00	36.33	0.04	0.33	25.66	0.21	101.6	72	244	VT
C97 1083	38.89	0.00	0.00	36.39	0.04	0.32	25.62	0.19	101.4	72	244	VT
C97 1083	39.17	0.02	0.00	36.58	0.02	0.33	26.07	0.18	102.4	71	244	VT
C97 1083	39.26	0.00	0.00	36.35	0.01	0.31	26.17	0.18	102.3	71	244	VT
C97 1083	39.11	0.01	0.00	36.66	0.02	0.34	26.14	0.20	102.5	71	244	VT

TS number	SiO_2	TiO_2	Al_2O_3	MgO	CaO	MnO	FeO	NiO	Total	Fo #	Depth	Rock
C97 1083	39.03	0.00	0.00	36.72	0.02	0.34	26.17	0.19	102.5	71	244	VT
C97 1083	39.08	0.02	0.00	36.50	0.03	0.31	26.00	0.20	102.1	71	244	VT
C97 1084	39.35	0.04	0.00	39.73	0.02	0.25	21.67	0.14	101.2	77	248.7	VT
C97 1084	39.25	0.03	0.00	39.71	0.03	0.24	21.72	0.13	101.1	77	248.7	VT
C97 1084	39.51	0.02	0.00	39.54	0.01	0.26	21.96	0.12	101.4	76	248.7	VT
C97 1084	39.68	0.04	0.01	39.55	0.02	0.24	21.78	0.11	101.4	76	248.7	VT
C97 1084	39.45	0.00	0.01	40.04	0.03	0.23	21.49	0.13	101.4	77	248.7	VT
C97 1084	39.70	0.02	0.04	40.37	0.03	0.26	21.27	0.12	101.8	77	248.7	VT
C97 1084	39.20	0.00	0.00	39.92	0.03	0.25	21.26	0.14	100.8	77	248.7	VT
C97 1084	39.74	0.04	0.01	39.99	0.02	0.25	21.46	0.13	101.6	77	248.7	VT
C97 1084	39.97	0.05	0.01	40.17	0.03	0.26	21.75	0.13	102.4	77	248.7	VT
C97 1084	39.86	0.00	0.01	40.12	0.02	0.27	21.67	0.13	102.1	77	248.7	VT
C97 1084	39.57	0.00	0.00	40.10	0.02	0.26	21.70	0.12	101.8	77	248.7	VT
C97 1084	39.64	0.01	0.01	39.99	0.02	0.25	21.85	0.13	101.9	77	248.7	VT
C97 1084	39.32	0.01	0.00	39.81	0.01	0.27	22.04	0.13	101.6	76	248.7	VT
C97 1084	39.55	0.00	0.00	39.69	0.02	0.27	22.12	0.13	101.8	76	248.7	VT
C97 1084	39.60	0.08	0.00	39.62	0.01	0.27	22.25	0.11	101.9	76	248.7	VT
C97 1084	39.52	0.02	0.00	39.71	0.01	0.27	22.26	0.12	101.9	76	248.7	VT
C97 1084	39.53	0.00	0.00	39.26	0.03	0.27	22.32	0.11	101.5	76	248.7	VT
C97 1084	39.19	0.02	0.01	39.47	0.01	0.27	22.19	0.13	101.3	76	248.7	VT
C97 1084	39.64	0.00	0.02	39.86	0.01	0.26	22.26	0.13	102.2	76	248.7	VT
C97 1084	39.85	0.01	0.01	39.93	0.02	0.26	21.84	0.13	102.0	77	248.7	VT
C97 1105	38.72	0.01	0.02	36.22	0.03	0.31	26.07	0.22	101.6	71	260.6	VT
C97 1105	38.51	0.00	0.00	35.77	0.04	0.32	26.36	0.21	101.2	71	260.6	VT
C97 1105	38.67	0.00	0.02	36.29	0.04	0.31	26.10	0.21	101.6	71	260.6	VT
C97 1105	38.77	0.00	0.00	36.23	0.02	0.29	26.29	0.22	101.8	71	260.6	VT
C97 1105	38.45	0.10	0.00	36.36	0.03	0.31	26.16	0.21	101.6	71	260.6	VT
C97 1105	38.72	0.01	0.00	36.34	0.01	0.31	26.16	0.22	101.8	71	260.6	VT
C97 1105	38.58	0.01	0.00	36.48	0.02	0.32	26.15	0.19	101.7	71	260.6	VT
C97 1105	38.61	0.00	0.00	36.19	0.01	0.33	26.45	0.21	101.8	71	260.6	VT
C97 1105	38.69	0.00	0.00	36.87	0.02	0.31	26.01	0.21	102.1	72	260.6	VT
C97 1105	38.82	0.01	0.00	36.49	0.01	0.32	26.45	0.18	102.3	71	260.6	VT
C97 1105	38.70	0.01	0.02	36.43	0.01	0.35	26.40	0.20	102.1	71	260.6	VT
C97 1105	36.30	0.01	0.00	35.36	0.01	0.33	25.90	0.21	98.1	71	260.6	VT
C97 1105	38.93	0.00	0.00	36.02	0.02	0.31	25.20	0.22	100.7	72	260.6	VT
C97 1105	38.77	0.02	0.00	36.33	0.01	0.32	26.47	0.21	102.1	71	260.6	VT
C97 1105	38.73	0.00	0.00	36.51	0.02	0.31	26.43	0.21	102.2	71	260.6	VT
C97 1105	38.83	0.02	0.00	36.27	0.01	0.30	26.33	0.21	102.0	71	260.6	VT
C97 1105	38.80	0.00	0.00	36.48	0.02	0.33	26.14	0.19	102.0	71	260.6	VT
C97 1105	38.94	0.02	0.00	36.31	0.04	0.32	26.04	0.18	101.9	71	260.6	VT
C97 1105	38.59	0.02	0.00	36.31	0.02	0.32	26.23	0.20	101.7	71	260.6	VT
C97 1105	38.69	0.02	0.00	36.27	0.04	0.31	26.23	0.21	101.8	71	260.6	VT
C97 1105	38.71	0.01	0.02	36.28	0.03	0.34	26.20	0.21	101.8	71	260.6	VT
C97 1105	38.52	0.02	0.00	36.06	0.02	0.33	26.23	0.22	101.4	71	260.6	VT
C97 1105	38.98	0.00	0.12	35.99	0.03	0.33	26.26	0.23	101.9	71	260.6	VT
C97 1105	38.50	0.01	0.14	35.93	0.03	0.33	25.91	0.22	101.1	71	260.6	VT
C97 1105	38.60	0.03	0.00	36.27	0.02	0.30	26.22	0.22	101.7	71	260.6	VT
C97 1105	38.90	0.00	0.01	36.38	0.01	0.33	25.96	0.22	101.8	71	260.6	VT
C97 1105	38.63	0.00	0.00	36.37	0.02	0.31	25.86	0.22	101.4	71	260.6	VT
C97 1105	38.52	0.00	0.04	36.24	0.02	0.32	26.04	0.21	101.4	71	260.6	VT
C97 1105	38.89	0.01	0.00	36.34	0.03	0.32	25.73	0.22	101.5	72	260.6	VT
C97 1105	38.75	0.00	0.00	36.37	0.04	0.30	25.46	0.21	101.1	72	260.6	VT
C97 1085	38.97	0.10	0.00	36.88	0.04	0.33	25.70	0.19	102.2	72	262	VT
C97 1085	39.12	0.00	0.00	36.91	0.02	0.32	25.59	0.19	102.1	72	262	VT

TS number	SiO_2	TiO_2	Al_2O_3	MgO	CaO	MnO	FeO	NiO	Total	Fo #	Depth	Rock
C97 1085	39.11	0.02	0.00	37.00	0.02	0.31	25.60	0.19	102.2	72	262	VT
C97 1085	39.06	0.00	0.00	37.01	0.02	0.31	25.61	0.20	102.2	72	262	VT
C97 1085	39.14	0.00	0.00	36.80	0.02	0.30	25.75	0.18	102.2	72	262	VT
C97 1085	38.93	0.03	0.00	36.97	0.03	0.31	25.53	0.20	102.0	72	262	VT
C97 1085	39.01	0.00	0.00	36.86	0.01	0.33	25.48	0.17	101.9	72	262	VT
C97 1085	39.06	0.00	0.00	36.99	0.00	0.33	25.85	0.18	102.4	72	262	VT
C97 1085	39.13	0.00	0.00	36.80	0.02	0.30	25.72	0.19	102.1	72	262	VT
C97 1085	39.17	0.03	0.01	36.78	0.02	0.30	25.61	0.18	102.1	72	262	VT
C97 1085	39.01	0.00	0.00	36.58	0.02	0.33	26.06	0.17	102.2	71	262	VT
C97 1085	39.09	0.00	0.00	36.59	0.02	0.32	25.97	0.18	102.2	72	262	VT
C97 1085	38.99	0.00	0.01	36.45	0.03	0.33	26.10	0.17	102.1	71	262	VT
C97 1085	39.23	0.03	0.00	36.86	0.02	0.30	25.54	0.17	102.1	72	262	VT
C97 1085	38.91	0.00	0.00	36.70	0.01	0.31	25.81	0.17	101.9	72	262	VT
C97 1085	38.72	0.05	0.00	36.16	0.02	0.33	25.87	0.17	101.3	71	262	VT
C97 1085	38.74	0.01	0.00	36.61	0.01	0.32	25.53	0.17	101.4	72	262	VT
C97 1085	38.86	0.00	0.00	36.99	0.02	0.29	25.32	0.19	101.7	72	262	VT
C97 1085	38.88	0.00	0.00	36.57	0.03	0.29	25.06	0.17	101.0	72	262	VT
C97 1085	38.93	0.00	0.01	36.78	0.02	0.32	25.35	0.17	101.6	72	262	VT
C97 1085	38.93	0.01	0.00	35.87	0.04	0.29	25.96	0.17	101.3	71	262	VT
C97 1085	39.15	0.00	0.00	36.80	0.02	0.33	25.55	0.16	102.0	72	262	VT
C97 1085	39.08	0.00	0.00	36.78	0.03	0.31	25.98	0.16	102.3	72	262	VT
C97 1085	39.08	0.00	0.01	36.84	0.02	0.30	25.95	0.15	102.3	72	262	VT
C97 1085	39.59	0.01	0.02	36.79	0.04	0.29	25.69	0.15	102.6	72	262	VT
C97 1085	39.05	0.00	0.00	36.79	0.02	0.31	25.84	0.15	102.2	72	262	VT
C97 1085	38.89	0.00	0.00	36.50	0.03	0.31	25.96	0.16	101.8	71	262	VT
C97 1085	39.09	0.07	0.00	36.99	0.02	0.30	25.39	0.15	102.0	72	262	VT
C97 1085	39.10	0.00	0.01	36.93	0.01	0.33	25.39	0.15	101.9	72	262	VT
C97 1085	38.93	0.00	0.00	36.86	0.01	0.32	25.01	0.15	101.3	72	262	VT
C97 1085	38.87	0.00	0.01	37.10	0.14	0.32	24.99	0.13	101.5	73	262	VT
C97 1085	39.07	0.01	0.00	36.88	0.01	0.30	25.18	0.14	101.6	72	262	VT
C97 1085	39.06	0.01	0.00	37.24	0.01	0.31	25.39	0.14	102.2	72	262	VT
C97 1085	39.01	0.00	0.00	36.92	0.01	0.32	25.55	0.14	102.0	72	262	VT
C97 1085	39.15	0.02	0.00	37.02	0.03	0.32	25.56	0.15	102.2	72	262	VT
C97 1085	39.20	0.02	0.00	37.33	0.01	0.32	25.27	0.13	102.3	72	262	VT
C97 1085	39.06	0.00	0.00	37.17	0.02	0.32	25.48	0.13	102.2	72	262	VT
C97 1085	39.24	0.00	0.00	37.47	0.03	0.33	25.13	0.15	102.4	73	262	VT
C97 1085	39.38	0.00	0.00	37.25	0.02	0.31	25.65	0.14	102.7	72	262	VT
C97 1085	39.49	0.05	0.00	37.61	0.02	0.30	25.14	0.12	102.7	73	262	VT
C97 1106	38.49	0.00	0.00	36.77	0.02	0.32	24.77	0.16	100.5	73	271.5	VT
C97 1106	38.61	0.00	0.00	37.04	0.03	0.29	24.69	0.18	100.8	73	271.5	VT
C97 1106	38.47	0.00	0.00	36.92	0.01	0.31	24.86	0.16	100.7	73	271.5	VT
C97 1106	38.79	0.00	0.00	37.52	0.01	0.30	24.54	0.17	101.3	73	271.5	VT
C97 1106	38.88	0.02	0.00	37.29	0.02	0.29	24.18	0.16	100.8	73	271.5	VT
C97 1106	38.46	0.02	0.06	37.20	0.01	0.29	24.68	0.15	100.9	73	271.5	VT
C97 1106	38.54	0.02	0.04	37.26	0.01	0.30	24.21	0.17	100.6	73	271.5	VT
C97 1106	38.77	0.02	0.00	37.49	0.02	0.30	24.32	0.16	101.1	73	271.5	VT
C97 1106	38.68	0.00	0.12	37.24	0.01	0.29	24.34	0.15	100.8	73	271.5	VT
C97 1106	38.72	0.14	0.03	37.38	0.02	0.29	24.26	0.15	101.0	73	271.5	VT
C97 1106	38.52	0.01	0.00	37.03	0.01	0.31	25.05	0.16	101.1	72	271.5	VT
C97 1107	37.04	0.04	0.16	35.10	0.02	0.32	26.14	0.11	98.9	71	274	VT
C97 1107	37.94	0.10	0.01	35.70	0.02	0.36	26.36	0.11	100.6	71	274	VT
C97 1107	37.79	0.01	0.00	35.76	0.01	0.34	26.25	0.11	100.3	71	274	VT
C97 1107	38.04	0.02	0.00	35.57	0.03	0.35	27.11	0.11	101.2	70	274	VT
C97 1107	38.83	0.00	0.00	36.99	0.03	0.33	25.25	0.10	101.5	72	274	VT

TS number	SiO_2	TiO_2	Al_2O_3	MgO	CaO	MnO	FeO	NiO	Total	Fo #	Depth	Rock
C97 1107	38.28	0.10	0.02	36.69	0.02	0.31	25.39	0.11	100.9	72	274	VT
C97 1107	38.74	0.08	0.01	36.86	0.02	0.32	25.41	0.11	101.5	72	274	VT
C97 1107	38.29	0.02	0.00	37.08	0.03	0.34	25.53	0.12	101.4	72	274	VT
C97 1107	38.66	0.01	0.01	36.53	0.01	0.33	25.71	0.10	101.4	72	274	VT
C97 1107	37.63	0.02	0.00	36.14	0.06	0.33	25.64	0.10	99.9	72	274	VT
C97 1107	38.55	0.01	0.01	36.84	0.03	0.33	25.70	0.11	101.6	72	274	VT
C97 1107	38.07	0.00	0.01	35.43	0.01	0.35	27.06	0.10	101.0	70	274	VT
C97 1107	37.93	0.00	0.00	35.82	0.01	0.32	27.07	0.10	101.3	70	274	VT
C97 1107	38.79	0.01	0.00	37.19	0.01	0.32	25.45	0.12	101.9	72	274	VT
C97 1107	37.49	0.00	0.02	36.37	0.24	0.31	25.83	0.12	100.4	72	274	VT
C97 1107	38.48	0.01	0.00	36.67	0.00	0.33	25.46	0.10	101.0	72	274	VT
C97 1107	38.59	0.00	0.01	37.07	0.02	0.31	25.48	0.11	101.6	72	274	VT
C97 1107	38.77	0.00	0.00	36.93	0.01	0.33	25.90	0.10	102.0	72	274	VT
C97 1107	37.89	0.01	0.00	36.57	0.04	0.32	25.17	0.11	100.1	72	274	VT
C97 1107	38.25	0.03	0.01	36.55	0.03	0.30	25.38	0.12	100.7	72	274	VT
C97 1107	38.44	0.01	0.02	36.77	0.00	0.31	25.21	0.10	100.9	72	274	VT
C97 1107	38.51	0.00	0.00	36.69	0.03	0.33	25.43	0.11	101.1	72	274	VT
C97 1107	38.26	0.02	0.05	36.77	0.03	0.34	25.42	0.10	101.0	72	274	VT
C97 1107	38.27	0.01	0.00	37.08	0.02	0.33	25.45	0.11	101.3	72	274	VT
C97 1107	37.93	0.01	0.00	36.73	0.00	0.32	25.26	0.12	100.4	72	274	VT
C97 1108	37.82	0.00	0.05	35.98	0.01	0.32	25.16	0.14	99.5	72	280	VT
C97 1108	37.54	0.01	0.00	35.73	0.01	0.32	25.55	0.15	99.3	71	280	VT
C97 1108	38.29	0.02	0.00	35.92	0.01	0.33	26.11	0.14	100.8	71	280	VT
C97 1108	38.15	0.02	0.00	36.05	0.03	0.33	26.03	0.15	100.7	71	280	VT
C97 1108	37.90	0.01	0.00	35.67	0.02	0.33	25.79	0.17	99.9	71	280	VT
C97 1108	37.53	0.00	0.01	35.39	0.02	0.31	25.95	0.17	99.4	71	280	VT
C97 1108	37.48	0.00	0.01	35.06	0.02	0.32	26.04	0.16	99.1	71	280	VT
C97 1108	37.59	0.00	0.00	34.56	0.03	0.32	27.09	0.18	99.8	69	280	VT
C97 1108	37.40	0.00	0.00	34.56	0.03	0.36	26.95	0.17	99.5	70	280	VT
C97 1108	37.39	0.00	0.00	35.50	0.02	0.32	26.37	0.17	99.8	71	280	VT
C97 1108	37.57	0.01	0.00	35.55	0.02	0.32	26.19	0.18	99.8	71	280	VT
C97 1108	37.95	0.00	0.00	35.74	0.02	0.33	26.29	0.17	100.5	71	280	VT
C97 1109	37.00	0.03	0.00	36.53	0.02	0.29	23.52	0.15	97.5	73	283.5	VT
C97 1109	37.09	0.04	0.02	36.79	0.01	0.30	23.71	0.15	98.1	73	283.5	VT
C97 1109	37.26	0.00	0.02	36.36	0.02	0.29	24.02	0.15	98.1	73	283.5	VT
C97 1109	36.52	0.00	0.01	36.36	0.02	0.28	23.85	0.14	97.2	73	283.5	VT
C97 1109	37.26	0.01	0.02	36.47	0.02	0.29	23.72	0.16	97.9	73	283.5	VT
C97 1109	37.85	0.00	0.01	37.54	0.01	0.27	23.94	0.15	99.8	74	283.5	VT
C97 1109	35.88	0.01	0.00	36.84	0.01	0.29	23.87	0.14	97.0	73	283.5	VT
C97 1109	37.87	0.04	0.00	37.11	0.01	0.29	24.26	0.14	99.7	73	283.5	VT
C97 1109	37.72	0.00	0.01	37.18	0.02	0.27	24.17	0.15	99.5	73	283.5	VT
C97 1109	37.58	0.05	0.02	36.96	0.03	0.29	24.24	0.15	99.3	73	283.5	VT
C97 1109	36.14	0.01	0.00	36.79	0.01	0.27	23.70	0.14	97.1	73	283.5	VT
C97 1110	38.75	0.01	0.01	36.50	0.03	0.32	25.77	0.17	101.5	72	290	VT
C97 1110	38.86	0.00	0.00	36.79	0.02	0.31	25.56	0.18	101.7	72	290	VT
C97 1110	38.68	0.02	0.00	37.25	0.01	0.30	25.30	0.16	101.7	72	290	VT
C97 1110	38.65	0.07	0.00	37.21	0.01	0.31	25.37	0.17	101.8	72	290	VT
C97 1110	38.60	0.01	0.00	36.94	0.01	0.31	25.34	0.18	101.4	72	290	VT
C97 1110	38.68	0.00	0.00	37.14	0.00	0.31	25.22	0.18	101.5	72	290	VT
C97 1110	38.72	0.01	0.00	37.21	0.02	0.32	25.10	0.18	101.6	73	290	VT
C97 1110	38.55	0.03	0.00	36.99	0.03	0.31	25.30	0.17	101.4	72	290	VT
C97 1110	38.82	0.01	0.01	37.37	0.02	0.32	25.22	0.17	101.9	73	290	VT
C97 1110	38.48	0.00	0.00	37.20	0.01	0.32	25.23	0.17	101.4	72	290	VT
C97 1110	38.64	0.04	0.02	37.16	0.09	0.31	25.29	0.17	101.7	72	290	VT

TS number	SiO_2	TiO_2	Al_2O_3	MgO	CaO	MnO	FeO	NiO	Total	Fo #	Depth	Rock
C97 1110	38.42	0.04	0.54	36.71	0.00	0.32	25.14	0.17	101.3	72	290	VT
C97 1110	38.56	0.00	0.00	36.83	0.01	0.30	25.22	0.18	101.1	72	290	VT
C97 1110	38.71	0.00	0.00	37.09	0.03	0.31	25.51	0.18	101.8	72	290	VT
C97 1110	38.75	0.00	0.01	36.31	0.01	0.32	26.00	0.17	101.6	71	290	VT
C97 1110	38.51	0.04	0.00	36.86	0.02	0.32	25.59	0.17	101.5	72	290	VT
C97 1110	38.41	0.02	0.00	36.92	0.02	0.32	25.19	0.18	101.0	72	290	VT
98/AV/297	38.42	0.01	0.00	37.98	0.02	0.27	23.01	0.18	99.9	75	294	VT
98/AV/297	38.13	0.00	0.00	38.15	0.01	0.26	23.09	0.18	99.8	75	294	VT
98/AV/297	38.76	0.02	0.00	38.08	0.02	0.26	23.11	0.18	100.4	75	294	VT
98/AV/297	38.54	0.01	0.00	38.41	0.02	0.25	22.92	0.19	100.3	75	294	VT
98/AV/297	38.71	0.01	0.00	38.30	0.02	0.25	22.95	0.18	100.4	75	294	VT
98/AV/297	39.92	0.01	0.00	39.18	0.02	0.27	22.88	0.18	102.5	75	294	VT
98/AV/297	38.88	0.01	0.00	38.27	0.02	0.27	23.02	0.18	100.6	75	294	VT
98/AV/297	38.88	0.00	0.00	38.37	0.02	0.28	23.25	0.19	101.0	75	294	VT
98/AV/297	38.76	0.02	0.00	38.45	0.03	0.26	23.04	0.18	100.7	75	294	VT
98/AV/297	38.65	0.01	0.02	38.39	0.03	0.25	23.05	0.18	100.6	75	294	VT
98/AV/297	38.67	0.01	0.00	38.42	0.02	0.26	22.92	0.18	100.5	75	294	VT
98/AV/297	38.67	0.01	0.00	38.37	0.01	0.27	23.22	0.18	100.7	75	294	VT
98/AV/297	38.43	0.00	0.00	38.23	0.01	0.27	23.13	0.20	100.3	75	294	VT
98/AV/297	38.68	0.01	0.00	38.25	0.02	0.27	23.01	0.18	100.4	75	294	VT
98/AV/297	38.44	0.02	0.01	37.71	0.02	0.28	23.11	0.19	99.8	74	294	VT
98/AV/297	38.65	0.00	0.00	38.28	0.01	0.26	23.11	0.18	100.5	75	294	VT
98/AV/297	38.66	0.00	0.00	38.64	0.03	0.25	23.11	0.18	100.9	75	294	VT
98/AV/297	38.73	0.01	0.00	38.62	0.03	0.27	22.99	0.19	100.8	75	294	VT
C97 1111	38.53	0.05	0.06	36.40	0.02	0.33	25.84	0.17	101.4	72	296	VT
C97 1111	38.67	0.00	0.04	36.33	0.03	0.31	26.15	0.19	101.7	71	296	VT
C97 1111	38.35	0.03	0.08	36.21	0.04	0.29	26.06	0.19	101.2	71	296	VT
C97 1111	38.74	0.00	0.02	36.47	0.01	0.33	26.20	0.18	101.9	71	296	VT
C97 1111	38.75	0.00	0.00	36.35	0.01	0.31	26.08	0.20	101.7	71	296	VT
C97 1111	38.90	0.00	0.01	36.73	0.01	0.32	26.00	0.18	102.1	72	296	VT
C97 1111	38.84	0.00	0.00	36.36	0.02	0.31	26.03	0.20	101.8	71	296	VT
C97 1111	38.74	0.00	0.00	36.65	0.03	0.33	26.11	0.20	102.1	71	296	VT
C97 1111	38.87	0.00	0.00	36.44	0.00	0.34	26.48	0.18	102.3	71	296	VT
C97 1111	38.74	0.00	0.01	36.29	0.02	0.33	26.27	0.19	101.9	71	296	VT
C97 1111	38.59	0.03	0.00	36.61	0.03	0.31	26.24	0.20	102.0	71	296	VT
C97 1111	38.75	0.01	0.01	36.53	0.06	0.34	26.11	0.19	102.0	71	296	VT
C97 1111	38.57	0.01	0.00	36.69	0.02	0.32	25.91	0.18	101.7	72	296	VT
C97 1111	38.59	0.00	0.00	36.61	0.02	0.33	26.21	0.18	101.9	71	296	VT
C97 1111	38.48	0.00	0.00	36.35	0.01	0.32	26.22	0.19	101.6	71	296	VT
C97 1111	38.72	0.00	0.03	36.17	0.03	0.31	26.21	0.19	101.7	71	296	VT
C97 1111	38.85	0.00	0.01	36.56	0.00	0.32	26.09	0.19	102.0	71	296	VT
C97 1111	38.30	0.00	0.00	35.90	0.02	0.31	26.12	0.19	100.9	71	296	VT
C97 1111	38.92	0.00	0.01	36.31	0.02	0.34	26.35	0.20	102.2	71	296	VT
C97 1111	38.68	0.00	0.00	36.73	0.01	0.31	26.20	0.21	102.1	71	296	VT
C97 1111	38.85	0.02	0.02	36.54	0.02	0.31	25.98	0.20	101.9	71	296	VT
C97 1111	38.74	0.00	0.01	36.65	0.01	0.32	26.09	0.20	102.0	71	296	VT
C97 1111	39.02	0.00	0.00	36.35	0.03	0.30	25.93	0.19	101.8	71	296	VT
C97 1111	38.86	0.01	0.01	36.40	0.01	0.33	26.45	0.20	102.3	71	296	VT
C97 1111	38.77	0.00	0.00	36.46	0.02	0.33	26.91	0.18	102.7	71	296	VT
C97 1111	38.32	0.00	0.00	35.64	0.01	0.35	27.54	0.18	102.0	70	296	VT
C97 1111	38.47	0.02	0.00	36.22	0.02	0.34	26.52	0.19	101.8	71	296	VT
C97 1111	38.75	0.00	0.00	36.46	0.02	0.33	26.30	0.20	102.1	71	296	VT
C97 1111	38.82	0.02	0.01	36.87	0.01	0.33	26.16	0.20	102.4	72	296	VT
C97 1111	38.54	0.01	0.00	36.78	0.02	0.31	26.07	0.18	101.9	72	296	VT

TS number	SiO_2	TiO_2	Al_2O_3	MgO	CaO	MnO	FeO	NiO	Total	Fo #	Depth	Rock
C97 1111	38.68	0.01	0.01	36.16	0.01	0.32	26.79	0.20	102.2	71	296	VT
C97 1111	38.65	0.00	0.00	36.37	0.02	0.30	26.18	0.21	101.7	71	296	VT
C97 1111	38.76	0.00	0.00	36.51	0.02	0.32	26.33	0.20	102.1	71	296	VT
C97 1111	38.55	0.02	0.02	36.31	0.04	0.33	26.03	0.21	101.5	71	296	VT
C97 1111	38.67	0.05	0.03	36.33	0.04	0.33	26.05	0.20	101.7	71	296	VT
C97 1072	39.10	0.01	0.00	36.77	0.03	0.32	25.42	0.13	101.8	72	304.5	VT
C97 1072	39.22	0.03	0.01	37.02	0.01	0.32	25.51	0.15	102.3	72	304.5	VT
C97 1072	38.87	0.01	0.00	37.24	0.03	0.33	25.14	0.14	101.8	73	304.5	VT
C97 1072	39.12	0.06	0.00	37.20	0.03	0.35	25.13	0.15	102.0	73	304.5	VT
C97 1072	39.15	0.01	0.01	36.98	0.02	0.31	25.37	0.14	102.0	72	304.5	VT
C97 1072	39.17	0.02	0.00	37.46	0.02	0.33	25.44	0.14	102.6	72	304.5	VT
C97 1072	39.04	0.02	0.02	37.26	0.03	0.33	25.38	0.15	102.2	72	304.5	VT
C97 1072	38.92	0.02	0.00	36.74	0.02	0.32	25.35	0.12	101.5	72	304.5	VT
C97 1072	39.17	0.03	0.01	37.14	0.02	0.32	25.74	0.15	102.6	72	304.5	VT
C97 1072	38.85	0.03	0.01	37.13	0.02	0.30	25.49	0.14	102.0	72	304.5	VT
C97 1072	38.99	0.04	0.01	36.91	0.01	0.31	25.39	0.14	101.8	72	304.5	VT
C97 1072	38.89	0.02	0.00	37.22	0.05	0.33	25.37	0.15	102.0	72	304.5	VT
C97 1072	39.17	0.02	0.01	37.09	0.02	0.33	25.34	0.13	102.1	72	304.5	VT
C97 1072	39.25	0.01	0.00	37.09	0.02	0.33	25.25	0.12	102.1	72	304.5	VT
C97 1072	38.91	0.00	0.00	36.57	0.03	0.30	24.94	0.13	100.9	72	304.5	VT
C97 1072	38.88	0.02	0.01	37.02	0.02	0.34	25.40	0.14	101.8	72	304.5	VT
C97 1072	38.89	0.00	0.00	36.95	0.04	0.31	25.31	0.12	101.6	72	304.5	VT
C97 1072	39.19	0.00	0.00	37.35	0.01	0.31	25.03	0.14	102.0	73	304.5	VT
C97 1072	39.05	0.01	0.01	37.14	0.01	0.34	25.33	0.13	102.0	72	304.5	VT
C97 1072	39.23	0.00	0.01	37.26	0.02	0.32	25.36	0.15	102.4	72	304.5	VT
C97 1073	39.62	0.01	0.00	37.95	0.02	0.30	24.49	0.12	102.5	73	312.2	VT
C97 1073	39.29	0.01	0.00	37.69	0.01	0.30	24.51	0.14	101.9	73	312.2	VT
C97 1073	39.61	0.01	0.00	38.25	0.02	0.31	24.61	0.14	102.9	73	312.2	VT
C97 1073	39.17	0.03	0.00	37.93	0.03	0.32	24.21	0.13	101.8	74	312.2	VT
C97 1073	39.26	0.01	0.00	37.68	0.02	0.31	24.84	0.13	102.3	73	312.2	VT
C97 1073	39.71	0.02	0.00	37.65	0.01	0.32	24.81	0.14	102.6	73	312.2	VT
C97 1073	39.08	0.01	0.01	37.34	0.02	0.31	24.66	0.11	101.5	73	312.2	VT
C97 1073	39.33	0.02	0.00	37.35	0.02	0.33	25.07	0.13	102.2	73	312.2	VT
C97 1073	39.12	0.00	0.01	37.11	0.03	0.31	24.91	0.12	101.6	73	312.2	VT
C97 1073	39.32	0.00	0.00	37.50	0.02	0.33	25.14	0.13	102.4	73	312.2	VT
C97 1073	39.11	0.00	0.00	38.08	0.03	0.31	24.08	0.13	101.7	74	312.2	VT
C97 1073	39.39	0.00	0.00	37.65	0.02	0.33	25.13	0.13	102.6	73	312.2	VT
C97 1073	39.28	0.00	0.00	37.52	0.03	0.33	24.83	0.13	102.1	73	312.2	VT
C97 1073	39.31	0.01	0.01	37.76	0.02	0.30	24.73	0.14	102.3	73	312.2	VT
C97 1073	39.40	0.00	0.03	37.32	0.01	0.31	24.84	0.14	102.0	73	312.2	VT
C97 1073	39.24	0.04	0.01	37.49	0.01	0.31	24.96	0.13	102.2	73	312.2	VT
C97 1073	39.15	0.00	0.00	37.27	0.01	0.30	24.93	0.15	101.8	73	312.2	VT
C97 1073	39.24	0.00	0.00	37.44	0.02	0.30	25.03	0.14	102.2	73	312.2	VT
C97 1073	39.31	0.06	0.00	37.55	0.02	0.30	25.04	0.13	102.4	73	312.2	VT
C97 1073	39.13	0.03	0.00	37.34	0.02	0.31	25.05	0.13	102.0	73	312.2	VT
C97 1074	38.98	0.05	0.01	37.88	0.02	0.28	23.63	0.14	101.0	74	327	VT
C97 1074	38.99	0.01	0.01	37.88	0.03	0.29	23.78	0.14	101.1	74	327	VT
C97 1074	38.99	0.01	0.01	37.76	0.02	0.29	23.80	0.13	101.0	74	327	VT
C97 1074	38.95	0.01	0.02	37.79	0.08	0.27	23.21	0.13	100.5	74	327	VT
C97 1074	39.28	0.00	0.01	38.06	0.01	0.28	23.68	0.15	101.5	74	327	VT
C97 1074	38.72	0.02	0.00	37.86	0.02	0.30	23.54	0.14	100.6	74	327	VT
C97 1074	39.47	0.00	0.02	38.06	0.02	0.28	23.57	0.15	101.6	74	327	VT
C97 1074	37.85	0.03	0.00	37.08	0.01	0.27	22.62	0.14	98.0	75	327	VT
C97 1074	39.47	0.04	0.00	38.58	0.02	0.29	22.96	0.14	101.5	75	327	VT

TS number	SiO_2	TiO_2	Al_2O_3	MgO	CaO	MnO	FeO	NiO	Total	Fo #	Depth	Rock
C97 1074	39.50	0.03	0.00	39.04	0.01	0.29	22.74	0.14	101.7	75	327	VT
C97 1074	39.39	0.01	0.00	38.28	0.01	0.28	23.60	0.17	101.7	74	327	VT
C97 1074	39.40	0.00	0.00	38.00	0.02	0.28	23.70	0.15	101.6	74	327	VT
C97 1074	39.11	0.02	0.00	37.95	0.02	0.30	24.05	0.17	101.6	74	327	VT
C97 1074	38.77	0.00	0.00	37.62	0.02	0.31	23.89	0.15	100.8	74	327	VT
C97 1074	39.05	0.02	0.00	37.51	0.03	0.28	24.15	0.17	101.2	73	327	VT
C97 1074	38.92	0.02	0.01	37.75	0.00	0.28	23.97	0.17	101.1	74	327	VT
C97 1074	39.03	0.04	0.00	37.63	0.03	0.30	23.77	0.15	100.9	74	327	VT
C97 1074	39.15	0.01	0.00	37.93	0.02	0.26	23.68	0.16	101.2	74	327	VT
C97 1074	39.03	0.02	0.00	37.64	0.03	0.30	23.93	0.17	101.1	74	327	VT
C97 1074	39.40	0.01	0.00	38.29	0.02	0.29	23.89	0.15	102.1	74	327	VT
C97 1075	39.50	0.03	0.00	38.53	0.02	0.25	22.89	0.19	101.4	75	332.5	VT
C97 1075	39.43	0.00	0.00	38.54	0.02	0.26	22.75	0.18	101.2	75	332.5	VT
C97 1075	39.54	0.15	0.00	38.57	0.03	0.29	22.75	0.19	101.5	75	332.5	VT
C97 1075	39.36	0.00	0.00	38.56	0.02	0.27	22.86	0.22	101.3	75	332.5	VT
C97 1075	39.09	0.10	0.01	38.31	0.01	0.29	22.89	0.22	100.9	75	332.5	VT
C97 1075	39.60	0.00	0.00	38.68	0.01	0.28	22.71	0.21	101.5	75	332.5	VT
C97 1075	39.60	0.00	0.00	38.60	0.01	0.28	22.68	0.18	101.4	75	332.5	VT
C97 1075	39.22	0.00	0.00	38.94	0.00	0.26	22.79	0.22	101.4	75	332.5	VT
C97 1075	39.70	0.01	0.00	38.77	0.03	0.28	22.80	0.17	101.7	75	332.5	VT
C97 1075	39.11	0.01	0.01	38.11	0.02	0.28	23.01	0.19	100.7	75	332.5	VT
C97 1075	39.64	0.01	0.00	38.83	0.02	0.28	23.04	0.18	102.0	75	332.5	VT
C97 1075	39.51	0.00	0.00	38.52	0.02	0.26	23.11	0.20	101.6	75	332.5	VT
C97 1075	39.52	0.01	0.00	38.74	0.00	0.27	22.84	0.20	101.6	75	332.5	VT
C97 1075	39.37	0.09	0.00	38.58	0.01	0.27	23.10	0.18	101.6	75	332.5	VT
C97 1075	39.46	0.04	0.00	38.44	0.02	0.28	22.97	0.19	101.4	75	332.5	VT
C97 1075	39.58	0.01	0.00	38.78	0.03	0.29	22.81	0.18	101.7	75	332.5	VT
C97 1075	39.19	0.04	0.01	38.42	0.01	0.26	22.58	0.19	100.7	75	332.5	VT
C97 1075	39.44	0.00	0.00	38.71	0.03	0.26	22.61	0.20	101.2	75	332.5	VT
C97 1075	39.20	0.02	0.00	38.55	0.03	0.28	22.59	0.21	100.9	75	332.5	VT
C97 1075	39.71	0.09	0.00	39.14	0.02	0.27	22.75	0.19	102.2	75	332.5	VT
C97 1077	39.36	0.03	0.00	38.79	0.01	0.28	23.15	0.18	101.8	75	350.5	VT
C97 1077	39.55	0.00	0.00	39.21	0.00	0.28	23.14	0.19	102.4	75	350.5	VT
C97 1077	39.47	0.08	0.01	39.28	0.02	0.30	22.89	0.20	102.3	75	350.5	VT
C97 1077	39.41	0.04	0.02	39.05	0.00	0.28	22.98	0.20	102.0	75	350.5	VT
C97 1077	39.32	0.01	0.15	39.18	0.05	0.27	22.91	0.19	102.1	75	350.5	VT
C97 1077	39.80	0.02	0.00	39.71	0.02	0.28	22.67	0.18	102.7	76	350.5	VT
C97 1077	39.34	0.00	0.01	39.14	0.03	0.27	22.65	0.19	101.6	75	350.5	VT
C97 1077	39.18	0.04	0.00	38.44	0.01	0.28	23.50	0.19	101.6	74	350.5	VT
C97 1077	39.12	0.02	0.01	38.83	0.02	0.30	23.28	0.19	101.8	75	350.5	VT
C97 1077	39.40	0.01	0.00	38.54	0.01	0.29	23.22	0.18	101.7	75	350.5	VT
C97 1077	39.52	0.01	0.01	39.19	0.01	0.29	23.14	0.19	102.4	75	350.5	VT
C97 1077	39.28	0.02	0.00	38.92	0.03	0.28	23.19	0.19	101.9	75	350.5	VT
C97 1077	39.14	0.09	0.00	38.75	0.04	0.30	23.43	0.18	101.9	75	350.5	VT
C97 1077	39.40	0.03	0.01	39.26	0.01	0.28	22.80	0.20	102.0	75	350.5	VT
C97 1077	38.67	0.04	0.00	39.34	0.03	0.27	22.70	0.20	101.2	76	350.5	VT
C97 1077	39.81	0.05	0.03	39.70	0.03	0.28	22.60	0.19	102.7	76	350.5	VT
C971077	39.39	0.02	0.01	39.04	0.03	0.28	23.02	0.19	102.0	75	350.5	VT
C97 1076	38.84	0.02	0.11	37.24	0.04	0.31	24.49	0.14	101.2	73	355.7	VT
C97 1076	39.20	0.04	0.00	37.51	0.01	0.33	24.78	0.14	102.0	73	355.7	VT
C97 1076	38.72	0.00	0.02	37.53	0.00	0.31	24.01	0.13	100.7	74	355.7	VT
C97 1076	39.10	0.01	0.00	37.58	0.01	0.33	24.85	0.14	102.0	73	355.7	VT
C97 1076	38.96	0.00	0.00	37.28	0.03	0.33	25.16	0.14	101.9	73	355.7	VT
C97 1076	39.09	0.02	0.01	37.47	0.01	0.33	25.17	0.14	102.2	73	355.7	VT

TS number	SiO_2	TiO_2	Al_2O_3	MgO	CaO	MnO	FeO	NiO	Total	Fo #	Depth	Rock
C97 1076	39.13	0.02	0.00	37.34	0.01	0.33	25.10	0.12	102.0	73	355.7	VT
C97 1076	38.98	0.00	0.00	37.40	0.02	0.32	25.12	0.14	102.0	73	355.7	VT
C97 1076	38.99	0.05	0.00	37.08	0.01	0.34	25.15	0.15	101.8	72	355.7	VT
C97 1076	38.82	0.00	0.05	36.94	0.02	0.33	24.97	0.14	101.3	73	355.7	VT
C97 1076	39.10	0.01	0.02	37.79	0.02	0.32	24.75	0.12	102.1	73	355.7	VT
C97 1076	39.09	0.08	0.00	38.34	0.02	0.30	24.06	0.13	102.0	74	355.7	VT
C97 1076	39.05	0.00	0.01	37.60	0.03	0.31	24.77	0.13	101.9	73	355.7	VT
C97 1076	38.93	0.00	0.00	37.27	0.03	0.32	25.35	0.15	102.0	72	355.7	VT
C97 1076	38.87	0.03	0.00	37.15	0.02	0.34	25.34	0.14	101.9	72	355.7	VT
C97 1076	38.92	0.00	0.01	37.34	0.03	0.32	25.05	0.15	101.8	73	355.7	VT
C97 1076	39.20	0.00	0.00	37.45	0.03	0.32	25.51	0.14	102.6	72	355.7	VT
C97 1076	39.19	0.00	0.01	37.66	0.01	0.32	24.72	0.14	102.0	73	355.7	VT
C97 1076	38.79	0.02	0.00	37.73	0.01	0.33	24.44	0.15	101.5	73	355.7	VT
C97 1076	39.25	0.00	0.00	38.09	0.02	0.33	24.38	0.15	102.2	74	355.7	VT
C97 1092	38.81	0.00	0.00	36.92	0.01	0.33	24.87	0.15	101.1	73	369	VT
C97 1092	38.90	0.01	0.00	37.15	0.01	0.33	24.90	0.16	101.4	73	369	VT
C97 1092	38.71	0.04	0.00	37.12	0.02	0.33	24.74	0.16	101.1	73	369	VT
C97 1092	39.02	0.04	0.00	37.12	0.02	0.32	24.83	0.16	101.5	73	369	VT
C97 1092	39.05	0.00	0.00	37.23	0.02	0.32	24.80	0.17	101.6	73	369	VT
C97 1092	38.33	0.00	0.00	35.86	0.02	0.30	24.78	0.15	99.4	72	369	VT
C97 1092	38.37	0.00	0.01	36.30	0.02	0.31	25.61	0.18	100.8	72	369	VT
C97 1092	38.87	0.00	0.02	36.36	0.01	0.31	25.27	0.16	101.0	72	369	VT
C97 1092	38.87	0.00	0.02	36.77	0.03	0.34	25.26	0.16	101.4	72	369	VT
C97 1092	38.87	0.01	0.00	36.71	0.02	0.34	25.35	0.16	101.5	72	369	VT
C97 1092	38.73	0.01	0.00	36.66	0.02	0.33	25.52	0.16	101.4	72	369	VT
C97 1092	38.85	0.00	0.01	36.60	0.01	0.32	25.35	0.16	101.3	72	369	VT
C97 1092	39.24	0.00	0.00	37.27	0.00	0.33	25.32	0.15	102.3	72	369	VT
C97 1092	38.74	0.00	0.01	36.91	0.02	0.32	25.23	0.16	101.4	72	369	VT
C97 1092	38.71	0.03	0.03	36.62	0.04	0.33	24.97	0.16	100.9	72	369	VT
C97 1092	38.88	0.03	0.00	36.83	0.02	0.32	25.58	0.16	101.8	72	369	VT
C97 1092	38.46	0.00	0.00	36.37	0.02	0.32	25.37	0.16	100.7	72	369	VT
C97 1092	39.04	0.02	0.00	36.87	0.01	0.33	25.47	0.16	101.9	72	369	VT
C97 1092	38.93	0.00	0.00	36.98	0.01	0.32	25.36	0.16	101.8	72	369	VT
C97 1092	38.43	0.00	0.00	36.95	0.03	0.35	25.42	0.16	101.3	72	369	VT
C97 1092	38.94	0.00	0.00	36.60	0.01	0.33	25.37	0.16	101.4	72	369	VT
C97 1092	38.96	0.00	0.00	36.79	0.01	0.31	25.54	0.16	101.8	72	369	VT
C97 1092	38.81	0.00	0.00	36.29	0.01	0.34	26.17	0.15	101.8	71	369	VT
C97 1092	38.75	0.00	0.00	36.28	0.03	0.32	26.02	0.16	101.6	71	369	VT
C97 1092	38.70	0.00	0.00	36.22	0.02	0.31	26.06	0.14	101.5	71	369	VT
C97 1092	38.75	0.00	0.01	36.40	0.01	0.31	25.91	0.14	101.5	71	369	VT
C97 1092	38.77	0.00	0.01	36.40	0.01	0.31	25.16	0.17	100.8	72	369	VT
C97 1092	38.60	0.01	0.00	36.66	0.01	0.32	25.67	0.15	101.4	72	369	VT
C97 1092	38.57	0.02	0.02	36.68	0.02	0.30	25.59	0.15	101.3	72	369	VT
C97 1092	38.74	0.02	0.00	36.65	0.02	0.34	25.18	0.16	101.1	72	369	VT
C97 1092	38.87	0.00	0.00	36.31	0.02	0.35	25.48	0.15	101.2	72	369	VT
C97 1092	38.96	0.03	0.00	36.98	0.02	0.32	24.97	0.13	101.4	73	369	VT
C97 1092	38.97	0.01	0.06	36.71	0.03	0.31	24.98	0.13	101.2	72	369	VT
C97 1092	38.44	0.02	0.01	36.63	0.02	0.32	24.81	0.15	100.4	72	369	VT
C97 1092	38.59	0.01	0.00	36.84	0.02	0.32	24.74	0.14	100.7	73	369	VT
C97 1092	38.83	0.01	0.00	37.10	0.01	0.33	24.98	0.15	101.4	73	369	VT
C97 1092	38.80	0.00	0.00	36.91	0.02	0.31	25.58	0.16	101.8	72	369	VT
C97 1092	38.91	0.00	0.00	37.02	0.01	0.33	25.53	0.18	102.0	72	369	VT
C97 1092	39.04	0.01	0.00	37.01	0.01	0.32	25.75	0.19	102.3	72	369	VT
C97 1092	38.86	0.00	0.00	37.07	0.03	0.33	25.46	0.18	101.9	72	369	VT

TS number	SiO_2	TiO_2	Al_2O_3	MgO	CaO	MnO	FeO	NiO	Total	Fo #	Depth	Rock
C97 1092	38.98	0.00	0.00	36.81	0.02	0.31	25.66	0.18	102.0	72	369	VT
C97 1092	38.96	0.02	0.00	37.00	0.01	0.31	25.49	0.18	102.0	72	369	VT
C97 1092	38.80	0.00	0.00	36.93	0.02	0.32	25.48	0.15	101.7	72	369	VT
C97 1092	38.75	0.00	0.00	36.88	0.02	0.32	25.19	0.16	101.3	72	369	VT
C97 1092	38.75	0.00	0.01	36.94	0.01	0.33	25.32	0.16	101.5	72	369	VT
C97 1092	38.79	0.00	0.00	37.04	0.00	0.33	25.37	0.15	101.7	72	369	VT
C97 1092	38.83	0.02	0.00	36.96	0.03	0.31	25.38	0.18	101.7	72	369	VT
C97 1092	38.61	0.02	0.01	36.88	0.02	0.33	25.14	0.16	101.2	72	369	VT
C97 1092	38.74	0.00	0.00	37.12	0.01	0.32	24.85	0.16	101.2	73	369	VT
C97 1092	39.14	0.03	0.00	37.12	0.01	0.32	25.13	0.14	101.9	72	369	VT
C97 1092	38.60	0.00	0.00	36.82	0.01	0.33	24.90	0.15	100.8	73	369	VT
C97 1093	38.85	0.00	0.00	36.92	0.02	0.31	25.51	0.14	101.8	72	375	VT
C97 1093	38.43	0.07	0.00	37.09	0.03	0.30	25.57	0.15	101.6	72	375	VT
C97 1093	38.56	0.03	0.00	36.93	0.03	0.32	25.22	0.16	101.2	72	375	VT
C97 1093	38.10	0.00	0.06	36.78	0.02	0.31	25.28	0.15	100.7	72	375	VT
C97 1093	38.58	0.04	0.00	36.82	0.02	0.31	25.07	0.14	101.0	72	375	VT
C97 1093	38.27	0.01	0.00	37.27	0.00	0.31	24.91	0.14	100.9	73	375	VT
C97 1093	38.19	0.00	0.01	36.93	0.03	0.33	25.00	0.14	100.6	72	375	VT
C97 1093	38.77	0.01	0.00	37.24	0.01	0.32	25.23	0.14	101.7	72	375	VT
C97 1093	38.34	0.00	0.01	37.12	0.01	0.34	24.93	0.15	100.9	73	375	VT
C97 1093	38.09	0.00	0.00	37.10	0.02	0.32	24.77	0.13	100.4	73	375	VT
C97 1093	38.73	0.00	0.00	37.20	0.01	0.32	24.95	0.14	101.3	73	375	VT
C97 1093	38.39	0.00	0.00	37.37	0.01	0.32	24.54	0.15	100.8	73	375	VT
C97 1093	37.77	0.04	0.00	37.36	0.01	0.29	24.55	0.14	100.2	73	375	VT
C97 1093	39.03	0.00	0.00	37.85	0.03	0.30	24.85	0.14	102.2	73	375	VT
C97 1093	38.73	0.01	0.00	36.98	0.02	0.32	25.36	0.14	101.5	72	375	VT
C97 1093	38.44	0.00	0.00	37.06	0.00	0.31	25.32	0.14	101.3	72	375	VT
C97 1093	37.96	0.00	0.02	37.08	0.01	0.29	25.11	0.14	100.6	72	375	VT
C97 1093	39.13	0.02	0.00	37.20	0.02	0.33	25.52	0.13	102.3	72	375	VT
C97 1093	37.85	0.01	0.00	36.65	0.02	0.32	25.33	0.14	100.3	72	375	VT
C97 1093	38.33	0.01	0.00	36.90	0.02	0.33	25.13	0.12	100.8	72	375	VT
C97 1093	38.00	0.01	0.00	36.83	0.02	0.33	25.39	0.12	100.7	72	375	VT
C97 1093	38.03	0.00	0.01	36.59	0.02	0.32	25.43	0.14	100.5	72	375	VT
C97 1093	38.77	0.00	0.00	36.98	0.02	0.35	25.79	0.14	102.1	72	375	VT
C97 1094	37.70	0.04	0.18	36.33	0.04	0.32	24.93	0.14	99.7	72	397	VT
C97 1094	38.43	0.01	0.00	36.40	0.01	0.32	25.60	0.15	100.9	72	397	VT
C97 1094	38.26	0.03	0.00	36.59	0.02	0.32	25.43	0.14	100.8	72	397	VT
C97 1094	38.82	0.03	0.01	36.67	0.03	0.32	25.71	0.14	101.7	72	397	VT
C97 1094	38.41	0.00	0.01	36.29	0.02	0.32	25.73	0.15	100.9	72	397	VT
C97 1094	38.14	0.00	0.00	36.47	0.02	0.32	25.55	0.13	100.6	72	397	VT
C97 1094	38.47	0.02	0.01	36.43	0.09	0.33	25.88	0.13	101.3	72	397	VT
C97 1094	38.21	0.01	0.00	36.30	0.02	0.34	25.61	0.15	100.6	72	397	VT
C97 1094	38.39	0.02	0.00	36.26	0.01	0.35	26.48	0.17	101.7	71	397	VT
C97 1094	39.11	0.01	0.01	36.82	0.02	0.33	25.80	0.15	102.3	72	397	VT
C97 1094	38.56	0.02	0.00	36.77	0.02	0.32	25.66	0.15	101.5	72	397	VT
C97 1094	38.71	0.01	0.00	36.87	0.02	0.33	26.03	0.16	102.1	72	397	VT
C97 1094	38.73	0.00	0.01	36.79	0.03	0.33	25.66	0.14	101.7	72	397	VT
C97 1094	38.68	0.00	0.00	36.99	0.01	0.32	25.55	0.15	101.7	72	397	VT
C97 1094	38.29	0.00	0.01	36.83	0.02	0.30	25.45	0.15	101.0	72	397	VT
C97 1094	38.38	0.01	0.00	36.82	0.02	0.36	25.60	0.14	101.3	72	397	VT
C97 1094	37.94	0.00	0.01	36.85	0.02	0.35	25.37	0.15	100.7	72	397	VT
C97 1094	38.89	0.07	0.18	36.92	0.03	0.31	25.54	0.14	102.1	72	397	VT
C97 1094	38.84	0.00	0.00	37.04	0.03	0.33	25.53	0.14	101.9	72	397	VT
C97 1096	38.49	0.02	0.00	37.52	0.02	0.34	24.33	0.17	100.9	73	404	VT

TS number	SiO_2	TiO_2	Al_2O_3	MgO	CaO	MnO	FeO	NiO	Total	Fo #	Depth	Rock
C97 1096	37.66	0.00	0.00	36.93	0.02	0.34	24.61	0.18	99.7	73	404	VT
C97 1096	37.73	0.00	0.00	36.88	0.00	0.34	24.54	0.16	99.6	73	404	VT
C97 1096	38.07	0.01	0.00	36.76	0.00	0.33	24.54	0.15	99.9	73	404	VT
C97 1096	38.52	0.00	0.00	36.80	0.02	0.34	25.23	0.16	101.1	72	404	VT
C97 1096	38.38	0.00	0.02	36.83	0.05	0.31	25.10	0.16	100.9	72	404	VT
C97 1096	38.38	0.00	0.00	37.06	0.01	0.33	24.62	0.18	100.6	73	404	VT
C97 1096	38.37	0.00	0.01	36.63	0.02	0.33	25.20	0.17	100.7	72	404	VT
C97 1096	38.66	0.00	0.01	36.58	0.02	0.34	25.60	0.16	101.4	72	404	VT
C97 1096	38.73	0.00	0.00	37.29	0.00	0.32	24.91	0.15	101.4	73	404	VT
C97 1096	38.32	0.01	0.02	37.40	0.00	0.34	24.54	0.16	100.8	73	404	VT
C97 1096	38.52	0.01	0.00	37.32	0.00	0.36	24.65	0.18	101.0	73	404	VT
C97 1096	38.76	0.01	0.01	37.33	0.00	0.33	24.86	0.17	101.5	73	404	VT
C97 1096	38.49	0.03	0.00	37.28	0.03	0.33	24.90	0.17	101.2	73	404	VT
C97 1096	38.41	0.00	0.00	37.30	0.01	0.32	25.03	0.19	101.3	73	404	VT
C97 1096	34.54	0.01	7.95	33.08	0.03	0.30	22.23	0.15	98.3	73	404	VT
C97 1096	37.87	0.00	0.00	36.98	0.00	0.33	24.68	0.17	100.1	73	404	VT
C97 1096	38.43	0.00	0.02	37.45	0.01	0.34	24.23	0.18	100.7	73	404	VT
C97 1096	38.91	0.01	0.00	37.73	0.00	0.33	24.46	0.18	101.6	73	404	VT
C97 1096	38.34	0.00	0.00	36.27	0.01	0.34	26.12	0.16	101.3	71	404	VT
C97 1096	38.35	0.00	0.00	37.35	0.00	0.33	24.51	0.19	100.7	73	404	VT
C97 1096	38.70	0.01	0.01	36.97	0.01	0.35	25.71	0.17	101.9	72	404	VT
C97 1096	38.29	0.02	0.01	37.44	0.00	0.33	24.19	0.17	100.5	73	404	VT
C97 1096	38.27	0.00	0.00	37.31	0.01	0.33	24.78	0.18	100.9	73	404	VT
C97 1096	38.54	0.00	0.01	37.61	0.01	0.34	24.64	0.18	101.3	73	404	VT
C97 1095	38.69	0.00	0.01	35.91	0.04	0.35	26.14	0.15	101.3	71	417	VT
C97 1095	38.49	0.01	0.00	35.80	0.03	0.32	26.01	0.14	100.8	71	417	VT
C97 1095	38.36	0.01	0.08	35.59	0.03	0.32	26.24	0.16	100.8	71	417	VT
C97 1095	35.82	0.00	0.00	35.46	0.01	0.32	25.69	0.16	97.5	71	417	VT
C97 1095	35.72	0.01	0.00	35.68	0.02	0.31	25.88	0.16	97.8	71	417	VT
C97 1095	38.76	0.05	0.00	36.21	0.02	0.31	26.31	0.15	101.8	71	417	VT
C97 1095	38.63	0.07	0.00	36.14	0.02	0.34	26.27	0.17	101.7	71	417	VT
C97 1095	38.85	0.05	0.00	36.34	0.03	0.34	26.10	0.17	101.9	71	417	VT
C97 1095	38.76	0.00	0.01	36.32	0.03	0.33	26.25	0.17	101.9	71	417	VT
C97 1095	38.82	0.03	0.00	36.24	0.02	0.34	26.29	0.16	101.9	71	417	VT
C97 1095	38.70	0.02	0.00	36.26	0.02	0.34	26.02	0.18	101.5	71	417	VT
C97 1095	39.44	0.04	0.02	35.89	0.02	0.27	22.88	0.18	98.7	74	417	VT
C97 1095	38.85	0.03	0.00	36.18	0.02	0.31	25.95	0.17	101.5	71	417	VT
C97 1095	38.74	0.10	0.01	36.34	0.01	0.32	25.63	0.18	101.3	72	417	VT
C97 1095	38.81	0.07	0.02	36.49	0.02	0.33	25.66	0.17	101.6	72	417	VT
C97 1095	38.95	0.05	0.00	36.65	0.02	0.31	25.66	0.18	101.8	72	417	VT
C97 1095	38.98	0.01	0.08	36.75	0.03	0.32	25.28	0.18	101.6	72	417	VT
C97 1095	39.26	0.00	0.00	36.80	0.02	0.32	25.57	0.18	102.2	72	417	VT
C97 1095	39.10	0.00	0.00	36.73	0.02	0.31	25.46	0.17	101.8	72	417	VT
C97 1095	38.81	0.00	0.00	36.47	0.02	0.33	25.85	0.17	101.7	72	417	VT
C97 1095	39.08	0.03	0.00	36.68	0.02	0.32	25.50	0.17	101.8	72	417	VT
C97 1095	39.06	0.00	0.00	36.50	0.03	0.34	25.53	0.17	101.6	72	417	VT
C97 1095	38.98	0.00	0.00	36.43	0.04	0.31	25.35	0.18	101.3	72	417	VT
C97 1095	39.15	0.02	0.01	36.60	0.01	0.34	25.67	0.18	102.0	72	417	VT
C97 1095	38.25	0.00	0.02	36.18	0.03	0.33	25.94	0.20	100.9	71	417	VT
C97 1095	38.88	0.03	0.00	36.70	0.03	0.32	25.95	0.17	102.1	72	417	VT
C97 1095	39.00	0.00	0.00	36.57	0.02	0.30	25.87	0.18	101.9	72	417	VT
C97 1095	38.80	0.01	0.00	36.82	0.00	0.30	25.51	0.18	101.6	72	417	VT
C97 1095	39.16	0.04	0.00	36.41	0.02	0.33	25.88	0.17	102.0	71	417	VT
C97 1095	38.95	0.00	0.00	36.82	0.01	0.32	25.97	0.17	102.2	72	417	VT

TS number	SiO_2	TiO_2	Al_2O_3	MgO	CaO	MnO	FeO	NiO	Total	Fo #	Depth	Rock
C97 1095	38.93	0.00	0.01	36.45	0.02	0.32	25.85	0.17	101.8	72	417	VT
C97 1095	39.02	0.00	0.00	36.62	0.02	0.31	25.85	0.17	102.0	72	417	VT
C97 1095	38.76	0.01	0.01	36.44	0.02	0.33	26.14	0.18	101.9	71	417	VT
C97 1095	38.78	0.00	0.00	36.51	0.02	0.33	26.14	0.17	102.0	71	417	VT
C97 1095	38.78	0.01	0.00	36.08	0.01	0.31	25.97	0.16	101.3	71	417	VT
C97 1095	39.01	0.01	0.00	36.44	0.02	0.31	26.07	0.17	102.0	71	417	VT
C97 1095	38.78	0.00	0.00	36.23	0.00	0.33	26.01	0.18	101.5	71	417	VT
C97 1095	38.82	0.00	0.00	36.21	0.02	0.34	26.30	0.16	101.8	71	417	VT
C97 1095	38.77	0.02	0.02	35.97	0.03	0.33	26.36	0.15	101.6	71	417	VT
C97 1095	38.78	0.01	0.01	36.00	0.01	0.32	26.00	0.15	101.3	71	417	VT
C97 1095	38.93	0.01	0.00	36.29	0.02	0.34	26.36	0.16	102.1	71	417	VT
C97 1095	38.72	0.00	0.01	36.19	0.02	0.34	26.47	0.14	101.9	71	417	VT
C97 1095	38.60	0.01	0.00	36.24	0.01	0.31	26.19	0.14	101.5	71	417	VT
C97 1095	38.61	0.00	0.02	35.88	0.02	0.32	26.45	0.14	101.4	71	417	VT
C97 1095	38.75	0.01	0.01	35.86	0.03	0.33	26.36	0.15	101.5	71	417	VT
C97 1095	38.71	0.00	0.00	36.16	0.02	0.33	26.32	0.16	101.7	71	417	VT
C97 1095	38.86	0.04	0.02	35.99	0.02	0.33	26.44	0.14	101.8	71	417	VT
C97 1095	38.76	0.00	0.00	36.15	0.02	0.34	26.33	0.16	101.8	71	417	VT
C97 1095	38.65	0.02	0.01	36.03	0.01	0.32	26.32	0.15	101.5	71	417	VT
C97 1095	38.81	0.00	0.01	36.15	0.01	0.33	26.37	0.15	101.8	71	417	VT
C97 1095	38.78	0.03	0.00	36.07	0.03	0.32	26.43	0.14	101.8	71	417	VT
C97 1095	38.63	0.01	0.00	36.42	0.01	0.32	26.06	0.17	101.6	71	417	VT
98/AV/300	36.98	0.00	0.00	35.56	0.00	0.33	26.22	0.17	99.3	71	418	VT
98/AV/300	37.71	0.01	0.00	35.48	0.02	0.34	26.34	0.17	100.1	71	418	VT
98/AV/300	37.58	0.04	0.00	35.76	0.02	0.36	26.32	0.18	100.3	71	418	VT
98/AV/300	37.59	0.01	0.00	35.65	0.02	0.33	26.65	0.18	100.4	70	418	VT
98/AV/300	38.24	0.00	0.00	35.80	0.01	0.33	26.14	0.17	100.7	71	418	VT
98/AV/300	37.73	0.02	0.00	35.82	0.03	0.33	26.19	0.17	100.3	71	418	VT
98/AV/300	38.21	0.00	0.00	35.92	0.01	0.33	26.23	0.17	100.9	71	418	VT
98/AV/300	38.17	0.02	0.00	35.86	0.02	0.33	26.08	0.18	100.7	71	418	VT
98/AV/300	38.08	0.02	0.01	35.95	0.02	0.33	26.11	0.17	100.7	71	418	VT
98/AV/300	38.26	0.00	0.00	36.02	0.01	0.33	25.99	0.17	100.8	71	418	VT
98/AV/300	38.36	0.03	0.00	35.91	0.03	0.34	26.09	0.18	100.9	71	418	VT
98/AV/300	38.08	0.00	0.00	36.06	0.01	0.34	26.36	0.19	101.0	71	418	VT
98/AV/300	37.95	0.01	0.01	35.81	0.00	0.33	25.87	0.18	100.2	71	418	VT
98/AV/300	38.02	0.00	0.00	35.95	0.00	0.35	25.86	0.17	100.3	71	418	VT
98/AV/300	38.25	0.00	0.00	35.97	0.01	0.33	26.04	0.18	100.8	71	418	VT
98/AV/300	38.35	0.00	0.00	35.73	0.02	0.33	26.02	0.18	100.6	71	418	VT
98/AV/300	37.74	0.00	0.00	35.75	0.03	0.31	26.04	0.20	100.1	71	418	VT
C97 1112	38.55	0.00	0.00	36.39	0.03	0.29	25.57	0.20	101.0	72	481	VT
C97 1112	38.71	0.03	0.00	36.46	0.04	0.32	25.56	0.19	101.3	72	481	VT
C97 1112	38.45	0.00	0.00	36.29	0.03	0.33	25.84	0.17	101.1	71	481	VT
C97 1112	38.58	0.00	0.00	36.01	0.04	0.32	26.12	0.20	101.3	71	481	VT
C97 1112	38.55	0.00	0.01	36.23	0.00	0.34	26.13	0.18	101.4	71	481	VT
C97 1112	38.57	0.01	0.14	36.71	0.03	0.30	25.45	0.18	101.4	72	481	VT
C97 1112	39.35	0.03	1.20	36.14	0.04	0.30	25.44	0.18	102.7	72	481	VT
C97 1112	38.45	0.02	0.00	36.12	0.02	0.33	26.39	0.18	101.5	71	481	VT
C97 1112	38.67	0.01	0.00	36.12	0.01	0.33	26.39	0.19	101.7	71	481	VT
C97 1112	38.19	0.00	0.00	36.12	0.03	0.33	26.37	0.17	101.2	71	481	VT
C97 1112	38.60	0.02	0.00	36.07	0.02	0.32	26.63	0.20	101.9	71	481	VT
C97 1112	38.31	0.01	0.02	35.92	0.04	0.32	26.02	0.17	100.8	71	481	VT
C97 1112	38.23	0.01	0.81	36.17	0.01	0.33	25.47	0.19	101.2	72	481	VT
C97 1116	38.84	0.00	0.01	37.65	0.03	0.30	24.49	0.15	101.5	73	597.4	VT
C97 1116	38.80	0.00	0.01	37.58	0.02	0.28	24.54	0.16	101.4	73	597.4	VT

TS number	SiO_2	TiO_2	Al_2O_3	MgO	CaO	MnO	FeO	NiO	Total	Fo #	Depth	Rock
C97 1116	37.75	0.00	0.02	36.08	0.02	0.27	25.74	0.16	100.0	71	597.4	VT
C97 1116	39.30	0.01	0.03	38.01	0.03	0.29	24.49	0.15	102.3	73	597.4	VT
C97 1116	38.86	0.00	0.07	37.42	0.00	0.27	24.09	0.15	100.9	73	597.4	VT
C97 1116	38.86	0.01	0.00	37.77	0.01	0.29	24.44	0.16	101.5	73	597.4	VT
C97 1116	38.85	0.00	0.00	37.57	0.01	0.28	25.00	0.16	101.9	73	597.4	VT
C97 1116	38.78	0.00	0.00	37.38	0.02	0.30	25.12	0.14	101.7	73	597.4	VT
C97 1116	39.07	0.02	0.00	37.41	0.02	0.28	24.81	0.14	101.7	73	597.4	VT
C97 1116	39.13	0.00	0.00	37.85	0.01	0.28	24.53	0.14	101.9	73	597.4	VT
C97 1116	39.28	0.01	0.01	38.40	0.01	0.28	24.33	0.17	102.5	74	597.4	VT
C97 1116	39.51	0.00	0.02	38.61	0.02	0.28	23.58	0.15	102.2	74	597.4	VT
C97 1116	39.06	0.00	0.00	38.15	0.02	0.28	24.45	0.16	102.1	74	597.4	VT
C97 1116	38.96	0.00	0.00	37.94	0.02	0.30	24.45	0.16	101.8	73	597.4	VT
C97 1116	37.21	0.00	0.02	36.60	0.03	0.26	23.18	0.15	97.4	74	597.4	VT
C97 1116	38.66	0.02	0.01	37.58	0.02	0.30	24.21	0.16	100.9	73	597.4	VT
C97 1116	38.81	0.01	0.02	37.58	0.03	0.30	24.35	0.15	101.3	73	597.4	VT
C97 1116	39.15	0.01	0.01	37.55	0.02	0.29	25.31	0.14	102.5	73	597.4	VT
C97 1116	39.27	0.04	0.01	37.80	0.02	0.28	24.94	0.16	102.5	73	597.4	VT
C97 1116	39.05	0.03	0.00	37.92	0.01	0.31	24.91	0.15	102.4	73	597.4	VT
C97 1116	38.94	0.02	0.00	37.68	0.00	0.29	24.90	0.15	102.0	73	597.4	VT
C97 1116	39.02	0.00	0.00	37.62	0.00	0.27	24.97	0.16	102.0	73	597.4	VT
C97 1116	36.74	0.04	0.13	35.48	0.04	0.26	26.49	0.15	99.3	70	597.4	VT
C97 1116	38.78	0.00	0.00	37.45	0.00	0.28	24.92	0.18	101.6	73	597.4	VT
C97 1116	38.57	0.00	0.00	36.99	0.03	0.30	25.55	0.15	101.6	72	597.4	VT
C97 1116	38.39	0.04	0.00	36.82	0.03	0.29	25.72	0.16	101.5	72	597.4	VT
C97 1116	38.89	0.00	0.02	36.91	0.00	0.28	25.91	0.15	102.2	72	597.4	VT
C97 1116	39.94	0.02	0.01	38.13	0.02	0.27	24.89	0.13	103.4	73	597.4	VT
C97 1116	38.64	0.00	0.17	36.73	0.03	0.28	24.95	0.14	100.9	72	597.4	VT
C97 1116	39.55	0.00	0.03	38.09	0.02	0.28	24.78	0.16	102.9	73	597.4	VT
C97 1116	38.99	0.01	0.00	37.83	0.01	0.29	24.92	0.17	102.2	73	597.4	VT
C97 1116	38.48	0.00	0.11	37.41	0.04	0.27	23.30	0.18	99.8	74	597.4	VT
C97 1116	39.35	0.00	0.00	38.06	0.02	0.29	24.69	0.14	102.5	73	597.4	VT
C97 1118	38.25	0.00	0.00	34.35	0.01	0.35	28.40	0.17	101.5	68	604.5	BBS
C97 1118	38.43	0.01	0.01	35.59	0.05	0.35	27.10	0.17	101.7	70	604.5	BBS
C97 1118	38.35	0.00	0.01	35.43	0.02	0.35	27.31	0.18	101.6	70	604.5	BBS
C97 1118	38.30	0.00	0.00	35.50	0.05	0.36	26.45	0.18	100.8	71	604.5	BBS
C97 1118	38.17	0.00	0.00	35.65	0.04	0.33	26.72	0.18	101.1	70	604.5	BBS
C97 1118	38.67	0.00	0.00	34.74	0.05	0.35	25.62	0.17	99.6	71	604.5	BBS
C97 1118	38.62	0.00	0.00	35.58	0.02	0.35	27.11	0.19	101.9	70	604.5	BBS
C97 1118	38.27	0.01	0.00	34.26	0.02	0.37	28.71	0.19	101.8	68	604.5	BBS
C97 1118	37.99	0.00	0.01	34.22	0.02	0.34	28.57	0.19	101.3	68	604.5	BBS
C97 1118	38.51	0.02	0.02	35.55	0.02	0.34	26.82	0.17	101.5	70	604.5	BBS
C97 1118	38.41	0.02	0.00	35.46	0.03	0.37	27.47	0.20	102.0	70	604.5	BBS
C97 1118	38.52	0.00	0.00	35.53	0.03	0.37	27.40	0.18	102.0	70	604.5	BBS
C97 1120	36.73	0.00	0.40	32.79	0.04	0.35	28.03	0.18	98.5	68	627	BBS
C97 1120	37.15	0.02	0.19	33.43	0.04	0.34	28.41	0.21	99.8	68	627	BBS
C97 1120	36.74	0.00	0.00	32.63	0.02	0.36	28.82	0.19	98.8	67	627	BBS
C97 1120	36.23	0.02	0.14	31.60	0.14	0.34	29.33	0.16	98.0	66	627	BBS
C97 1120	36.58	0.00	0.01	32.29	0.02	0.34	29.30	0.18	98.7	66	627	BBS
C97 1120	36.97	0.01	0.00	32.72	0.03	0.36	29.31	0.19	99.6	67	627	BBS
C97 1120	36.79	0.01	0.00	32.97	0.03	0.36	28.70	0.19	99.0	67	627	BBS
C97 1120	37.02	0.01	0.01	32.86	0.03	0.37	28.84	0.20	99.3	67	627	BBS
C97 1120	36.44	0.00	0.01	32.90	0.04	0.36	27.93	0.19	97.9	68	627	BBS
C97 1120	36.68	0.00	0.00	32.56	0.01	0.37	29.24	0.18	99.0	66	627	BBS
C97 1120	36.58	0.00	0.00	32.55	0.03	0.36	28.85	0.18	98.6	67	627	BBS

TS number	SiO_2	TiO_2	Al_2O_3	MgO	CaO	MnO	FeO	NiO	Total	Fo #	Depth	Rock
C97 2557	38.74	0.00	0.00	35.29	0.00	0.32	27.82	0.15	102.3	69	637	BBS
C97 2557	38.48	0.02	0.01	35.50	0.02	0.30	27.53	0.16	102.0	70	637	BBS
C97 2557	38.05	0.00	0.00	34.74	0.03	0.31	27.55	0.18	100.8	69	637	BBS
C97 2557	38.28	0.02	0.01	35.07	0.01	0.31	27.83	0.16	101.7	69	637	BBS
C97 2557	38.63	0.00	0.00	35.50	0.01	0.31	27.68	0.16	102.3	70	637	BBS
C97 2557	38.39	0.02	0.01	35.17	0.00	0.32	27.63	0.17	101.7	69	637	BBS
C97 2557	38.45	0.00	0.00	35.48	0.00	0.33	27.76	0.16	102.2	69	637	BBS
C97 2557	38.31	0.01	0.00	34.78	0.01	0.33	28.15	0.16	101.7	69	637	BBS
C97 2557	38.37	0.03	0.00	34.62	0.02	0.32	28.48	0.16	102.0	68	637	BBS
C97 2557	38.34	0.00	0.00	34.51	0.03	0.33	28.54	0.15	101.9	68	637	BBS
C97 2557	38.55	0.01	0.00	34.83	0.00	0.32	28.36	0.14	102.2	69	637	BBS
C97 2557	38.63	0.00	0.00	35.54	0.02	0.32	27.66	0.17	102.3	70	637	BBS
C97 2557	38.58	0.01	0.00	35.59	0.00	0.33	27.59	0.17	102.3	70	637	BBS
C97 2557	38.62	0.00	0.00	35.57	0.00	0.32	27.65	0.17	102.3	70	637	BBS
C97 2557	38.60	0.01	0.00	35.44	0.10	0.31	27.58	0.17	102.2	70	637	BBS
C97 2557	38.36	0.00	0.00	35.68	0.02	0.32	27.49	0.17	102.1	70	637	BBS
C97 2557	38.63	0.02	0.00	35.92	0.02	0.31	27.56	0.19	102.6	70	637	BBS
C97 2557	38.02	0.01	0.00	35.83	0.01	0.32	27.17	0.17	101.5	70	637	BBS
C97 2557	38.94	0.00	0.02	35.24	0.01	0.27	25.50	0.16	100.2	71	637	BBS
C97 2557	38.56	0.00	0.00	35.06	0.01	0.31	27.87	0.15	102.0	69	637	BBS
C97 2557	38.37	0.01	0.00	34.58	0.00	0.34	28.53	0.17	102.0	68	637	BBS
C97 2557	38.29	0.00	0.02	34.11	0.04	0.29	25.35	0.14	98.2	71	637	BBS
C97 2557	35.60	0.03	3.55	31.95	0.02	0.26	25.14	0.15	96.7	69	637	BBS
C97 2557	37.71	0.02	1.28	34.44	0.01	0.30	26.75	0.18	100.7	70	637	BBS
C97 2557	38.53	0.00	0.00	35.29	0.02	0.32	27.54	0.14	101.8	70	637	BBS
C97 2557	38.36	0.01	0.00	35.32	0.01	0.33	27.80	0.15	102.0	69	637	BBS
C97 2557	38.66	0.00	0.00	34.92	0.01	0.33	28.37	0.17	102.5	69	637	BBS
C97 2557	38.40	0.00	0.01	35.56	0.01	0.33	27.96	0.17	102.4	69	637	BBS
C97 2557	38.46	0.00	0.00	35.92	0.00	0.30	27.36	0.16	102.2	70	637	BBS

Table A.4 sulphide microprobe data

TS number	C97 801	C97 801	C97 801	C97 801	C97 801	C97 801	C97 801	C97 801	C97 801
Wt% S	38.75	34.65	34.66	38.66	32.99	32.85	34.31	38.86	39.04
Wt% Fe	58.35	29.82	29.86	58.17	28.59	28.47	29.89	58.45	58.59
Wt% Co	0.07	0.02	0.01	0.05	2.16	2.11	0.03	0.06	0.04
Wt% Ni	0.74	0.01	0.00	0.72	36.34	35.94	0.12	0.70	0.65
Wt% Cu	0.00	35.02	35.11	0.04	0.00	0.00	35.14	0.00	0.00
Total	97.94	99.53	99.65	97.65	100.09	99.39	99.51	98.07	98.32
Atomic% S	53.30	49.89	49.85	53.32	46.85	46.94	49.52	53.36	53.44
Atomic% Fe	46.07	24.65	24.65	46.06	23.30	23.36	24.76	46.07	46.05
Atomic% Co	0.05	0.02	0.01	0.03	1.67	1.64	0.03	0.05	0.03
Atomic% Ni	0.56	0.01	0.00	0.54	28.18	28.05	0.10	0.52	0.49
Atomic% Cu	0.00	25.44	25.48	0.03	0.00	0.00	25.59	0.00	0.00
Host	BBS	BBS	BBS	BBS	BBS	BBS	BBS	BBS	BBS
Hole	VB96356	VB96356	VB96356	VB96356	VB96356	VB96356	VB96356	VB96356	VB96356
Depth	1189.00	1189.00	1189.00	1189.00	1189.00	1189.00	1189.00	1189.00	1189.00
Easting	560803.2	560803.2	560803.2	560803.2	560803.2	560803.2	560803.2	560803.2	560803.2
Northing	6242137.3	6242137.3	6242137.3	6242137.3	6242137.3	6242137.3	6242137.3	6242137.3	6242137.3

TS number	C97 801	C97 801	C97 801	C97 801	C97 801	C97 801	C97 801	C97 801	C97 801
Wt% S	39.04	33.07	38.78	33.30	33.10	39.08	39.35	33.03	39.21
Wt% Fe	58.59	28.53	58.14	28.81	28.73	58.67	58.69	28.68	58.58
Wt% Co	0.04	1.96	0.08	1.92	1.93	0.07	0.07	2.05	0.06
Wt% Ni	0.65	36.43	0.76	36.62	36.43	0.72	0.62	36.05	0.67
Wt% Cu	0.00	0.00	0.00	0.00	0.00	0.01	0.01	0.00	0.02
Total	98.32	99.99	97.75	100.64	100.19	98.56	98.74	99.82	98.55
Atomic% S	53.44	46.97	53.40	46.98	46.93	53.38	53.59	46.98	53.53
Atomic% Fe	46.05	23.26	45.97	23.33	23.38	46.01	45.89	23.42	45.91
Atomic% Co	0.03	1.51	0.06	1.48	1.49	0.05	0.05	1.59	0.04
Atomic% Ni	0.49	28.26	0.57	28.21	28.20	0.54	0.46	28.00	0.50
Atomic% Cu	0.00	0.00	0.00	0.00	0.00	0.00	0.01	0.00	0.01
Host	BBS	BBS	BBS	BBS	BBS	BBS	BBS	BBS	BBS
Hole	VB96356	VB96356	VB96356	VB96356	VB96356	VB96356	VB96356	VB96356	VB96356
Depth	1189.00	1189.00	1189.00	1189.00	1189.00	1189.00	1189.00	1189.00	1189.00
Easting	560803.2	560803.2	560803.2	560803.2	560803.2	560803.2	560803.2	560803.2	560803.2
Northing	6242137.3	6242137.3	6242137.3	6242137.3	6242137.3	6242137.3	6242137.3	6242137.3	6242137.3

TS number	C97 801	C97 801	C97 801	C96 2557	C96 2557	C96 2557	C96 2557	C96 2557	C97 1106
Wt% S	33.43	34.56	39.58	38.06	38.29	33.16	32.98	33.85	37.75
Wt% Fe	28.46	29.98	58.12	59.62	59.21	30.54	30.51	29.47	59.59
Wt% Co	2.20	0.01	0.06	0.03	0.03	1.20	1.25	0.01	0.03
Wt% Ni	36.67	0.00	0.67	0.45	0.47	34.64	34.97	0.01	0.38
Wt% Cu	0.00	35.14	0.02	0.00	0.00	0.00	0.00	34.49	0.00
Total	100.77	99.69	98.54	98.16	98.01	99.54	99.70	97.82	97.75
Atomic% S	47.09	49.72	53.91	52.46	52.77	47.20	46.93	49.65	52.29
Atomic% Fe	23.01	24.77	45.45	47.18	46.84	24.95	24.93	24.82	47.39
Atomic% Co	1.69	0.01	0.05	0.02	0.02	0.93	0.97	0.01	0.03
Atomic% Ni	28.21	0.00	0.50	0.34	0.36	26.92	27.17	0.00	0.28
Atomic% Cu	0.00	25.51	0.02	0.00	0.00	0.00	0.00	25.52	0.00
Host	BBS	BBS	BBS	BBS	BBS	BBS	BBS	BBS	BBS
Hole	VB96356	VB96356	VB96356	VB96266	VB96266	VB96266	VB96266	VB96266	VB96266
Depth	1189.00	1189.00	1189.00	637.00	637.00	637.00	637.00	637.00	271.50
Easting	560803.2	560803.2	560803.2	556965.8	556965.8	556965.8	556965.8	556965.8	556965.8
Northing	6242137.3	6242137.3	6242137.3	6242466.0	6242466.0	6242466.0	6242466.0	6242466.0	6242466.0

TS number	C97 1106	C97 1106	C97 1106	C97 1106	C97 1106	C97 1106	C97 1106	C97 1106	C97 1106
Wt% S	31.86	38.25	33.82	32.86	37.85	37.83	32.92	37.72	33.94
Wt% Fe	30.51	59.46	29.71	32.25	59.43	59.63	31.03	59.92	29.63
Wt% Co	1.25	0.04	0.01	1.09	0.03	0.04	1.23	0.04	0.02
Wt% Ni	33.17	0.39	0.03	32.97	0.33	0.39	34.80	0.28	0.00
Wt% Cu	0.00	0.01	34.76	0.00	0.00	0.00	0.00	0.01	34.80
Total	96.80	98.16	98.37	99.18	97.65	97.90	99.99	97.97	98.39
Atomic% S	46.73	52.66	49.41	46.96	52.45	52.33	46.76	52.17	49.53
Atomic% Fe	25.69	47.00	24.92	26.46	47.27	47.34	25.30	47.58	24.82
Atomic% Co	1.00	0.03	0.01	0.85	0.03	0.03	0.95	0.03	0.02
Atomic% Ni	26.57	0.30	0.02	25.73	0.25	0.30	26.99	0.21	0.00
Atomic% Cu	0.00	0.01	25.62	0.00	0.00	0.00	0.00	0.01	25.63
Host	BBS	BBS	BBS	BBS	BBS	BBS	BBS	BBS	BBS
Hole	VB96266	VB96266	VB96266	VB96266	VB96266	VB96266	VB96266	VB96266	VB96266
Depth	271.50	271.50	271.50	271.50	271.50	271.50	271.50	271.50	271.50
Easting	556965.8	556965.8	556965.8	556965.8	556965.8	556965.8	556965.8	556965.8	556965.8
Northing	6242466.0	6242466.0	6242466.0	6242466.0	6242466.0	6242466.0	6242466.0	6242466.0	6242466.0

TS number	C97 1106	C97 1106	C97 1106	C97 1106	C97 1106	C97 1106	C97 1106	C97 1106	C97 1106
Wt% S	33.22	38.14	32.85	34.08	37.69	37.64	37.66	32.78	37.44
Wt% Fe	32.05	59.69	31.92	29.77	59.84	59.74	59.58	31.48	59.85
Wt% Co	1.31	0.05	1.54	0.02	0.04	0.04	0.05	1.27	0.04
Wt% Ni	33.32	0.23	33.25	0.07	0.23	0.29	0.29	34.03	0.27
Wt% Cu	0.00	0.01	0.00	34.89	0.00	0.00	0.00	0.00	0.02
Total	99.91	98.14	99.57	98.82	97.79	97.70	97.57	99.57	97.62
Atomic% S	47.10	52.56	46.81	49.52	52.21	52.19	52.27	46.74	52.02
Atomic% Fe	26.09	47.22	26.12	24.83	47.59	47.56	47.47	25.77	47.73
Atomic% Co	1.01	0.04	1.20	0.01	0.03	0.03	0.04	0.98	0.03
Atomic% Ni	25.80	0.17	25.88	0.05	0.17	0.22	0.22	26.50	0.20
Atomic% Cu	0.00	0.01	0.00	25.58	0.00	0.00	0.00	0.00	0.02
Host	BBS	BBS	BBS	BBS	BBS	BBS	BBS	BBS	BBS
Hole	VB96266	VB96266	VB96266	VB96266	VB96266	VB96266	VB96266	VB96266	VB96266
Depth	271.50	271.50	271.50	271.50	271.50	271.50	271.50	271.50	271.50
Easting	556965.8	556965.8	556965.8	556965.8	556965.8	556965.8	556965.8	556965.8	556965.8
Northing	6242466.0	6242466.0	6242466.0	6242466.0	6242466.0	6242466.0	6242466.0	6242466.0	6242466.0

TS number	C97 1106	C97 1106	C97 1106	C97 1106	C97 1106	C97 1106	C97 1106	C97 1106	C97 1106
Wt% S	32.58	37.77	34.25	37.93	32.60	38.02	32.94	31.85	37.64
Wt% Fe	31.40	59.54	29.95	59.47	30.68	59.54	31.06	30.65	59.65
Wt% Co	1.28	0.03	0.01	0.05	1.39	0.04	1.17	1.14	0.05
Wt% Ni	34.03	0.35	0.00	0.38	34.65	0.35	34.78	33.89	0.41
Wt% Cu	0.00	0.05	34.79	0.00	0.00	0.00	0.00	0.00	0.03
Total	99.33	97.74	99.01	97.83	99.34	97.97	99.95	97.54	97.78
Atomic% S	46.61	52.33	49.63	52.46	46.64	52.50	46.79	46.45	52.17
Atomic% Fe	25.79	47.35	24.92	47.22	25.19	47.20	25.33	25.66	47.47
Atomic% Co	0.99	0.02	0.01	0.03	1.08	0.03	0.91	0.91	0.04
Atomic% Ni	26.58	0.27	0.00	0.29	27.07	0.27	26.98	26.99	0.31
Atomic% Cu	0.00	0.04	25.43	0.00	0.00	0.00	0.00	0.00	0.02
Host	BBS	BBS	BBS	BBS	BBS	BBS	BBS	BBS	BBS
Hole	VB96266	VB96266	VB96266	VB96266	VB96266	VB96266	VB96266	VB96266	VB96266
Depth	271.50	271.50	271.50	271.50	271.50	271.50	271.50	271.50	271.50
Easting	556965.8	556965.8	556965.8	556965.8	556965.8	556965.8	556965.8	556965.8	556965.8
Northing	6242466.0	6242466.0	6242466.0	6242466.0	6242466.0	6242466.0	6242466.0	6242466.0	6242466.0

TS number	C99 1118	C99 1118	C99 1118	C99 1118	C99 1118	C99 1118	C96 2655	C96 2655	C96 2655
Wt% S	38.98	34.10	33.07	32.98	38.82	32.86	38.15	34.02	38.24
Wt% Fe	58.41	29.76	29.24	29.31	58.34	29.10	59.21	30.25	59.15
Wt% Co	0.04	0.01	1.29	1.21	0.04	1.13	0.04	0.02	0.04
Wt% Ni	0.64	0.01	36.52	36.60	0.61	36.86	0.58	0.00	0.61
Wt% Cu	0.00	34.94	0.00	0.00	0.00	0.00	0.01	34.68	0.00
Total	98.08	98.81	100.13	100.11	97.80	99.95	98.00	98.97	98.04
Atomic% S	53.48	49.55	46.91	46.81	53.42	46.73	52.63	49.38	52.70
Atomic% Fe	46.01	24.82	23.81	23.88	46.09	23.76	46.89	25.20	46.80
Atomic% Co	0.03	0.01	0.99	0.94	0.03	0.87	0.03	0.02	0.03
Atomic% Ni	0.48	0.00	28.29	28.37	0.46	28.63	0.44	0.00	0.46
Atomic% Cu	0.00	25.61	0.00	0.00	0.00	0.00	0.00	25.40	0.00
Host	BBS	BBS	BBS	BBS	BBS	BBS	BBS	BBS	BBS
Hole	VB96266	VB96266	VB96266	VB96266	VB96266	VB96266	VB96362	VB96362	VB96362
Depth	604.5	604.5	604.5	604.5	604.5	604.5	391.00	391.00	391.00
Easting	556965.8	556965.8	556965.8	556965.8	556965.8	556965.8	553679.5	553679.5	553679.5
Northing	6242466.0	6242466.0	6242466.0	6242466.0	6242466.0	6242466.0	6243235.6	6243235.6	6243235.6

TS number	C96 2655	C96 2655	C96 2655	C96 2655	C96 2655	C96 2655	C96 2655	C96 2655	C96 2655
Wt% S	34.36	38.26	33.15	38.19	33.17	34.28	38.21	38.22	38.15
Wt% Fe	30.08	59.09	29.70	59.18	29.78	30.06	59.39	59.28	59.20
Wt% Co	0.02	0.05	1.89	0.03	1.97	0.02	0.04	0.05	0.07
Wt% Ni	0.00	0.59	35.46	0.53	35.35	0.00	0.66	0.66	0.65
Wt% Cu	34.89	0.07	0.00	0.00	0.00	35.25	0.00	0.01	0.01
Total	99.34	98.08	100.20	97.93	100.28	99.60	98.31	98.22	98.10
Atomic% S	49.63	52.72	46.96	52.70	46.95	49.44	52.56	52.61	52.60
Atomic% Fe	24.94	46.74	24.15	46.88	24.20	24.89	46.90	46.84	46.85
Atomic% Co	0.01	0.04	1.46	0.02	1.52	0.01	0.03	0.03	0.05
Atomic% Ni	0.00	0.44	27.43	0.40	27.33	0.00	0.50	0.50	0.49
Atomic% Cu	25.42	0.05	0.00	0.00	0.00	25.65	0.00	0.00	0.01
Host	BBS	BBS	BBS	BBS	BBS	BBS	BBS	BBS	BBS
Hole	VB96362	VB96362	VB96362	VB96362	VB96362	VB96362	VB96362	VB96362	VB96362
Depth	391.00	391.00	391.00	391.00	391.00	391.00	391.00	391.00	391.00
Easting	553679.5	553679.5	553679.5	553679.5	553679.5	553679.5	553679.5	553679.5	553679.5
Northing	6243235.6	6243235.6	6243235.6	6243235.6	6243235.6	6243235.6	6243235.6	6243235.6	6243235.6

TS number	C96 2655	C96 2655	C96 2655	C96 2655	C96 2655	C96 2655	C96 2655	C96 2655	C96 2655
Wt% S	38.00	38.20	32.97	34.16	34.13	34.08	33.96	37.67	37.63
Wt% Fe	59.36	59.29	29.83	30.02	29.88	29.81	29.97	59.05	58.93
Wt% Co	0.05	0.07	1.82	0.01	0.01	0.03	0.01	0.03	0.05
Wt% Ni	0.64	0.61	34.12	0.00	0.00	0.00	0.00	0.59	0.65
Wt% Cu	0.02	0.01	1.14	35.25	35.39	35.30	35.24	0.01	0.01
Total	98.08	98.19	99.90	99.46	99.42	99.22	99.20	97.35	97.27
Atomic% S	52.44	52.61	46.90	49.37	49.36	49.37	49.25	52.38	52.37
Atomic% Fe	47.02	46.87	24.36	24.91	24.80	24.79	24.95	47.14	47.08
Atomic% Co	0.04	0.05	1.41	0.01	0.01	0.02	0.01	0.02	0.04
Atomic% Ni	0.49	0.46	26.50	0.00	0.00	0.00	0.00	0.45	0.50
Atomic% Cu	0.01	0.01	0.82	25.70	25.82	25.81	25.78	0.00	0.01
Host	BBS	BBS	BBS	BBS	BBS	BBS	BBS	BBS	BBS
Hole	VB96362	VB96362	VB96362	VB96362	VB96362	VB96362	VB96362	VB96362	VB96362
Depth	391.00	391.00	391.00	391.00	391.00	391.00	391.00	391.00	391.00
Easting	553679.5	553679.5	553679.5	553679.5	553679.5	553679.5	553679.5	553679.5	553679.5
Northing	6243235.6	6243235.6	6243235.6	6243235.6	6243235.6	6243235.6	6243235.6	6243235.6	6243235.6

TS number	C96 2655	C96 2655	C96 2655	C96 2655	C96 2655	C96 2655	C96 2655	C96 2655	C96 2655
Wt% S	37.51	37.43	37.64	37.13	37.64	37.50	37.46	37.16	37.12
Wt% Fe	58.89	58.94	58.80	58.56	58.83	58.63	58.63	58 52	58.65
Wt% Co	0.04	0.06	0.04	0.04	0.06	0.05	0.05	0.05	0.07
Wt% Ni	0.67	0.64	0.64	0.55	0.65	0.66	0.66	0.67	0.66
Wt% Cu	0.00	0.00	0.00	0.00	0.00	0.02	0.03	0.00	0.00
Total	97.12	97.08	97.12	96.30	97.21	96.88	96.84	96.41	96.50
Atomic% S	52.31	52.24	52.44	52.24	52.41	52.40	52.37	52.23	52 14
Atomic% Fe	47.14	47.22	47.03	47.30	47.03	47.03	47.06	47.21	47.30
Atomic% Co	0.03	0.04	0.03	0.03	0.05	0.04	0.04	0.03	0.05
Atomic% Ni	0.51	0.49	0.48	0.42	0.50	0.51	0.51	0.52	0.51
Atomic% Cu	0.00	0.00	0.00	0.00	0.00	0.02	0.02	0.00	0.00
Host	BBS	BBS	BBS	BBS	BBS	BBS	BBS	BBS	BBS
Hole	VB96362	VB96362	VB96362	VB96362	VB96362	VB96362	VB96362	VB96362	VB96362
Depth	391.00	391.00	391.00	391.00	391.00	391.00	391.00	391.00	391.00
Easting	553679.5	553679.5	553679.5	553679.5	553679.5	553679.5	553679.5	553679.5	553679.5
Northing	6243235.6	6243235.6	6243235.6	6243235.6	6243235.6	6243235.6	6243235.6	6243235.6	6243235.6

TS number	C96 2655	C96 2655	C96 2655	C96 2655	C96 2655	C96 2655	C96 2655	C96 2655	C96 2655
Wt% S	34.51	34.44	34.51	38.02	38.27	38.43	33.91	34.46	34.16
Wt% Fe	29.99	29.97	30.11	59.32	59.27	59.30	30.02	29.99	30.05
Wt% Co	0.01	0.02	0.01	0.04	0.04	0.04	0.02	0.01	0.02
Wt% Ni	0.00	0.00	0.01	0.44	0.35	0.48	0.00	0.01	0.01
Wt% Cu	35.26	35.17	35.14	0.10	0.01	0.04	35.16	35.14	35.33
Total	99.77	99.61	99.78	97.91	97.95	98.28	99.13	99.61	99.68
Atomic% S	49.64	49.62	49.63	52.52	52.78	52.81	49.21	49.65	49.29
Atomic% Fe	24.77	24.79	24.86	47.05	46.92	46.78	25.02	24.80	24.89
Atomic% Co	0.01	0.02	0.01	0.03	0.03	0.03	0.02	0.01	0.02
Atomic% Ni	0.00	0.00	0.01	0.33	0.27	0.36	0.00	0.00	0.01
Atomic% Cu	25.59	25.57	25.50	0.07	0.01	0.03	25.75	25.54	25.72
Host	BBS	BBS	BBS	BBS	BBS	BBS	BBS	BBS	BBS
Hole	VB96362	VB96362	VB96362	VB96362	VB96362	VB96362	VB96362	VB96362	VB96362
Depth	391.00	391.00	391.00	391.00	391.00	391.00	391.00	391.00	391.00
Easting	553679.5	553679.5	553679.5	553679.5	553679.5	553679.5	553679.5	553679.5	553679.5
Northing	6243235.6	6243235.6	6243235.6	6243235.6	6243235.6	6243235.6	6243235.6	6243235.6	6243235.6

TS number	C96 2655	C96 2655	C96 2655	C96 2655	C96 2655	C96 2655	C96 2655	C96 2655	C96 2655
Wt% S	34.14	34.35	36.17	38.24	38.10	38.18	38.09	38.17	38.06
Wt% Fe	29.98	30.17	50.76	59.35	59.28	59.33	59.13	59.14	59.25
Wt% Co	0.01	0.03	0.05	0.05	0.04	0.04	0.04	0.05	0.05
Wt% Ni	0.00	0.00	0.28	0.62	0.66	0.65	0.66	0.68	0.69
Wt% Cu	35.25	35.09	9.47	0.00	0.00	0.00	0.00	0.00	0.00
Total	99.39	99.66	96.76	98.26	98.07	98.19	97.94	98.04	98.07
Atomic% S	49.38	49.50	51.47	52.62	52.55	52.58	52.59	52.64	52.51
Atomic% Fe	24.89	24.96	41.46	46.88	46.93	46.90	46.87	46.81	46.92
Atomic% Co	0.01	0.02	0.04	0.03	0.03	0.03	0.03	0.04	0.04
Atomic% Ni	0.00	0.00	0.22	0.47	0.50	0.49	0.50	0.51	0.52
Atomic% Cu	25.72	25.51	6.80	0.00	0.00	0.00	0.00	0.00	0.00
Host	BBS	BBS	BBS	BBS	BBS	BBS	BBS	BBS	BBS
Hole	VB96362	VB96362	VB96362	VB96362	VB96362	VB96362	VB96362	VB96362	VB96362
Depth	391.00	391.00	391.00	391.00	391.00	391.00	391.00	391.00	391.00
Easting	553679.5	553679.5	553679.5	553679.5	553679.5	553679.5	553679.5	553679.5	553679.5
Northing	6243235.6	6243235.6	6243235.6	6243235.6	6243235.6	6243235.6	6243235.6	6243235.6	6243235.6

TS number	C96 2655	C96 2655	C96 2655	C96 2655	C96 2655	C96 2655	C96 2655	C96 2655	C96 2655
Wt% S	38.16	38.17	38.90	38.85	38.76	38.07	33.01	37.94	38.06
Wt% Fe	59.19	59.33	58.98	59.26	59.08	59.32	29.78	59.31	59.30
Wt% Co	0.05	0.05	0.04	0.06	0.05	0.04	1.90	0.04	0.04
Wt% Ni	0.69	0.67	0.38	0.41	0.38	0.62	35.63	0.71	0.70
Wt% Cu	0.00	0.00	0.01	0.02	0.00	0.02	0.00	0.00	0.00
Total	98.10	98.22	98.30	98.58	98.27	98.09	100.32	98.00	98.12
Atomic% S	52.60	52.56	53.29	53.12	53.17	52.51	46.76	52.40	52.49
Atomic% Fe	46.84	46.90	46.39	46.52	46.52	46.97	24.22	47.03	46.95
Atomic% Co	0.04	0.04	0.03	0.04	0.04	0.03	1.46	0.03	0.03
Atomic% Ni	0.52	0.50	0.28	0.30	0.28	0.47	27.57	0.54	0.52
Atomic% Cu	0.00	0.00	0.01	0.01	0.00	0.01	0.00	0.00	0.00
Host	BBS	BBS	BBS	BBS	BBS	BBS	BBS	BBS	BBS
Hole	VB96362	VB96362	VB96362	VB96362	VB96362	VB96362	VB96362	VB96362	VB96362
Depth	391.00	391.00	391.00	391.00	391.00	391.00	391.00	391.00	391.00
Easting	553679.5	553679.5	553679.5	553679.5	553679.5	553679.5	553679.5	553679.5	553679.5
Northing	6243235.6	6243235.6	6243235.6	6243235.6	6243235.6	6243235.6	6243235.6	6243235.6	6243235.6

TS number	C96 2655	C96 2655	C96 2655	C96 2655	C96 2655	C96 2655	C96 2655	C96 2655	C96 2655
Wt% S	37.91	38.07	37.99	38.50	38.22	38.29	37.90	38.01	38.14
Wt% Fe	59.05	59.21	59.29	59.14	58.92	58.98	58.83	58.95	59.20
Wt% Co	0.05	0.04	0.05	0.04	0.04	0.06	0.05	0.06	0.02
Wt% Ni	0.70	0.68	0.62	0.51	0.68	0.68	0.64	0.59	0.71
Wt% Cu	0.00	0.01	0.00	0.02	0.00	0.00	0.00	0.00	0.00
Total	97.70	98.01	97.96	98.22	97.87	98.04	97.42	97.61	98.07
Atomic% S	52.49	52.54	52.48	52.91	52.76	52.77	52.60	52.64	52.59
Atomic% Fe	46.94	46.91	47.02	46.66	46.69	46.66	46.88	46.87	46.86
Atomic% Co	0.04	0.03	0.04	0.03	0.03	0.04	0.04	0.05	0.02
Atomic% Ni	0.53	0.51	0.47	0.38	0.51	0.51	0.49	0.45	0.53
Atomic% Cu	0.00	0.01	0.00	0.02	0.00	0.00	0.00	0.00	0.00
Host	BBS	BBS	BBS	BBS	BBS	BBS	BBS	BBS	BBS
Hole	VB96362	VB96362	VB96362	VB96362	VB96362	VB96362	VB96362	VB96362	VB96362
Depth	391.00	391.00	391.00	391.00	391.00	391.00	391.00	391.00	391.00
Easting	553679.5	553679.5	553679.5	553679.5	553679.5	553679.5	553679.5	553679.5	553679.5
Northing	6243235.6	6243235.6	6243235.6	6243235.6	6243235.6	6243235.6	6243235.6	6243235.6	6243235.6

TS number	C96 2655	C96 2655	C96 2655	C96 2655	C96 2655	C96 2655	C96 2655	C96 2655	C96 2655
Wt% S	38.74	38.63	38.53	38.76	38.42	38.88	38.72	38.55	38.72
Wt% Fe	59.34	59.29	59.37	59.31	59.11	59.08	58.21	59.32	59.35
Wt% Co	0.03	0.04	0.06	0.04	0.04	0.05	0.11	0.04	0.05
Wt% Ni	0.71	0.68	0.67	0.68	0.64	0.29	1.81	0.63	0.70
Wt% Cu	0.00	0.02	0.00	0.00	0.02	0.01	0.00	0.01	0.00
Total	98.81	98.68	98.64	98.80	98.24	98.31	98.86	98.55	98.84
Atomic% S	52.92	52.86	52.77	52.95	52.82	53.27	52.90	52.83	52.89
Atomic% Fe	46.53	46.57	46.68	46.51	46.65	46.47	45.66	46.66	46.54
Atomic% Co	0.03	0.03	0.04	0.03	0.03	0.03	0.08	0.03	0.04
Atomic% Ni	0.53	0.51	0.50	0.51	0.48	0.21	1.35	0.47	0.52
Atomic% Cu	0.00	0.01	0.00	0.00	0.02	0.00	0.00	0.01	0.00
Host	BBS	BBS	BBS	BBS	BBS	BBS	BBS	BBS	BBS
Hole	VB96362	VB96362	VB96362	VB96362	VB96362	VB96362	VB96362	VB96362	VB96362
Depth	391.00	391.00	391.00	391.00	391.00	391.00	391.00	391.00	391.00
Easting	553679.5	553679.5	553679.5	553679.5	553679.5	553679.5	553679.5	553679.5	553679.5
Northing	6243235.6	6243235.6	6243235.6	6243235.6	6243235.6	6243235.6	6243235.6	6243235.6	6243235.6

TS number	C96 2655	C96 2655	C96 2655	C96 2655	C96 2655	C96 2655	C96 2655	C96 2655	C96 2655
Wt% S	38.17	37.95	38.47	33.00	38.00	38.39	32.82	37.92	38.03
Wt% Fe	59.17	59.08	59.15	30.17	59.27	59.45	30.53	59.58	59.44
Wt% Co	0.05	0.06	0.03	1.69	0.05	0.04	1.63	0.03	0.03
Wt% Ni	0.69	0.72	0.47	34.78	0.53	0.36	34.89	0.39	0.40
Wt% Cu	0.00	0.01	0.00	0.00	0.00	0.01	0.00	0.00	0.00
Total	98.08	97.83	98.12	99.64	97.86	98.26	99.88	97.93	97.90
Atomic% S	52.62	52.49	52.91	46.99	52.53	52.77	46.70	52.41	52.54
Atomic% Fe	46.82	46.91	46.71	24.66	47.03	46.92	24.93	47.27	47.14
Atomic% Co	0.04	0.05	0.02	1.31	0.04	0.03	1.26	0.02	0.02
Atomic% Ni	0.52	0.55	0.36	27.05	0.40	0.27	27.10	0.30	0.30
Atomic% Cu	0.00	0.01	0.00	0.00	0.00	0.01	0.00	0.00	0.00
Host	BBS	BBS	BBS	BBS	BBS	BBS	BBS	BBS	BBS
Hole	VB96362	VB96362	VB96362	VB96362	VB96362	VB96362	VB96362	VB96362	VB96362
Depth	391.00	391.00	391.00	391.00	391.00	391.00	391.00	391.00	391.00
Easting	553679.5	553679.5	553679.5	553679.5	553679.5	553679.5	553679.5	553679.5	553679.5
Northing	6243235.6	6243235.6	6243235.6	6243235.6	6243235.6	6243235.6	6243235.6	6243235.6	6243235.6

TS number	C96 2655	C96 2655	C96 2655	C96 2655	C96 2655	C96 2655	C96 2655	C96 2655	C96 2655
Wt% S	33.05	34.08	34.38	38.57	34.45	34.62	34.00	38.10	37.89
Wt% Fe	30.45	29.67	29.63	59.34	29.87	30.00	29.94	59.19	59.12
Wt% Co	1.73	0.06	0.02	0.05	0.01	0.02	0.03	0.05	0.06
Wt% Ni	35.00	0.37	0.00	0.52	0.00	0.00	0.00	0.54	0.66
Wt% Cu	0.00	34.22	34.80	0.00	35.14	35.10	35.24	0.00	0.00
Total	100.23	98.40	98.83	98.47	99.47	99.73	99.20	97.89	97.72
Atomic% S	46.82	49.67	49.85	52.87	49.69	49.77	49.29	52.62	52.47
Atomic% Fe	24.77	24.82	24.67	46.70	24.73	24.76	24.92	46.92	46.99
Atomic% Co	1.34	0.05	0.01	0.03	0.00	0.02	0.02	0.04	0.04
Atomic% Ni	27.08	0.29	0.00	0.39	0.00	0.00	0.00	0.41	0.50
Atomic% Cu	0.00	25.17	25.47	0.00	25.57	25.46	25.77	0.00	0.00
Host	BBS	BBS	BBS	BBS	BBS	BBS	BBS	BBS	BBS
Hole	VB96362	VB96362	VB96362	VB96362	VB96362	VB96362	VB96362	VB96362	VB96362
Depth	391.00	391.00	391.00	391.00	391.00	391.00	391.00	391.00	391.00
Easting	553679.5	553679.5	553679.5	553679.5	553679.5	553679.5	553679.5	553679.5	553679.5
Northing	6243235.6	6243235.6	6243235.6	6243235.6	6243235.6	6243235.6	6243235.6	6243235.6	6243235.6

TS number	C96 2655	C96 2655	C96 2655	C96 2655	C96 2655	C96 2655	C96 2655	C96 2655	C96 2655
Wt% S	33.20	33.09	32.87	24.83	32.40	30.52	33.04	32.56	32.84
Wt% Fe	30.55	30.61	30.64	28.59	30.44	29.17	30.73	30.57	30.44
Wt% Co	1.74	1.72	1.72	1.25	1.72	1.68	1.73	1.74	1.77
Wt% Ni	34.80	34.96	34.98	25.25	33.56	32.61	34.71	34.35	34.62
Wt% Cu	0.00	0.00	0.00	0.00	0.00	0.00	0.00	0.00	0.00
Total	100.29	100.38	100.21	79.92	98.13	93.99	100.23	99.23	99.69
Atomic% S	46.97	46.81	46.63	44.56	46.86	46.25	46.80	46.64	46.79
Atomic% Fe	24.81	24.86	24.95	29.46	25.28	25.37	25.00	25.14	24.89
Atomic% Co	1.34	1.33	1.33	1.23	1.35	1.38	1.34	1.36	1.37
Atomic% Ni	26.88	27.01	27.09	24.75	26.51	26.98	26.86	26.87	26.93
Atomic% Cu	0.00	0.00	0.00	0.00	0.00	0.00	0.00	0.00	0.00
Host	BBS	BBS	BBS	BBS	BBS	BBS	BBS	BBS	BBS
Hole	VB96362	VB96362	VB96362	VB96362	VB96362	VB96362	VB96362	VB96362	VB96362
Depth	391.00	391.00	391.00	391.00	391.00	391.00	391.00	391.00	391.00
Easting	553679.5	553679.5	553679.5	553679.5	553679.5	553679.5	553679.5	553679.5	553679.5
Northing	6243235.6	6243235.6	6243235.6	6243235.6	6243235.6	6243235.6	6243235.6	6243235.6	6243235.6

TS number	C96 2655	C96 2655	C96 2655	C96 2655	C96 2655	C96 2655	C96 2655	C96 2655	C96 2655
Wt% S	33.71	34.03	34.23	34.32	34.26	34.12	37.95	37.92	37.86
Wt% Fe	29.85	29.97	29.91	29.94	29.98	29.91	59.55	59.55	59.49
Wt% Co	0.01	0.01	0.02	0.01	0.02	0.03	0.04	0.03	0.03
Wt% Ni	0.00	0.00	0.00	0.00	0.00	0.00	0.50	0.53	0.56
Wt% Cu	35.28	35.20	35.21	35.21	35.07	35.23	0.00	0.02	0.00
Total	98.86	99.21	99.39	99.50	99.33	99.29	98.04	98.04	97.96
Atomic% S	49.10	49.32	49.47	49.53	49.53	49.39	52.39	52.36	52.33
Atomic% Fe	24.96	24.93	24.82	24.80	24.88	24.85	47.20	47.21	47.21
Atomic% Co	0.01	0.01	0.02	0.00	0.02	0.02	0.03	0.02	0.03
Atomic% Ni	0.00	0.00	0.00	0.00	0.00	0.00	0.38	0.40	0.42
Atomic% Cu	25.92	25.74	25.68	25.64	25.58	25.73	0.00	0.01	0.00
Host	BBS	BBS	BBS	BBS	BBS	BBS	BBS	BBS	BBS
Hole	VB96362	VB96362	VB96362	VB96362	VB96362	VB96362	VB96362	VB96362	VB96362
Depth	391.00	391.00	391.00	391.00	391.00	391.00	391.00	391.00	391.00
Easting	553679.5	553679.5	553679.5	553679.5	553679.5	553679.5	553679.5	553679.5	553679.5
Northing	6243235.6	6243235.6	6243235.6	6243235.6	6243235.6	6243235.6	6243235.6	6243235.6	6243235.6

TS number	C96 2655	C96 2655	C96 2655	C96 2655	C96 2655	C96 2655	C96 2655	C96 2655	C96 2655
Wt% S	37.85	37.92	38.01	34.15	37.89	37.43	34.02	38.01	34.01
Wt% Fe	59.39	59.39	59.23	30.02	58.14	59.14	30.07	59.17	29.71
Wt% Co	0.06	0.05	0.03	0.01	0.07	0.05	0.02	0.03	0.02
Wt% Ni	0.60	0.60	0.69	0.01	1.76	0.62	0.00	0.62	0.00
Wt% Cu	0.00	0.00	0.00	35.05	0.00	0.00	35.07	0.00	35.09
Total	97.90	97.97	97.96	99.29	97.88	97.24	99.18	97.84	98.83
Atomic% S	52.34	52.39	52.49	49.42	52.43	52.17	49.32	52.54	49.45
Atomic% Fe	47.16	47.10	46.97	24.94	46.18	47.33	25.02	46.96	24.80
Atomic% Co	0.04	0.04	0.02	0.01	0.05	0.03	0.02	0.02	0.02
Atomic% Ni	0.45	0.45	0.52	0.01	1.33	0.47	0.00	0.47	0.00
Atomic% Cu	0.00	0.00	0.00	25.59	0.00	0.00	25.65	0.00	25.74
Host	BBS	BBS	BBS	BBS	BBS	BBS	BBS	BBS	BBS
Hole	VB96362	VB96362	VB96362	VB96362	VB96362	VB96362	VB96362	VB96362	VB96362
Depth	391.00	391.00	391.00	391.00	391.00	391.00	391.00	391.00	391.00
Easting	553679.5	553679.5	553679.5	553679.5	553679.5	553679.5	553679.5	553679.5	553679.5
Northing	6243235.6	6243235.6	6243235.6	6243235.6	6243235.6	6243235.6	6243235.6	6243235.6	6243235.6

TS number	C96 2655	C96 2655	C97 0842	C97 0842	C97 0842	C97 0842	C97 0842	C97 0842	C97 0842
Wt% S	33.04	37.63	38.16	38.72	37.35	38.16	33.08	38.16	31.49
Wt% Fe	30.54	59.37	59.07	58.29	57.07	58.81	27.48	59.19	26.32
Wt% Co	1.66	0.04	0.05	0.04	0.05	0.05	0.01	0.04	0.01
Wt% Ni	35.38	0.57	0.38	0.23	0.30	0.32	0.02	0.35	0.01
Wt% Cu	0.00	0.00	0.03	0.00	0.01	0.01	33.68	0.00	32.40
Total	100.63	97.61	97.72	97.30	94.79	97.34	94.28	97.74	90.24
Atomic% S	46.66	52.23	52.75	53.53	53.12	52.91	50.23	52.74	50.02
Atomic% Fe	24.77	47.31	46.88	46.26	46.60	46.81	23.95	46.97	24.00
Atomic% Co	1.27	0.03	0.04	0.03	0.04	0.03	0.01	0.03	0.01
Atomic% Ni	27.29	0.43	0.29	0.18	0.24	0.24	0.02	0.26	0.00
Atomic% Cu	0.00	0.00	0.02	0.00	0.01	0.00	25.80	0.00	25.97
Host	BBS	BBS	BBS	BBS	BBS	BBS	BBS	BBS	BBS
Hole	VB96362	VB96362	VB95162	VB95162	VB95162	VB95162	VB95162	VB95162	VB95162
Depth	391.00	391.00	263.30	263.30	263.30	263.30	263.30	263.30	263.30
Easting	553679.5	553679.5	555047.7	555047.7	555047.7	555047.7	555047.7	555047.7	555047.7
Northing	6243235.6	6243235.6	6243528.6	6243528.6	6243528.6	6243528.6	6243528.6	6243528.6	6243528.6

TS number	C97 0842	C97 0842	C97 0842	C97 0842	C97 0842	C97 0842	C97 0842	C97 0842	C97 0842
Wt% S	32.95	33.51	38.21	32.36	32.04	32.69	38.06	38.25	34.17
Wt% Fe	30.47	30.96	59.26	30.50	30.40	30.46	58.81	59.18	29.44
Wt% Co	1.31	1.64	0.05	1.49	1.52	1.50	0.03	0.03	0.01
Wt% Ni	33.83	33.90	0.28	32.77	32.57	33.14	0.25	0.30	0.00
Wt% Cu	0.07	0.00	0.00	0.00	0.00	0.00	0.00	0.03	34.68
Total	98.65	100.03	97.80	97.13	96.53	97.79	97.17	97.78	98.30
Atomic% S	47.29	47.40	52.77	47.19	47.05	47.32	52.87	52.82	49.83
Atomic% Fe	25.10	25.14	46.98	25.53	25.62	25.31	46.90	46.91	24.64
Atomic% Co	1.03	1.26	0.04	1.18	1.22	1.18	0.03	0.02	0.01
Atomic% Ni	26.52	26.18	0.21	26.09	26.12	26.20	0.19	0.22	0.00
Atomic% Cu	0.05	0.00	0.00	0.00	0.00	0.00	0.00	0.02	25.52
Host	BBS	BBS	BBS	BBS	BBS	BBS	BBS	BBS	BBS
Hole	VB95162	VB95162	VB95162	VB95162	VB95162	VB95162	VB95162	VB95162	VB95162
Depth	263.30	263.30	263.30	263.30	263.30	263.30	263.30	263.30	263.30
Easting	555047.7	555047.7	555047.7	555047.7	555047.7	555047.7	555047.7	555047.7	555047.7
Northing	6243528.6	6243528.6	6243528.6	6243528.6	6243528.6	6243528.6	6243528.6	6243528.6	6243528.6

TS number	C97 0842	C97 0842	C97 0842	C97 0842	C97 0842	C97 0842	C97 0842	C97 0842	C97 0842
Wt% S	32.15	32.96	37.81	34.76	33.24	34.64	38.60	33.27	33.31
Wt% Fe	31.15	31.26	58.62	29.31	31.18	29.04	59.65	32.99	32.97
Wt% Co	1.54	1.62	0.04	0.03	1.46	0.02	0.04	1.29	1.31
Wt% Ni	33.27	33.96	0.32	0.00	33.09	0.00	0.24	33.08	32.97
Wt% Cu	0.00	0.00	0.04	34.64	0.00	34.47	0.01	0.00	0.00
Total	98.12	99.79	96.82	98.74	98.97	98.16	98.54	100.63	100.57
Atomic% S	46.57	46.87	52.76	50.32	47.49	50.41	52.87	46.88	46.95
Atomic% Fe	25.90	25.51	46.95	24.36	25.57	24.26	46.91	26.68	26.67
Atomic% Co	1.21	1.25	0.03	0.02	1.13	0.02	0.03	0.99	1.01
Atomic% Ni	26.31	26.37	0.24	0.00	25.81	0.00	0.18	25.45	25.38
Atomic% Cu	0.00	0.00	0.03	25.30	0.00	25.31	0.01	0.00	0.00
Host	BBS	BBS	BBS	BBS	BBS	BBS	BBS	BBS	BBS
Hole	VB95162	VB95162	VB95162	VB95162	VB95162	VB95162	VB95162	VB95162	VB95162
Depth	263.30	263.30	263.30	263.30	263.30	263.30	263.30	263.30	263.30
Easting	555047.7	555047.7	555047.7	555047.7	555047.7	555047.7	555047.7	555047.7	555047.7
Northing	6243528.6	6243528.6	6243528.6	6243528.6	6243528.6	6243528.6	6243528.6	6243528.6	6243528.6

TS number	C97 0842	C97 0842	C97 0842	C97 0842	C97 0842	C97 0842	C97 0842	C97 0842	C97 0842
Wt% S	33.49	33.08	38.15	38.65	33.17	35.12	34.95	38.46	32.97
Wt% Fe	33.09	32.78	59.92	59.59	32.23	29.99	30.07	59.85	32.30
Wt% Co	1.47	1.56	0.04	0.04	1.54	0.02	0.02	0.04	1.55
Wt% Ni	32.74	32.73	0.27	0.27	33.55	0.00	0.00	0.22	33.10
Wt% Cu	0.00	0.00	0.00	0.02	0.00	35.17	35.07	0.01	0.00
Total	100.80	100.16	98.39	98.58	100.49	100.29	100.11	98.59	99.92
Atomic% S	47.06	46.84	52.46	52.91	46.83	50.11	49.98	52.71	46.82
Atomic% Fe	26.69	26.65	47.30	46.83	26.12	24.56	24.69	47.09	26.32
Atomic% Co	1.12	1.20	0.03	0.03	1.18	0.02	0.02	0.03	1.19
Atomic% Ni	25.12	25.31	0.20	0.20	25.87	0.00	0.00	0.16	25.67
Atomic% Cu	0.00	0.00	0.00	0.02	0.00	25.32	25.31	0.01	0.00
Host	BBS	BBS	BBS	BBS	BBS	BBS	BBS	BBS	BBS
Hole	VB95162	VB95162	VB95162	VB95162	VB95162	VB95162	VB95162	VB95162	VB95162
Depth	263.30	263.30	263.30	263.30	263.30	263.30	263.30	263.30	263.30
Easting	555047.7	555047.7	555047.7	555047.7	555047.7	555047.7	555047.7	555047.7	555047.7
Northing	6243528.6	6243528.6	6243528.6	6243528.6	6243528.6	6243528.6	6243528.6	6243528.6	6243528.6

TS number	C97 0842	C97 0842	C97 0842	C97 0842	C97 0842	C97 0842	C97 0842	C97 0842	C97 0842
Wt% S	34.28	38.65	33.12	33.22	34.13	38.16	38.44	38.27	31.36
Wt% Fe	29.56	59.88	31.99	31.93	29.87	59.79	59.90	59.93	30.93
Wt% Co	0.02	0.05	1.56	1.51	0.05	0.05	0.03	0.03	1.41
Wt% Ni	0.04	0.26	33.63	33.86	0.36	0.29	0.32	0.33	32.60
Wt% Cu	34.29	0.01	0.00	0.00	34.78	0.00	0.00	0.01	0.00
Total	98.21	98.86	100.29	100.52	99.19	98.29	98.71	98.58	96.31
Atomic% S	49.97	52.79	46.85	46.88	49.43	52.51	52.64	52.51	46.33
Atomic% Fe	24.74	46.96	25.98	25.87	24.84	47.24	47.08	47.21	26.23
Atomic% Co	0.02	0.04	1.20	1.16	0.04	0.03	0.02	0.02	1.14
Atomic% Ni	0.03	0.19	25.98	26.09	0.28	0.22	0.24	0.25	26.30
Atomic% Cu	25.22	0.01	0.00	0.00	25.41	0.00	0.00	0.01	0.00
Host	BBS	BBS	BBS	BBS	BBS	BBS	BBS	BBS	BBS
Hole	VB95162	VB95162	VB95162	VB95162	VB95162	VB95162	VB95162	VB95162	VB95162
Depth	263.30	263.30	263.30	263.30	263.30	263.30	263.30	263.30	263.30
Easting	555047.7	555047.7	555047.7	555047.7	555047.7	555047.7	555047.7	555047.7	555047.7
Northing	6243528.6	6243528.6	6243528.6	6243528.6	6243528.6	6243528.6	6243528.6	6243528.6	6243528.6

TS number	C97 0842	C97 0842	C96 0197	C96 0197	C96 0197	C96 0197	C96 0197	C96 0197	C96 0197
Wt% S	34.58	38.37	37.89	37.93	32.98	38.35	38.01	34.27	32.97
Wt% Fe	29.83	59.91	59.50	59.44	29.53	59.39	59.53	29.97	29.97
Wt% Co	0.01	0.05	0.04	0.05	3.12	0.04	0.04	0.02	2.85
Wt% Ni	0.01	0.21	0.54	0.54	34.18	0.51	0.44	0.00	34.32
Wt% Cu	35.14	0.02	0.01	0.01	0.00	0.00	0.00	35.12	0.00
Total	99.59	98.55	97.98	97.97	99.82	98.28	98.04	99.39	100.12
Atomic% S	49.79	52.63	52.36	52.40	46.92	52.72	52.46	49.52	46.79
Atomic% Fe	24.66	47.17	47.20	47.15	24.11	46.87	47.16	24.86	24.42
Atomic% Co	0.01	0.03	0.03	0.04	2.42	0.03	0.03	0.01	2.20
Atomic% Ni	0.01	0.16	0.41	0.41	26.55	0.38	0.33	0.00	26.59
Atomic% Cu	25.53	0.01	0.01	0.01	0.00	0.00	0.00	25.60	0.00
Host	BBS	BBS	BBS	BBS	BBS	BBS	BBS	BBS	BBS
Hole	VB95162	VB95162	VB98461c	VB98461c	VB98461c	VB98461c	VB98461c	VB98461c	VB98461c
Depth	263.30	263.30	1560.60	1560.60	1560.60	1560.60	1560.60	1560.60	1560.60
Easting	555047.7	555047.7	554897.6	554897.6	554897.6	554897.6	554897.6	554897.6	554897.6
Northing	6243528.6	6243528.6	6242852.3	6242852.3	6242852.3	6242852.3	6242852.3	6242852.3	6242852.3

TS number	C96 0197	C96 0197	C96 0197	C96 0197	C96 0197	C96 0197	C96 0197	C96 0197	C96 0197
Wt% S	38.11	38.18	34.44	34.28	38.06	38.08	32.75	38.09	38.01
Wt% Fe	59.28	59.33	30.02	29.97	59.37	59.20	29.77	59.47	59.45
Wt% Co	0.05	0.05	0.01	0.02	0.04	0.05	2.95	0.05	0.06
Wt% Ni	0.53	0.53	0.00	0.00	0.52	0.59	34.29	0.58	0.57
Wt% Cu	0.02	0.02	34.86	34.80	0.01	0.01	0.00	0.00	0.01
Total	97.99	98.11	99.33	99.10	98.00	97.94	99.79	98.19	98.12
Atomic% S	52.59	52.62	49.73	49.63	52.53	52.58	46.67	52.48	52.43
Atomic% Fe	46.96	46.94	24.88	24.91	47.04	46.92	24.35	47.04	47.08
Atomic% Co	0.04	0.03	0.01	0.02	0.03	0.04	2.29	0.04	0.05
Atomic% Ni	0.40	0.40	0.00	0.00	0.39	0.45	26.68	0.43	0.43
Atomic% Cu	0.02	0.02	25.39	25.42	0.01	0.01	0.00	0.00	0.00
Host	BBS	BBS	BBS	BBS	BBS	BBS	BBS	BBS	BBS
Hole	VB98461c	VB98461c	VB98461c	VB98461c	VB98461c	VB98461c	VB98461c	VB98461c	VB98461c
Depth	1560.60	1560.60	1560.60	1560.60	1560.60	1560.60	1560.60	1560.60	1560.60
Easting	554897.6	554897.6	554897.6	554897.6	554897.6	554897.6	554897.6	554897.6	554897.6
Northing	6242852.3	6242852.3	6242852.3	6242852.3	6242852.3	6242852.3	6242852.3	6242852.3	6242852.3

TS number	C96 0197	C96 0197	C96 0197	C96 0197	C96 0197	C96 0197	C96 0197	C96 0197	C96 0197
Wt% S	32.98	32.77	38.09	38.04	33.98	37.84	38.27	38.41	34.76
Wt% Fe	29.91	29.79	59.59	59.51	30.06	59.45	59.48	59.56	30.24
Wt% Co	2.99	2.92	0.04	0.04	0.01	0.05	0.05	0.05	0.03
Wt% Ni	33.57	33.64	0.40	0.55	0.00	0.52	0.57	0.53	0.00
Wt% Cu	0.00	0.00	0.00	0.00	34.93	0.03	0.02	0.00	34.70
Total	99.45	99.15	98.13	98.17	98.99	97.90	98.40	98.56	99.73
Atomic% S	47.04	46.92	52.51	52.44	49.34	52.34	52.59	52.68	49.91
Atomic% Fe	24.50	24.49	47.16	47.09	25.06	47.20	46.92	46.89	24.93
Atomic% Co	2.32	2.28	0.03	0.03	0.01	0.04	0.04	0.04	0.02
Atomic% Ni	26.15	26.30	0.30	0.41	0.00	0.39	0.43	0.40	0.00
Atomic% Cu	0.00	0.00	0.00	0.00	25.59	0.02	0.02	0.00	25.14
Host	BBS	BBS	BBS	BBS	BBS	BBS	BBS	BBS	BBS
Hole	VB98461c	VB98461c	VB98461c	VB98461c	VB98461c	VB98461c	VB98461c	VB98461c	VB98461c
Depth	1560.60	1560.60	1560.60	1560.60	1560.60	1560.60	1560.60	1560.60	1560.60
Easting	554897.6	554897.6	554897.6	554897.6	554897.6	554897.6	554897.6	554897.6	554897.6
Northing	6242852.3	6242852.3	6242852.3	6242852.3	6242852.3	6242852.3	6242852.3	6242852.3	6242852.3

TS number	C96 0197	C96 0197	C96 0197	C99 0363	C99 0363	C99 0363	C99 0363	C99 0363	C99 0363
Wt% S	38.28	34.52	37.93	32.95	38.81	39.30	37.78	33.42	39.29
Wt% Fe	59.51	29.85	59.42	25.95	59.31	59.07	57.16	29.06	58.55
Wt% Co	0.06	0.02	0.03	9.62	0.11	0.10	0.15	6.23	0.13
Wt% Ni	0.50	0.00	0.45	32.04	0.38	0.40	0.09	31.22	0.58
Wt% Cu	0.01	35.13	0.00	0.00	0.03	0.00	0.01	0.60	0.16
Total	98.37	99.52	97.83	100.55	98.67	98.88	95.19	100.55	98.71
Atomic% S	52.61	49.74	52.46	46.69	53.04	53.48	53.42	47.16	53.55
Atomic% Fe	46.95	24.70	47.18	21.11	46.54	46.14	46.39	23.54	45.81
Atomic% Co	0.04	0.02	0.02	7.41	0.08	0.08	0.12	4.78	0.10
Atomic% Ni	0.37	0.00	0.34	24.79	0.28	0.30	0.07	24.06	0.43
Atomic% Cu	0.01	25.54	0.00	0.00	0.02	0.00	0.01	0.43	0.11
Host	BBS	BBS	BBS	BBS	BBS	BBS	BBS	BBS	BBS
Hole	VB98461c	VB98461c	VB98461c	VB98478	VB98478	VB98478	VB98478	VB98478	VB98478
Depth	1560.60	1560.60	1560.60	555.00	555.00	555.00	555.00	555.00	555.00
Easting	554897.6	554897.6	554897.6	556846.9	556846.9	556846.9	556846.9	556846.9	556846.9
Northing	6242852.3	6242852.3	6242852.3	6243167.0	6243167.0	6243167.0	6243167.0	6243167.0	6243167.0

TS number	C99 0363	C99 0363	C99 0363	C99 0318	C99 0318	C99 0318	C99 0318	C99 0318	C99 0318
Wt% S	38.53	39.02	39.13	34.45	37.52	38.04	32.71	33.78	37.67
Wt% Fe	59.53	58.84	58.88	30.01	59.52	59.71	30.50	29.92	59.35
Wt% Co	0.07	0.09	0.09	0.01	0.04	0.04	1.53	0.01	0.04
Wt% Ni	0.27	0.47	0.46	0.00	0.57	0.52	35.35	0.01	0.51
Wt% Cu	0.26	0.00	0.03	35.10	0.01	0.00	0.00	35.13	0.00
Total	98.68	98.43	98.59	99.58	97.66	98.32	100.10	98.85	97.58
Atomic% S	52.76	53.37	53.43	49.64	52.09	52.38	46.49	49.17	52.28
Atomic% Fe	46.80	46.20	46.15	24.82	47.44	47.20	24.89	25.01	47.30
Atomic% Co	0.05	0.07	0.06	0.01	0.03	0.03	1.19	0.01	0.03
Atomic% Ni	0.20	0.35	0.34	0.00	0.43	0.39	27.43	0.01	0.39
Atomic% Cu	0.18	0.00	0.02	25.52	0.01	0.00	0.00	25.80	0.00
Host	BBS	BBS	BBS	BBS	BBS	BBS	BBS	BBS	BBS
Hole	VB98478	VB98478	VB98478	VB99492	VB99492	VB99492	VB99492	VB99492	VB99492
Depth	555.00	555.00	555.00	1995.00	1995.00	1995.00	1995.00	1995.00	1995.00
Easting	556846.9	556846.9	556846.9	N/A	N/A	N/A	N/A	N/A	N/A
Northing	6243167.0	6243167.0	6243167.0	N/A	N/A	N/A	N/A	N/A	N/A

TS number	C99 0318	C99 0318	C99 0318	C99 0318	C99 0318	C99 0318	C99 0318	C99 0318	C99 0318
Wt% S	37.74	37.96	32.89	33.87	32.51	34.07	37.48	37.22	33.92
Wt% Fe	59.53	59.70	30.07	30.43	30.20	29.99	60.02	60.29	29.85
Wt% Co	0.04	0.04	1.40	0.03	1.47	0.03	0.06	0.04	0.01
Wt% Ni	0.52	0.52	35.48	0.00	35.14	0.00	0.26	0.24	0.01
Wt% Cu	0.00	0.01	0.00	34.69	0.00	35.11	0.00	0.02	34.99
Total	97.82	98.23	99.83	99.05	99.31	99.20	97.82	97.82	98.78
Atomic% S	52.26	52.33	46.80	49.18	46.55	49.37	51.98	51.70	49.36
Atomic% Fe	47.32	47.24	24.56	25.36	24.83	24.94	47.78	48.07	24.94
Atomic% Co	0.03	0.03	1.08	0.03	1.14	0.02	0.04	0.03	0.01
Atomic% Ni	0.39	0.39	27.56	0.00	27.48	0.00	0.20	0.18	0.01
Atomic% Cu	0.00	0.01	0.00	25.42	0.00	25.66	0.00	0.01	25.69
Host	BBS	BBS	BBS	BBS	BBS	BBS	BBS	BBS	BBS
Hole	VB99492	VB99492	VB99492	VB99492	VB99492	VB99492	VB99492	VB99492	VB99492
Depth	1995.00	1995.00	1995.00	1995.00	1995.00	1995.00	1995.00	1995.00	1995.00
Easting	N/A	N/A	N/A	N/A	N/A	N/A	N/A	N/A	N/A
Northing	N/A	N/A	N/A	N/A	N/A	N/A	N/A	N/A	N/A

TS number	C99 0318	C99 0318	C99 0318	C99 0263	C99 0263	C99 0263	C99 0263	C99 0263	C99 0263
Wt% S	35.65	32.86	37.98	38.47	38.80	38.70	32.84	32.16	39.21
Wt% Fe	57.75	32.06	58.96	59.68	58.87	59.09	30.06	30.08	58.72
Wt% Co	0.03	1.63	0.04	0.03	0.05	0.06	1.00	1.09	0.04
Wt% Ni	0.26	33.47	0.29	0.39	0.38	0.30	32.45	34.63	0.29
Wt% Cu	0.00	0.00	0.00	0.03	0.06	0.04	2.94	0.10	0.08
Total	93.68	100.01	97.28	98.60	98.17	98.21	99.41	98.07	98.35
Atomic% S	51.70	46.66	52.74	52.72	53.25	53.13	46.98	46.62	53.61
Atomic% Fe	48.08	26.14	47.00	46.95	46.39	46.57	24.68	25.03	46.08
Atomic% Co	0.02	1.26	0.03	0.02	0.04	0.04	0.78	0.86	0.03
Atomic% Ni	0.21	25.95	0.22	0.29	0.28	0.22	25.35	27.41	0.22
Atomic% Cu	0.00	0.00	0.00	0.02	0.04	0.03	2.12	0.08	0.06
Host	BBS	BBS	BBS	BBS	BBS	BBS	BBS	BBS	BBS
Hole	VB99492	VB99492	VB99492	VB99495	VB99495	VB99495	VB99495	VB99495	VB99495
Depth	1995.00	1995.00	1995.00	1146.00	1146.00	1146.00	1146.00	1146.00	1146.00
Easting	N/A	N/A	N/A	N/A	N/A	N/A	N/A	N/A	N/A
Northing	N/A	N/A	N/A	N/A	N/A	N/A	N/A	N/A	N/A

TS number	C99 0263	C99 0263	C99 0263	C99 0263	C99 0263	C99 0263	C99 0263	C99 0263	C99 0263
Wt% S	34.91	39.27	38.44	33.19	33.30	34.39	38.36	33.19	33.42
Wt% Fe	30.06	58.69	59.43	30.56	30.56	30.01	59.52	30.22	30.25
Wt% Co	0.02	0.04	0.03	1.52	1.53	0.02	0.03	1.12	1.01
Wt% Ni	0.00	0.37	0.55	35.12	35.28	0.00	0.51	36.18	36.34
Wt% Cu	34.97	0.02	0.01	0.00	0.00	35.15	0.01	0.00	0.00
Total	99.98	98.41	98.45	100.39	100.67	99.57	98.43	100.71	101.03
Atomic% S	49.99	53.64	52.75	46.92	46.94	49.58	52.67	46.81	46.95
Atomic% Fe	24.71	46.03	46.82	24.80	24.73	24.84	46.91	24.47	24.40
Atomic% Co	0.02	0.03	0.02	1.17	1.18	0.01	0.02	0.86	0.77
Atomic% Ni	0.00	0.28	0.41	27.12	27.16	0.00	0.38	27.86	27.88
Atomic% Cu	25.27	0.02	0.01	0.00	0.00	25.57	0.01	0.00	0.00
Host	BBS	BBS	BBS	BBS	BBS	BBS	BBS	BBS	BBS
Hole	VB99495	VB99495	VB99495	VB99495	VB99495	VB99495	VB99495	VB99495	VB99495
Depth	1146.00	1146.00	1146.00	1146.00	1146.00	1146.00	1146.00	1146.00	1146.00
Easting	N/A	N/A	N/A	N/A	N/A	N/A	N/A	N/A	N/A
Northing	N/A	N/A	N/A	N/A	N/A	N/A	N/A	N/A	N/A

TS number	C99 0263	C99 0263	C99 0263	C99 0263	C99 0263	C99 0263	C99 0263	C99 0263	C99 0263
Wt% S	38.52	38.48	38.68	34.82	38.46	38.37	38.42	38.48	33.33
Wt% Fe	59.25	59.32	59.24	29.81	59.20	59.40	59.29	59.27	30.52
Wt% Co	0.03	0.05	0.03	0.00	0.05	0.03	0.04	0.04	1.07
Wt% Ni	0.50	0.59	0.52	0.00	0.62	0.63	0.60	0.65	35.41
Wt% Cu	0.02	0.01	0.02	34.73	0.01	0.01	0.04	0.00	0.00
Total	98.32	98.46	98.49	99.37	98.34	98.44	98.38	98.43	100.34
Atomic% S	52.89	52.78	52.99	50.13	52.82	52.68	52.76	52.80	47.09
Atomic% Fe	46.70	46.72	46.59	24.64	46.67	46.82	46.74	46.69	24.75
Atomic% Co	0.02	0.04	0.02	0.00	0.04	0.02	0.03	0.03	0.82
Atomic% Ni	0.37	0.44	0.39	0.00	0.47	0.47	0.45	0.48	27.33
Atomic% Cu	0.01	0.01	0.01	25.23	0.00	0.01	0.03	0.00	0.00
Host	BBS	BBS	BBS	BBS	BBS	BBS	BBS	BBS	BBS
Hole	VB99495	VB99495	VB99495	VB99495	VB99495	VB99495	VB99495	VB99495	VB99495
Depth	1146.00	1146.00	1146.00	1146.00	1146.00	1146.00	1146.00	1146.00	1146.00
Easting	N/A	N/A	N/A	N/A	N/A	N/A	N/A	N/A	N/A
Northing	N/A	N/A	N/A	N/A	N/A	N/A	N/A	N/A	N/A

TS number	C99 0263	C99 0263	C99 0263	C99 0263	C99 0263	C99 0263	C97 0263	C97-1080	C97-1080
Wt% S	34.46	38.57	34.21	32.62	33.45	33.30	34.96	38.21	38.90
Wt% Fe	29.80	59.49	29.62	29.44	30.37	30.40	29.57	61.35	60.69
Wt% Co	0.01	0.04	0.01	1.06	1.17	1.10	0.02	0.04	0.05
Wt% Ni	0.01	0.62	0.02	35.53	35.48	35.36	0.01	0.27	0.18
Wt% Cu	35.07	0.00	34.70	0.00	0.00	0.01	34.81	0.06	0.03
Total	99.35	98.74	98.56	98.64	100.48	100.16	99.37	99.93	99.85
Atomic% S	49.75	52.77	49.77	46.93	47.18	47.12	50.30	51.90	52.65
Atomic% Fe	24.70	46.73	24.74	24.32	24.59	24.70	24.42	47.83	47.16
Atomic% Co	0.01	0.03	0.01	0.83	0.90	0.85	0.01	0.00	0.00
Atomic% Ni	0.01	0.46	0.01	27.92	27.32	27.33	0.00	0.03	0.04
Atomic% Cu	25.54	0.00	25.47	0.00	0.00	0.00	25.27	0.20	0.13
Host	BBS	BBS	BBS	BBS	BBS	BBS	BBS	Troc	Troc
Hole	VB99495	VB99495	VB99495	VB99495	VB99495	VB99495	VB99495	VB96266	VB96266
Depth	1146.00	1146.00	1146.00	1146.00	1146.00	1146.00	1146.00	211.50	211.50
Easting	N/A	N/A	N/A	N/A	N/A	N/A	N/A	556965.8	556965.8
Northing	N/A	N/A	N/A	N/A	N/A	N/A	N/A	6242466.0	6242466.0

TS number	C97-1080	C97-1080	C97-1080	C97-1080	C97-1080	C97-1080	C97-1080	C97-1080	C97-1080
Wt% S	34.45	38.69	33.03	32.92	39.02	38.54	35.09	33.39	38.83
Wt% Fe	29.64	60.71	31.01	30.79	61.07	61.16	30.59	32.17	61.39
Wt% Co	0.01	0.03	1.27	1.26	0.05	0.03	0.02	1.63	0.04
Wt% Ni	0.00	0.29	34.48	34.20	0.33	0.29	0.00	34.06	0.32
Wt% Cu	34.08	0.02	0.02	0.00	0.05	0.01	35.05	0.00	0.00
Total	98.19	99.75	99.83	99.17	100.53	100.03	100.78	101.25	100.59
Atomic% S	50.17	52.47	46.94	47.06	52.51	52.20	49.87	46.80	52.27
Atomic% Fe	24.78	47.27	25.30	25.27	47.18	47.56	24.96	25.88	47.45
Atomic% Co	0.00	0.01	0.00	0.00	0.00	0.00	0.01	0.01	0.01
Atomic% Ni	0.01	0.02	0.99	0.98	0.03	0.03	0.02	1.25	0.03
Atomic% Cu	0.00	0.22	26.76	26.70	0.24	0.22	0.00	26.07	0.24
Host	Troc	Troc	Troc	Troc	Troc	Troc	Troc	Troc	Troc
Hole	VB96266	VB96266	VB96266	VB96266	VB96266	VB96266	VB96266	VB96266	VB96266
Depth	211.50	211.50	211.50	211.50	211.50	211.50	211.50	211.50	211.50
Easting	556965.8	556965.8	556965.8	556965.8	556965.8	556965.8	556965.8	556965.8	556965.8
Northing	6242466.0	6242466.0	6242466.0	6242466.0	6242466.0	6242466.0	6242466.0	6242466.0	6242466.0

TS number	C97-1080	C97-1080	C97-1080	C97-1080	C97-1080	C97-1080	C97-1080	C97-1080	C97-1114
Wt% S	32.64	38.87	33.55	38.67	33.37	34.54	38.50	33.41	35.32
Wt% Fe	31.59	61.09	31.97	61.15	32.03	30.48	61.73	33.71	29.71
Wt% Co	1.22	0.03	1.52	0.04	1.44	0.02	0.05	1.49	0.00
Wt% Ni	33.91	0.37	34.70	0.34	34.68	0.01	0.13	32.97	0.01
Wt% Cu	0.00	0.03	0.00	0.03	0.00	34.72	0.02	0.00	34.40
Total	99.36	100.39	101.73	100.24	101.51	99.77	100.44	101.60	99.44
Atomic% S	46.65	52.40	46.81	52.26	46.69	49.64	51.99	46.67	50.64
Atomic% Fe	25.92	47.28	25.60	47.44	25.72	25.15	47.86	27.03	24.46
Atomic% Co	0.00	0.00	0.00	0.00	0.00	0.00	0.00	0.00	0.00
Atomic% Ni	0.95	0.02	1.15	0.03	1.09	0.02	0.03	1.13	0.00
Atomic% Cu	26.47	0.27	26.43	0.25	26.49	0.01	0.10	25.15	0.01
Host	Troc	Troc	Troc	Troc	Troc	Troc	Troc	Troc	Troc
Hole	VB96266	VB96266	VB96266	VB96266	VB96266	VB96266	VB96266	VB96266	VB96266
Depth	211.50	211.50	211.50	211.50	211.50	211.50	211.50	211.50	529.00
Easting	556965.8	556965.8	556965.8	556965.8	556965.8	556965.8	556965.8	556965.8	556965.8
Northing	6242466.0	6242466.0	6242466.0	6242466.0	6242466.0	6242466.0	6242466.0	6242466.0	6242466.0

TS number	C97-1114	C97-1114	C97-1114	C97-1114	C97-1114	C97-1114	C97-1114	C97-1114	C97-1114
Wt% S	33.59	39.10	38.98	33.17	34.87	39.21	33.13	34.92	39.07
Wt% Fe	29.99	60.05	60.43	31.07	30.43	60.27	29.96	30.39	60.18
Wt% Co	1.04	0.02	0.02	1.20	0.02	0.05	1.05	0.20	0.06
Wt% Ni	35.94	0.66	0.46	35.45	0.06	0.62	35.86	6.57	0.58
Wt% Cu	0.07	0.04	0.04	0.00	34.61	0.00	0.00	28.39	0.02
Total	100.64	99.87	99.97	100.88	99.99	100.14	100.01	100.48	99.92
Atomic% S	47.29	52.87	52.70	46.71	49.93	52.86	47.00	49.61	52.81
Atomic% Fe	24.24	46.60	46.90	25.12	25.01	46.65	24.40	24.79	46.70
Atomic% Co	0.00	0.00	0.01	0.00	0.00	0.00	0.00	0.01	0.01
Atomic% Ni	0.79	0.02	0.02	0.92	0.01	0.04	0.81	0.15	0.04
Atomic% Cu	27.63	0.49	0.34	27.26	0.05	0.45	27.78	5.10	0.43
Host	Troc	Troc	Troc	Troc	Troc	Troc	Troc	Troc	Troc
Hole	VB96266	VB96266	VB96266	VB96266	VB96266	VB96266	VB96266	VB96266	VB96266
Depth	529.00	529.00	529.00	529.00	529.00	529.00	529.00	529.00	529.00
Easting	556965.8	556965.8	556965.8	556965.8	556965.8	556965.8	556965.8	556965.8	556965.8
Northing	6242466.0	6242466.0	6242466.0	6242466.0	6242466.0	6242466.0	6242466.0	6242466.0	6242466.0

TS number	C97-1114	C97-1114	C97-1114	C97-1114	C97-1114	C97-1114	C97-1114	C97-1114	C97-1114
Wt% S	33.29	39.01	32.83	33.55	35.07	39.26	33.19	33.88	35.05
Wt% Fe	30.12	60.34	30.61	30.76	30.74	60.23	30.75	29.96	30.36
Wt% Co	1.20	0.04	0.95	0.99	0.01	0.02	1.10	0.02	0.04
Wt% Ni	35.20	0.69	35.98	36.14	0.00	0.62	36.01	0.08	0.00
Wt% Cu	0.00	0.00	0.00	0.00	34.94	0.00	0.00	34.35	34.49
Total	99.80	100.09	100.37	101.44	100.76	100.13	101.05	98.28	100.00
Atomic% S	47.25	52.68	46.53	46.93	49.85	52.92	46.67	49.48	50.12
Atomic% Fe	24.54	46.77	24.90	24.71	25.08	46.60	24.83	25.13	24.92
Atomic% Co	0.00	0.01	0.00	0.00	0.00	0.00	0.00	0.00	0.03
Atomic% Ni	0.92	0.03	0.73	0.75	0.01	0.01	0.84	0.02	0.03
Atomic% Cu	27.28	0.51	27.84	27.61	0.00	0.46	27.66	0.06	0.00
Host	Troc	Troc	Troc	Troc	Troc	Troc	Troc	Troc	Troc
Hole	VB96266	VB96266	VB96266	VB96266	VB96266	VB96266	VB96266	VB96266	VB96266
Depth	529.00	529.00	529.00	529.00	529.00	529.00	529.00	529.00	529.00
Easting	556965.8	556965.8	556965.8	556965.8	556965.8	556965.8	556965.8	556965.8	556965.8
Northing	6242466.0	6242466.0	6242466.0	6242466.0	6242466.0	6242466.0	6242466.0	6242466.0	6242466.0

TS number	C97-1114	C97-1114	C97-1112	C97-1112	C97-1112	C97-1112	C97-1112	C97-1112	C97-1112
Wt% S	39.77	33.52	36.44	33.13	34.98	36.86	38.29	33.04	33.11
Wt% Fe	59.81	30.14	62.33	35.21	30.02	62.96	61.27	34.25	31.25
Wt% Co	0.03	0.97	0.03	1.15	0.01	0.02	0.03	1.08	0.45
Wt% Ni	0.50	36.53	0.00	30.17	0.00	0.01	0.05	31.97	14.71
Wt% Cu	0.01	0.00	0.02	0.00	34.59	0.00	0.03	0.00	18.18
Total	100.12	101.16	98.84	99.67	99.61	99.86	99.69	100.33	97.70
Atomic% S	53.45	47.01	50.43	47.03	50.20	50.47	52.07	46.70	48.33
Atomic% Fe	46.15	24.27	49.52	28.69	24.74	49.49	47.84	27.79	26.19
Atomic% Co	0.00	0.00	0.01	0.00	0.00	0.01	0.01	0.00	0.00
Atomic% Ni	0.03	0.74	0.02	0.89	0.01	0.02	0.02	0.83	0.36
Atomic% Cu	0.37	27.98	0.00	23.39	0.00	0.01	0.04	24.68	11.73
Host	Troc	Troc	Troc	Troc	Troc	Troc	Troc	Troc	Troc
Hole	VB96266	VB96266	VB96266	VB96266	VB96266	VB96266	VB96266	VB96266	VB96266
Depth	529.00	529.00	481.00	481.00	481.00	481.00	481.00	481.00	481.00
Easting	556965.8	556965.8	556965.8	556965.8	556965.8	556965.8	556965.8	556965.8	556965.8
Northing	6242466.0	6242466.0	6242466.0	6242466.0	6242466.0	6242466.0	6242466.0	6242466.0	6242466.0

TS number	C97-1112	C97-1112	C97-1112	C97-1112	C97-1112	C97-1112	C97-1112	C97-1112	C97-1112
Wt% S	34.66	36.91	38.78	34.06	32.87	38.89	38.24	35.00	33.02
Wt% Fe	30.28	63.59	60.60	29.96	33.95	60.98	61.44	30.22	33.03
Wt% Co	0.01	0.04	0.05	0.02	0.93	0.03	0.05	0.01	1.32
Wt% Ni	0.00	0.01	0.18	0.02	32.40	0.19	0.15	0.00	32.81
Wt% Cu	34.72	0.00	0.01	33.88	0.00	0.03	0.02	34.72	0.02
Total	99.67	100.55	99.63	97.95	100.15	100.13	99.90	99.97	100.21
Atomic% S	49.83	50.26	52.62	49.81	46.58	52.53	51.93	50.09	46.75
Atomic% Fe	24.99	49.70	47.20	25.15	27.62	47.28	47.90	24.82	26.85
Atomic% Co	0.00	0.00	0.01	0.00	0.00	0.01	0.01	0.01	0.00
Atomic% Ni	0.01	0.03	0.03	0.02	0.72	0.02	0.03	0.01	1.02
Atomic% Cu	0.00	0.01	0.13	0.02	25.08	0.14	0.11	0.00	25.37
Host	Troc	Troc	Troc	Troc	Troc	Troc	Troc	Troc	Troc
Hole	VB96266	VB96266	VB96266	VB96266	VB96266	VB96266	VB96266	VB96266	VB96266
Depth	481.00	481.00	481.00	481.00	481.00	481.00	481.00	481.00	481.00
Easting	556965.8	556965.8	556965.8	556965.8	556965.8	556965.8	556965.8	556965.8	556965.8
Northing	6242466.0	6242466.0	6242466.0	6242466.0	6242466.0	6242466.0	6242466.0	6242466.0	6242466.0

TS number	C97-1110	C97-1110	C97-1110	C97-1110	C97-1110	C97-1074	C97-1074	C97-1074	C97-1074
Wt% S	37.85	33.02	34.17	38.60	35.66	34.88	33.20	36.29	36.49
Wt% Fe	62.03	32.30	30.03	61.27	37.17	30.31	34.17	62.82	62.76
Wt% Co	0.02	1.54	0.02	0.04	0.02	0.02	1.64	0.04	0.04
Wt% Ni	0.13	33.78	0.11	0.25	0.14	0.03	31.34	0.02	0.02
Wt% Cu	0.03	0.05	34.60	0.04	27.48	34.60	0.06	0.05	0.04
Total	100.08	100.70	98.93	100.21	100.47	99.83	100.41	99.22	99.37
Atomic% S	51.45	46.59	49.56	52.19	50.26	50.00	46.86	50.12	50.28
Atomic% Fe	48.40	26.16	25.01	47.56	30.08	24.94	27.69	49.81	49.64
Atomic% Co	0.02	0.00	0.00	0.01	0.00	0.00	0.00	0.00	0.00
Atomic% Ni	0.02	1.18	0.01	0.03	0.01	0.01	1.26	0.03	0.03
Atomic% Cu	0.10	26.03	0.09	0.18	0.11	0.03	24.16	0.01	0.02
Host	Troc	Troc	Troc	Troc	Troc	Troc	Troc	Troc	Troc
Hole	VB96266	VB96266	VB96266	VB96266	VB96266	VB96266	VB96266	VB96266	VB96266
Depth	290.00	290.00	290.00	290.00	290.00	327.00	327.00	327.00	327.00
Easting	556965.8	556965.8	556965.8	556965.8	556965.8	556965.8	556965.8	556965.8	556965.8
Northing	6242466.0	6242466.0	6242466.0	6242466.0	6242466.0	6242466.0	6242466.0	6242466.0	6242466.0

TS number	C97-1074	C97-1074	C97-1074	C97-1074	C97-1074	C97-1074	C97-1074	C97-1074	C97-1074
Wt% S	33.04	36.05	34.46	36.99	36.82	33.28	38.40	33.43	38.13
Wt% Fe	33.99	62.52	30.40	62.36	62.78	34.03	60.84	34.15	61.27
Wt% Co	1.38	0.02	0.00	0.04	0.03	1.23	0.04	1.30	0.04
Wt% Ni	32.01	0.01	0.00	0.15	0.02	32.37	0.18	32.02	0.12
Wt% Cu	0.01	0.05	34.74	0.11	0.03	0.02	0.01	0.00	0.03
Total	100.44	98.65	99.60	99.66	99.69	100.93	99.46	100.92	99.59
Atomic% S	46.67	50.08	49.63	50.71	50.50	46.76	52.28	46.92	51.94
Atomic% Fe	27.57	49.86	25.13	49.07	49.43	27.45	47.55	27.52	47.92
Atomic% Co	0.01	0.00	0.00	0.00	0.00	0.00	0.00	0.01	0.00
Atomic% Ni	1.06	0.01	0.00	0.03	0.02	0.94	0.03	0.99	0.03
Atomic% Cu	24.69	0.01	0.00	0.12	0.01	24.83	0.13	24.55	0.09
Host	Troc	Troc	Troc	Troc	Troc	Troc	Troc	Troc	Troc
Hole	VB96266	VB96266	VB96266	VB96266	VB96266	VB96266	VB96266	VB96266	VB96266
Depth	327.00	327.00	327.00	327.00	327.00	327.00	327.00	327.00	327.00
Easting	556965.8	556965.8	556965.8	556965.8	556965.8	556965.8	556965.8	556965.8	556965.8
Northing	6242466.0	6242466.0	6242466.0	6242466.0	6242466.0	6242466.0	6242466.0	6242466.0	6242466.0

TS number	C97-1074	C97-1074	C97-1074	C97-1074	C97-1074	C97-1074	C97-1074	C97-1074	C97-1074
Wt% S	36.50	32.69	36.45	38.56	37.32	34.57	38.27	33.61	34.47
Wt% Fe	63.24	33.11	63.33	61.01	62.25	29.31	61.13	32.98	30.08
Wt% Co	0.04	1.30	0.04	0.03	0.03	0.01	0.04	1.28	0.01
Wt% Ni	0.03	31.86	0.00	0.14	0.05	0.00	0.15	32.54	0.04
Wt% Cu	0.02	0.02	0.06	0.04	0.03	34.45	0.03	0.07	34.58
Total	99.82	99.00	99.88	99.78	99.70	98.35	99.62	100.49	99.20
Atomic% S	50.10	46.82	50.03	52.32	51.04	50.26	52.08	47.31	49.80
Atomic% Fe	49.84	27.22	49.90	47.53	48.87	24.46	47.76	26.65	24.95
Atomic% Co	0.00	0.01	0.00	0.00	0.00	0.01	0.00	0.00	0.00
Atomic% Ni	0.03	1.01	0.03	0.02	0.03	0.01	0.03	0.98	0.01
Atomic% Cu	0.02	24.91	0.00	0.10	0.03	0.00	0.11	25.01	0.03
Host	Troc	Troc	Troc	Troc	Troc	Troc	Troc	Troc	Troc
Hole	VB96266	VB96266	VB96266	VB96266	VB96266	VB96266	VB96266	VB96266	VB96266
Depth	327.00	327.00	327.00	327.00	327.00	327.00	327.00	327.00	327.00
Easting	556965.8	556965.8	556965.8	556965.8	556965.8	556965.8	556965.8	556965.8	556965.8
Northing	6242466.0	6242466.0	6242466.0	6242466.0	6242466.0	6242466.0	6242466.0	6242466.0	6242466.0

TS number	C97-1075	C97-1075	C97-1075	C97-1075	C97-1075	C97-1075	C97-1075	C97-1075	C97-1075
Wt% S	36.56	36.68	35.02	33.54	36.57	33.33	36.40	33.41	34.27
Wt% Fe	62.20	62.89	30.32	38.59	63.11	38.54	62.92	38.92	30.42
Wt% Co	0.05	0.05	0.01	0.76	0.04	0.91	0.04	0.80	0.03
Wt% Ni	0.00	0.00	0.07	27.32	0.00	27.42	0.02	27.10	0.22
Wt% Cu	0.03	0.03	34.40	0.04	0.02	0.00	0.01	0.00	34.70
Total	98.83	99.64	99.82	100.39	99.76	100.20	99.41	100.24	99.65
Atomic% S	50.56	50.37	50.15	47.17	50.20	46.99	50.16	47.06	49.40
Atomic% Fe	49.38	49.57	24.93	31.15	49.74	31.20	49.78	31.48	25.17
Atomic% Co	0.00	0.00	0.00	0.09	0.01	0.00	0.01	0.00	0.00
Atomic% Ni	0.04	0.04	0.01	0.59	0.03	0.69	0.03	0.62	0.03
Atomic% Cu	0.00	0.00	0.05	20.98	0.00	21.12	0.01	20.85	0.18
Host	Troc	Troc	Troc	Troc	Troc	Troc	Troc	Troc	Troc
Hole	VB96266	VB96266	VB96266	VB96266	VB96266	VB96266	VB96266	VB96266	VB96266
Depth	332.50	332.50	332.50	332.50	332.50	332.50	332.50	332.50	332.50
Easting	556965.8	556965.8	556965.8	556965.8	556965.8	556965.8	556965.8	556965.8	556965.8
Northing	6242466.0	6242466.0	6242466.0	6242466.0	6242466.0	6242466.0	6242466.0	6242466.0	6242466.0

TS number	C97-1075	C97-1075	C97-1075	C97-1075	C97-1075	C97-1075	C97-1075	C97-1075	C97-1075
Wt% S	36.34	33.53	33.80	36.41	33.89	36.47	33.57	34.58	33.53
Wt% Fe	63.09	39.22	30.87	63.01	30.90	62.94	39.12	31.66	39.48
Wt% Co	0.05	1.07	0.10	0.03	0.12	0.05	1.07	0.02	1.01
Wt% Ni	0.05	26.71	5.29	0.00	3.54	0.00	26.90	0.15	26.78
Wt% Cu	0.02	0.00	28.40	0.01	30.87	0.01	0.00	33.09	0.00
Total	99.56	100.53	98.47	99.47	99.33	99.48	100.67	99.51	100.80
Atomic% S	50.04	47.08	49.13	50.15	48.97	50.20	47.09	49.73	46.98
Atomic% Fe	49.87	31.62	25.76	49.82	25.63	49.74	31.49	26.13	31.76
Atomic% Co	0.01	0.00	0.00	0.01	0.01	0.00	0.00	0.00	0.00
Atomic% Ni	0.04	0.82	0.08	0.02	0.09	0.04	0.82	0.02	0.77
Atomic% Cu	0.03	20.48	4.20	0.00	2.79	0.00	20.60	0.12	20.49
Host	Troc	Troc	Troc	Troc	Troc	Troc	Troc	Troc	Troc
Hole	VB96266	VB96266	VB96266	VB96266	VB96266	VB96266	VB96266	VB96266	VB96266
Depth	332.50	332.50	332.50	332.50	332.50	332.50	332.50	332.50	332.50
Easting	556965.8	556965.8	556965.8	556965.8	556965.8	556965.8	556965.8	556965.8	556965.8
Northing	6242466.0	6242466.0	6242466.0	6242466.0	6242466.0	6242466.0	6242466.0	6242466.0	6242466.0

TS number	C97-1075	C97-1075	C97-1075	C97-1075	C97-1075	C97-1075	C97-1075	C97-1075	C97-1075
Wt% S	36.28	33.16	33.28	36.29	33.44	36.41	33.43	34.42	36.64
Wt% Fe	62.86	39.28	39.15	63.22	39.06	63.03	38.95	30.37	62.80
Wt% Co	0.03	1.03	1.03	0.04	0.91	0.04	1.02	0.02	0.04
Wt% Ni	0.02	26.76	27.19	0.00	27.09	0.00	27.43	0.37	0.00
Wt% Cu	0.03	0.01	0.00	0.03	0.02	0.04	0.00	33.59	0.02
Total	99.22	100.24	100.66	99.60	100.53	99.52	100.84	98.77	99.52
Atomic% S	50.11	46.78	46.77	49.97	46.99	50.13	46.87	49.87	50.38
Atomic% Fe	49.83	31.81	31.58	49.97	31.51	49.82	31.35	25.26	49.57
Atomic% Co	0.00	0.00	0.00	0.01	0.01	0.00	0.00	0.00	0.01
Atomic% Ni	0.02	0.79	0.79	0.03	0.70	0.03	0.78	0.02	0.03
Atomic% Cu	0.01	20.61	20.86	0.00	20.79	0.00	21.00	0.29	0.00
Host	Troc	Troc	Troc	Troc	Troc	Troc	Troc	Troc	Troc
Hole	VB96266	VB96266	VB96266	VB96266	VB96266	VB96266	VB96266	VB96266	VB96266
Depth	332.50	332.50	332.50	332.50	332.50	332.50	332.50	332.50	332.50
Easting	556965.8	556965.8	556965.8	556965.8	556965.8	556965.8	556965.8	556965.8	556965.8
Northing	6242466.0	6242466.0	6242466.0	6242466.0	6242466.0	6242466.0	6242466.0	6242466.0	6242466.0

TS number	C97-1075	C97-1075	C97-1075	C97-1075	C97-1075	C97-1078	C97-1078	C97-1078	C97-1078
Wt% S	34.97	34.22	33.42	36.46	32.56	53.02	38.84	38.20	33.17
Wt% Fe	30.77	33.56	38.95	62.97	38.20	44.84	35.66	60.34	30.92
Wt% Co	0.03	0.29	1.01	0.03	0.90	1.91	1.26	0.04	2.11
Wt% Ni	0.39	11.60	26.96	0.00	26.40	0.53	24.68	0.29	33.81
Wt% Cu	34.01	20.69	0.00	0.02	0.65	0.78	0.70	0.03	0.00
Total	100.28	100.36	100.34	99.48	98.72	101.10	101.13	98.90	100.01
Atomic% S	49.90	48.60	47.04	50.19	46.70	65.87	52.61	52.31	47.02
Atomic% Fe	25.21	27.36	31.47	49.77	31.45	31.98	27.73	47.42	25.16
Atomic% Co	0.08	0.00	0.00	0.00	0.00	0.00	0.00	0.00	0.00
Atomic% Ni	0.02	0.22	0.77	0.02	0.70	1.29	0.93	0.03	1.63
Atomic% Cu	0.30	9.00	20.72	0.00	20.68	0.36	18.26	0.22	26.18
Host	Troc	Troc	Troc	Troc	Troc	Troc	Troc	Troc	Troc
Hole	VB96266	VB96266	VB96266	VB96266	VB96266	VB96266	VB96266	VB96266	VB96266
Depth	332.50	332.50	332.50	332.50	332.50	192.50	192.50	192.50	192.50
Easting	556965.8	556965.8	556965.8	556965.8	556965.8	556965.8	556965.8	556965.8	556965.8
Northing	6242466.0	6242466.0	6242466.0	6242466.0	6242466.0	6242466.0	6242466.0	6242466.0	6242466.0

TS number	C97-1078	C97-1078	C97-1078	C97-1078	C97-1078	C97-1078	C97-1078	C97-1078	C97-1078
Wt% S	38.34	33.27	32.83	38.56	38.59	33.48	38.56	38.58	33.23
Wt% Fe	60.78	31.59	31.05	60.92	60.84	31.52	60.97	60.74	31.65
Wt% Co	0.04	1.10	1.09	0.02	0.05	1.28	0.04	0.02	1.24
Wt% Ni	0.39	35.19	34.69	0.39	0.39	34.98	0.39	0.38	34.90
Wt% Cu	0.00	0.00	0.01	0.00	0.03	0.00	0.00	0.00	0.01
Total	99.56	101.15	99.67	99.90	99.90	101.26	99.96	99.72	101.03
Atomic% S	52.18	46.72	46.77	52.28	52.31	46.91	52.25	52.37	46.72
Atomic% Fe	47.49	25.47	25.39	47.42	47.34	25.35	47.43	47.33	25.54
Atomic% Co	0.00	0.00	0.00	0.00	0.00	0.00	0.00	0.00	0.00
Atomic% Ni	0.03	0.84	0.84	0.02	0.04	0.98	0.03	0.01	0.94
Atomic% Cu	0.29	26.98	26.99	0.29	0.29	26.76	0.29	0.28	26.79
Host	Troc	Troc	Troc	Troc	Troc	Troc	Troc	Troc	Troc
Hole	VB96266	VB96266	VB96266	VB96266	VB96266	VB96266	VB96266	VB96266	VB96266
Depth	192.50	192.50	192.50	192.50	192.50	192.50	192.50	192.50	192.50
Easting	556965.8	556965.8	556965.8	556965.8	556965.8	556965.8	556965.8	556965.8	556965.8
Northing	6242466.0	6242466.0	6242466.0	6242466.0	6242466.0	6242466.0	6242466.0	6242466.0	6242466.0

TS number	C97-1078	C97-1078	C97-1078	C97-1078	C97-1078	C97-1078	C97-1078	C97-1079	C97-1079
Wt% S	38.42	35.22	53.72	38.52	34.43	34.47	38.45	38.44	34.84
Wt% Fe	60.86	30.48	45.06	60.65	30.82	30.78	60.97	60.01	29.53
Wt% Co	0.05	0.01	2.46	0.05	0.28	0.00	0.05	0.03	0.01
Wt% Ni	0.32	0.00	0.01	0.48	10.17	0.00	0.35	0.40	0.00
Wt% Cu	0.07	34.90	0.00	0.03	24.18	35.09	0.01	0.01	34.25
Total	99.72	100.66	101.25	99.72	99.92	100.34	99.85	98.90	98.63
Atomic% S	52.20	50.06	66.38	52.31	49.15	49.35	52.18	52.57	50.43
Atomic% Fe	47.48	24.87	31.96	47.28	25.25	25.30	47.50	47.11	24.54
Atomic% Co	0.00	0.03	0.00	0.00	0.02	0.00	0.00	0.00	0.00
Atomic% Ni	0.03	0.01	1.65	0.03	0.22	0.00	0.04	0.02	0.01
Atomic% Cu	0.24	0.00	0.01	0.36	7.93	0.00	0.26	0.30	0.00
Host	Troc	Troc	Troc	Troc	Troc	Troc	Troc	Troc	Troc
Hole	VB96266	VB96266	VB96266	VB96266	VB96266	VB96266	VB96266	VB96266	VB96266
Depth	192.50	192.50	192.50	192.50	192.50	192.50	192.50	206.50	206.50
Easting	556965.8	556965.8	556965.8	556965.8	556965.8	556965.8	556965.8	556965.8	556965.8
Northing	6242466.0	6242466.0	6242466.0	6242466.0	6242466.0	6242466.0	6242466.0	6242466.0	6242466.0

TS number	C97-1079	C97-1079	C97-1079	C97-1079	C97-1079	C97-1079	C97-1079	C97-1079	C97-1079
Wt% S	38.54	34.88	33.41	33.29	38.45	38.85	34.84	33.45	33.10
Wt% Fe	60.48	30.10	31.24	31.00	60.82	60.53	30.48	31.31	31.30
Wt% Co	0.03	0.01	1.13	1.14	0.05	0.02	0.00	0.92	0.90
Wt% Ni	0.34	0.04	34.65	34.77	0.39	0.48	0.00	35.24	35.41
Wt% Cu	0.02	34.47	0.00	0.00	0.00	0.02	34.49	0.05	0.00
Total	99.41	99.50	100.43	100.20	99.70	99.90	100.22	100.97	100.71
Atomic% S	52.45	50.13	47.14	47.09	52.25	52.58	49.82	46.98	46.69
Atomic% Fe	47.25	24.83	25.30	25.18	47.44	47.04	25.02	25.25	25.35
Atomic% Co	0.00	0.01	0.00	0.00	0.00	0.00	0.28	0.00	0.00
Atomic% Ni	0.02	0.01	0.87	0.88	0.03	0.02	0.00	0.70	0.69
Atomic% Cu	0.25	0.03	26.70	26.86	0.29	0.35	0.00	27.03	27.27
Host	Troc	Troc	Troc	Troc	Troc	Troc	Troc	Troc	Troc
Hole	VB96266	VB96266	VB96266	VB96266	VB96266	VB96266	VB96266	VB96266	VB96266
Depth	206.50	206.50	206.50	206.50	206.50	206.50	206.50	206.50	206.50
Easting	556965.8	556965.8	556965.8	556965.8	556965.8	556965.8	556965.8	556965.8	556965.8
Northing	6242466.0	6242466.0	6242466.0	6242466.0	6242466.0	6242466.0	6242466.0	6242466.0	6242466.0

TS number	C97-1079	C97-1079	C97-1079	C97-1079	C97-1079	C97-1079	C97-1079	C97-1079	C97-1079
Wt% S	38.82	38.57	33.36	38.73	34.97	33.45	33.38	38.67	38.70
Wt% Fe	60.36	60.38	31.17	60.56	30.52	31.24	31.33	60.47	60.52
Wt% Co	0.04	0.03	1.22	0.04	0.01	1.20	1.11	0.03	0.03
Wt% Ni	0.47	0.56	35.23	0.54	0.01	35.25	35.26	0.55	0.34
Wt% Cu	0.01	0.01	0.00	0.00	34.73	0.00	0.00	0.00	0.00
Total	99.71	99.54	100.97	99.89	100.25	101.14	101.08	99.71	99.60
Atomic% S	52.63	52.43	46.89	52.47	49.94	46.92	46.87	52.47	52.54
Atomic% Fe	46.98	47.12	25.15	47.09	25.02	25.16	25.25	47.10	47.18
Atomic% Co	0.00	0.00	0.00	0.01	0.00	0.00	0.00	0.00	0.01
Atomic% Ni	0.03	0.02	0.93	0.03	0.01	0.92	0.85	0.02	0.02
Atomic% Cu	0.35	0.42	27.04	0.40	0.01	27.00	27.03	0.41	0.25
Host	Troc	Troc	Troc	Troc	Troc	Troc	Troc	Troc	Troc
Hole	VB96266	VB96266	VB96266	VB96266	VB96266	VB96266	VB96266	VB96266	VB96266
Depth	206.50	206.50	206.50	206.50	206.50	206.50	206.50	206.50	206.50
Easting	556965.8	556965.8	556965.8	556965.8	556965.8	556965.8	556965.8	556965.8	556965.8
Northing	6242466.0	6242466.0	6242466.0	6242466.0	6242466.0	6242466.0	6242466.0	6242466.0	6242466.0

TS number	C97-1079	C97-1079	C97-1079	C97-1079	C97-1079	C97-1083	C97-1083	C97-1083	C97-1083
Wt% S	33.37	34.62	38.54	33.45	34.63	38.77	33.98	39.62	33.09
Wt% Fe	31.91	30.31	60.76	33.08	30.41	59.56	30.71	59.85	30.53
Wt% Co	1.12	0.01	0.04	1.08	0.00	0.03	0.03	0.03	1.36
Wt% Ni	34.49	0.01	0.28	33.46	0.02	0.23	0.07	0.29	35.36
Wt% Cu	0.05	34.83	0.01	0.00	34.76	0.17	34.21	0.01	0.00
Total	100.94	99.80	99.62	101.07	99.82	98.76	99.03	99.80	100.34
Atomic% S	46.90	49.73	52.37	46.92	49.72	52.97	49.28	53.43	46.83
Atomic% Fe	25.74	25.00	47.39	26.64	25.07	46.71	25.57	46.33	24.80
Atomic% Co	0.00	0.01	0.00	0.00	0.00	0.00	0.00	0.00	0.00
Atomic% Ni	0.85	0.01	0.03	0.82	0.00	0.02	0.02	0.02	1.05
Atomic% Cu	26.47	0.01	0.21	25.62	0.02	0.17	0.06	0.22	27.32
Host	Troc	Troc	Troc	Troc	Troc	Troc	Troc	Troc	Troc
Hole	VB96266	VB96266	VB96266	VB96266	VB96266	VB96266	VB96266	VB96266	VB96266
Depth	206.50	206.50	206.50	206.50	206.50	244.00	244.00	244.00	244.00
Easting	556965.8	556965.8	556965.8	556965.8	556965.8	556965.8	556965.8	556965.8	556965.8
Northing	6242466.0	6242466.0	6242466.0	6242466.0	6242466.0	6242466.0	6242466.0	6242466.0	6242466.0

TS number	C97-1083	C97-1083	C97-1083	C97-1083	C97-1083	C97-1083	C97-1083	C97-1083	C97-1083
Wt% S	39.19	34.36	32.59	34.52	39.60	33.16	39.14	32.48	32.98
Wt% Fe	59.80	30.52	30.01	30.47	59.78	30.03	59.81	30.26	30.62
Wt% Co	0.05	0.01	1.27	0.01	0.03	1.13	0.05	1.15	1.16
Wt% Ni	0.38	0.00	35.56	0.07	0.41	35.33	0.37	35.34	35.67
Wt% Cu	0.02	34.52	0.00	34.35	0.00	0.00	0.02	0.00	0.00
Total	99.44	99.41	99.44	99.53	99.83	99.65	99.38	99.23	100.43
Atomic% S	53.13	49.58	46.60	49.72	53.40	47.17	53.10	46.55	46.67
Atomic% Fe	46.54	25.28	24.64	25.19	46.27	24.52	46.58	24.90	24.87
Atomic% Co	0.01	0.00	0.01	0.07	0.00	0.00	0.00	0.00	0.00
Atomic% Ni	0.04	0.01	0.99	0.00	0.03	0.88	0.03	0.90	0.89
Atomic% Cu	0.28	0.00	27.77	0.06	0.30	27.44	0.28	27.65	27.56
Host	Troc	Troc	Troc	Troc	Troc	Troc	Troc	Troc	Troc
Hole	VB96266	VB96266	VB96266	VB96266	VB96266	VB96266	VB96266	VB96266	VB96266
Depth	244.00	244.00	244.00	244.00	244.00	244.00	244.00	244.00	244.00
Easting	556965.8	556965.8	556965.8	556965.8	556965.8	556965.8	556965.8	556965.8	556965.8
Northing	6242466.0	6242466.0	6242466.0	6242466.0	6242466.0	6242466.0	6242466.0	6242466.0	6242466.0

TS number	C97-1083	C97-1083	C97-1083	C97-1083	C97-1083	C97-1083	C97-1083	C97-1083	C97-1083
Wt% S	34.74	39.32	39.41	34.86	33.02	39.38	34.35	33.03	39.41
Wt% Fe	30.46	59.96	59.67	30.61	30.55	59.95	30.47	30.37	59.81
Wt% Co	0.02	0.04	0.04	0.02	1.17	0.04	0.01	1.25	0.05
Wt% Ni	0.00	0.37	0.35	0.00	35.71	0.28	0.00	35.68	0.46
Wt% Cu	34.41	0.01	0.02	34.39	0.00	0.04	34.35	0.00	0.00
Total	99.70	99.69	99.49	99.88	100.45	99.71	99.18	100.32	99.72
Atomic% S	49.89	53.16	53.33	49.95	46.70	53.21	49.66	46.77	53.25
Atomic% Fe	25.11	46.54	46.37	25.17	24.81	46.51	25.29	24.68	46.39
Atomic% Co	0.05	0.00	0.00	0.00	0.00	0.01	0.00	0.00	0.00
Atomic% Ni	0.02	0.03	0.03	0.02	0.90	0.03	0.01	0.96	0.03
Atomic% Cu	0.00	0.27	0.26	0.00	27.58	0.21	0.00	27.59	0.34
Host	Troc	Troc	Troc	Troc	Troc	Troc	Troc	Troc	Troc
Hole	VB96266	VB96266	VB96266	VB96266	VB96266	VB96266	VB96266	VB96266	VB96266
Depth	244.00	244.00	244.00	244.00	244.00	244.00	244.00	244.00	244.00
Easting	556965.8	556965.8	556965.8	556965.8	556965.8	556965.8	556965.8	556965.8	556965.8
Northing	6242466.0	6242466.0	6242466.0	6242466.0	6242466.0	6242466.0	6242466.0	6242466.0	6242466.0

TS number	C97-1083	C97-1083	C97-1083	C97-1083	C97-1083	C97-1083	C97-1083	C97-1083	C97-1085
Wt% S	39.47	33.07	34.70	32.81	39.35	39.76	32.96	34.79	33.00
Wt% Fe	59.86	30.54	30.52	30.40	59.85	59.79	30.21	30.53	30.88
Wt% Co	0.04	1.18	0.01	1.23	0.04	0.04	1.27	0.03	1.28
Wt% Ni	0.37	35.52	0.01	35.67	0.35	0.35	35.64	0.17	34.49
Wt% Cu	0.03	0.00	34.63	0.00	0.02	0.03	0.00	34.57	0.00
Total	99.77	100.31	99.87	100.11	99.60	99.97	100.08	100.09	99.67
Atomic% S	53.29	46.82	49.78	46.60	53.23	53.51	46.78	49.79	46.97
Atomic% Fe	46.39	24.82	25.14	24.79	46.48	46.18	24.61	25.08	25.23
Atomic% Co	0.00	0.00	0.00	0.00	0.00	0.00	0.01	0.00	0.01
Atomic% Ni	0.03	0.91	0.01	0.95	0.03	0.03	0.98	0.02	0.99
Atomic% Cu	0.27	27.46	0.01	27.66	0.26	0.25	27.62	0.13	26.80
Host	Troc	Troc	Troc	Troc	Troc	Troc	Troc	Troc	Troc
Hole	VB96266	VB96266	VB96266	VB96266	VB96266	VB96266	VB96266	VB96266	VB96266
Depth	244.00	244.00	244.00	244.00	244.00	244.00	244.00	244.00	262.00
Easting	556965.8	556965.8	556965.8	556965.8	556965.8	556965.8	556965.8	556965.8	556965.8
Northing	6242466.0	6242466.0	6242466.0	6242466.0	6242466.0	6242466.0	6242466.0	6242466.0	6242466.0

TS number	C97-1085	C97-1085	C97-1085	C97-1085	C97-1085	C97-1085	C97-1085	C97-1085	C97-1085
Wt% S	38.96	34.85	34.72	33.24	38.81	38.64	33.34	33.59	38.69
Wt% Fe	60.34	29.88	30.05	30.56	60.24	60.16	30.99	31.28	60.77
Wt% Co	0.03	0.02	0.00	1.36	0.03	0.04	1.36	1.33	0.04
Wt% Ni	0.46	0.00	0.00	34.18	0.37	0.41	34.76	34.39	0.33
Wt% Cu	0.01	34.27	34.40	0.00	0.00	0.02	0.00	0.00	0.02
Total	99.82	99.06	99.23	99.34	99.45	99.26	100.45	100.59	99.86
Atomic% S	52.74	50.27	50.06	47.36	52.72	52.62	47.06	47.28	52.43
Atomic% Fe	46.88	24.74	24.88	25.00	46.98	47.03	25.11	25.27	47.27
Atomic% Co	0.00	0.04	0.03	0.00	0.00	0.00	0.00	0.00	0.01
Atomic% Ni	0.03	0.01	0.00	1.05	0.02	0.03	1.04	1.02	0.03
Atomic% Cu	0.34	0.00	0.00	26.59	0.27	0.31	26.79	26.43	0.25
Host	Troc	Troc	Troc	Troc	Troc	Troc	Troc	Troc	Troc
Hole	VB96266	VB96266	VB96266	VB96266	VB96266	VB96266	VB96266	VB96266	VB96266
Depth	262.00	262.00	262.00	262.00	262.00	262.00	262.00	262.00	262.00
Easting	556965.8	556965.8	556965.8	556965.8	556965.8	556965.8	556965.8	556965.8	556965.8
Northing	6242466.0	6242466.0	6242466.0	6242466.0	6242466.0	6242466.0	6242466.0	6242466.0	6242466.0

TS number	C97-1086	C97-1086	C97-1086	C97-1086	C97-1086	C97-1086	C97-1086	C97-1086	C97-1086
Wt% S	33.70	37.09	34.71	36.70	32.90	36.57	33.21	34.89	36.59
Wt% Fe	35.07	63.04	30.25	63.16	34.73	63.25	34.36	30.67	63.14
Wt% Co	1.35	0.04	0.02	0.04	1.32	0.03	1.38	0.03	0.03
Wt% Ni	30.25	0.01	0.05	0.01	31.17	0.00	31.47	0.00	0.00
Wt% Cu	0.05	0.08	34.62	0.02	0.00	0.05	0.00	34.63	0.04
Total	100.43	100.37	99.64	99.94	100.14	99.90	100.42	100.22	99.81
Atomic% S	47.39	50.51	49.89	50.27	46.60	50.15	46.85	49.86	50.20
Atomic% Fe	28.31	49.29	24.96	49.67	28.25	49.79	27.84	25.15	49.73
Atomic% Co	0.00	0.00	0.00	0.00	0.00	0.00	0.00	0.00	0.01
Atomic% Ni	1.04	0.03	0.01	0.03	1.01	0.03	1.06	0.02	0.03
Atomic% Cu	23.23	0.01	0.04	0.01	24.12	0.00	24.25	0.00	0.00
Host	Troc	Troc	Troc	Troc	Troc	Troc	Troc	Troc	Troc
Hole	VB96266	VB96266	VB96266	VB96266	VB96266	VB96266	VB96266	VB96266	VB96266
Depth	136.30	136.30	136.30	136.30	136.30	136.30	136.30	136.30	136.30
Easting	556965.8	556965.8	556965.8	556965.8	556965.8	556965.8	556965.8	556965.8	556965.8
Northing	6242466.0	6242466.0	6242466.0	6242466.0	6242466.0	6242466.0	6242466.0	6242466.0	6242466.0

TS number	C97-1086	C97-1086	C97-1086	C97-1086	C97-1086	C97-1086	C97-1086	C97-1086	C97-1086
Wt% S	36.59	36.58	36.36	33.25	36.45	34.93	33.57	33.46	36.63
Wt% Fe	63.14	63.12	63.46	34.84	63.23	30.51	36.33	34.35	63.11
Wt% Co	0.03	0.03	0.02	1.48	0.03	0.02	1.13	1.30	0.03
Wt% Ni	0.00	0.00	0.02	31.00	0.00	0.00	29.41	31.33	0.00
Wt% Cu	0.04	0.04	0.01	0.00	0.05	34.48	0.00	0.00	0.01
Total	99.81	99.77	99.89	100.57	99.76	99.98	100.45	100.44	99.79
Atomic% S	50.20	50.21	49.93	46.84	50.07	49.99	47.21	47.13	50.26
Atomic% Fe	49.73	49.74	50.02	28.18	49.86	25.07	29.33	27.77	49.71
Atomic% Co	0.01	0.00	0.00	0.00	0.00	0.02	0.01	0.00	0.00
Atomic% Ni	0.03	0.02	0.02	1.13	0.02	0.02	0.86	1.00	0.02
Atomic% Cu	0.00	0.00	0.01	23.85	0.00	0.00	22.59	24.10	0.00
Host	Troc	Troc	Troc	Troc	Troc	Troc	Troc	Troc	Troc
Hole	VB96266	VB96266	VB96266	VB96266	VB96266	VB96266	VB96266	VB96266	VB96266
Depth	136.30	136.30	136.30	136.30	136.30	136.30	136.30	136.30	136.30
Easting	556965.8	556965.8	556965.8	556965.8	556965.8	556965.8	556965.8	556965.8	556965.8
Northing	6242466.0	6242466.0	6242466.0	6242466.0	6242466.0	6242466.0	6242466.0	6242466.0	6242466.0

TS number	C97-1086	C97-1086	C97-1086	C97-1086	C97-1090	C97-1090	C97-1090	C97-1090	C97-1090
Wt% S	33.37	36.56	34.74	33.72	38.22	37.48	34.95	33.10	38.66
Wt% Fe	35.88	62.93	30.50	34.67	59.97	61.83	29.87	31.85	60.18
Wt% Co	1.19	0.04	0.02	1.36	0.04	0.03	0.02	0.98	0.04
Wt% Ni	30.22	0.00	0.03	30.12	0.28	0.09	0.09	33.78	0.27
Wt% Cu	0.00	0.02	34.33	0.40	0.00	0.01	34.07	0.00	0.00
Total	100.66	99.55	99.62	100.26	98.51	99.44	99.03	99.71	99.15
Atomic% S	46.92	50.27	49.91	47.49	52.48	51.31	50.39	47.05	52.69
Atomic% Fe	28.97	49.68	25.16	28.03	47.27	48.59	24.72	25.98	47.08
Atomic% Co	0.00	0.00	0.00	0.00	0.00	0.00	0.00	0.00	0.00
Atomic% Ni	0.91	0.03	0.01	1.04	0.03	0.02	0.02	0.76	0.03
Atomic% Cu	23.21	0.00	0.03	23.16	0.21	0.07	0.07	26.22	0.20
Host	Troc	Troc	Troc	Troc	Troc	Troc	Troc	Troc	Troc
Hole	VB96266	VB96266	VB96266	VB96266	VB96266	VB96266	VB96266	VB96266	VB96266
Depth	136.30	136.30	136.30	136.30	167.00	167.00	167.00	167.00	167.00
Easting	556965.8	556965.8	556965.8	556965.8	556965.8	556965.8	556965.8	556965.8	556965.8
Northing	6242466.0	6242466.0	6242466.0	6242466.0	6242466.0	6242466.0	6242466.0	6242466.0	6242466.0

TS number	C97-1090	C97-1090	C97-1090	C97-1090	C97-1090	C97-1090	C97-1090	C97-1090	C97-1090
Wt% S	34.13	38.65	34.78	33.61	38.58	33.46	35.07	38.33	33.40
Wt% Fe	38.29	60.49	29.78	32.16	60.98	32.94	30.65	60.94	32 82
Wt% Co	0.78	0.04	0.02	1.31	0.03	1.17	0.00	0.04	1.13
Wt% Ni	26.87	0.29	0.00	33.10	0.27	33.02	0.00	0.27	33.46
Wt% Cu	0.00	0.02	33.80	0.00	0.01	0.00	34.77	0.00	0.00
Total	100.08	99.50	98.39	100.19	99.87	100.59	100.48	99.59	100.81
Atomic% S	47.93	52.54	50.45	47.43	52.31	47.10	49.95	52.16	46.96
Atomic% Fe	30.87	47.20	24.80	26.05	47.46	26.62	25.06	47.60	26.49
Atomic% Co	0.00	0.00	0.00	0.00	0.01	0.00	0.00	0.00	0.00
Atomic% Ni	0.60	0.03	0.01	1.01	0.03	0.90	0.00	0.03	0.87
Atomic% Cu	20.61	0.22	0.00	25.50	0.20	25.38	0.00	0.20	25.68
Host	Troc	Troc	Troc	Troc	Troc	Troc	Troc	Troc	Troc
Hole	VB96266	VB96266	VB96266	VB96266	VB96266	VB96266	VB96266	VB96266	VB96266
Depth	167.00	167.00	167.00	167.00	167.00	167.00	167.00	167.00	167.00
Easting	556965.8	556965.8	556965.8	556965.8	556965.8	556965.8	556965.8	556965.8	556965.8
Northing	6242466.0	6242466.0	6242466.0	6242466.0	6242466.0	6242466.0	6242466.0	6242466.0	6242466.0

TS number	C97-1090	C97-1090	C97-1090	C97-1090	C97-1090	98/AV/310	98/AV/310	98/AV/310	98/AV/310
Wt% S	33.43	38.71	35.05	33.17	39.05	34.77	38.08	33.21	38.98
Wt% Fe	32.70	59.95	29.67	31.63	60.06	31.31	61.77	31.43	62.05
Wt% Co	1.17	0.05	0.01	1.26	0.03	0.06	0.03	1.97	0.04
Wt% Ni	33.42	0.32	0.03	33.29	0.29	0.39	0.47	34.17	0.50
Wt% Cu	0.00	0.01	34.22	0.00	0.00	31.98	0.01	0.00	0.00
Total	100.72	99.05	98.98	99.36	99.43	98.50	100.38	100.79	101.58
Atomic% S	47.03	52.78	50.53	47.26	52.99	50.30	51.58	46.79	52.05
Atomic% Fe	26.41	46.93	24.55	25.87	46.78	26.00	48.03	25.42	47.56
Atomic% Co	0.00	0.01	0.00	0.00	0.00	0.00	0.02	0.00	0.00
Atomic% Ni	0.89	0.04	0.01	0.98	0.02	0.05	0.03	1.51	0.03
Atomic% Cu	25.67	0.24	0.02	25.90	0.22	0.31	0.35	26.29	0.37
Host	Troc	Troc	Troc	Troc	Troc	MASU	MASU	MASU	MASU
Hole	VB96266	VB96266	VB96266	VB96266	VB96266	VB96266	VB96266	VB96266	VB96266
Depth	167.00	167.00	167.00	167.00	167.00	653.50	653.50	653.50	653.50
Easting	556965.8	556965.8	556965.8	556965.8	556965.8	556965.8	556965.8	556965.8	556965.8
Northing	6242466.0	6242466.0	6242466.0	6242466.0	6242466.0	6242466.0	6242466.0	6242466.0	6242466.0

TS number	98/AV/310	98/AV/310	98/AV/310	98/AV/310	98/AV/310	98/AV/310	98/AV/310	98/AV/310	98/AV/310
Wt% S	39.19	38.86	39.03	35.34	39.13	39.20	33.38	38.99	39.20
Wt% Fe	62.20	61.45	61.67	41.35	61.75	61.90	31.55	61.86	62.15
Wt% Co	0.04	0.03	0.04	1.29	0.03	0.03	1.81	0.03	0.04
Wt% Ni	0.53	0.54	0.53	23.21	0.51	0.40	33.69	0.40	0.50
Wt% Cu	0.00	0.00	0.00	0.00	0.00	0.01	0.00	0.01	0.00
Total	101.95	100.88	101.28	101.20	101.44	101.55	100.42	101.29	101.89
Atomic% S	52.11	52.20	52.21	48.77	52.26	52.28	47.10	52.17	52.14
Atomic% Fe	47.48	47.38	47.37	32.76	47.34	47.40	25.56	47.51	47.46
Atomic% Co	0.00	0.00	0.00	0.01	0.01	0.01	0.00	0.00	0.00
Atomic% Ni	0.03	0.02	0.03	0.97	0.02	0.02	1.39	0.02	0.03
Atomic% Cu	0.38	0.40	0.39	17.49	0.37	0.29	25.96	0.29	0.37
Host	MASU	MASU	MASU	MASU	MASU	MASU	MASU	MASU	MASU
Hole	VB96266	VB96266	VB96266	VB96266	VB96266	VB96266	VB96266	VB96266	VB96266
Depth	653.50	653.50	653.50	653.50	653.50	653.50	653.50	653.50	653.50
Easting	556965.8	556965.8	556965.8	556965.8	556965.8	556965.8	556965.8	556965.8	556965.8
Northing	6242466.0	6242466.0	6242466.0	6242466.0	6242466.0	6242466.0	6242466.0	6242466.0	6242466.0

TS number	98/AV/310	98/AV/310	98/AV/310	98/AV/310	98/AV/310	98/AV/310	98/AV/310	98/AV/310	98/AV/310
Wt% S	38.93	39.04	33.33	39.06	33.17	39.01	31.60	39.06	39.07
Wt% Fe	61.80	61.82	31.36	62.30	31.45	61.91	31.38	61.79	61.67
Wt% Co	0.04	0.03	1.99	0.03	2.00	0.03	1.91	0.04	0.03
Wt% Ni	0.51	0.47	34.42	0.42	34.11	0.41	33.57	0.53	0.47
Wt% Cu	0.00	0.00	0.00	0.01	0.00	0.00	0.00	0.01	0.00
Total	101.28	101.36	101.12	101.82	100.73	101.37	98.50	101.43	101.26
Atomic% S	52.11	52.19	46.80	52.03	46.76	52.16	45.80	52.19	52.26
Atomic% Fe	47.49	47.45	25.28	47.64	25.45	47.52	26.11	47.39	47.36
Atomic% Co	0.00	0.00	0.01	0.00	0.00	0.00	0.03	0.00	0.02
Atomic% Ni	0.03	0.02	1.52	0.02	1.54	0.02	1.50	0.03	0.02
Atomic% Cu	0.37	0.35	26.39	0.31	26.26	0.30	26.57	0.39	0.34
Host	MASU	MASU	MASU	MASU	MASU	MASU	MASU	MASU	MASU
Hole	VB96266	VB96266	VB96266	VB96266	VB96266	VB96266	VB96266	VB96266	VB96266
Depth	653.50	653.50	653.50	653.50	653.50	653.50	653.50	653.50	653.50
Easting	556965.8	556965.8	556965.8	556965.8	556965.8	556965.8	556965.8	556965.8	556965.8
Northing	6242466.0	6242466.0	6242466.0	6242466.0	6242466.0	6242466.0	6242466.0	6242466.0	6242466.0

TS number	98/AV/310	98/AV/310	98/AV/310	98/AV/310	98/AV/310	98/AV/310	98/AV/310	98/AV/310	98/AV/310
Wt% S	33.23	39.12	33.26	31.47	38.96	39.13	33.09	39.07	38.77
Wt% Fe	31.71	61.63	31.46	31.31	61.55	61.49	31.00	62.01	61.64
Wt% Co	2.08	0.04	2.09	2.02	0.02	0.02	2.05	0.02	0.04
Wt% Ni	33.46	0.46	33.39	32.54	0.35	0.52	33.04	0.40	0.48
Wt% Cu	0.00	0.00	0.00	0.00	0.00	0.00	0.00	0.00	0.00
Total	100.48	101.27	100.20	97.35	100.88	101.16	99.18	101.49	100.94
Atomic% S	46.91	52.31	47.06	46.07	52.30	52.37	47.25	52.16	52.08
Atomic% Fe	25.69	47.31	25.55	26.31	47.43	47.24	25.41	47.54	47.54
Atomic% Co	0.00	0.01	0.00	0.00	0.00	0.00	0.00	0.00	0.00
Atomic% Ni	1.60	0.03	1.61	1.61	0.02	0.01	1.59	0.01	0.03
Atomic% Cu	25.79	0.33	25.79	26.01	0.25	0.38	25.76	0.29	0.35
Host	MASU	MASU	MASU	MASU	MASU	MASU	MASU	MASU	MASU
Hole	VB96266	VB96266	VB96266	VB96266	VB96266	VB96266	VB96266	VB96266	VB96266
Depth	653.50	653.50	653.50	653.50	653.50	653.50	653.50	653.50	653.50
Easting	556965.8	556965.8	556965.8	556965.8	556965.8	556965.8	556965.8	556965.8	556965.8
Northing	6242466.0	6242466.0	6242466.0	6242466.0	6242466.0	6242466.0	6242466.0	6242466.0	6242466.0

TS number	98/AV/310	98/AV/310	98/AV/310	98/AV/310	98/AV/310	98/AV/310	98/AV/310	98/AV/310	98/AV/310
Wt% S	33.37	34.91	34.81	38.43	32.99	33.14	38.92	38.95	33.60
Wt% Fe	31.95	31.28	31.21	61.07	31.20	31.58	61.90	61.84	31.40
Wt% Co	2.17	0.03	0.00	0.03	1.96	2.11	0.03	0.04	2.26
Wt% Ni	33.51	0.03	0.00	0.38	33.58	33.24	0.49	0.52	34.54
Wt% Cu	0.00	33.29	32.89	0.01	0.00	0.00	0.00	0.00	0.00
Total	100.99	99.53	98.90	99.92	99.73	100.10	101.35	101.36	101.79
Atomic% S	46.87	50.09	50.21	52.13	46.92	46.95	52.07	52.10	46.85
Atomic% Fe	25.77	25.77	25.85	47.56	25.48	25.68	47.54	47.48	25.13
Atomic% Co	0.00	0.00	0.00	0.00	0.00	0.02	0.01	0.01	0.00
Atomic% Ni	1.66	0.02	0.00	0.02	1.52	1.63	0.02	0.03	1.71
Atomic% Cu	25.70	0.02	0.00	0.28	26.08	25.72	0.36	0.38	26.30
Host	MASU	MASU	MASU	MASU	MASU	MASU	MASU	MASU	MASU
Hole	VB96266	VB96266	VB96266	VB96266	VB96266	VB96266	VB96266	VB96266	VB96266
Depth	653.50	653.50	653.50	653.50	653.50	653.50	653.50	653.50	653.50
Easting	556965.8	556965.8	556965.8	556965.8	556965.8	556965.8	556965.8	556965.8	556965.8
Northing	6242466.0	6242466.0	6242466.0	6242466.0	6242466.0	6242466.0	6242466.0	6242466.0	6242466.0

TS number	98/AV/314	98/AV/314	98/AV/314	98/AV/314	98/AV/314	98/AV/314	98/AV/314	98/AV/314	98/AV/314
Wt% S	39.04	39.45	33.80	35.04	38.88	38.99	34.12	38.84	0.01
Wt% Fe	61.44	61.58	31.93	30.90	61.59	61.83	30.18	60.75	66.10
Wt% Co	0.04	0.03	1.62	0.01	0.04	0.04	0.01	0.03	0.03
Wt% Ni	0.55	0.33	28.03	0.00	0.36	0.42	0.01	0.43	0.04
Wt% Cu	0.03	0.05	5.23	32.97	0.00	0.00	32.60	0.00	0.00
Total	101.10	101.45	100.60	98.91	100.87	101.28	96.92	100.05	66.18
Atomic% S	52.30	52.58	47.64	50.48	52.21	52.17	50.25	52.51	0.02
Atomic% Fe	47.25	47.12	25.83	25.55	47.48	47.50	25.52	47.15	99.87
Atomic% Co	0.01	0.00	0.00	0.00	0.01	0.00	0.00	0.01	0.02
Atomic% Ni	0.03	0.02	1.24	0.01	0.03	0.03	0.01	0.02	0.04
Atomic% Cu	0.40	0.24	21.57	0.00	0.27	0.30	0.01	0.32	0.06
Host	MASU	MASU	MASU	MASU	MASU	MASU	MASU	MASU	MASU
Hole	VB96266	VB96266	VB96266	VB96266	VB96266	VB96266	VB96266	VB96266	VB96266
Depth	675.00	675.00	675.00	675.00	675.00	675.00	675.00	675.00	675.00
Easting	556965.8	556965.8	556965.8	556965.8	556965.8	556965.8	556965.8	556965.8	556965.8
Northing	6242466.0	6242466.0	6242466.0	6242466.0	6242466.0	6242466.0	6242466.0	6242466.0	6242466.0

TS number	98/AV/314	98/AV/314	98/AV/314	98/AV/314	98/AV/314	98/AV/314	98/AV/314	98/AV/314	98/AV/314
Wt% S	38.98	33.30	39.11	38.95	38.96	33.43	34.91	33.10	38.87
Wt% Fe	62.01	31.36	62.18	61.92	61.99	31.13	31.41	31.34	61.97
Wt% Co	0.05	2.00	0.03	0.03	0.04	1.76	0.02	1.90	0.05
Wt% Ni	0.49	34.44	0.43	0.47	0.50	31.49	0.08	33.92	0.53
Wt% Cu	0.00	0.00	0.02	0.00	0.00	2.45	33.34	0.00	0.00
Total	101.52	101.12	101.79	101.39	101.51	100.46	99.77	100.26	101.41
Atomic% S	52.07	46.76	52.10	52.08	52.05	47.22	50.00	46.85	51.99
Atomic% Fe	47.55	25.29	47.55	47.54	47.55	25.25	25.83	25.47	47.59
Atomic% Co	0.00	0.02	0.01	0.02	0.01	0.14	0.00	0.00	0.00
Atomic% Ni	0.03	1.53	0.02	0.02	0.03	1.36	0.02	1.46	0.03
Atomic% Cu	0.36	26.41	0.32	0.34	0.37	24.29	0.06	26.22	0.39
Host	MASU	MASU	MASU	MASU	MASU	MASU	MASU	MASU	MASU
Hole	VB96266	VB96266	VB96266	VB96266	VB96266	VB96266	VB96266	VB96266	VB96266
Depth	675.00	675.00	675.00	675.00	675.00	675.00	675.00	675.00	675.00
Easting	556965.8	556965.8	556965.8	556965.8	556965.8	556965.8	556965.8	556965.8	556965.8
Northing	6242466.0	6242466.0	6242466.0	6242466.0	6242466.0	6242466.0	6242466.0	6242466.0	6242466.0

TS number	98/AV/314	98/AV/314	98/AV/314	98/AV/314	98/AV/314	98/AV/314	98/AV/314	98/AV/314	98/AV/314
Wt% S	32.99	33.62	38.87	33.43	38.93	38.87	39.13	33.47	33.44
Wt% Fe	31.70	31.04	61.44	31.40	62.18	61.99	62.06	31.37	31.84
Wt% Co	1.91	1.91	0.03	1.88	0.04	0.03	0.02	1.98	2.16
Wt% Ni	33.74	33.85	0.50	33.66	0.50	0.51	0.45	34.14	33.80
Wt% Cu	0.00	0.00	0.00	0.00	0.02	0.00	0.00	0.00	0.00
Total	100.34	100.41	100.84	100.37	101.68	101.41	101.66	100.95	101.26
Atomic% S	46.70	47.38	52.23	47.17	51.95	52.00	52.17	47.01	46.86
Atomic% Fe	25.76	25.11	47.39	25.44	47.64	47.60	47.49	25.29	25.61
Atomic% Co	0.00	0.00	0.00	0.00	0.01	0.00	0.00	0.00	0.01
Atomic% Ni	1.47	1.46	0.02	1.44	0.03	0.02	0.02	1.51	1.65
Atomic% Cu	26.08	26.05	0.36	25.94	0.37	0.37	0.33	26.19	25.87
Host	MASU	MASU	MASU	MASU	MASU	MASU	MASU	MASU	MASU
Hole	VB96266	VB96266	VB96266	VB96266	VB96266	VB96266	VB96266	VB96266	VB96266
Depth	675.00	675.00	675.00	675.00	675.00	675.00	675.00	675.00	675.00
Easting	556965.8	556965.8	556965.8	556965.8	556965.8	556965.8	556965.8	556965.8	556965.8
Northing	6242466.0	6242466.0	6242466.0	6242466.0	6242466.0	6242466.0	6242466.0	6242466.0	6242466.0

TS number	98/AV/314	98/AV/314	98/AV/314	98AV/304	98AV/304	98AV/304	98AV/304	98AV/304	98AV/304
Wt% S	38.95	38.97	33.63	39.02	35.25	39.06	38.97	0.00	38.27
Wt% Fe	62.24	62.03	31.38	62.45	31.59	62.44	62.38	28.60	60.15
Wt% Co	0.03	0.04	2.00	0.01	0.02	0.04	0.03	0.00	0.04
Wt% Ni	0.49	0.43	34.68	0.23	0.00	0.06	0.27	0.01	0.38
Wt% Cu	0.00	0.01	0.00	0.04	33.69	0.17	0.01	0.00	0.00
Total	101.71	101.47	101.71	101.75	100.55	101.77	101.66	28.61	98.85
Atomic% S	51.96	52.07	46.92	52.01	50.07	52.05	52.00	0.00	52.40
Atomic% Fe	47.66	47.58	25.13	47.79	25.77	47.77	47.78	99.95	47.28
Atomic% Co	0.00	0.00	0.02	0.00	0.00	0.01	0.00	0.00	0.01
Atomic% Ni	0.02	0.03	1.52	0.01	0.01	0.03	0.02	0.02	0.03
Atomic% Cu	0.36	0.31	26.42	0.17	0.00	0.04	0.20	0.02	0.28
Host	MASU	MASU	MASU	Troc	Troc	Troc	Troc	Troc	Troc
Hole	VB96266	VB96266	VB96266	VB96266	VB96266	VB96266	VB96266	VB96266	VB96266
Depth	675.00	675.00	675.00	499.30	499.30	499.30	499.30	499.30	499.30
Easting	556965.8	556965.8	556965.8	556965.8	556965.8	556965.8	556965.8	556965.8	556965.8
Northing	6242466.0	6242466.0	6242466.0	6242466.0	6242466.0	6242466.0	6242466.0	6242466.0	6242466.0

TS number	98AV/304	98AV/304	98AV/304	98AV/304	98AV/304	98AV/304	98AV/304	98AV/304	98AV/304
Wt% S	33.47	33.01	39.29	33.63	39.24	39.21	33.50	39.37	35.06
Wt% Fe	32.15	30.97	61.75	31.93	62.07	61.31	31.74	62.22	31.55
Wt% Co	1.34	1.32	0.03	0.92	0.02	0.03	1.05	0.04	0.02
Wt% Ni	34.95	33.76	0.71	35.47	0.68	0.69	35.69	0.72	0.00
Wt% Cu	0.00	0.00	0.00	0.00	0.00	0.00	0.00	0.00	33.88
Total	101.90	99.06	101.78	101.97	102.01	101.23	101.99	102.38	100.50
Atomic% S	46.65	47.20	52.29	46.81	52.14	52.42	46.67	52.13	49.90
Atomic% Fe	25.73	25.42	47.17	25.52	47.35	47.06	25.38	47.30	25.77
Atomic% Co	0.00	0.00	0.00	0.01	0.00	0.00	0.01	0.02	0.00
Atomic% Ni	1.01	1.02	0.02	0.70	0.01	0.02	0.79	0.03	0.01
Atomic% Cu	26.61	26.36	0.52	26.96	0.49	0.50	27.15	0.52	0.00
Host	Troc	Troc	Troc	Troc	Troc	Troc	Troc	Troc	Troc
Hole	VB96266	VB96266	VB96266	VB96266	VB96266	VB96266	VB96266	VB96266	VB96266
Depth	499.30	499.30	499.30	499.30	499.30	499.30	499.30	499.30	499.30
Easting	556965.8	556965.8	556965.8	556965.8	556965.8	556965.8	556965.8	556965.8	556965.8
Northing	6242466.0	6242466.0	6242466.0	6242466.0	6242466.0	6242466.0	6242466.0	6242466.0	6242466.0

TS number	98AV/304	98AV/304	98AV/304	98AV/304	98AV/304	98AV/304	98AV/304	98AV/304	98AV/304
Wt% S	35.45	38.95	35.07	33.46	39.43	39.25	33.54	39.31	39.45
Wt% Fe	31.58	60.99	31.61	31.93	62.00	61.95	31.84	61.85	62.05
Wt% Co	0.02	0.03	0.01	0.95	0.03	0.04	1.02	0.03	0.04
Wt% Ni	0.00	0.47	0.00	35.28	0.56	0.69	35.80	0.72	0.70
Wt% Cu	33.88	0.02	34.09	0.00	0.00	0.01	0.00	0.00	0.00
Total	101.01	100.45	100.80	101.63	102.03	101.96	102.19	101.93	102.25
Atomic% S	50.12	52.47	49.80	46.75	52.33	52.18	46.63	52.25	52.27
Atomic% Fe	25.64	47.16	25.77	25.61	47.24	47.27	25.41	47.19	47.19
Atomic% Co	0.05	0.00	0.00	0.00	0.00	0.01	0.00	0.01	0.01
Atomic% Ni	0.02	0.02	0.01	0.72	0.02	0.03	0.78	0.02	0.03
Atomic% Cu	0.00	0.35	0.00	26.92	0.41	0.50	27.18	0.53	0.50
Host	Troc	Troc	Troc	Troc	Troc	Troc	Troc	Troc	Troc
Hole	VB96266	VB96266	VB96266	VB96266	VB96266	VB96266	VB96266	VB96266	VB96266
Depth	499.30	499.30	499.30	499.30	499.30	499.30	499.30	499.30	499.30
Easting	556965.8	556965.8	556965.8	556965.8	556965.8	556965.8	556965.8	556965.8	556965.8
Northing	6242466.0	6242466.0	6242466.0	6242466.0	6242466.0	6242466.0	6242466.0	6242466.0	6242466.0

TS number	98AV/304	98AV/304	98AV/304	98AV/304	98AV/304	98AV/304	98AV/304	98AV/304	98AV/304
Wt% S	33.66	39.23	33.54	39.17	33.70	39.06	39.36	33.74	39.41
Wt% Fe	31.59	61.79	31.76	61.94	31.79	62.28	62.36	31.78	62.02
Wt% Co	1.09	0.03	1.07	0.04	1.23	0.04	0.04	0.97	0.03
Wt% Ni	35.68	0.61	35.38	0.47	35.81	0.65	0.77	35.85	0.67
Wt% Cu	0.00	0.01	0.00	0.00	0.00	0.00	0.03	0.00	0.00
Total	102.03	101.68	101.75	101.62	102.53	102.03	102.59	102.35	102.16
Atomic% S	46.83	52.26	46.79	52.23	46.70	51.95	52.04	46.81	52.26
Atomic% Fe	25.23	47.26	25.44	47.41	25.28	47.55	47.34	25.31	47.21
Atomic% Co	0.00	0.01	0.00	0.00	0.00	0.00	0.03	0.00	0.02
Atomic% Ni	0.83	0.02	0.82	0.03	0.93	0.03	0.03	0.73	0.02
Atomic% Cu	27.11	0.44	26.96	0.34	27.10	0.47	0.55	27.15	0.49
Host	Troc	Troc	Troc	Troc	Troc	Troc	Troc	Troc	Troc
Hole	VB96266	VB96266	VB96266	VB96266	VB96266	VB96266	VB96266	VB96266	VB96266
Depth	499.30	499.30	499.30	499.30	499.30	499.30	499.30	499.30	499.30
Easting	556965.8	556965.8	556965.8	556965.8	556965.8	556965.8	556965.8	556965.8	556965.8
Northing	6242466.0	6242466.0	6242466.0	6242466.0	6242466.0	6242466.0	6242466.0	6242466.0	6242466.0

TS number	98AV/304	98/AV040	98/AV040	98/AV040	98/AV040	98/AV040	98/AV040	98/AV040	98/AV040
Wt% S	39.12	38.93	39.04	38.76	33.12	39.19	38.84	38.91	38.80
Wt% Fe	61.91	62.56	62.44	62.36	32.77	62.76	63.00	62.36	62.32
Wt% Co	0.05	0.02	0.05	0.04	1.59	0.03	0.04	0.04	0.03
Wt% Ni	0.74	0.31	0.37	0.37	34.13	0.31	0.34	0.40	0.39
Wt% Cu	0.00	0.00	0.01	0.00	0.00	0.00	0.00	0.00	0.00
Total	101.80	101.86	101.92	101.53	101.61	102.29	102.23	101.71	101.56
Atomic% S	52.10	51.88	51.96	51.84	46.37	51.97	51.64	51.91	51.86
Atomic% Fe	47.33	47.86	47.72	47.87	26.34	47.78	48.08	47.76	47.82
Atomic% Co	0.00	0.02	0.03	0.03	1.21	0.02	0.03	0.03	0.02
Atomic% Ni	0.03	0.23	0.27	0.27	26.09	0.22	0.25	0.29	0.28
Atomic% Cu	0.54	0.00	0.01	0.00	0.00	0.00	0.00	0.00	0.00
Host	Troc	MASU	MASU	MASU	MASU	MASU	MASU	MASU	MASU
Hole	VB96266	PD006	PD006	PD006	PD006	PD006	PD006	PD006	PD006
Depth	499.30	80.00	80.00	80.00	80.00	80.00	80.00	80.00	80.00
Easting	556965.8	555837.1	555837.1	555837.1	555837.1	555837.1	555837.1	555837.1	555837.1
Northing	6242466.0	6243322.9	6243322.9	6243322.9	6243322.9	6243322.9	6243322.9	6243322.9	6243322.9

TS number	98/AV040	98/AV040	98/AV040	98/AV040	98/AV040	98/AV040	98/AV040	98/AV040	98/AV040
Wt% S	38.71	38.91	38.61	33.24	38.56	33.55	35.13	38.98	35.81
Wt% Fe	62.71	62.46	62.64	32.96	62.39	33.04	31.44	62.29	38.80
Wt% Co	0.03	0.04	0.03	1.68	0.06	1.61	0.03	0.04	0.02
Wt% Ni	0.33	0.38	0.31	34.18	0.36	34.00	0.07	0.31	0.27
Wt% Cu	0.01	0.01	0.00	0.00	0.02	0.00	34.22	0.00	26.78
Total	101.79	101.82	101.59	102.09	101.38	102.20	100.89	101.62	101.68
Atomic% S	51.67	51.87	51.65	46.33	51.68	46.63	49.83	52.02	49.91
Atomic% Fe	48.06	47.80	48.11	26.37	48.00	26.36	25.60	47.72	31.04
Atomic% Co	0.02	0.03	0.02	1.28	0.04	1.22	0.02	0.03	0.02
Atomic% Ni	0.24	0.28	0.23	26.01	0.26	25.80	0.06	0.22	0.20
Atomic% Cu	0.01	0.01	0.00	0.00	0.01	0.00	24.49	0.00	18.83
Host	MASU	MASU	MASU	MASU	MASU	MASU	MASU	MASU	MASU
Hole	PD006	PD006	PD006	PD006	PD006	PD006	PD006	PD006	PD006
Depth	80.00	80.00	80.00	80.00	80.00	80.00	80.00	80.00	80.00
Easting	555837.1	555837.1	555837.1	555837.1	555837.1	555837.1	555837.1	555837.1	555837.1
Northing	6243322.9	6243322.9	6243322.9	6243322.9	6243322.9	6243322.9	6243322.9	6243322.9	6243322.9

TS number	98/AV040	98/AV040	98/AV040	98/AV040	98/AV040	98/AV040	98/AV040	98/AV040	98/AV040
Wt% S	38.88	38.66	38.68	39.13	32.86	38.76	33.84	35.02	38.69
Wt% Fe	62.25	62.14	61.95	61.85	33.03	61.40	32.18	31.52	61.59
Wt% Co	0.05	0.03	0.04	0.04	1.59	0.04	1.71	0.01	0.04
Wt% Ni	0.36	0.40	0.33	0.34	33.85	0.38	33.79	0.00	0.39
Wt% Cu	0.00	0.00	0.01	0.00	0.00	0.00	0.00	34.02	0.00
Total	101.54	101.23	101.01	101.37	101.33	100.57	101.53	100.59	100.72
Atomic% S	51.96	51.85	51.96	52.28	46.17	52.22	47.19	49.82	52.08
Atomic% Fe	47.75	47.84	47.76	47.44	26.64	47.48	25.76	25.75	47.60
Atomic% Co	0.03	0.02	0.03	0.03	1.22	0.03	1.30	0.01	0.03
Atomic% Ni	0.26	0.29	0.24	0.25	25.97	0.28	25.74	0.00	0.29
Atomic% Cu	0.00	0.00	0.01	0.00	0.00	0.00	0.00	24.42	0.00
Host	MASU	MASU	MASU	MASU	MASU	MASU	MASU	MASU	MASU
Hole	PD006	PD006	PD006	PD006	PD006	PD006	PD006	PD006	PD006
Depth	80.00	80.00	80.00	80.00	80.00	80.00	80.00	80.00	80.00
Easting	555837.1	555837.1	555837.1	555837.1	555837.1	555837.1	555837.1	555837.1	555837.1
Northing	6243322.9	6243322.9	6243322.9	6243322.9	6243322.9	6243322.9	6243322.9	6243322.9	6243322.9

TS number	98/AV040	98/AV040	98/AV040	98/AV040	98/AV040	98/AV040	98/AV040	98/AV040	98/AV040
Wt% S	39.02	38.55	39.09	33.69	35.38	38.89	39.14	33.23	38.56
Wt% Fe	61.84	61.62	62.74	31.85	33.32	62.43	62.83	32.71	63.06
Wt% Co	0.03	0.04	0.03	2.00	0.07	0.03	0.03	1.76	0.03
Wt% Ni	0.39	0.36	0.33	34.44	0.42	0.37	0.36	34.18	0.31
Wt% Cu	0.00	0.01	0.01	0.00	31.89	0.02	0.01	0.00	0.01
Total	101.28	100.58	102.20	101.99	101.08	101.73	102.37	101.89	102.00
Atomic% S	52.20	51.99	51.91	46.87	49.92	51.89	51.89	46.39	51.44
Atomic% Fe	47.50	47.71	47.83	25.44	26.99	47.81	47.82	26.22	48.29
Atomic% Co	0.02	0.03	0.02	1.51	0.05	0.02	0.02	1.34	0.03
Atomic% Ni	0.28	0.26	0.24	26.17	0.32	0.27	0.26	26.05	0.23
Atomic% Cu	0.00	0.01	0.01	0.00	22.70	0.01	0.00	0.00	0.00
Host	MASU	MASU	MASU	MASU	MASU	MASU	MASU	MASU	MASU
Hole	PD006	PD006	PD006	PD006	PD006	PD006	PD006	PD006	PD006
Depth	80.00	80.00	80.00	80.00	80.00	80.00	80.00	80.00	80.00
Easting	555837.1	555837.1	555837.1	555837.1	555837.1	555837.1	555837.1	555837.1	555837.1
Northing	6243322.9	6243322.9	6243322.9	6243322.9	6243322.9	6243322.9	6243322.9	6243322.9	6243322.9

TS number	98/AV040	98/AV040	98/AV040	98/AV040	98/AV040	98/AV040	98/AV040	98/AV040	98/AV040
Wt% S	33.45	32.50	38.98	35.11	33.21	39.01	39.05	39.13	33.58
Wt% Fe	32.99	32.76	62.43	31.72	33.02	62.34	62.15	62.26	33.10
Wt% Co	1.67	1.70	0.04	0.01	1.64	0.04	0.03	0.03	1.70
Wt% Ni	34.30	33.45	0.22	0.00	33.96	0.31	0.36	0.32	33.86
Wt% Cu	0.00	0.00	0.00	34.09	0.00	0.00	0.00	0.00	0.00
Total	102.42	100.42	101.67	100.98	101.83	101.70	101.59	101.74	102.23
Atomic% S	46.44	46.10	52.00	49.77	46.38	52.02	52.11	52.13	46.64
Atomic% Fe	26.29	26.68	47.81	25.81	26.48	47.73	47.61	47.61	26.39
Atomic% Co	1.26	1.31	0.03	0.01	1.25	0.03	0.02	0.02	1.28
Atomic% Ni	26.00	25.91	0.16	0.00	25.90	0.22	0.26	0.24	25.68
Atomic% Cu	0.00	0.00	0.00	24.38	0.00	0.00	0.00	0.00	0.00
Host	MASU	MASU	MASU	MASU	MASU	MASU	MASU	MASU	MASU
Hole	PD006	PD006	PD006	PD006	PD006	PD006	PD006	PD006	PD006
Depth	80.00	80.00	80.00	80.00	80.00	80.00	80.00	80.00	80.00
Easting	555837.1	555837.1	555837.1	555837.1	555837.1	555837.1	555837.1	555837.1	555837.1
Northing	6243322.9	6243322.9	6243322.9	6243322.9	6243322.9	6243322.9	6243322.9	6243322.9	6243322.9

TS number	98/AV040	98/AV040	98/AV040	98/AV040	98/AV040	98/AV/076	98/AV/076	98/AV/076	98/AV/076
Wt% S	39.42	33.03	33.60	38.48	36.47	39.08	33.57	33.47	39.33
Wt% Fe	62.54	33.12	33.11	63.36	61.42	62.41	31.66	31.52	62.28
Wt% Co	0.04	1.26	1.66	0.03	0.03	0.04	2.67	2.63	0.04
Wt% Ni	0.22	27.04	33.87	0.24	0.34	0.47	34.33	34.53	0.45
Wt% Cu	0.00	5.90	0.00	0.03	0.00	0.00	0.02	0.00	0.00
Total	102.22	100.34	102.32	102.16	98.26	102.00	102.25	102.16	102.11
Atomic% S	52.24	46.88	46.63	51.29	50.70	47.65	25.26	25.18	47.45
Atomic% Fe	47.57	26.98	26.39	48.48	49.02	0.34	26.06	26.24	0.33
Atomic% Co	0.03	0.97	1.25	0.02	0.02	0.03	2.02	1.99	0.03
Atomic% Ni	0.16	20.95	25.67	0.18	0.26	0.00	0.01	0.00	0.00
Atomic% Cu	0.00	4.22	0.00	0.02	0.00	0.00	0.00	0.00	0.00
Host	MASU	MASU	MASU	MASU	MASU	MASU	MASU	MASU	MASU
Hole	PD006	PD006	PD006	PD006	PD006	VB96300	VB96300	VB96300	VB96300
Depth	80.00	80.00	80.00	80.00	80.00	764.00	764.00	764.00	764.00
Easting	555837.1	555837.1	555837.1	555837.1	555837.1	553779.1	553779.1	553779.1	553779.1
Northing	6243322.9	6243322.9	6243322.9	6243322.9	6243322.9	6243011.7	6243011.7	6243011.7	6243011.7

TS number	98/AV/076	98/AV/076	98/AV/076	98/AV/076	98/AV/076	98/AV/076	98/AV/076	98/AV/076	98/AV/076
Wt% S	39.21	38.87	39.05	39.06	33.33	38.94	33.54	39.18	33.24
Wt% Fe	61.99	62.15	62.06	62.18	31.28	61.50	31.42	62.23	31.26
Wt% Co	0.05	0.03	0.03	0.04	2.46	0.04	2.49	0.05	2.63
Wt% Ni	0.52	0.49	0.51	0.47	35.13	0.45	34.72	0.39	34.70
Wt% Cu	0.00	0.00	0.00	0.00	0.02	0.03	0.01	0.03	0.00
Total	101.77	101.54	101.64	101.75	102.22	100.97	102.18	101.89	101.84
Atomic% S	47.39	47.68	47.52	47.57	25.00	47.37	25.09	47.53	25.07
Atomic% Fe	0.38	0.36	0.37	0.34	26.71	0.33	26.37	0.29	26.48
Atomic% Co	0.03	0.02	0.02	0.03	1.87	0.03	1.89	0.04	2.00
Atomic% Ni	0.00	0.00	0.00	0.00	0.01	0.02	0.01	0.02	0.00
Atomic% Cu	0.00	0.00	0.00	0.00	0.00	0.00	0.00	0.00	0.00
Host	MASU	MASU	MASU	MASU	MASU	MASU	MASU	MASU	MASU
Hole	VB96300	VB96300	VB96300	VB96300	VB96300	VB96300	VB96300	VB96300	VB96300
Depth	764.00	764.00	764.00	764.00	764.00	764.00	764.00	764.00	764.00
Easting	553779.1	553779.1	553779.1	553779.1	553779.1	553779.1	553779.1	553779.1	553779.1
Northing	6243011.7	6243011.7	6243011.7	6243011.7	6243011.7	6243011.7	6243011.7	6243011.7	6243011.7

TS number	98/AV/076	98/AV/076	98/AV/076	98/AV/076	98/AV/076	98/AV/076	98/AV/076	98/AV/076	98/AV/076
Wt% S	39.53	39.36	39.23	39.23	33.33	39.08	39.28	33.59	39.01
Wt% Fe	61.96	62.22	62.22	61.95	31.10	61.84	62.53	31.36	62.18
Wt% Co	0.04	0.03	0.04	0.05	2.49	0.04	0.05	2.51	0.04
Wt% Ni	0.38	0.46	0.52	0.45	35.19	0.46	0.44	34.89	0.40
Wt% Cu	0.01	0.00	0.04	0.00	0.01	0.00	0.01	0.00	0.02
Total	101.91	102.06	102.06	101.68	102.11	101.43	102.31	102.35	101.64
Atomic% S	47.22	47.41	47.45	47.38	24.88	47.43	47.58	25.00	47.63
Atomic% Fe	0.27	0.33	0.38	0.33	26.78	0.34	0.32	26.46	0.29
Atomic% Co	0.03	0.02	0.03	0.04	1.89	0.03	0.04	1.90	0.03
Atomic% Ni	0.01	0.00	0.02	0.00	0.00	0.00	0.01	0.00	0.01
Atomic% Cu	0.00	0.00	0.01	0.00	0.00	0.00	0.00	0.00	0.00
Host	MASU	MASU	MASU	MASU	MASU	MASU	MASU	MASU	MASU
Hole	VB96300	VB96300	VB96300	VB96300	VB96300	VB96300	VB96300	VB96300	VB96300
Depth	764.00	764.00	764.00	764.00	764.00	764.00	764.00	764.00	764.00
Easting	553779.1	553779.1	553779.1	553779.1	553779.1	553779.1	553779.1	553779.1	553779.1
Northing	6243011.7	6243011.7	6243011.7	6243011.7	6243011.7	6243011.7	6243011.7	6243011.7	6243011.7

TS number	98/AV/076	98/AV/076	98/AV/076	98/AV/076	98/AV/076	98/AV/076	98/AV/076	98/AV/076	98/AV/076
Wt% S	33.56	39.39	33.61	39.30	33.01	39.24	34.29	39.41	33.99
Wt% Fe	31.17	62.69	32.62	62.48	31.53	61.79	31.01	62.62	33.43
Wt% Co	2.44	0.04	2.36	0.04	2.36	0.02	2.60	0.05	2.54
Wt% Ni	34.61	0.42	33.87	0.45	34.51	0.46	33.82	0.46	32.76
Wt% Cu	0.00	0.00	0.00	0.01	0.00	0.00	0.03	0.01	0.00
Total	101.77	102.54	102.46	102.27	101.41	101.51	101.74	102.55	102.72
Atomic% S	24.96	47.59	25.97	47.55	25.41	47.31	24.73	47.52	26.49
Atomic% Fe	26.36	0.30	25.65	0.32	26.45	0.33	25.65	0.33	24.69
Atomic% Co	1.85	0.03	1.78	0.03	1.81	0.02	1.96	0.04	1.91
Atomic% Ni	0.00	0.00	0.00	0.01	0.00	0.00	0.02	0.01	0.00
Atomic% Cu	0.00	0.00	0.00	0.00	0.00	0.00	0.00	0.00	0.00
Host	MASU	MASU	MASU	MASU	MASU	MASU	MASU	MASU	MASU
Hole	VB96300	VB96300	VB96300	VB96300	VB96300	VB96300	VB96300	VB96300	VB96300
Depth	764.00	764.00	764.00	764.00	764.00	764.00	764.00	764.00	764.00
Easting	553779.1	553779.1	553779.1	553779.1	553779.1	553779.1	553779.1	553779.1	553779.1
Northing	6243011.7	6243011.7	6243011.7	6243011.7	6243011.7	6243011.7	6243011.7	6243011.7	6243011.7

TS number	98/AV/076	98/AV/076	98/AV/076	98/AV/076	98/AV/076	98/AV/076	98/AV/076	98/AV/076	98/AV/076
Wt% S	39.10	39.23	39.29	39.28	39.33	33.25	35.21	39.13	39.12
Wt% Fe	62.33	62.44	62.47	62.52	62.20	31.40	31.83	62.21	62.53
Wt% Co	0.04	0.03	0.04	0.05	0.03	2.59	0.01	0.07	0.05
Wt% Ni	0.50	0.49	0.52	0.47	0.44	34.99	0.00	0.76	0.48
Wt% Cu	0.00	0.00	0.00	0.00	0.02	0.01	0.00	0.00	0.03
Total	101.98	102.19	102.33	102.32	102.02	102.24	101.22	102.17	102.22
Atomic% S	47.60	47.57	47.53	47.56	47.41	25.11	25.84	47.43	47.66
Atomic% Fe	0.36	0.36	0.38	0.34	0.32	26.62	0.00	0.55	0.35
Atomic% Co	0.03	0.02	0.03	0.03	0.02	1.96	0.01	0.05	0.04
Atomic% Ni	0.00	0.00	0.00	0.00	0.01	0.00	0.00	0.00	0.02
Atomic% Cu	0.01	0.00	0.00	0.01	0.00	0.00	24.38	0.00	0.00
Host	MASU	MASU	MASU	MASU	MASU	MASU	MASU	MASU	MASU
Hole	VB96300	VB96300	VB96300	VB96300	VB96300	VB96300	VB96300	VB96300	VB96300
Depth	764.00	764.00	764.00	764.00	764.00	764.00	764.00	764.00	764.00
Easting	553779.1	553779.1	553779.1	553779.1	553779.1	553779.1	553779.1	553779.1	553779.1
Northing	6243011.7	6243011.7	6243011.7	6243011.7	6243011.7	6243011.7	6243011.7	6243011.7	6243011.7

TS number	98/AV/076	98/AV/076	98/AV/076	98/AV/076	98/AV/076	98/AV/076	98/AV/076	98/AV/076	98/AV/076
Wt% S	33.43	39.35	39.07	33.52	39.15	39.03	33.50	33.67	35.21
Wt% Fe	31.43	62.60	62.14	32.00	62.30	62.54	31.70	31.59	31.76
Wt% Co	2.45	0.03	0.04	2.59	0.04	0.03	2.63	2.60	0.02
Wt% Ni	34.98	0.44	0.52	34.28	0.45	0.50	34.52	34.66	0.04
Wt% Cu	0.02	0.00	0.00	0.00	0.01	0.02	0.00	0.00	0.00
Total	102.31	102.43	101.77	102.40	101.95	102.12	102.35	102.52	101.15
Atomic% S	25.09	47.57	47.53	25.51	47.57	47.72	25.29	25.13	25.80
Atomic% Fe	26.56	0.32	0.38	25.99	0.32	0.36	26.19	26.24	0.03
Atomic% Co	1.85	0.02	0.03	1.96	0.03	0.02	1.99	1.96	0.02
Atomic% Ni	0.02	0.00	0.00	0.00	0.01	0.01	0.00	0.00	0.00
Atomic% Cu	0.00	0.01	0.00	0.00	0.00	0.00	0.00	0.00	24.35
Host	MASU	MASU	MASU	MASU	MASU	MASU	MASU	MASU	MASU
Hole	VB96300	VB96300	VB96300	VB96300	VB96300	VB96300	VB96300	VB96300	VB96300
Depth	764.00	764.00	764.00	764.00	764.00	764.00	764.00	764.00	764.00
Easting	553779.1	553779.1	553779.1	553779.1	553779.1	553779.1	553779.1	553779.1	553779.1
Northing	6243011.7	6243011.7	6243011.7	6243011.7	6243011.7	6243011.7	6243011.7	6243011.7	6243011.7

TS number	98/AV/076	98/AV/076	98/AV/076	98/AV/076	98/AV/076	98/AV/076	98/AV/076	98/AV/076	98/AV/076
Wt% S	39.33	39.57	36.41	39.27	39.33	33.41	33.33	39.25	39.24
Wt% Fe	62.27	62.20	45.41	62.41	62.36	31.79	31.66	62.52	62.22
Wt% Co	0.02	0.04	1.39	0.03	0.04	2.65	2.50	0.03	0.03
Wt% Ni	0.46	0.44	19.67	0.46	0.40	34.74	34.83	0.42	0.47
Wt% Cu	0.00	0.00	0.00	0.00	0.03	0.00	0.00	0.00	0.00
Total	102.08	102.25	102.88	102.17	102.16	102.59	102.32	102.23	101.96
Atomic% S	47.44	47.27	35.24	47.54	47.49	25.32	25.28	47.61	47.48
Atomic% Fe	0.33	0.32	14.52	0.33	0.29	26.32	26.46	0.31	0.34
Atomic% Co	0.01	0.03	1.02	0.02	0.03	2.00	1.89	0.03	0.02
Atomic% Ni	0.00	0.00	0.00	0.00	0.02	0.00	0.00	0.00	0.00
Atomic% Cu	0.01	0.01	0.00	0.00	0.00	0.00	0.00	0.00	0.00
Host	MASU	MASU	MASU	MASU	MASU	MASU	MASU	MASU	MASU
Hole	VB96300	VB96300	VB96300	VB96300	VB96300	VB96300	VB96300	VB96300	VB96300
Depth	764.00	764.00	764.00	764.00	764.00	764.00	764.00	764.00	764.00
Easting	553779.1	553779.1	553779.1	553779.1	553779.1	553779.1	553779.1	553779.1	553779.1
Northing	6243011.7	6243011.7	6243011.7	6243011.7	6243011.7	6243011.7	6243011.7	6243011.7	6243011.7

TS number	98/AV/076	98/AV/076	98/AV/076	98/AV/076	98/AV/076	98/AV/076	98/AV/076	98/AV/076	98/AV/076
Wt% S	39.23	33.61	39.40	33.60	39.30	39.14	37.14	39.33	39.23
Wt% Fe	62.05	31.84	62.44	31.83	62.48	62.21	49.17	62.16	62.71
Wt% Co	0.03	2.41	0.04	2.56	0.04	0.05	0.97	0.04	0.04
Wt% Ni	0.45	34.79	0.45	34.73	0.43	0.49	15.65	0.47	0.47
Wt% Cu	0.00	0.00	0.03	0.00	0.03	0.00	0.00	0.04	0.00
Total	101.77	102.65	102.35	102.73	102.28	101.89	102.93	102.03	102.45
Atomic% S	47.42	25.32	47.46	25.30	47.55	47.53	37.92	47.38	47.68
Atomic% Fe	0.33	26.31	0.33	26.26	0.31	0.36	11.48	0.34	0.34
Atomic% Co	0.03	1.81	0.03	1.93	0.03	0.03	0.71	0.03	0.03
Atomic% Ni	0.00	0.00	0.02	0.00	0.02	0.00	0.00	0.02	0.00
Atomic% Cu	0.01	0.00	0.00	0.00	0.00	0.00	0.00	0.00	0.00
Host	MASU	MASU	MASU	MASU	MASU	MASU	MASU	MASU	MASU
Hole	VB96300	VB96300	VB96300	VB96300	VB96300	VB96300	VB96300	VB96300	VB96300
Depth	764.00	764.00	764.00	764.00	764.00	764.00	764.00	764.00	764.00
Easting	553779.1	553779.1	553779.1	553779.1	553779.1	553779.1	553779.1	553779.1	553779.1
Northing	6243011.7	6243011.7	6243011.7	6243011.7	6243011.7	6243011.7	6243011.7	6243011.7	6243011.7

TS number	98/AV/076	98/AV/076	98/AV/076	98/AV/076	98/AV/076	98/AV/076	98/AV/076	98/AV/076	98/AV/076
Wt% S	35.47	35.18	35.08	33.41	39.34	38.24	39.31	39.20	40.01
Wt% Fe	31.76	32.11	31.78	32.12	62.51	55.57	62.53	62.58	61.58
Wt% Co	0.00	0.02	0.01	2.56	0.04	0.58	0.04	0.06	0.04
Wt% Ni	0.00	0.02	0.00	34.64	0.49	8.13	0.50	0.53	0.45
Wt% Cu	0.00	0.05	0.04	0.00	0.00	0.00	0.00	0.00	0.03
Total	101.54	101.63	101.26	102.73	102.39	102.53	102.37	102.38	102.11
Atomic% S	25.68	25.99	25.81	25.56	47.51	42.59	47.55	47.61	46.74
Atomic% Fe	0.00	0.01	0.00	26.22	0.36	5.93	0.36	0.39	0.33
Atomic% Co	0.00	0.01	0.01	1.93	0.03	0.42	0.03	0.04	0.03
Atomic% Ni	0.00	0.03	0.03	0.00	0.00	0.00	0.00	0.00	0.02
Atomic% Cu	24.37	24.37	24.52	0.00	0.01	0.00	0.00	0.01	0.00
Host	MASU	MASU	MASU	MASU	MASU	MASU	MASU	MASU	MASU
Hole	VB96300	VB96300	VB96300	VB96300	VB96300	VB96300	VB96300	VB96300	VB96300
Depth	764.00	764.00	764.00	764.00	764.00	764.00	764.00	764.00	764.00
Easting	553779.1	553779.1	553779.1	553779.1	553779.1	553779.1	553779.1	553779.1	553779.1
Northing	6243011.7	6243011.7	6243011.7	6243011.7	6243011.7	6243011.7	6243011.7	6243011.7	6243011.7

TS number	98/AV/076	98/AV/076	98/AV/076	98/AV/076	98/AV/076	98/AV/076	98/AV/076	98/AV/076	C97-1074
Wt% S	39.32	35.02	33.91	39.33	39.45	33.74	33.76	33.68	34.88
Wt% Fe	62.53	38.73	31.30	62.37	62.54	31.85	32.07	31.81	30.31
Wt% Co	0.03	1.99	2.85	0.04	0.03	2.50	2.74	2.72	0.02
Wt% Ni	0.47	27.03	34.75	0.36	0.37	34.64	34.43	34.45	0.03
Wt% Cu	0.01	0.02	0.01	0.00	0.02	0.02	0.00	0.00	34.60
Total	102.36	102.79	102.82	102.11	102.41	102.75	103.00	102.66	99.83
Atomic% S	47.55	30.41	24.81	47.51	47.50	25.28	25.41	25.28	50.00
Atomic% Fe	0.34	20.19	26.20	0.26	0.27	26.16	25.95	26.05	24.94
Atomic% Co	0.02	1.48	2.14	0.03	0.02	1.88	2.05	2.04	0.01
Atomic% Ni	0.01	0.02	0.01	0.00	0.01	0.01	0.00	0.00	0.03
Atomic% Cu	0.00	0.00	0.00	0.00	0.00	0.00	0.00	0.00	25.02
Host	MASU	MASU	MASU	MASU	MASU	MASU	MASU	MASU	Troc
Hole	VB96300	VB96300	VB96300	VB96300	VB96300	VB96300	VB96300	VB96300	VB96266
Depth	764.00	764.00	764.00	764.00	764.00	764.00	764.00	764.00	327.00
Easting	553779.1	553779.1	553779.1	553779.1	553779.1	553779.1	553779.1	553779.1	556965.8
Northing	6243011.7	6243011.7	6243011.7	6243011.7	6243011.7	6243011.7	6243011.7	6243011.7	6242466.0

TS number	C97-1074	C97-1074	C97-1074	C97-1074	C97-1074	C97-1074	C97-1074	C97-1074	C97-1074
Wt% S	33.20	36.29	36.49	33.04	36.05	34.46	36.99	36.82	33.28
Wt% Fe	34.17	62.82	62.76	33.99	62.52	30.40	62.36	62.78	34.03
Wt% Co	1.64	0.04	0.04	1.38	0.02	0.00	0.04	0.03	1.23
Wt% Ni	31.34	0.02	0.02	32.01	0.01	0.00	0.15	0.02	32.37
Wt% Cu	0.06	0.05	0.04	0.01	0.05	34.74	0.11	0.03	0.02
Total	100.41	99.22	99.37	100.44	98.65	99.60	99.66	99.69	100.93
Atomic% S	46.86	50.12	50.28	46.67	50.08	49.63	50.71	50.50	46.76
Atomic% Fe	27.69	49.81	49.64	27.57	49.86	25.13	49.07	49.43	27.45
Atomic% Co	1.26	0.03	0.03	1.06	0.01	0.00	0.03	0.02	0.94
Atomic% Ni	24.16	0.01	0.02	24.69	0.01	0.00	0.12	0.01	24.83
Atomic% Cu	0.04	0.03	0.03	0.00	0.04	25.24	0.08	0.02	0.01
Host	Troc	Troc	Troc	Troc	Troc	Troc	Troc	Troc	Troc
Hole	VB96266	VB96266	VB96266	VB96266	VB96266	VB96266	VB96266	VB96266	VB96266
Depth	327.00	327.00	327.00	327.00	327.00	327.00	327.00	327.00	327.00
Easting	556965.8	556965.8	556965.8	556965.8	556965.8	556965.8	556965.8	556965.8	556965.8
Northing	6242466.0	6242466.0	6242466.0	6242466.0	6242466.0	6242466.0	6242466.0	6242466.0	6242466.0

TS number	C97-1074	C97-1074	C97-1074	C97-1074	C97-1074	C97-1074	C97-1074	C97-1074	C97-1074
Wt% S	38.40	33.43	38.13	36.50	32.69	36.45	38.56	37.32	34.57
Wt% Fe	60.84	34.15	61.27	63.24	33.11	63.33	61.01	62.25	29.31
Wt% Co	0.04	1.30	0.04	0.04	1.30	0.04	0.03	0.03	0.01
Wt% Ni	0.18	32.02	0.12	0.03	31.86	0.00	0.14	0.05	0.00
Wt% Cu	0.01	0.00	0.03	0.02	0.02	0.06	0.04	0.03	34.45
Total	99.46	100.92	99.59	99.82	99.00	99.88	99.78	99.70	98.35
Atomic% S	52.28	46.92	51.94	50.10	46.82	50.03	52.32	51.04	50.26
Atomic% Fe	47.55	27.52	47.92	49.84	27.22	49.90	47.53	48.87	24.46
Atomic% Co	0.03	0.99	0.03	0.03	1.01	0.03	0.02	0.03	0.01
Atomic% Ni	0.13	24.55	0.09	0.02	24.91	0.00	0.10	0.03	0.00
Atomic% Cu	0.01	0.00	0.02	0.01	0.01	0.04	0.03	0.02	25.27
Host	Troc	Troc	Troc	Troc	Troc	Troc	Troc	Troc	Troc
Hole	VB96266	VB96266	VB96266	VB96266	VB96266	VB96266	VB96266	VB96266	VB96266
Depth	327.00	327.00	327.00	327.00	327.00	327.00	327.00	327.00	327.00
Easting	556965.8	556965.8	556965.8	556965.8	556965.8	556965.8	556965.8	556965.8	556965.8
Northing	6242466.0	6242466.0	6242466.0	6242466.0	6242466.0	6242466.0	6242466.0	6242466.0	6242466.0

TS number	C97-1074	C97-1074	C97-1074	C97-1075	C97-1075	C97-1075	C97-1075	C97-1075	C97-1075
Wt% S	38.27	33.61	34.47	36.56	36.68	35.02	33.54	36.57	33.33
Wt% Fe	61.13	32.98	30.08	62.20	62.89	30.32	38.59	63.11	38.54
Wt% Co	0.04	1.28	0.01	0.05	0.05	0.01	0.76	0.04	0.91
Wt% Ni	0.15	32.54	0.04	0.00	0.00	0.07	27.32	0.00	27.42
Wt% Cu	0.03	0.07	34.58	0.03	0.03	34.40	0.04	0.02	0.00
Total	99.62	100.49	99.20	98.83	99.64	99.82	100.39	99.76	100.20
Atomic% S	52.08	47.31	49.80	50.56	50.37	50.15	47.17	50.20	46.99
Atomic% Fe	47.76	26.65	24.95	49.38	49.57	24.93	31.15	49.74	31.20
Atomic% Co	0.03	0.98	0.01	0.04	0.04	0.01	0.59	0.03	0.69
Atomic% Ni	0.11	25.01	0.03	0.00	0.00	0.05	20.98	0.00	21.12
Atomic% Cu	0.02	0.05	25.21	0.02	0.02	24.85	0.03	0.01	0.00
Host	Troc	Troc	Troc	Troc	Troc	Troc	Troc	Troc	Troc
Hole	VB96266	VB96266	VB96266	VB96266	VB96266	VB96266	VB96266	VB96266	VB96266
Depth	327.00	327.00	327.00	332.50	332.50	332.50	332.50	332.50	332.50
Easting	556965.8	556965.8	556965.8	556965.8	556965.8	556965.8	556965.8	556965.8	556965.8
Northing	6242466.0	6242466.0	6242466.0	6242466.0	6242466.0	6242466.0	6242466.0	6242466.0	6242466.0

TS number	C97-1075	C97-1075	C97-1075	C97-1075	C97-1075	C97-1075	C97-1075	C97-1075	C97-1075
Wt% S	36.40	33.41	34.27	36.34	33.53	33.80	36.41	33.89	36.47
Wt% Fe	62.92	38.92	30.42	63.09	39.22	30.87	63.01	30.90	62.94
Wt% Co	0.04	0.80	0.03	0.05	1.07	0.10	0.03	0.12	0.05
Wt% Ni	0.02	27.10	0.22	0.05	26.71	5.29	0.00	3.54	0.00
Wt% Cu	0.01	0.00	34.70	0.02	0.00	28.40	0.01	30.87	0.01
Total	99.41	100.24	99.65	99.56	100.53	98.47	99.47	99.33	99.48
Atomic% S	50.16	47.06	49.40	50.04	47.08	49.13	50.15	48.97	50.20
Atomic% Fe	49.78	31.48	25.17	49.87	31.62	25.76	49.82	25.63	49.74
Atomic% Co	0.03	0.62	0.03	0.04	0.82	0.08	0.02	0.09	0.04
Atomic% Ni	0.01	20.85	0.18	0.03	20.48	4.20	0.00	2.79	0.00
Atomic% Cu	0.01	0.00	25.23	0.01	0.00	20.82	0.01	22.51	0.01
Host	Troc	Troc	Troc	Troc	Troc	Troc	Troc	Troc	Troc
Hole	VB96266	VB96266	VB96266	VB96266	VB96266	VB96266	VB96266	VB96266	VB96266
Depth	332.50	332.50	332.50	332.50	332.50	332.50	332.50	332.50	332.50
Easting	556965.8	556965.8	556965.8	556965.8	556965.8	556965.8	556965.8	556965.8	556965.8
Northing	6242466.0	6242466.0	6242466.0	6242466.0	6242466.0	6242466.0	6242466.0	6242466.0	6242466.0

TS number	C97-1075	C97-1075	C97-1075	C97-1075	C97-1075	C97-1075	C97-1075	C97-1075	C97-1075
Wt% S	33.57	34.58	33.53	36.28	33.16	33.28	36.29	33.44	36.41
Wt% Fe	39.12	31.66	39.48	62.86	39.28	39.15	63.22	39.06	63.03
Wt% Co	1.07	0.02	1.01	0.03	1.03	1.03	0.04	0.91	0.04
Wt% Ni	26.90	0.15	26.78	0.02	26.76	27.19	0.00	27.09	0.00
Wt% Cu	0.00	33.09	0.00	0.03	0.01	0.00	0.03	0.02	0.04
Total	100.67	99.51	100.80	99.22	100.24	100.66	99.60	100.53	99.52
Atomic% S	47.09	49.73	46.98	50.11	46.78	46.77	49.97	46.99	50.13
Atomic% Fe	31.49	26.13	31.76	49.83	31.81	31.58	49.97	31.51	49.82
Atomic% Co	0.82	0.02	0.77	0.02	0.79	0.79	0.03	0.70	0.03
Atomic% Ni	20.60	0.12	20.49	0.01	20.61	20.86	0.00	20.79	0.00
Atomic% Cu	0.00	24.00	0.00	0.02	0.01	0.00	0.02	0.01	0.03
Host	Troc	Troc	Troc	Troc	Troc	Troc	Troc	Troc	Troc
Hole	VB96266	VB96266	VB96266	VB96266	VB96266	VB96266	VB96266	VB96266	VB96266
Depth	332.50	332.50	332.50	332.50	332.50	332.50	332.50	332.50	332.50
Easting	556965.8	556965.8	556965.8	556965.8	556965.8	556965.8	556965.8	556965.8	556965.8
Northing	6242466.0	6242466.0	6242466.0	6242466.0	6242466.0	6242466.0	6242466.0	6242466.0	6242466.0

TS number	C97-1075	C97-1075	C97-1075	C97-1075	C97-1075	C97-1075	C97-1075	C97-1075	C97-1078
Wt% S	33.43	34.42	36.64	34.97	34.22	33.42	36.46	32.56	53.02
Wt% Fe	38.95	30.37	62.80	30.77	33.56	38.95	62.97	38.20	44.84
Wt% Co	1.02	0.02	0.04	0.03	0.29	1.01	0.03	0.90	1.91
Wt% Ni	27.43	0.37	0.00	0.39	11.60	26.96	0.00	26.40	0.53
Wt% Cu	0.00	33.59	0.02	34.01	20.69	0.00	0.02	0.65	0.78
Total	100.84	98.77	99.52	100.28	100.36	100.34	99.48	98.72	101.10
Atomic% S	46.87	49.87	50.38	49.90	48.60	47.04	50.19	46.70	65.87
Atomic% Fe	31.35	25.26	49.57	25.21	27.36	31.47	49.77	31.45	31.98
Atomic% Co	0.78	0.02	0.03	0.02	0.22	0.77	0.02	0.70	1.29
Atomic% Ni	21.00	0.29	0.00	0.30	9.00	20.72	0.00	20.68	0.36
Atomic% Cu	0.00	24.56	0.01	24.48	14.82	0.00	0.02	0.47	0.49
Host	Troc	Troc	Troc	Troc	Troc	Troc	Troc	Troc	Troc
Hole	VB96266	VB96266	VB96266	VB96266	VB96266	VB96266	VB96266	VB96266	VB96266
Depth	332.50	332.50	332.50	332.50	332.50	332.50	332.50	332.50	192.50
Easting	556965.8	556965.8	556965.8	556965.8	556965.8	556965.8	556965.8	556965.8	556965.8
Northing	6242466.0	6242466.0	6242466.0	6242466.0	6242466.0	6242466.0	6242466.0	6242466.0	6242466.0

TS number	C97-1078	C97-1078	C97-1078	C97-1078	C97-1078	C97-1078	C97-1078	C97-1078	C97-1078
Wt% S	38.84	38.20	33.17	38.34	33.27	32.83	38.56	38.59	33.48
Wt% Fe	35.66	60.34	30.92	60.78	31.59	31.05	60.92	60.84	31.52
Wt% Co	1.26	0.04	2.11	0.04	1.10	1.09	0.02	0.05	1.28
Wt% Ni	24.68	0.29	33.81	0.39	35.19	34.69	0.39	0.39	34.98
Wt% Cu	0.70	0.03	0.00	0.00	0.00	0.01	0.00	0.03	0.00
Total	101.13	98.90	100.01	99.56	101.15	99.67	99.90	99.90	101.26
Atomic% S	52.61	52.31	47.02	52.18	46.72	46.77	52.28	52.31	46.91
Atomic% Fe	27.73	47.42	25.16	47.49	25.47	25.39	47.42	47.34	25.35
Atomic% Co	0.93	0.03	1.63	0.03	0.84	0.84	0.02	0.04	0.98
Atomic% Ni	18.26	0.22	26.18	0.29	26.98	26.99	0.29	0.29	26.76
Atomic% Cu	0.48	0.02	0.00	0.00	0.00	0.01	0.00	0.02	0.00
Host	Troc	Troc	Troc	Troc	Troc	Troc	Troc	Troc	Troc
Hole	VB96266	VB96266	VB96266	VB96266	VB96266	VB96266	VB96266	VB96266	VB96266
Depth	192.50	192.50	192.50	192.50	192.50	192.50	192.50	192.50	192.50
Easting	556965.8	556965.8	556965.8	556965.8	556965.8	556965.8	556965.8	556965.8	556965.8
Northing	6242466.0	6242466.0	6242466.0	6242466.0	6242466.0	6242466.0	6242466.0	6242466.0	6242466.0

TS number	C97-1078	C97-1078	C97-1078	C97-1078	C97-1078	C97-1078	C97-1078	C97-1078	C97-1078
Wt% S	38.56	38.58	33.23	38.42	35.22	53.72	38.52	34.43	34.47
Wt% Fe	60.97	60.74	31.65	60.86	30.48	45.06	60.65	30.82	30.78
Wt% Co	0.04	0.02	1.24	0.05	0.01	2.46	0.05	0.28	0.00
Wt% Ni	0.39	0.38	34.90	0.32	0.00	0.01	0.48	10.17	0.00
Wt% Cu	0.00	0.00	0.01	0.07	34.90	0.00	0.03	24.18	35.09
Total	99.96	99.72	101.03	99.72	100.66	101.25	99.72	99.92	100.34
Atomic% S	52.25	52.37	46.72	52.20	50.06	66.38	52.31	49.15	49.35
Atomic% Fe	47.43	47.33	25.54	47.48	24.87	31.96	47.28	25.25	25.30
Atomic% Co	0.03	0.01	0.94	0.03	0.01	1.65	0.03	0.22	0.00
Atomic% Ni	0.29	0.28	26.79	0.24	0.00	0.01	0.36	7.93	0.00
Atomic% Cu	0.00	0.00	0.01	0.05	25.03	0.00	0.02	17.42	25.35
Host	Troc	Troc	Troc	Troc	Troc	Troc	Troc	Troc	Troc
Hole	VB96266	VB96266	VB96266	VB96266	VB96266	VB96266	VB96266	VB96266	VB96266
Depth	192.50	192.50	192.50	192.50	192.50	192.50	192.50	192.50	192.50
Easting	556965.8	556965.8	556965.8	556965.8	556965.8	556965.8	556965.8	556965.8	556965.8
Northing	6242466.0	6242466.0	6242466.0	6242466.0	6242466.0	6242466.0	6242466.0	6242466.0	6242466.0

TS number	C97-1078	C97-1079	C97-1079	C97-1079	C97-1079	C97-1079	C97-1079	C97-1079	C97-1079
Wt% S	38.45	38.44	34.84	38.54	34.88	33.41	33.29	38.45	38.85
Wt% Fe	60.97	60.01	29.53	60.48	30.10	31.24	31.00	60.82	60.53
Wt% Co	0.05	0.03	0.01	0.03	0.01	1.13	1.14	0.05	0.02
Wt% Ni	0.35	0.40	0.00	0.34	0.04	34.65	34.77	0.39	0.48
Wt% Cu	0.01	0.01	34.25	0.02	34.47	0.00	0.00	0.00	0.02
Total	99.85	98.90	98.63	99.41	99.50	100.43	100.20	99.70	99.90
Atomic% S	52.18	52.57	50.43	52.45	50.13	47.14	47.09	52.25	52.58
Atomic% Fe	47.50	47.11	24.54	47.25	24.83	25.30	25.18	47.44	47.04
Atomic% Co	0.04	0.02	0.01	0.02	0.01	0.87	0.88	0.03	0.02
Atomic% Ni	0.26	0.30	0.00	0.25	0.03	26.70	26.86	0.29	0.35
Atomic% Cu	0.01	0.01	25.01	0.02	24.99	0.00	0.00	0.00	0.01
Host	Troc	Troc	Troc	Troc	Troc	Troc	Troc	Troc	Troc
Hole	VB96266	VB96266	VB96266	VB96266	VB96266	VB96266	VB96266	VB96266	VB96266
Depth	192.50	206.50	206.50	206.50	206.50	206.50	206.50	206.50	206.50
Easting	556965.8	556965.8	556965.8	556965.8	556965.8	556965.8	556965.8	556965.8	556965.8
Northing	6242466.0	6242466.0	6242466.0	6242466.0	6242466.0	6242466.0	6242466.0	6242466.0	6242466.0

TS number	C97-1079	C97-1079	C97-1079	C97-1079	C97-1079	C97-1079	C97-1079	C97-1079	C97-1079
Wt% S	34.84	33.45	33.10	38.82	38.57	33.36	38.73	34.97	33.45
Wt% Fe	30.48	31.31	31.30	60.36	60.38	31.17	60.56	30.52	31.24
Wt% Co	0.00	0.92	0.90	0.04	0.03	1.22	0.04	0.01	1.20
Wt% Ni	0.00	35.24	35.41	0.47	0.56	35.23	0.54	0.01	35.25
Wt% Cu	34.49	0.05	0.00	0.01	0.01	0.00	0.00	34.73	0.00
Total	100.22	100.97	100.71	99.71	99.54	100.97	99.89	100.25	101.14
Atomic% S	49.82	46.98	46.69	52.63	52.43	46.89	52.47	49.94	46.92
Atomic% Fe	25.02	25.25	25.35	46.98	47.12	25.15	47.09	25.02	25.16
Atomic% Co	0.00	0.70	0.69	0.03	0.02	0.93	0.03	0.01	0.92
Atomic% Ni	0.00	27.03	27.27	0.35	0.42	27.04	0.40	0.01	27.00
Atomic% Cu	24.88	0.03	0.00	0.01	0.01	0.00	0.00	25.03	0.00
Host	Troc	Troc	Troc	Troc	Troc	Troc	Troc	Troc	Troc
Hole	VB96266	VB96266	VB96266	VB96266	VB96266	VB96266	VB96266	VB96266	VB96266
Depth	206.50	206.50	206.50	206.50	206.50	206.50	206.50	206.50	206.50
Easting	556965.8	556965.8	556965.8	556965.8	556965.8	556965.8	556965.8	556965.8	556965.8
Northing	6242466.0	6242466.0	6242466.0	6242466.0	6242466.0	6242466.0	6242466.0	6242466.0	6242466.0

TS number	C97-1079	C97-1079	C97-1079	C97-1079	C97-1079	C97-1079	C97-1079	C97-1079	C97-1083
Wt% S	33.38	38.67	38.70	33.37	34.62	38.54	33.45	34.63	38.77
Wt% Fe	31.33	60.47	60.52	31.91	30.31	60.76	33.08	30.41	59.56
Wt% Co	1.11	0.03	0.03	1.12	0.01	0.04	1.08	0.00	0.03
Wt% Ni	35.26	0.55	0.34	34.49	0.01	0.28	33.46	0.02	0.23
Wt% Cu	0.00	0.00	0.00	0.05	34.83	0.01	0.00	34.76	0.17
Total	101.08	99.71	99.60	100.94	99.80	99.62	101.07	99.82	98.76
Atomic% S	46.87	52.47	52.54	46.90	49.73	52.37	46.92	49.72	52.97
Atomic% Fe	25.25	47.10	47.18	25.74	25.00	47.39	26.64	25.07	46.71
Atomic% Co	0.85	0.02	0.02	0.85	0.01	0.03	0.82	0.00	0.02
Atomic% Ni	27.03	0.41	0.25	26.47	0.01	0.21	25.62	0.02	0.17
Atomic% Cu	0.00	0.00	0.00	0.04	25.24	0.00	0.00	25.19	0.11
Host	Troc	Troc	Troc	Troc	Troc	Troc	Troc	Troc	Troc
Hole	VB96266	VB96266	VB96266	VB96266	VB96266	VB96266	VB96266	VB96266	VB96266
Depth	206.50	206.50	206.50	206.50	206.50	206.50	206.50	206.50	244.00
Easting	556965.8	556965.8	556965.8	556965.8	556965.8	556965.8	556965.8	556965.8	556965.8
Northing	6242466.0	6242466.0	6242466.0	6242466.0	6242466.0	6242466.0	6242466.0	6242466.0	6242466.0

TS number	C97-1083	C97-1083	C97-1083	C97-1083	C97-1083	C97-1083	C97-1083	C97-1083	C97-1083
Wt% S	33.98	39.62	33.09	39.19	34.36	32.59	34.52	39.60	33.16
Wt% Fe	30.71	59.85	30.53	59.80	30.52	30.01	30.47	59.78	30.03
Wt% Co	0.03	0.03	1.36	0.05	0.01	1.27	0.01	0.03	1.13
Wt% Ni	0.07	0.29	35.36	0.38	0.00	35.56	0.07	0.41	35.33
Wt% Cu	34.21	0.01	0.00	0.02	34.52	0.00	34.35	0.00	0.00
Total	99.03	99.80	100.34	99.44	99.41	99.44	99.53	99.83	99.65
Atomic% S	49.28	53.43	46.83	53.13	49.58	46.60	49.72	53.40	47.17
Atomic% Fe	25.57	46.33	24.80	46.54	25.28	24.64	25.19	46.27	24.52
Atomic% Co	0.02	0.02	1.05	0.04	0.01	0.99	0.00	0.03	0.88
Atomic% Ni	0.06	0.22	27.32	0.28	0.00	27.77	0.06	0.30	27.44
Atomic% Cu	25.04	0.01	0.00	0.01	25.13	0.00	24.96	0.00	0.00
Host	Troc	Troc	Troc	Troc	Troc	Troc	Troc	Troc	Troc
Hole	VB96266	VB96266	VB96266	VB96266	VB96266	VB96266	VB96266	VB96266	VB96266
Depth	244.00	244.00	244.00	244.00	244.00	244.00	244.00	244.00	244.00
Easting	556965.8	556965.8	556965.8	556965.8	556965.8	556965.8	556965.8	556965.8	556965.8
Northing	6242466.0	6242466.0	6242466.0	6242466.0	6242466.0	6242466.0	6242466.0	6242466.0	6242466.0

TS number	C97-1083	C97-1083	C97-1083	C97-1083	C97-1083	C97-1083	C97-1083	C97-1083	C97-1083
Wt% S	39.14	32.48	32.98	34.74	39.32	39.41	34.86	33.02	39.38
Wt% Fe	59.81	30.26	30.62	30.46	59.96	59.67	30.61	30.55	59.95
Wt% Co	0.05	1.15	1.16	0.02	0.04	0.04	0.02	1.17	0.04
Wt% Ni	0.37	35.34	35.67	0.00	0.37	0.35	0.00	35.71	0.28
Wt% Cu	0.02	0.00	0.00	34.41	0.01	0.02	34.39	0.00	0.04
Total	99.38	99.23	100.43	99.70	99.69	99.49	99.88	100.45	99.71
Atomic% S	53.10	46.55	46.67	49.89	53.16	53.33	49.95	46.70	53.21
Atomic% Fe	46.58	24.90	24.87	25.11	46.54	46.37	25.17	24.81	46.51
Atomic% Co	0.03	0.90	0.89	0.02	0.03	0.03	0.02	0.90	0.03
Atomic% Ni	0.28	27.65	27.56	0.00	0.27	0.26	0.00	27.58	0.21
Atomic% Cu	0.01	0.00	0.00	24.93	0.01	0.02	24.86	0.00	0.03
Host	Troc	Troc	Troc	Troc	Troc	Troc	Troc	Troc	Troc
Hole	VB96266	VB96266	VB96266	VB96266	VB96266	VB96266	VB96266	VB96266	VB96266
Depth	244.00	244.00	244.00	244.00	244.00	244.00	244.00	244.00	244.00
Easting	556965.8	556965.8	556965.8	556965.8	556965.8	556965.8	556965.8	556965.8	556965.8
Northing	6242466.0	6242466.0	6242466.0	6242466.0	6242466.0	6242466.0	6242466.0	6242466.0	6242466.0

TS number	C97-1083	C97-1083	C97-1083	C97-1083	C97-1083	C97-1083	C97-1083	C97-1083	C97-1083
Wt% S	34.35	33.03	39.41	39.47	33.07	34.70	32.81	39.35	39.76
Wt% Fe	30.47	30.37	59.81	59.86	30.54	30.52	30.40	59.85	59.79
Wt% Co	0.01	1.25	0.05	0.04	1.18	0.01	1.23	0.04	0.04
Wt% Ni	0.00	35.68	0.46	0.37	35.52	0.01	35.67	0.35	0.35
Wt% Cu	34.35	0.00	0.00	0.03	0.00	34.63	0.00	0.02	0.03
Total	99.18	100.32	99.72	99.77	100.31	99.87	100.11	99.60	99.97
Atomic% S	49.66	46.77	53.25	53.29	46.82	49.78	46.60	53.23	53.51
Atomic% Fe	25.29	24.68	46.39	46.39	24.82	25.14	24.79	46.48	46.18
Atomic% Co	0.01	0.96	0.03	0.03	0.91	0.01	0.95	0.03	0.03
Atomic% Ni	0.00	27.59	0.34	0.27	27.46	0.01	27.66	0.26	0.25
Atomic% Cu	25.05	0.00	0.00	0.02	0.00	25.07	0.00	0.01	0.02
Host	Troc	Troc	Troc	Troc	Troc	Troc	Troc	Troc	Troc
Hole	VB96266	VB96266	VB96266	VB96266	VB96266	VB96266	VB96266	VB96266	VB96266
Depth	244.00	244.00	244.00	244.00	244.00	244.00	244.00	244.00	244.00
Easting	556965.8	556965.8	556965.8	556965.8	556965.8	556965.8	556965.8	556965.8	556965.8
Northing	6242466.0	6242466.0	6242466.0	6242466.0	6242466.0	6242466.0	6242466.0	6242466.0	6242466.0

TS number	C97-1083	C97-1083	C97-1085	C97-1085	C97-1085	C97-1085	C97-1085	C97-1085	C97-1085
Wt% S	32.96	34.79	33.00	38.96	34.85	34.72	33.24	38.81	38.64
Wt% Fe	30.21	30.53	30.88	60.34	29.88	30.05	30.56	60.24	60.16
Wt% Co	1.27	0.03	1.28	0.03	0.02	0.00	1.36	0.03	0.04
Wt% Ni	35.64	0.17	34.49	0.46	0.00	0.00	34.18	0.37	0.41
Wt% Cu	0.00	34.57	0.00	0.01	34.27	34.40	0.00	0.00	0.02
Total	100.08	100.09	99.67	99.82	99.06	99.23	99.34	99.45	99.26
Atomic% S	46.78	49.79	46.97	52.74	50.27	50.06	47.36	52.72	52.62
Atomic% Fe	24.61	25.08	25.23	46.88	24.74	24.88	25.00	46.98	47.03
Atomic% Co	0.98	0.02	0.99	0.03	0.01	0.00	1.05	0.02	0.03
Atomic% Ni	27.62	0.13	26.80	0.34	0.00	0.00	26.59	0.27	0.31
Atomic% Cu	0.00	24.96	0.00	0.01	24.94	25.03	0.00	0.00	0.01
Host	Troc	Troc	Troc	Troc	Troc	Troc	Troc	Troc	Troc
Hole	VB96266	VB96266	VB96266	VB96266	VB96266	VB96266	VB96266	VB96266	VB96266
Depth	244.00	244.00	262.00	262.00	262.00	262.00	262.00	262.00	262.00
Easting	556965.8	556965.8	556965.8	556965.8	556965.8	556965.8	556965.8	556965.8	556965.8
Northing	6242466.0	6242466.0	6242466.0	6242466.0	6242466.0	6242466.0	6242466.0	6242466.0	6242466.0

TS number	C97-1085	C97-1085	C97-1085	C97-1086	C97-1086	C97-1086	C97-1086	C97-1086	C97-1086
Wt% S	33.34	33.59	38.69	33.70	37.09	34.71	36.70	32.90	36.57
Wt% Fe	30.99	31.28	60.77	35.07	63.04	30.25	63.16	34.73	63.25
Wt% Co	1.36	1.33	0.04	1.35	0.04	0.02	0.04	1.32	0.03
Wt% Ni	34.76	34.39	0.33	30.25	0.01	0.05	0.01	31.17	0.00
Wt% Cu	0.00	0.00	0.02	0.05	0.08	34.62	0.02	0.00	0.05
Total	100.45	100.59	99.86	100.43	100.37	99.64	99.94	100.14	99.90
Atomic% S	47.06	47.28	52.43	47.39	50.51	49.89	50.27	46.60	50.15
Atomic% Fe	25.11	25.27	47.27	28.31	49.29	24.96	49.67	28.25	49.79
Atomic% Co	1.04	1.02	0.03	1.04	0.03	0.01	0.03	1.01	0.03
Atomic% Ni	26.79	26.43	0.25	23.23	0.01	0.04	0.01	24.12	0.00
Atomic% Cu	0.00	0.00	0.01	0.04	0.05	25.10	0.02	0.00	0.03
Host	Troc	Troc	Troc	Troc	Troc	Troc	Troc	Troc	Troc
Hole	VB96266	VB96266	VB96266	VB96266	VB96266	VB96266	VB96266	VB96266	VB96266
Depth	262.00	262.00	262.00	136.30	136.30	136.30	136.30	136.30	136.30
Easting	556965.8	556965.8	556965.8	556965.8	556965.8	556965.8	556965.8	556965.8	556965.8
Northing	6242466.0	6242466.0	6242466.0	6242466.0	6242466.0	6242466.0	6242466.0	6242466.0	6242466.0

TS number	C97-1086	C97-1086	C97-1086	C97-1086	C97-1086	C97-1086	C97-1086	C97-1086	C97-1086
Wt% S	33.21	34.89	36.59	36.58	36.36	33.25	36.45	34.93	33.57
Wt% Fe	34.36	30.67	63.14	63.12	63.46	34.84	63.23	30.51	36.33
Wt% Co	1.38	0.03	0.03	0.03	0.02	1.48	0.03	0.02	1.13
Wt% Ni	31.47	0.00	0.00	0.00	0.02	31.00	0.00	0.00	29.41
Wt% Cu	0.00	34.63	0.04	0.04	0.01	0.00	0.05	34.48	0.00
Total	100.42	100.22	99.81	99.77	99.89	100.57	99.76	99.98	100.45
Atomic% S	46.85	49.86	50.20	50.21	49.93	46.84	50.07	49.99	47.21
Atomic% Fe	27.84	25.15	49.73	49.74	50.02	28.18	49.86	25.07	29.33
Atomic% Co	1.06	0.02	0.03	0.02	0.02	1.13	0.02	0.02	0.86
Atomic% Ni	24.25	0.00	0.00	0.00	0.01	23.85	0.00	0.00	22.59
Atomic% Cu	0.00	24.97	0.03	0.03	0.01	0.00	0.03	24.90	0.00
Host	Troc	Troc	Troc	Troc	Troc	Troc	Troc	Troc	Troc
Hole	VB96266	VB96266	VB96266	VB96266	VB96266	VB96266	VB96266	VB96266	VB96266
Depth	136.30	136.30	136.30	136.30	136.30	136.30	136.30	136.30	136.30
Easting	556965.8	556965.8	556965.8	556965.8	556965.8	556965.8	556965.8	556965.8	556965.8
Northing	6242466.0	6242466.0	6242466.0	6242466.0	6242466.0	6242466.0	6242466.0	6242466.0	6242466.0

TS number	C97-1086	C97-1086	C97-1086	C97-1086	C97-1086	C97-1086	C97-1090	C97-1090	C97-1090
Wt% S	33.46	36.63	33.37	36.56	34.74	33.72	38.22	37.48	34.95
Wt% Fe	34.35	63.11	35.88	62.93	30.50	34.67	59.97	61.83	29.87
Wt% Co	1.30	0.03	1.19	0.04	0.02	1.36	0.04	0.03	0.02
Wt% Ni	31.33	0.00	30.22	0.00	0.03	30.12	0.28	0.09	0.09
Wt% Cu	0.00	0.01	0.00	0.02	34.33	0.40	0.00	0.01	34.07
Total	100.44	99.79	100.66	99.55	99.62	100.26	98.51	99.44	99.03
Atomic% S	47.13	50.26	46.92	50.27	49.91	47.49	52.48	51.31	50.39
Atomic% Fe	27.77	49.71	28.97	49.68	25.16	28.03	47.27	48.59	24.72
Atomic% Co	1.00	0.02	0.91	0.03	0.01	1.04	0.03	0.02	0.02
Atomic% Ni	24.10	0.00	23.21	0.00	0.03	23.16	0.21	0.07	0.07
Atomic% Cu	0.00	0.01	0.00	0.01	24.89	0.28	0.00	0.01	24.78
Host	Troc	Troc	Troc	Troc	Troc	Troc	Troc	Troc	Troc
Hole	VB96266	VB96266	VB96266	VB96266	VB96266	VB96266	VB96266	VB96266	VB96266
Depth	136.30	136.30	136.30	136.30	136.30	136.30	197.00	197.00	197.00
Easting	556965.8	556965.8	556965.8	556965.8	556965.8	556965.8	556965.8	556965.8	556965.8
Northing	6242466.0	6242466.0	6242466.0	6242466.0	6242466.0	6242466.0	6242466.0	6242466.0	6242466.0

TS number	C97-1090	C97-1090	C97-1090	C97-1090	C97-1090	C97-1090	C97-1090	C97-1090	C97-1090
Wt% S	33.10	38.66	34.13	38.65	34.78	33.61	38.58	33.46	35.07
Wt% Fe	31.85	60.18	38.29	60.49	29.78	32.16	60.98	32.94	30.65
Wt% Co	0.98	0.04	0.78	0.04	0.02	1.31	0.03	1.17	0.00
Wt% Ni	33.78	0.27	26.87	0.29	0.00	33.10	0.27	33.02	0.00
Wt% Cu	0.00	0.00	0.00	0.02	33.80	0.00	0.01	0.00	34.77
Total	99.71	99.15	100.08	99.50	98.39	100.19	99.87	100.59	100.48
Atomic% S	47.05	52.69	47.93	52.54	50.45	47.43	52.31	47.10	49.95
Atomic% Fe	25.98	47.08	30.87	47.20	24.80	26.05	47.46	26.62	25.06
Atomic% Co	0.76	0.03	0.60	0.03	0.01	1.01	0.03	0.90	0.00
Atomic% Ni	26.22	0.20	20.61	0.22	0.00	25.50	0.20	25.38	0.00
Atomic% Cu	0.00	0.00	0.00	0.02	24.74	0.00	0.00	0.00	24.99
Host	Troc	Troc	Troc	Troc	Troc	Troc	Troc	Troc	Troc
Hole	VB96266	VB96266	VB96266	VB96266	VB96266	VB96266	VB96266	VB96266	VB96266
Depth	197.00	197.00	197.00	197.00	197.00	197.00	197.00	197.00	197.00
Easting	556965.8	556965.8	556965.8	556965.8	556965.8	556965.8	556965.8	556965.8	556965.8
Northing	6242466.0	6242466.0	6242466.0	6242466.0	6242466.0	6242466.0	6242466.0	6242466.0	6242466.0

TS number	C97-1090	C97-1090	C97-1090	C97-1090	C97-1090	C97-1090	C97-1090	C97 1084	C97 1084
Wt% S	38.33	33.40	33.43	38.71	35.05	33.17	39.05	36.15	37.66
Wt% Fe	60.94	32.82	32.70	59.95	29.67	31.63	60.06	63.96	61.93
Wt% Co	0.04	1.13	1.17	0.05	0.01	1.26	0.03	0.04	0.04
Wt% Ni	0.27	33.46	33.42	0.32	0.03	33.29	0.29	0.03	0.37
Wt% Cu	0.00	0.00	0.00	0.01	34.22	0.00	0.00	0.02	0.00
Total	99.59	100.81	100.72	99.05	98.98	99.36	99.43	100.24	100.00
Atomic% S	52.16	46.96	47.03	52.78	50.53	47.26	52.99	49.56	51.28
Atomic% Fe	47.60	26.49	26.41	46.93	24.55	25.87	46.78	50.34	48.41
Atomic% Co	0.03	0.87	0.89	0.04	0.01	0.98	0.02	0.03	0.03
Atomic% Ni	0.20	25.68	25.67	0.24	0.02	25.90	0.22	0.02	0.28
Atomic% Cu	0.00	0.00	0.00	0.01	24.89	0.00	0.00	0.01	0.00
Host	Troc	Troc	Troc	Troc	Troc	Troc	Troc	Troc	Troc
Hole	VB96266	VB96266	VB96266	VB96266	VB96266	VB96266	VB96266	VB96266	VB96266
Depth	197.00	197.00	197.00	197.00	197.00	197.00	197.00	248.70	248.70
Easting	556965.8	556965.8	556965.8	556965.8	556965.8	556965.8	556965.8	556965.8	556965.8
Northing	6242466.0	6242466.0	6242466.0	6242466.0	6242466.0	6242466.0	6242466.0	6242466.0	6242466.0

TS number	C97 1084	C97 1084	C97 1084	C97 1084	C97 1089	C97 1089	C97 1089	C97 1089	C97 1089
Wt% S	32.91	33.95	37.95	33.79	36.00	35.75	32.85	37.96	33.13
Wt% Fe	35.27	30.74	62.15	29.92	61.13	58.72	31.02	61.64	33.53
Wt% Co	2.02	0.02	0.04	0.02	0.06	0.05	1.21	0.05	1.18
Wt% Ni	30.87	0.05	0.07	0.01	0.12	0.22	36.04	0.23	33.84
Wt% Cu	0.19	34.34	0.01	33.82	0.02	0.00	0.00	0.04	0.00
Total	101.30	99.12	100.22	97.61	97.34	94.74	101.12	99.92	101.68
Atomic% S	46.20	49.22	51.50	49.63	50.56	51.36	46.28	51.64	46.34
Atomic% Fe	28.42	25.58	48.41	25.23	49.28	48.42	25.08	48.13	26.92
Atomic% Co	1.54	0.02	0.03	0.01	0.05	0.04	0.92	0.04	0.90
Atomic% Ni	23.66	0.04	0.05	0.01	0.09	0.17	27.72	0.17	25.85
Atomic% Cu	0.14	25.12	0.00	25.06	0.01	0.00	0.00	0.03	0.00
Host	Troc	Troc	Troc	Troc	Troc	Troc	Troc	Troc	Troc
Hole	VB96266	VB96266	VB96266	VB96266	VB96266	VB96266	VB96266	VB96266	VB96266
Depth	248.70	248.70	248.70	248.70	156.50	156.50	156.50	156.50	156.50
Easting	556965.8	556965.8	556965.8	556965.8	556965.8	556965.8	556965.8	556965.8	556965.8
Northing	6242466.0	6242466.0	6242466.0	6242466.0	6242466.0	6242466.0	6242466.0	6242466.0	6242466.0

TS number	C97 1089	C97 1089	C97 1089	C97 1089	C97 1089	C97 1089	C97 1089	C97 1089	C97 1089
Wt% S	38.21	37.56	37.96	32.28	37.96	34.01	32.92	38.07	37.20
Wt% Fe	61.84	62.35	61.08	33.16	61.94	31.16	33.83	61.91	63.04
Wt% Co	0.04	0.04	0.05	1.04	0.04	0.02	1.03	0.06	0.05
Wt% Ni	0.25	0.23	0.20	33.35	0.18	0.04	33.97	0.25	0.19
Wt% Cu	0.05	0.01	0.01	0.00	0.02	35.22	0.00	0.00	0.00
Total	100.42	100.18	99.33	99.83	100.17	100.45	101.75	100.30	100.51
Atomic% S	51.69	51.10	51.87	46.05	51.53	48.79	46.08	51.60	50.58
Atomic% Fe	48.04	48.70	47.91	27.16	48.27	25.67	27.18	48.17	49.21
Atomic% Co	0.03	0.03	0.04	0.81	0.03	0.02	0.78	0.04	0.03
Atomic% Ni	0.18	0.17	0.15	25.98	0.13	0.03	25.96	0.19	0.14
Atomic% Cu	0.04	0.01	0.01	0.00	0.02	25.50	0.00	0.00	0.00
Host	Troc	Troc	Troc	Troc	Troc	Troc	Troc	Troc	Troc
Hole	VB96266	VB96266	VB96266	VB96266	VB96266	VB96266	VB96266	VB96266	VB96266
Depth	156.50	156.50	156.50	156.50	156.50	156.50	156.50	156.50	156.50
Easting	556965.8	556965.8	556965.8	556965.8	556965.8	556965.8	556965.8	556965.8	556965.8
Northing	6242466.0	6242466.0	6242466.0	6242466.0	6242466.0	6242466.0	6242466.0	6242466.0	6242466.0

TS number	C97 1089	C97 1089	C97 1089	C97 1089	C97 1091	C97 1091	C97 1091	C97 1091	C97 1091
Wt% S	36.06	38.26	33.35	33.91	37.87	37.98	37.49	34.36	32.96
Wt% Fe	63.47	62.05	34.36	30.17	61.89	61.39	62.24	30.59	33.63
Wt% Co	0.04	0.04	0.98	0.02	0.04	0.04	0.04	0.03	1.15
Wt% Ni	0.02	0.14	33.36	0.17	0.08	0.08	0.09	0.01	33.15
Wt% Cu	0.03	0.02	0.00	34.48	0.03	0.06	0.03	35.14	0.05
Total	99.64	100.51	102.06	98.75	99.91	99.54	99.90	100.13	100.93
Atomic% S	49.70	51.71	46.43	49.34	51.54	51.80	51.14	49.32	46.41
Atomic% Fe	50.22	48.15	27.46	25.20	48.35	48.07	48.74	25.20	27.18
Atomic% Co	0.03	0.03	0.74	0.02	0.03	0.03	0.03	0.02	0.88
Atomic% Ni	0.01	0.11	25.36	0.14	0.06	0.06	0.07	0.01	25.49
Atomic% Cu	0.02	0.01	0.00	25.31	0.02	0.04	0.02	25.44	0.04
Host	Troc	Troc	Troc	Troc	Troc	Troc	Troc	Troc	Troc
Hole	VB96266	VB96266	VB96266	VB96266	VB96266	VB96266	VB96266	VB96266	VB96266
Depth	156.50	156.50	156.50	156.50	187.00	187.00	187.00	187.00	187.00
Easting	556965.8	556965.8	556965.8	556965.8	556965.8	556965.8	556965.8	556965.8	556965.8
Northing	6242466.0	6242466.0	6242466.0	6242466.0	6242466.0	6242466.0	6242466.0	6242466.0	6242466.0

TS number	C97 1091	C97 1091	C97 1091	C97 1091	C97 1091	C97 1091	C97 1091	C97 1091	C97 1091
Wt% S	33.13	36.63	31.84	34.63	34.42	33.02	34.88	38.38	37.01
Wt% Fe	33.89	63.26	33.02	31.07	30.93	34.47	32.11	61.69	63.08
Wt% Co	1.10	0.05	1.14	0.01	0.02	1.55	0.03	0.04	0.04
Wt% Ni	32.76	0.06	32.61	0.06	0.08	32.79	0.03	0.16	0.07
Wt% Cu	0.00	0.01	0.00	35.25	34.94	0.00	34.28	0.04	0.02
Total	100.88	100.01	98.63	101.02	100.41	101.83	101.33	100.34	100.22
Atomic% S	46.62	50.17	45.99	49.27	49.26	46.15	49.38	51.91	50.50
Atomic% Fe	27.37	49.74	27.38	25.38	25.42	27.65	26.09	47.90	49.41
Atomic% Co	0.84	0.04	0.90	0.01	0.01	1.18	0.03	0.03	0.03
Atomic% Ni	25.17	0.05	25.72	0.05	0.06	25.02	0.02	0.12	0.05
Atomic% Cu	0.00	0.01	0.00	25.30	25.23	0.00	24.48	0.03	0.01
Host	Troc	Troc	Troc	Troc	Troc	Troc	Troc	Troc	Troc
Hole	VB96266	VB96266	VB96266	VB96266	VB96266	VB96266	VB96266	VB96266	VB96266
Depth	187.00	187.00	187.00	187.00	187.00	187.00	187.00	187.00	187.00
Easting	556965.8	556965.8	556965.8	556965.8	556965.8	556965.8	556965.8	556965.8	556965.8
Northing	6242466.0	6242466.0	6242466.0	6242466.0	6242466.0	6242466.0	6242466.0	6242466.0	6242466.0

TS number	C97 1091	C97 1091	C97 1091	C97 1091	C97 1091	C97 1091	C97 1091	C97 1091	C97 1091
Wt% S	34.31	37.31	37.38	38.27	38.45	33.14	34.38	37.83	36.86
Wt% Fe	31.02	62.57	62.75	61.68	61.73	34.17	31.02	62.19	63.59
Wt% Co	0.01	0.05	0.04	0.05	0.04	1.18	0.02	0.05	0.03
Wt% Ni	0.00	0.13	0.11	0.20	0.17	33.25	0.00	0.19	0.03
Wt% Cu	35.16	0.03	0.03	0.02	0.00	0.00	35.27	0.03	0.01
Total	100.54	100.12	100.31	100.23	100.39	101.74	100.81	100.30	100.55
Atomic% S	49.10	50.86	50.85	51.83	51.96	46.31	49.08	51.35	50.21
Atomic% Fe	25.48	48.97	49.01	47.96	47.89	27.41	25.42	48.45	49.72
Atomic% Co	0.01	0.04	0.03	0.04	0.03	0.90	0.01	0.04	0.02
Atomic% Ni	0.00	0.10	0.08	0.15	0.13	25.38	0.00	0.14	0.02
Atomic% Cu	25.38	0.02	0.02	0.02	0.00	0.00	25.40	0.02	0.00
Host	Troc	Troc	Troc	Troc	Troc	Troc	Troc	Troc	Troc
Hole	VB96266	VB96266	VB96266	VB96266	VB96266	VB96266	VB96266	VB96266	VB96266
Depth	187.00	187.00	187.00	187.00	187.00	187.00	187.00	187.00	187.00
Easting	556965.8	556965.8	556965.8	556965.8	556965.8	556965.8	556965.8	556965.8	556965.8
Northing	6242466.0	6242466.0	6242466.0	6242466.0	6242466.0	6242466.0	6242466.0	6242466.0	6242466.0

TS number	C97 1091	C97 1092	C97 1092	C97 1092	C97 1092	C97 1092	C97 1072	C97 1072	C97 1072
Wt% S	38.24	35.96	36.10	31.74	36.42	26.50	36.50	36.38	38.12
Wt% Fe	61.78	63.85	64.40	35.77	63.97	33.75	63.48	63.99	61.85
Wt% Co	0.05	0.04	0.04	1.35	0.04	1.04	0.14	0.12	0.27
Wt% Ni	0.16	0.00	0.02	27.86	0.03	28.75	0.03	0.04	0.05
Wt% Cu	0.02	0.00	0.01	0.00	0.05	0.00	0.02	0.17	0.01
Total	100.24	99.85	100.57	96.74	100.56	90.05	100.21	100.70	100.29
Atomic% S	51.80	49.51	49.38	46.51	49.74	42.64	49.96	49.64	51.65
Atomic% Fe	48.04	50.46	50.57	30.10	50.15	31.18	49.88	50.13	48.11
Atomic% Co	0.03	0.03	0.03	1.08	0.03	0.91	0.02	0.03	0.03
Atomic% Ni	0.12	0.00	0.02	22.30	0.02	25.26	0.11	0.09	0.20
Atomic% Cu	0.01	0.00	0.01	0.00	0.04	0.00	0.02	0.12	0.01
Host	Troc	Troc	Troc	Troc	Troc	Troc	Troc	Troc	Troc
Hole	VB96266	VB96266	VB96266	VB96266	VB96266	VB96266	VB96266	VB96266	VB96266
Depth	187.00	369.00	369.00	369.00	369.00	369.00	304.50	304.50	304.50
Easting	556965.8	556965.8	556965.8	556965.8	556965.8	556965.8	556965.8	556965.8	556965.8
Northing	6242466.0	6242466.0	6242466.0	6242466.0	6242466.0	6242466.0	6242466.0	6242466.0	6242466.0

TS number	C97 1072	C97 1072	C97 1072	C97 1072	C97 1072	C97 1072	C97 1072	C97 1072	C97 1072
Wt% S	32.70	35.94	33.64	32.81	37.76	36.62	33.14	38.01	32 89
Wt% Fe	32.89	63.91	30.59	32.90	61.52	60.47	32.43	61.74	33.20
Wt% Co	33.49	0.00	0.06	33.36	0.24	0.24	32.82	0.20	33.09
Wt% Ni	1.67	0.06	0.02	1.78	0.03	0.04	1.62	0.04	1.70
Wt% Cu	0.00	0.02	34.50	0.00	0.01	0.22	0.62	0.00	0.00
Total	100.74	99.93	98.81	100.85	99.59	97.58	100.71	100.21	100.90
Atomic% S	46.20	49.45	49.01	46.29	51.55	51.15	46.73	51.56	46.35
Atomic% Fe	26.67	50.49	25.58	26.65	48.22	48.48	26.25	48.08	26.86
Atomic% Co	1.28	0.04	0.01	1.37	0.02	0.03	1.24	0.03	1.31
Atomic% Ni	25.84	0.00	0.05	25.70	0.18	0.19	25.27	0.15	25.46
Atomic% Cu	0.00	0.01	25.35	0.00	0.01	0.16	0.44	0.00	0.00
Host	Troc	Troc	Troc	Troc	Troc	Troc	Troc	Troc	Troc
Hole	VB96266	VB96266	VB96266	VB96266	VB96266	VB96266	VB96266	VB96266	VB96266
Depth	304.50	304.50	304.50	304.50	304.50	304.50	304.50	304.50	304.50
Easting	556965.8	556965.8	556965.8	556965.8	556965.8	556965.8	556965.8	556965.8	556965.8
Northing	6242466.0	6242466.0	6242466.0	6242466.0	6242466.0	6242466.0	6242466.0	6242466.0	6242466.0

TS number	C97 1072	C97 1072	C97 1072	C97 1072	C97 1072	C97 1072	C97 1072	C97 1072	C97 1073
Wt% S	36.11	38.05	36.59	37.09	37.37	33.14	36.32	36.36	37.17
Wt% Fe	63.94	61.67	62.51	62.82	62.86	33.95	63.77	64.13	62.75
Wt% Co	0.03	0.19	0.31	0.13	0.10	32.83	0.01	0.02	0.10
Wt% Ni	0.03	0.04	0.05	0.04	0.03	1.71	0.05	0.05	0.04
Wt% Cu	0.00	0.01	0.00	0.04	0.04	0.00	0.02	0.02	0.00
Total	100.13	99.98	99.49	100.12	100.42	101.65	100.19	100.57	100.08
Atomic% S	49.56	51.71	50.34	50.62	50.81	46.35	49.77	49.66	50.72
Atomic% Fe	50.38	48.11	49.37	49.22	49.06	27.26	50.16	50.28	49.16
Atomic% Co	0.02	0.03	0.03	0.03	0.03	1.30	0.04	0.03	0.03
Atomic% Ni	0.03	0.14	0.23	0.10	0.08	25.08	0.01	0.01	0.08
Atomic% Cu	0.00	0.01	0.00	0.03	0.03	0.00	0.01	0.01	0.00
Host	Troc	Troc	Troc	Troc	Troc	Troc	Troc	Troc	Troc
Hole	VB96266	VB96266	VB96266	VB96266	VB96266	VB96266	VB96266	VB96266	VB96266
Depth	304.50	304.50	304.50	304.50	304.50	304.50	304.50	304.50	312.20
Easting	556965.8	556965.8	556965.8	556965.8	556965.8	556965.8	556965.8	556965.8	556965.8
Northing	6242466.0	6242466.0	6242466.0	6242466.0	6242466.0	6242466.0	6242466.0	6242466.0	6242466.0

TS number	C97 1073	C97 1073	C97 1073	C97 1073	C97 1073	C97 1073	C97 1073	C97 1073	C97 1073
Wt% S	37.75	38.32	31.99	38.07	37.63	33.22	34.46	37.79	35.33
Wt% Fe	60.72	61.55	31.95	61.59	62.25	33.19	30.08	62.07	57.14
Wt% Co	0.22	0.28	32.83	0.20	0.19	33.40	0.08	0.12	6.68
Wt% Ni	0.04	0.04	2.20	0.05	0.05	1.83	0.03	0.04	0.82
Wt% Cu	0.04	0.00	0.00	0.00	0.00	0.00	33.94	0.00	0.00
Total	98.77	100.22	98.97	99.91	100.16	101.65	98.68	100.03	100.09
Atomic% S	51.88	51.90	46.05	51.76	51.18	46.45	49.96	51.40	48.87
Atomic% Fe	47.90	47.85	26.41	48.06	48.60	26.65	25.04	48.46	45.37
Atomic% Co	0.03	0.03	1.73	0.04	0.03	1.39	0.03	0.03	0.61
Atomic% Ni	0.16	0.21	25.82	0.15	0.14	25.51	0.07	0.09	5.05
Atomic% Cu	0.02	0.00	0.00	0.00	0.00	0.00	24.82	0.00	0.00
Host	Troc	Troc	Troc	Troc	Troc	Troc	Troc	Troc	Troc
Hole	VB96266	VB96266	VB96266	VB96266	VB96266	VB96266	VB96266	VB96266	VB96266
Depth	312.20	312.20	312.20	312.20	312.20	312.20	312.20	312.20	312.20
Easting	556965.8	556965.8	556965.8	556965.8	556965.8	556965.8	556965.8	556965.8	556965.8
Northing	6242466.0	6242466.0	6242466.0	6242466.0	6242466.0	6242466.0	6242466.0	6242466.0	6242466.0

TS number	C97 1073	C97 1073	C97 1073	C97 1076	C97 1076	C97 1076	C97 1076	C97 1076	C97 1076
Wt% S	34.19	36.90	34.02	33.64	35.60	36.16	33.06	36.29	35.97
Wt% Fe	30.91	63.00	30.95	35.42	63.71	64.13	39.23	63.58	64.24
Wt% Co	0.00	0.07	0.00	1.25	0.01	0.01	27.09	0.01	0.00
Wt% Ni	0.02	0.03	0.01	0.05	0.05	0.04	1.65	0.03	0.06
Wt% Cu	35.21	0.02	35.01	27.43	0.01	0.02	0.01	0.03	0.02
Total	100.49	100.06	100.13	100.19	99.41	100.35	101.06	100.02	100.30
Atomic% S	48.98	50.44	48.91	48.27	49.29	49.52	46.38	49.79	49.35
Atomic% Fe	25.42	49.44	25.54	29.17	50.64	50.43	31.59	50.08	50.59
Atomic% Co	0.02	0.03	0.01	0.04	0.04	0.03	1.26	0.03	0.04
Atomic% Ni	0.00	0.05	0.00	0.98	0.01	0.01	20.75	0.01	0.00
Atomic% Cu	25.44	0.02	25.39	19.86	0.00	0.01	0.00	0.02	0.01
Host	Troc	Troc	Troc	Troc	Troc	Troc	Troc	Troc	Troc
Hole	VB96266	VB96266	VB96266	VB96266	VB96266	VB96266	VB96266	VB96266	VB96266
Depth	312.20	312.20	312.20	355.70	355.70	355.70	355.70	355.70	355.70
Easting	556965.8	556965.8	556965.8	556965.8	556965.8	556965.8	556965.8	556965.8	556965.8
Northing	6242466.0	6242466.0	6242466.0	6242466.0	6242466.0	6242466.0	6242466.0	6242466.0	6242466.0

TS number	C97 1076	C97 1076	C97 1076	C97 1076	C97 1076	C97 1076	C97 1076	C97 1076	C97 1081
Wt% S	33.07	34.06	35.59	33.05	32.97	32.75	35.60	36.16	35.75
Wt% Fe	36.37	30.73	64.18	36.28	36.25	36.18	63.90	63.91	63.63
Wt% Co	30.51	0.03	0.02	30.59	30.30	30.19	0.01	0.00	0.02
Wt% Ni	1.39	0.02	0.05	1.34	1.51	1.54	0.06	0.04	0.04
Wt% Cu	0.00	34.72	0.00	0.01	0.02	0.00	0.01	0.00	0.01
Total	101.37	99.55	99.83	101.39	101.05	100.65	99.61	100.11	99.45
Atomic% S	46.33	49.19	49.11	46.31	46.33	46.24	49.22	49.62	49.44
Atomic% Fe	29.25	25.48	50.85	29.18	29.25	29.32	50.71	50.35	50.51
Atomic% Co	1.06	0.01	0.03	1.02	1.15	1.18	0.05	0.03	0.03
Atomic% Ni	23.34	0.02	0.01	23.40	23.25	23.27	0.01	0.00	0.01
Atomic% Cu	0.00	25.30	0.00	0.00	0.01	0.00	0.01	0.00	0.00
Host	Troc	Troc	Troc	Troc	Troc	Troc	Troc	Troc	Troc
Hole	VB96266	VB96266	VB96266	VB96266	VB96266	VB96266	VB96266	VB96266	VB96266
Depth	355.70	355.70	355.70	355.70	355.70	355.70	355.70	355.70	224.00
Easting	556965.8	556965.8	556965.8	556965.8	556965.8	556965.8	556965.8	556965.8	556965.8
Northing	6242466.0	6242466.0	6242466.0	6242466.0	6242466.0	6242466.0	6242466.0	6242466.0	6242466.0

TS number	C97 1081	C97 1081	C97 1081	C97 1081	C97 1081	C97 1081	C97 1081	C97 1081	C97 1081
Wt% S	33.06	37.77	35.68	32.43	36.78	32.70	36.21	36.72	37.18
Wt% Fe	33.10	61.25	62.29	32.79	62.85	32.70	63.77	63.64	62.17
Wt% Co	32.47	0.21	0.02	30.60	0.14	34.32	0.01	0.03	0.16
Wt% Ni	1.82	0.04	0.06	2.72	0.04	1.65	0.03	0.04	0.04
Wt% Cu	0.00	0.00	0.02	0.00	0.09	0.00	0.00	0.00	0.00
Total	100.46	99.27	98.08	98.53	99.89	101.37	100.03	100.43	99.56
Atomic% S	46.71	51.69	49.90	46.70	50.38	45.99	49.70	50.10	50.94
Atomic% Fe	26.84	48.12	50.01	27.11	49.43	26.40	50.26	49.85	48.90
Atomic% Co	1.40	0.03	0.04	2.13	0.03	1.26	0.02	0.03	0.03
Atomic% Ni	25.05	0.16	0.02	24.06	0.11	26.35	0.01	0.02	0.12
Atomic% Cu	0.00	0.00	0.01	0.00	0.06	0.00	0.00	0.00	0.00
Host	Troc	Troc	Troc	Troc	Troc	Troc	Troc	Troc	Troc
Hole	VB96266	VB96266	VB96266	VB96266	VB96266	VB96266	VB96266	VB96266	VB96266
Depth	224.00	224.00	224.00	224.00	224.00	224.00	224.00	224.00	224.00
Easting	556965.8	556965.8	556965.8	556965.8	556965.8	556965.8	556965.8	556965.8	556965.8
Northing	6242466.0	6242466.0	6242466.0	6242466.0	6242466.0	6242466.0	6242466.0	6242466.0	6242466.0

TS number	C97 1095	C97 1095	C97 1095	C97 1095	C97 1095	C97 1095	C97 1095	C97 1095	C97 1095
Wt% S	37.90	37.10	37.00	33.25	37.68	36.01	33.05	36.27	33.06
Wt% Fe	60.97	62.08	62.35	33.03	61.58	63.69	30.11	63.17	31.88
Wt% Co	0.17	0.03	0.04	1.59	0.05	0.03	0.01	0.04	0.47
Wt% Ni	0.13	0.04	0.06	31.66	0.14	0.01	0.01	0.11	11.55
Wt% Cu	0.08	0.08	0.05	0.00	0.07	0.10	34.60	0.05	23.02
Total	99.27	99.34	99.50	99.54	99.52	99.83	97.77	99.63	100.04
Atomic% S	51.84	50.94	50.77	47.25	51.49	49.57	48.75	49.94	47.52
Atomic% Fe	47.87	48.94	49.12	26.94	48.31	50.33	25.50	49.92	26.31
Atomic% Co	0.13	0.02	0.03	1.23	0.03	0.02	0.01	0.03	0.37
Atomic% Ni	0.10	0.03	0.05	24.57	0.11	0.01	0.00	0.08	9.07
Atomic% Cu	0.05	0.06	0.04	0.00	0.05	0.07	25.75	0.03	16.70
Host	Troc	Troc	Troc	Troc	Troc	Troc	Troc	Troc	Troc
Hole	VB96266	VB96266	VB96266	VB96266	VB96266	VB96266	VB96266	VB96266	VB96266
Depth	417.00	417.00	417.00	417.00	417.00	417.00	417.00	417.00	417.00
Easting	556965.8	556965.8	556965.8	556965.8	556965.8	556965.8	556965.8	556965.8	556965.8
Northing	6242466.0	6242466.0	6242466.0	6242466.0	6242466.0	6242466.0	6242466.0	6242466.0	6242466.0

TS number	C97 1095	C97 1095	C97 1095	C97 1095	C97 1095	C97 1095	C97 1095	C97 1095	C97 1095
Wt% S	36.06	34.49	36.86	32.73	36.17	34.22	34.19	37.75	33.05
Wt% Fe	63.75	30.77	62.78	34.46	63.70	30.83	31.30	61.72	34.03
Wt% Co	0.03	0.03	0.03	1.50	0.04	0.03	0.27	0.02	1.48
Wt% Ni	0.04	0.03	0.09	32.00	0.04	0.02	5.52	0.13	32.54
Wt% Cu	0.04	34.93	0.09	0.01	0.08	35.14	29.37	0.02	0.00
Total	99.92	100.26	99.86	100.73	100.04	100.29	100.84	99.65	101.12
Atomic% S	49.59	49.41	50.49	46.21	49.66	49.10	48.68	51.52	46.44
Atomic% Fe	50.33	25.30	49.36	27.94	50.22	25.39	25.59	48.35	27.45
Atomic% Co	0.03	0.02	0.02	1.15	0.03	0.03	0.21	0.02	1.14
Atomic% Ni	0.03	0.02	0.06	24.68	0.03	0.02	4.29	0.10	24.97
Atomic% Cu	0.03	25.24	0.06	0.01	0.05	25.44	21.10	0.01	0.00
Host	Troc	Troc	Troc	Troc	Troc	Troc	Troc	Troc	Troc
Hole	VB96266	VB96266	VB96266	VB96266	VB96266	VB96266	VB96266	VB96266	VB96266
Depth	417.00	417.00	417.00	417.00	417.00	417.00	417.00	417.00	417.00
Easting	556965.8	556965.8	556965.8	556965.8	556965.8	556965.8	556965.8	556965.8	556965.8
Northing	6242466.0	6242466.0	6242466.0	6242466.0	6242466.0	6242466.0	6242466.0	6242466.0	6242466.0

TS number	C97 1095	C97 1095	C97 1095	C97 1095	C97 1095	C97 1095	C97 1103	C97 1103	C97 1103
Wt% S	36.49	34.21	32.85	37.51	34.06	32.92	35.89	33.82	35.99
Wt% Fe	63.07	30.97	34.53	62.28	31.04	35.15	62.85	30.73	63.60
Wt% Co	0.04	0.01	1.23	0.04	0.01	1.39	0.05	0.01	0.03
Wt% Ni	0.07	0.00	32.60	0.03	0.00	31.46	0.00	0.57	0.07
Wt% Cu	0.02	35.17	0.00	0.13	35.39	0.04	0.00	34.11	0.07
Total	99.70	100.37	101.22	100.01	100.49	100.98	98.79	99.27	99.77
Atomic% S	50.15	49.05	46.17	51.12	48.84	46.33	49.85	49.02	49.57
Atomic% Fe	49.76	25.49	27.86	48.73	25.55	28.40	50.11	25.56	50.29
Atomic% Co	0.03	0.01	0.94	0.03	0.01	1.07	0.04	0.00	0.02
Atomic% Ni	0.05	0.00	25.02	0.02	0.00	24.18	0.00	0.45	0.05
Atomic% Cu	0.01	25.44	0.00	0.09	25.60	0.03	0.00	24.94	0.05
Host	Troc	Troc	Troc	Troc	Troc	Troc	Troc	Troc	Troc
Hole	VB96266	VB96266	VB96266	VB96266	VB96266	VB96266	VB96266	VB96266	VB96266
Depth	417.00	417.00	417.00	417.00	417.00	417.00	109.00	109.00	109.00
Easting	556965.8	556965.8	556965.8	556965.8	556965.8	556965.8	556965.8	556965.8	556965.8
Northing	6242466.0	6242466.0	6242466.0	6242466.0	6242466.0	6242466.0	6242466.0	6242466.0	6242466.0

TS number	C97 1103	C97 1103	C97 1103	C97 1103	C97 1103	C97 1103	C97 1103	C97 1103	C97 1103
Wt% S	33.28	33.25	36.06	32.99	34.17	34.34	35.97	32.72	35.92
Wt% Fe	39.05	29.78	63.67	39.48	31.94	30.73	63.46	35.00	63.17
Wt% Co	0.77	0.01	0.04	0.88	0.04	0.03	0.04	0.78	0.04
Wt% Ni	27.43	0.07	0.00	26.90	0.54	0.20	0.00	29.55	0.02
Wt% Cu	0.02	33.75	0.03	0.02	33.13	34.90	0.01	0.36	0.02
Total	100.55	96.92	99.81	100.28	99.82	100.20	99.48	98.40	99.20
Atomic% S	46.80	49.28	49.63	46.57	49.14	49.26	49.66	47.04	49.72
Atomic% Fe	31.53	25.34	50.31	32.00	26.36	25.31	50.30	28.89	50.20
Atomic% Co	0.59	0.01	0.03	0.68	0.03	0.03	0.03	0.61	0.03
Atomic% Ni	21.07	0.05	0.00	20.74	0.42	0.16	0.00	23.20	0.02
Atomic% Cu	0.02	25.24	0.02	0.01	24.04	25.25	0.01	0.26	0.02
Host	Troc	Troc	Troc	Troc	Troc	Troc	Troc	Troc	Troc
Hole	VB96266	VB96266	VB96266	VB96266	VB96266	VB96266	VB96266	VB96266	VB96266
Depth	109.00	109.00	109.00	109.00	109.00	109.00	109.00	109.00	109.00
Easting	556965.8	556965.8	556965.8	556965.8	556965.8	556965.8	556965.8	556965.8	556965.8
Northing	6242466.0	6242466.0	6242466.0	6242466.0	6242466.0	6242466.0	6242466.0	6242466.0	6242466.0

TS number	C97 1103	C97 1103	C97 1103	C97 1103	C97 1103	C97 1103	C97 1103	C97 1103	C97 1103
Wt% S	34.62	32.85	33.03	36.07	32.93	36.23	33.26	34.32	33.11
Wt% Fe	30.42	35.39	35.22	63.30	35.41	63.92	36.34	30.57	37.16
Wt% Co	0.01	0.69	0.68	0.05	0.82	0.05	0.84	0.01	0.80
Wt% Ni	0.00	30.68	30.73	0.00	30.08	0.01	30.43	0.01	29.84
Wt% Cu	34.68	0.00	0.00	0.01	0.00	0.02	0.00	34.77	0.00
Total	99.74	99.62	99.66	99.43	99.24	100.23	100.87	99.67	100.91
Atomic% S	49.75	46.73	46.92	49.80	46.96	49.65	46.72	49.44	46.52
Atomic% Fe	25.10	28.90	28.72	50.16	28.99	50.29	29.30	25.28	29.97
Atomic% Co	0.01	0.54	0.52	0.03	0.63	0.04	0.64	0.01	0.61
Atomic% Ni	0.00	23.83	23.83	0.00	23.42	0.01	23.34	0.01	22.90
Atomic% Cu	25.15	0.00	0.00	0.01	0.00	0.01	0.00	25.27	0.00
Host	Troc	Troc	Troc	Troc	Troc	Troc	Troc	Troc	Troc
Hole	VB96266	VB96266	VB96266	VB96266	VB96266	VB96266	VB96266	VB96266	VB96266
Depth	109.00	109.00	109.00	109.00	109.00	109.00	109.00	109.00	109.00
Easting	556965.8	556965.8	556965.8	556965.8	556965.8	556965.8	556965.8	556965.8	556965.8
Northing	6242466.0	6242466.0	6242466.0	6242466.0	6242466.0	6242466.0	6242466.0	6242466.0	6242466.0

TS number	C97 1103	C97 1103	C97 1103	C97 1105	C97 1105	C97 1105	C97 1105	C97 1105	C97 1105
Wt% S	36.22	34.33	36.13	33.37	34.51	38.51	38.19	38.19	32.87
Wt% Fe	63.56	31.14	63.85	29.61	30.20	60.29	60.33	61.21	32.10
Wt% Co	0.05	0.02	0.04	1.15	0.01	0.05	0.04	0.04	1.16
Wt% Ni	0.01	0.00	0.00	35.23	0.02	0.49	0.45	0.39	34.69
Wt% Cu	0.00	34.54	0.01	0.00	34.74	0.06	0.06	0.01	0.00
Total	99.84	100.04	100.04	99.37	99.48	99.40	99.08	99.85	100.83
Atomic% S	49.80	49.30	49.62	47.52	49.74	52.43	52.22	51.91	46.37
Atomic% Fe	50.16	25.67	50.34	24.20	24.99	47.13	47.36	47.76	26.00
Atomic% Co	0.03	0.01	0.03	0.89	0.01	0.04	0.03	0.03	0.89
Atomic% Ni	0.01	0.00	0.00	27.39	0.01	0.37	0.33	0.29	26.73
Atomic% Cu	0.00	25.02	0.01	0.00	25.26	0.04	0.04	0.00	0.00
Host	Troc	Troc	Troc	Troc	Troc	Troc	Troc	Troc	Troc
Hole	VB96266	VB96266	VB96266	VB96266	VB96266	VB96266	VB96266	VB96266	VB96266
Depth	109.00	109.00	109.00	260.60	260.60	260.60	260.60	260.60	260.60
Easting	556965.8	556965.8	556965.8	556965.8	556965.8	556965.8	556965.8	556965.8	556965.8
Northing	6242466.0	6242466.0	6242466.0	6242466.0	6242466.0	6242466.0	6242466.0	6242466.0	6242466.0

TS number	C97 1105	C97 1105	C97 1105	C97 1105	C97 1105	C97 1105	C97 1105	C97 1105	C97 1105
Wt% S	34.30	38.16	32.93	38.52	33.10	38.14	34.29	32.85	38.05
Wt% Fe	30.81	61.15	31.35	60.33	30.54	60.63	30.69	31.06	58.64
Wt% Co	0.02	0.05	1.17	0.05	1.32	0.04	0.03	1.35	0.04
Wt% Ni	0.01	0.35	34.62	0.57	35.56	0.53	0.00	35.32	0.31
Wt% Cu	34.92	0.03	0.00	0.01	0.00	0.02	34.83	0.00	0.03
Total	100.10	99.74	100.11	99.47	100.53	99.38	99.83	100.59	97.06
Atomic% S	49.25	51.92	46.71	52.41	46.77	52.05	49.35	46.46	52.91
Atomic% Fe	25.40	47.76	25.53	47.13	24.78	47.50	25.35	25.22	46.81
Atomic% Co	0.02	0.03	0.91	0.04	1.02	0.03	0.02	1.04	0.03
Atomic% Ni	0.01	0.26	26.82	0.42	27.44	0.40	0.00	27.28	0.24
Atomic% Cu	25.30	0.02	0.00	0.00	0.00	0.01	25.29	0.00	0.02
Host	Troc	Troc	Troc	Troc	Troc	Troc	Troc	Troc	Troc
Hole	VB96266	VB96266	VB96266	VB96266	VB96266	VB96266	VB96266	VB96266	VB96266
Depth	260.60	260.60	260.60	260.60	260.60	260.60	260.60	260.60	260.60
Easting	556965.8	556965.8	556965.8	556965.8	556965.8	556965.8	556965.8	556965.8	556965.8
Northing	6242466.0	6242466.0	6242466.0	6242466.0	6242466.0	6242466.0	6242466.0	6242466.0	6242466.0

TS number	C97 1105	C97 1105	C97 1105	C97 1105	C97 1105	C97 1105	C97 1105	C97 1105	C97 1105
Wt% S	38.15	38.41	34.61	38.97	38.68	31.74	34.52	38.58	34.50
Wt% Fe	59.36	60.63	30.18	60.51	60.56	30.46	30.68	60.68	30.56
Wt% Co	0.04	0.05	0.02	0.06	0.05	1.26	0.01	0.03	0.02
Wt% Ni	0.60	0.50	0.00	0.34	0.45	34.82	0.01	0.59	0.02
Wt% Cu	0.03	0.03	34.67	0.01	0.02	0.11	34.97	0.02	34.78
Total	98.17	99.61	99.48	99.91	99.78	98.41	100.18	99.93	99.90
Atomic% S	52.55	52.24	49.84	52.70	52.46	46.01	49.47	52.29	49.55
Atomic% Fe	46.94	47.34	24.95	46.98	47.15	25.35	25.24	47.22	25.20
Atomic% Co	0.03	0.03	0.02	0.04	0.04	0.99	0.01	0.02	0.02
Atomic% Ni	0.45	0.37	0.00	0.25	0.33	27.56	0.01	0.43	0.01
Atomic% Cu	0.02	0.02	25.19	0.00	0.01	0.08	25.28	0.01	25.21
Host	Troc	Troc	Troc	Troc	Troc	Troc	Troc	Troc	Troc
Hole	VB96266	VB96266	VB96266	VB96266	VB96266	VB96266	VB96266	VB96266	VB96266
Depth	260.60	260.60	260.60	260.60	260.60	260.60	260.60	260.60	260.60
Easting	556965.8	556965.8	556965.8	556965.8	556965.8	556965.8	556965.8	556965.8	556965.8
Northing	6242466.0	6242466.0	6242466.0	6242466.0	6242466.0	6242466.0	6242466.0	6242466.0	6242466.0

TS number	C97 1105	C97 1105	C97 1105	C97 1105	C97 1105	C97 1111	C97 1111	C97 1111	C97 1111
Wt% S	33.11	38.45	38.47	34.15	33.09	38.16	37.04	33.06	38.54
Wt% Fe	30.88	61.17	60.34	30.08	31.00	60.87	59.75	31.72	61.22
Wt% Co	1.32	0.04	0.04	0.02	1.19	0.02	0.05	1.44	0.03
Wt% Ni	35.40	0.35	0.49	0.00	35.24	0.31	0.38	35.41	0.48
Wt% Cu	0.00	0.04	0.01	34.43	0.00	0.06	0.01	0.00	0.03
Total	100.70	100.05	99.35	98.67	100.53	99.42	97.24	101.66	100.31
Atomic% S	46.71	52.10	52.41	49.64	46.75	52.06	51.75	46.30	52.10
Atomic% Fe	25.01	47.58	47.19	25.10	25.15	47.66	47.92	25.50	47.50
Atomic% Co	1.01	0.03	0.03	0.01	0.91	0.02	0.04	1.09	0.02
Atomic% Ni	27.27	0.26	0.36	0.00	27.19	0.23	0.29	27.08	0.36
Atomic% Cu	0.00	0.02	0.01	25.25	0.00	0.04	0.01	0.00	0.02
Host	Troc	Troc	Troc	Troc	Troc	Troc	Troc	Troc	Troc
Hole	VB96266	VB96266	VB96266	VB96266	VB96266	VB96266	VB96266	VB96266	VB96266
Depth	260.60	260.60	260.60	260.60	260.60	296.00	296.00	296.00	296.00
Easting	556965.8	556965.8	556965.8	556965.8	556965.8	556965.8	556965.8	556965.8	556965.8
Northing	6242466.0	6242466.0	6242466.0	6242466.0	6242466.0	6242466.0	6242466.0	6242466.0	6242466.0

TS number	C97 1111	C97 1111	C97 1111	C97 1111	C97 1111	C97 1111	C97 1111	C97 1111	C97 1111
Wt% S	38.16	33.19	34.25	37.99	37.94	38.58	36.18	38.23	34 32
Wt% Fe	61.54	31.99	30.78	61.42	61.73	61.35	47.61	61.69	31.79
Wt% Co	0.04	1.38	0.02	0.03	0.04	0.03	0.05	0.03	0.00
Wt% Ni	0.31	34.64	0.04	0.28	0.27	0.36	0.16	0.43	0.01
Wt% Cu	0.10	0.11	34.98	0.00	0.00	0.14	14.17	0.00	34.72
Total	100.15	101.31	100.07	99.72	99.98	100.45	98.17	100.39	100.84
Atomic% S	51.75	46.56	49.21	51.75	51.59	52.08	51.12	51.74	48.96
Atomic% Fe	47.92	25.76	25.38	48.03	48.18	47.54	38.62	47.92	26.04
Atomic% Co	0.03	1.06	0.01	0.02	0.03	0.03	0.04	0.02	0.00
Atomic% Ni	0.23	26.54	0.03	0.21	0.20	0.26	0.12	0.32	0.01
Atomic% Cu	0.07	0.08	25.35	0.00	0.00	0.09	10.10	0.00	24.99
Host	Troc	Troc	Troc	Troc	Troc	Troc	Troc	Troc	Troc
Hole	VB96266	VB96266	VB96266	VB96266	VB96266	VB96266	VB96266	VB96266	VB96266
Depth	296.00	296.00	296.00	296.00	296.00	296.00	296.00	296.00	296.00
Easting	556965.8	556965.8	556965.8	556965.8	556965.8	556965.8	556965.8	556965.8	556965.8
Northing	6242466.0	6242466.0	6242466.0	6242466.0	6242466.0	6242466.0	6242466.0	6242466.0	6242466.0

TS number	C97 1111	C97 1111	C97 1111	C97 1111	C97 1111
Wt% S	32.57	33.08	37.84	32.96	37.88
Wt% Fe	31.57	31.85	62.09	32.89	61.10
Wt% Co	1.25	1.30	0.05	1.33	0.05
Wt% Ni	34.23	35.02	0.34	34.23	0.36
Wt% Cu	0.00	0.00	0.01	0.00	0.01
Total	99.64	101.25	100.34	101.40	99.42
Atomic% S	46.48	46.46	51.33	46.26	51.75
Atomic% Fe	25.86	25.68	48.36	26.50	47.92
Atomic% Co	0.97	0.99	0.04	1.02	0.03
Atomic% Ni	26.67	26.86	0.25	26.23	0.27
Atomic% Cu	0.00	0.00	0.00	0.00	0.00
Host	Troc	Troc	Troc	Troc	Troc
Hole	VB96266	VB96266	VB96266	VB96266	VB96266
Depth	296.00	296.00	296.00	296.00	296.00
Easting	556965.8	556965.8	556965.8	556965.8	556965.8
Northing	6242466.0	6242466.0	6242466.0	6242466.0	6242466.0

Table A5a Pb isotope ratios Voisey's Bay sulphides (OU)

Sample	98/AV/041ms	98/AV/191ms	98/AV/197ms	98/AV/189ms	98/AV/222po	98/AV/244ms	98/AV/012po
Core	PD006	VB 98 461	VB 98 461	VB 98 461	VB 97 391	AG 95 01	VB 95 151
Location	Ovoid	N.E.D	N.E.D	N.E.D	R.B.Z	Mushaua	E.Deeps
Easting	555688.7	554897.6	554897.6	554897.6	553583.4	554218.8	556421.1
Northing	6243337.8	6242852.3	6242852.3	6242852.3	6243212.4	6240197.4	6242801.7
Depth	87.2	1568.5	15886.2	1554.6	348.3	121.6	319.4
Type	Troctolite	Troctolite	Tasiuyak	Troctolite	Tasiuyak	Tasiuyak	Troctolite
$^{208}Pb/^{204}Pb$	35.200	36.467	38.271	36.140	36.923	36.923	35.404
error	0.024	0.063	0.094	0.014	0.014	0.070	0.056
$^{207}Pb/^{204}Pb$	15.120	15.341	15.562	15.313	15.313	15.406	15.127
error	0.010	0.027	0.038	0.006	0.006	0.030	0.024
$^{206}Pb/^{204}Pb$	15.296	15.895	17.407	15.859	15.859	16.216	15.373
error	0.010	0.027	0.043	0.006	0.006	0.032	0.024

Sample	98/AV/234pent	98/AV/053ms	98/AV/294ms	98/AV/307ms	98/AV/142po	98/AV/222ms	98/AV/240pent
Core	VB 98 454	VB 97 368	VB 96 266	VB 96 266	VB 98 276	VB 97 391	AG 95 01
Location	Red Dog	R.B.Z	E. Deeps	E. Deeps	R.B.Z	R.B.Z	Mushaua
Easting	558800.5	553583.4	556965.8	556965.8	553778.5	553583.4	554218.8
Northing	6241071.2	6243211.7	6242466.0	6242466.0	6243211.7	6243212.4	6240197.4
Depth	1025.3	313.5	211.5	599.6	508	348.1	34.8
Type	Troctolite	Troctolite	Troctolite	Troctolite	MASU	Tasiuyak	Tasiuyak
$^{208}Pb/^{204}Pb$	35.330	36.267	35.756	35.309	36.279	36.400	35.905
error	0.073	0.068	0.081	0.070	0.066	0.037	0.052
$^{207}Pb/^{204}Pb$	15.112	15.347	15.218	15.085	15.153	15.366	15.380
error	0.031	0.022	0.035	0.030	0.027	0.017	0.023
$^{206}Pb/^{204}Pb$	15.299	15.881	15.755	15.446	16.306	16.113	16.084
error	0.032	0.034	0.035	0.030	0.029	0.016	0.023

Sample	98/AV/242po	98/AV/314cpy	98/AV/167po	98/AV/205cpy	98/AV/142cpy	98/AV/314pent	98/AV/186ms
Core	AG 95 01	VB 96 266	VB 96 461	VB 97 391	VB 98 276	VB 96 266	VB 98 461
Location	Mushaua	E. Deeps	N.E.D	R.B.Z	R.B.Z	E.Deeps	N.E.D
Easting	554218.8	556965.8	554897.6	553583.4	553778.5	556965.8	554897.6
Northing	6240197.4	6242466.0	6242852.3	6243212.4	6243211.7	6242466.0	6242852.3
Depth	65.6	675.7	1695	197.3	207.6	675.7	1546.4
Type	Tasiuyak	MASU	Tasiuyak	MASU	MASU	MASU	Troctolite
$^{208}Pb/^{204}Pb$	35.613	35.438	37.392	36.423	36.369	35.222	36.160
error	0.076	0.047	0.055	0.112	0.048	0.021	0.154
$^{207}Pb/^{204}Pb$	15.315	15.139	15.217	15.367	15.230	15.054	15.183
error	0.032	0.018	0.021	0.042	0.019	0.009	0.063
$^{206}Pb/^{204}Pb$	16.419	15.489	15.878	15.935	15.781	15.387	16.214
error	0.033	0.016	0.023	0.041	0.020	0.008	0.067

Sample	98/AV/185ms	98/AV/240ms	98/AV/023cpy	98/AV/199po	98/AV/033cpy	98/AV/166ms	98/AV/295ms
Core	VB 98 461	AG 95 01	VB 96 271	VB 95 08	VB 96 277	VB 98 461	VB 96 266
Location	N.E.D	Mushaua	E. Deeps	Ovoid	Far E.Deeps	N.E.D	E. Deeps
Easting	554897.6	554218.8	556718.7	555831.6	557985.2	554897.6	556965.8
Northing	6242852.3	6240197.4	6242741.6	6243051.5	6242178.2	6242852.3	6242466.0
Depth	1542.2	34.8	451.5	34.9	943.2	1692.3	258.4
Type	Troctolite	Tasiuyak	MASU	MASU	MASU	Tasiuyak	Troctolite
$^{208}Pb/^{204}Pb$	36.019	35.134	34.500	34.964	32.153	34.738	33.956
error	0.036	0.086	0.075	0.036	0.077	0.101	0.058
$^{207}Pb/^{204}Pb$	15.240	14.903	14.728	14.895	13.746	14.680	14.465
error	0.014	0.036	0.032	0.015	0.033	0.042	0.024
$^{206}Pb/^{204}Pb$	15.798	15.472	15.018	15.354	14.043	15.435	14.933
error	0.015	0.038	0.031	0.015	0.033	0.042	0.025

Sample	98/AV/222cpy	98/AV/199cpy	98/AV/057po	98/AV/012cpy	98/AV/240ms	98/AV/166po	98/AV/294ms
Core	VB 97 391	VB 95 08	VB 97 368	VB 95 151	AG 95 01	VB 98 461	VB 96 266
Location	R.B.Z	Ovoid	R.B.Z	E.Deeps	Mushaua	N.E.D	E. Deeps
Easting	553583.4	555831.6	553583.4	556421.1	554218.8	554897.6	556965.8
Northing	6243212.4	6243051.5	6243211.7	6242801.7	6240197.4	6242852.3	6242466.0
Depth	348.1	34.9	317.7	319.4	34.8	1692.3	211.5
Type	Tasiuyak	MASU	MASU	Troctolite	Tasiuyak	Tasiuyak	Troctolite
$^{208}Pb/^{204}Pb$	36.070	35.336	34.414	35.130	35.042	34.736	35.746
error	0.020	0.048	0.109	0.105	0.043	0.848	0.048
$^{207}Pb/^{204}Pb$	15.244	15.051	14.542	15.034	14.981	14.585	15.220
error	0.007	0.021	0.046	0.042	0.017	0.406	0.019
$^{206}Pb/^{204}Pb$	15.979	15.519	15.097	15.115	15.191	15.386	15.759
error	0.011	0.020	0.048	0.042	0.016	0.479	0.019

Sample	98/AV/191ms	98/AV/041ms	98/AV/197po
Core	VB 98 461	PD006	VB 98 461
Location	N.E.D	Ovoid	N.E.D
Easting	554897.6	555688.7	554897.6
Northing	6242852.3	6243337.8	6242852.3
Depth	1538.4	86.7	1586.2
Type	Troctolite	Troctolite	Tasiuyak
$^{208}Pb/^{204}Pb$	36.579	35.214	39.903
error	0.070	0.056	0.129
$^{207}Pb/^{204}Pb$	15.392	15.131	15.667
error	0.029	0.020	0.050
$^{206}Pb/^{204}Pb$	15.949	15.307	18.238
error	0.030	0.017	0.057

Table A.5a. Pb isotope data derived from analyses of sulphide minerals at the Open University by MC-ICP-MS. Quoted errors are within run to ±2 S.E.

Table A5b Pb isotope ratios Voisey's Bay sulphides (INCO)

Sample	RX313682CP	65CP	65PO	66CP	66PN	66PO	67CP
Core	VB 95 25	VB 96 363	VB 96 363	VB 96 363	VB 96 363	VB 96 363	VB 96 363
Location	Ovoid	RBZ	RBZ	RBZ	RBZ	RBZ	RBZ
Easting	555782.8	554073.6	554073.6	554073.6	554073.6	554073.6	554073.6
Northing	6243107.8	6243286.3	6243286.3	6243286.3	6243286.3	6243286.3	6243286.3
Type	MASU	MASU	MASU	MASU	Tasiuyak	Tasiuyak	Tasiuyak
$^{208}Pb/^{204}Pb$	35.754	36.046	36.140	36.435	37.050	36.425	36.104
error	0.053	0.043	0.204	0.133	0.068	0.114	0.057
$^{207}Pb/^{204}Pb$	15.232	15.271	15.283	15.315	15.584	15.342	15.276
error	0.056	0.045	0.204	0.132	0.067	0.115	0.056
$^{206}Pb/^{204}Pb$	15.692	15.848	15.915	15.986	17.252	16.197	15.848
error	0.056	0.043	0.210	0.136	0.067	0.117	0.057

Sample	67PO	69CP	69PO	70CP	70PO	71CP	71PN
Core	VB 96 363	VB 96 282	VB 96 282	VB 96 282	VB 96 282	VB 96 282	VB 96 282
Location	RBZ	RBZ	RBZ	RBZ	RBZ	RBZ	RBZ
Easting	554073.6	554073.6	553777.2	553777.2	553777.2	553777.2	553777.2
Northing	6243286.3	6243286.3	6243335.5	6243335.5	6243335.5	6243335.5	6243335.5
Type	Tasiuyak	MASU	MASU	MASU	MASU	MASU	Tasiuyak
$^{208}Pb/^{204}Pb$	36.452	36.417	35.895	36.995	36.240	35.928	35.818
error	0.180	0.025	0.024	0.058	0.125	0.032	0.097
$^{207}Pb/^{204}Pb$	15.347	15.249	15.215	15.281	15.276	15.254	15.229
error	0.174	0.024	0.022	0.058	0.125	0.003	0.097
$^{206}Pb/^{204}Pb$	16.182	16.016	15.695	15.941	15.981	15.740	15.817
error	0.173	0.021	0.022	0.058	0.127	0.027	0.101

Sample	71PO	72CP	72PO	77CP	77PN	77PO	78PO
Core	VB 96 282	VB 96 41	VB 96 41	VB 96 41	VB 95 27	VB 95 27	VB 95 27
Location	RBZ	Ovoid	Ovoid	Ovoid	Ovoid	Ovoid	Ovoid
Easting	553777.2	555931.4	555931.4	555931.4	555781.9	555781.9	555781.9
Northing	6243335.5	6242945.1	6242945.1	6242945.1	6243057.8	6243057.8	6243057.8
Type	Tasiuyak	MASU	MASU	MASU	MASU	MASU	Troctolite
$^{208}Pb/^{204}Pb$	36.003	35.726	35.738	35.794	35.899	35.720	35.326
error	0.143	0.023	0.025	0.085	0.157	0.041	0.019
$^{207}Pb/^{204}Pb$	15.259	15.221	15.220	15.233	15.263	15.215	15.133
error	0.143	0.023	0.024	0.087	0.160	0.039	0.020
$^{206}Pb/^{204}Pb$	16.005	15.672	15.689	15.746	15.942	15.696	15.460
error	0.146	0.023	0.024	0.087	0.161	0.036	0.020

Sample	79CP	79PO	82PO
Core	VB 95 27	VB 95 27	VB 95 25
Location	Ovoid	Ovoid	Ovoid
Easting	555781.9	555781.9	555782.8
Northing	6243057.8	6243057.8	6243107.8
Type	Troctolite	Troctolite	MASU
$^{208}Pb/^{204}Pb$	35.288	35.498	35.790
error	0.108	0.106	0.285
$^{207}Pb/^{204}Pb$	15.131	15.167	15.219
error	0.112	0.108	0.288
$^{206}Pb/^{204}Pb$	15.434	15.641	15.786
error	0.114	0.110	0.287

Table A.5b Pb isotope data for the sulphides analysed on behalf of INCO by the University of Toronto using thermal ionisation mass spectrometry (TIMS). Errors are within run and are to ±2 S.E. These data are unpublished.

Table A.6 Electron microprobe analyses of spinel

TS number	C97 617	C97 617	C97 617	C97 617	C97 617	C97 617	C97 617	C97 617	C97 617
SiO_2	n/a	n/a	n/a	n/a	n/a	n/a	n/a	n/a	n/a
TiO_2	0.03	0.004	0.025	0.053	0.039	0.031	0.04	0.028	0.012
Al_2O_3	60.149	60.95	60.324	60.838	60.43	59.114	61.686	61.42	62.054
V_2O_3	n/a	n/a	n/a	n/a	n/a	n/a	n/a	n/a	n/a
Cr_2O_3	0.428	0.353	0.196	0.536	0.271	0.664	0.229	0.205	0.193
MgO	10.928	11.168	11.328	10.607	11.262	10.934	11.654	11.561	12.268
CaO	n/a	n/a	n/a	n/a	n/a	n/a	n/a	n/a	n/a
MnO	0.221	0.212	0.221	0.23	0.159	0.182	0.195	0.196	0.204
FeO	26.722	24.985	25.318	27.203	26.687	27.733	25.314	25.806	24.407
NiO	0.227	0.232	0.267	0.269	0.259	0.241	0.334	0.336	0.349
ZnO	0.127	0.101	0.131	0.12	0.174	0.199	0.093	0.112	0.189
Total	98.832	98.005	97.81	99.856	99.281	99.098	99.545	99.664	99.676
Hole	VB96319	VB96319	VB96319	VB96319	VB96319	VB96319	VB96319	VB96319	VB96319
Depth	978	978	978	978	978	978	978	978	978
Easting	558241	558241	558241	558241	558241	558241	558241	558241	558241
Northing	6242202	6242202	6242202	6242202	6242202	6242202	6242202	6242202	6242202

TS number	C97 617	C97 617	C97 617	C97 617	C97 617	C97 617	C97 617	C97 617	C97 617
SiO_2	n/a	n/a	n/a	n/a	n/a	n/a	n/a	n/a	n/a
TiO_2	0.158	0.042	0.042	0.031	0.092	0.057	0.022	0.01	0.027
Al_2O_3	61.921	61.347	64.948	61.098	61.383	60.617	61.404	61.598	61.789
V_2O_3	n/a	n/a	n/a	n/a	n/a	n/a	n/a	n/a	n/a
Cr_2O_3	0.239	0.158	0.172	0.244	0.144	0.276	0.136	0.107	0.074
MgO	12.638	11.714	12.818	11.998	11.468	11.099	11.512	11.748	11.78
CaO	n/a	n/a	n/a	n/a	n/a	n/a	n/a	n/a	n/a
MnO	0.163	0.219	0.196	0.233	0.222	0.217	0.202	0.189	0.171
FeO	23.761	25.078	23.681	25.326	26.303	26.39	25.475	24.955	24.772
NiO	0.356	0.332	0.372	0.379	0.398	0.379	0.338	0.348	0.347
ZnO	0.149	0.139	0.148	0.143	0.201	0.117	0.119	0.119	0.146
Total	99.385	99.029	102.377	99.452	100.211	99.152	99.208	99.074	99.106
Hole	VB96319	VB96319	VB96319	VB96319	VB96319	VB96319	VB96319	VB96319	VB96319
Depth	978	978	978	978	978	978	978	978	978
Easting	558241	558241	558241	558241	558241	558241	558241	558241	558241
Northing	6242202	6242202	6242202	6242202	6242202	6242202	6242202	6242202	6242202

TS number	C97 617	C97 617	C97 617	C97 617	C97 617	C97 617	C97 617	C97 617	C97 617
SiO_2	n/a	n/a	n/a	n/a	n/a	n/a	n/a	n/a	n/a
TiO_2	0.041	0.005	0.009	0	0.006	0.033	0.052	0.01	0
Al_2O_3	59.619	61.464	62.194	61.274	61.785	61.626	57.263	59.124	62.116
V_2O_3	n/a	n/a	n/a	n/a	n/a	n/a	n/a	n/a	n/a
Cr_2O_3	0.089	0.121	0.093	0.079	0.186	0.149	0.147	0.192	0.164
MgO	11.239	10.501	10.672	10.381	10.697	10.695	10.334	10.056	10.828
CaO	n/a	n/a	n/a	n/a	n/a	n/a	n/a	n/a	n/a
MnO	0.174	0.209	0.174	0.193	0.193	0.195	0.176	0.2	0.188
FeO	24.659	26.39	26.112	26.882	26.557	26.452	25.31	24.562	25.539
NiO	0.31	0.268	0.245	0.258	0.252	0.261	0.253	0.225	0.24
ZnO	0.11	0.096	0.057	0.091	0.046	0.135	0.113	0.14	0.075
Total	96.241	99.054	99.556	99.158	99.722	99.546	93.648	94.509	99.15
Hole	VB96319	VB96319	VB96319	VB96319	VB96319	VB96319	VB96319	VB96319	VB96319
Depth	978	978	978	978	978	978	978	978	978
Easting	558241	558241	558241	558241	558241	558241	558241	558241	558241
Northing	6242202	6242202	6242202	6242202	6242202	6242202	6242202	6242202	6242202

TS number	C97 617	C97 617	C97 617	C97 617	C96 2569	C96 2569	C96 2569	C96 2569	C96 2569
SiO_2	n/a	n/a	n/a	n/a	VB96247	VB96247	VB96247	VB96247	VB96247
TiO_2	0	0.022	0.025	0.026	947	947	947	947	947
Al_2O_3	61.753	61.993	61.781	61.952	557783	557783	557783	557783	557783
V_2O_3	n/a	n/a	n/a	n/a	6242163	6242163	6242163	6242163	6242163
Cr_2O_3	0.21	0.202	0.179	0.155	n/a	n/a	n/a	n/a	n/a
MgO	10.871	10.893	10.78	10.832	0.438	9.968	0.242	0.591	0.526
CaO	n/a	n/a	n/a	n/a	33.073	30.675	35.629	29.883	34.251
MnO	0.2	0.189	0.192	0.207	n/a	n/a	n/a	n/a	n/a
FeO	26.225	26.035	26.426	25.927	22.837	15.435	20.857	22.542	22.757
NiO	0.259	0.242	0.248	0.239	5.542	5.39	5.811	5.817	6.263
ZnO	0.052	0.103	0.066	0.132	n/a	n/a	n/a	n/a	n/a
Total	99.57	99.679	99.697	99.47	0.285	0.368	0.271	0.274	0.281
Hole	VB96319	VB96319	VB96319	VB96319	33.985	34.43	34.096	37.358	34.59
Depth	978	978	978	978	0.08	0.064	0.084	0.045	0.079
Easting	558241	558241	558241	558241	3.322	2.499	3.135	1.996	1.862
Northing	6242202	6242202	6242202	6242202	99.562	98.829	100.125	98.506	100.609

TS number	C96 2569	C96 2569	C96 2569	C96 2569	C97 0915	C97 0915	C97 0915	C97 0915	C97 0915
SiO_2	n/a	n/a	n/a	n/a	n/a	n/a	n/a	n/a	n/a
TiO_2	50.8	0.554	0.635	4.034	0.084	0.052	0.047	0.069	0.046
Al_2O_3	0.019	29.594	29.478	18.583	57.441	57.017	57.299	55.301	55.848
V_2O_3	n/a	n/a	n/a	n/a	n/a	n/a	n/a	n/a	n/a
Cr_2O_3	0.08	25.473	24.637	20.565	0.15	0.241	0.171	0.184	0.185
MgO	2.305	4.545	4.696	3.542	10.235	9.305	9.529	9.216	9.467
CaO	n/a	n/a	n/a	n/a	n/a	n/a	n/a	n/a	n/a
MnO	0.528	0.34	0.323	0.335	0.186	0.228	0.229	0.22	0.207
FeO	44.36	37.845	37.647	49.393	27.81	29.878	28.762	32.065	30.512
NiO	0.026	0.07	0.07	0.106	0.271	0.297	0.295	0.298	0.288
ZnO	0.021	1.759	1.984	0.875	0.993	0.871	0.889	0.929	1.003
Total	98.139	100.18	99.47	97.433	97.17	97.889	97.221	98.282	97.556
Hole	VB96247	VB96247	VB96247	VB96247	VB95139	VB95139	VB95139	VB95139	VB95139
Depth	947	947	947	947	76	76	76	76	76
Easting	557783	557783	557783	557783	556169	556169	556169	556169	556169
Northing	6242163	6242163	6242163	6242163	6242802	6242802	6242802	6242802	6242802

TS number	C97 0915	C97 0915	C97 0915	C97 0915	C97 0915	C97 0915	C97 0915	C97 0915	C97 0915
SiO_2	n/a	n/a	n/a	n/a	n/a	n/a	n/a	n/a	n/a
TiO_2	0.04	0.052	0.097	0.105	0.325	0.109	0.095	0.041	0.149
Al_2O_3	56.334	57.379	55.035	57.92	55.323	56.098	57.246	55.621	56.604
V_2O_3	n/a	n/a	n/a	n/a	n/a	n/a	n/a	n/a	n/a
Cr_2O_3	0.353	0.116	0.128	0.23	0.252	n/a	n/a	n/a	n/a
MgO	9.434	10.227	9.941	10.209	10.215	10.338	11.421	11.025	10.98
CaO	n/a	n/a	n/a	n/a	n/a	n/a	n/a	n/a	n/a
MnO	0.217	0.214	0.215	0.235	0.208	0.222	0.216	0.198	0.228
FeO	30.041	30.08	31.251	29.215	32.195	30.558	28.626	31.882	28.951
NiO	0.276	0.292	0.269	0.301	0.295	n/a	n/a	n/a	n/a
ZnO	1.095	1.419	0.941	0.7	0.564	n/a	n/a	n/a	n/a
Total	97.79	99.779	97.877	98.915	99.377	97.35	97.617	98.816	96.921
Hole	VB95139	VB95139	VB95139	VB95139	VB95139	VB95139	VB95139	VB95139	VB95139
Depth	76	76	76	76	76	76	76	76	76
Easting	556169	556169	556169	556169	556169	556169	556169	556169	556169
Northing	6242802	6242802	6242802	6242802	6242802	6242802	6242802	6242802	6242802

TS number	C97 0915	C97 0915	C97 0915	C97 0915	C97 0915	C97 0915	C97 0915	C97 0915	C96 2557
SiO_2	n/a	n/a	n/a	n/a	n/a	n/a	n/a	n/a	n/a
TiO_2	0.098	0.037	0.021	0.496	0.026	0.033	0.04	50.433	0.008
Al_2O_3	57.474	57.232	58.083	55.793	56.499	58.239	55.762	0.036	61.56
V_2O_3	n/a	n/a	n/a	n/a	n/a	n/a	n/a	n/a	n/a
Cr_2O_3	n/a	n/a	n/a	n/a	n/a	n/a	n/a	0.086	0.902
MgO	11.139	11.065	11.419	10.84	9.96	10.284	9.392	1.527	12.804
CaO	n/a	n/a	n/a	n/a	n/a	n/a	n/a	n/a	n/a
MnO	0.235	0.24	0.227	0.245	0.22	0.248	0.262	0.743	0.188
FeO	28.688	28.633	28.18	29.161	29.457	28.29	30.952	45.415	22.788
NiO	n/a	n/a	n/a	n/a	n/a	n/a	n/a	0.011	0.302
ZnO	n/a	n/a	n/a	n/a	n/a	n/a	n/a	0	0.208
Total	97.663	97.233	97.959	96.637	96.221	97.14	96.482	98.251	98.76
Hole	VB95139	VB95139	VB95139	VB95139	VB95139	VB95139	VB95139	VB95139	VB96266
Depth	76	76	76	76	76	76	76	76	637
Easting	556169	556169	556169	556169	556169	556169	556169	556169	556966
Northing	6242802	6242802	6242802	6242802	6242802	6242802	6242802	6242802	6242466

TS number	C96 2557	C96 2557	C96 2557	C96 2557	C96 2557	C96 2557	C96 2557	C96 2557	C96 2557
SiO_2	n/a	n/a	n/a	n/a	n/a	n/a	n/a	n/a	n/a
TiO_2	0	0.004	0.011	0.015	0.01	0.064	0.015	0.02	0.028
Al_2O_3	60.256	61.575	61.591	61.606	61.147	59.198	63.243	62.445	56.231
V_2O_3	n/a	n/a	n/a	n/a	n/a	n/a	n/a	n/a	n/a
Cr_2O_3	2.32	1.214	0.919	0.9	1.289	1.472	1.979	1.985	4.026
MgO	12.566	13.167	12.884	12.952	12.949	12.468	9.708	10.513	11.417
CaO	n/a	n/a	n/a	n/a	n/a	n/a	n/a	n/a	n/a
MnO	0.219	0.178	0.183	0.178	0.172	0.124	0.119	0.109	0.139
FeO	23.022	22.641	22.903	22.958	22.829	24.276	19.341	20.553	26.313
NiO	0.24	0.303	0.342	0.304	0.266	0.248	0.24	0.24	0.206
ZnO	0.238	0.275	0.232	0.297	0.219	1.201	0.914	1.081	0.631
Total	98.861	99.357	99.065	99.21	98.881	99.051	95.559	96.946	98.991
Hole	VB96266	VB96266	VB96266	VB96266	VB96266	VB96266	VB96266	VB96266	VB96266
Depth	637	637	637	637	637	637	637	637	637
Easting	556966	556966	556966	556966	556966	556966	556966	556966	556966
Northing	6242466	6242466	6242466	6242466	6242466	6242466	6242466	6242466	6242466

TS number	C96 2557	C96 2557	C96 2557	C96 2557	C96 2557	C96 2557	C96 2569	C96 2569	C96 2569
SiO_2	n/a	n/a	n/a	n/a	n/a	n/a	n/a	n/a	n/a
TiO_2	0.025	0.014	0.033	0.005	0.041	0.056	18.066	42.197	41.134
Al_2O_3	57.076	59.91	58.338	60.012	60.299	60.205	17.168	6.912	12.667
V_2O_3	n/a	n/a	n/a	n/a	n/a	n/a	n/a	n/a	n/a
Cr_2O_3	3.365	0.527	0.319	0.343	0.44	0.537	5.965	1.892	1.596
MgO	11.693	12.864	12.164	12.839	12.504	12.702	6.185	3.617	4.226
CaO	n/a	n/a	n/a	n/a	n/a	n/a	n/a	n/a	n/a
MnO	0.158	0.136	0.137	0.119	0.139	0.12	1.04	1.093	0.858
FeO	25.832	24.538	24.534	24.396	24.923	24.648	49.237	40.215	39.189
NiO	0.232	0.283	0.275	0.295	0.284	0.295	0.04	0.042	0.028
ZnO	0.654	0.628	0.593	0.562	0.596	0.614	0.726	0.265	0.439
Total	99.035	98.9	96.393	98.571	99.226	99.177	98.427	96.233	100.137
Hole	VB96266	VB96266	VB96266	VB96266	VB96266	VB96266	VB96247	VB96247	VB96247
Depth	637	637	637	637	637	637	947	947	947
Easting	556966	556966	556966	556966	556966	556966	557783	557783	557783
Northing	6242466	6242466	6242466	6242466	6242466	6242466	6242163	6242163	6242163

TS number	C96 2569	C96 2569	C96 2569	C96 2569	C96 2569	C96 2569	C96 2569	C96 2569	C96 2569
SiO_2	n/a	n/a	n/a	n/a	n/a	n/a	n/a	n/a	n/a
TiO_2	13.243	0.018	0.015	0.008	52.004	0.494	52.298	50.888	51.002
Al_2O_3	36.341	59.047	58.95	59.401	0.064	31.402	0.02	0.06	0.031
V_2O_3	n/a	n/a	n/a	n/a	n/a	n/a	n/a	n/a	n/a
Cr_2O_3	6.437	0.402	0.374	0.455	0.047	22.737	0.364	0.222	0.214
MgO	9.03	11.999	11.892	12.016	1.772	4.469	3.044	3.066	2.933
CaO	n/a	n/a	n/a	n/a	n/a	n/a	n/a	n/a	n/a
MnO	0.676	0.178	0.138	0.181	1.002	0.31	0.536	0.459	0.471
FeO	30.092	26.375	26.636	26.142	43.931	36.228	42.25	43.809	43.335
NiO	0.066	0.228	0.201	0.201	0.049	0.054	0.042	0.011	0
ZnO	1.854	1.077	1.031	1.086	0	3.012	0.038	0	0
Total	97.739	99.324	99.237	99.49	98.869	98.706	98.592	98.515	97.986
Hole	VB96247	VB96247	VB96247	VB96247	VB96247	VB96247	VB96247	VB96247	VB96247
Depth	947	947	947	947	947	947	947	947	947
Easting	557783	557783	557783	557783	557783	557783	557783	557783	557783
Northing	6242163	6242163	6242163	6242163	6242163	6242163	6242163	6242163	6242163

TS number	C96 2557	C96 2557	C96 2557	C96 2569	C96 2569	C96 2569	C96 2569	C96 2569	C96 2569
SiO_2	n/a	n/a	n/a	n/a	n/a	n/a	n/a	n/a	n/a
TiO_2	49.892	50.347	49.373	7.112	11.371	9.246	8.709	5.27	8.362
Al_2O_3	0.054	0.058	0.064	5.64	5.737	4.849	5.091	6.595	5.683
V_2O_3	n/a	n/a	n/a	n/a	n/a	n/a	n/a	n/a	n/a
Cr_2O_3	0.1	0.11	0.042	17.4	17.08	15.433	16.082	18.51	17.213
MgO	0.044	2.978	1.29	1.204	1.503	1.713	1.309	1.266	1.508
CaO	n/a	n/a	n/a	n/a	n/a	n/a	n/a	n/a	n/a
MnO	0.642	0.472	0.538	0.371	0.411	0.391	0.44	0.374	0.381
FeO	46.927	43.035	45.284	61.749	58.552	60.289	62.549	62.615	62.123
NiO	0	0.015	0.008	0.142	0.127	0.143	0.167	0.106	0.16
ZnO	0	0.022	0	0.334	0.438	0.21	0.187	0.241	0.245
Total	97.659	97.037	96.599	93.952	95.219	92.274	94.534	94.977	95.675
Hole	VB96266	VB96266	VB96266	VB96247	VB96247	VB96247	VB96247	VB96247	VB96247
Depth	637	637	637	947	947	947	947	947	947
Easting	556966	556966	556966	557783	557783	557783	557783	557783	557783
Northing	6242466	6242466	6242466	6242163	6242163	6242163	6242163	6242163	6242163

TS number	C96 2569	C96 2569	C96 2569	C96 2569	C97 2658	C97 2658	C97 2658	C97 2658	C97 2658
SiO_2	n/a	n/a	n/a	n/a	0	0.248	0.422	0	0
TiO_2	5.324	7.587	0.924	7.173	0.067	0.054	0.055	0.045	0.052
Al_2O_3	6.933	7.429	1.109	5.328	55.638	55.465	55.089	55.536	55.934
V_2O_3	n/a	n/a	n/a	n/a	n/a	n/a	n/a	n/a	n/a
Cr_2O_3	18.787	17.17	4.18	16.792	0.139	0.154	0.162	0.345	0.223
MgO	1.188	3.854	0.173	0.863	5.651	5.493	5.588	5.579	5.694
CaO	n/a	n/a	n/a	n/a	0.041	0.066	0.115	0.068	0.061
MnO	0.396	0.401	0.082	0.389	0.313	0.33	0.33	0.31	0.298
FeO	62.077	57.761	83.837	62.887	37.59	36.541	36.517	37.313	37.016
NiO	0.146	0.127	0.097	0.145	0.297	0.305	0.286	0.307	0.285
ZnO	0.266	0.229	0.033	0.333	2.015	2.025	2.018	1.782	1.995
Total	95.117	94.558	90.435	93.91	101.751	100.681	100.582	101.285	101.558
Hole	VB96247	VB96247	VB96247	VB96247	OVOID	OVOID	OVOID	OVOID	OVOID
Depth	947	947	947	947	N/A	N/A	N/A	N/A	N/A
Easting	557783	557783	557783	557783	N/A	N/A	N/A	N/A	N/A
Northing	6242163	6242163	6242163	6242163	N/A	N/A	N/A	N/A	N/A

TS number	C97 2658	C97 2658	C97 2658	C97 2658	C97 2658	C97 2658	C97 2658	C97 2658	C97 2658
SiO_2	0.278	2.891	0.038	0.063	1.528	0	0.023	0.674	1.293
TiO_2	0.106	0.05	0.059	0.064	48.626	0.042	0.054	0.079	8.881
Al_2O_3	54.45	54.14	55.635	55.467	1.054	54.829	55.507	55.249	0.99
V_2O_3	n/a	n/a	n/a	n/a	n/a	n/a	n/a	n/a	n/a
Cr_2O_3	0.77	0.399	0.376	0.347	0.194	0.209	0.257	0.307	0.958
MgO	5.26	5.294	5.452	5.281	0.581	5.438	5.59	5.624	0.334
CaO	0.054	0.203	0.03	0.054	0.01	0.032	0.036	0.039	0.096
MnO	0.312	0.295	0.328	0.338	1.391	0.314	0.323	0.299	0.522
FeO	37.419	35.339	37.764	37.904	45.992	37.696	37.852	37.807	81.995
NiO	0.283	0.267	0.273	0.275	0.014	0.285	0.295	0.295	0.081
ZnO	2.048	1.982	2.304	2.3	3.024	1.936	1.969	2.01	0
Total	100.98	100.86	102.259	102.093	102.414	100.781	101.906	102.383	95.15
Hole	OVOID	OVOID	OVOID	OVOID	OVOID	OVOID	OVOID	OVOID	OVOID
Depth	N/A	N/A	N/A	N/A	N/A	N/A	N/A	N/A	N/A
Easting	N/A	N/A	N/A	N/A	N/A	N/A	N/A	N/A	N/A
Northing	N/A	N/A	N/A	N/A	N/A	N/A	N/A	N/A	N/A

TS number	C97 2658	C97 2658	C97 2658	C97 2658	C97 2658	C97 2658	C97 2658	C97 2658	C97 2658
SiO_2	0	0.215	0	0	0.509	0.284	0	0.201	0.147
TiO_2	0.05	0.041	0.028	0.066	1.421	2.086	0.043	0.952	2.381
Al_2O_3	55.994	55.933	56.489	56.624	0.854	1.505	54.741	0.716	1.222
V_2O_3	n/a	n/a	n/a	n/a	n/a	n/a	n/a	n/a	n/a
Cr_2O_3	0.241	0.315	0.329	0.22	0.902	1.845	1.039	0.372	0.357
MgO	5.579	5.472	5.735	5.676	0.061	0.104	5.14	0	0.061
CaO	0.042	0.067	0.056	0.06	0.046	0.01	0.12	0.124	0.094
MnO	0.333	0.319	0.305	0.321	0.093	0.1	0.325	0.043	0.133
FeO	36.915	37.053	36.237	36.718	91.04	89.955	37.949	92.795	91.51
NiO	0.265	0.268	0.289	0.262	0.072	0.084	0.25	0.087	0.086
ZnO	2.408	2.578	2.338	2.525	0	0	2.247	0.03	0.006
Total	101.827	102.261	101.806	102.472	94.998	95.973	101.854	95.32	95.997
Hole	OVOID	OVOID	OVOID	OVOID	OVOID	OVOID	OVOID	OVOID	OVOID
Depth	N/A	N/A	N/A	N/A	N/A	N/A	N/A	N/A	N/A
Easting	N/A	N/A	N/A	N/A	N/A	N/A	N/A	N/A	N/A
Northing	N/A	N/A	N/A	N/A	N/A	N/A	N/A	N/A	N/A

TS number	C97 2658	C97 2658	C97 2658	C97 2658	C97 2658	C97 2658	C97 2658	C97 2658	C97 2658
SiO_2	0.077	0	0	0.097	0	0	0.106	0	0
TiO_2	0.056	0.06	0.055	51.599	0.136	0.084	51.746	0.093	0.105
Al_2O_3	55.683	55.539	55.913	0.025	55.038	56.735	0.028	56.95	55.926
V_2O_3	n/a	n/a	n/a	n/a	n/a	n/a	n/a	n/a	n/a
Cr_2O_3	0.263	0.287	0.221	0.016	0.231	0.228	0.016	0.234	0.196
MgO	6.11	6.174	6.249	0.893	6.213	6.269	0.414	6.102	5.905
CaO	0	0	0.017	0.011	0.009	0.034	0.011	0.019	0.018
MnO	0.281	0.296	0.305	0.808	0.277	0.304	0.781	0.272	0.296
FeO	37.702	37.758	37.709	48.095	38.266	37.145	48.76	36.951	37.616
NiO	0.29	0.296	0.289	0.006	0.296	0.273	0.018	0.283	0.292
ZnO	1.384	1.381	1.437	0	1.408	1.488	0	1.442	1.368
Total	101.846	101.791	102.195	101.55	101.874	102.56	101.88	102.346	101.722
Hole	OVOID	OVOID	OVOID	OVOID	OVOID	OVOID	OVOID	OVOID	OVOID
Depth	N/A	N/A	N/A	N/A	N/A	N/A	N/A	N/A	N/A
Easting	N/A	N/A	N/A	N/A	N/A	N/A	N/A	N/A	N/A
Northing	N/A	N/A	N/A	N/A	N/A	N/A	N/A	N/A	N/A

TS number	C97 2658	C97 2658	C97 2658	C97 2658	C97 2658	C97 2658	C97 2658	C97 2658	C97 2658
SiO_2	1.478	0	0.118	36.987	37.797	37.464	0.12	0.527	0.109
TiO_2	0.051	0.109	1.417	1.677	2.226	2.023	0.051	0.05	0.033
Al_2O_3	51.505	55.881	1.424	17.694	16.663	17.324	57.006	57.692	56.706
V_2O_3	n/a	n/a	n/a	n/a	n/a	n/a	n/a	n/a	n/a
Cr_2O_3	0.356	0.214	0.719	0.069	0.053	0.14	0.647	0.914	0.647
MgO	6.661	5.931	0.053	14.721	16.083	15.783	6.363	6.158	6.322
CaO	0.015	0.005	0	0.044	0.021	0.057	0.072	0.084	0.025
MnO	0.282	0.305	0.06	0.11	0.055	0.056	0.313	0.328	0.316
FeO	37.231	38.364	92.747	18.874	15.517	14.184	35.537	35.906	36.104
NiO	0.315	0.294	0.056	0.069	0.085	0.128	0.23	0.242	0.26
ZnO	1.267	1.338	0	0.035	0.018	0.016	2.938	2.854	2.652
Total	99.161	102.441	96.594	90.28	88.518	87.175	103.277	104.755	103.174
Hole	OVOID	OVOID	OVOID	OVOID	OVOID	OVOID	OVOID	OVOID	OVOID
Depth	N/A	N/A	N/A	N/A	N/A	N/A	N/A	N/A	N/A
Easting	N/A	N/A	N/A	N/A	N/A	N/A	N/A	N/A	N/A
Northing	N/A	N/A	N/A	N/A	N/A	N/A	N/A	N/A	N/A

TS number	C97 2658	C97 2658	PTS 4501	PTS 4501	PTS 4501	PTS 4501	PTS 4501	PTS 4501	PTS 4501
SiO_2	0.703	0	3.091	0.424	0	1.009	0	0	1.924
TiO_2	0.027	0.083	0.106	0.115	5.451	0.147	0.084	0.125	0.175
Al_2O_3	55.784	56.193	57.466	59.687	56.98	63.82	60.597	60.7	57.337
V_2O_3	n/a	n/a	n/a	n/a	n/a	n/a	n/a	n/a	n/a
Cr_2O_3	1.23	1.115	0.28	0.314	0.084	0.138	0.141	0.059	0.051
MgO	6.198	6.165	13.488	14.144	14.538	15.471	14.089	14.154	13.034
CaO	0.293	0.043	1.224	0.095	0.037	0.5	0.037	0.076	0.145
MnO	0.282	0.292	0.157	0.148	0.184	0.135	0.149	0.158	0.168
FeO	35.397	36.686	23.084	24.828	25.268	23.207	25.28	24.906	26.202
NiO	0.242	0.252	0.152	0.174	0.14	0.172	0.178	0.178	0.168
ZnO	2.636	2.691	0.136	0.167	0.126	0.13	0.117	0.12	0.135
Total	102.792	103.52	99.184	100.096	102.808	104.729	100.672	100.476	99.339
Hole	OVOID	OVOID	VB95006	VB95006	VB95006	VB95006	VB95006	VB95006	VB95006
Depth	N/A	N/A	86	86	86	86	86	86	86
Easting	N/A	N/A	555837	555837	555837	555837	555837	555837	555837
Northing	N/A	N/A	6243323	6243323	6243323	6243323	6243323	6243323	6243323

TS number	PTS 4501	PTS 4501	PTS 4501	PTS 4501	PTS 4501	C99 0197	C99 0197	C99 0197	C99 0197
SiO_2	9.202	0	0	0	1.03	0	0	0	0
TiO_2	0.079	0.102	0.102	0.156	0.097	0.1	0.059	0.066	0.069
Al_2O_3	55.611	59.024	60.213	59.906	59.145	58.658	58.594	58.03	58.165
V_2O_3	n/a	n/a	n/a	n/a	n/a	n/a	n/a	n/a	n/a
Cr_2O_3	0.049	0.128	0.151	0.136	0.132	1.151	1.231	1.143	1.114
MgO	11.375	12.978	13.551	13.444	13.795	8.571	8.354	8.741	8.758
CaO	2.048	0.007	0.033	0.037	0.074	0.018	0.01	0	0.023
MnO	0.146	0.16	0.159	0.171	0.164	0.276	0.262	0.257	0.284
FeO	21.993	27.542	26.301	26.169	25.787	31.178	30.657	30.746	30.899
NiO	0.162	0.183	0.179	0.191	0.19	0.121	0.14	0.139	0.133
ZnO	0.037	0.093	0.096	0.129	0.093	2.203	2.197	2.261	2.17
Total	100.702	100.217	100.785	100.339	100.507	102.276	101.504	101.383	101.615
Hole	VB95006	VB95006	VB95006	VB95006	VB95006	VB98461c	VB98461c	VB98461c	VB98461c
Depth	86	86	86	86	86	1560	1560	1560	1560
Easting	555837	555837	555837	555837	555837	554898	554898	554898	554898
Northing	6243323	6243323	6243323	6243323	6243323	6242852	6242852	6242852	6242852

TS number	C99 0197	C99 0197	C99 0197	C97 1106	C97 1106	C97 1106	C97 1106	C97 1106	C97 1106
SiO_2	0	0	0	0.047	0.433	0.16	0	0.226	0.726
TiO_2	0.074	0.083	0.106	0.042	0.245	0.028	0.046	0.387	0.017
Al_2O_3	58.551	57.522	57.969	58.144	65.557	57.364	58.471	57.374	56.201
V_2O_3	n/a	n/a	n/a	n/a	n/a	n/a	n/a	n/a	n/a
Cr_2O_3	1.282	1.181	1.245	2.645	2.817	2.779	2.532	2.767	3.281
MgO	8.381	8.714	8.617	13.73	8.599	13.672	13.738	13.572	13.455
CaO	0.021	0	0.008	0.124	0.045	0.071	0.073	0.062	0.241
MnO	0.284	0.253	0.267	0.152	0.104	0.153	0.17	0.192	0.159
FeO	30.964	30.381	30.851	25.063	17.553	25.743	25.859	25.7	25.991
NiO	0.145	0.13	0.126	0.246	0.261	0.262	0.246	0.246	0.263
ZnO	2.226	2.985	2.959	0.549	0.325	0.527	0.483	0.59	0.818
Total	101.928	101.249	102.148	100.742	95.939	100.759	101.618	101.116	101.152
Hole	VB98461c	VB98461c	VB98461c	VB96266	VB96266	VB96266	VB96266	VB96266	VB96266
Depth	1560	1560	1560	271	271	271	271	271	271
Easting	554898	554898	554898	556966	556966	556966	556966	556966	556966
Northing	6242852	6242852	6242852	6242466	6242466	6242466	6242466	6242466	6242466

TS number	C97 1106	C97 1106	C97 0862	C97 0862	C97 0862	C97 0862	C97 0862	C97 0862	C97 0862
SiO_2	2.01	0.249	0	0	0	0	0	0.097	0
TiO_2	0.069	0.07	0.037	0.063	0.058	0.047	0.027	52.619	0.172
Al_2O_3	55.488	58.695	57.986	59.891	59.789	59.896	59.622	0.005	57.214
V_2O_3	n/a	n/a	0.197	0.184	0.207	0.18	0.175	2.368	0.253
Cr_2O_3	1.282	1.742	0.187	0.202	0.201	0.202	0.227	0.085	2.262
MgO	13.82	14.312	8.947	8.948	9.089	9.4	9.449	0.592	8.367
CaO	0.493	0.093	0.052	0.004	0	0.016	0.017	0.002	0.028
MnO	0.139	0.165	0.158	0.145	0.154	0.155	0.136	0.663	0.115
FeO	23.642	24.22	28.684	29.721	29.653	29.395	29.146	46.05	28.543
NiO	0.303	0.269	0.179	0.18	0.2	0.183	0.189	0.015	0.143
ZnO	0.634	0.692	0.856	0.817	0.813	0.85	0.796	0	4.269
Total	97.88	100.507	97.283	100.155	100.164	100.324	99.784	102.496	101.366
Hole	VB96266	VB96266	VB97368	VB97368	VB97368	VB97368	VB97368	VB97368	VB97368
Depth	271	271	311	311	311	311	311	311	311
Easting	556966	556966	553583	553583	553583	553583	553583	553583	553583
Northing	6242466	6242466	6243212	6243212	6243212	6243212	6243212	6243212	6243212

TS number	C97 0862	C97 0862	C97 0862	C97 0862	C97 0862	C97 0862	C97 0862	C97 0862	C97 0862
SiO_2	0	0	0.817	0	0.11	0	0	0.165	0.037
TiO_2	0.042	0.022	0.014	0.22	0.045	0.036	0.061	52.157	0.047
Al_2O_3	59.424	58.877	58.631	59.554	59.146	59.658	59.289	0.059	59.35
V_2O_3	0.236	0.254	0.247	0.207	0.239	0.169	0.207	2.272	0.196
Cr_2O_3	0.411	0.433	0.533	0.496	0.465	0.283	0.408	0.053	0.528
MgO	9.449	9.392	9.212	9.624	9.681	9.665	9.728	0.352	9.613
CaO	0.017	0.062	0.182	0.022	0.019	0.024	0.001	0.138	0.011
MnO	0.148	0.144	0.148	0.14	0.138	0.155	0.142	0.985	0.138
FeO	29.211	28.913	28.935	28.758	28.97	28.928	28.872	46.178	29.015
NiO	0.168	0.168	0.152	0.163	0.163	0.164	0.168	0	0.163
ZnO	1.312	1.211	1.216	1.249	1.285	1.363	1.42	0.003	1.316
Total	100.418	99.476	100.087	100.433	100.261	100.445	100.296	102.362	100.414
Hole	VB97368	VB97368	VB97368	VB97368	VB97368	VB97368	VB97368	VB97368	VB97368
Depth	311	311	311	311	311	311	311	311	311
Easting	553583	553583	553583	553583	553583	553583	553583	553583	553583
Northing	6243212	6243212	6243212	6243212	6243212	6243212	6243212	6243212	6243212

TS number	C97 0862	C97 0862	C97 0862	C97 0862	C97 0862	C97 0862	C97 0862	C97 0862	C97 0862
SiO_2	0.096	4.048	0.021	0	0	0	10.319	21.151	0
TiO_2	52.409	0.056	0.049	0.041	0.015	0.039	0.088	0.023	0.05
Al_2O_3	0.043	53.224	58.21	58.66	58.85	59.093	48.962	27.656	58.182
V_2O_3	2.249	0.177	0.214	0.241	0.214	0.232	0.183	0.131	0.255
Cr_2O_3	0.011	0.444	0.488	0.644	0.624	0.607	0.448	0.399	0.653
MgO	0.241	8.3	1.491	8.92	8.939	9.179	6.575	15.391	8.809
CaO	0.047	0.767	0.03	0	0	0.036	1.083	0.869	0
MnO	0.574	0.125	0.134	0.135	0.129	0.125	0.126	0.295	0.133
FeO	47.352	26.466	29.148	29.883	30.327	29.576	23.233	34.461	30.001
NiO	0.01	0.147	0.166	0.169	0.163	0.175	0.143	0.1	0.164
ZnO	0	1.222	1.303	1.841	1.889	1.778	1.258	0.807	1.81
Total	103.032	94.976	91.254	100.534	101.15	100.84	92.418	101.283	100.057
Hole	VB97368	VB97368	VB97368	VB97368	VB97368	VB97368	VB97368	VB97368	VB97368
Depth	311	311	311	311	311	311	311	311	311
Easting	553583	553583	553583	553583	553583	553583	553583	553583	553583
Northing	6243212	6243212	6243212	6243212	6243212	6243212	6243212	6243212	6243212

TS number	C97 0862	C97 0862	C97 0862	C97 0862	C97 0862	C97 0862	C97 0862	C97 0862	C97 0862
SiO_2	0	0	1.322	0	0	6.244	0	0	35.091
TiO_2	0.04	0.026	0.099	0.037	0.038	0.726	0.041	0.023	0
Al_2O_3	58.488	55.526	56.943	58.52	58.501	42.339	59.309	58.957	0.023
V_2O_3	0.195	0.224	0.219	0.24	0.249	0.182	0.22	0.225	0.009
Cr_2O_3	0.541	0.553	0.479	0.509	0.424	0.415	0.407	0.621	0.009
MgO	8.9	7.936	8.684	9.006	9.037	9.069	9.55	8.949	23.565
CaO	0.041	0.041	0.716	0.084	0	0.036	0.153	0.034	0.046
MnO	0.138	0.135	0.117	0.132	0.111	0.102	0.133	0.122	0.409
FeO	29.796	29.68	27.911	29.291	29.897	25.417	28.569	29.893	40.9
NiO	0.159	0.164	0.169	0.175	0.176	0.138	0.15	0.155	0.049
ZnO	1.664	1.618	1.606	1.629	1.71	1.274	1.506	1.659	0
Total	99.962	95.903	98.265	99.623	100.143	85.942	100.038	100.638	100.101
Hole	VB97368	VB97368	VB97368	VB97368	VB97368	VB97368	VB97368	VB97368	VB97368
Depth	311	311	311	311	311	311	311	311	311
Easting	553583	553583	553583	553583	553583	553583	553583	553583	553583
Northing	6243212	6243212	6243212	6243212	6243212	6243212	6243212	6243212	6243212

TS number	C97 0862	C97 0862	C97 0862	C97 0862	C97 0862	C97 0862	C97 0862	C97 0862	C97 0862
SiO_2	0	0.3	7.448	0.027	0	0.026	0	0.09	0.181
TiO_2	0.019	0.039	0.038	0.051	0.037	0.048	0.063	0.08	52.215
Al_2O_3	58.756	59.284	39.776	58.533	58.387	57.685	59.249	58.863	0.029
V_2O_3	0.238	0.217	0.183	0.191	0.211	0.248	0.224	0.235	2.249
Cr_2O_3	0.524	0.518	0.489	0.486	0.585	0.617	0.626	0.639	0.073
MgO	9.005	8.865	10.569	8.833	8.736	8.816	9.08	8.952	0.632
CaO	0.146	0.184	0.032	0.098	0.078	0.09	0.009	0.023	0.069
MnO	0.132	0.125	0.118	0.117	0.145	0.131	0.129	0.142	0.6
FeO	28.999	29.382	34.606	29.089	29.63	29.033	29.735	29.15	46.583
NiO	0.167	0.168	0.129	0.175	0.173	0.173	0.171	0.171	0.014
ZnO	1.688	1.654	1.248	1.616	1.579	1.669	1.689	1.681	0.005
Total	99.674	100.736	94.636	99.216	99.561	98.536	100.975	100.026	102.65
Hole	VB97368	VB97368	VB97368	VB97368	VB97368	VB97368	VB97368	VB97368	VB97368
Depth	311	311	311	311	311	311	311	311	311
Easting	553583	553583	553583	553583	553583	553583	553583	553583	553583
Northing	6243212	6243212	6243212	6243212	6243212	6243212	6243212	6243212	6243212

TS number	C97 0862	C97 0862	C97 0862	C97 0862	C97 0862	C97 0862	C97 0862	C97 0862	C97 0862
SiO_2	0.266	7.633	3.891	11.962	46.829	47.383	0	35.609	0
TiO_2	0.063	0.021	0	0.048	0	0.03	0.037	0.007	0.05
Al_2O_3	57.818	50.172	55.771	47.892	31.66	29.302	59.186	0.16	58.857
V_2O_3	0.26	0.18	0.206	0.185	0.001	0	0.246	0.009	0.264
Cr_2O_3	0.505	0.411	0.51	0.531	0.021	0.028	0.485	0.034	0.663
MgO	9.085	11.381	8.208	6.298	0.163	0.688	9.092	23.156	9.215
CaO	0.181	0.031	0.963	2.781	15.637	14.187	0.104	0.033	0.019
MnO	0.156	0.19	0.119	0.123	0.012	0	0.15	0.421	0.133
FeO	28.751	31.93	27.827	23.946	1.196	1.15	28.888	40.258	29.407
NiO	0.166	0.148	0.165	0.139	0.011	0.002	0.173	0.074	0.17
ZnO	1.232	1.377	1.635	1.271	0.012	0.019	1.647	0.01	1.823
Total	98.483	103.474	99.295	95.176	95.542	92.789	100.008	99.771	100.601
Hole	VB97368	VB97368	VB97368	VB97368	VB97368	VB97368	VB97368	VB97368	VB97368
Depth	311	311	311	311	311	311	311	311	311
Easting	553583	553583	553583	553583	553583	553583	553583	553583	553583
Northing	6243212	6243212	6243212	6243212	6243212	6243212	6243212	6243212	6243212

TS number	C97 0862	C97 0862	C97 0862	C97 0862	C97 0862	C97 0862	C97 0862	C97 0862	C97 0862
SiO_2	7.276	0	0.116	0	6.412	0.132	2.742	0.107	0
TiO_2	0.041	0.144	52.507	0.03	0.025	0.039	0.094	52.471	0.057
Al_2O_3	52.082	58.216	0.008	58.77	47.97	58.285	53.988	0.009	58.704
V_2O_3	0.202	0.242	2.174	0.241	0.221	0.251	0.266	2.272	0.259
Cr_2O_3	0.577	0.678	0.038	0.656	0.764	0.657	0.586	0.025	0.623
MgO	7.39	9.115	0.49	9.117	10.936	9.218	10.105	0.749	9.171
CaO	2.76	0.021	0.019	0.023	0.012	0.006	0.01	0.005	0
MnO	0.112	0.119	0.565	0.136	0.167	0.128	0.157	0.596	0.127
FeO	24.772	29.418	46.995	29.347	31.229	29.481	30.65	46.538	29.545
NiO	0.146	0.167	0.016	0.17	0.149	0.179	0.162	0.005	0.159
ZnO	1.538	1.938	0.024	1.835	1.643	1.861	1.72	0.011	1.928
Total	96.896	100.058	102.952	100.325	99.528	100.237	100.48	102.788	100.573
Hole	VB97368	VB97368	VB97368	VB97368	VB97368	VB97368	VB97368	VB97368	VB97368
Depth	311	311	311	311	311	311	311	311	311
Easting	553583	553583	553583	553583	553583	553583	553583	553583	553583
Northing	6243212	6243212	6243212	6243212	6243212	6243212	6243212	6243212	6243212

TS number	C97 0862	C97 0862	C97 0862	C97 0862	C97 0862	C97 0862	C97 0862	C97 0862	C97 0862
SiO_2	0	6.771	4.015	0	0.1	0	13.553	0	34.881
TiO_2	0.051	0.002	0.195	0.04	0.03	0.056	0.044	0.02	0.006
Al_2O_3	58.649	48.057	51.33	58.639	56.852	58.277	51.123	58.153	0.006
V_2O_3	0.287	0.17	0.216	0.248	0.269	0.252	0.223	0.262	0.016
Cr_2O_3	1.154	1.037	0.989	1.086	1.426	1.622	1.139	1.327	0
MgO	8.914	11.245	10.168	9.069	8.785	8.944	6.101	8.905	22.473
CaO	0.009	0.018	0.012	0.005	0.042	0.02	3.97	0.06	0.09
MnO	0.143	0.186	0.188	0.127	0.124	0.133	0.1	0.16	0.469
FeO	29.801	32.024	31.224	29.705	29.852	29.353	24.364	29.018	42.865
NiO	0.157	0.14	0.143	0.161	0.158	0.153	0.119	0.161	0.07
ZnO	2.251	1.768	1.934	2.263	2.529	2.602	1.84	1.701	0.008
Total	101.416	101.418	100.414	101.343	100.167	101.412	102.576	99.767	100.884
Hole	VB97368	VB97368	VB97368	VB97368	VB97368	VB97368	VB97368	VB97368	VB97368
Depth	311	311	311	311	311	311	311	311	311
Easting	553583	553583	553583	553583	553583	553583	553583	553583	553583
Northing	6243212	6243212	6243212	6243212	6243212	6243212	6243212	6243212	6243212

TS number	C97 0801	C97 0801	C97 0801	C97 0801	C97 0801	C97 0801	C97 0801	C97 0801	C97 0801
SiO_2	0	0	0	0.255	0.445	0.739	0.123	0	3.419
TiO_2	0.019	0.029	0.011	0.227	45.149	0.654	0.576	0.026	0.054
Al_2O_3	58.458	58.962	58.576	0.617	4.856	1.82	0.742	58.092	51.366
V_2O_3	0.089	0.07	0.109	0.638	1.973	0.623	0.709	0.079	0.038
Cr_2O_3	0.193	0.2	0.198	0.4	0.48	0.436	0.262	0.205	0.264
MgO	10.551	10.619	10.28	0.131	1.219	0.462	0.05	10.34	10.741
CaO	0	0	0.023	0.019	0.006	0	0.002	0	0.01
MnO	0.266	0.239	0.24	0.019	1.391	0.03	0.033	0.246	0.213
FeO	28.668	28.581	29.43	90.828	43.686	88.898	90.656	28.976	26.725
NiO	0.245	0.234	0.238	0.109	0.052	0.109	0.075	0.221	0.224
ZnO	2.444	2.488	2.439	0.004	2.964	0.006	0.005	2.417	2.067
Total	100.933	101.422	101.544	93.247	102.221	93.777	93.233	100.602	95.121
Hole	VB96356	VB96356	VB96356	VB96356	VB96356	VB96356	VB96356	VB96356	VB96356
Depth	1189	1189	1189	1189	1189	1189	1189	1189	1189
Easting	560803	560803	560803	560803	560803	560803	560803	560803	560803
Northing	6242137	6242137	6242137	6242137	6242137	6242137	6242137	6242137	6242137

TS number	C97 0801	C97 0801	C97 0801	C97 0862	C97 0862	C97 0862	C97 0862	C97 0862	C97 0862
SiO_2	0.089	52.144	6.049	34.929	34.997	35.173	34.96	35.318	35.146
TiO_2	50.994	0.017	41.419	0.002	0	0.031	0.009	0	0
Al_2O_3	0.026	26.63	3.759	0	0	0.017	0	0	0.019
V_2O_3	2.059	0.027	1.624	0.006	0.031	0.053	0	0	0
Cr_2O_3	0.036	0.049	0.081	0.025	0.017	0.014	0.031	0	0
MgO	1.328	0.103	4.493	24.031	23.98	23.69	23.898	24.212	24.242
CaO	0.006	10.912	0.316	0.018	0.039	0.019	0.043	0.04	0.048
MnO	0.638	0	1.595	0.427	0.413	0.442	0.426	0.427	0.447
FeO	47.571	0.522	38.914	41.403	41.28	42.202	41.458	41.019	41.256
NiO	0.021	0	0.035	0.067	0.072	0.066	0.066	0.073	0.066
ZnO	0.005	0.038	0.003	0.025	0.054	0.036	0.016	0.01	0.02
Total	102.773	90.442	98.288	100.933	100.883	101.743	100.907	101.099	101.244
Hole	VB96356	VB96356	VB96356	VB97368	VB97368	VB97368	VB97368	VB97368	VB97368
Depth	1189	1189	1189	311	311	311	311	311	311
Easting	560803	560803	560803	553583	553583	553583	553583	553583	553583
Northing	6242137	6242137	6242137	6243212	6243212	6243212	6243212	6243212	6243212

TS number	C97 0862	C97 0862	C97 0862	C97 0862	C97 0862	C97 0862	C97 0862	C97 0862	C97 0862
SiO_2	35.159	35.485	35.289	35.255	35.144	34.717	35.046	35.297	35.365
TiO_2	0.02	0.016	0	0	0	0	0	0.008	0.02
Al_2O_3	0	0	0.006	0.001	0	0.004	0	0	0
V_2O_3	0.018	0.014	0.023	0.01	0	0.005	0.011	0.024	0
Cr_2O_3	0.005	0.027	0.005	0	0.033	0	0.002	0.007	0.027
MgO	24.126	24.123	24.101	24.18	24.051	23.714	23.931	24.303	24.605
CaO	0.012	0.013	0.065	0.02	0.011	0	0.027	0	0.011
MnO	0.426	0.412	0.406	0.421	0.431	0.432	0.414	0.431	0.422
FeO	41.45	41.222	40.776	41.167	41.476	41.515	41.286	41.196	41.674
NiO	0.077	0.076	0.082	0.071	0.078	0.075	0.081	0.077	0.071
ZnO	0.017	0.053	0.02	0.005	0.017	0.025	0	0.022	0.02
Total	101.31	101.441	100.773	101.13	101.241	100.487	100.798	101.365	102.215
Hole	VB97368	VB97368	VB97368	VB97368	VB97368	VB97368	VB97368	VB97368	VB97368
Depth	311	311	311	311	311	311	311	311	311
Easting	553583	553583	553583	553583	553583	553583	553583	553583	553583
Northing	6243212	6243212	6243212	6243212	6243212	6243212	6243212	6243212	6243212

TS number	C97 0862	C97 0862	C97 0862	C97 0862	C97 0862	C97 0862	C97 0862	C97 0862	C97 0862
SiO_2	34.896	34.677	0 4.037	0	34.883	35.273	0	35.356	0
TiO_2	0	0	0.037	0.018	0.004	0.018	0.05	0	0.032
Al_2O_3	0	0	28.579	59.168	0	0.003	58.751	0.001	59 418
V_2O_3	0.01	0.016	0.092	0.211	0.001	0	0.221	0	0.213
Cr_2O_3	0.035	0.003	0.355	0.398	0.037	0.03	0.482	0	0.481
MgO	24.309	24.039	11.061	9.255	24.011	23.745	9.133	24.347	9.233
CaO	0.002	0.001	0.018	0	0.003	0.02	0.001	0.007	0
MnO	0.461	0.432	0.177	0.136	0.437	0.435	0.135	0.432	0.144
FeO	41.325	41.982	31.886	30.188	41.518	41.568	29.753	41.641	29.897
NiO	0.074	0.076	0.158	0.179	0.076	0.077	0.164	0.084	0.168
ZnO	0.032	0.017	1.402	1.663	0.003	0	1.639	0	1.656
Total	101.144	101.243	77.802	101.216	100.973	101.169	100.329	101.868	101.242
Hole	VB97368	VB97368	VB97368	VB97368	VB97368	VB97368	VB97368	VB97368	VB97368
Depth	311	311	311	311	311	311	311	311	311
Easting	553583	553583	553583	553583	553583	553583	553583	553583	553583
Northing	6243212	6243212	6243212	6243212	6243212	6243212	6243212	6243212	6243212

TS number	C97 1118	C97 1118	C97 1118	C97 1118	C97 1118	C97 1118	C97 1118	C97 1118	C97 1118
SiO_2	0.835	0.142	0.021	0.432	0.445	2 0.000	5.085	1.015	0
TiO_2	6.037	0.454	0.029	0.086	0.033	0.015	0.032	0.04	0.028
Al_2O_3	1.622	0.693	59.744	58.277	58.679	57.984	53.946	58.238	58.571
V_2O_3	0.769	0.568	0.061	0.051	0.075	0.103	0.05	0.071	0.078
Cr_2O_3	0.606	0.598	0.21	0.238	0.3	0.237	0.28	0.268	0.244
MgO	0.475	0.036	11.37	10.651	10.704	10.479	10.306	10.734	10.579
CaO	0.035	0.001	0.012	0.213	0.068	0.007	0.223	0.471	0.03
MnO	0.132	0.031	0.239	0.249	0.238	0.243	0.206	0.253	0.263
FeO	85.254	91.879	27.504	27.433	28.206	29.508	27.646	27.57	28.796
NiO	0.183	0.165	0.4	0.398	0.378	0.395	0.896	0.366	0.366
ZnO	0.05	0.045	2.144	2.135	2.121	2.03	1.73	2.067	2.098
Total	95.998	94.612	101.734	100.163	101.247	101.001	100.4	101.093	101.053
Hole	VB96266	VB96266	VB96266	VB96266	VB96266	VB96266	VB96266	VB96266	VB96266
Depth	604	604	604	604	604	604	604	604	604
Easting	556966	556966	556966	556966	556966	556966	556966	556966	556966
Northing	6242466	6242466	6242466	6242466	6242466	6242466	6242466	6242466	6242466

TS number	C97 1118	C97 1118	C97 1118	C97 1118	C97 1118	C97 0482	C97 0482	C97 0482	C97 0482
SiO_2	0.376	4.698	0	0.125	0	0	0	0	0
TiO_2	0.021	0.031	0.03	0.528	0.016	0.037	0.054	0.04	0.034
Al_2O_3	57.696	53.932	58.8	0.758	59.161	58.58	58.321	58.474	58.778
V_2O_3	0.057	0.065	0.049	0.491	0.065	0.041	0.051	0.071	0.044
Cr_2O_3	0.248	0.308	0.247	0.186	0.212	0.134	0.146	0.144	0.109
MgO	10.406	10.156	10.821	0.062	10.672	9.41	9.512	9.489	9.791
CaO	0.074	1.587	0.008	0.009	0.003	0.034	0.025	0.02	0.018
MnO	0.276	0.228	0.269	0.066	0.26	0.216	0.201	0.2	0.204
FeO	28.674	26.303	28.687	92.444	29.042	29.801	30.734	30.349	29.235
NiO	0.36	0.329	0.344	0.158	0.369	0.232	0.239	0.246	0.229
ZnO	2.112	1.879	2.246	0.013	2.214	3.674	3.411	3.445	3.329
Total	100.3	99.516	101.501	94.84	102.014	102.159	102.694	102.478	101.771
Hole	VB96266	VB96266	VB96266	VB96266	VB96266	VB95162	VB95162	VB95162	VB95162
Depth	604	604	604	604	604	263	263	263	263
Easting	556966	556966	556966	556966	556966	555048	555048	555048	555048
Northing	6242466	6242466	6242466	6242466	6242466	6243529	6243529	6243529	6243529

TS number	C97 0482	C97 0482	C97 0482	C97 0482	C97 0482	C97 0482	C97 0482	C97 0482	C97 0482
SiO_2	0	0.004	0	0	0	0	0	0	0.003
TiO_2	0.147	0.065	0.084	0.066	0.065	0.091	0.074	0.106	0.252
Al_2O_3	57.885	58.478	58.632	58.797	58.982	58.554	58.233	58.242	58.31
V_2O_3	0.129	0.101	0.132	0.134	0.129	0.144	0.109	0.158	0.119
Cr_2O_3	0.134	0.136	0.159	0.105	0.18	0.121	0.108	0.184	0.164
MgO	10.256	10.251	10.217	10.382	10.279	10.234	10.368	10.461	10.481
CaO	0.024	0.021	0.025	0.031	0.018	0.021	0.019	0.014	0.007
MnO	0.201	0.215	0.221	0.201	0.235	0.209	0.227	0.213	0.209
FeO	30.151	29.908	30.144	29.751	29.844	30.377	29.708	29.875	29.873
NiO	0.225	0.24	0.222	0.222	0.226	0.233	0.235	0.236	0.212
ZnO	1.276	1.365	1.546	1.182	1.198	1.249	1.11	0.974	0.864
Total	100.428	100.784	101.382	100.871	101.156	101.233	100.191	100.463	100.494
Hole	VB95162	VB95162	VB95162	VB95162	VB95162	VB95162	VB95162	VB95162	VB95162
Depth	263	263	263	263	263	263	263	263	263
Easting	555048	555048	555048	555048	555048	555048	555048	555048	555048
Northing	6243529	6243529	6243529	6243529	6243529	6243529	6243529	6243529	6243529

TS number	C97 0482	C97 0482	C97 0482	C97 0482	C97 0482	C97 0482	C97 0482	C97 0482	C97 0482
SiO_2	0	0.12	0.59	0	0	0.259	0	0	0
TiO_2	0.075	0.074	0.08	0.08	0.056	0.047	0.067	0.081	0.094
Al_2O_3	57.582	59.305	59.149	59.815	60.623	58.707	58.859	58.596	58.811
V_2O_3	0.108	0.143	0.153	0.146	0.173	0.175	0.155	0.178	0.185
Cr_2O_3	0.13	0.164	0.157	0.125	0.194	0.171	0.166	0.172	0.184
MgO	9.755	12.101	11.983	12.046	12.192	10.795	10.443	10.414	10.284
CaO	0.022	0.013	0.034	0.019	0.029	0.022	0.001	0	0
MnO	0.229	0.185	0.196	0.214	0.202	0.194	0.193	0.217	0.214
FeO	30.667	27.043	26.845	26.919	26.419	29.547	30.213	30.218	30.411
NiO	0.249	0.196	0.206	0.2	0.196	0.23	0.239	0.235	0.235
ZnO	0.841	0.271	0.24	0.253	0.188	0.337	0.325	0.36	0.378
Total	99.658	99.615	99.633	99.817	100.272	100.484	100.661	100.471	100.796
Hole	VB95162	VB95162	VB95162	VB95162	VB95162	VB95162	VB95162	VB95162	VB95162
Depth	263	263	263	263	263	263	263	263	263
Easting	555048	555048	555048	555048	555048	555048	555048	555048	555048
Northing	6243529	6243529	6243529	6243529	6243529	6243529	6243529	6243529	6243529

TS number	C97 0482	C97 0482	C97 0482	C97 0482	C97 0482	C97 0482	C97 0482	C97 0482	C99 0263
SiO_2	0	0	0	0	0	0	0	0	0
TiO_2	0.129	0.069	0.08	0.049	0.14	0.049	0.074	0.077	0.054
Al_2O_3	58.628	58.403	57.9	58.49	58.824	59.055	58.89	59.477	60.184
V_2O_3	0.181	0.173	0.199	0.186	0.177	0.185	0.18	0.163	0.176
Cr_2O_3	0.185	0.172	0.173	0.168	0.142	0.164	0.108	0.128	0.458
MgO	10.172	10.146	10.128	10.545	10.83	10.847	10.789	11.057	12.275
CaO	0.005	0.004	0	0	0.006	0.034	0.008	0.024	0.024
MnO	0.213	0.22	0.222	0.227	0.253	0.216	0.212	0.231	0.168
FeO	30.33	30.629	30.483	30.123	29.975	29.616	29.589	29.315	26.251
NiO	0.237	0.246	0.244	0.254	0.232	0.221	0.239	0.239	0.266
ZnO	0.345	0.315	0.324	0.303	0.31	0.313	0.259	0.3	1.261
Total	100.425	100.377	99.753	100.345	100.889	100.7	100.348	101.011	101.117
Hole	VB95162	VB95162	VB95162	VB95162	VB95162	VB95162	VB95162	VB95162	VB99495
Depth	263	263	263	263	263	263	263	263	1146
Easting	555048	555048	555048	555048	555048	555048	555048	555048	N/A
Northing	6243529	6243529	6243529	6243529	6243529	6243529	6243529	6243529	N/A

TS number	C99 0263	C99 0263	C99 0263	C99 0263	C97 2655	C97 2655	C97 2655	C97 2655	C97 2655
SiO_2	0	0.314	0	0	0.615	0.086	0	0	0
TiO_2	0.044	0	0.011	0.03	0.072	0.111	0.037	0.062	0.038
Al_2O_3	59.187	59.49	59.875	59.068	55.337	55.382	57.606	57.176	56.288
V_2O_3	0.18	0.206	0.137	0.172	0.159	0.25	0.208	0.201	0.234
Cr_2O_3	0.436	0.372	0.36	0.727	0.714	0.305	0.267	0.625	0.253
MgO	11.936	12.362	12.311	12.24	6.437	6.404	6.437	6.495	6.084
CaO	0.014	0.036	0.056	0.002	0.076	0.104	0.067	0.115	0.037
MnO	0.183	0.148	0.164	0.164	0.21	0.224	0.239	0.219	0.235
FeO	26.995	25.906	25.935	26.298	32.48	34.813	35.125	34.746	36.055
NiO	0.307	0.325	0.322	0.289	0.264	0.267	0.298	0.262	0.266
ZnO	1.259	1.263	1.238	1.451	1.964	1.947	1.984	2.204	1.871
Total	100.541	100.422	100.409	100.441	98.328	99.893	102.268	102.105	101.361
Hole	VB99495	VB99495	VB99495	VB99495	OVOID	OVOID	OVOID	OVOID	OVOID
Depth	1146	1146	1146	1146	N/A	N/A	N/A	N/A	N/A
Easting	N/A	N/A	N/A	N/A	N/A	N/A	N/A	N/A	N/A
Northing	N/A	N/A	N/A	N/A	N/A	N/A	N/A	N/A	N/A

TS number	C97 2655	C97 2655	C97 2655	C97 2655	C97 2655	C97 2655	C97 2655	C97 2655	C97 2655
SiO_2	16.65	0.458	0	2.753	0.031	0	0	0	0
TiO_2	0.159	0.051	0.135	0.067	0.022	0.039	0.04	0.025	0.063
Al_2O_3	49.805	56.568	56.651	49.78	58.622	57.016	56.446	56.911	57.735
V_2O_3	0.108	0.118	0.134	0.08	0.107	0.14	0.143	0.143	0.12
Cr_2O_3	0.159	0.196	0.165	0.222	0.146	0.219	0.252	0.23	0.178
MgO	5.334	7.077	6.813	6.096	7.138	6.536	6.537	6.669	6.656
CaO	3.154	0.033	0.015	0.38	0.049	0.036	0.025	0.02	0.022
MnO	0.165	0.219	0.211	0.163	0.222	0.217	0.228	0.221	0.223
FeO	27.672	33.922	35.368	25.542	33.492	35.35	35.56	35.122	35.427
NiO	0.17	0.364	0.281	0.236	0.305	0.294	0.285	0.277	0.277
ZnO	2.125	1.691	1.573	1.249	1.643	1.615	1.639	1.497	1.393
Total	105.501	100.697	101.346	86.568	101.777	101.462	101.155	101.115	102.094
Hole	OVOID	OVOID	OVOID	OVOID	OVOID	OVOID	OVOID	OVOID	OVOID
Depth	N/A	N/A	N/A	N/A	N/A	N/A	N/A	N/A	N/A
Easting	N/A	N/A	N/A	N/A	N/A	N/A	N/A	N/A	N/A
Northing	N/A	N/A	N/A	N/A	N/A	N/A	N/A	N/A	N/A

TS number	C97 2655	C97 2655	C97 2655	C97 2655	C97 2655	C97 2655	C99 0363	C99 0363	C99 0363
SiO_2	0	3.261	0	0	0	0.495	1.105	0	0
TiO_2	0.056	0.143	0.1	0.039	0.073	0.025	0.021	0.047	0.033
Al_2O_3	56.45	55.641	56.22	57.114	56.971	56.624	58.572	59.061	58.85
V_2O_3	0.139	0.13	0.129	0.122	0.126	0.095	0.057	0.044	0.042
Cr_2O_3	0.249	0.191	0.17	0.195	0.164	0.162	0.129	0.103	0.124
MgO	6.28	7.533	6.366	6.401	6.559	6.295	9.091	8.966	8.923
CaO	0.025	0.052	0.021	0.046	0.027	0.04	0.03	0	0.008
MnO	0.214	0.228	0.211	0.227	0.227	0.215	0.257	0.247	0.238
FeO	36.157	33.935	37.131	34.518	35.195	34.935	29.955	30.814	30.616
NiO	0.288	0.263	0.26	0.258	0.284	0.258	0.121	0.132	0.131
ZnO	1.135	2.551	2.687	3.047	2.736	3.246	2.943	3.025	3.071
Total	100.993	103.928	103.295	101.967	102.362	102.39	102.281	102.439	102.036
Hole	OVOID	OVOID	OVOID	OVOID	OVOID	OVOID	VB98478	VB98478	VB98478
Depth	N/A	N/A	N/A	N/A	N/A	N/A	555	555	555
Easting	N/A	N/A	N/A	N/A	N/A	N/A	556847	556847	556847
Northing	N/A	N/A	N/A	N/A	N/A	N/A	6243167	6243167	6243167

TS number	C99 0363	C99 0363	C99 0363	C99 0363	C99 0363	C99 0363	C99 0363	C99 0363	C99 0363
SiO_2	0	0	0	0.045	0.851	0	0	0	0
TiO_2	0.086	0.038	0.021	0.038	0.011	0.026	0.037	0.024	0.053
Al_2O_3	60.118	58.674	59.735	58.985	56.408	60.204	59.875	60.408	60.273
V_2O_3	0.045	0.05	0.153	0.148	0.166	0.142	0.156	0.135	0.159
Cr_2O_3	0.12	0.117	0.366	0.193	0.179	0.129	0.127	0.116	0.12
MgO	9.077	8.69	8.647	8.932	9.566	9.805	9.568	9.754	9.74
CaO	0	0.01	0.03	0.01	0.012	0	0.024	0.005	0.017
MnO	0.246	0.248	0.229	0.236	0.223	0.26	0.29	0.256	0.261
FeO	30.307	30.971	33.261	32.897	32.068	29.907	29.797	29.759	29.865
NiO	0.127	0.097	0.083	0.086	0.09	0.082	0.08	0.074	0.084
ZnO	3.034	3.045	0.327	0.358	0.304	0.238	0.22	0.233	0.243
Total	103.16	101.94	102.852	101.928	99.878	100.793	100.174	100.764	100.815
Hole	VB98478	VB98478	VB98478	VB98478	VB98478	VB98478	VB98478	VB98478	VB98478
Depth	555	555	555	555	555	555	555	555	555
Easting	556847	556847	556847	556847	556847	556847	556847	556847	556847
Northing	6243167	6243167	6243167	6243167	6243167	6243167	6243167	6243167	6243167

TS number	C99 0363	C99 0363	C99 0363	C99 0363	C99 0363	C99 0363	C99 0318	C99 0318	C99 0318
SiO_2	0	0	0	0	0	1.208	0	0	0
TiO_2	0.076	0.034	0.045	0.042	0.022	0.043	0.011	0.026	0.028
Al_2O_3	60.37	59.703	60.116	60.385	60.404	58.744	63.375	62.698	62.999
V_2O_3	0.17	0.167	0.175	0.169	0.165	0.135	0.175	0.187	0.173
Cr_2O_3	0.161	0.152	0.114	0.118	0.138	0.134	0.129	0.145	0.19
MgO	9.721	9.453	9.691	9.844	9.954	10.475	14.905	14.864	14.71
CaO	0.028	0.005	0.009	0.002	0.015	0.001	0.006	0	0.111
MnO	0.247	0.262	0.281	0.291	0.257	0.249	0.159	0.178	0.174
FeO	29.677	30.165	29.649	29.619	29.402	28.633	21.56	21.616	21.346
NiO	0.079	0.096	0.087	0.079	0.063	0.083	0.475	0.488	0.463
ZnO	0.262	0.216	0.206	0.189	0.251	0.207	0.212	0.208	0.153
Total	100.791	100.253	100.373	100.738	100.671	99.912	101.007	100.41	100.347
Hole	VB98478	VB98478	VB98478	VB98478	VB98478	VB98478	VB99492	VB99492	VB99492
Depth	555	555	555	555	555	555	1005	1005	1005
Easting	556847	556847	556847	556847	556847	556847	N/A	N/A	N/A
Northing	6243167	6243167	6243167	6243167	6243167	6243167	N/A	N/A	N/A

TS number	C99 0318	C99 0318	C99 0318	C99 0318	C99 0318	C99 0318	C99 0318	C99 0318	C99 0318
SiO_2	0	0.083	0	0.254	0	0	0	0	0
TiO_2	0.001	0.017	0.023	0.024	0.013	0.037	0.018	0.014	0.111
Al_2O_3	63.317	62.303	62.613	62.349	62.83	63.096	62.69	63.063	62.79
V_2O_3	0.193	0.175	0.192	0.161	0.156	0.182	0.188	0.172	0.163
Cr_2O_3	0.188	0.17	0.17	0.154	0.176	0.153	0.145	0.157	0.15
MgO	14.072	14.394	14.625	14.882	14.602	14.882	14.773	14.921	14.701
CaO	0.08	0.101	0.072	0.009	0.011	0.061	0.068	0.113	0.072
MnO	0.183	0.166	0.195	0.187	0.189	0.184	0.183	0.194	0.18
FeO	21.015	21.349	21.511	21.451	21.775	21.511	21.538	20.978	21.2
NiO	0.441	0.458	0.485	0.478	0.479	0.491	0.439	0.446	0.47
ZnO	0.175	0.175	0.174	0.214	0.163	0.232	0.23	0.179	0.171
Total	99.665	99.391	100.06	100.163	100.394	100.829	100.272	100.237	100.008
Hole	VB99492	VB99492	VB99492	VB99492	VB99492	VB99492	VB99492	VB99492	VB99492
Depth	1005	1005	1005	1005	1005	1005	1005	1005	1005
Easting	N/A	N/A	N/A	N/A	N/A	N/A	N/A	N/A	N/A
Northing	N/A	N/A	N/A	N/A	N/A	N/A	N/A	N/A	N/A

TS number	C99 0318	C99 0318	C99 0318	C99 0318	C99 0318	C99 0318	C99 0318	C99 0318	C99 0318
SiO_2	0	0.162	0	0.114	0	0	0.285	0.092	0
TiO_2	0.016	0.032	0.007	53.294	0.131	0.041	51.835	53.322	0.041
Al_2O_3	62.801	62.722	62.565	0.094	61.644	63.047	3.288	0.066	64.195
V_2O_3	0.145	0.128	0.167	1.767	0.133	0.159	1.672	1.652	0.187
Cr_2O_3	0.151	0.161	0.146	0.019	0.15	0.142	0.111	0.07	0.199
MgO	14.697	14.791	14.704	3.478	15.467	15.712	3.338	3.54	16.179
CaO	0.093	0.073	0.017	0	0.003	0	0.004	0	0
MnO	0.185	0.166	0.187	0.711	0.113	0.133	0.73	0.692	0.152
FeO	21.174	20.892	21.588	43.333	18.285	19.303	42.602	43.145	18.561
NiO	0.47	0.455	0.481	0.031	0.451	0.478	0.045	0.045	0.486
ZnO	0.189	0.199	0.226	0.012	0.181	0.211	0.011	0	0.207
Total	99.921	99.781	100.088	102.853	96.558	99.226	103.921	102.624	100.207
Hole	VB99492	VB99492	VB99492	VB99492	VB99492	VB99492	VB99492	VB99492	VB99492
Depth	1005	1005	1005	1005	1005	1005	1005	1005	1005
Easting	N/A	N/A	N/A	N/A	N/A	N/A	N/A	N/A	N/A
Northing	N/A	N/A	N/A	N/A	N/A	N/A	N/A	N/A	N/A

TS number	C99 0318	C99 0318	C99 0318	C99 0318	C99 0318	C99 0318	C99 0318	C99 0318
SiO_2	0.186	0	0	0	0	0	0	0
TiO_2	0.011	0.039	0.031	0.029	0.033	0.041	0.034	0.054
Al_2O_3	63.114	60.446	60.859	61.137	61.633	61.219	62.261	60.905
V_2O_3	0.171	0.215	0.237	0.203	0.206	0.183	0.193	0.263
Cr_2O_3	0.26	0.513	0.273	0.306	0.243	0.198	0.233	0.486
MgO	15.237	14.355	14.561	14.576	14.885	14.977	15.082	14.19
CaO	0.021	0.004	0.001	0.019	0.018	0.019	0.034	0.014
MnO	0.141	0.165	0.171	0.162	0.15	0.156	0.144	0.152
FeO	19.61	23.924	23.5	23.263	23.043	23.143	22.408	23.599
NiO	0.46	0.327	0.329	0.336	0.339	0.341	0.34	0.307
ZnO	0.257	0.322	0.302	0.282	0.301	0.308	0.28	0.321
Total	99.468	100.31	100.264	100.313	100.851	100.585	101.009	100.291
Hole	VB99492	VB99492	VB99492	VB99492	VB99492	VB99492	VB99492	VB99492
Depth	1005	1005	1005	1005	1005	1005	1005	1005
Easting	N/A	N/A	N/A	N/A	N/A	N/A	N/A	N/A
Northing	N/A	N/A	N/A	N/A	N/A	N/A	N/A	N/A

Appendix B

B.1.1 Introduction

The lead isotope analyses were carried out at the Open University using the Nu Plasma magnetic sector inductively coupled multi collector mass spectrometer (MC-ICP-MS). The sample solution was introduced into the spray chamber via an Aridus nebuliser/desolvator. The Pb was ionised in an argon plasma and extracted from the plasma through standard sample and skimmer cones. Ions were accelerated behind the skimmer cone and focussed onto an intermediate circular aperture. Two Einzel lenses were used to match this beam onto the defining slit of the mass spectrometer. The ion beam was then transmitted through a 35cm radius electrostatic analyser followed by a 25cm radius magnet. Two quadrupole lenses were used to adjust the peak separations of the isotopes to that of the separation of the fixed detectors. The detectors consist of an array of 12 Faraday buckets with gold and graphite coatings.

The masses ^{208}Pb, ^{207}Pb, ^{206}Pb, ^{208}Pb, and ^{204}Pb were measured along with ^{204}Hg and ^{202}Hg to monitor the Hg interference on ^{204}Pb. In addition, a Tl spike was added with known $^{205}Tl/^{203}Tl$ ratio to allow a mass fractionation correction to be made. 100 8-second integrations were collected for each sample.

All data were normalised to the values of NBS 981 as reported by Galer and Abouchami (1998). To assess contamination, total procedure blanks were run with each batch of samples. Pb blanks were below 0.5 ng.

The materials analysed were sulphides, chosen based on their habit, i.e. disseminated, semi-massive, or massive, and the host lithology. Samples were also picked to represent different locations within the deposit. Sulphides are not present in any quantity in the Nain

and Enderbite gneisses, so these rocks are not represented. Massive sulphides were sampled from the Ovoid, the Eastern Deeps, the Discovery Hill Zone and Red Dog.

B.1.2 Sample Preparation

The sulphide-bearing whole rocks were crushed in steel jaw mill. Between each sample the mill was cleaned by crushing two aliquots of clean quartz. The jaws were then removed, washed in hot water and Decon 90. The jaws were then thoroughly rinsed in hot water and excess water blown off using compressed air. Before the jaws were reinstalled into the mill, they were dried using lab-wipes and isopropyl alcohol (IPA) known to be isotopically clean.

To remove fines, the crushates were washed, using deionised water and Decon 90. The samples were then dried in an 80°C forced air oven for approximately two hours. Samples were then sieved using stainless steel sieves, constructed using lead-free solder. As an extra precaution, all soldered joints were sealed using silicone sealant. The sieve sizes used were 2.0mm, 1.0mm, 500μm, 250μm, and 125μm. It was not considered necessary to sieve below the 125μm fraction because of the difficulties picking minerals at this size. Between each sample, the sieves were carefully brushed clean to remove all loose material. The sieves were then cleaned in an ultrasonic bath for two minutes in deionised water, removed and carefully blown dry using compressed air. Drying was completed by leaving the sieves in a warm room until no moisture could be detected. The sieves were dried at room temperature as it was felt that the temperatures in an oven might compromise the sealing on the sieves' soldered joints.

The sulphide minerals were picked from the 250μm and 125μm sieved fractions using a binocular microscope and tweezers. Different sulphide minerals were separated and placed into labelled screw-top glass vials. To ensure complete and rapid dissolution all samples

were crushed using a 100mm agate pestle and mortar. Between samples, the pestle and mortar were washed using reverse osmosis (RO) water, dried using laboratory wipes, and then washed again in RO water and dried. To ensure dryness, IPA and laboratory wipes were used as a final cleaning process.

So that contamination with environmental lead was minimised, all samples were washed in three changes of isotopically clean IPA and dried down in a clean-room fume hood using infrared lamps.

Prior to dissolution, sample material was transferred into 7 ml Teflon savillex screw-top beakers of known mass. All beakers were labelled with sample identity using indelible marker. Considerable difficulty was experienced transferring the samples, because of the effects of static electricity. This was overcome by transferring the samples as slurry in IPA and then evaporating off the fluid in fume hoods using heat lamps. After evaporation was complete, the beakers were re-weighed and the sample masses recorded.

The dissolution procedure used is based on Oversby (1970) and was carried out using Teflon-distilled (TD) acids. TD reagents are high purity and are produced by sub-boiling distillation in Teflon stills rather than boiling distillation used to produce quartz-distilled reagents. The use of sub-boiling distillation results in higher purity reagents as fewer contaminants are carried into the finished product. The Pb separation procedure used small volumes of resin and reagents to minimise the blank component. The first stage of dissolution used ~1 ml of 2 x TD 15M HNO_3 followed by 2-3 ml of 2 x TD HF. The beakers were then sealed and left to stand for 24-48 hours before being dried down under evaporating hoods. The hoods were fed by a continuous supply of filtered compressed air. Care was taken not to over-bake the samples as this might cause insoluble fluorides to form. Approximately 2 ml of 2x TD 15M HNO_3 was then added to the residue and the

beakers were sealed and placed on a hotplate for 12-24 hours before being evaporated to dryness. After this, ~2 ml of 2 x TD 6M HCl were added and the beakers placed on a hotplate for 12-24 hours and then evaporated to dryness. The HCl and HNO_3 stages were repeated using decreased reagent volumes until the samples were fully dissolved. When complete dissolution had taken place, the HCl was evaporated to dryness and the residue left to dissolve in cold ~1 ml 1M TD HBr for 12-24 hours.

Columns were prepared from 1 ml pipette tips by placing a Teflon frit at the narrowest end. The columns were then cleaned by rinsing in QD 6M HCl, followed by immersion in QD 6M HCl overnight on a hotplate. The columns were removed from the HCl, rinsed with RO H_2O and placed in the column racks. The columns were then rinsed with further RO H_2O and QD 6M HCl. In each case, the amount of RO H_2O and HCl used was 1 column volume (CV). Following this, 5 drops (approximately 100 µl) of Dowex 200-400 mesh anion exchange resin was added. The resin was washed using 1 CV of 2 x TD 6M HCl followed by 1 CV of 2 X TD H_2O. This was repeated before preconditioning the resin with 0.5 CV of TD 1M HBr.

Sample solutions were loaded into the column using a 1 ml pipette tip cleaned with 1M TD HBr. Care was taken to avoid taking up any residue that remained in the beaker, as this would have blocked the column. The sample was washed into the resin using 0.5 CV of 1M TD HBr followed by a further CV of the same acid. The Pb fraction was collected in a cleaned beaker by eluting with 2 CV of 2 x TD 6M HCl. To remove the Br from this fraction 50 µl of 2 x TD 15M HNO_3 was added. The sample was then evaporated to dryness and then dissolved in few drops of HBr ready for a second pass through the columns. During the period that that the samples were being dried down, the columns were cleaned using 2 x TD 6M HCl and 2 x TD H_2O. Before the second pass, the columns were preconditioned with 0.5 CV of TD HBr.

Aliquots of the Pb fraction prepared using column chemistry were then diluted using TD 15 % HCl with a 0.3 ppm Tl spike preparatory to analyses by MC-ICP-MS. The total sample volume following dilution was 2 ml. This volume was sufficient to allow for 100 8-second integrations. The amount of dilutant used was determined by the need to match the sample Pb concentration to that of the NBS981 standard and the Tl spike, i.e. 0.2 and 0.3 ppm respectively. The sulphide samples were assumed to contain 1000 ppm Pb and the amount that was added to the Tl/HCl solution was determined by the sample masses.

Because mass fractionation is an intrinsic problem with isotopic analysis, repeated analyses of an international standard (NBS 981) spiked with 0.3 ppm of Tl of known isotopic composition throughout the analytical programme were undertaken. Because the isotopic ratios of Pb in NBS 981 are well constrained (Galer and Abouchami, 1998), and a Tl spike was included, the repeated analysis of NBS981 provided the means to correct fractionation effects very accurately. Additionally, the repeated analyses of NBS 981 provided a means of assessing the reproducibility of the data.

B.1.3 Standards data

The results of analysing NBS 981 are presented in Table A1. Typically the $^{206}Pb/^{204}Pb$, $^{207}Pb/^{204}Pb$ and $^{208}Pb/^{204}Pb$ values are within 100 ppm of those obtained by Galer and Abouchami (1998), with a few values deviating by up to 300 ppm. Within run errors (2 σ) are 0.02 for $^{206}Pb/^{204}Pb$ and $^{207}Pb/^{204}Pb$ and 0.04 for $^{208}Pb/^{204}Pb$.

A graphical representation of these data is given in Figures A1-3, graphs of total beam intensity in volts versus $^{208}Pb/^{204}Pb$, $^{207}Pb/^{204}Pb$ and $^{206}Pb/^{204}Pb$ respectively. Included on each of these figures is the appropriate ratio for NBS 981 according to Galer and Abouchami (1998). Examination of these figures reveals that the measured values of NBS

981 are in close agreement with those published by Galer and Abouchami (1998) for a wide range of beam intensities. However, when the total beam intensity falls below ~1 volt, the agreement between measured and published values for NBS 981 is poor. As a consequence of this, data for low beam intensities was discarded.

.

DATE	$^{208}Pb/^{204}Pb$	error	dev	$^{207}Pb/^{204}Pb$	error	dev	$^{206}Pb/^{204}Pb$	error	dev	Intensity
G&A	36.722	0.004		15.496	0.002		16.941	0.002		
11/21/01	36.724	0.020	57.086	15.497	0.008	31.319	16.939	0.008	-88.406	7.02
11/21/01	36.723	0.020	39.855	15.497	0.008	48.312	16.939	0.008	-88.168	6.51
11/21/01	36.724	0.018	63.148	15.497	0.007	20.010	16.939	0.008	-83.158	6.20
11/21/01	36.722	0.023	10.626	15.497	0.009	55.694	16.939	0.010	-66.320	5.05
11/21/01	36.725	0.019	75.041	15.497	0.008	20.349	16.939	0.008	-95.390	5.33
11/21/01	36.726	0.036	118.219	15.496	0.012	-19.437	16.939	0.011	-98.782	3.91
11/22/01	36.724	0.020	54.674	15.497	0.007	31.318	16.939	0.007	-85.992	5.70
11/22/01	36.722	0.021	8.394	15.498	0.008	79.918	16.939	0.008	-88.312	5.77
11/22/01	36.722	0.025	-6.303	15.498	0.010	100.392	16.939	0.009	-94.089	5.54
11/22/01	36.722	0.030	-8.821	15.498	0.011	117.036	16.939	0.010	-108.214	4.96
11/22/01	36.722	0.019	9.906	15.498	0.007	87.818	16.939	0.007	-97.724	4.71
11/23/01	36.727	0.047	127.387	15.496	0.016	-3.183	16.938	0.014	-124.204	3.82
11/23/01	36.725	0.050	88.888	15.497	0.018	26.229	16.939	0.016	-115.117	3.35
11/23/01	36.725	0.053	80.425	15.497	0.019	32.419	16.939	0.018	-112.844	3.35
11/24/01	36.718	0.017	-97.789	15.499	0.006	174.267	16.939	0.005	-76.478	8.97
11/24/01	36.717	0.031	-134.396	15.500	0.010	216.257	16.939	0.008	-81.861	8.75
11/24/01	36.715	0.027	-192.145	15.501	0.010	278.402	16.939	0.008	-86.257	8.67
11/24/01	36.713	0.022	-229.429	15.501	0.009	324.394	16.939	0.008	-94.965	8.25
11/24/01	36.713	0.034	-253.774	15.502	0.012	350.395	16.939	0.010	-96.622	8.15
11/25/01	36.711	0.048	-305.089	15.502	0.017	385.057	16.939	0.012	-79.968	6.33
11/25/01	36.712	0.032	-270.301	15.502	0.010	352.034	16.939	0.009	-81.733	6.46
11/25/01	36.711	0.071	-295.088	15.502	0.028	386.688	16.939	0.028	-91.600	6.77
11/25/01	36.714	0.031	-202.533	15.501	0.009	286.836	16.939	0.010	-84.303	10.51
11/26/01	36.718	0.031	-117.634	15.499	0.010	190.875	16.939	0.010	-73.241	12.29
11/26/01	36.719	0.019	-69.473	15.499	0.009	148.312	16.939	0.009	-78.838	13.45
11/26/01	36.719	0.027	-86.641	15.499	0.009	169.519	16.939	0.008	-82.878	13.79
U of T	36.706			15.493			16.937			
U of T	36.712			15.499			16.944			

Table B.1. Data derived from the repeated analyses of NBS 981. The values for NBS 981 after Galer and Abouchami (1998) are shown in the first row. The dev values are deviation relative to the values derived by Galer and Abouchami (1998) expressed in ppm. Quoted errors are within run to ±2 S.E. U of T values are University of Toronto and relate to the data supplied by Dr Peter C. Lightfoot.

Crystal 1												
Run	1	2	3	4	5	6	7	8	9	10	Average	S.D
SiO2	39.55	40.01	39.94	40.14	40.33	40.53	40.46	40.80	41.16	41.34		
TiO2	5.64	5.68	5.72	5.69	5.89	5.73	5.72	5.84	5.80	5.83	5.75	0.08
Al2O3	13.60	13.85	13.97	14.08	14.18	14.29	14.24	14.49	14.46	14.55	14.17	0.30
FeO	9.33	9.50	9.42	0.39	9.56	9.42	9.52	9.46	9.49	9.10	8.52	2.86
MnO	0.09	0.07	0.07	0.08	0.09	0.07	0.08	0.08	0.08	0.09	0.08	0.01
MgO	12.89	13.04	13.07	13.13	13.32	13.16	13.24	13.43	13.49	13.57	13.23	0.22
CaO	10.12	10.10	10.08	10.10	9.68	9.99	10.10	10.05	9.98	10.03	10.02	0.13
Na2O	2.62	2.68	2.66	2.68	2.63	2.69	2.69	2.77	2.86	2.80	2.71	0.08
K2O	1.99	1.89	1.92	2.00	2.21	1.94	1.94	1.99	1.89	1.95	1.97	0.09
Total	95.83	96.82	96.85	88.29	97.89	97.82	97.99	98.91	99.21	99.26	96.89	
Crystal 2												
Run	11.00	12.00	13.00	14.00	15.00	16.00	17.00	18.00	19.00	20.00		
SiO2	39.85	40.14	40.10	40.03	39.87	40.14	40.32	40.53	40.46	40.68	40.21	0.28
TiO2	5.63	5.55	5.73	5.71	5.62	5.61	5.65	5.75	5.57	5.70	5.65	0.07
Al2O3	14.08	14.02	14.13	14.09	14.15	14.30	14.26	14.33	14.45	14.43	14.22	0.15
FeO	9.45	9.53	9.47	9.44	9.53	9.47	9.40	9.48	9.46	9.33	9.46	0.06
MnO	0.07	0.08	0.08	0.08	0.08	0.08	0.08	0.08	0.09	0.08	0.08	0.00
MgO	13.13	13.09	13.14	13.13	13.18	13.31	13.29	13.23	13.36	13.40	13.23	0.11
CaO	10.02	10.10	10.06	10.15	10.03	10.03	9.98	10.02	10.03	10.09	10.05	0.05
Na2O	2.65	2.68	2.70	2.68	2.68	2.69	2.67	2.73	2.72	2.73	2.69	0.03
K2O	1.99	1.98	2.03	2.01	2.00	2.04	1.98	2.00	1.99	1.94	2.00	0.03
Total	96.87	97.17	97.44	97.32	97.14	97.67	97.63	98.15	98.13	98.38	97.59	
Crystal 3												
Run	21.00	22.00	23.00	24.00	25.00	26.00	27.00	28.00	29.00	30.00		
SiO2	40.44	40.49	40.10	40.26	40.20	39.93	39.98	40.00	40.09	39.66	40.12	0.25
TiO2	5.93	5.97	5.88	5.96	5.88	5.98	6.07	5.85	6.00	5.99	5.95	0.07
Al2O3	14.24	14.20	14.10	14.22	14.03	14.14	14.22	14.05	14.07	13.88	14.12	0.11
FeO	9.63	9.68	9.61	9.64	9.66	9.66	9.59	9.68	9.64	9.68	9.65	0.03
MnO	0.09	0.08	0.10	0.09	0.08	0.07	0.07	0.08	0.09	0.09	0.08	0.01
MgO	13.20	13.19	13.18	13.06	13.15	13.20	13.19	13.08	13.02	12.92	13.12	0.10
CaO	10.07	10.14	10.11	10.02	10.04	9.86	9.91	9.95	10.02	10.03	10.02	0.09
Na2O	2.69	2.69	2.69	2.68	2.74	2.63	2.66	2.74	2.64	2.64	2.68	0.04
K2O	1.99	2.00	1.99	2.00	1.98	2.17	2.03	2.01	2.00	2.02	2.02	0.06
Total	98.28	98.44	97.76	97.93	97.76	97.64	97.72	97.44	97.57	96.91	97.75	
Crystal 4												
Run	31.00	32.00	33.00	34.00	35.00	36.00	37.00	38.00	39.00	40.00		
SiO2	40.76	40.85	41.03	41.39	41.34	41.60	41.85	41.65	42.02	42.21	41.47	0.49
TiO2	5.66	5.73	5.61	5.71	5.63	5.69	5.62	5.65	5.68	5.72	5.67	0.04
Al2O3	14.58	14.59	14.67	14.64	14.60	14.64	14.73	14.75	14.92	14.95	14.71	0.13
FeO	9.51	9.52	9.51	9.46	9.47	9.46	9.57	9.34	9.49	9.47	9.48	0.06
MnO	0.80	0.07	0.09	0.08	0.08	0.07	0.08	0.08	0.08	0.09	0.15	0.23
MgO	13.58	13.76	13.76	13.76	13.92	13.89	13.86	13.92	13.95	13.97	13.84	0.12
CaO	9.86	10.00	9.93	9.85	9.88	9.97	9.99	10.06	9.98	10.03	9.96	0.07
Na2O	2.79	2.83	2.83	2.84	2.87	2.90	2.88	2.86	2.84	2.94	2.86	0.04
K2O	1.97	1.93	2.00	1.98	1.97	1.97	1.99	1.94	1.99	1.97	1.97	0.02
Total	99.51	99.28	99.43	99.71	99.76	100.19	100.57	100.25	100.95	101.35	100.10	

Table B.2 Results of repeated analyses on different kaersutite crystal with the Open University Cameca SX100 electron microprobe. Standard deviations are to 1 σ. The different kaersutite crystals have differing compositions and this is reflected in the data. These analyses were carried out throughout the experimental programme when a new filament was fitted to the microprobe. The inter-run results on each crystal give and indication of the reproducibility on heterogeneous minerals.

Crystal	fo 1-a	fo 1-b	fo 1-c	fo 1-d	fo 1-e	fo 1-f	fo 1-g	fo 1-h	fo 1-i	fo 1-j	average	2s.d.
SiO_2	41.49	41.56	41.65	41.36	41.60	41.40	41.38	41.34	40.93	41.00	41.4	0.5
TiO_2	0.00	0.00	0.02	0.02	0.00	0.01	0.01	0.00	0.00	0.00	0.0	0.0
Al_2O_3	0.01	0.01	0.00	0.01	0.01	0.00	0.01	0.01	0.01	0.01	0.0	0.0
Cr_2O_3	0.02	0.01	0.01	0.00	0.01	0.00	0.00	0.00	0.00	0.00	0.0	0.0
Fe2O3	0.00	0.00	0.00	0.00	0.00	0.00	0.00	0.00	0.00	0.00	0.0	0.0
FeO	8.81	9.00	8.90	8.82	8.80	8.93	8.89	9.02	8.81	8.84	8.9	0.2
MnO	0.13	0.13	0.12	0.15	0.13	0.13	0.12	0.14	0.13	0.14	0.1	0.0
MgO	49.37	49.38	49.41	49.10	49.40	49.26	49.16	49.28	49.01	49.02	49.2	0.3
CaO	0.02	0.03	0.01	0.04	0.03	0.04	0.03	0.04	0.03	0.03	0.0	0.0
Na_2O	0.01	0.00	0.01	0.03	0.00	0.02	0.00	0.02	0.01	0.00	0.0	0.0
K_2O	0.00	0.01	0.00	0.01	0.00	0.00	0.01	0.00	0.01	0.00	0.0	0.0
P_2O_5	0.00	0.01	0.02	0.01	0.01	0.00	0.01	0.00	0.00	0.00	0.0	0.0
NiO	0.39	0.40	0.40	0.39	0.39	0.40	0.38	0.40	0.38	0.40	0.4	0.0
Total	100.24	100.55	100.54	99.93	100.38	100.19	100.02	100.24	99.32	99.43		
Si	1.01	1.01	1.01	1.01	1.01	1.01	1.01	1.01	1.01	1.01	1.009	0.003
Ti	0.00	0.00	0.00	0.00	0.00	0.00	0.00	0.00	0.00	0.00	0.000	0.000
Al	0.00	0.00	0.00	0.00	0.00	0.00	0.00	0.00	0.00	0.00	0.000	0.000
Cr	0.00	0.00	0.00	0.00	0.00	0.00	0.00	0.00	0.00	0.00	0.000	0.000
Fe^{+3}	0.00	0.00	0.00	0.00	0.00	0.00	0.00	0.00	0.00	0.00	0.000	0.000
Fe^{+2}	0.18	0.18	0.18	0.18	0.18	0.18	0.18	0.18	0.18	0.18	0.181	0.003
Mn	0.00	0.00	0.00	0.00	0.00	0.00	0.00	0.00	0.00	0.00	0.003	0.000
Mg	1.79	1.79	1.79	1.79	1.79	1.79	1.79	1.79	1.80	1.79	1.789	0.006
Ca	0.00	0.00	0.00	0.00	0.00	0.00	0.00	0.00	0.00	0.00	0.001	0.001
Na	0.00	0.00	0.00	0.00	0.00	0.00	0.00	0.00	0.00	0.00	0.000	0.001
K	0.00	0.00	0.00	0.00	0.00	0.00	0.00	0.00	0.00	0.00	0.000	0.000
P	0.00	0.00	0.00	0.00	0.00	0.00	0.00	0.00	0.00	0.00	0.000	0.000
Ni	0.01	0.01	0.01	0.01	0.01	0.01	0.01	0.01	0.01	0.01	0.008	0.000
Total	2.99	2.99	2.99	2.99	2.99	2.99	2.99	2.99	2.99	2.99	2.991	0.004
Forsterite	0.909	0.907	0.908	0.908	0.909	0.908	0.908	0.907	0.908	0.908	0.908	0.001

Crystal	fo-a 1	fo-a 2	fo-a 3	fo-a 4	fo-a 5	fo-a 6	fo-a 7	fo-a 8	fo-a 9	fo-a 10	average	2s.d.
SiO_2	41.61	41.42	41.48	41.62	41.62	41.69	41.61	41.50	41.59	41.66	41.6	0.2
TiO_2	0.01	0.00	0.00	0.00	0.00	0.00	0.01	0.01	0.00	0.00	0.0	0.0
Al_2O_3	0.01	0.01	0.01	0.01	0.00	0.01	0.00	0.00	0.01	0.00	0.0	0.0
Cr_2O_3	0.01	0.01	0.02	0.00	0.00	0.00	0.00	0.02	0.00	0.01	0.0	0.0
Fe2O3	0.00	0.00	0.00	0.00	0.00	0.00	0.00	0.00	0.00	0.00	0.0	0.0
FeO	8.81	8.94	8.91	8.77	8.74	8.88	8.89	8.87	8.88	8.85	8.9	0.1
MnO	0.14	0.13	0.14	0.13	0.14	0.15	0.14	0.14	0.14	0.12	0.1	0.0
MgO	49.21	49.23	49.04	49.00	48.90	49.00	49.22	49.09	49.17	49.04	49.1	0.2
CaO	0.03	0.03	0.03	0.02	0.02	0.04	0.02	0.03	0.01	0.02	0.0	0.0
Na_2O	0.00	0.02	0.00	0.01	0.04	0.02	0.00	0.01	0.01	0.01	0.0	0.0
K_2O	0.00	0.00	0.00	0.00	0.03	0.01	0.00	0.01	0.00	0.00	0.0	0.0
P_2O_5	0.01	0.01	0.00	0.00	0.00	0.01	0.01	0.00	0.00	0.00	0.0	0.0
NiO	0.40	0.39	0.39	0.39	0.38	0.38	0.39	0.40	0.40	0.39	0.4	0.0
Total	100.22	100.17	100.03	99.96	99.87	100.17	100.29	100.08	100.20	100.10		
Si	1.01	1.01	1.01	1.02	1.01	1.02	1.01	1.01	1.02	1.02	1.014	0.012
Ti	0.00	0.00	0.00	0.00	0.00	0.00	0.00	0.00	0.00	0.00	0.000	0.000
Al	0.00	0.00	0.00	0.00	0.00	0.00	0.00	0.00	0.00	0.00	0.000	0.000
Cr	0.00	0.00	0.00	0.00	0.00	0.00	0.00	0.00	0.00	0.00	0.000	0.000
Fe^{+3}	0.00	0.00	0.00	0.00	0.00	0.00	0.00	0.00	0.00	0.00	0.000	0.000
Fe^{+2}	0.18	0.18	0.18	0.18	0.18	0.18	0.18	0.18	0.18	0.18	0.180	0.003
Mn	0.00	0.00	0.00	0.00	0.00	0.00	0.00	0.00	0.00	0.00	0.003	0.000
Mg	1.78	1.78	1.77	1.78	1.77	1.78	1.79	1.78	1.80	1.79	1.784	0.019
Ca	0.00	0.00	0.00	0.00	0.00	0.00	0.00	0.00	0.00	0.00	0.001	0.000
Na	0.00	0.00	0.00	0.00	0.00	0.00	0.00	0.00	0.00	0.00	0.001	0.001
K	0.00	0.00	0.00	0.00	0.00	0.00	0.00	0.00	0.00	0.00	0.000	0.001
P	0.00	0.00	0.00	0.00	0.00	0.00	0.00	0.00	0.00	0.00	0.000	0.000
Ni	0.01	0.01	0.01	0.01	0.01	0.01	0.01	0.01	0.01	0.01	0.008	0.000
Total	2.99	2.98	2.97	2.99	2.97	2.99	3.00	2.99	3.02	3.01	2.990	0.030
Forsterite	0.909	0.908	0.907	0.909	0.909	0.908	0.908	0.908	0.908	0.908	0.908	0.001

Crystal	Fo-a 11	Fo-a 12	Fo-a 13	Fo-a 14	Fo-a 15	Fo-a 16	Fo-a 17	Fo-a 18	Fo-a 19	Fo-a 20	average	2s.d.
SiO_2	41.60	41.45	41.43	41.46	41.54	41.56	41.56	41.59	41.57	41.50	41.5	0.1
TiO_2	0.00	0.00	0.00	0.00	0.00	0.00	0.00	0.00	0.02	0.01	0.0	0.0
Al_2O_3	0.00	0.00	0.01	0.00	0.00	0.02	0.01	0.00	0.00	0.00	0.0	0.0
Cr_2O_3	0.00	0.01	0.01	0.01	0.01	0.00	0.00	0.00	0.03	0.02	0.0	0.0
Fe2O3	0.00	0.00	0.00	0.00	0.00	0.00	0.00	0.00	0.00	0.00	0.0	0.0
FeO	8.81	8.81	8.83	8.88	8.75	8.81	8.73	8.83	8.87	8.87	8.8	0.1
MnO	0.11	0.12	0.13	0.12	0.13	0.13	0.12	0.12	0.12	0.14	0.1	0.0
MgO	48.94	48.90	49.01	49.24	49.16	49.08	48.93	49.12	49.21	49.25	49.1	0.3
CaO	0.03	0.04	0.03	0.02	0.03	0.03	0.02	0.02	0.03	0.03	0.0	0.0
Na_2O	0.01	0.01	0.02	0.00	0.01	0.00	0.00	0.00	0.01	0.01	0.0	0.0
K_2O	0.00	0.01	0.00	0.00	0.00	0.01	0.01	0.00	0.01	0.00	0.0	0.0
P_2O_5	0.00	0.01	0.01	0.01	0.02	0.01	0.00	0.01	0.01	0.00	0.0	0.0
NiO	0.39	0.40	0.39	0.39	0.39	0.40	0.40	0.39	0.37	0.39	0.4	0.0
Total	99.89	99.76	99.85	100.14	100.02	100.05	99.77	100.08	100.25	100.22		
Si	1.01	1.01	1.00	1.01	1.01	1.01	1.01	1.01	1.02	1.02	1.012	0.010
Ti	0.00	0.00	0.00	0.00	0.00	0.00	0.00	0.00	0.00	0.00	0.000	0.000
Al	0.00	0.00	0.00	0.00	0.00	0.00	0.00	0.00	0.00	0.00	0.000	0.000
Cr	0.00	0.00	0.00	0.00	0.00	0.00	0.00	0.00	0.00	0.00	0.000	0.000
Fe^{+3}	0.00	0.00	0.00	0.00	0.00	0.00	0.00	0.00	0.00	0.00	0.000	0.000
Fe^{+2}	0.18	0.18	0.18	0.18	0.18	0.18	0.18	0.18	0.18	0.18	0.180	0.003
Mn	0.00	0.00	0.00	0.00	0.00	0.00	0.00	0.00	0.00	0.00	0.003	0.000
Mg	1.77	1.77	1.77	1.79	1.78	1.78	1.78	1.78	1.80	1.80	1.782	0.021
Ca	0.00	0.00	0.00	0.00	0.00	0.00	0.00	0.00	0.00	0.00	0.001	0.000
Na	0.00	0.00	0.00	0.00	0.00	0.00	0.00	0.00	0.00	0.00	0.000	0.001
K	0.00	0.00	0.00	0.00	0.00	0.00	0.00	0.00	0.00	0.00	0.000	0.000
P	0.00	0.00	0.00	0.00	0.00	0.00	0.00	0.00	0.00	0.00	0.000	0.000
Ni	0.01	0.01	0.01	0.01	0.01	0.01	0.01	0.01	0.01	0.01	0.008	0.000
Total	2.977	2.967	2.968	2.997	2.978	2.986	2.982	2.988	3.019	3.015	2.985	0.032
Forsterite	0.908	0.908	0.908	0.908	0.909	0.908	0.909	0.908	0.908	0.908	0.908	0.001

Crystal	fo-a 1	fo-a 2	fo-a 3	fo-a 4	fo-a 5	fo-a 6	fo-a 7	fo-a 8	fo-a 9	fo-a 10	average	2s.d.
SiO_2	41.93	41.69	41.84	41.96	41.81	41.71	41.56	41.74	41.72	41.71	41.8	0.2
TiO_2	0.01	0.01	0.00	0.00	0.00	0.00	0.00	0.00	0.00	0.00	0.0	0.0
Al_2O_3	0.00	0.00	0.00	0.01	0.01	0.01	0.02	0.01	0.00	0.03	0.0	0.0
Cr_2O_3	0.02	0.01	0.02	0.00	0.01	0.00	0.01	0.01	0.00	0.00	0.0	0.0
Fe2O3	0.00	0.00	0.00	0.00	0.00	0.00	0.00	0.00	0.00	0.00	0.0	0.0
FeO	8.94	8.87	9.04	8.94	8.92	8.94	9.00	8.89	8.83	8.89	8.9	0.1
MnO	0.13	0.13	0.13	0.13	0.14	0.13	0.13	0.13	0.13	0.13	0.1	0.0
MgO	49.09	49.13	49.32	49.23	49.18	49.05	49.01	48.97	49.16	49.03	49.1	0.2
CaO	0.02	0.01	0.03	0.02	0.04	0.01	0.03	0.03	0.02	0.03	0.0	0.0
Na_2O	0.01	0.00	0.00	0.01	0.00	0.01	0.00	0.01	0.00	0.00	0.0	0.0
K_2O	0.01	0.01	0.00	0.00	0.00	0.00	0.00	0.00	0.01	0.01	0.0	0.0
P_2O_5	0.01	0.00	0.01	0.00	0.00	0.00	0.00	0.00	0.00	0.00	0.0	0.0
NiO	0.38	0.39	0.39	0.39	0.39	0.39	0.38	0.38	0.40	0.40	0.4	0.0
Total	100.55	100.26	100.77	100.68	100.50	100.24	100.14	100.15	100.27	100.21		
Si	1.02	1.01	1.01	1.02	1.02	1.02	1.01	1.02	1.03	1.02	1.018	0.010
Ti	0.00	0.00	0.00	0.00	0.00	0.00	0.00	0.00	0.00	0.00	0.000	0.000
Al	0.00	0.00	0.00	0.00	0.00	0.00	0.00	0.00	0.00	0.00	0.000	0.000
Cr	0.00	0.00	0.00	0.00	0.00	0.00	0.00	0.00	0.00	0.00	0.000	0.000
Fe^{+3}	0.00	0.00	0.00	0.00	0.00	0.00	0.00	0.00	0.00	0.00	0.000	0.000
Fe^{+2}	0.18	0.18	0.18	0.18	0.18	0.18	0.18	0.18	0.18	0.18	0.182	0.002
Mn	0.00	0.00	0.00	0.00	0.00	0.00	0.00	0.00	0.00	0.00	0.003	0.000
Mg	1.78	1.78	1.78	1.79	1.78	1.78	1.78	1.78	1.80	1.79	1.785	0.016
Ca	0.00	0.00	0.00	0.00	0.00	0.00	0.00	0.00	0.00	0.00	0.001	0.000
Na	0.00	0.00	0.00	0.00	0.00	0.00	0.00	0.00	0.00	0.00	0.000	0.000
K	0.00	0.00	0.00	0.00	0.00	0.00	0.00	0.00	0.00	0.00	0.000	0.000
P	0.00	0.00	0.00	0.00	0.00	0.00	0.00	0.00	0.00	0.00	0.000	0.000
Ni	0.01	0.01	0.01	0.01	0.01	0.01	0.01	0.01	0.01	0.01	0.008	0.000
Total	2.994	2.981	2.993	3.010	2.989	2.991	2.991	2.987	3.019	3.013	2.997	0.025
Forsterite	0.907	0.908	0.907	0.908	0.908	0.907	0.907	0.908	0.908	0.908	0.908	0.001

Crystal	fo-a 11	fo-a 12	fo-a 13	fo-a 14	fo-a 15	fo-a 16	fo-a 17	fo-a 18	fo-a 19	fo-a 20	average	2s.d.
SiO_2	41.73	41.81	41.61	41.72	41.89	41.82	41.94	41.78	41.72	41.93	41.8	0.2
TiO_2	0.00	0.00	0.01	0.00	0.00	0.00	0.01	0.00	0.00	0.00	0.0	0.0
Al_2O_3	0.00	0.00	0.01	0.00	0.00	0.01	0.00	0.01	0.01	0.00	0.0	0.0
Cr_2O_3	0.02	0.02	0.00	0.00	0.00	0.02	0.01	0.00	0.01	0.00	0.0	0.0
Fe2O3	0.00	0.00	0.00	0.00	0.00	0.00	0.00	0.00	0.00	0.00	0.0	0.0
FeO	8.99	8.85	8.85	9.01	8.92	8.91	8.96	8.85	8.92	8.89	8.9	0.1
MnO	0.13	0.13	0.13	0.13	0.14	0.12	0.14	0.12	0.12	0.13	0.1	0.0
MgO	49.17	49.11	49.12	48.91	49.15	49.05	49.03	48.95	49.11	49.25	49.1	0.2
CaO	0.03	0.03	0.03	0.04	0.02	0.03	0.03	0.02	0.03	0.02	0.0	0.0
Na_2O	0.00	0.00	0.02	0.01	0.00	0.02	0.01	0.02	0.01	0.01	0.0	0.0
K_2O	0.00	0.00	0.01	0.01	0.00	0.00	0.01	0.00	0.01	0.00	0.0	0.0
P_2O_5	0.00	0.01	0.00	0.00	0.01	0.01	0.00	0.00	0.00	0.01	0.0	0.0
NiO	0.39	0.39	0.37	0.38	0.38	0.40	0.39	0.38	0.37	0.39	0.4	0.0
Total	100.46	100.36	100.16	100.22	100.51	100.38	100.50	100.14	100.30	100.64		
Si	1.02	1.01	1.01	1.02	1.02	1.02	1.02	1.02	1.03	1.03	1.019	0.011
Ti	0.00	0.00	0.00	0.00	0.00	0.00	0.00	0.00	0.00	0.00	0.000	0.000
Al	0.00	0.00	0.00	0.00	0.00	0.00	0.00	0.00	0.00	0.00	0.000	0.000
Cr	0.00	0.00	0.00	0.00	0.00	0.00	0.00	0.00	0.00	0.00	0.000	0.000
Fe^{+3}	0.00	0.00	0.00	0.00	0.00	0.00	0.00	0.00	0.00	0.00	0.000	0.000
Fe^{+2}	0.18	0.18	0.18	0.18	0.18	0.18	0.18	0.18	0.18	0.18	0.182	0.003
Mn	0.00	0.00	0.00	0.00	0.00	0.00	0.00	0.00	0.00	0.00	0.003	0.000
Mg	1.78	1.78	1.78	1.78	1.78	1.78	1.78	1.78	1.80	1.80	1.784	0.018
Ca	0.00	0.00	0.00	0.00	0.00	0.00	0.00	0.00	0.00	0.00	0.001	0.000
Na	0.00	0.00	0.00	0.00	0.00	0.00	0.00	0.00	0.00	0.00	0.001	0.001
K	0.00	0.00	0.00	0.00	0.00	0.00	0.00	0.00	0.00	0.00	0.000	0.000
P	0.00	0.00	0.00	0.00	0.00	0.00	0.00	0.00	0.00	0.00	0.000	0.000
Ni	0.01	0.01	0.01	0.01	0.01	0.01	0.01	0.01	0.01	0.01	0.008	0.000
Total	2.993	2.983	2.977	2.994	2.989	2.994	3.000	2.987	3.019	3.026	2.996	0.031
Forsterite	0.907	0.908	0.908	0.906	0.908	0.908	0.907	0.908	0.908	0.908	0.908	0.001

Table B3 Results of repeated analyses on different olivine crystals on the Open University Cameca SX100 electron microprobe. The inter-run variations indicate the reproducibility achievable is around 0.002 forsterite units.

Analysis	S	Fe	Co	Ni	Cu	Zn	Total
1	32.9	29.9	1.7	35.3	0.0	0.0	99.8
2	33.1	29.9	1.8	35.2	0.0	0.0	100.0
3	33.0	29.9	1.7	35.0	0.0	0.0	99.5
4	33.0	29.9	1.8	35.3	0.0	0.0	100.0
5	33.0	30.1	1.8	35.0	0.0	0.0	99.9
6	32.9	30.2	1.8	35.1	0.0	0.0	100.0
7	33.1	30.1	1.7	34.9	0.0	0.0	99.8
8	33.1	30.2	1.7	35.0	0.0	0.0	100.0
9	32.9	30.3	1.7	35.0	0.0	0.0	99.9
10	32.8	30.2	1.7	35.1	0.0	0.0	99.8
11	33.0	30.3	1.7	34.7	0.0	0.0	99.8
12	32.8	30.2	1.7	35.1	0.0	0.0	99.8
13	33.1	30.3	1.8	35.0	0.0	0.0	100.2
14	33.0	30.2	1.8	34.9	0.0	0.0	99.9
15	32.9	30.1	1.8	35.0	0.0	0.0	99.8
16	33.1	30.2	1.8	34.9	0.0	0.0	99.9
17	33.1	30.3	1.7	34.9	0.0	0.0	100.0
18	33.2	30.1	1.7	35.0	0.0	0.0	100.0
19	33.0	29.9	1.8	35.3	0.0	0.0	100.0
20	32.9	30.0	1.8	35.2	0.0	0.0	99.9
Error	0.2	0.3	0.1	0.3	0.0	0.0	0.3

Table B.4 Results of repeated analyses of pentlandite standard on the Open University Cameca SX100 electron microprobe. Errors are presented as two standard deviations. The variability in these data is thought to represent heterogeneity in the standard.

	Approx. Det.Lt.	Expected Values	BHVO-1 23/01/04	BHVO-1 23/01/04	BHVO-1 16/02/04	BHVO-1 16/02/04	BHVO-1 26/02/04	BHVO-1 26/02/04	BHVO-1 27/02/04	BHVO-1 27/02/04	Error 2 St Dev
Rb	2	11	10	10	9	9	10	10	10	10	1
Sr	2	403	408	404	404	404	400	405	401	406	5
Y	2.0	27.6	27.1	26.8	27.5	27.1	28.3	27.9	27.7	27.9	1.0
Zr	2	179	180	176	177	178	179	180	179	179	3
Nb	1.5	19.0	18.3	17.3	18.3	17.8	17.8	19.0	17.4	18.2	1.1
Ba	12	139	148	147	155	146	146	149	154	147	7
Pb	5	3	4	3	3	3	3	2	4	5	2
Th	4	1	0	3	3	0	1	2	4	2	3
U	3	0.4	0	3	1	2	3	0	2	0	2
Sc	5	32	34	34	35	32	34	36	34	32	2
V	5	317	319	325	318	322	316	321	316	307	11
Cr	4	289	286	289	291	286	294	289	288	289	5
Co	2	45	44	44	45	45	42	44	46	50	5
Ni	3	121	121	123	122	119	119	119	119	119	3
Cu	3	136	136	137	136	136	136	138	135	136	2
Zn	3	105	107	105	102	105	109	105	104	105	4
Ga	3	21	21	21	21	19	22	21	21	21	1
Mo	2	1	0	0	0	0	0	0	0	0	0
As	5	0	4	2	2	1	0	0	3	0	3
S	50	102	78	80	81	83	80	77	81	82	4

	Approx. Det.Lt.	Expected Values	BHVO-1 28/02/04	BHVO-1 28/02/04	BHVO-1 01/03/04	BHVO-1 01/03/04	BHVO-1 15/03/04	BHVO-1 15/03/04	BHVO-1 29/03/04	BHVO-1 29/03/04	Error 2 St Dev
Rb	2	11	10	9	9.1	9.2	10	10	10	10	1
Sr	2	403	401	401	406	405	407	406	402	404	5
Y	2.0	27.6	27.5	27.9	27.7	28.3	28.4	28.8	28.5	26.8	1.3
Zr	2	179	178	176	180	179	182	180	180	180	4
Nb	1.5	19.0	18.0	17.8	16.9	18.3	17.7	17.3	17.9	18.1	0.9
Ba	12	139	156	151	148.8	140.5	148	149	139	141	12
Pb	5	3	4	2	0.8	4.6	4	3	4	5	3
Th	4	1	0	2	0	1.3	3	1	1	2	2
U	3	0.4	1	1	1.2	0.1	0	0	0	0	1
Sc	5	32	35	37	33.3	34.7	35	36	33	36	2
V	5	317	328	326	314.3	313.8	323	323	327	313	12
Cr	4	289	293	294	291.8	288.4	288	289	291	290	4
Co	2	45	45	42	43.5	45.1	47	42	48	47	5
Ni	3	121	120	118	123.9	124.4	121	120	118	123	5
Cu	3	136	136	134	137.3	135	138	135	136	136	3
Zn	3	105	105	104	105.6	104.2	107	105	105	104	2
Ga	3	21	21	21	20.2	20.7	22	19	21	21	1
Mo	2	1	0	0	0	0	0	0	0	0	0
As	5	0	2	3	2.4	0.3	3	0	0	0	3
S	50	102	78	79	80	79.2	80	79	77	83	3

Table B.5 Results of repeated analyses of Hawaiian basalt BHVO1 using SGS XRAL laboratories XRF data. The detection limits, expected values, and errors are given. Errors are presented as two standard deviations.

Appendix C

CHAPTER 2

Aggregate partial melting is calculated thus:

$$\overline{C_L} = \frac{C_O}{F}\left[1-\left(1-\frac{PF}{D_O}\right)^{\frac{1}{P}}\right]$$

Where $\overline{C}_L$ is the averaged concentration of a trace element in a mixed melt.

C_O is the concentration in the original solid.

F is the fraction of melting.

D_O is the bulk partition coefficient for the trace element.

P is the bulk distribution of the minerals that make up the melt

CHAPTER 3

Epsilon Sr is calculated thus:

$$\varepsilon_{Sr}^{t} = \left[\frac{(^{87}Sr/^{86}Sr)_R^i}{(^{87}Sr/^{86}Sr)_{UR}^t} - 1\right]\times 10^4$$

Where:

$\left(\frac{^{87}Sr}{^{86}Sr}\right)_R^i$ = Initial value of this ratio in the sample at time of crystallisation.

$\left(\frac{^{87}Sr}{^{86}Sr}\right)_{UR}^t$ = Value of this ratio in the uniform reservoir at any time t in the past.

The value of $\left(^{87}Sr/^{86}Sr\right)_{UR}^t$ can be calculated using:

$$\left(\frac{^{87}Sr}{^{86}Sr}\right)_{UR}^t = \left(\frac{^{87}Sr}{^{86}Sr}\right)_{UR}^0 - \left(\frac{^{87}Rb}{^{86}Sr}\right)_{UR}^0 \left(e^{\lambda t}-1\right)$$

Where:

$\left(\frac{^{87}Sr}{^{86}Sr}\right)^{0}_{UR}$ = Value of this ratio in the uniform reservoir at the present and is equal to 0.7045.

$\left(\frac{^{87}Rb}{^{86}Sr}\right)^{0}_{UR}$ = Value of this ratio in the uniform reservoir at the present and is equal to 0.0816. (Faure, 1986)

e = Natural logarithm

λ = Decay constant of ^{87}Rb $=1.42\times10^{-11}\,y^{-1}$.

t = Time before present in millions of years.

Epsilon Nd is calculated using:

$$\varepsilon^{t}_{CHUR} = \left[\frac{(^{143}Nd/^{144}Nd)_{i}}{(^{143}Nd/^{144}Nd)^{t}_{CHUR}} - 1\right]\times10^{4}$$

Where:

$(^{143}Nd/^{144}Nd)_{i}$ = The value of this ratio in the sample corrected for age of crystallisation.

$(^{143}Nd/^{144}Nd)^{t}_{CHUR}$ = The value of this ratio in CHUR (chondritic uniform reservoir) corrected to the time of crystallisation of the samples.

$(^{143}Nd/^{144}Nd)^{t}_{CHUR}$ is calculated thus:

$$(^{143}Nd/^{144}Nd)^{t}_{CHUR} = (^{147}Sm/^{144}Nd)^{0}_{CHUR}(e^{\lambda t} - 1)$$

Where:

$(^{147}Sm/^{144}Nd)^{0}_{CHUR}$ = This ratio in CHUR at the present. Equal to 0.1967.

$\left(^{143}Nd/^{144}Nd\right)_{CHUR}$ = This ratio in CHUR at the present, 0.512638 (Faure, 1986)

e = Natural logarithm.

λ = Decay constant of ^{147}Sm, $6.54 \times 10^{-12}\, y^{-1}$

t = Time before present in millions of years.

CHAPTER 4

Calculating the Fe/Mg ratio and Mg# for the normal troctolite:

Inferred primary olivine forsterite = 80

Therefore Fe/Mg ratio of olivine is:

$$\frac{1-(Fo/100)}{(Fo/100)} = \frac{1-0.8}{0.8} = 0.25$$

Because Roeder and Emslie (1970) state:

$$\left(\frac{(Fe/Mg)_{\text{Olivine}}}{(Fe/Mg)_{\text{Melt}}}\right) = 0.3 \pm 0.03$$

The Fe/Mg ratio of the melt is:

$$\frac{0.25}{0.3} = 0.833\dot{3}$$

Therefore the Mg# of the parental melt is:

$$100 \times \left[1 - \left(\frac{0.833\dot{3}}{1+0.833\dot{3}}\right)\right] = 55$$

a

b

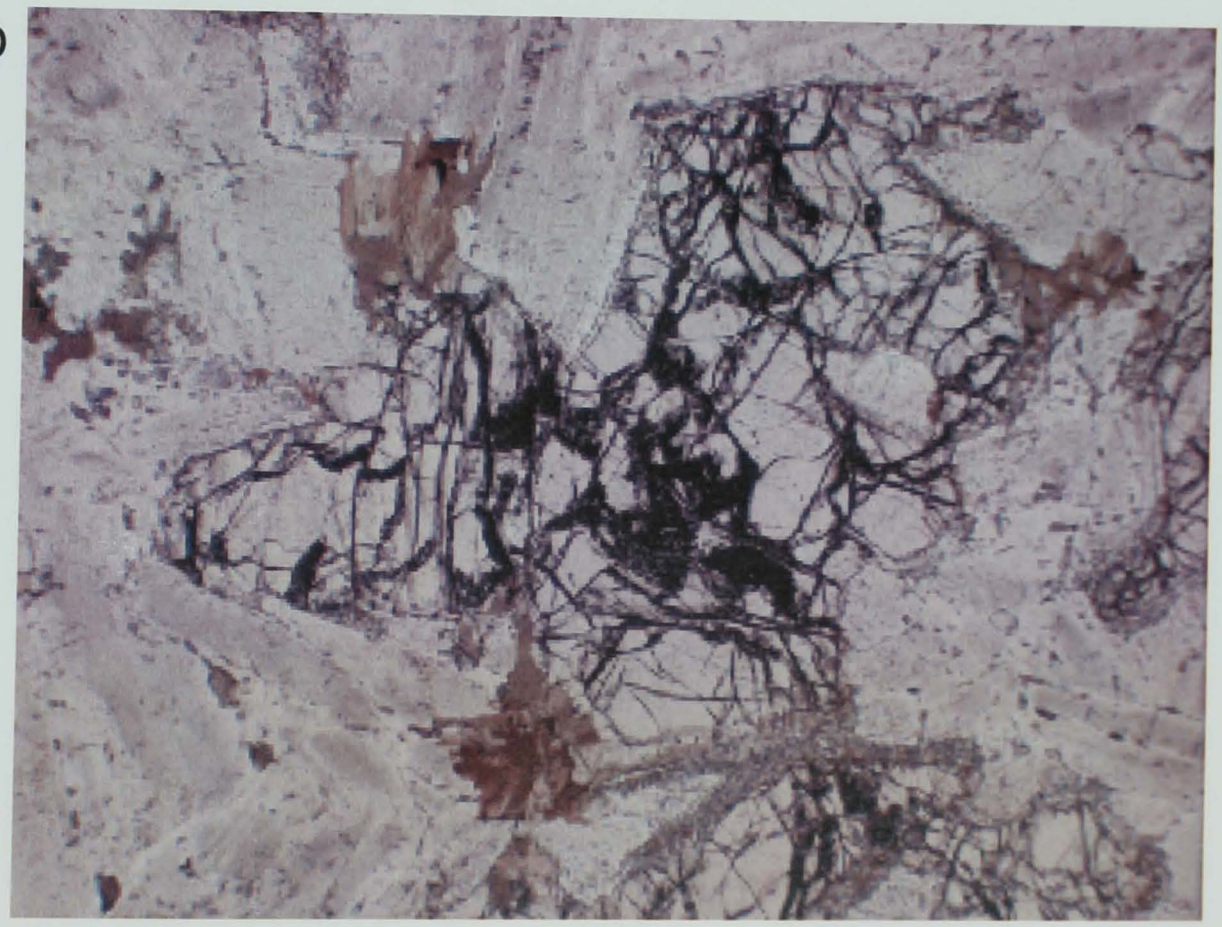

Figure D1a and b. Normal Troctolite, both sections shown in PPL. Both have clear plagioclase with litle evidence of hydration and alteration of sericite. Olivine grains are near pristine with only very slight corona textures of ortho and clinopyroxene. Field of view is approximately 5mm.

a

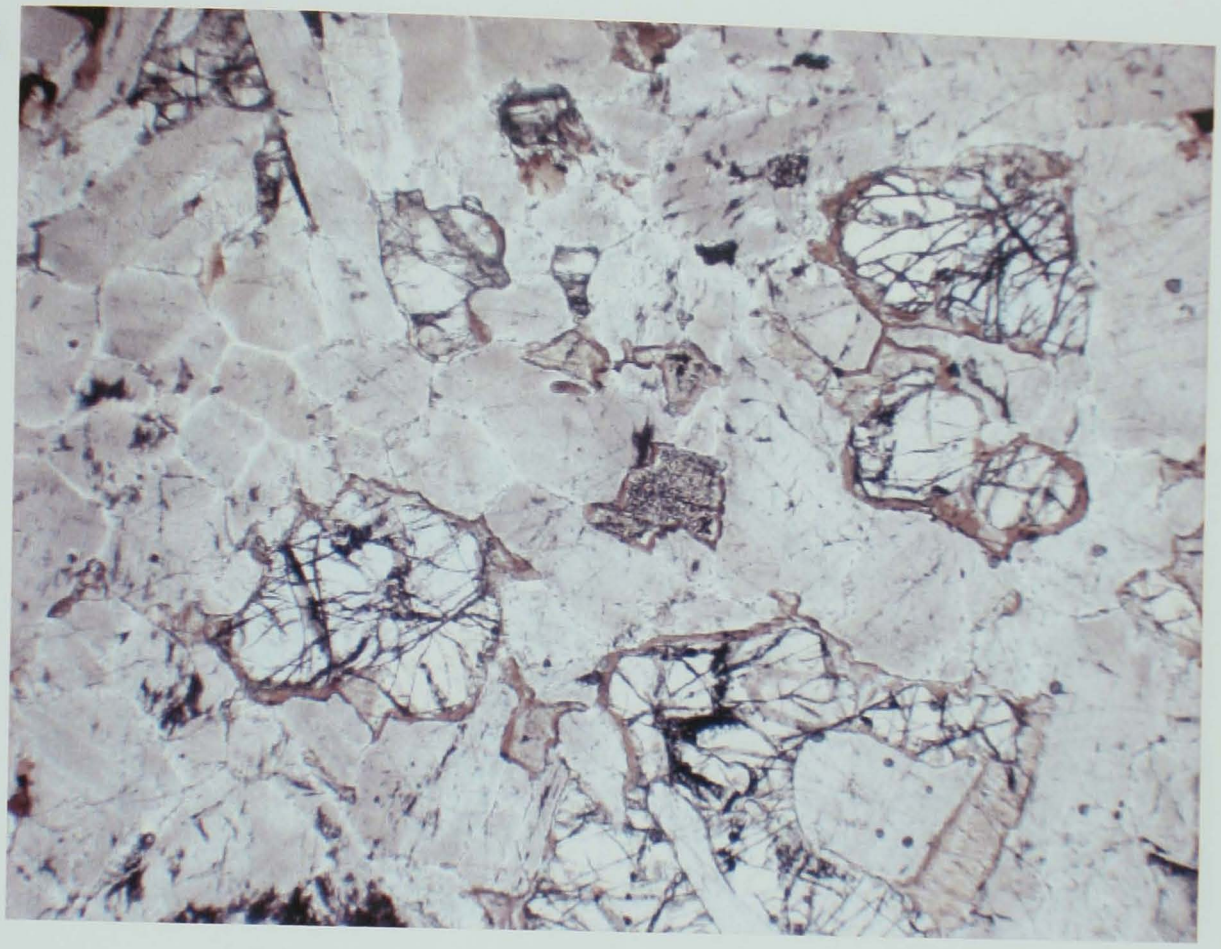

b

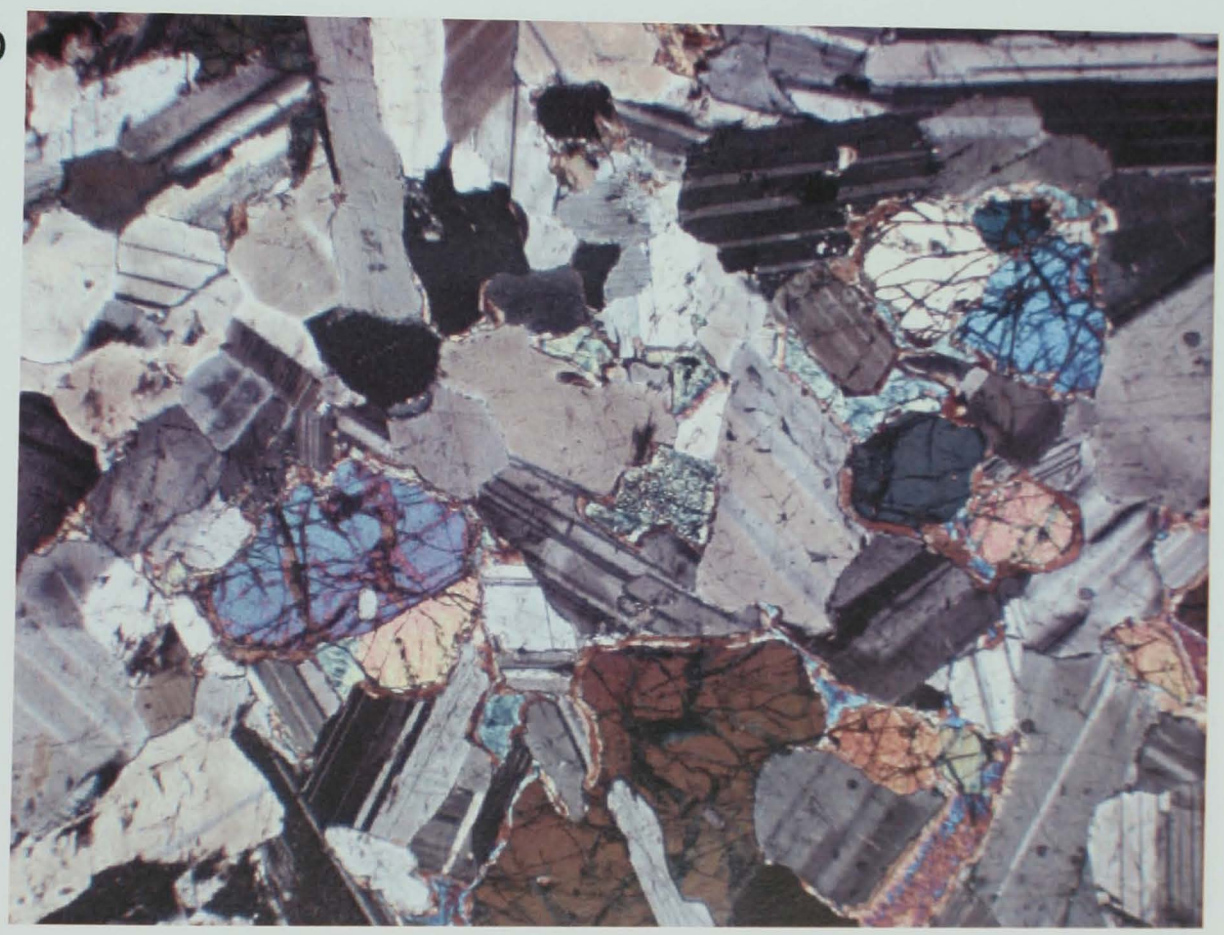

Figure D2a and b. Variable Troctolite. Here, instead of the pristine texture observed in the Normal troctolite, the olivine grains have corona textures of orthopyroxene and clinopyroxene and some embayment can be detected. Plagioclase is beginning to hydrate, perhaps to sericite and has a 'dusty' appearance. Figure a is in PPL, Figure b is in XPL. Field of view is approximately 5 mm in both cases.

a

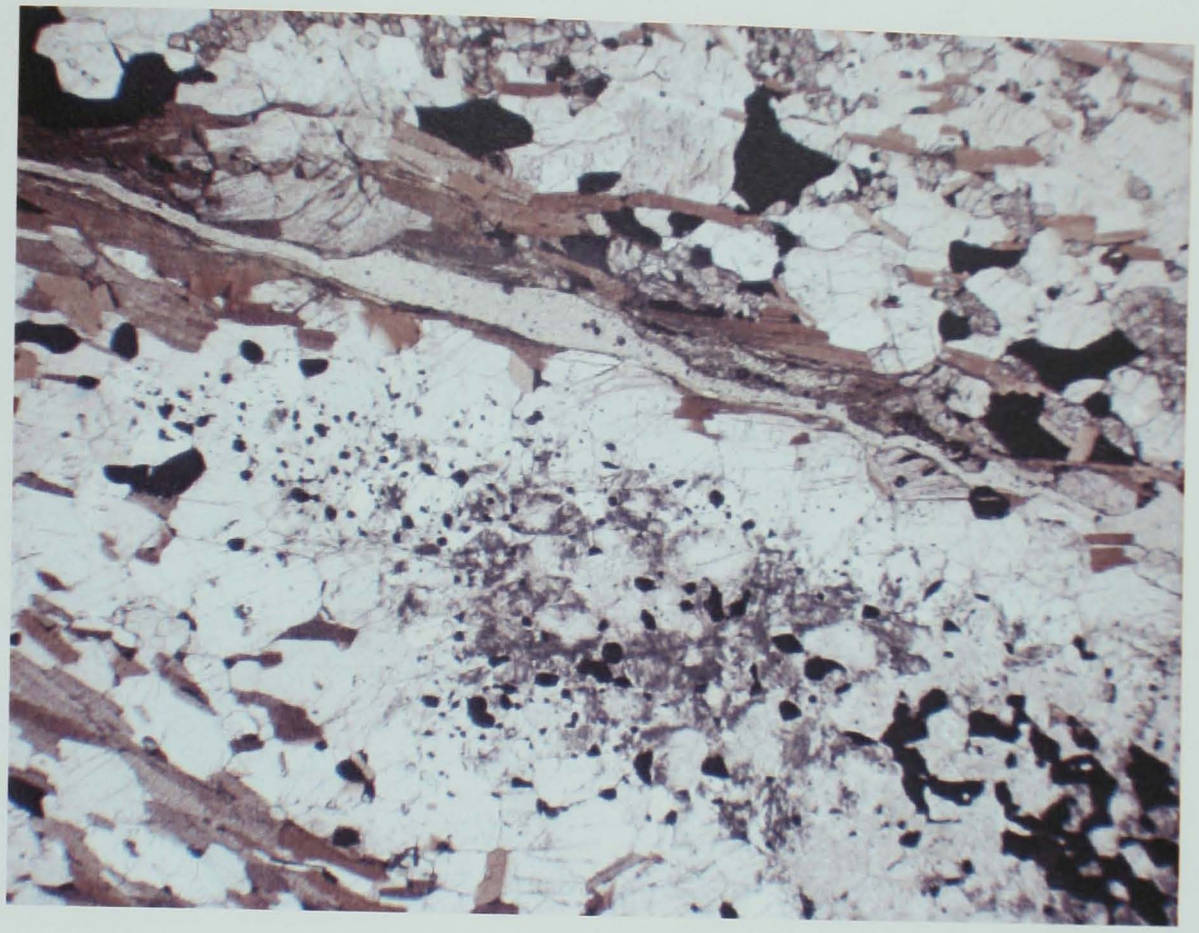

b

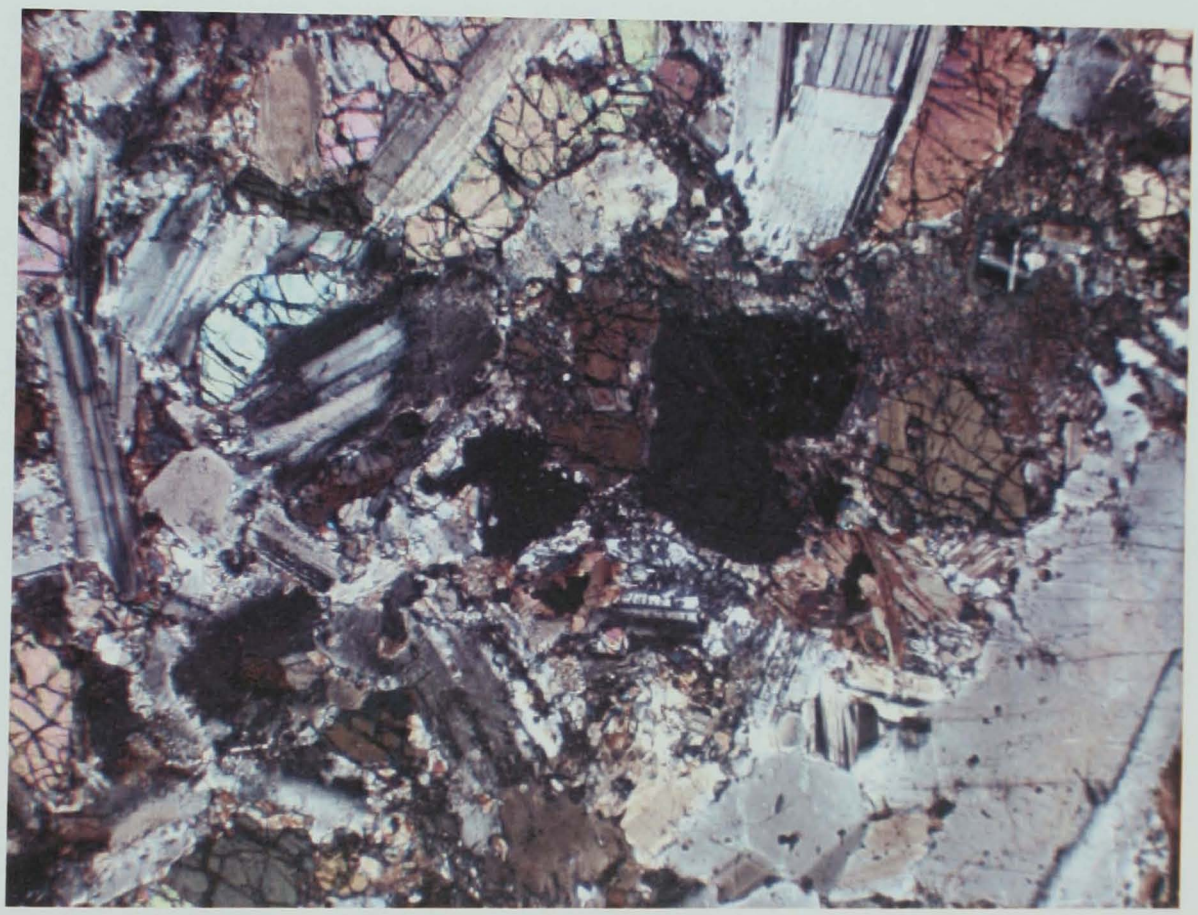

Figure D3 a and b. Breccia sequence rocks under PPL and XPL respectively. The field of view is approximately 5.5mm across. Almost central in D3a is a gneiss fragment with extensive alteration of feldspars to sericite. Thin section D3b is of a different part of the section, here olivine is seen altered to clinopyroxene. Opaque grains are sulphide, mostly pyrrhotite though some chalcopyrite and pentlandite are observed. Relict gneiss textures can be still be detected.

a

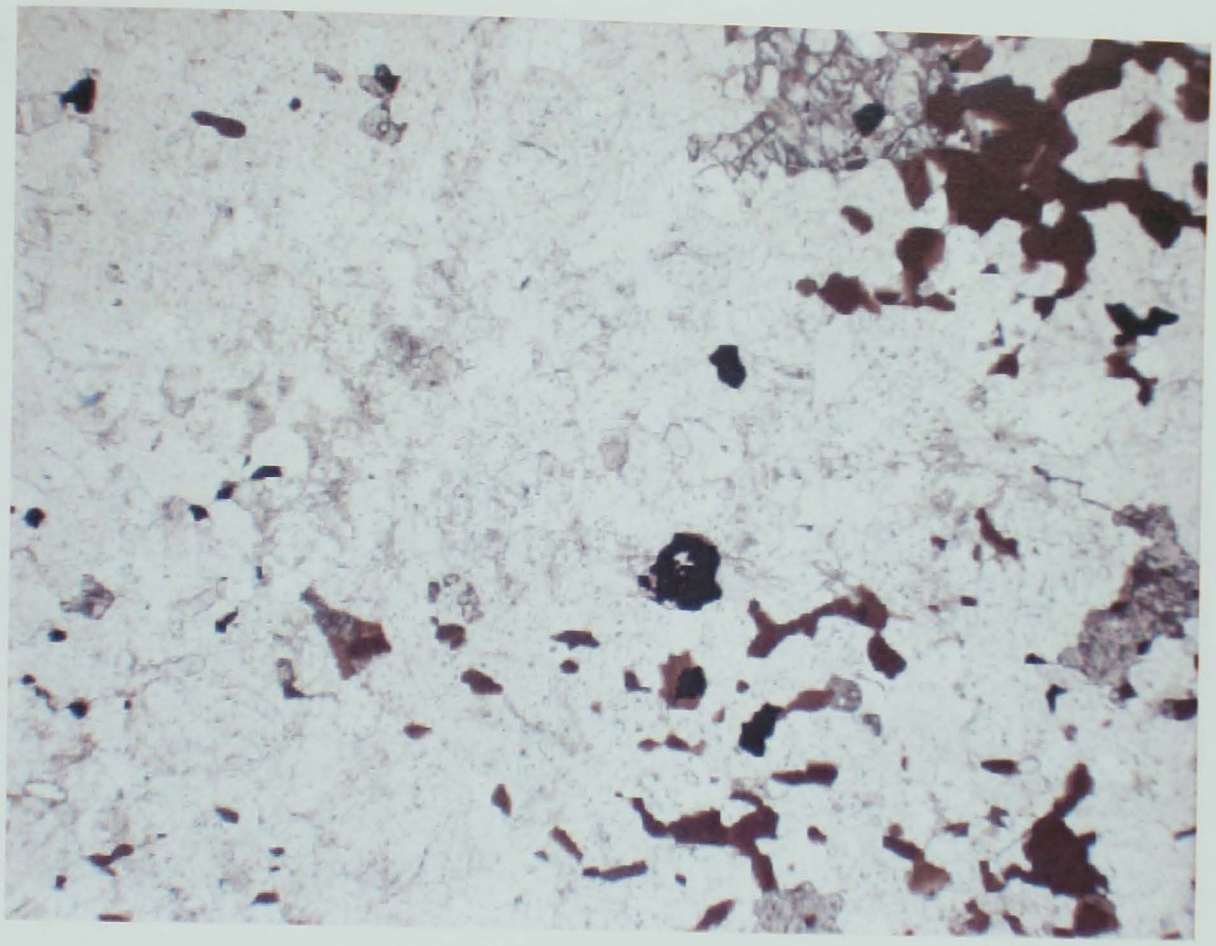

b

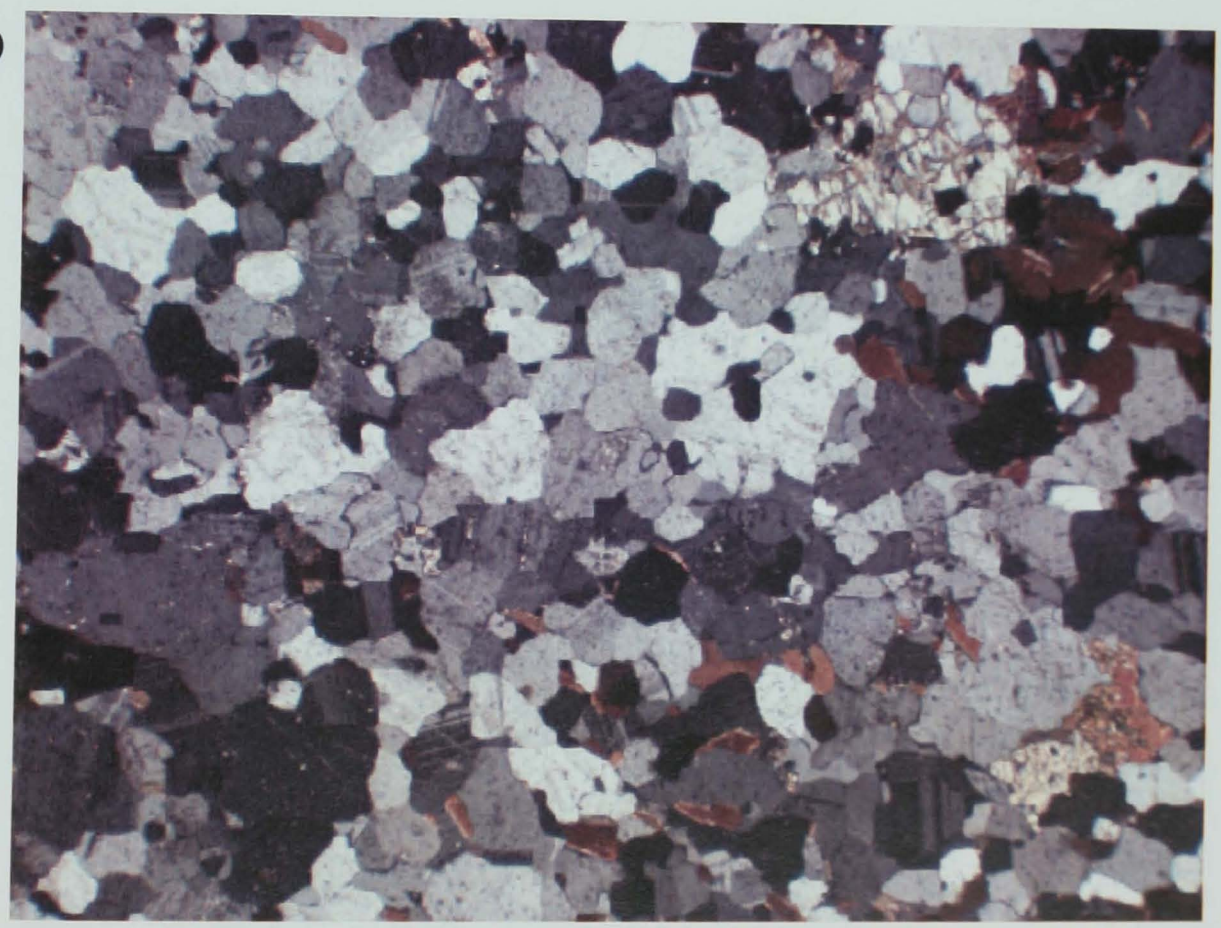

Figure D4 a and b. Nain gneiss, a quartzofeldspathic orthogneiss with accessory amphibole and biotite. Figure D4a is in PPL while Figure D4b is in XPL. Field of view is approximately 5mm in both cases.

a

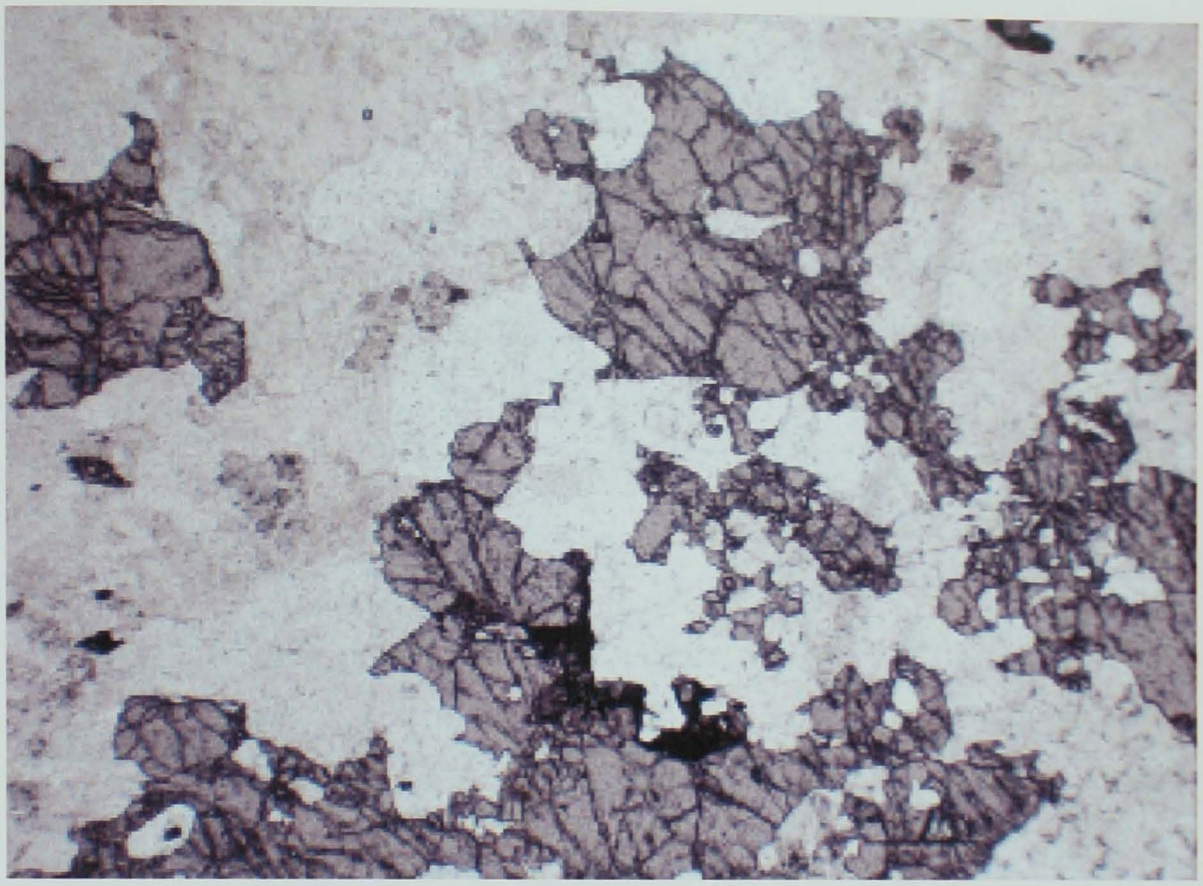

b

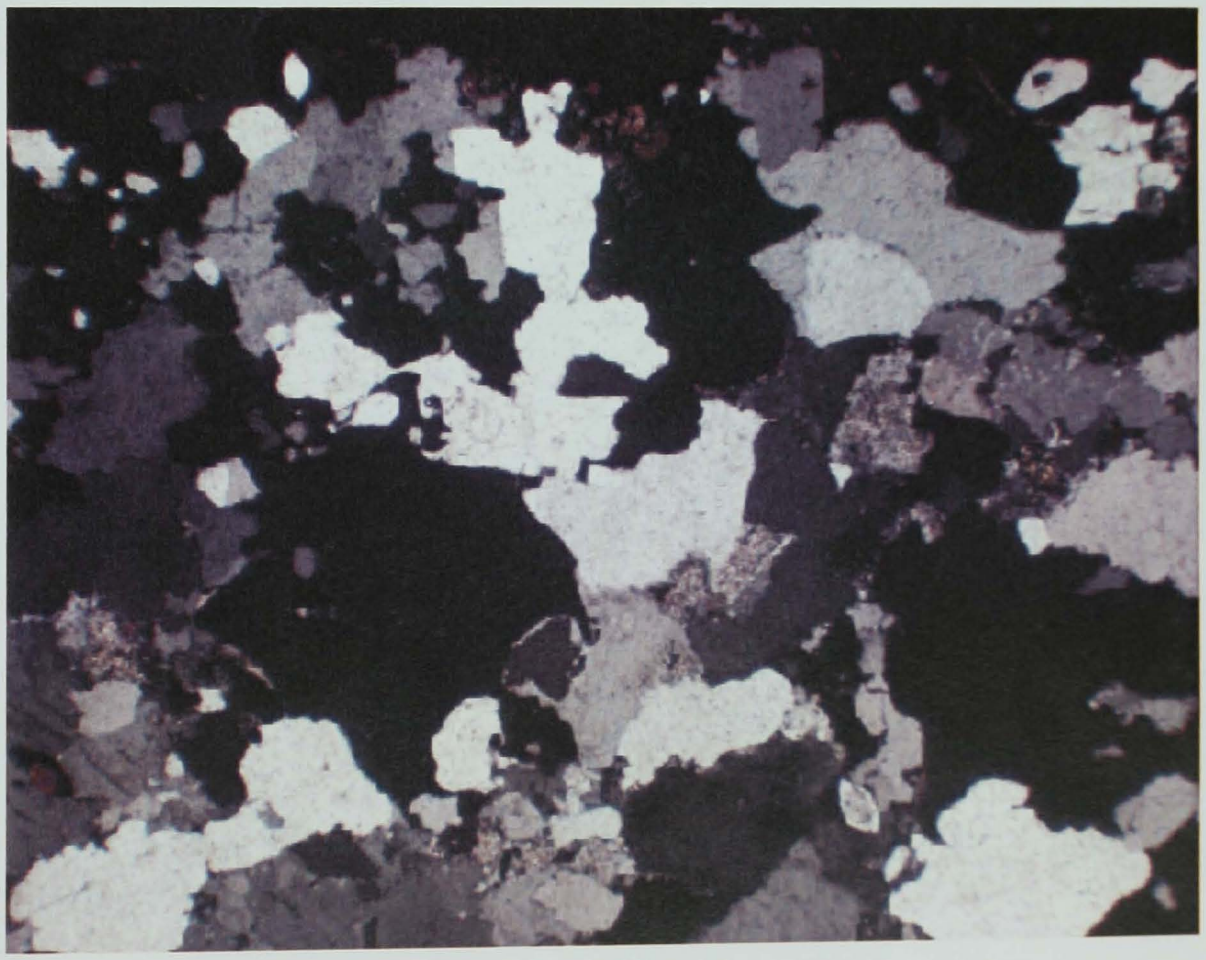

FigureD5 a and b. Tasiuyak gneiss. A quartzofeldspathic garnetiferous paragneiss. Clearly evident here are the garnet grains, high relief in PPL (Figure a) and isotropic in XPL (Figure b). Feldspars in this sample are typical of the rock in that they are significantly altered. Field of view is approximately 5mm.

a

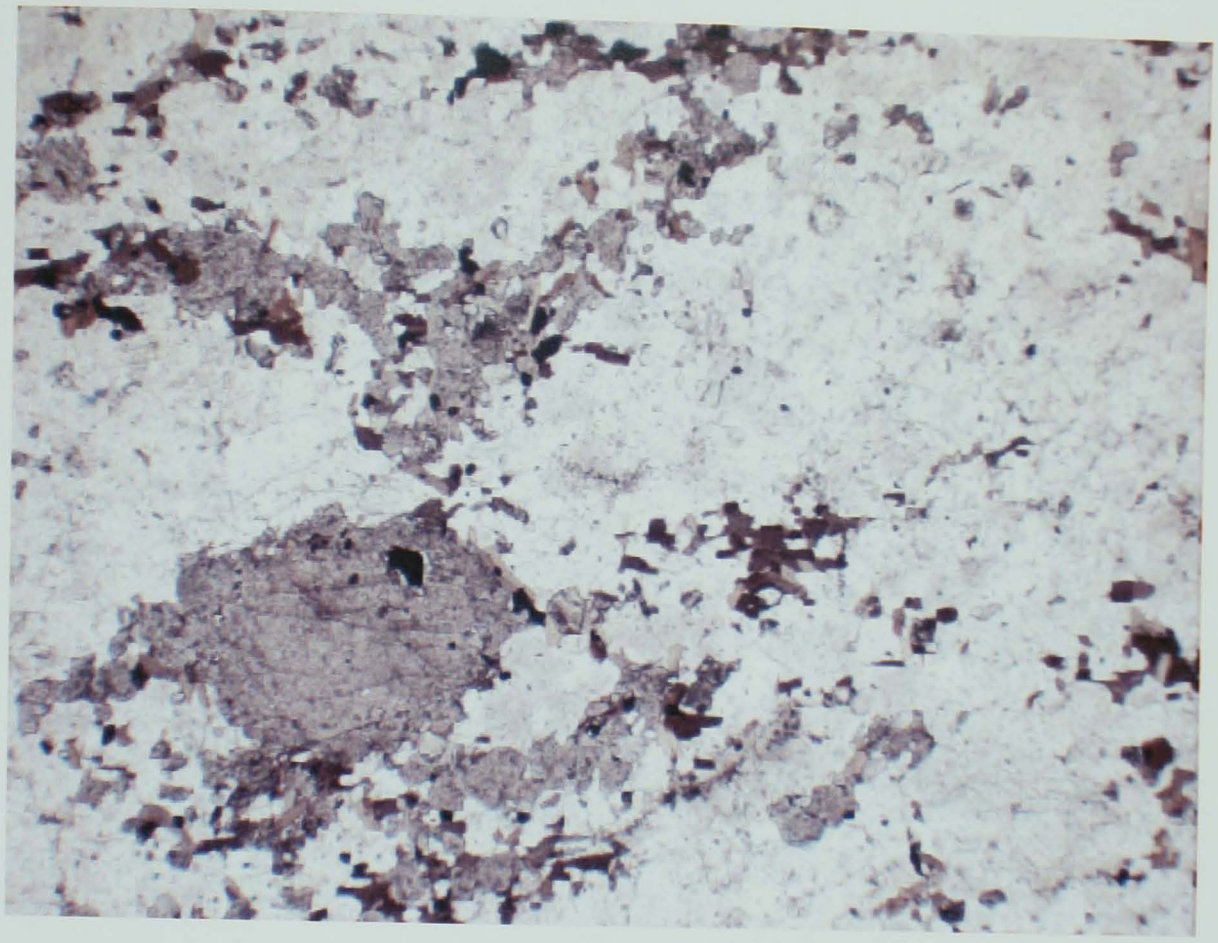

b

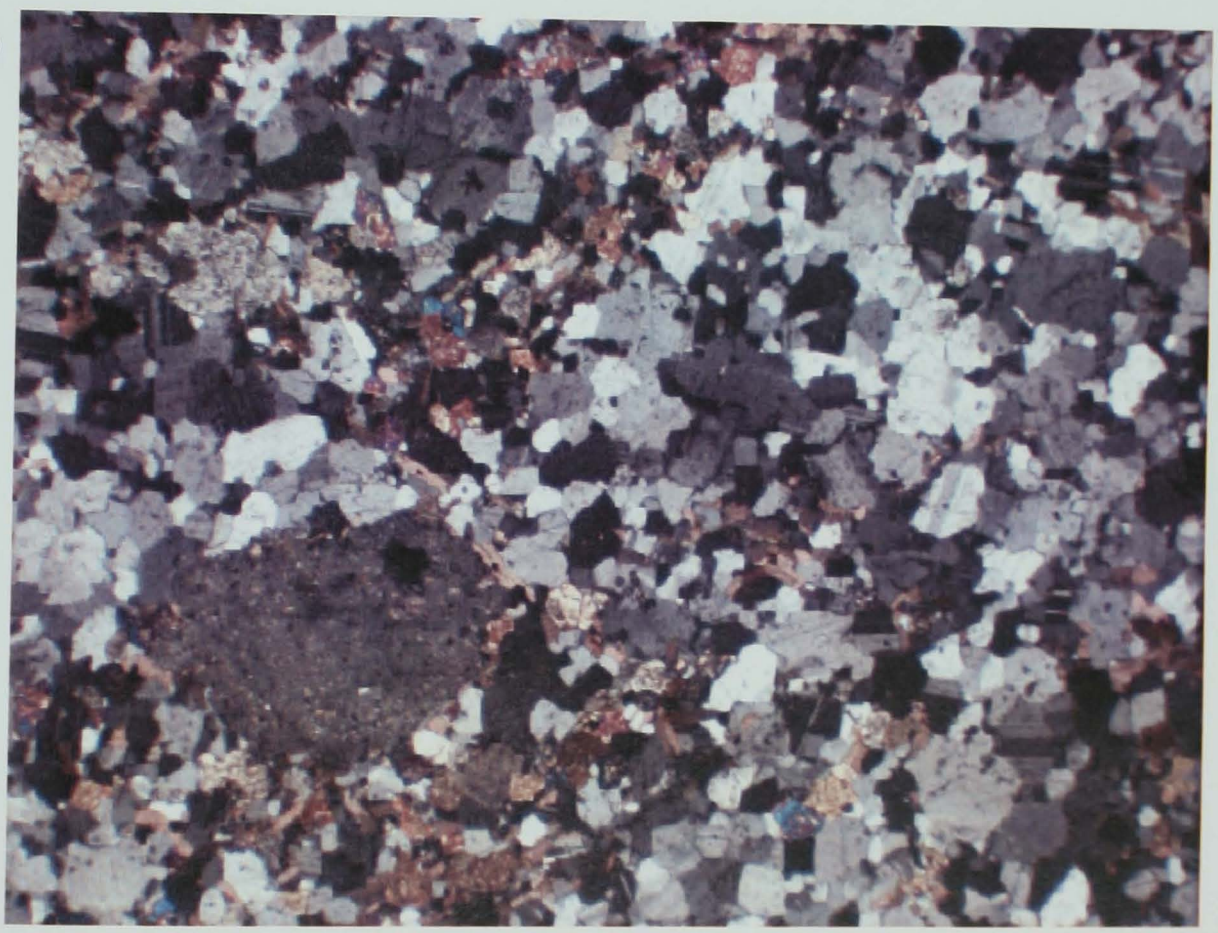

Figure D6 a and b. Enderbite gneiss. A quartzofeldspathic orthogneiss with abundant amphibole and biotite mica grains. Isolated opaques are sulphides, predominantly pyrrhotite. Figure a is PPL and Figure b XPL. Field of view is ~5mm in both cases.